Security Algorithms and Risk Management using Fuzzy Sets

Lead Guest Editor: Kifayat Ullah
Guest Editors: Tahir Mahmood, Qaisar Khan, and Shouzhen Zeng

Security Algorithms and Risk Management using Fuzzy Sets

Security Algorithms and Risk Management using Fuzzy Sets

Lead Guest Editor: Kifayat Ullah
Guest Editors: Tahir Mahmood, Qaisar Khan, and
Shouzhen Zeng

De Rosal Ignatius Moses Setiadi iD,
Indonesia
Wenbo Shi, China
Ghanshyam Singh iD, South Africa
Vasco Soares, Portugal
Salvatore Sorce iD, Italy
Abdulhamit Subasi, Saudi Arabia
Zhiyuan Tan iD, United Kingdom
Keke Tang iD, China
Je Sen Teh iD, Australia
Bohui Wang, China
Guojun Wang, China
Jinwei Wang iD, China
Qichun Wang iD, China
Hu Xiong iD, China
Chang Xu iD, China
Xuehu Yan iD, China
Anjia Yang iD, China
Jiachen Yang iD, China
Yu Yao iD, China
Yinghui Ye, China
Kuo-Hui Yeh iD, Taiwan
Yong Yu iD, China
Xiaohui Yuan iD, USA
Sherali Zeadally, USA
Leo Y. Zhang, Australia
Tao Zhang, China
Youwen Zhu iD, China
Zhengyu Zhu iD, China

Contents

Contents

WILEY | Hindawi

Retraction

Retracted: Analysis of Economic Relationship Using the Concept of Complex Pythagorean Fuzzy Information

Security and Communication Networks

This article has been retracted by Hindawi following an investigation undertaken by the publisher [1]. This investigation has uncovered evidence of one or more of the following indicators of systematic manipulation of the publication process:

(1) Discrepancies in scope

(2) Discrepancies in the description of the research reported

(3) Discrepancies between the availability of data and the research described

(4) Inappropriate citations

(5) Incoherent, meaningless and/or irrelevant content included in the article

(6) Manipulated or compromised peer review

The presence of these indicators undermines our confidence in the integrity of the article's content and we cannot, therefore, vouch for its reliability. Please note that this notice is intended solely to alert readers that the content of this article is unreliable. We have not investigated whether authors were aware of or involved in the systematic manipulation of the publication process.

Wiley and Hindawi regrets that the usual quality checks did not identify these issues before publication and have since put additional measures in place to safeguard research integrity.

We wish to credit our own Research Integrity and Research Publishing teams and anonymous and named external researchers and research integrity experts for contributing to this investigation.

The corresponding author, as the representative of all authors, has been given the opportunity to register their agreement or disagreement to this retraction. We have kept a record of any response received.

References

[1] N. Jan, S. U. Rehman, A. Nasir, H. Aydi, and S. U. Khan, "Analysis of Economic Relationship Using the Concept of Complex Pythagorean Fuzzy Information," *Security and Communication Networks*, vol. 2021, Article ID 4513992, 12 pages, 2021.

WILEY | Hindawi

Retraction

Retracted: An IoT-Based Water Level Detection System Enabling Fuzzy Logic Control and Optical Fiber Sensor

Security and Communication Networks

This article has been retracted by Hindawi following an investigation undertaken by the publisher [1]. This investigation has uncovered evidence of one or more of the following indicators of systematic manipulation of the publication process:

(1) Discrepancies in scope

(2) Discrepancies in the description of the research reported

(3) Discrepancies between the availability of data and the research described

(4) Inappropriate citations

(5) Incoherent, meaningless and/or irrelevant content included in the article

(6) Manipulated or compromised peer review

The presence of these indicators undermines our confidence in the integrity of the article's content and we cannot, therefore, vouch for its reliability. Please note that this notice is intended solely to alert readers that the content of this article is unreliable. We have not investigated whether authors were aware of or involved in the systematic manipulation of the publication process.

Wiley and Hindawi regrets that the usual quality checks did not identify these issues before publication and have since put additional measures in place to safeguard research integrity.

We wish to credit our own Research Integrity and Research Publishing teams and anonymous and named external researchers and research integrity experts for contributing to this investigation.

The corresponding author, as the representative of all authors, has been given the opportunity to register their agreement or disagreement to this retraction. We have kept a record of any response received.

References

[1] Y. Zheng, G. Dhiman, A. Sharma, A. Sharma, and M. A. Shah, "An IoT-Based Water Level Detection System Enabling Fuzzy Logic Control and Optical Fiber Sensor," *Security and Communication Networks*, vol. 2021, Article ID 4229013, 11 pages, 2021.

Retraction

Retracted: More General Form of Interval-Valued Fuzzy Ideals of BCK/BCI-Algebras

Security and Communication Networks

This article has been retracted by Hindawi following an investigation undertaken by the publisher [1]. This investigation has uncovered evidence of one or more of the following indicators of systematic manipulation of the publication process:

(1) Discrepancies in scope

(2) Discrepancies in the description of the research reported

(3) Discrepancies between the availability of data and the research described

(4) Inappropriate citations

(5) Incoherent, meaningless and/or irrelevant content included in the article

(6) Manipulated or compromised peer review

The presence of these indicators undermines our confidence in the integrity of the article's content and we cannot, therefore, vouch for its reliability. Please note that this notice is intended solely to alert readers that the content of this article is unreliable. We have not investigated whether authors were aware of or involved in the systematic manipulation of the publication process.

Wiley and Hindawi regrets that the usual quality checks did not identify these issues before publication and have since put additional measures in place to safeguard research integrity.

We wish to credit our own Research Integrity and Research Publishing teams and anonymous and named external researchers and research integrity experts for contributing to this investigation.

The corresponding author, as the representative of all authors, has been given the opportunity to register their agreement or disagreement to this retraction. We have kept a record of any response received.

References

[1] G. Muhiuddin, D. Al-Kadi, and A. Mahboob, "More General Form of Interval-Valued Fuzzy Ideals of BCK/BCI-Algebras," *Security and Communication Networks*, vol. 2021, Article ID 9930467, 10 pages, 2021.

Retraction

Retracted: Hamacher Weighted Aggregation Operators Based on Picture Cubic Fuzzy Sets and Their Application to Group Decision-Making Problems

Security and Communication Networks

This article has been retracted by Hindawi, as publisher, following an investigation undertaken by the publisher [1]. This investigation has uncovered evidence of systematic manipulation of the publication and peer-review process. We cannot, therefore, vouch for the reliability or integrity of this article.

Please note that this notice is intended solely to alert readers that the peer-review process of this article has been compromised.

Wiley and Hindawi regret that the usual quality checks did not identify these issues before publication and have since put additional measures in place to safeguard research integrity.

We wish to credit our Research Integrity and Research Publishing teams and anonymous and named external researchers and research integrity experts for contributing to this investigation.

The corresponding author, as the representative of all authors, has been given the opportunity to register their agreement or disagreement to this retraction. We have kept a record of any response received.

References

[1] L. Yanhong, R. Ambrin, M. Ibrar, and M. Ali Khan, "Hamacher Weighted Aggregation Operators Based on Picture Cubic Fuzzy Sets and Their Application to Group Decision-Making Problems," *Security and Communication Networks*, vol. 2022, Article ID 1651017, 39 pages, 2022.

WILEY | Hindawi

Retraction

Retracted: Fixed Point of Rational Contractions and Its Application for Secure Dynamic Routing in Wireless Sensor Networks

Security and Communication Networks

This article has been retracted by Hindawi following an investigation undertaken by the publisher [1]. This investigation has uncovered evidence of one or more of the following indicators of systematic manipulation of the publication process:

(1) Discrepancies in scope

(2) Discrepancies in the description of the research reported

(3) Discrepancies between the availability of data and the research described

(4) Inappropriate citations

(5) Incoherent, meaningless and/or irrelevant content included in the article

(6) Peer-review manipulation

The presence of these indicators undermines our confidence in the integrity of the article's content and we cannot, therefore, vouch for its reliability. Please note that this notice is intended solely to alert readers that the content of this article is unreliable. We have not investigated whether authors were aware of or involved in the systematic manipulation of the publication process.

Wiley and Hindawi regrets that the usual quality checks did not identify these issues before publication and have since put additional measures in place to safeguard research integrity.

We wish to credit our own Research Integrity and Research Publishing teams and anonymous and named external researchers and research integrity experts for contributing to this investigation.

The corresponding author, as the representative of all authors, has been given the opportunity to register their agreement or disagreement to this retraction. We have kept a record of any response received.

References

[1] A. Asif, E. Savas, H. AlSalman, M. Arshad, A. Gumaei, and A. Rehman, "Fixed Point of Rational Contractions and Its Application for Secure Dynamic Routing in Wireless Sensor Networks," *Security and Communication Networks*, vol. 2021, Article ID 9939546, 10 pages, 2021.

Retraction

Retracted: Cross-Border E-Commerce Supply Chain Risk Evaluation with FUZZY-ISM Model

Security and Communication Networks

This article has been retracted by Hindawi following an investigation undertaken by the publisher [1]. This investigation has uncovered evidence of one or more of the following indicators of systematic manipulation of the publication process:

(1) Discrepancies in scope

(2) Discrepancies in the description of the research reported

(3) Discrepancies between the availability of data and the research described

(4) Inappropriate citations

(5) Incoherent, meaningless and/or irrelevant content included in the article

(6) Peer-review manipulation

The presence of these indicators undermines our confidence in the integrity of the article's content and we cannot, therefore, vouch for its reliability. Please note that this notice is intended solely to alert readers that the content of this article is unreliable. We have not investigated whether authors were aware of or involved in the systematic manipulation of the publication process.

Wiley and Hindawi regrets that the usual quality checks did not identify these issues before publication and have since put additional measures in place to safeguard research integrity.

We wish to credit our own Research Integrity and Research Publishing teams and anonymous and named external researchers and research integrity experts for contributing to this investigation.

The corresponding author, as the representative of all authors, has been given the opportunity to register their agreement or disagreement to this retraction. We have kept a record of any response received.

References

[1] Z. Fang and Q. Wang, "Cross-Border E-Commerce Supply Chain Risk Evaluation with FUZZY-ISM Model," *Security and Communication Networks*, vol. 2021, Article ID 5155524, 14 pages, 2021.

Retraction

Retracted: Face Security Authentication System Based on Deep Learning and Homomorphic Encryption

Security and Communication Networks

This article has been retracted by Hindawi following an investigation undertaken by the publisher [1]. This investigation has uncovered evidence of one or more of the following indicators of systematic manipulation of the publication process:

(1) Discrepancies in scope

(2) Discrepancies in the description of the research reported

(3) Discrepancies between the availability of data and the research described

(4) Inappropriate citations

(5) Incoherent, meaningless and/or irrelevant content included in the article

(6) Peer-review manipulation

The presence of these indicators undermines our confidence in the integrity of the article's content and we cannot, therefore, vouch for its reliability. Please note that this notice is intended solely to alert readers that the content of this article is unreliable. We have not investigated whether authors were aware of or involved in the systematic manipulation of the publication process.

Wiley and Hindawi regrets that the usual quality checks did not identify these issues before publication and have since put additional measures in place to safeguard research integrity.

We wish to credit our own Research Integrity and Research Publishing teams and anonymous and named external researchers and research integrity experts for contributing to this investigation.

The corresponding author, as the representative of all authors, has been given the opportunity to register their agreement or disagreement to this retraction. We have kept a record of any response received.

References

[1] D. Sun, H. Huang, D. Zheng, H. Hu, C. Bi, and R. Wang, "Face Security Authentication System Based on Deep Learning and Homomorphic Encryption," *Security and Communication Networks*, vol. 2022, Article ID 7752292, 8 pages, 2022.

Retraction

Retracted: Some Novel Geometric Aggregation Operators of Spherical Cubic Fuzzy Information with Application

Security and Communication Networks

This article has been retracted by Hindawi following an investigation undertaken by the publisher [1]. This investigation has uncovered evidence of one or more of the following indicators of systematic manipulation of the publication process:

(1) Discrepancies in scope

(2) Discrepancies in the description of the research reported

(3) Discrepancies between the availability of data and the research described

(4) Inappropriate citations

(5) Incoherent, meaningless and/or irrelevant content included in the article

(6) Peer-review manipulation

The presence of these indicators undermines our confidence in the integrity of the article's content and we cannot, therefore, vouch for its reliability. Please note that this notice is intended solely to alert readers that the content of this article is unreliable. We have not investigated whether authors were aware of or involved in the systematic manipulation of the publication process.

Wiley and Hindawi regrets that the usual quality checks did not identify these issues before publication and have since put additional measures in place to safeguard research integrity.

We wish to credit our own Research Integrity and Research Publishing teams and anonymous and named external researchers and research integrity experts for contributing to this investigation.

The corresponding author, as the representative of all authors, has been given the opportunity to register their agreement or disagreement to this retraction. We have kept a record of any response received.

References

[1] Z. Ullah, H. Bashir, R. Anjum et al., "Some Novel Geometric Aggregation Operators of Spherical Cubic Fuzzy Information with Application," *Security and Communication Networks*, vol. 2021, Article ID 3774353, 14 pages, 2021.

WILEY | Hindawi

Retraction

Retracted: The Segmentation of Road Scenes Based on Improved ESPNet Model

Security and Communication Networks

This article has been retracted by Hindawi following an investigation undertaken by the publisher [1]. This investigation has uncovered evidence of one or more of the following indicators of systematic manipulation of the publication process:

(1) Discrepancies in scope

(2) Discrepancies in the description of the research reported

(3) Discrepancies between the availability of data and the research described

(4) Inappropriate citations

(5) Incoherent, meaningless and/or irrelevant content included in the article

(6) Peer-review manipulation

The presence of these indicators undermines our confidence in the integrity of the article's content and we cannot, therefore, vouch for its reliability. Please note that this notice is intended solely to alert readers that the content of this article is unreliable. We have not investigated whether authors were aware of or involved in the systematic manipulation of the publication process.

Wiley and Hindawi regrets that the usual quality checks did not identify these issues before publication and have since put additional measures in place to safeguard research integrity.

We wish to credit our own Research Integrity and Research Publishing teams and anonymous and named external researchers and research integrity experts for contributing to this investigation.

The corresponding author, as the representative of all authors, has been given the opportunity to register their agreement or disagreement to this retraction. We have kept a record of any response received.

References

[1] R. Jin, T. Yu, X. Han, and Y. Liu, "The Segmentation of Road Scenes Based on Improved ESPNet Model," *Security and Communication Networks*, vol. 2021, Article ID 1681952, 11 pages, 2021.

Retraction

Retracted: Intuitionistic Fuzzy Double Controlled Metric Spaces and Related Results

Security and Communication Networks

This article has been retracted by Hindawi following an investigation undertaken by the publisher [1]. This investigation has uncovered evidence of one or more of the following indicators of systematic manipulation of the publication process:

(1) Discrepancies in scope

(2) Discrepancies in the description of the research reported

(3) Discrepancies between the availability of data and the research described

(4) Inappropriate citations

(5) Incoherent, meaningless and/or irrelevant content included in the article

(6) Peer-review manipulation

The presence of these indicators undermines our confidence in the integrity of the article's content and we cannot, therefore, vouch for its reliability. Please note that this notice is intended solely to alert readers that the content of this article is unreliable. We have not investigated whether authors were aware of or involved in the systematic manipulation of the publication process.

Wiley and Hindawi regrets that the usual quality checks did not identify these issues before publication and have since put additional measures in place to safeguard research integrity.

We wish to credit our own Research Integrity and Research Publishing teams and anonymous and named external researchers and research integrity experts for contributing to this investigation.

The corresponding author, as the representative of all authors, has been given the opportunity to register their agreement or disagreement to this retraction. We have kept a record of any response received.

References

[1] M. Farheen, K. Ahmed, K. Javed, V. Parvaneh, F. U. Din, and U. Ishtiaq, "Intuitionistic Fuzzy Double Controlled Metric Spaces and Related Results," *Security and Communication Networks*, vol. 2022, Article ID 6254055, 15 pages, 2022.

WILEY | Hindawi

Retraction

Retracted: A Systematic Analysis of Regression Test Case Selection: A Multi-Criteria-Based Approach

Security and Communication Networks

This article has been retracted by Hindawi following an investigation undertaken by the publisher [1]. This investigation has uncovered evidence of one or more of the following indicators of systematic manipulation of the publication process:

(1) Discrepancies in scope

(2) Discrepancies in the description of the research reported

(3) Discrepancies between the availability of data and the research described

(4) Inappropriate citations

(5) Incoherent, meaningless and/or irrelevant content included in the article

(6) Peer-review manipulation

The presence of these indicators undermines our confidence in the integrity of the article's content and we cannot, therefore, vouch for its reliability. Please note that this notice is intended solely to alert readers that the content of this article is unreliable. We have not investigated whether authors were aware of or involved in the systematic manipulation of the publication process.

Wiley and Hindawi regrets that the usual quality checks did not identify these issues before publication and have since put additional measures in place to safeguard research integrity.

We wish to credit our own Research Integrity and Research Publishing teams and anonymous and named external researchers and research integrity experts for contributing to this investigation.

The corresponding author, as the representative of all authors, has been given the opportunity to register their agreement or disagreement to this retraction. We have kept a record of any response received.

References

[1] M. Rehan, N. Senan, M. Aamir et al., "A Systematic Analysis of Regression Test Case Selection: A Multi-Criteria-Based Approach," *Security and Communication Networks*, vol. 2021, Article ID 5834807, 11 pages, 2021.

WILEY | Hindawi

Retraction

Retracted: Hybrid Structures Applied to Subalgebras of BCH-Algebras

Security and Communication Networks

This article has been retracted by Hindawi following an investigation undertaken by the publisher [1]. This investigation has uncovered evidence of one or more of the following indicators of systematic manipulation of the publication process:

(1) Discrepancies in scope

(2) Discrepancies in the description of the research reported

(3) Discrepancies between the availability of data and the research described

(4) Inappropriate citations

(5) Incoherent, meaningless and/or irrelevant content included in the article

(6) Peer-review manipulation

The presence of these indicators undermines our confidence in the integrity of the article's content and we cannot, therefore, vouch for its reliability. Please note that this notice is intended solely to alert readers that the content of this article is unreliable. We have not investigated whether authors were aware of or involved in the systematic manipulation of the publication process.

Wiley and Hindawi regrets that the usual quality checks did not identify these issues before publication and have since put additional measures in place to safeguard research integrity.

We wish to credit our own Research Integrity and Research Publishing teams and anonymous and named external researchers and research integrity experts for contributing to this investigation.

The corresponding author, as the representative of all authors, has been given the opportunity to register their agreement or disagreement to this retraction. We have kept a record of any response received.

References

[1] G. Muhiuddin, D. Al-Kadi, W. Khan, and C. Jana, "Hybrid Structures Applied to Subalgebras of BCH-Algebras," *Security and Communication Networks*, vol. 2021, Article ID 8960437, 8 pages, 2021.

Retraction

Retracted: Intuitionistic Fuzzy Double Controlled Metric Spaces and Related Results

Security and Communication Networks

This article has been retracted by Hindawi following an investigation undertaken by the publisher [1]. This investigation has uncovered evidence of one or more of the following indicators of systematic manipulation of the publication process:

(1) Discrepancies in scope

(2) Discrepancies in the description of the research reported

(3) Discrepancies between the availability of data and the research described

(4) Inappropriate citations

(5) Incoherent, meaningless and/or irrelevant content included in the article

(6) Peer-review manipulation

The presence of these indicators undermines our confidence in the integrity of the article's content and we cannot, therefore, vouch for its reliability. Please note that this notice is intended solely to alert readers that the content of this article is unreliable. We have not investigated whether authors were aware of or involved in the systematic manipulation of the publication process.

Wiley and Hindawi regrets that the usual quality checks did not identify these issues before publication and have since put additional measures in place to safeguard research integrity.

We wish to credit our own Research Integrity and Research Publishing teams and anonymous and named external researchers and research integrity experts for contributing to this investigation.

The corresponding author, as the representative of all authors, has been given the opportunity to register their agreement or disagreement to this retraction. We have kept a record of any response received.

References

[1] M. Farheen, K. Ahmed, K. Javed, V. Parvaneh, F. U. Din, and U. Ishtiaq, "Intuitionistic Fuzzy Double Controlled Metric Spaces and Related Results," *Security and Communication Networks*, vol. 2022, Article ID 6254055, 15 pages, 2022.

WILEY | Hindawi

Research Article

Intuitionistic Fuzzy Double Controlled Metric Spaces and Related Results

Misbah Farheen ⓘ,[1] **Khalil Ahmed,**[2] **Khalil Javed ⓘ,**[2] **Vahid Parvaneh,**[3] **Fahim Ud Din ⓘ,**[4] **and Umar Ishtiaq ⓘ**[5]

[1]*Department of Mathematics, Quaid-I-Azam University, Islamabad, Pakistan*
[2]*Department of Math & Stats, International Islamic University, Islamabad, Pakistan*
[3]*Department of Mathematics, Gilan-E-Gharb Branch, Islamic Azad University, Gilan-E-Gharb, Iran*
[4]*Abdus Salam School of Mathematical Sciences, Government College University, Lahore, Pakistan*
[5]*Office of Research, Innovation and Commercialization, University of Management and Technology, Lahore, Pakistan*

Correspondence should be addressed to Khalil Javed; khalil.msma551@iiu.edu.pk

In this article, we introduce the concept of intuitionistic fuzzy double controlled metric spaces that generalizes the concept of intuitionistic fuzzy b-metric spaces. For this purpose, two noncomparable functions are used in triangle inequalities. We generalize the concepts of the Banach contraction principle and fuzzy contractive mappings by giving authentic proof of these mappings in the sense of intuitionistic fuzzy double controlled metric spaces. To validate the superiority of these results, examples are imparted. A possible application to solving integral equations is also set forth towards the end of this work to support the proposed results.

1. Introduction

The concept of metric spaces and the Banach contraction principle are the backbone of the field of fixed point theory. Since the axiomatic interpretations of metric space, it has attracted researchers due to its spaciousness. So far, different developments in metric space have appeared in the literature, either by improving contraction conditions or by relaxing the axioms of metric space.

Zadeh [1] was the first to put forward the concept of fuzzy sets and this idea has deeply influenced many scientific fields since its inception. Using the concepts of probabilistic metric space and fuzzy sets, fuzzy metric space was introduced in [2]. Afterward, the utility of FMS appeared in applied sciences such as fixed-point theory, image and signal processing, medical imaging, and decision-making. This concept succeeded in shifting a lot of mathematical structures within itself. In this continuation, Kramosil and Michalek [3] initiated the notion of fuzzy

metric spaces. Khalil et al. [4] generalized this concept by introducing fuzzy b-metric-like spaces. Fuzzy metric space only discusses membership functions, so for dealing with membership and nonmembership functions, the notion of intuitionistic fuzzy metric spaces introduced by Park [5] and this concept was generalized into intuitionistic fuzzy b-metric spaces by Konwar [6]. In this connectedness, many important results appeared in the literature, such as fixed point theorems on intuitionistic fuzzy metric space [7], fixed point theorems for a generalized intuitionistic fuzzy contraction in intuitionistic fuzzy metric spaces [8], extension of fixed point results in intuitionistic fuzzy b-metric spaces [6], fixed points in intuitionistic fuzzy metric spaces [4], fuzzy fixed point [9], and some more work in generalized metric space in [10], ordered defined in fuzzy b-metric [11], partial metric defining the relation in [12], orthogonal neutrosophic metric space [13], and orthogonal partial metric space [14]. More details related to generalized metric spaces can be seen in [15].

Recently, Saleem et al. [10] introduced the notion of fuzzy double controlled metric spaces and generalized the Banach contraction principle. This result was generalized in different spaces and different structures were attained using this topic. One may recall some basic results related to this topic, such as controlled fuzzy metric spaces and some related fixed point results in [16], controlled metric type spaces, and the related contraction principle in [17] and orthogonally controlled metric type spaces in [18], and very recently, the new aspects of metric spaces in [19].

In this article, we aim to generalize the concept of intuitionistic fuzzy b-metric spaces and introduce the concept of intuitionistic fuzzy double controlled metric spaces. Some nontrivial examples are given and an application to solving integral equations is also imparted in this work. Table 1 of abbreviations of notions will be used throughout this study.

1.1. Preliminaries.

First, we define some necessary definitions that are helpful for readers to understand the main results.

Definition 1 (see [2]). A binary operation $* : [0, 1] \times [0, 1] \longrightarrow [0, 1]$ is called a CTN if

(1) $\pi * \mu = \mu * \pi, (\forall)\pi, \mu \in [0, 1]$;

(2) $*$ is continuous;

(3) $\pi * 1 = \pi, (\forall)\pi \in [0, 1]$;

(4) $(\pi * \mu) * \rho = \pi * (\mu * \rho), (\forall)\pi, \mu, \rho \in [0, 1]$;

(5) $\pi \le \rho$ and $\mu \le d$, with $\pi, \mu, \rho, d \in [0, 1]$, then $\pi * \mu \le \rho * d$.

Example 1 (see [20]). Some fundamental examples of CTNs are $\pi * \mu = \pi \cdot \mu, \pi * \mu = \min\{\pi, \mu\}$ and $\pi * \mu = \max\{\pi + \mu - 1, 0\}$.

Definition 2 (see [2]). A binary operation $\bigcirc: [0, 1] \times [0, 1] \longrightarrow [0, 1]$ is called a CTCN if it meets the following assertions:

(1) $\pi \bigcirc \mu = \mu \bigcirc \pi$, or all $\pi, \mu \in [0, 1]$

(2) $\bigcirc$ is continuous;

(3) $\pi \bigcirc 0 = 0$, for all $\pi \in [0, 1]$;

(4) $(\pi \bigcirc \mu) \bigcirc \rho = \pi \bigcirc (\mu \bigcirc \rho)$, for all $\pi, \mu, \rho \in [0, 1]$;

(5) If $\pi \le \rho$ and $\mu \le d$, with $\pi, \mu, \rho, d \in [0, 1]$, then $\pi \bigcirc \mu \le \rho \bigcirc d$.

Example 2 (see [2]). $\pi \bigcirc \mu = \max\{\pi, \mu\}$ and $\pi \bigcirc \mu = \min\{\pi + \mu, 1\}$ are examples of CTCNs.

Definition 3 (see [21]). Let functions $\phi, \eta: \mathfrak{B} \times \mathfrak{B} \longrightarrow [1, \infty)$ be noncomparable. Let $\partial: \mathfrak{B} \times \mathfrak{B} \longrightarrow [0, \infty)$ be fulfilling:

(a) $\partial(x, y) = 0$ if $x = y$;

(b) $\partial(x, y) = \partial(y, x)$;

(c) $\partial(x, y) \le \phi(x, z)\partial(x, z) + \eta(z, y)\partial(z, y)$, for all $x, y, z \in \mathfrak{B}$. Then, ∂ is called a double controlled

metric and $(\mathfrak{B}, \partial)$ is called a double controlled metric space.

Definition 4 (see [21]). Let $\mathfrak{B} \ne \varnothing$ and $\phi, \eta: \mathfrak{B} \times \mathfrak{B} \longrightarrow [1, \infty)$ be given noncomparable functions, and $*$ is a CTN and P be a FS on $\mathfrak{B} \times \mathfrak{B} \times (0, \infty)$ which is called fuzzy double controlled metric on $\mathfrak{B}$; if for all $x, y, z \in \mathfrak{B}$, the below circumstances are fulfilling:

(I) $P(x, y, 0) = 0$;

(II) $P(x, y, t) = 1$ for all $t > 0$, if and only if $x = y$;

(III) $P(x, y, t) = P(y, x, t)$;

(IV) $P(x, z, t + s) \ge P(x, y, t/\phi(x, y)) * P(y, z, s/\eta(y, z))$;

(V) $P(x, y, \cdot): (0, \infty) \longrightarrow [0, 1]$ is left continuous.

Then, $(\mathfrak{B}, P, Q, *)$ is named a FDCMS.

Definition 5 (see [6]). Take $\mathfrak{B} \ne \varnothing$. Let $*$ be a CTN, $\bigcirc$ be a CTCN, $b \ge 1$, and P, Q be FSs on $\mathfrak{B} \times \mathfrak{B} \times (0, \infty)$, if the following for all $x, y \in \mathfrak{B}$ and $s, t > 0$:

(I) $P(x, y, t) + Q(x, y, t) \le 1$;

(II) $P(x, y, t) > 0$;

(III) $P(x, y, t) = 1 \Leftrightarrow x = y$;

(IV) $P(x, y, t) = P(y, x, t)$;

(V) $P(x, z, b(t + s)) \ge P(x, y, t) * P(y, z, s)$;

(VI) $P(x, y, \cdot)$ is a nondecreasing function of $\mathbb{R}^+$ and $\lim_{t \longrightarrow \infty} P(x, y, t) = 1$;

(VII) $Q(x, y, t) > 0$;

(VIII) $Q(x, y, t) = 0 \Leftrightarrow x = y$;

(IX) $Q(x, y, t) = Q(y, x, t)$;

(X) $Q(x, z, b(t + s)) \le Q(x, y, t)\bigcirc Q(y, z, s)$;

(XI) $Q(x, y, \cdot)$ is a nonincreasing function of $\mathbb{R}^+$ and $\lim_{t \longrightarrow \infty} Q(x, y, t) = 0$, then $(\mathfrak{B}, P, Q, *, \bigcirc)$ is an IFBMS.

2. Main Results

In this section, we introduce the concept of IFDCMSs and prove some fixed point (FP) results.

Definition 6. Let $\mathfrak{B} \ne \varnothing$ and $\phi, \eta: \mathfrak{B} \times \mathfrak{B} \longrightarrow [1, \infty)$ be given noncomparable functions, and $*$ is a CTN and $\bigcirc$ is a CTCN. P, Q are FSs on $\mathfrak{B} \times \mathfrak{B} \times (0, \infty)$ which are named intuitionistic fuzzy double controlled metrics on $\mathfrak{B}$; if for all $x, y, z \in \mathfrak{B}$, the below circumstances are fulfilling:

(I) $P(x, y, t) + Q(x, y, t) \le 1$

(II) $P(x, y, t) > 0$;

(III) $P(x, y, t) = 1$ for all $t > 0$, if and only if $x = y$;

(IV) $P(x, y, t) = P(y, x, t)$;

(V)
$P(x, z, t + s) \ge P(x, y, t/\phi(x, y)) * P(y, z, s/\eta(y, z))$;

(VI) $P(x, y, \cdot): (0, \infty) \longrightarrow [0, 1]$ is left continuous;

Table 1: Abbreviations.

Abbreviations	Meanings
FSs	Fuzzy sets
FMSs	Fuzzy metric spaces
IFBMSs	Intuitionistic fuzzy b-metric spaces
FDCMSs	Fuzzy double controlled metric spaces
IFDCMSs	Intuitionistic fuzzy double controlled metric spaces
CTN	Continuous triangle norm
CTCN	Continuous triangle conorm

(VII) $Q(x, y, t) < 1$;

(VIII) $Q(x, y, t) = 0$ for all $t > 0$, if and only if $x = y$;

(IX) $Q(x, y, t) = Q(y, x, t)$;

(X) $Q(x, z, t + s) \leq Q(x, y, t/\Phi(x, y)) \bigcirc Q (y, z, s/\eta(y, z))$;

(XI) $Q(x, y, \cdot): (0, \infty) \longrightarrow [0, 1]$ is left continuous.

Then, $(\mathfrak{B}, P, Q, *, \bigcirc)$ is called an IFDCMS.

Remark 1. If we take $\Phi(x, y) = \eta(y, z) = b \geq 1$, then IFDCMS becomes an IFBMS.

Example 3. Let $\mathfrak{B} = \{1, 2, 3\}$ and $\Phi, \eta: \mathfrak{B} \times \mathfrak{B} \longrightarrow [1, \infty)$ be two noncomparable functions given by $\Phi(x, y) = x + y + 1$ and $\eta(x, y) = x^2 + y^2 - 1$. Define $P, Q: \mathfrak{B} \times \mathfrak{B} \times (0, \infty) \longrightarrow [0, 1]$ as

$$P(x, y, t) = \begin{cases} 1, & \text{if } x = y, \\ \dfrac{t}{t + \max\{x, y\}}, & \text{if otherwise.} \end{cases} \tag{1}$$

$$Q(x, y, t) = \begin{cases} 1, & \text{if } x = y, \\ \dfrac{t}{t + \max\{x, y\}}, & \text{if otherwise.} \end{cases}$$

Then, $(\mathfrak{B}, P, Q, *, \bigcirc)$ is an IFDCMS with CTN $\pi * \mu = \pi\mu$ and CTCN $\pi \bigcirc \mu = \max\{\pi, \mu\}$.

Proof. Conditions (i)–(iv), (vi)–(ix), and (xi) are easy to examine Here, we prove (v) and (x).

Let $x = 1, y = 2$, and $z = 3$. Then,

$$P(1, 3, t + s) = \frac{t + s}{t + s + \max\{1, 3\}} \tag{2}$$

$$= \frac{t + s}{t + s + 3}.$$

On the other hand,

$$P\left(1, 2, \frac{t}{\Phi(1, 2)}\right) = \frac{t/\Phi(1, 2)}{\Phi(1, 2) + \max\{1, 2\}}$$

$$= \frac{t/4}{t/4 + 2} = \frac{t}{t + 8}. \tag{3}$$

$$P\left(2, 3, \frac{s}{\eta(2, 3)}\right) = \frac{s/\eta(2, 3)}{s/\eta(2, 3) + \max\{2, 3\}}$$

$$= \frac{s/12}{s/12 + 3} = \frac{s}{s + 36}.$$

That is,

$$\frac{t + s}{t + s + 3} \geq \frac{t}{t + 8} \cdot \frac{s}{s + 36}. \tag{4}$$

Then, it satisfies for all $t, s > 0$. Hence,

$$P(x, z, t + s) \geq P\left(x, y, \frac{t}{\Phi(x, y)}\right) * P\left(y, z, \frac{s}{\Phi(y, z)}\right). \tag{5}$$

Now,

$$Q(1, 3, t + s) = \frac{\max\{1, 3\}}{t + s + \max\{1, 3\}} \tag{6}$$

$$= \frac{3}{t + s + 3}.$$

On the other hand,

$$Q\left(1, 2, \frac{t}{\eta(1, 2)}\right) = \frac{\max\{1, 2\}}{t/\eta(1, 2) + \max\{1, 2\}}$$

$$= \frac{2}{t/4 + 2} = \frac{8}{t + 8}. \tag{7}$$

$$Q\left(2, 3, \frac{s}{\eta(2, 3)}\right) = \frac{\max\{2, 3\}}{s/\eta(2, 3) + \max\{2, 3\}}$$

$$= \frac{3}{s/12 + 3} = \frac{36}{s + 36}.$$

That is,

$$\frac{3}{t + s + 3} \leq \max\left\{\frac{8}{t + 8}, \frac{36}{s + 36}\right\}. \tag{8}$$

Then, it satisfies for all $t, s > 0$. Hence,

$$Q(x, z, t + s) \leq Q\left(x, y, \frac{t}{\Phi(x, y)}\right) \bigcirc Q\left(y, z, \frac{s}{\Phi(y, z)}\right). \tag{9}$$

On the same lines, one can examine all other cases. Hence, $(\mathfrak{B}, P, Q, *, \bigcirc)$ is an IFDCMS. $\square$

Remark 2. The above example also satisfied for CTN $\pi * \mu = \min\{\pi, \mu\}$ and CTCN $\pi \bigcirc \mu = \max\{\pi, \mu\}$.

Example 4. Let $\mathfrak{B} = (0, \infty)$ and $\phi, \eta\colon \mathfrak{B} \times \mathfrak{B} \longrightarrow [1, \infty)$ be two noncomparable functions given by $\phi(x, y) = x + y + 1$ and $\eta(x, y) = x^2 + y^2 - 1$.

Define P, Q: $\mathfrak{B} \times \mathfrak{B} \times (0, \infty) \longrightarrow [0, 1]$ as

$$P(x, y, t) = \frac{t}{t + |x - y|^2},$$

$$Q(x, y, t) = \frac{|x - y|^2}{t + |x - y|^2}.$$

(10)

Then, $(\mathfrak{B}, P, Q, *, \bigcirc)$ is an IFDCMS with CTN $\pi * \mu = \pi\mu$ and CTCN $\pi\bigcirc\mu = \max\{\pi, \mu\}$.

Remark 3. The above example also holds for

$$\phi(x, y) = \begin{cases} 1, & \text{if } x = y, \\ \dfrac{1 + \max\{x, y\}}{\min\{x, y\}}, & \text{if } x \neq y, \end{cases}$$

$$\eta(x, y) = \begin{cases} 1, & \text{if } x = y, \\ \dfrac{1 + \max\{x^2, y^2\}}{\min\{x^2, y^2\}}, & \text{if } x \neq y. \end{cases}$$

(11)

Remark 4. The above example is also satisfied for CTN $\pi * \mu = \min\{\pi, \mu\}$ and CTCN $\pi\bigcirc\mu = \max\{\pi, \mu\}$.

Example 5. Let $\mathfrak{B} = \{1, 2, 3\}$ and $\phi, \eta\colon \mathfrak{B} \times \mathfrak{B} \longrightarrow [1, \infty)$ be two noncomparable functions given by $\phi(x, y) = x + y + 1$ and $\eta(x, y) = x^2 + y^2 - 1$. Define P, Q: $\mathfrak{B} \times \mathfrak{B} \times (0, \infty) \longrightarrow [0, 1]$ as

$$P(x, y, t) = \frac{t + \min\{x, y\}}{t + \max\{x, y\}},$$

$$Q(x, y, t) = 1 - \frac{t + \min\{x, y\}}{t + \max\{x, y\}}.$$

(12)

Then, $(\mathfrak{B}, P, Q, *, \bigcirc)$ is an IFDCMS with CTN $\pi * \mu = \pi\mu$ and CTCN $\pi\bigcirc\mu = \max\{\pi, \mu\}$.

Proof. It is easy to examine the line of the above example.   □

Remark 5. The above example is not IFDCMS if we take CTN $\pi * \mu = \min\{\pi, \mu\}$, CTCN $\pi\bigcirc\mu = \max\{\pi, \mu\}$, and $x = 1, y = 2, z = 3, t = 0.02, s = 0.03$ with $\phi(x, y) = x + y + 1$ and $\eta(x, y) = x^2 + y^2 - 1$.

Proposition 1. *Let $\mathfrak{B} = [0, 1]$ and $\phi, \eta\colon \mathfrak{B} \times \mathfrak{B} \longrightarrow [0, 1]$ be two noncomparable functions given by $\phi(x, y) = 2(x + y + 1)$ and $\eta(x, y) = 2(x^2 + y^2 + 1)$. Define Q, P as*

$$P(x, y, t^n) = e^{-\left((x-y)^2/t^n\right)},$$

$$Q(x, y, t^n) = 1 - e^{-\left((x-y)^2/t^n\right)} \text{ for all } x, y \in \mathfrak{B}, t > 0.$$

(13)

Then, $(\mathfrak{B}, P, Q, *, \bigcirc)$ *is an IFDCMS with CTN $\pi * \mu = \pi\mu$ and CTCN $\pi\bigcirc\mu = \max\{\pi, \mu\}$.*

Remark 6. The above proposition is also satisfied for CTN $\pi * \mu = \min\{\pi, \mu\}$ and CTCN $\pi\bigcirc\mu = \max\{\pi, \mu\}$.

Proposition 2. *Let $\mathfrak{B} = [0, 1]$ and $\phi, \eta\colon \mathfrak{B} \times \mathfrak{B} \longrightarrow [0, 1]$ be two noncomparable functions given by $\phi(x, y) = 2(x + y + 1)$ and $\eta(x, y) = 2(x^2 + y^2 + 1)$. Define Q, P as*

$$P(x, y, t^n) = \left[e^{-\left((x-y)^2/t^n\right)}\right]^{-1},$$

$$Q(x, y, t^n) = 1 - \left[e^{-\left((x-y)^2/t^n\right)}\right]^{-1} \quad \text{for all } x, y \in \mathfrak{B}, t > 0.$$

(14)

Then, $(\mathfrak{B}, P, Q, *, \bigcirc)$ *is an IFDCMS with CTN $\pi * \mu = \pi\mu$ and CTCN $\pi\bigcirc\mu = \max\{\pi, \mu\}$.*

Remark 7. The above proposition is also satisfied for CTN $\pi * \mu = \min\{\pi, \mu\}$ and CTCN $\pi\bigcirc\mu = \max\{\pi, \mu\}$.

Definition 7. Let $(\mathfrak{B}, P, Q, *, \bigcirc)$ be an IFDCMS. Then, we define an open ball $B(x, r, t)$ with center x, radius $r, 0 < r < 1$, and $t > 0$ as follows:

$$B(x, r, t) = \{y \in \mathfrak{B}\colon P(x, y, t) > 1 - r, Q(x, y, t) < r\}. \quad (15)$$

Remark 8. An IFDCMS $(\mathfrak{B}, P, Q, *, \bigcirc)$ needs not to be a Hausdorff.

Proof. Let $\mathfrak{B} = \{1, 2, 3\}$ and $\phi, \eta\colon \mathfrak{B} \times \mathfrak{B} \longrightarrow [1, \infty)$ be two noncomparable functions given by $\phi(x, y) = x + y + 1$ and $\eta(x, y) = x^2 + y^2 - 1$. Define P, Q: $\mathfrak{B} \times \mathfrak{B} \times (0, \infty) \longrightarrow [0, 1]$ as

$$P(x, y, t) = \frac{t + \min\{x, y\}}{t + \max\{x, y\}},$$

$$Q(x, y, t) = 1 - \frac{t + \min\{x, y\}}{t + \max\{x, y\}}.$$

(16)

Then, $(\mathfrak{B}, P, Q, *, \bigcirc)$ is an IFDCMS with CTN $\pi * \mu = \pi\mu$ and CTCN $\pi\bigcirc\mu = \max\{\pi, \mu\}$. Consider the open ball $B(1, 0.4, 6)$ centered at 1, with radius $r = 0.4$ and $t = 6$. Then,

$$B(1, 0.4, 6) = \{y \in \mathfrak{B}\colon P(1, y, 6) > 0.6, Q(1, y, 6) < 0.4\}.$$

(17)

Now,

$$P(1,2,6) = \frac{1+6}{2+6}$$

$$= \frac{7}{8} = 0.875,$$

$$Q(1,2,6) = 1 - \frac{1+6}{2+6}$$

$$= 1 - \frac{7}{8} = 1 - 0.875$$

$$= 0.125,$$

$$P(1,3,6) = \frac{1+6}{3+6}$$

$$= \frac{7}{9} = 0.777,$$

$$Q(1,3,6) = 1 - \frac{1+6}{3+6}$$

$$= 1 - \frac{7}{9} = 1 - 0.777$$

$$= 0.223. \tag{18}$$

Thus, $B(1, 0.4, 6) = \{2, 3\}$. Now, consider the open ball $B(2, 0.6, 12)$ with radius $r = 0.6$, centered at 2, and $t = 12$. Then,

$$B(2, 0.6, 12) = \{y \in \mathfrak{B} : P(2, y, 12) > 0.4, Q(2, y, 12) < 0.6\}. \tag{19}$$

Now,

$$P(2,1,12) = \frac{1+12}{2+12}$$

$$= \frac{13}{14} = 0.928,$$

$$Q(2,1,12) = 1 - \frac{1+12}{2+12}$$

$$= 1 - \frac{13}{14}$$

$$= 0.071,$$

$$P(2,3,12) = \frac{2+12}{3+12}$$

$$= \frac{14}{15} = 0.933,$$

$$Q(2,3,12) = 1 - \frac{2+12}{3+12}$$

$$= 1 - \frac{14}{15} = 1 - 0.933$$

$$= 0.066. \tag{20}$$

Thus, $B(2, 0.6, 12) = \{1, 3\}$. Now,

$$B(1, 0.4, 6) \cap B(2, 0.6, 12) = \{2, 3\} \cap \{1, 3\},$$
$$= \{3\} \neq . \tag{21}$$

Hence, an IFDCMS is not necessarily Hausdorff. $\quad\square$

Definition 8. Let $(\mathfrak{B}, P, Q, *, \bigcirc)$ be an IFDCMS and $\{x_n\}$ be a sequence in $\mathfrak{B}$. Then, $\{x_n\}$ is named to be

(a) Convergent, if there exists $x \in \mathfrak{B}$ such that

$$\lim_{n \to \infty} P(x_n, x, t) = 1,$$

$$\lim_{n \to \infty} Q(x_n, x, t) = 0, \text{for all } t > 0. \tag{22}$$

(b) A Cauchy sequence (CS), if and only if for each $\mu > 0, t > 0$, there exists $n_0 \in \mathbb{N}$ such that

$$P(x_n, x_{n+q}, t) \geq 1 - \mu,$$

$$Q(x_n, x_{n+q}, t) \leq \mu, \text{ for all } n, m \geq n_0. \tag{23}$$

If every Cauchy sequence is convergent in $\mathfrak{B}$, then $(\mathfrak{B}, P, Q, *, \bigcirc)$ is called a complete IFDCMS.

Lemma 1. *Let $\{x_n\}$ be a Cauchy sequence in IFDCMS $(\mathfrak{B}, P, Q, *, \bigcirc)$ such that $x_n \neq x_m$ whenever $m, n \in \mathbb{N}$ with $n \neq m$. Then, the sequence $\{x_n\}$ can converge to at most one limit point.*

Proof. Ccontrarily, assume that $x_n \longrightarrow x$ and $x_n \longrightarrow y$, for $x \neq y$. Then, $\lim_{n \to \infty} P(x_n, x, t) = 1, \lim_{n \to \infty} Q(x_n, x, t) = 0$ and $\lim_{n \to \infty} P(x_n, y, t) = 1, \lim_{n \to \infty} Q(x_n, y, t) = 0$, for all $t > 0$. Therefore,

$$P(x, y, t) \geq P\left(x, x_n, \frac{t}{2\phi(x, x_n)}\right) * P\left(x_n, y, \frac{t}{2\eta(x_n, y)}\right)$$

$$\longrightarrow 1 * 1, \text{as } n \longrightarrow \infty,$$

$$Q(x, y, t) \leq Q\left(x, x_n, \frac{t}{2\phi(x, x_n)}\right) \bigcirc Q\left(x_n, y, \frac{t}{2\eta(x_n, y)}\right)$$

$$\longrightarrow 0 \bigcirc 0, \text{as } n \longrightarrow \infty. \tag{24}$$

That is, $P(x, y, t) \geq 1 * 1 = 1$ and $Q(x, y, t) \leq 0 \bigcirc 0 = 0$. Hence, $x = y$, that is, the sequence converges to at most one limit point. $\quad\square$

Lemma 2. *Let $(\mathfrak{B}, P, Q, *, \bigcirc)$ be an IFDCMS. If for some $0 < \theta < 1$ and for any $x, y \in \mathfrak{B}, t > 0$,*

$$P(x, y, t) \geq P\left(x, y, \frac{t}{\theta}\right),$$

$$Q(x, y, t) \leq Q\left(x, y, \frac{t}{\theta}\right). \tag{25}$$

then $x = y$.

Proof. (1) implies that

$$P(x, y, t) \geq P\left(x, y, \frac{t}{\theta^n}\right),$$

$$Q(x, y, t) \leq Q\left(x, y, \frac{t}{\theta^n}\right), \quad n \in \mathbb{N}, t > 0. \tag{26}$$

Now,

$$P(x, y, t) \geq \lim_{n \to \infty} P\left(x, y, \frac{t}{\theta^n}\right) = 1,$$

$$Q(x, y, t) \leq \lim_{n \to \infty} Q\left(x, y, \frac{t}{\theta^n}\right) = 0, \quad t > 0. \tag{27}$$

By (iii) and (viii), then $x = y$.

At this time, we prove the intuitionistic fuzzy controlled Banach contraction result. $\square$

Theorem 1. *Suppose that* $(\mathfrak{B}, P, Q, *, \bigcirc)$ *is a complete IFDCMS in the company of* $\varphi, \eta: \mathfrak{B} \times \mathfrak{B} \longrightarrow [1, 1/\theta)$ *with* $0 < \theta < 1$ *and suppose that*

$$\lim_{t \to \infty} P(x, y, t) = 1 \text{ and } \lim_{t \to \infty} Q(x, y, t) = 0. \tag{28}$$

for all $x, y \in \mathfrak{B}$, *and* $t > 0$. *Let* $\Psi: \mathfrak{B} \longrightarrow \mathfrak{B}$ *be a mapping satisfying for all* $x, y \in \mathfrak{B}$ *and* $t > 0$. *Then,* Ψ *has a unique FP.*

Proof. Let x_0 be a random integer of $\mathfrak{B}$ and describe a sequence x_n by $x_n = \Psi^n x_0 = \Psi x_{n-1}, n \in \mathbb{N}$. By using (2) for all $t > 0$, we have

$$P(x_n, x_{n+1}, \theta t) = P(\Psi x_{n-1}, \Psi x_n, \theta t) \geq P(x_{n-1}, x_n, t) \geq P\left(x_{n-2}, x_{n-1}, \frac{t}{\theta}\right)$$

$$\geq P\left(x_{n-3}, x_{n-2}, \frac{t}{\theta^2}\right) \geq \cdots \geq P\left(x_0, x_1, \frac{t}{\theta^{n-1}}\right),$$

$$Q(x_n, x_{n+1}, \theta t) = Q(\Psi x_{n-1}, \Psi x_n, \theta t) \leq Q(x_{n-1}, x_n, t) \leq Q\left(x_{n-2}, x_{n-1}, \frac{t}{\theta}\right), \tag{29}$$

$$\leq Q\left(x_{n-3}, x_{n-2}, \frac{t}{\theta^2}\right) \leq \cdots \leq Q\left(x_0, x_1, \frac{t}{\theta^{n-1}}\right).$$

We obtain

$$P(x_n, x_{n+1}, \theta t) \geq P\left(x_0, x_1, \frac{t}{\theta^{n-1}}\right),$$

$$Q(x_n, x_{n+1}, \theta t) \leq Q\left(x_0, x_1, \frac{t}{\theta^{n-1}}\right). \tag{30}$$

For any $q \in \mathbb{N}$, using (v) and (x), we deduce

$$P(x_n, x_{n+q}, t) \geq P\left(x_n, x_{n+1}, \frac{t}{2(\varphi(x_n, x_{n+1}))}\right) * P\left(x_{n+1}, x_{n+q}, \frac{t}{2(\eta(x_{n+1}, x_{n+q}))}\right)$$

$$\geq P\left(x_n, x_{n+1}, \frac{t}{2(\varphi(x_n, x_{n+1}))}\right) * P\left(x_{n+1}, x_{n+2}, \frac{t}{(2)^2(\eta(x_{n+1}, x_{n+q})\varphi(x_{n+1}, x_{n+2}))}\right)$$

$$* P_\varphi\left(x_{n+2}, x_{n+q}, \frac{t}{(2)^2(\eta(x_{n+1}, x_{n+q})\eta(x_{n+2}, x_{n+q}))}\right)$$

$$\geq P\left(x_n, x_{n+1}, \frac{t}{2(\varphi(x_n, x_{n+1}))}\right) * P\left(x_{n+1}, x_{n+2}, \frac{t}{(2)^2(\eta(x_{n+1}, x_{n+q})\varphi(x_{n+1}, x_{n+2}))}\right)$$

$$* P\left(x_{n+2}, x_{n+3}, \frac{t}{(2)^3(\eta(x_{n+1}, x_{n+q})\eta(x_{n+2}, x_{n+q})\varphi(x_{n+2}, x_{n+3}))}\right)$$

$$* P\left(x_{n+3}, x_{n+q}, \frac{t}{(2)^3(\eta(x_{n+1}, x_{n+q})\eta(x_{n+2}, x_{n+q})\eta(x_{n+3}, x_{n+q}))}\right)$$

$$\geq P\left(x_n, x_{n+1}, \frac{t}{2(\phi(x_n, x_{n+1}))}\right) * P\left(x_{n+1}, x_{n+2}, \frac{t}{(2)^2(\eta(x_{n+1}, x_{n+q})\phi(x_{n+1}, x_{n+2}))}\right)$$

$$* P\left(x_{n+2}, x_{n+3}, \frac{t}{(2)^3(\eta(x_{n+1}, x_{n+q})\eta(x_{n+2}, x_{n+q})\phi(x_{n+2}, x_{n+3}))}\right)$$

$$* P\left(x_{n+3}, x_{n+4}, \frac{t}{(2)^4(\eta(x_{n+1}, x_{n+q})\eta(x_{n+2}, x_{n+q})\eta(x_{n+3}, x_{n+q})\phi(x_{n+3}, x_{n+4}))}\right) * \cdots *$$

$$P\left(x_{n+q-2}, x_{n+q-1}, \frac{t}{(2)^{q-1}(\eta(x_{n+1}, x_{n+q})\eta(x_{n+2}, x_{n+q})\cdots\eta(x_{n+q-2}, x_{n+q})\phi(x_{n+q-2}, x_{n+q-1}))}\right)$$

$$* P\left(x_{n+q-1}, x_{n+q}, \frac{t}{(2)^{q-1}(\eta(x_{n+1}, x_{n+q})\eta(x_{n+2}, x_{n+q})\cdots(x_{n+q-1}, x_{n+q}))}\right),$$

$$Q(x_n, x_{n+q}, t) \leq Q\left(x_n, x_{n+1}, \frac{t}{2(\phi(x_n, x_{n+1}))}\right)Q\left(x_{n+1}, x_{n+q}, \frac{t}{2(\eta(x_{n+1}, x_{n+q}))}\right),$$

$$\leq Q\left(x_n, x_{n+1}, \frac{t}{2(\phi(x_n, x_{n+1}))}\right) \circ Q\left(x_{n+1}, x_{n+2}, \frac{t}{(2)^2(\eta(x_{n+1}, x_{n+q})\phi(x_{n+1}, x_{n+2}))}\right),$$

$$\circ Q\left(x_{n+2}, x_{n+q}, \frac{t}{(2)^2(\eta(x_{n+1}, x_{n+q})\eta(x_{n+2}, x_{n+q}))}\right),$$

$$\leq Q\left(x_n, x_{n+1}, \frac{t}{2(\phi(x_n, x_{n+1}))}\right) \circ Q\left(x_{n+1}, x_{n+2}, \frac{t}{(2)^2(\eta(x_{n+1}, x_{n+q})\phi(x_{n+1}, x_{n+2}))}\right),$$

$$\circ Q\left(x_{n+2}, x_{n+3}, \frac{t}{(2)^3(\eta(x_{n+1}, x_{n+q})\eta(x_{n+2}, x_{n+q})\phi(x_{n+2}, x_{n+3}))}\right),$$

$$\circ Q\left(x_{n+3}, x_{n+q}, \frac{t}{(2)^3(\eta(x_{n+1}, x_{n+q})\eta(x_{n+2}, x_{n+q})\eta(x_{n+3}, x_{n+q}))}\right),$$

$$\leq Q\left(x_n, x_{n+1}, \frac{t}{2(\phi(x_n, x_{n+1}))}\right) \circ Q\left(x_{n+1}, x_{n+2}, \frac{t}{(2)^2(\eta(x_{n+1}, x_{n+q})\phi(x_{n+1}, x_{n+2}))}\right),$$

$$\circ Q\left(x_{n+2}, x_{n+3}, \frac{t}{(2)^3(\eta(x_{n+1}, x_{n+q})\eta(x_{n+2}, x_{n+q})\phi(x_{n+2}, x_{n+3}))}\right),$$

$$\circ Q\left(x_{n+3}, x_{n+4}, \frac{t}{(2)^4(\eta(x_{n+1}, x_{n+q})\eta(x_{n+2}, x_{n+q})\eta(x_{n+3}, x_{n+q})\phi(x_{n+3}, x_{n+4}))}\right) \circ \cdots \circ,$$

$$Q\left(x_{n+q-2}, x_{n+q-1}, \frac{t}{(2)^{q-1}(\eta(x_{n+1}, x_{n+q})\eta(x_{n+2}, x_{n+q})\cdots\eta(x_{n+q-2}, x_{n+q})\phi(x_{n+q-2}, x_{n+q-1}))}\right),$$

$$\circ Q\left(x_{n+q-1}, x_{n+q}, \frac{t}{(2)^{q-1}(\eta(x_{n+1}, x_{n+q})\eta(x_{n+2}, x_{n+q})\eta(x_{n+3}, x_{n+q})\cdots\eta(x_{n+q-1}, x_{n+q}))}\right).$$

$$(31)$$

Using (4) in the above inequalities, we deduce

$$
\geq P\left(x_0, x_1, \frac{t}{2(\theta)^{n-1}(\phi(x_n, x_{n+1}))}\right) * P\left(x_0, x_1, \frac{t}{(2)^2(\theta)^n(\eta(x_{n+1}, x_{n+q})\phi(x_{n+1}, x_{n+2}))}\right),
$$

$$
* P\left(x_0, x_1, \frac{t}{(2)^3(\theta)^{n+1}(\eta(x_{n+1}, x_{n+q})\eta(x_{n+2}, x_{n+q})\phi(x_{n+2}, x_{n+3}))}\right),
$$

$$
* P\left(x_0, x_1, \frac{t}{(2)^4(\theta)^{n+2}(\eta(x_{n+1}, x_{n+q})\eta(x_{n+2}, x_{n+q})\eta(x_{n+3}, x_{n+q})\phi(x_{n+3}, x_{n+4}))}\right) * \cdots *,
$$

$$
P\left(x_0, x_1, \frac{t}{(2)^{q-1}(\theta)^{n+q-2}(\eta(x_{n+1}, x_{n+q})\eta(x_{n+2}, x_{n+q})\cdots\eta(x_{n+q-2}, x_{n+q})\phi(x_{n+q-2}, x_{n+q-1}))}\right),
$$

$$
* P\left(x_0, x_1, \frac{t}{(2)^{q-1}(\theta)^{n+q-1}(\eta(x_{n+1}, x_{n+q})\eta(x_{n+2}, x_{n+q})\eta(x_{n+3}, x_{n+q})\cdots\eta(x_{n+q-1}, x_{n+q}))}\right),
$$

$$
\leq Q\left(x_0, x_1, \frac{t}{2(\theta)^{n-1}(\phi(x_n, x_{n+1}))}\right) Q\left(x_0, x_1, \frac{t}{(2)^2(\theta)^n(\eta(x_{n+1}, x_{n+q})\phi(x_{n+1}, x_{n+2}))}\right), \tag{32}
$$

$$
\bigcirc Q\left(x_0, x_1, \frac{t}{(2)^3(\theta)^{n+1}(\eta(x_{n+1}, x_{n+q})\eta(x_{n+2}, x_{n+q})\phi(x_{n+2}, x_{n+3}))}\right),
$$

$$
\bigcirc Q\left(x_0, x_1, \frac{t}{(2)^4(\theta)^{n+2}((x_{n+1}, x_{n+q})\eta(x_{n+2}, x_{n+q})\eta(x_{n+3}, x_{n+q})\phi(x_{n+3}, x_{n+4}))}\right),
$$

$$
\bigcirc \cdots \bigcirc
$$

$$
Q\left(x_0, x_1, \frac{t}{(2)^{q-1}(\theta)^{n+q-2}(\eta(x_{n+1}, x_{n+q})\eta(x_{n+2}, x_{n+q})\cdots\eta(x_{n+q-2}, x_{n+q})\phi(x_{n+q-2}, x_{n+q-1}))}\right),
$$

$$
\bigcirc Q\left(x_0, x_1, \frac{t}{(2)^{q-1}(\theta)^{n+q-1}(\eta(x_{n+1}, x_{n+q})\eta(x_{n+2}, x_{n+q})\eta(x_{n+3}, x_{n+q})\cdots\eta(x_{n+q-1}, x_{n+q}))}\right).
$$

Using (2), if $n \longrightarrow \infty$, we deduce

$$
\lim_{n \longrightarrow \infty} P(x_n, x_{n+q}, t) = 1 * 1 * \cdots * 1 = 1,
$$
$$
\lim_{n \longrightarrow \infty} Q(x_n, x_{n+q}, t) = 0 \bigcirc 0 \bigcirc 0 \cdots \bigcirc 0 = 0, \tag{33}
$$

i.e., $\{x_n\}$ is a CS. Since $(\mathfrak{B}, P, Q, *, \bigcirc)$ is a complete IFDCMS, there exists

$$
\lim_{n \longrightarrow \infty} x_n = x. \tag{34}
$$

Now, we investigate that x is a FP of Ψ. Using (v), (x), and (2), we obtain

$$
P(x, \Psi x, t) \geq P\left(x, x_{n+1}, \frac{t}{2(\phi(x, x_{n+1}))}\right) * P\left(x_{n+1}, \Psi x, \frac{t}{2(\eta(x_{n+1}, \Psi x))}\right)
$$

$$
\geq P\left(x, x_{n+1}, \frac{t}{2(\phi(x, x_{n+1}))}\right) * P\left(\Psi x_n, \Psi x, \frac{t}{2(\eta(x_{n+1}, \Psi x))}\right) \tag{35}
$$

$$
\geq P\left(x, x_{n+1}, \frac{t}{2(\phi(x, x_{n+1}))}\right) * P\left(x_n, x, \frac{t}{2\theta(\eta(x_{n+1}, \Psi x))}\right) \longrightarrow 1 * 1 = 1,
$$

as $n \longrightarrow \infty$, and

$$Q(x, \Psi x, t) \leq Q\left(x, x_{n+1}, \frac{t}{2\left(\varphi\left(x, x_{n+1}\right)\right)}\right) \bigcirc Q\left(x_{n+1}, \Psi x, \frac{t}{2\left(\eta\left(x_{n+1}, \Psi x\right)\right)}\right)$$

$$\leq Q\left(x, x_{n+1}, \frac{t}{2\left(\varphi\left(x, x_{n+1}\right)\right)}\right) \bigcirc Q\left(\Psi x_n, \Psi x, \frac{t}{2\left(\eta\left(x_{n+1}, \Psi x\right)\right)}\right)$$

$$\leq Q\left(x, x_{n+1}, \frac{t}{2\left(\varphi\left(x, x_{n+1}\right)\right)}\right) \bigcirc Q\left(x_n, x, \frac{t}{2\theta\left(\eta\left(x_{n+1}, \Psi x\right)\right)}\right) \longrightarrow 0 \bigcirc 0 = 0, \tag{36}$$

as $n \longrightarrow \infty$. This implies that $\Psi x = x$, a FP. Now, we show the uniqueness. Suppose that $\Psi \rho = \rho$ for some $\rho \in \mathfrak{B}$. Then,

$$1 \geq P(\rho, x, t) = P(\Psi \rho, \Psi x, t) \geq P\left(\rho, x, \frac{t}{\theta}\right) = P\left(\Psi \rho, \Psi x, \frac{t}{\theta}\right)$$

$$\geq P\left(\rho, x, \frac{t}{\theta^2}\right) \geq \cdots \geq P\left(\rho, x, \frac{t}{\theta^n}\right) \longrightarrow 1 \text{ as } n \longrightarrow \infty$$

$$0 \leq Q(\rho, x, t) = Q(\Psi \rho, \Psi x, t) \leq Q\left(\rho, x, \frac{t}{\theta}\right) = Q\left(\Psi \rho, \Psi x, \frac{t}{\theta}\right)$$

$$\leq Q\left(\rho, x, \frac{t}{\theta^2}\right) \leq \cdots \leq Q\left(\rho, x, \frac{t}{\theta^n}\right) \longrightarrow 0 \text{ as } n \longrightarrow \infty. \tag{37}$$

By using (iii)and (viii), then $x = \rho$. □

Corollary 1. *Suppose that* $(\mathfrak{B}, P, Q, *, \bigcirc)$ *is a complete IFDCMS in the company of* $\varphi, \eta: \mathfrak{B} \times \mathfrak{B} \longrightarrow [1, 1/\theta)$ *with* $0 < \theta < 1$ *and suppose that*

$$\lim_{t \longrightarrow \infty} P(x, y, t) = 1,$$
$$\lim_{t \longrightarrow \infty} Q(x, y, t) = 0, \tag{38}$$

for all $x, y \in \mathfrak{B}$ *and* $t > 0$. *Let* $\Psi: \mathfrak{B} \longrightarrow \mathfrak{B}$ *be a mapping satisfying*

$$P(\Psi x, \Psi y, \theta t) \geq \min\{P(x, y, t), P(x, \Psi x, t), P(y, \Psi y, t)\},$$
$$Q(\Psi x, \Psi y, \theta t) \leq \min\{Q(x, y, t), Q(x, \Psi x, t), Q(y, \Psi y, t)\}, \tag{39}$$

for all $x, y \in \mathfrak{B}$, *and* $t > 0$. *Then,* Ψ *has a unique FP.*

Proof. It is easy to prove by using Theorem 1 and Lemma 2. □

Definition 9. Let $(\mathfrak{B}, P, Q, *, \bigcirc)$ be an IFDCMS. A map $\Psi: \mathfrak{B} \longrightarrow \mathfrak{B}$ is a D-controlled intuitionistic fuzzy contraction if there exists $0 < \theta < 1$, such that

$$\frac{1}{P_\varphi(\Psi x, \Psi y, t)} - 1 \leq \theta\left[\frac{1}{P_\varphi(x, y, t)} - 1\right],$$

$$Q_\varphi(\Psi x, \Psi y, t) \leq \theta Q_\varphi(x, y, t), \tag{40}$$

for all $x, y \in \mathfrak{B}$ and $t > 0$.

Now, we prove a theorem for D-controlled intuitionistic fuzzy contractions.

Theorem 2. *Let* $(\mathfrak{B}, P, Q, *, \bigcirc)$ *be a complete IFDCMS with* $\varphi, \eta: \mathfrak{B} \times \mathfrak{B} \longrightarrow [1, \infty)$ *and suppose that*

$$\lim_{t \longrightarrow \infty} P(x, y, t) = 1,$$
$$\lim_{t \longrightarrow \infty} Q(x, y, t) = 0, \tag{41}$$

for all $x, y \in \mathfrak{B}$ *and* $t > 0$. *Let* $\Psi: \mathfrak{B} \longrightarrow \mathfrak{B}$ *be a D-controlled intuitionistic fuzzy contraction. Further, suppose that for an arbitrary* $x_0 \in \mathfrak{B}$, *and* $n, q \in \mathbb{N}$, $x_n = \Psi^n x_0 = \Psi x_{n-1}$. *Then,* Ψ *has a unique FP.*

Proof. Let x_0 be a random integer of $\mathfrak{B}$ and describe a sequence x_n by $x_n = \Psi^n x_0 = \Psi x_{n-1}, n \in \mathbb{N}$. By using (5) and (6) for all $t > 0$, $n > q$, we have

$$\frac{1}{P(x_n, x_{n+1}, t)} - 1 = \frac{1}{P(\Psi x_{n-1}, x_n, t)} - 1$$

$$\leq \theta\left[\frac{1}{P(x_{n-1}, x_n, t)} - 1\right] = \frac{\theta}{P(x_{n-1}, x_n, t)} - \theta$$

$$\Rightarrow \frac{1}{P(x_n, x_{n+1}, t)} \leq \frac{\theta}{P(x_{n-1}, x_n, t)} + (1 - \theta)$$

$$\leq \frac{\theta^2}{P(x_{n-2}, x_{n-1}, t)} + \theta(1 - \theta) + (1 - \theta). \tag{42}$$

Continuing in this way, we get

$$\frac{1}{P(x_n, x_{n+1}, t)} \leq \frac{\theta^n}{P(x_0, x_1, t)} + \theta^{n-1}(1 - \theta) + \theta^{n-2}(1 - \theta) + \cdots + \theta(1 - \theta) + (1 - \theta)$$

$$\leq \frac{\theta^n}{P(x_0, x_1, t)} + \left(\theta^{n-1} + \theta^{n-2} + \cdots + 1\right)(1 - \theta) \leq \frac{\theta^n}{P(x_0, x_1, t)} + (1 - \theta^n). \tag{43}$$

We obtain   for any $q \in \mathbb{N}$Using (v) and (x), we deduce

$$\frac{1}{\theta^n / \mathrm{P}(x_0, x_1, t) + (1 - \theta^n)} \leq \mathrm{P}(x_n, x_{n+1}, t),$$

$$Q(x_n, x_{n+1}, t) = Q(\Psi x_{n-1}, x_n, t) \leq \theta Q(x_{n-1}, x_n, t) \qquad (44)$$

$$= Q(\Psi x_{n-2}, x_{n-1}, t),$$

$$\leq \theta^2 Q(x_{n-2}, x_{n-1}, t) \leq \cdots \leq \theta^n Q(x_0, x_1, t),$$

$$\mathrm{P}(x_n, x_{n+q}, t) \geq \mathrm{P}\left(x_n, x_{n+1}, \frac{t}{2(\phi(x_n, x_{n+1}))}\right) * \mathrm{P}\left(x_{n+1}, x_{n+q}, \frac{t}{2(\eta(x_{n+1}, x_{n+q}))}\right),$$

$$\geq \mathrm{P}\left(x_n, x_{n+1}, \frac{t}{2(\phi(x_n, x_{n+1}))}\right) * \mathrm{P}\left(x_{n+1}, x_{n+2}, \frac{t}{(2)^2(\eta(x_{n+1}, x_{n+q})\phi(x_{n+1}, x_{n+2}))}\right),$$

$$* \mathrm{P}\left(x_{n+2}, x_{n+q}, \frac{t}{(2)^2(\eta(x_{n+1}, x_{n+q})\eta(x_{n+2}, x_{n+q}))}\right),$$

$$\geq \mathrm{P}\left(x_n, x_{n+1}, \frac{t}{2(\phi(x_n, x_{n+1}))}\right) * \mathrm{P}\left(x_{n+1}, x_{n+2}, \frac{t}{(2)^2(\eta(x_{n+1}, x_{n+q})\phi(x_{n+1}, x_{n+2}))}\right),$$

$$* \mathrm{P}\left(x_{n+2}, x_{n+3}, \frac{t}{(2)^3(\eta(x_{n+1}, x_{n+q})\eta(x_{n+2}, x_{n+q})\phi(x_{n+2}, x_{n+3}))}\right),$$

$$* \mathrm{P}\left(x_{n+3}, x_{n+q}, \frac{t}{(2)^3(\eta(x_{n+1}, x_{n+q})\eta(x_{n+2}, x_{n+q})\eta(x_{n+3}, x_{n+q}))}\right),$$

$$\geq \mathrm{P}\left(x_n, x_{n+1}, \frac{t}{2(\phi(x_n, x_{n+1}))}\right) * \mathrm{P}\left(x_{n+1}, x_{n+2}, \frac{t}{(2)^2(\eta(x_{n+1}, x_{n+q})\phi(x_{n+1}, x_{n+2}))}\right),$$

$$* \mathrm{P}\left(x_{n+2}, x_{n+3}, \frac{t}{(2)^3(\eta(x_{n+1}, x_{n+q})\eta(x_{n+2}, x_{n+q})\phi(x_{n+2}, x_{n+3}))}\right),$$

$$* \mathrm{P}\left(x_{n+3}, x_{n+4}, \frac{t}{(2)^4(\eta(x_{n+1}, x_{n+q})\eta(x_{n+2}, x_{n+q})\eta(x_{n+3}, x_{n+q})\phi(x_{n+3}, x_{n+4}))}\right) * \cdots *,$$

$$\mathrm{P}\left(x_{n+q-2}, x_{n+q-1}, \frac{t}{(2)^{q-1}(\eta(x_{n+1}, x_{n+q})\eta(x_{n+2}, x_{n+q}) \cdots \eta(x_{n+q-2}, x_{n+q})\phi(x_{n+q-2}, x_{n+q-1}))}\right),$$

$$* \mathrm{P}\left(x_{n+q-1}, x_{n+q}, \frac{t}{(2)^{q-1}(\eta(x_{n+1}, x_{n+q})\eta(x_{n+2}, x_{n+q})\eta(x_{n+3}, x_{n+q}) \cdots \eta(x_{n+q-1}, x_{n+q}))}\right),$$

$$Q(x_n, x_{n+q}, t) \leq Q\left(x_n, x_{n+1}, \frac{t}{2(\phi(x_n, x_{n+1}))}\right) \bigcirc Q\left(x_{n+1}, x_{n+q}, \frac{t}{2(\eta(x_{n+1}, x_{n+q}))}\right),$$

$$\leq Q\left(x_n, x_{n+1}, \frac{t}{2\left(\phi(x_n, x_{n+1})\right)}\right) \bigcirc Q\left(x_{n+1}, x_{n+2}, \frac{t}{(2)^2\left(\eta(x_{n+1}, x_{n+q})\phi(x_{n+1}, x_{n+2})\right)}\right),$$

$$\bigcirc Q\left(x_{n+2}, x_{n+q}, \frac{t}{(2)^2\left(\eta(x_{n+1}, x_{n+q})\eta(x_{n+2}, x_{n+q})\right)}\right),$$

$$\leq Q\left(x_n, x_{n+1}, \frac{t}{2\left(\phi(x_n, x_{n+1})\right)}\right) \bigcirc Q\left(x_{n+1}, x_{n+2}, \frac{t}{(2)^2\left(\eta(x_{n+1}, x_{n+q})\phi(x_{n+1}, x_{n+2})\right)}\right),$$

$$\bigcirc Q\left(x_{n+2}, x_{n+3}, \frac{t}{(2)^3\left(\eta(x_{n+1}, x_{n+q})\eta(x_{n+2}, x_{n+q})\phi(x_{n+2}, x_{n+3})\right)}\right),$$

$$\bigcirc Q\left(x_{n+3}, x_{n+q}, \frac{t}{(2)^3\left(\eta(x_{n+1}, x_{n+q})\eta(x_{n+2}, x_{n+q})\eta(x_{n+3}, x_{n+q})\right)}\right),$$

$$\leq Q\left(x_n, x_{n+1}, \frac{t}{2\left(\phi(x_n, x_{n+1})\right)}\right) \bigcirc Q\left(x_{n+1}, x_{n+2}, \frac{t}{(2)^2\left(\eta(x_{n+1}, x_{n+q})\phi(x_{n+1}, x_{n+2})\right)}\right),$$

$$\bigcirc Q\left(x_{n+2}, x_{n+3}, \frac{t}{(2)^3\left(\eta(x_{n+1}, x_{n+q})\eta(x_{n+2}, x_{n+q})\phi(x_{n+2}, x_{n+3})\right)}\right),$$

$$\bigcirc Q\left(x_{n+3}, x_{n+4}, \frac{t}{(2)^4\left(\eta(x_{n+1}, x_{n+q})\eta(x_{n+2}, x_{n+q})\eta(x_{n+3}, x_{n+q})\phi(x_{n+3}, x_{n+4})\right)}\right) \bigcirc \cdots \bigcirc,$$

$$Q\left(x_{n+q-2}, x_{n+q-1}, \frac{t}{(2)^{q-1}\left(\eta(x_{n+1}, x_{n+q})\eta(x_{n+2}, x_{n+q})\cdots\eta(x_{n+q-2}, x_{n+q})\phi(x_{n+q-2}, x_{n+q-1})\right)}\right),$$

$$\bigcirc Q\left(x_{n+q-1}, x_{n+q}, \frac{t}{(2)^{q-1}\left(\eta(x_{n+1}, x_{n+q})\eta(x_{n+2}, x_{n+q})\eta(x_{n+3}, x_{n+q})\cdots\eta(x_{n+q-1}, x_{n+q})\right)}\right),$$

$$P(x_n, x_{n+q}, t) \geq \frac{1}{\theta^n / P\left(x_0, x_1, t/2\left(\phi(x_n, x_{n+1})\right)\right) + (1 - \theta^n)} * \frac{1}{\theta^{n+1} / P\left(x_0, x_1, t/(2)^2\left(\eta(x_{n+1}, x_{n+q})\phi(x_{n+1}, x_{n+2})\right)\right) + (1 - \theta^{n+1})},$$

$$* \frac{1}{\theta^{n+2} / P\left(x_0, x_1, t/(2)^3\left(\eta(x_{n+1}, x_{n+q})\eta(x_{n+2}, x_{n+q})\phi(x_{n+2}, x_{n+3})\right)\right) + (1 - \theta^{n+2})} * \cdots *,$$

$$\frac{1}{\theta^{n+q-2} / P\left(x_0, x_1, t/(2)^{q-1}\left(\eta(x_{n+1}, x_{n+q})\eta(x_{n+2}, x_{n+q})\cdots\eta(x_{n+q-2}, x_{n+q})\phi(x_{n+q-2}, x_{n+q-1})\right)\right) + (1 - \theta^{n+q-2})},$$

$$* \frac{1}{\theta^{n+q-1} / P\left(x_0, x_1, t/(2)^{q-1}\left(\eta(x_{n+1}, x_{n+q})\eta(x_{n+2}, x_{n+q})\eta(x_{n+3}, x_{n+q})\cdots\eta(x_{n+q-1}, x_{n+q})\right)\right) + (1 - \theta^{n+q-1})},$$

$$Q(x_n, x_{n+q}, t) \leq \theta^n Q\left(x_0, x_1, \frac{t}{2\left(\phi(x_n, x_{n+1})\right)}\right) \bigcirc \theta^{n+1} Q\left(x_0, x_1, \frac{t}{(2)^2\left(\eta(x_{n+1}, x_{n+q})\phi(x_{n+1}, x_{n+2})\right)}\right),$$

$$\bigcirc \theta^{n+2} Q\left(x_0, x_1, \frac{t}{(2)^3\left(\eta(x_{n+1}, x_{n+q})\eta(x_{n+2}, x_{n+q})\phi(x_{n+2}, x_{n+3})\right)}\right) \bigcirc \cdots \bigcirc,$$

$$\theta^{n+q-2} Q\left(x_0, x_1, \frac{t}{(2)^{q-1}\left(\eta(x_{n+1}, x_{n+q})\eta(x_{n+2}, x_{n+q})\cdots\eta(x_{n+q-2}, x_{n+q})\phi(x_{n+q-2}, x_{n+q-1})\right)}\right),$$

$$\bigcirc \theta^{n+q-1} Q\left(x_0, x_1, \frac{t}{(2)^{q-1}\left(\eta(x_{n+1}, x_{n+q})\eta(x_{n+2}, x_{n+q})\eta(x_{n+3}, x_{n+q})\cdots\eta(x_{n+q-1}, x_{n+q})\right)}\right).$$

$$(45)$$

Therefore,

$$\lim_{n \to \infty} P(x_n, x_{n+q}, t) = 1 * 1 * \cdots * 1 = 1,$$
$$\lim_{n \to \infty} Q(x_n, x_{n+q}, t) = 0 \bigcirc 0 \bigcirc \cdots \bigcirc 0 = 0, \tag{46}$$

i.e., $\{x_n\}$ is a CS. Since $(\mathfrak{B}, P, Q, *, \bigcirc)$ is a complete IFDCMS, there exists

$$\lim_{n \to \infty} x_n = x. \tag{47}$$

Now, we investigate that x is a FP of Ψ. Using (v) and (x), we obtain

$$P(x, \Psi x, t) \geq P\left(x, x_{n+1}, \frac{t}{2\varphi(x, x_{n+1})}\right) * P\left(x_{n+1}, \Psi x, \frac{t}{2\eta(x_{n+1}, \Psi x)}\right)$$

$$\geq P\left(x, x_{n+1}, \frac{t}{2\varphi(x, x_{n+1})}\right) * P\left(\Psi x_n, \Psi x, \frac{t}{2\eta(x_{n+1}, \Psi x)}\right) \tag{49}$$

$$\geq P\left(x_n, x_{n+1}, \frac{t}{(2\varphi(x, x_{n+1}))}\right) * \frac{1}{\theta/P(x_n, x, t/2\eta(x_{n+1}, \Psi x)) + (1 - \theta)} \longrightarrow 1 * 1 = 1,$$

as $n \to \infty$, and

$$Q(x, \Psi x, t) \leq Q\left(x, x_{n+1}, \frac{t}{2\varphi(x, x_{n+1})}\right) \bigcirc Q\left(x_{n+1}, \Psi x, \frac{t}{2\eta(x_{n+1}, \Psi x)}\right)$$

$$\leq Q\left(x, x_{n+1}, \frac{t}{2\varphi(x, x_{n+1})}\right) \bigcirc Q\left(\Psi x_n, \Psi x, \frac{t}{2\eta(x_{n+1}, \Psi x)}\right) \tag{50}$$

$$\leq Q\left(x_n, x_{n+1}, \frac{t}{2\varphi(x, x_{n+1})}\right) \bigcirc \theta Q\left(x_n, x, \frac{t}{2\eta(x_{n+1}, \Psi x)}\right) \longrightarrow 0 \bigcirc 0 = 0 \ as \ n \to \infty.$$

This implies that $\Psi x = x$, a FP. Now, we show the uniqueness. Suppose that $\Psi \rho = \rho$ for some $\rho \in \mathfrak{B}$. Then,

$$\frac{1}{P(x, \rho, t)} - 1 = \frac{1}{P(\Psi x, \Psi \rho, t)} - 1$$
$$\leq \theta\left[\frac{1}{P(x, \rho, t)} - 1\right] < \frac{1}{P(x, \rho, t)} - 1, \tag{51}$$

a contradiction, and

$$Q(x, \rho, t) = Q(\Psi x, \Psi \rho, t) \leq \theta Q(x, \rho, t) < Q(x, \rho, t), \tag{52}$$

a contradiction. Therefore, we must have $P(x, \rho, t) = 1$ and $Q(x, \rho, t) = 0$, hence $x = \rho$. □

Example 6. Let $\mathfrak{B} = [0, 1]$ and $\varphi, \eta: \mathfrak{B} \times \mathfrak{B} \longrightarrow [1, \infty)$ be two noncomparable functions given by

$$\frac{1}{P(\Psi x_n, \Psi x, t)} - 1 \leq \theta\left[\frac{1}{P(x_n, x, t)} - 1\right] = \frac{\theta}{P(x_n, x, t)} - \theta$$

$$\Rightarrow \frac{1}{\theta/P(x_n, x, t) + (1 - \theta)} \leq P(\Psi x_n, \Psi x, t). \tag{48}$$

Using the above inequality, we obtain

$$\varphi(x, y) = \begin{cases} 1, & \text{if } x = y, \\ \dfrac{1 + \max\{x, y\}}{\min\{x, y\}}, & \text{if } x \neq y \neq 0. \end{cases}$$

$$\eta(x, y) = \begin{cases} 1, & \text{if } x = y, \\ \dfrac{1 + \max\{x^2, y^2\}}{\min\{x^2, y^2\}}, & \text{if } x \neq y. \end{cases} \tag{53}$$

Define $P, Q: \mathfrak{B} \times \mathfrak{B} \times (0, \infty) \longrightarrow [0, 1]$ as

$$P(x, y, t) = \frac{t}{t + |x - y|^2},$$

$$Q(x, y, t) = \frac{|x - y|^2}{t + |x - y|^2}. \tag{54}$$

Then, $(\mathfrak{B}, P, Q, *, \bigcirc)$ is a complete IFDCMS with CTN $\pi * \mu = \pi\mu$ and CTCN $\pi\bigcirc\mu = \max\{\pi, \mu\}$.

Define $\Psi: \mathfrak{B} \longrightarrow \mathfrak{B}$ by $\Psi(x) = 1 - 2^{-x}/3$ and take $\theta \in [1/2, 1)$. Then,

$$P(\Psi x, \Psi y, \theta t) = P\left(\frac{1 - 2^{-x}}{3}, \frac{1 - 2^{-y}}{3}, \theta t\right)$$

$$= \frac{\theta t}{\theta t + \left|1 - 2^{-x}/3 - 1 - 2^{-y}/3\right|^2}$$

$$= \frac{\theta t}{\theta t + \left|2^{-x} - 2^{-y}\right|^2/9}$$

$$\geq \frac{\theta t}{\theta t + |x - y|^2/9} = \frac{9\theta t}{9\theta t + |x - y|^2} \geq \frac{t}{t + |x - y|^2} = P(x, y, t),$$

$$Q(\Psi x, \Psi y, \theta t) = Q\left(\frac{1 - 2^{-x}}{3}, \frac{1 - 2^{-y}}{3}, \theta t\right)$$

$$= \frac{\left|1 - 2^{-x}/3 - 1 - 2^{-y}/3\right|^2}{\theta t + \left|1 - 2^{-x}/3 - 1 - 2^{-y}/3\right|^2}$$

$$= \frac{\left|2^{-x} - 2^{-y}\right|^2/9}{\theta t + \left|2^{-x} - 2^{-y}\right|^2/9}$$

$$= \frac{\left|2^{-x} - 2^{-y}\right|^2}{9\theta t + \left|2^{-x} - 2^{-y}\right|^2} \leq \frac{|x - y|^2}{9\theta t + |x - y|^2} \leq \frac{|x - y|^2}{t + |x - y|^2} = Q(x, y, t).$$

(55)

Hence, all circumstances of Theorem 1 are fulfilled and 0 is a unique fixed point for Ψ.

3. Application to Fuzzy Fredholm Integral Equation

Let $\mathfrak{B} = C([e, g], \mathbb{R})$ be the set of the entire continuous functions so that their domain is real values and defined on $[e, g]$.

Now, we consider the following fuzzy integral equation:

$$x(l) = f(j) + \delta \int_e^g F(l, j) x(l) \mathrm{d}j, \quad \text{for } j \in [e, g], \quad (56)$$

where $\delta > 0$, $f(j)$ is a fuzzy function of $j: j \in [e, g]$ and $F \in \mathfrak{B}$

Define P and Q by

$$P(x(l), y(l), t) = \sup_{l \in [e,g]} \frac{t}{t + |x(l) - y(l)|^2} \quad \text{for all } x, y \in \mathfrak{B} \text{ and } t > 0,$$

$$P(x(l), y(l), t) = 1 - \sup_{l \in [e,g]} \frac{t}{t + |x(l) - y(l)|^2} \quad \text{for all } x, y \in \mathfrak{B} \text{ and } t > 0,$$

(57)

with CTN and CTCN defined by $\pi * \mu = \pi$. μ and $\pi\bigcirc\mu = \max\{\pi, \mu\}$.

Define $\phi, \eta: \mathfrak{B} \times \mathfrak{B} \longrightarrow [1, \infty)$ as

$$\varphi(x, y) = \begin{cases} 1, & \text{if} \quad x = y, \\ \dfrac{1 + \max\{x, y\}}{\min\{x, y\}}, & \text{if} \quad x \neq y \neq 0. \end{cases}$$

$$\eta(x, y) = \begin{cases} 1, & \text{if} \quad x = y, \\ \dfrac{1 + \max\{x^2, y^2\}}{\min\{x^2, y^2\}}, & \text{if} \quad x \neq y. \end{cases} \tag{58}$$

Then, $(\mathfrak{B}, P, P, *, \bigcirc)$ is a complete IFDCMS. Assume that

$$|F(l, j)x(l) - F(l, j)y(l)| \leq |x(l) - y(l)|, \tag{59}$$

for $x, y \in \mathfrak{B}$, $\theta \in (0, 1)$ and for all $l, j \in [e, g]$.

Also, consider $(\delta \pi \int_e^g \mathrm{d}j)^2 \leq \theta < 1$. Then, the fuzzy integral equation in equation (56) has a unique solution.

Proof: . Define $\Psi: \mathfrak{B} \longrightarrow \mathfrak{B}$ by

$$\Psi x(l) = f(j) + \delta \int_e^g F(l, j)e(l)\mathrm{d}j, \quad \text{for all } j \in [e, g]. \tag{60}$$

Scrutinize that survival of an FP of the operator Ψ has come to the survival of solution of the fuzzy integral equation.

Now, for all $x, y \in \mathfrak{B}$, we obtain

$$
\begin{aligned}
P(\Psi x(l), \Psi y(l), \theta t) &= \sup_{l \in [e, g]} \frac{\theta t}{\theta t + |\Psi x(l) - \Psi y(l)|^2} \\
&= \sup_{l \in [e, g]} \frac{\theta t}{\theta t + \left| f(j) + \delta \int_e^g F(l, j)e(l)\mathrm{d}j - f(j) - \delta \int_e^g F(l, j)e(l)\mathrm{d}j \right|^2} \\
&= \sup_{l \in [e, g]} \frac{\theta t}{\theta t + \left| \delta \int_e^g F(l, j)e(l)\mathrm{d}j - \delta \int_e^g F(l, j)e(l)\mathrm{d}j \right|^2} \\
&= \sup_{l \in [e, g]} \frac{\theta t}{\theta t + |F(l, j)x(l) - F(l, j)y(l)|^2 \left(\delta \int_e^g \mathrm{d}j \right)^2} \\
&\geq \sup_{l \in [e, g]} \frac{t}{t + |x(l) - y(l)|^2} \\
&\geq P(x(l), y(l), t)
\end{aligned}
$$

$$
\begin{aligned}
Q(\Psi x(l), \Psi y(l), \theta t) &= 1 - \sup_{l \in [e, g]} \frac{\theta t}{\theta t + |\Psi x(l) - \Psi y(l)|^2} \\
&= 1 - \sup_{l \in [e, g]} \frac{\theta t}{\theta t + \left| f(j) + \delta \int_e^g F(l, j)e(l)\mathrm{d}j - f(j) - \delta \int_e^g F(l, j)e(l)\mathrm{d}j \right|^2} \\
&= 1 - \sup_{l \in [e, g]} \frac{\theta t}{\theta t + \left| \delta \int_e^g F(l, j)e(l)\mathrm{d}j - \delta \int_e^g F(l, j)e(l)\mathrm{d}j \right|^2} \\
&= 1 - \sup_{l \in [e, g]} \frac{\theta t}{\theta t + |F(l, j)x(l) - F(l, j)y(l)|^2 \left(\delta \int_e^g \mathrm{d}j \right)^2} \\
&\leq 1 - \sup_{l \in [e, g]} \frac{t}{t + |x(l) - y(l)|^2} \\
&\leq Q(x(l), y(l), t).
\end{aligned}
$$

$$\tag{61}$$

Therefore, all circumstances of Theorem 1 are fulfilled. Hence, operator Ψ has a single FP. This implies that fuzzy integral (56) has a single solution. $\square$

Retraction

Retracted: Hamacher Weighted Aggregation Operators Based on Picture Cubic Fuzzy Sets and Their Application to Group Decision-Making Problems

Security and Communication Networks

This article has been retracted by Hindawi, as publisher, following an investigation undertaken by the publisher [1]. This investigation has uncovered evidence of systematic manipulation of the publication and peer-review process. We cannot, therefore, vouch for the reliability or integrity of this article.

Please note that this notice is intended solely to alert readers that the peer-review process of this article has been compromised.

Wiley and Hindawi regret that the usual quality checks did not identify these issues before publication and have since put additional measures in place to safeguard research integrity.

We wish to credit our Research Integrity and Research Publishing teams and anonymous and named external researchers and research integrity experts for contributing to this investigation.

The corresponding author, as the representative of all authors, has been given the opportunity to register their agreement or disagreement to this retraction. We have kept a record of any response received.

References

[1] L. Yanhong, R. Ambrin, M. Ibrar, and M. Ali Khan, "Hamacher Weighted Aggregation Operators Based on Picture Cubic Fuzzy Sets and Their Application to Group Decision-Making Problems," *Security and Communication Networks*, vol. 2022, Article ID 1651017, 39 pages, 2022.

WILEY | Hindawi

Research Article

Hamacher Weighted Aggregation Operators Based on Picture Cubic Fuzzy Sets and Their Application to Group Decision-Making Problems

Li Yanhong,[1] Rabia Ambrin,[2] Muhammad Ibrar ⓘ,[2] and Muhammad Ali Khan[3]

[1]*School of Physic and Mathematics, Hebei University of Architecture, Zhangjiakou 075000, China*
[2]*Department of Mathematics, University of Science and Technology Bannu, Bannu, Pakistan*
[3]*Department of Mathematics, Abdul Wali Khan University Mardan, Mardan, Pakistan*

Correspondence should be addressed to Muhammad Ibrar; m.ibrar@ustb.edu.pk

In this study, an extended version of intuitionistic cubic fuzzy Hamacher weighted aggregation operators is the primary objective of the expected study. We establish new concept, picture cubic fuzzy set, and utilize this new concept for ranking in decision analysis. Picture cubic fuzzy Hamacher weighted averaging operator, picture cubic fuzzy Hamacher order weighted averaging, and picture cubic fuzzy Hamacher hybrid averaging operator are developed on the basis of picture cubic fuzzy sets. Some unique cases and few suitable properties of these proposed operators are also examined. In addition, based on these expected operators, we are designing a new multicriteria group decision-making framework. The proposed aggregation operators can be used in the performance evaluation of energy projects and security systems and devices. We give an illustrative example for the selection of small hydropower plants locations as an implementation and appropriateness of the proposed algorithm. Finally, we perform a comparative review of the designed algorithm with intuitionistic cubic fuzzy Hamacher weighted averaging operators to expose the new algorithm efficiency, feasibility, and goodness.

1. Introduction

Need for electricity globally is continuously increasing due to rapid growing of the demographic and comparison of growth in agricultural and global industries. Electricity is typically derived from two kinds of energy sources, such as nontraditional (renewable) and traditional (nonrenewable) energy sources. Nonrenewable or conventional sources of energy, such as flammable gas, oil, coal, and atomic separation, are normally used in the energy production, and a greater part of the exact areas of management limitation is represented. While renewable energy sources include hydropower, solar, biomass, hydroelectric, and air, the generate electricity from alternative sources of energy provides a smaller amount of the overall generation capacity, and this segment should also be unambiguously committed to an expected returns in the energy circumstance. Hydropower accounts with about 24% of the combined production of power, and in the all-out amounts of electricity produced annually, this was one of the prominent renewable energy sources [1]. Hydropower projects are divided into groups on the basis of power generation capacity, namely, large hydropower plant (LHPP) and small hydropower plant (SHPP). SHPP is typically the sort of run-of-the-stream or stream dependent and refers to hydroelectric plants with such a consumption level of less than 25 MW, while LHPP is almost always linked to a large dam built over a stream, and it refers to a plant with a productivity level greater than 25 MW.

Karimi Azari et al. [2] followed the method to order of preference by similarity to ideal solution (TOPSIS) to pick a fair risk management framework for development projects. Chen et al. [3] reported out research on the design of procurement systems China's development programs. The

best range of SHPP construction projects is a significant task, as the parameters are often in disagreement between each other. The choice among the most favorable SHPP is therefore absolutely MCGDM issue. Many multicriteria group decision-making (MCGDM) issues (such as strategic financial management, and medical diagnosis and business) have been generated by aggregation operators [4, 5]. In 2018, Fahmi et al. [6] utilized some geometric operators under triangular cubic linguistic hesitant fuzzy environment and constructed a framework to group decision-making (GDM) complications. Weighted average rating algorithm, designed by [7], to solve group decision-making issues based on triangular cubic fuzzy hybrid aggregation. In [8], cubic fuzzy Einstein aggregation operators are introduced and its uses to decision-making (DM) issues. Triangular cubic linguistic hesitant fuzzy aggregation operators introduced by Aliya et al. [9], including its participation within group decision-making problem. Also, in 2018, Fahmi et al. [10] introduced planned values of aggregation operators based on cubic trapezoidal fuzzy value and their approach to the problems of MCDM. He [11] initiated typhoon disaster assessment focused on Dombi hesitant fuzzy data aggregation operators. In 2019, Jana et al. [12] initiated the notion of picture fuzzy Dombi aggregation operators and their approach to MCDM issues. Gagandeep and Harish [13] defined generalized cubic intuitionist fuzzy (CIF) aggregation operators through t-norm (TN) operations and their approach to GDM framework. Several linguistic intuitionist fuzzy aggregation operators and its uses to MAD issues are initiated by Peide and Peng [14]. Amiri et al. [15] designed a new fuzzy best-worst method technique for analyzing and choosing a supplier which is competitive in supply chain management. Utilizing Einstein t-norm and t-conorm and its approach to DM, generalize intuitionist fuzzy (IF) interactive geometric interaction operators [16]. Harish generalized the notion of IF multiplicative interactive geometric operators and its uses to MCDM [17]. Khan and Saleem [18] developed the concept of cubic aggregation operators. Liu [19] presented some interval-valued intuitionistic fuzzy (IVIF) Hamacher aggregation operators and applied it to the issue of MCGDM. Liang et al. [20] initiated the notion of GDM framework for multicriteria focused on generalized intuitionistic trapezoidal fuzzy prioritized aggregation operators. A few other IF Dombi Bonferroni mean operators including its connection to MAGDM are presented by Liu et al. [21]. Cubic hesitant fuzzy sets and respective approaches to DM under various parameters are defined in [22]. Only with the support of the new proposal of PF similarity, Haseeb and Singh present a novel framework recognized as the picture fuzzy inferior ratio method to solve MADM issues in the PF setting, which is focused on the very same concept as TOPSIS, taken into consideration both PIS and NIS similarities in [23]. Dombi operations are applied to neutrosophic cubic sets and proposed a neutrosophic cubic Dombi weighted arithmetic average operator and neutrosophic cubic Dombi weighted geometric average operator [24]. Ullah et al. [25] utilized the GRA method on the basis of picture hesitant fuzzy sets and discussed its application in GDM problems. Minxia and Huifeng defined

transformation algorithm for a picture fuzzy value and trapezoidal fuzzy value and suggested a PF multiplication operation and an image fuzzy power operation on the basis of this procedure [26]. The creation of a modern hybrid model based on PFSs through linear assignment and its first cases involve for the design of sustainable transportation systems [27]. To determine the distinct requirements of the option between the DM methods, many aggregation operators (AOs), named PF Yager aggregation, under the PF data [28] have been developed. Two correlation coefficients for PFSs obtaining their values in [−1, 1] have been introduced by Haseeb et al. while explaining the significance of the correlation more sufficiently [29].

In the field of DM environment, it is really tough to select real criterion values. In 1965, Zadeh coined his remarkable theory of fuzzy set (FS) to deal with uncertainty [30]. The notion of bi-parametric distance and similarity measures for PFSs was extended by Khan et al. [31]. The description of the PFS entropy measure has been developed by Thao [32]. They also analyzed such similarity measures caused by entropy measures at same period and then utilized it is applicable in MCDM issue regarding supplier selection. Focused on picture fuzzy numbers, Egrioglu et al. [33] model fuzzy time-series and a single-variable high-order PF time-series model are established. They also propose a better method of forecasting PF time series. Few operators were developed by Akram et al. [34], to aggregate CPF information, namely, complex picture fuzzy Hamacher weighted averaging, ordered weighted averaging, hybrid averaging and complex picture fuzzy Hamacher weighted geometric, ordered weighted geometric and hybrid geometric operators, gaining from standard Hamacher operations, and averaging geometric aggregation. Many PF geometric operators have been established by Chunyong et al. and its basic properties are examined [35]. In [36, 37], Xu and Yager initiated the concept of aggregation operators such as IF hybrid averaging (IFHA) operator, IF order weighted averaging (IFOWA) operator, IF weighted averaging (IFWA) operator, IF hybrid geometric (IFHG) operator, IF order weighted geometric (IFOWG) operator, and IF weighted geometric (IFWG) operator and utilized these proposed operators to MCGDM.

Hamacher operator (HO) [38] is an alloy of Einstein triangular cubic number, algebraic t-norm, and t-conorm [39]. Li studied Hamacher correlated averaging operator based on interval-valued IF (IVIF) information [40]. Hung introduced the concept of IF Hamacher aggregation (IFHA) operator and utilized this operator to MAGDM issues [41]. Garg [42] introduced IF Hamacher aggregation (IFHA) operators under depends on entropy weight and applied them to MCGDM problems.

Picture fuzzy Hamacher aggregation operator is presented by Jana and Pal [43], for assessment of enterprise performance. Xiao provided an order weighted Hamacher geometric operator [44], on the basis of IVIF environment. Hamacher and other aggregation operator functions are applied to the introduced MAGDM method [45,46]. Abdullah and Ashraf [47] established the concept of cubic picture fuzzy set and utilized this concept to evaluate the

petroleum circulation center problem. Muneeza et al. [48] presented intuitionistic cubic fuzzy Hamacher weighted aggregation (ICFHWA) operators and applied them to the MCGDM method. In this study, we want to define picture cubic fuzzy set (PCFS) and some picture cubic fuzzy Hamacher weighted aggregation (PCFHWA) operator based on HOs [49]. PCFS has a ground-breaking ability to appear the unpredictable information of the real life problem. PCFS is a forceful ability to model the uncertain information of real world. From the literature study of HOs, there is a broad range of works matching to application of fuzzy aggregation algorithms in MAGDM issues; by means of this encouragement, we utilized PCFHWA operator, PCFHOWA operator, and PCFHHA operator based on PCF numbers, to obtain the best SHPP as a manufacture project for the developer.

Based on the internal characteristics of unmanned ground delivery vehicles (UGDVs), a multicriteria comprehensive evaluation system for UGDVs is constructed [50]. In [51], Zeng et al. proposed a multicriteria model based on a social network for assessing a digital reform under an intuitionistic fuzzy environment. Xie et al., in [52], introduced a novel progressively under the sampling method based on the density peaks sequence for imbalanced data. In [53], the concept of SFS and T-spherical fuzzy set (T-SFS) is introduced as a generalization of FS, IFS, and PFS. The principle of Bonferroni mean (BM) operators with interval-valued T-spherical fuzzy set (IVTSFS) to develop the principle of the intervalued T-spherical fuzzy (IVTSF) BM (IVTSFBM) operator, the IVTSF-weighted BM (IVTSFWBM) operator, the IVTSF geometric BM (IVTSFGBM) operator, and the IVTSF-weighted geometric BM (IVTSFWGBM) operator is introduced in [54]. Ullah et al. developed the concept of picture fuzzy Maclaurin symmetric mean (PFMSM) operators and investigated their validity [55].

The aim of this study is to propose a new concept called "picture cubic fuzzy set" (PCFS), as an extension of intuitionistic cubic fuzzy set (ICFS). The addition of a neutral membership degree to ICFS makes PCFS as generalized form of ICFS. The uniqueness of this new theory lies in the capability to attain the wider range with the help of degree of neutral membership, nonmembership, and membership. Hamacher aggregation operator is one such operator which is based on Hamacher t-norm and t-conorm. It is observed that the Hamacher aggregation operators of intuitionistic cubic fuzzy set have some limitations in their applicability. To overcome these limitations, some Hamacher aggregation operators based on picture cubic fuzzy numbers are introduced.

In 2020, Muneeza et al. [48] presented the concept of ICFS and utilized this concept in MADM problems. Since PFS is a generalized concept to IFS, so, we gave attention to bring the notion of PCFS and defined Hamacher aggregation operators on the bases of PCFS and utilized PCFHA operators for selection of SHPP. The proposed aggregation operators can be used in the performance evaluation of energy projects, security systems and devices, etc.

Based on to what is discussed with regard to the abovementioned studies, the contribution of this study is given as below:

(1) Propose an idea of PCF set and discuss its basic properties; also, few Hamacher operators for PCFS are established

(2) Propose PCF Hamacher weighted aggregation operators

(3) Propose new-MCGDM algorithm based on these planned operators

(4) Solve SHPP place choice on the basis of new algorithm

(5) Discuss the comparison analysis to describe the validity of the proposed new-MCGDM algorithm

The leftovers of this study are planned below. In Section 2, we shortly review of essential definitions and HCs on PFS. In Section 3, we first describe the idea of PCFS and discuss its different basic properties. Several Hamacher operators for PCFSs are established. In Section 4, a number of PCFHA operators are given, such as PCFHWA operator, PCFHOWA operator, and PCFHHA operator, and study some of their properties. In Section 5, we state a new-MCGDM algorithm on the basis of these planned operators. In Section 6, we utilize descriptive example of SHPP locations selection and conduct a comparison analysis. In Section 7, conclusion is presented.

2. Preliminaries

The study provides a brief overview of the basic concepts of PFS, as well as their operation and operators. We also go through several more well-known concepts that will be essential in the upcoming analysis.

2.1. Fuzzy Set (FS)

Definition 1 (see [30]). *A FS R in $\check{T} \neq \phi$ is expressed as*

$$R = \left\{ \langle \check{t}, \mu_R(\check{t}) \rangle | \check{t} \in \check{T} \right\}, \tag{1}$$

where $\mu_R(\check{t}) \in [0, 1]$ is a membership degree of $\check{t}$ in R.

Definition 2 (see [56]). *An interval-valued intuitionistic fuzzy set* (IVIFS)R *in $\check{T} \neq \phi$ is expressed as*

$$R = \left\{ \langle \check{t}, [\mu_R^-(\check{t}), \mu_R^+(\check{t})], [\nu_R^-(\check{t}), \nu_R^+(\check{t})] \rangle | \check{t} \in \check{T} \right\}, \tag{2}$$

where $[\mu_R^-(\check{t}), \mu_R^+(\check{t})]$ indicates the membership function and $[\nu_R^-(\check{t}), \nu_R^+(\check{t})]$ denotes the nonmembership function.

Definition 3 (see [57]). *A cubic fuzzy set* (CFS)R *in $\check{T} \neq \phi$ is expressed as*

$$R = \left\{ \langle \check{t}, [\mu_R^-(\check{t}), \mu_R^+(\check{t})], \nu_R(\check{t}) \rangle | \check{t} \in \check{T} \right\}, \tag{3}$$

where the first value is the IVF number, indicates the degree of membership, and the second value is a simple fuzzy number, indicates the nonmembership degree.

2.2. Hamacher Aggregation Operators on ICFS

Definition 4 (see [48]). An ICFS R in $\check{T} \neq \phi$ is expressed as

$$R = \left\{ \check{t}, \langle a_R, b_R \rangle | \check{t} \in \check{T} \right\},$$

$$\text{or,} \tag{4}$$

$$R = \left\{ \left(\check{t}, \langle [a^-, a^+], \check{\lambda} \rangle, \langle [b^-, b^+], \check{\delta} \rangle \right) | \check{t} \in \check{T} \right\},$$

where $\check{\lambda}$ and $\check{\delta}$ represent degree of membership and degree of nonmembership, respectively, $\langle [a^-, a^+], \check{\lambda} \rangle$ denotes the exact degree of membership, and $\langle [b^-, b^+], \check{\delta} \rangle$ denotes the exact degree of non-membership of ICFS. $[a^-, a^+]$ and $[b^-, b^+] \subset [0, 1]$ and $\check{\lambda}: \check{T} \longrightarrow [0, 1]$ and $\delta: \check{T} \longrightarrow [0, 1]$ under restriction $\text{Sup}[a^-, a^+] + \text{Sup}[b^-, b^+] \leq 1$ and $\check{\lambda} + \check{\delta} \leq 1$. Besides, we obtain

$$\check{\pi}(R) = \left\{ \langle [1, 1] - [[a^-, a^+] + [b^-, b^+]] \rangle, \langle 1 - (\check{\lambda} + \check{\delta}) \rangle \right\},$$

$$\check{\pi}(R) = \left\{ [1 - (a^- + b^-), 1 - (a^+ + b^+)], 1 - (\check{\lambda} + \check{\delta}) \right\},$$

$$\tag{5}$$

is called index of ICFS or indeterminacy degree of $\check{t} \in \check{T}$ for R. For simplicity, an ICFN is represented by R, that is, $R = (\langle [a^-, a^+], \check{\lambda} \rangle, \langle [b^-, b^+], \check{\delta} \rangle)$.

Definition 5 (see [48]). Let $R_z = \langle a_{R_z}, b_{R_z} \rangle$ ($z = 1, 2, \ldots, g$) be a collection of ICFNs in $\check{T}$, and suppose ICFHWA operator of dimension g is a function of ICFHWA: $\Omega^g \longrightarrow \Omega$; thus,

$$\text{ICFHWA}_\omega \left(R_1, R_2, R_3, \ldots, R_g \right) = \oplus_{z=1}^g \omega_z R_z,$$

$$= \left\{ \left(\left[\frac{\prod_{z=1}^g \left(1 + (d-1)a_z^-\right)^{\omega_z} - \prod_{z=1}^g \left(1 - a_z^-\right)^{\omega_z}}{\prod_{z=1}^g \left(1 + (d-1)a_z^-\right)^{\omega_z} + (d-1)\prod_{z=1}^g \left(1 - a_z^-\right)^{\omega_z}}, \right. \right. \right.$$

$$\left. \frac{\prod_{z=1}^g \left(1 + (d-1)a_z^+\right)^{\omega_z} - \prod_{z=1}^g \left(1 - a_z^+\right)^{\omega_z}}{\prod_{z=1}^g \left(1 + (d-1)a_z^+\right)^{\omega_z} + (d-1)\prod_{z=1}^g \left(1 - a_z^+\right)^{\omega_z}} \right],$$

$$\left. \frac{\prod_{z=1}^g \left(1 + (d-1)\check{\lambda}_z\right)^{\omega_z} - \prod_{z=1}^g \left(1 - \check{\lambda}_z\right)^{\omega_z}}{\prod_{z=1}^g \left(1 + (d-1)\lambda_z\right)^{\omega_z} + (d-1)\prod_{z=1}^g \left(1 - \check{\lambda}_z\right)^{\omega_z}} \right),$$

$$\left(\left[\frac{d\prod_{z=1}^g \left(b_z^-\right)^{\omega_z}}{\prod_{z=1}^g \left(1 + (d-1)\left(1 - b_z^-\right)\right)^{\omega_z} + (d-1)\prod_{z=1}^g \left(b_z^-\right)^{\omega_z}}, \right. \right.$$

$$\left. \frac{k\prod_{z=1}^g \left(b_z^+\right)^{\omega_z}}{\prod_{z=1}^g \left(1 + (d-1)\left(1 - b_z^+\right)\right)^{\omega_z} + (d-1)\prod_{z=1}^g \left(b_z^+\right)^{\omega_z}} \right],$$

$$\left. \left. \frac{d\prod_{z=1}^g \left(\delta_z\right)^{\omega_z}}{\prod_{z=1}^g \left(1 + (d-1)\left(1 - \check{\delta}_z\right)\right)^{\omega_z} + (d-1)\prod_{z=1}^g \left(\check{\delta}_z\right)^{\omega_z}} \right) \right\},$$

$$\tag{6}$$

where $\omega = (\omega_1, \omega_2, \omega_3, \ldots, \omega_g)^T$ are weight vector of R_z $(z = 1, 2, 3, \ldots, g)$ by $\sum_{z=1}^{g} \omega_z = 1$ and $\omega_z \in [0, 1]$.

Definition 6 (see [48]). Let $R_z = \langle a_{R_z}, b_{R_z} \rangle$ $(z = 1, 2, \ldots, g)$ be a collection of ICFNs in $\check{T}$, and suppose ICFHOWA operator of dimension g is a function of ICFHOWA: $\Omega^g \longrightarrow \Omega$; thus,

$$\text{ICFHOWA}_{\omega}\left(R_1, R_2, R_3, \ldots, R_g\right) = \oplus_{z=1}^{g} \omega_z R_{\sigma_{(z)}},$$

$$= \left\{ \left(\left[\frac{\prod_{z=1}^{g}\left(1 + (d-1)a_{\sigma_{(z)}}^{-}\right)^{\omega_z} - \prod_{z=1}^{g}\left(1 - a_{\sigma_{(z)}}^{-}\right)^{\omega_z}}{\prod_{z=1}^{g}\left(1 + (d-1)a_{\sigma_{(z)}}^{-}\right)^{\omega_z} + (d-1)\prod_{z=1}^{g}\left(1 - a_{\sigma_{(z)}}^{-}\right)^{\omega_z}}, \right. \right. \right.$$

$$\left. \frac{\prod_{z=1}^{g}\left(1 + (d-1)a_{\sigma_{(z)}}^{+}\right)^{\omega_z} - \prod_{z=1}^{g}\left(1 - a_{\sigma_{(z)}}^{+}\right)^{\omega_z}}{\prod_{z=1}^{g}\left(1 + (d-1)a_{\sigma_{(z)}}^{+}\right)^{\omega_z} + (d-1)\prod_{z=1}^{g}\left(1 - a_{\sigma_{(z)}}^{+}\right)^{\omega_z}} \right],$$

$$\left. \frac{\prod_{z=1}^{g}\left(1 + (d-1)\breve{\lambda}_{\sigma_{(z)}}\right)^{\omega_z} - \prod_{z=1}^{g}\left(1 - \breve{\lambda}_{\sigma_{(z)}}\right)^{\omega_z}}{\prod_{z=1}^{g}\left(1 + (d-1)\breve{\lambda}_{\sigma_{(z)}}\right)^{\omega_z} + (d-1)\prod_{z=1}^{g}\left(1 - \breve{\lambda}_{\sigma_{(z)}}\right)^{\omega_z}} \right),$$

$$\left(\left[\frac{d\prod_{z=1}^{g}\left(b_{\sigma_{(z)}}^{-}\right)^{\omega_z}}{\prod_{z=1}^{g}\left(1 + (d-1)\left(1 - b_{\sigma_{(z)}}^{-}\right)\right)^{\omega_z} + (d-1)\prod_{z=1}^{g}\left(b_{\sigma_{(z)}}^{-}\right)^{\omega_z}}, \right. \right.$$

$$\left. \frac{k\prod_{z=1}^{g}\left(b_{\sigma_{(z)}}^{+}\right)^{\omega_z}}{\prod_{z=1}^{g}\left(1 + (d-1)\left(1 - b_{\sigma_{(z)}}^{+}\right)\right)^{\omega_z} + (d-1)\prod_{z=1}^{g}\left(b_{\sigma_{(z)}}^{+}\right)^{\omega_z}} \right],$$

$$\left. \left. \frac{d\prod_{z=1}^{g}\left(\breve{\delta}_{\sigma_{(z)}}\right)^{\omega_z}}{\prod_{z=1}^{g}\left(1 + (d-1)\left(1 - \breve{\delta}_{\sigma_{(z)}}\right)\right)^{\omega_z} + (d-1)\prod_{z=1}^{g}\left(\breve{\delta}_{\sigma_{(z)}}\right)^{\omega_z}} \right) \right] \right\}, \tag{7}$$

where $\omega = (\omega_1, \omega_2, \ldots, \omega_g)^T$ are weight vector of R_z $(z = 1, 2, \ldots, g)$ by $\sum_{z=1}^{g} \omega_z = 1$ and $\omega_z \in [0, 1]$. For all z, $R_{\sigma_{(z-1)}} \geq R_{\sigma_{(z)}}$ and $(\sigma_{(1)}, \sigma_{(2)}, \ldots, \sigma_{(g)})$ are permutation of $(1, 2, \ldots, g)$.

Definition 7 (see [48]). Let $R_z = \langle a_{R_z}, b_{R_z} \rangle (z = 1, 2, \ldots, g)$ be a collection of ICFNs in $\check{T}$, and let ICFHWA operator of dimension g be a function of ICFHHA: $\Omega^g \longrightarrow \Omega$, with weight vector $\omega = (\omega_1, \omega_2, \ldots, \omega_g)^T$ which is the weight

vector of R_z $(z = 1, 2, \ldots, g)$ with $\sum_{z=1}^g \varpi_z = 1$ and $\varpi_z \in [0, 1]$ and $\varpi_z > 0$; thus,

$$\text{ICFHHA}_{w,v}(R_1, R_2, R_3, \ldots, R_z) = \mathring{\mathrm{A}}_{z=1}^g v_z \widetilde{R}_{\sigma_{(z)}}, \quad (8)$$

where $w = (w_1, w_2, \ldots, w_g)^T$ are weight of R_z with $\sum_{z=1}^g w_z = 1$ and $w_z \in [0, 1]$. Here, $\widetilde{R}_{\sigma_{(z)}}$ is the zth largest of the weighted ICFNs $\widetilde{R}_z$ and $\widetilde{R}_{\sigma_{(z)}} = gw_z R_{\sigma_{(z)}} = (\langle [\widetilde{a}_{\sigma_{(z)}}^-, \widetilde{a}_{\sigma_{(z)}}^+], \widetilde{\lambda}_{\sigma_{(z)}} \rangle, \langle [\widetilde{b}_{\sigma_{(z)}}^-, \widetilde{b}_{\sigma_{(z)}}^+], \widetilde{\delta}_{\sigma_{(z)}} \rangle)$ $(z = 1, 2, 3, \ldots, g)$, where

$$\widetilde{a}_{\sigma_{(z)}}^- = \left(1 + (d-1)a_{\sigma_{(z)}}^-\right)^{gw_z} - \frac{\left(1 - a_{\sigma_{(z)}}^-\right)^{gw_z}}{\left(1 + (d-1)a_{\sigma_{(z)}}^-\right)^{gw_p} + (d-1)\left(1 - a_{\sigma_{(z)}}^-\right)^{gw_z}},$$

$$\widetilde{a}_{\sigma_{(z)}}^+ = \left(1 + (d-1)a_{\sigma_{(z)}}^+\right)^{gw_z} - \frac{\left(1 - a_{\sigma_{(z)}}^-\right)^{gw_z}}{\left(1 + (d-1)a_{\sigma_{(z)}}^+\right)^{gw_p} + (d-1)\left(1 - a_{\sigma_{(z)}}^+\right)^{gw_z}},$$

$$\widetilde{\lambda}_{\sigma_{(z)}} = \frac{\left(1 + (d-1)\breve{\lambda}_{\sigma_{(z)}}\right)^{gw_z} - \left(1 - \breve{\lambda}_{\sigma_{(z)}}\right)^{gw_z}}{\left(1 + (d-1)\breve{\lambda}_{\sigma_{(z)}}\right)^{gw_z} + (d-1)\left(1 - \breve{\lambda}_{\sigma_{(z)}}\right)^{gw_z}},$$

$$\widetilde{b}_{\sigma_{(z)}}^- = \frac{d\left(b_{\sigma_{(z)}}^-\right)^{gw_z}}{1 + (d-1)\left(1 - b_{\sigma_{(z)}}^-\right)^{gw_z} + (d-1)\left(b_{\sigma_{(z)}}^-\right)^{gw_z}},$$

$$\widetilde{b}_{\sigma_{(z)}}^+ = \frac{d\left(b_{\sigma_{(z)}}^+\right)^{gw_z}}{1 + (d-1)\left(1 - b_{\sigma_{(z)}}^+\right)^{gw_z} + (d-1)\left(b_{\sigma_{(z)}}^+\right)^{gw_z}},$$

$$\widetilde{\delta}_{\sigma_{(z)}} = \frac{d\left(\breve{\delta}_{\sigma_{(z)}}\right)^{gw_z}}{1 + (d-1)\left(1 - \breve{\delta}_{\sigma_{(z)}}\right)^{gw_z} + (d-1)\left(\breve{\delta}_{\sigma_{(z)}}\right)^{gw_z}},$$

$$(9)$$

where g is the balancing coefficient, which keeps the proper balance.

2.3. Picture Fuzzy set (PFS)

Definition 8 (see [58]). *A PFS R in $\breve{T} \neq \phi$ is identified as*

$$R = \left\{\langle \breve{t}, \mu_R(\breve{t}), \eta_R(\breve{t}), \nu_R(\breve{t}) \rangle | \breve{t} \in \breve{T}\right\}, \quad (10)$$

where $\mu_R(\breve{t})$, $\eta_R(\breve{t})$, and $\nu_R(\breve{t})$ in unit closed interval ($[0, 1]$) are called positive-membership, neutral-membership, and negative-membership degrees respectively, under restriction $0 \leq \mu_R(\breve{t}) + \eta_R(\breve{t}) + \nu_R(\breve{t}) \leq 1 \forall \breve{t} \in \breve{T}$. Furthermore, $\Psi_R = 1 - (\mu_R(\breve{t}) + \eta_R(\breve{t}) + \nu_R(\breve{t}))$ for all $\breve{t} \in \breve{T}$ is said to be the refusal-membership degree of the function. The pair (μ_R, η_R, ν_R) is called PF value (PFV) or PF number (PFN). Keep in mind that each one IFS can be expressed as

$$R = \left\{\langle \mu_R(\breve{t}), 0, \nu_R(\breve{t}) \rangle | \breve{t} \in \breve{T}\right\}. \quad (11)$$

If we put $\eta_R(\breve{t}) \neq 0$, in equation (2), then we get PFS.

2.4. Hamacher Operations (HOs).
Basically, t-operator are union and intersection operators in fuzzy set theory which are represent by t-conorm (T) and t-norm (T^*), respectively [59]. The generalized intersection and union of IFSs on the basis of t-conorm and t-norm were introduced by Deschrijver and Kerre [60]. Hamacher initiated HOs, so called as Hamacher sum ($\oplus$) and Hamacher product ($\otimes$), in 1978 [38], the t-conorm and t-norm examples, respectively. Hamacher T and Hamacher T^* are given in the following definition:

$$T_H(s, t) = s \otimes t = \frac{st}{d + (1-d)(s + t - st)},$$

$$T_H^*(s, t) = s \oplus t = \frac{s + t - st - (1-d)st}{1 - (1-d)st}. \quad (12)$$

When $d = 1$, at that time, Hamacher T^* and T will change to the form:

$$T_H(s, t) = s \otimes t = st, \quad (13)$$

$$T_H^*(s, t) = s \oplus t = s + t - st, \quad (14)$$

which represent algebraic T and T^*. When $d = 2$, at that time, Hamacher T^* and T will change to the form:

$$T_H(s,t) = s \otimes t = \frac{st}{1 + (1-s)(1-t)}, \quad (15)$$

$$T_H^*(s,t) = s \oplus t = \frac{s+t}{1+st}, \quad (16)$$

called Einstein T and T^*, respectively.

2.5. Hamacher Operations (HOs) of PFS.

Several Hamacher operations (HOs) on picture fuzzy values (PFVs) are given, which are introduced by Wei [49]. Suppose R_1 and R_2 be any two picture fuzzy set and $n > 0$. Then, the Hamacher sum and Hamacher product of R_1 and R_2 are represented by $(R_1 \oplus R_2)$ and $(R_1 \otimes R_2)$ and defined by

(1) $(R_1 \oplus R_2) = (\mu_1 + \mu_2 - \mu_1\mu_2 - (1-d)\mu_1\mu_2/1 - (1-d)\mu_1\mu_2, \eta_1\eta_2/d + (1-d)(\eta_1 + \eta_2 - \eta_1\eta_2), \nu_1\nu_2/d + (1-d)(\nu_1 + \nu_2 - \nu_1\nu_2))$

(2) $(R_1 \otimes R_2) = (\mu_1\mu_2/d + (1-d)(\mu_1 + \mu_2 - \mu_1\mu_2), \eta_1 + \eta_2 - \eta_1\eta_2 - (1-d)\eta_1\eta_2/1 - (1-d)\eta_1\eta_2, \nu_1 + \nu_2 - \mu_1\nu_2 - (1-d)\nu_1\nu_2/1 - (1-d)\nu_1\nu_2)$

(3) $nR_1 = \{((1 + (d-1)\mu_1)^n - (1 - \mu_1)^n/(1 + (d-1)\mu_1)^n + (d-1)(1-\mu_1)^n), (d(\eta_1)^n/(1 + (d-1)(1-\eta_1))^n + (d-1)(\eta_1)^n), (d(\nu_1)^n/(1 + (d-1)(1-\nu_1))^n + (d-1)(\nu_1)^n)\}$

(4) $R_1^n = \{(d(\mu_1)^n/(1 + (d-1)(1-\mu_1))^n + (d-1)(\mu_1)^n), ((1 + (d-1)\eta_1)^n - (1-\eta_1)^n/(1 + (d-1)\eta_1)^n + (d-1)(1-\eta_1)^n), ((1 + (d-1)\nu_1)^n - (1-\nu_1)^n/(1 + (d-1)\nu_1)^n + (d-1)(1-\nu_1)^n)\}.$

3. PCFS and Its Fundamental Relations and Operations

Definition 9. A picture cubic fuzzy set (PCFS) P in $\check{T} \neq \phi$ is defined as

$$P = \{\check{t}, \langle a_P, c_P, b_P \rangle | \check{t} \in \check{T}\}, \quad (17)$$

or

$$P = \left\{ \left(\check{t}, \langle [a^-, a^+], \check{\lambda} \rangle, \langle [c^-, c^+], \check{\psi} \rangle, \langle [b^-, b^+], \check{\delta} \rangle \right) | \check{t} \in \check{T} \right\}, \quad (18)$$

where $\langle [a^-, a^+], \check{\lambda} \rangle$ denotes the exact degree of membership, $\langle [c^-, c^+], \check{\psi} \rangle$ denotes the exact degree of neutral, and $\langle [b^-, b^+], \check{\delta} \rangle$ denotes the exact degree of nonmembership of P. On this spot $[a^-, a^+][c^-, c^+]$ and $[b^-, b^+] \subset [0,1]$, $\check{\lambda}: \check{T} \longrightarrow [0,1], \check{\psi}: \check{T} \longrightarrow [0,1],$ and $\check{\delta}: \check{T} \longrightarrow [0,1]$ subject to $\text{Sup}[a^-, a^+] + \text{Sup}[c^-, c^+] + \text{Sup}[b^-, b^+] \leq 1$ and $\check{\lambda} + \check{\psi} + \check{\delta} \leq 1$. Thus, we have

$$\check{\pi}(R) = \left\{ \langle [1,1] - [[a^-, a^+] + [c^-, c^+] + [b^-, b^+]] \rangle, \langle 1 - (\check{\lambda} + \check{\psi} + \check{\delta}) \rangle \right\},$$

$$\check{\pi}(R) = \left\{ [1 - (a^- + c^- + b^-), 1 - (a^+ + c^+ + b^+)], 1 - (\check{\lambda} + \check{\psi} + \check{\delta}) \right\}, \quad (19)$$

which is called index of PCFS or indeterminacy degree of $\check{t} \in \check{T}$ for PCFS. For simplicity, an PCFN is denoted by P, that is, $P = (\langle (a^-, a^+), \check{\lambda} \rangle, \langle [c^-, c^+], \check{\psi} \rangle, \langle [b^-, b^+], \check{\delta} \rangle)$.

Example 1. Let us have $\check{T} = \{\check{t}_1, \check{t}_2, \check{t}_3, \check{t}_4\}$ a set, and suppose P be a set given by

$$P = \left\{ \begin{array}{l} (\check{t}_1, ([0.1, 0.15], 0.4), ([0.25, 0.3], 0.1), ([0.4, 0.5], 0.3)), \\ (\check{t}_2, ([0.1, 0.4], 0.2), ([0.35, 0.4], 0.6), ([0.1, 0.15], 0.2)), \\ (\check{t}_3, ([0.2, 0.3], 0.1), ([0.1, 0.2], 0.35), ([0.2, 0.4], 0.3)), \\ (\check{t}_4, ([0.1, 0.5], 0.4), ([0.15, 0.2], 0.3), ([0.2, 0.3], 0.3)) \end{array} \right\}. \quad (20)$$

Thus, P satisfies the definition of PCFS. Hence, P is PCFS. Based on PCFN, we defined score function $S(P)$ and accuracy function $A(P)$.

Definition 10. Suppose $P = (\langle [a^-, a^+], \check{\lambda} \rangle, \langle [c^-, c^+], \check{\psi} \rangle, \langle [b^-, b^+], \check{\delta} \rangle)$ be a picture cubic fuzzy number. $S(P)$ is expressed as

$$S(P) = \left(\frac{a^- + a^+ + \check{\lambda} - (c^- + c^+ + \check{\psi} + b^- + b^+ + \check{\delta})}{3} \right), \quad (21)$$

so as $S(P) \in [-1, 1]$. The function $S(P)$ computes the score of PCFN P.

Definition 11. Suppose $P = (\langle[a^-, a^+], \breve{\lambda}\rangle, \langle[c^-, c^+], \breve{\psi}\rangle, \langle[b^-, b^+], \breve{\delta}\rangle)$ *be a PCFN. The accuracy function $A(P)$ is expressed as*

$$A(P) = \left(\frac{a^- + a^+ + \breve{\lambda} + c^- + c^+ + \breve{\psi} + b^- + b^+ + \breve{\delta}}{3} \right), \quad (22)$$

where $A(P) \in [0, 1]$.

Definition 12. Suppose

$$P_1 = \left(\langle[a_1^-, a_1^+], \breve{\lambda}_1\rangle, \langle[c_1^-, c_1^+], \breve{\psi}_1\rangle, \langle[b_1^-, b_1^+], \breve{\delta}_1\rangle \right),$$
$$P_2 = \left(\langle[a_2^-, a_2^+], \breve{\lambda}_2\rangle, \langle[c_2^-, c_2^+], \breve{\psi}_2\rangle, \langle[b_2^-, b_2^+], \breve{\delta}_2\rangle \right), \quad (23)$$

are two PCFNs, $S(P_1)$ and $S(P_2)$ are the score function of P_1 and P_2, and $A(P_1)$ and $A(P_2)$ are the accuracy function of P_1 and P_2, respectively. Then,

   (1) If $S(P_1) < S(P_2) \Rightarrow P_1 < P_2$
   (2) If $S(P_1) = S(P_2), A(P_1) = A(P_2)$, then $P_1 = P_2$
   (3) If $S(P_1) = S(P_2)$ and $A(P_1) < A(P_2) \Rightarrow P_1 = P_2$

3.1. Hamacher Operations in PCFS. Let

$$P_1 = \left\{ \left(\langle[a_1^-, a_1^+], \breve{\lambda}_1\rangle, \langle[c_1^-, c_1^+], \breve{\psi}_1\rangle, \langle[b_1^-, b_1^+], \breve{\delta}_1\rangle \right) \right\},$$
$$P_2 = \left\{ \left(\langle[a_2^-, a_2^+], \breve{\lambda}_2\rangle, \langle[c_2^-, c_2^+], \breve{\psi}_2\rangle, \langle[b_2^-, b_2^+], \breve{\delta}_2\rangle \right) \right\}, \quad (24)$$

be two PCFN and $n > 0$; we introduce the below fundamental Hamacher operators in PCFS:

(1) $P_1 \oplus P_2 = \{ \ (\ [\ a_1^- + a_2^- - a_1^- a_2^- - (1-d)a_1^- a_2^-/1 - (1-d)a_1^- a_2^-, a_1^+ + a_2^+ - a_1^+ a_2^+ - (1-d)a_1^+ a_2^+/1 - (1-d)a_1^+ a_2^+], \breve{\lambda}_1 + \breve{\lambda}_2 - \breve{\lambda}_1\breve{\lambda}_2 - (1-d)\breve{\lambda}_1\breve{\lambda}_2/1 - (1-d)\breve{\lambda}_1\breve{\lambda}_2),$

$\left(\begin{bmatrix} c_1^- c_2^-/d + (1-d)(c_1^- + c_2^- - c_1^- c_2^-), \\ c_1^+ c_2^+/d + (1-d)(c_1^+ + c_2^+ - c_1^+ c_2^+) \end{bmatrix}, \\ \breve{\psi}_1\breve{\psi}_2/d + (1-d)(\breve{\psi}_1 + \breve{\psi}_2 - \breve{\psi}_1\breve{\psi}_2) \right)$

$\left(\begin{bmatrix} b_1^- b_2^-/d + (1-d)(b_1^- + b_2^- - b_1^- b_2^-), \\ b_1^+ b_2^+/d + (1-d)(b_1^+ + b_2^+ - b_1^+ b_2^+) \end{bmatrix}, \\ \breve{\delta}_1\breve{\delta}_2/d + (1-d)(\breve{\delta}_1 + \breve{\delta}_2 - \breve{\delta}_1\breve{\delta}_2) \right), \}$

(2) $P_1 \otimes P_2 = \{ \ (\ [\ a_1^- a_2^-/d + (1-d) \ (a_1^- + a_2^- - a_1^- a_2^-), a_1^+ a_2^+/d + (1-d)(a_1^+ + a_2^+ - a_1^+ a_2^+)], \breve{\lambda}_1\breve{\lambda}_2/d + (1-d)(\breve{\lambda}_1 + \breve{\lambda}_2 - \breve{\lambda}_1\breve{\lambda}_2)), \ (\ [\ c_1^- + c_2^- - c_1^- c_2^- - (1-d)c_1^- c_2^-/1 - (1-d)c_1^- c_2^-, c_1^+ + c_2^+ - c_1^+ c_2^+ - (1-d)c_1^+ c_2^+/1 - (1-d)c_1^+ c_2^+], \breve{\psi}_1 + \breve{\psi}_2 - \breve{\psi}_1\breve{\psi}_2 - (1-d)\breve{\psi}_1\breve{\psi}_2/1 - (1-d)\breve{\psi}_1\breve{\psi}_2), \ (\ [\ b_1^- + b_2^- - b_1^- b_2^- - (1-d)b_1^- b_2^-/1 - (1-d)b_1^- b_2^-, b_1^+ + b_2^+ - b_1^+ b_2^+ - (1-d)b_1^+ b_2^+/1 - (1-d)b_1^+ b_2^+], \delta_1 + \delta_2 - \delta_1\delta_2 - (1-d)\delta_1\delta_2/1 - (1-d)\delta_1\delta_2)\}$

(3) $nP_1 = \{ \ (\ [\ (1 + (d-1)a_1^-)^n - (1 - a_1^-)^n/(1 + (d-1)a_1^-)^n + (d-1)(1 - a_1^-)^n, (1 + (d-1)a_1^+)^n - (1 - a_1^+)^n/(1 + (d-1)a_1^+)^n + (d-1)(1 - a_1^+)^n], (1 + (d-1)\breve{\lambda}_1)^n - (1 - \breve{\lambda}_1)^n/(1 + (d-1)\breve{\lambda}_1)^n + (d-1)(1 - \breve{\lambda}_1)^n) (\ [\ k(c_1^-)^n/ \quad (1 + (d-1)(1 - c_1^-))^n + (d-1)(c_1^-)^n, k(c_1^+)^n/(1 + (d-1)(1 - c_1^+))^n + (d-1)(c_1^+)^n], d(\breve{\psi}_1)^n/(1 + (d-1)(1 - \breve{\psi}_1))^n + (d-$

$1)(\breve{\psi}_1)^n), (\ [\ d(b_1^-)^n/(1 + (1 - d) \ (1 - b_1^-))^n + (1-d)(b_1^-)^n, d(b_4^+)^n/(1 + (1 - d)(1 - b_4^+))^n + (1-d)(b_1^+)^n], d(\delta_1)^n/(1 + (1 - d)(1 - \delta_1))^n + (1 - d)(\delta_1)^n)\}$

(4) $(P_1)^n = \{ \ (\ [\ d(a_1^-)^n/ \quad (1 + (d-1)(1 - a_1^-))^n + (d-1)(a_1^-)^n, d(a_1^+)^n/(1 + (d-1)(1 - a_1^+))^n + (d-1)(a_1^+)^n], d(\breve{\lambda}_1)^n/(1 + (d-1)(1 - \breve{\lambda}_1))^n + (d-1)(\breve{\lambda}_1)^n) (\ [\ (1 + (d-1)c_1^-)^n - (1 - c_1^-)^n/(1 + (d-1)c_1^-)^n + (d-1)(1 - c_1^-)^n, (1 + (d-1)c_1^+)^n - (1 - c_1^+)^n/(1 + (d-1)c_1^+)^n + (d-1)(1 - c_1^+)^n], (1 + (d-1)\breve{\psi}_1)^n - (1 - \breve{\psi}_1)^n/(1 + (d-1)\breve{\psi}_1)^n + (d-1)(1 - \breve{\psi}_1)^n), (\ [\ (1 + (d-1)b_1^-)^n - (1 - b_1^-)^n/(1 + (d-1)b_1^-)^n + (d-1)(1 - b_1^-)^n, (1 + (d-1)b_1^+)^n - (1 - b_1^+)^n/(1 + (d-1)b_1^+)^n + (d-1)(1 - b_1^+)^n], (1 + (d-1)\delta_1)^n - (1 - \delta_1)^n/(1 + (d-1)\delta_1)^n + (d-1)(1 - \delta_1)^n)\}$

Proposition 1. *Let*

$$P_1 = \left\{ \left(\langle[a_1^-, a_1^+], \breve{\lambda}_1\rangle, \langle[c_1^-, c_1^+], \breve{\psi}_1\rangle, \langle[b_1^-, b_1^+], \breve{\delta}_1\rangle \right) \right\},$$
$$P_2 = \left\{ \left(\langle[a_2^-, a_2^+], \breve{\lambda}_2\rangle, \langle[c_1^-, c_1^+], \breve{\psi}_2\rangle, \langle[b_2^-, b_2^+], \breve{\delta}_2\rangle \right) \right\}, \quad (25)$$

be two PCFN and $n_1, n_2 > 0$; then, we have

   (1) $P_1 \oplus P_2 = P_2 \oplus P_1$
   (2) $P_1 \otimes P_2 = P_2 \otimes P_1$
   (3) $n(P_1 \oplus P_2) = nP_1 \oplus nP_2$
   (4) $n(P_1 \otimes P_2) = nP_1 \otimes nP_2$
   (5) $(P_1 \otimes P_2)^n = P_1^n \otimes P_2^n$
   (6) $(P_1 \oplus P_2)^n = P_1^n \oplus P_2^n$
   (7) $(P_1^{n_1})^{n_2} = (P_1)^{n_1 n_2}$.

4. Picture Cubic Fuzzy Hamacher Weighted Aggregation (PCFHWA) Operators

Here, we establish a number of PCFHA operators and describe few of its basic properties.

4.1. PCFHWA Operator

Definition 13. Suppose $P_r = \langle a_{P_r}, c_{P_r}, b_{P_r} \rangle$ $(r = 1, 2, \ldots, g)$ *is a set of PCFVs in $\breve{T}$. A PCFHWA operator of dimension g is a function PCFHWA: $\Omega^g \longrightarrow \Omega$, such that*

$$\text{PCFHWA}_{\varpi}(P_1, P_2, P_3, \ldots, P_g) = \oplus_{r=1}^g \varpi_r P_r, \quad (26)$$

where Ω is the set of all PCFVs and $\varpi = (\varpi_1, \varpi_2, \varpi_3, \ldots, \varpi_g)^T$ is the weight vector of P_r $(r = 1, 2, \ldots, g)$ with $\sum_{r=1}^g \varpi_r = 1$ and $\varpi_r \in [0, 1]$.

Under the Hamacher operational rules of the PCFNs, we get the theorem as given below.

Theorem 1. *Suppose that $P_r = \langle a_{P_r}, c_{P_r}, b_{P_r} \rangle$ $(r = 1, 2, \ldots, g)$ is a set of PCFVs in $\breve{T}$; then, the aggregated value of them utilizing PCFHWA operator is again a PCFV and is given as*

$$PCFHWA_{\omega}\left(P_1, P_2, P_3, \ldots, P_g\right),$$

$$= \left\{ \left(\left[\frac{\prod_{r=1}^{g}\left(1+(d-1)a_r^-\right)^{\omega_r} - \prod_{r=1}^{g}\left(1-a_r^-\right)^{\omega_r}}{\prod_{r=1}^{g}\left(1+(d-1)a_r^-\right)^{\omega_r} + (d-1)\prod_{r=1}^{g}\left(1-a_r^-\right)^{\omega_r}}, \right. \right. \right.$$
$$\left. \frac{\prod_{r=1}^{g}\left(1+(k-1)a_r^+\right)^{\omega_r} - \prod_{r=1}^{g}\left(1-a_r^+\right)^{\omega_r}}{\prod_{r=1}^{g}\left(1+(d-1)a_r^+\right)^{\omega_r} + (d-1)\prod_{r=1}^{g}\left(1-a_r^+\right)^{\omega_r}} \right],$$
$$\left. \frac{\prod_{r=1}^{g}\left(1+(d-1)\breve{\lambda}_r\right)^{\omega_r} - \prod_{r=1}^{g}\left(1-\breve{\lambda}_r\right)^{\omega_r}}{\prod_{r=1}^{g}\left(1+(d-1)\breve{\lambda}_r\right)^{\omega_r} + (d-1)\prod_{r=1}^{g}\left(1-\breve{\lambda}_r\right)^{\omega_r}} \right),$$

$$\left(\left[\frac{d\prod_{r=1}^{g}\left(c_r^-\right)^{\omega_r}}{\prod_{r=1}^{g}\left(1+(d-1)\left(1-c_r^-\right)\right)^{\omega_r} + (d-1)\prod_{r=1}^{g}\left(c_r^-\right)^{\omega_r}}, \right. \right.$$
$$\left. \frac{d\prod_{r=1}^{g}\left(c_r^+\right)^{\omega_r}}{\prod_{r=1}^{g}\left(1+(d-1)\left(1-c_r^+\right)\right)^{\omega_r} + (d-1)\prod_{r=1}^{g}\left(c_r^+\right)^{\omega_r}} \right],$$
$$\left. \frac{d\prod_{r=1}^{g}\left(\breve{\psi}_r\right)^{\omega_r}}{\prod_{r=1}^{g}\left(1+(d-1)\left(1-\breve{\psi}_r\right)\right)^{\omega_r} + (d-1)\prod_{r=1}^{g}\left(\breve{\psi}_r\right)^{\omega_r}} \right),$$

$$\left(\left[\frac{d\prod_{r=1}^{g}\left(b_r^-\right)^{\omega_r}}{\prod_{r=1}^{g}\left(1+(d-1)\left(1-b_r^-\right)\right)^{\omega_r} + (d-1)\prod_{r=1}^{g}\left(b_r^-\right)^{\omega_r}}, \right. \right.$$
$$\left. \frac{d\prod_{r=1}^{g}\left(b_r^+\right)^{\omega_r}}{\prod_{r=1}^{g}\left(1+(d-1)\left(1-b_r^+\right)\right)^{\omega_r} + (d-1)\prod_{r=1}^{g}\left(b_r^+\right)^{\omega_r}} \right],$$
$$\left. \left. \frac{d\prod_{r=1}^{g}\left(\breve{\delta}_r\right)^{\omega_r}}{\prod_{r=1}^{g}\left(1+(d-1)\left(1-\breve{\delta}_r\right)\right)^{\omega_r} + (d-1)\prod_{r=1}^{g}\left(\breve{\delta}_r\right)^{\omega_r}} \right) \right\}, \tag{27}$$

where $\omega = (\omega_1, \omega_2, \omega_3, \ldots, \omega_m)^T$ is the weight vector of P_r $(r = 1, 2, .., g)$ with $\sum_{r=1}^{g} \omega_r = 1$ and $\omega_r > 0$.

Proof. For proof, see Appendix A. □

4.2. Parameter d Effect on PCFHWA Operator. Subsequently, we suppose that two appropriate cases for the PCFHWA operator whenever $d = 1$ or 2.

Case (i): in case that $d = 1$, at that time, PCFHWA operator will change to PCFWA operator:

$$\text{PCFWA}_{\omega}\left(P_1, P_2, P_3, \ldots, P_g\right),$$

$$= \left\{ \begin{array}{c} \left(\left(\begin{bmatrix} 1 - \prod_{r=1}^{g} \left(1 - a_r^-\right)^{\omega_r}, \\ 1 - \prod_{r=1}^{g} \left(1 - a_r^+\right)^{\omega_r} \end{bmatrix}, \\ 1 - \prod_{r=1}^{g} \left(1 - \breve{\lambda}_r\right)^{\omega_r} \end{array} \right), \\ \left(\begin{bmatrix} \prod_{r=1}^{g} \left(c_r^-\right)^{\omega_r}, \\ \prod_{r=1}^{g} \left(c_r^+\right)^{\omega_r} \end{bmatrix}, \\ \prod_{r=1}^{g} \left(\breve{\psi}_r\right)^{\omega_r} \end{array} \right), \\ \left(\begin{bmatrix} \prod_{r=1}^{g} \left(b_r^-\right)^{\omega_r}, \\ \prod_{r=1}^{g} \left(b_r^+\right)^{\omega_r} \end{bmatrix}, \\ \prod_{r=1}^{g} \left(\breve{\delta}_r\right)^{\omega_r} \end{array} \right) \end{array} \right\}. \quad (28)$$

Case (ii): if $d = 2$, then the PCFHWA operator will change to picture cubic fuzzy Einstein weighted averaging (PCFEWA) operator:

$$\text{PCFEWA}_{\omega}\left(P_1, P_2, P_3, \ldots, P_g\right),$$

$$= \left\{ \begin{array}{c} \left(\left(\begin{bmatrix} \dfrac{\prod_{r=1}^{g} \left(1 + a_r^-\right)^{\omega_r} - \prod_{r=1}^{g} \left(1 - a_r^-\right)^{\omega_r}}{\prod_{r=1}^{g} \left(1 + a_r^-\right)^{\omega_r} + \prod_{r=1}^{g} \left(1 - a_r^-\right)^{\omega_r}}, \\ \dfrac{\prod_{r=1}^{g} \left(1 + a_r^+\right)^{\omega_r} - \prod_{r=1}^{g} \left(1 - a_r^+\right)^{\omega_r}}{\prod_{r=1}^{g} \left(1 + a_r^+\right)^{\omega_r} + \prod_{r=1}^{g} \left(1 - a_r^+\right)^{\omega_r}} \end{bmatrix}, \\ \dfrac{\prod_{r=1}^{g} \left(1 + \breve{\lambda}_r\right)^{\omega_r} - \prod_{r=1}^{g} \left(1 - \breve{\lambda}_r\right)^{\omega_r}}{\prod_{r=1}^{g} \left(1 + \breve{\lambda}_r\right)^{\omega_r} + \prod_{r=1}^{g} \left(1 - \breve{\lambda}_r\right)^{\omega_r}} \end{array} \right), \\ \left(\begin{bmatrix} \dfrac{2 \prod_{r=1}^{g} \left(c_r^-\right)^{\omega_r}}{\prod_{r=1}^{g} \left(2 - c_r^-\right)^{\omega_r} + \prod_{r=1}^{g} \left(c_r^-\right)^{\omega_r}}, \\ \dfrac{2 \prod_{r=1}^{g} \left(c_r^+\right)^{\omega_r}}{\prod_{r=1}^{g} \left(2 - c_r^+\right)^{\omega_r} + \prod_{r=1}^{g} \left(c_r^+\right)^{\omega_r}} \end{bmatrix}, \\ \dfrac{2 \prod_{r=1}^{g} \left(\breve{\psi}_r\right)^{\omega_r}}{\prod_{r=1}^{g} \left(2 - \breve{\psi}_r\right)^{\omega_r} + \prod_{r=1}^{g} \left(\breve{\psi}_r\right)^{\omega_r}} \end{array} \right), \\ \left(\begin{bmatrix} \dfrac{2 \prod_{r=1}^{g} \left(b_r^-\right)^{\omega_r}}{\prod_{r=1}^{g} \left(2 - b_r^-\right)^{\omega_r} + \prod_{r=1}^{g} \left(b_r^-\right)^{\omega_r}}, \\ \dfrac{2 \prod_{r=1}^{g} \left(b_r^+\right)^{\omega_r}}{\prod_{r=1}^{g} \left(2 - b_r^+\right)^{\omega_r} + \prod_{r=1}^{g} \left(b_r^+\right)^{\omega_r}} \end{bmatrix}, \\ \dfrac{2 \prod_{r=1}^{g} \left(\breve{\delta}_r\right)^{\omega_r}}{\prod_{r=1}^{g} \left(2 - \breve{\delta}_r\right)^{\omega_r} + \prod_{r=1}^{g} \left(\breve{\delta}_r\right)^{\omega_r}} \end{array} \right) \end{array} \right\}.$$

$$(29)$$

Proposition 2. *Suppose that* $P_r = \langle a_{P_r}, c_{P_r}, b_{P_r} \rangle$ *(r = 1, 2, ..., g) is a set of PCFVs in* $\breve{T}$, $\varpi = (\varpi_1, \varpi_2, \varpi_3, \ldots, \varpi_g)^T$ *are the weight vector of* P_r *with* $\sum_{r=1}^{g} \varpi_r = 1$, *and* ϖ_r *is the element of unit closed interval ([0,1]); then, the coming properties are initiated.*

Idempotency Property. If all $P_r = \langle a_{P_r}, c_{P_r}, b_{P_r} \rangle$ *(r = 1, 2, ..., g) are equal, that is,* $P_r = P$, *then*

$$\text{PCFHWA}_\varpi(P_1, P_2, \ldots, P_g) = P. \tag{30}$$

Proof. For proof, see Appendix B.

Boundedness Property. For every ϖ,

$$P^- \leq \text{PCFHWA}_\varpi(P_1, P_2, P_3, \ldots, P_g) \leq P^+, \tag{31}$$

where

$$P^+ = \left\{ \begin{array}{l} \left([\min a^-, \max a^+], \max \breve{\lambda}\right), \\ \left([\max c^-, \min c^+], \min \breve{\psi}\right), \\ \left([\max b^-, \min b^+], \min \breve{\delta}\right) \end{array} \right\}, \tag{32}$$

$$P^- = \left\{ \begin{array}{l} \left([\min a^-, \max a^+], \min \breve{\lambda}\right), \\ \left([\max c^-, \min c^+], \max \breve{\psi}\right), \\ [\max b^-, \min b^+], \min \breve{\delta} \end{array} \right\}.$$

Monotonicity property : let

$$P_r^* = \left\{ \left(\langle [a_r^{*-}, a_r^{*+}], \breve{\lambda}_r^* \rangle, \langle [c_r^{*-}, c_r^{*+}], \breve{\psi}_r^* \rangle, \langle [b_r^{*-}, b_r^{*+}], \breve{\delta}_r^* \rangle \right) \right\}, \tag{33}$$

where $(r = 1, 2, .., g)$ be a group of PCFNs if

$$[a_r^-, a_r^+] \leq [a_r^{*-}, a_r^{*+}], \breve{\lambda}_r \leq \breve{\lambda}_r^*, [c_r^{*-}, c_r^{*+}] \leq [c_r^-, c_r^+], \breve{\psi}_r^* \leq \breve{\psi}_r,$$

$$[b_r^{*-}, b_r^{*+}] \leq [b_r^-, b_r^+], \breve{\delta}_r^* \leq \breve{\delta}_r, \tag{34}$$

for all r. Then,

$$\text{PCFHWA}_\varpi(P_1, P_2, \ldots, P_g) \leq \text{PCFHWA}_\varpi(P_1^*, P_2^*, \ldots, P_g^*). \tag{35}$$

$\square$

Proof. See Appendix C. $\square$

4.3. PCFHOWA Operator

Definition 14. Let $P_r = \langle a_{P_r}, c_{P_r}, b_{P_r} \rangle (r = 1, 2, \ldots, g)$ *be a set of PCFVs in* $\breve{T}$. *A PCFHOWA operator of g dimension is a function PCFHOWA:* $\Omega^g \longrightarrow \Omega$, *such that*

$$\text{PCFHOWA}_\varpi(P_1, P_2, \ldots, P_g) = \oplus_{r=1}^{g} \varpi_r P_{\sigma_{(r)}}. \tag{36}$$

For all $r P_{\sigma_{(r-1)}} \geq P_{\sigma_{(r)}}$, $(\sigma_{(1)}, \sigma_{(2)}, .., \sigma_{(g)})$ *is a permutation of* $(1, 2, .., g)$. Ω *is the set of all PCFVs and* $\varpi = (\varpi_1, \varpi_2, .., \varpi_g)^T$ *is the weight vector of* $P_r (r = 1, 2, .., g)$ *with* $\sum_{r=1}^{g} \varpi_r = 1$ *and* $\varpi_r \in [0, 1]$.

Hence, under the Hamacher operational rules of the PCFNs, we get the theorem as given below.

Theorem 2. *Suppose that* $P_r = \langle a_{P_r}, c_{P_r}, b_{P_r} \rangle$ *(r = 1, 2, ..., g) is a set of PCFVs in* $\breve{X}$; *then, the aggregated value of the utilizing PCFHOWA operator is also a PCFV and is written as*

$$\mathrm{PCFHOWA}_\omega\left(P_1, P_2, \ldots, P_g\right),$$

$$= \left\{ \left(\left[\frac{\prod_{r=1}^{g}\left(1+(d-1)a_{\sigma_{(r)}}^-\right)^{\omega_r} - \prod_{r=1}^{g}\left(1-a_{\sigma_{(r)}}^-\right)^{\omega_r}}{\prod_{r=1}^{g}\left(1+(d-1)a_{\sigma_{(r)}}^-\right)^{\omega_r} + (d-1)\prod_{r=1}^{g}\left(1-a_{\sigma_{(r)}}^-\right)^{\omega_r}}, \right. \right. \right.$$

$$\left. \frac{\prod_{r=1}^{g}\left(1+(d-1)a_{\sigma_{(r)}}^+\right)^{\omega_r} - \prod_{r=1}^{g}\left(1-a_{\sigma_{(r)}}^+\right)^{\omega_r}}{\prod_{r=1}^{g}\left(1+(d-1)a_{\sigma_{(r)}}^+\right)^{\omega_r} + (d-1)\prod_{r=1}^{g}\left(1-a_{\sigma_{(r)}}^+\right)^{\omega_r}} \right],$$

$$\left. \frac{\prod_{r=1}^{g}\left(1+(d-1)\breve{\lambda}_{\sigma_{(r)}}\right)^{\omega_r} - \prod_{r=1}^{g}\left(1-\breve{\lambda}_{\sigma_{(r)}}\right)^{\omega_r}}{\prod_{r=1}^{g}\left(1+(d-1)\breve{\lambda}_{\sigma_{(r)}}\right)^{\omega_r} + (d-1)\prod_{r=1}^{g}\left(1-\breve{\lambda}_{\sigma_{(r)}}\right)^{\omega_r}} \right),$$

$$\left(\left[\frac{d\prod_{r=1}^{g}\left(c_{\sigma_{(r)}}^-\right)^{\omega_r}}{\prod_{r=1}^{g}\left(1+(d-1)\left(1-c_{\sigma_{(r)}}^-\right)\right)^{\omega_r} + (d-1)\prod_{r=1}^{g}\left(c_{\sigma_{(r)}}^-\right)^{\omega_r}}, \right. \right.$$

$$\left. \frac{d\prod_{r=1}^{g}\left(c_{\sigma_{(r)}}^+\right)^{\omega_r}}{\prod_{r=1}^{g}\left(1+(d-1)\left(1-c_{\sigma_{(r)}}^+\right)\right)^{\omega_r} + (d-1)\prod_{r=1}^{g}\left(c_{\sigma_{(r)}}^+\right)^{\omega_r}} \right],$$

$$\left. \frac{d\prod_{r=1}^{g}\left(\breve{\psi}_{\sigma_{(r)}}\right)^{\omega_r}}{\prod_{r=1}^{g}\left(1+(d-1)\left(1-\breve{\psi}_{\sigma_{(r)}}\right)\right)^{\omega_r} + (d-1)\prod_{r=1}^{g}\left(\breve{\psi}_{\sigma_{(r)}}\right)^{\omega_r}} \right),$$

$$\left(\left[\frac{d\prod_{r=1}^{g}\left(b_{\sigma_{(r)}}^-\right)^{\omega_r}}{\prod_{r=1}^{g}\left(1+(d-1)\left(1-b_{\sigma_{(r)}}^-\right)\right)^{\omega_r} + (d-1)\prod_{r=1}^{g}\left(b_{\sigma_{(r)}}^-\right)^{\omega_r}}, \right. \right.$$

$$\left. \frac{d\prod_{r=1}^{g}\left(b_{\sigma_{(r)}}^+\right)^{\omega_r}}{\prod_{r=1}^{m}\left(1+(d-1)\left(1-b_{\sigma_{(r)}}^+\right)\right)^{\omega_r} + (d-1)\prod_{r=1}^{g}\left(b_{\sigma_{(r)}}^+\right)^{\omega_r}} \right],$$

$$\left. \left. \frac{d\prod_{r=1}^{g}\left(\breve{\delta}_{\sigma_{(r)}}\right)^{\omega_r}}{\prod_{r=1}^{g}\left(1+(d-1)\left(1-\breve{\delta}_{\sigma_{(r)}}\right)\right)^{\omega_r} + (d-1)\prod_{r=1}^{g}\left(\breve{\delta}_{\sigma_{(r)}}\right)^{\omega_r}} \right) \right\}. \tag{37}$$

The weight vector of P_r $(r = 1, 2, .., g)$ is $\varpi = (\varpi_1, \varpi_2, .., \varpi_g)^T$ with $\sum_{r=1}^{g} \varpi_r = 1$ and $\varpi_r > 0$.

4.4. Parameter d Effect on PCFHOWA Operator.

Subsequently, we suppose that two appropriate cases for the PCFHOWA operator when the parameter $d = 1$ or 2.

Case (i): whenever $d = 1$, at that time, the PCFHOWA operator will reduce to PCFOWA operator:

$$
\text{PCFOWA}_{\varpi}\left(P_1, P_2, \ldots, P_g\right)
$$

$$
= \left\{
\begin{array}{l}
\left(\left(\begin{bmatrix} 1 - \prod_{r=1}^{g}\left(1 - a_{\sigma_{(r)}}^{-}\right)^{\varpi_r}, \\ 1 - \prod_{r=1}^{g}\left(1 - a_{\sigma_{(r)}}^{+}\right)^{\varpi_r} \end{bmatrix} \right), \\ \left(1 - \prod_{r=1}^{g}\left(1 - \breve{\lambda}_{\sigma_{(r)}}\right)^{\varpi_r} \right) \right), \\[20pt]
\left(\begin{bmatrix} \prod_{r=1}^{g}\left(c_{\sigma_{(r)}}^{-}\right)^{\varpi_r}, \\ \prod_{r=1}^{g}\left(c_{\sigma_{(r)}}^{+}\right)^{\varpi_r} \end{bmatrix}, \\ \prod_{r=1}^{g}\left(\breve{\psi}_{\sigma_{(r)}}\right)^{\varpi_r} \right), \\[20pt]
\left(\begin{bmatrix} \prod_{r=1}^{g}\left(b_{\sigma_{(r)}}^{-}\right)^{\varpi_r}, \\ \prod_{r=1}^{g}\left(b_{\sigma_{(r)}}^{+}\right)^{\varpi_r} \end{bmatrix}, \\ \prod_{r=1}^{g}\left(\breve{\delta}_{\sigma_{(r)}}\right)^{\varpi_r} \right)
\end{array}
\right\}. \tag{38}
$$

Case (ii): if $d = 2$, then the PCFHOWA operator will change to PCF Einstein weighted averaging (PCFEWA) operator:

$$\text{PCFEOWA}_{\omega}\left(P_1, P_2, \ldots, P_g\right)$$

$$= \left\{ \left(\left[\frac{\prod_{r=1}^{g}\left(1+a_{\sigma_{(r)}}^{-}\right)^{\omega_r} - \prod_{r=1}^{g}\left(1-a_{\sigma_{(r)}}^{-}\right)^{\omega_r}}{\prod_{r=1}^{g}\left(1+a_{\sigma_{(r)}}^{-}\right)^{\omega_r} + \prod_{r=1}^{g}\left(1-a_{\sigma_{(r)}}^{-}\right)^{\omega_r}}, \right. \right. \right.$$
$$\left. \left. \left. \frac{\prod_{r=1}^{g}\left(1+a_{\sigma_{(r)}}^{+}\right)^{\omega_r} - \prod_{r=1}^{g}\left(1-a_{\sigma_{(r)}}^{+}\right)^{\omega_r}}{\prod_{r=1}^{g}\left(1+a_{\sigma_{(r)}}^{+}\right)^{\omega_r} + \prod_{r=1}^{g}\left(1-a_{\sigma_{(r)}}^{+}\right)^{\omega_r}} \right], \right. \right.$$
$$\left. \left. \frac{\prod_{r=1}^{g}\left(1+\breve{\lambda}_{\sigma_{(r)}}\right)^{\omega_r} - \prod_{r=1}^{g}\left(1-\breve{\lambda}_{\sigma_{(r)}}\right)^{\omega_r}}{\prod_{r=1}^{g}\left(1+\breve{\lambda}_{\sigma_{(r)}}\right)^{\omega_r} + \prod_{r=1}^{g}\left(1-\breve{\lambda}_{\sigma_{(r)}}\right)^{\omega_r}} \right),$$

$$\left(\left[\frac{2\prod_{r=1}^{g}\left(c_{\sigma_{(r)}}^{-}\right)^{\omega_r}}{\prod_{r=1}^{g}\left(2-c_{\sigma_{(r)}}^{-}\right)^{\omega_r} + \prod_{r=1}^{g}\left(c_{\sigma_{(r)}}^{-}\right)^{\omega_r}}, \right. \right.$$
$$\left. \frac{2\prod_{r=1}^{g}\left(c_{\sigma_{(r)}}^{+}\right)^{\omega_r}}{\prod_{r=1}^{g}\left(2-c_{\sigma_{(r)}}^{+}\right)^{\omega_r} + \prod_{r=1}^{g}\left(c_{\sigma_{(r)}}^{+}\right)^{\omega_r}} \right],$$
$$\left. \frac{2\prod_{r=1}^{g}\left(\breve{\psi}_{\sigma_{(r)}}\right)^{\omega_r}}{\prod_{r=1}^{g}\left(2-\breve{\psi}_{\sigma_{(r)}}\right)^{\omega_r} + \prod_{r=1}^{g}\left(\breve{\psi}_{\sigma_{(r)}}\right)^{\omega_r}} \right),$$

$$\left. \left(\left[\frac{2\prod_{r=1}^{g}\left(b_{\sigma_{(r)}}^{-}\right)^{\omega_r}}{\prod_{r=1}^{g}\left(2-b_{\sigma_{(r)}}^{-}\right)^{\omega_r} + \prod_{r=1}^{g}\left(b_{\sigma_{(r)}}^{-}\right)^{\omega_r}}, \right. \right. \right.$$
$$\left. \left. \frac{2\prod_{r=1}^{g}\left(b_{\sigma_{(r)}}^{+}\right)^{\omega_r}}{\prod_{r=1}^{g}\left(2-b_{\sigma_{(r)}}^{+}\right)^{\omega_r} + \prod_{r=1}^{g}\left(b_{\sigma_{(r)}}^{+}\right)^{\omega_r}} \right], \right.$$
$$\left. \left. \frac{2\prod_{r=1}^{g}\left(\breve{\delta}_{\sigma_{(r)}}\right)^{\omega_r}}{\prod_{r=1}^{g}\left(2-\breve{\delta}_{\sigma_{(r)}}\right)^{\omega_r} + \prod_{r=1}^{g}\left(\breve{\delta}_{\sigma_{(r)}}\right)^{\omega_r}} \right) \right\}. \tag{39}$$

Proposition 3. *Suppose that $P_r = \langle a_{P_r}, c_{P_r}, b_{P_r} \rangle$ $(r = 1, 2, 3, \ldots, g)$ be a set of PCFVs in T and $\varpi = (\varpi_1, \varpi_2, \varpi_3, \ldots, \varpi_g)^T$ is the weight vector of P_r with $\sum_{r=1}^{g} \varpi_r = 1$, and ϖ_r is the element of unit closed interval $([0,1])$; then, the coming properties are initiated.*

Idempotency Property. If all $P_r = \langle a_{P_r}, c_{P_r}, b_{P_r} \rangle$ $(r = 1, 2, 3, \ldots, g)$ are equal, that is, $P_r = P$, then

$$\text{PCFHOWA}_\varpi(P_1, P_2, P_3, \ldots, P_g) = P. \tag{40}$$

Boundedness Property. For every ϖ,

$$P^- \leq \text{PCFHOWA}_\varpi(P_1, P_2, P_3, \ldots, P_g) \leq P^+, \tag{41}$$

where

$$P^+ = \left\{ \begin{array}{l} \left(\left[\min a_{\sigma_{(r)}}^-, \max a_{\sigma_{(r)}}^+ \right], \max \breve{\lambda}_{\sigma_{(r)}} \right), \\ \left(\left[\max c_{\sigma_{(r)}}^-, \min c_{\sigma_{(r)}}^+ \right], \min \breve{\psi}_{\sigma_{(r)}} \right), \\ \left(\left[\max b_{\sigma_{(r)}}^-, \min b_{\sigma_{(r)}}^+ \right], \min \breve{\delta}_{\sigma_{(r)}} \right) \end{array} \right\},$$

$$P^- = \left\{ \begin{array}{l} \left(\left[\min a_{\sigma_{(r)}}^-, \max a_{\sigma_{(r)}}^+ \right], \min \breve{\lambda}_{\sigma_{(r)}} \right), \\ \left(\left[\max c_{\sigma_{(r)}}^-, \min c_{\sigma_{(r)}}^+ \right], \max \breve{\psi}_{\sigma_{(r)}} \right), \\ \left(\left[\max b_{\sigma_{(r)}}^-, \min b_{\sigma_{(r)}}^+ \right], \max \breve{\delta}_{\sigma_{(r)}} \right) \end{array} \right\}. \tag{42}$$

Monotonicity Property. Let

$$P_r^* = \left\{ \left(\left\langle \left[a_{\sigma_{(r)}}^{*-}, a_{\sigma_{(r)}}^{*+} \right], \breve{\lambda}_{\sigma_{(r)}}^* \right\rangle, \left\langle \left[c_{\sigma_{(r)}}^{*-}, c_{\sigma_{(r)}}^{*+} \right], \breve{\psi}_{\sigma_{(r)}}^* \right\rangle, \left\langle \left[b_{\sigma_{(r)}}^{*-}, b_{\sigma_{(r)}}^{*+} \right], \breve{\delta}_{\sigma_{(r)}}^* \right\rangle \right) \right\}, \tag{43}$$

where $(r = 1, 2, 3, \ldots, g)$ is a group of PCFNs if

$$\begin{aligned} \left[a_{\sigma_{(r)}}^-, a_{\sigma_{(r)}}^+ \right] &\leq \left[a_{\sigma_{(r)}}^{*-}, a_{\sigma_{(r)}}^{*+} \right], \breve{\lambda}_{\sigma_{(r)}} \leq \breve{\lambda}_{\sigma_{(r)}}^*, \\ \left[c_{\sigma_{(r)}}^{*-}, c_{\sigma_{(r)}}^{*+} \right] &\leq \left[c_{\sigma_{(r)}}^-, c_{\sigma_{(r)}}^+ \right], \breve{\psi}_{\sigma_{(r)}}^* \leq \breve{\psi}_{\sigma_{(r)}}, \\ \left[b_{\sigma_{(r)}}^{*-}, b_{\sigma_{(r)}}^{*+} \right] &\leq \left[b_{\sigma_{(r)}}^-, b_{\sigma_{(r)}}^+ \right], \breve{\delta}_{\sigma_{(r)}}^* \leq \breve{\delta}_{\sigma_{(r)}}. \end{aligned} \tag{44}$$

Then,

$$\begin{aligned} &\text{PCFHOWA}_\varpi(P_1, P_2, P_3, \ldots, P_g) \\ &\leq \text{PCFOHWA}_\varpi(P_1^*, P_2^*, P_3^* \ldots, P_g^*). \end{aligned} \tag{45}$$

4.5. PCFHHA Operator

Definition 15. Let $P_r = \langle a_{P_r}, c_{P_r}, b_{P_r} \rangle$ $(r = 1, 2, 3, \ldots, g)$ be a set of PCFVs in T, and suppose PCFHHA operator of g dimension is a function of PCFHHA: $\Omega^g \longrightarrow \Omega$, having $\varpi = (\varpi_1, \varpi_2, \varpi_3, \ldots, \varpi_g)^T$ which are the weight vector of P_r $(r = 1, 2, \ldots, g)$ with $\sum_{r=1}^g \varpi_r = 1$ and ϖ_r is the element of unit closed interval $([0,1])$ and $\varpi_r > 0$ such that

$$\text{PCFHHA}_{w,\varpi}(P_1, P_2, \ldots, P_g) = \oplus_{r=1}^g \varpi_r \widetilde{P}_{\sigma_{(r)}}, \tag{46}$$

which is the weight of P_r $w = (w_1, w_2, \ldots, w_g)^T$, with $\sum_{r=1}^m w_r = 1$, and w_r is the element of unit closed interval $([0,1])$. Here, $\widetilde{P}_{\sigma_{(r)}}$ is the gth greatest of the weighted PCFNs $\widetilde{P}_r$ and $\widetilde{P}_{\sigma_{(r)}} = g w_r P_{\sigma_{(r)}} = (\langle [\widetilde{a}_{\sigma_{(r)}}^-, \widetilde{a}_{\sigma_{(r)}}^+], \breve{\lambda}_{\sigma_{(r)}} \rangle, \langle [\widetilde{c}_{\sigma_{(r)}}^-, \widetilde{c}_{\sigma_{(r)}}^+], \breve{\psi}_{\sigma_{(r)}} \rangle, \langle [\widetilde{b}_{\sigma_{(r)}}^-, \widetilde{b}_{\sigma_{(r)}}^+], \breve{\delta}_{\sigma_{(r)}} \rangle)$ $(r = 1, 2, \ldots, g)$, where

$$\widetilde{a}_{\sigma_{(r)}}^- = \frac{\left(1 + (d-1)a_{\sigma_{(r)}}^-\right)^{g w_r} - \left(1 - a_{\sigma_{(r)}}^-\right)^{g w_r}}{\left(1 + (d-1)a_{\sigma_{(r)}}^-\right)^{g w_r} + (d-1)\left(1 - a_{\sigma_{(r)}}^-\right)^{g w_r}},$$

$$\widetilde{a}_{\sigma_{(r)}}^+ = \frac{\left(1 + (d-1)a_{\sigma_{(r)}}^+\right)^{g w_r} - \left(1 - a_{\sigma_{(r)}}^+\right)^{g w_r}}{\left(1 + (d-1)a_{\sigma_{(r)}}^+\right)^{g w_r} + (g-1)\left(1 - a_{\sigma_{(r)}}^+\right)^{g w_r}},$$

$$\breve{\widetilde{\lambda}}_{\sigma_{(r)}} = \frac{\left(1 + (d-1)\breve{\lambda}_{\sigma_{(r)}}\right)^{g w_r} - \left(1 - \breve{\lambda}_{\sigma_{(r)}}\right)^{g w_r}}{\left(1 + (d-1)\breve{\lambda}_{\sigma_{(r)}}\right)^{g w_r} + (d-1)\left(1 - \breve{\lambda}_{\sigma_{(r)}}\right)^{g w_r}},$$

$$\widetilde{c}_{\sigma_{(r)}}^- = \frac{d\left(c_{\sigma_{(r)}}^-\right)^{g w_r}}{1 + (d-1)\left(1 - c_{\sigma_{(r)}}^-\right)^{g w_r} + (d-1)\left(c_{\sigma_{(r)}}^-\right)^{g w_r}},$$

$$\widetilde{c}^{+}_{\sigma_{(r)}} = \frac{d\left(c^{+}_{\sigma_{(r)}}\right)^{gw_r}}{1 + (d-1)\left(1 - c^{+}_{\sigma_{(r)}}\right)^{gw_r} + (d-1)\left(c^{+}_{\sigma_{(r)}}\right)^{gw_r}},$$

$$\widetilde{\widetilde{\breve{\psi}}}_{\sigma_{(r)}} = \frac{g\left(\breve{\psi}_{\sigma_{(r)}}\right)^{gw_r}}{1 + (d-1)\left(1 - \breve{\psi}_{\sigma_{(r)}}\right)^{gw_r} + (d-1)\left(\breve{\psi}_{\sigma_{(r)}}\right)^{gw_r}},$$

$$\widetilde{b}^{-}_{\sigma_{(r)}} = \frac{d\left(b^{-}_{\sigma_{(r)}}\right)^{gw_r}}{1 + (d-1)\left(1 - b^{-}_{\sigma_{(r)}}\right)^{gw_r} + (d-1)\left(b^{-}_{\sigma_{(r)}}\right)^{gw_r}}, \tag{47}$$

$$\widetilde{b}^{+}_{\sigma_{(r)}} = \frac{d\left(b^{+}_{\sigma_{(r)}}\right)^{gw_r}}{1 + (d-1)\left(1 - b^{+}_{\sigma_{(r)}}\right)^{gw_r} + (d-1)\left(b^{+}_{\sigma_{(r)}}\right)^{gw_r}},$$

$$\widetilde{\widetilde{\breve{\psi}}}_{\sigma_{(r)}} = \frac{d\left(\breve{\delta}_{\sigma_{(r)}}\right)^{gw_r}}{1 + (d-1)\left(1 - \breve{\delta}_{\sigma_{(r)}}\right)^{gw_r} + (d-1)\left(\breve{\delta}_{\sigma_{(r)}}\right)^{gw_r}}.$$

Here, the coefficient of balancing is m, which maintains the appropriate balance; particularly, whenever $\omega = (1/g, 1/g, 1/g, \ldots, 1/g)^T$, then the PCFHWA and PCFHOWA operators are considered as an important case of PCFHHA operator.

Hence, under Hamacher operational rules of PCFNs, we get the theorem as given below.

Theorem 3. *Suppose that $P_r = \langle a_{P_r}, c_{P_r}, b_{P_r} \rangle$ ($r = 1, 2, \ldots, g$) is the set of PCFVs in $\breve{T}$; then, the aggregated value of them utilizing PCFHHA operator is also a PCFV and is given below:*

$$PCFHHA_{\omega}\left(P_1, P_2, .., P_g\right)$$

$$= \left\{ \begin{array}{l} \left(\left[\dfrac{\prod_{r=1}^{g}\left(1+(d-1)\widetilde{a}_{\sigma_{(r)}}^{-}\right)^{\omega_r} - \prod_{r=1}^{g}\left(1-\widetilde{a}_{\sigma_{(r)}}^{-}\right)^{\omega_r}}{\prod_{r=1}^{g}\left(1+(d-1)\widetilde{a}_{\sigma_{(r)}}^{-}\right)^{\omega_r} + (d-1)\prod_{r=1}^{g}\left(1-\widetilde{a}_{\sigma_{(r)}}^{-}\right)^{\omega_r}}, \right. \right. \\[4em] \left. \left. \dfrac{\prod_{r=1}^{g}\left(1+(d-1)\widetilde{a}_{\sigma_{(r)}}^{+}\right)^{\omega_r} - \prod_{r=1}^{g}\left(1-\widetilde{a}_{\sigma_{(r)}}^{+}\right)^{\omega_r}}{\prod_{r=1}^{g}\left(1+(d-1)\widetilde{a}_{\sigma_{(r)}}^{+}\right)^{\omega_r} + (d-1)\prod_{r=1}^{g}\left(1-\widetilde{a}_{\sigma_{(r)}}^{+}\right)^{\omega_r}} \right], \right. \\[4em] \left. \dfrac{\prod_{r=1}^{g}\left(1+(d-1)\widetilde{\widetilde{\lambda}}_{\sigma_{(r)}}\right)^{\omega_r} - \prod_{r=1}^{g}\left(1-\widetilde{\widetilde{\lambda}}_{\sigma_{(r)}}\right)^{\omega_r}}{\prod_{r=1}^{g}\left(1+(d-1)\widetilde{\widetilde{\lambda}}_{\sigma_{(r)}}\right)^{\omega_r} + (d-1)\prod_{r=1}^{g}\left(1-\widetilde{\widetilde{\lambda}}_{\sigma_{(r)}}\right)^{\omega_r}} \right), \\[5em] \left(\left[\dfrac{d\prod_{r=1}^{g}\left(\widetilde{c}_{\sigma_{(r)}}^{-}\right)^{\omega_r}}{\prod_{r=1}^{g}\left(1+(d-1)\left(1-\widetilde{c}_{\sigma_{(r)}}^{-}\right)\right)^{\omega_r} + \prod_{r=1}^{g}\left(\widetilde{c}_{\sigma_{(r)}}^{-}\right)^{\omega_r}(d-1)}, \right. \right. \\[4em] \left. \left. \dfrac{k\prod_{r=1}^{g}\left(\widetilde{c}_{\sigma_{(r)}}^{+}\right)^{\omega_r}}{\prod_{r=1}^{g}\left(1+(d-1)\left(1-\widetilde{c}_{\sigma_{(r)}}^{+}\right)\right)^{\omega_r} + (d-1)\prod_{r=1}^{g}\left(\widetilde{c}_{\sigma_{(r)}}^{+}\right)^{\omega_r}} \right], \right. \\[4em] \left. \dfrac{d\prod_{r=1}^{g}\left(\widetilde{\widetilde{\psi}}_{\sigma_{(r)}}\right)^{\omega_r}}{\prod_{r=1}^{g}\left(1+(d-1)\left(1-\widetilde{\widetilde{\psi}}_{\sigma_{(r)}}\right)\right)^{\omega_r} + (d-1)\prod_{r=1}^{g}\left(\widetilde{\widetilde{\psi}}_{\sigma_{(r)}}\right)^{\omega_r}} \right), \\[5em] \left(\left[\dfrac{d\prod_{r=1}^{g}\left(\widetilde{b}_{\sigma_{(r)}}^{-}\right)^{\omega_r}}{\prod_{r=1}^{g}\left(1+(d-1)\left(1-\widetilde{b}_{\sigma_{(r)}}^{-}\right)\right)^{\omega_r} + (d-1)\prod_{r=1}^{g}\left(\widetilde{b}_{\sigma_{(r)}}^{-}\right)^{\omega_r}}, \right. \right. \\[4em] \left. \left. \dfrac{d\prod_{r=1}^{g}\left(\widetilde{b}_{\sigma_{(r)}}^{+}\right)^{\omega_r}}{\prod_{r=1}^{g}\left(1+(d-1)\left(1-\widetilde{b}_{\sigma_{(r)}}^{+}\right)\right)^{\omega_r} + (d-1)\prod_{r=1}^{m}\left(\widetilde{b}_{\sigma_{(r)}}^{+}\right)^{\omega_r}} \right], \right. \\[4em] \left. \dfrac{d\prod_{r=1}^{g}\left(\widetilde{\widetilde{\delta}}_{\sigma_{(r)}}\right)^{\omega_r}}{\prod_{r=1}^{g}\left(1+(d-1)\left(1-\widetilde{\widetilde{\delta}}_{\sigma_{(r)}}\right)\right)^{\omega_r} + (d-1)\prod_{r=1}^{g}\left(\widetilde{\widetilde{\delta}}_{\sigma_{(r)}}\right)^{\omega_r}} \right) \end{array} \right\}. \tag{48}$$

The weight vector of P_r $(r = 1, 2, \ldots, g)$ *are* $\omega = (\omega_1, \omega_2, .., \omega_g)^T$, *with* $\sum_{r=1}^{g} \omega_r = 1$ *and* $\omega_r > 0$.

4.6. Parameter d Effect on PCFHHA Operator.

Subsequently, we suppose that two appropriate cases for the PCFHHA operator when $d = 1$ or 2.

Case (i): whenever $d = 1$, at that time, the PCFHHA operator will change to picture cubic fuzzy hybrid averaging (PCFHA) operator:

$$
\mathrm{PCFHA}_{\omega}\left(P_1, P_2, P_3, \ldots, P_g\right)
$$

$$
= \left\{ \begin{pmatrix} \begin{bmatrix} 1 - \prod_{r=1}^{g}\left(1 - \widetilde{a}_{\sigma_{(r)}}^{-}\right)^{\omega_r}, \\ 1 - \prod_{r=1}^{g}\left(1 - \widetilde{a}_{\sigma_{(r)}}^{+}\right)^{\omega_r} \end{bmatrix}, \\ 1 - \prod_{r=1}^{g}\left(1 - \widetilde{\lambda}_{\sigma_{(r)}}\right)^{\omega_r} \end{pmatrix}, \begin{pmatrix} \begin{bmatrix} \prod_{r=1}^{g}\left(\widetilde{c}_{\sigma_{(r)}}^{-}\right)^{\omega_r}, \\ \prod_{r=1}^{g}\left(\widetilde{c}_{\sigma_{(r)}}^{+}\right)^{\omega_r} \end{bmatrix}, \\ \prod_{r=1}^{g}\left(\widetilde{\widetilde{\psi}}_{\sigma_{(r)}}\right)^{\omega_r} \end{pmatrix}, \begin{pmatrix} \begin{bmatrix} \prod_{r=1}^{g}\left(\widetilde{b}_{\sigma_{(r)}}^{-}\right)^{\omega_r}, \\ \prod_{r=1}^{g}\left(\widetilde{b}_{\sigma_{(r)}}^{+}\right)^{\omega_r} \end{bmatrix}, \\ \prod_{r=1}^{g}\left(\widetilde{\widetilde{\delta}}_{\sigma_{(r)}}\right)^{\omega_r} \end{pmatrix} \end{matrix} \right\}. \tag{49}
$$

Case (ii): whenever $d = 2$, at that time, the PCFHHA operator will change to PCF Einstein hybrid averaging (PCFEHA) operator:

$$
\mathrm{PCFEHA}_{\omega}\left(P_1, P_2, P_3, \ldots, P_g\right)
$$

$$
= \left\{ \begin{pmatrix} \begin{bmatrix} \dfrac{\prod_{r=1}^{g}\left(1 + \widetilde{a}_{\sigma_{(r)}}^{-}\right)^{\omega_r} - \prod_{r=1}^{g}\left(1 + \widetilde{a}_{\sigma_{(r)}}^{-}\right)^{\omega_r}}{\prod_{r=1}^{g}\left(1 + \widetilde{a}_{\sigma_{(r)}}^{-}\right)^{\omega_r} + \prod_{r=1}^{g}\left(1 + \widetilde{a}_{\sigma_{(r)}}^{-}\right)^{\omega_r}}, \\[4mm] \dfrac{\prod_{r=1}^{g}\left(1 + \widetilde{a}_{\sigma_{(r)}}^{+}\right)^{\omega_r} - \prod_{r=1}^{g}\left(1 + \widetilde{a}_{\sigma_{(r)}}^{+}\right)^{\omega_r}}{\prod_{r=1}^{g}\left(1 + \widetilde{a}_{\sigma_{(r)}}^{+}\right)^{\omega_r} + \prod_{r=1}^{g}\left(1 + \widetilde{a}_{\sigma_{(r)}}^{+}\right)^{\omega_r}} \end{bmatrix}, \\[4mm] \dfrac{\prod_{r=1}^{g}\left(1 + \widetilde{\lambda}_{\sigma_{(r)}}\right) - \prod_{r=1}^{g}\left(1 + \widetilde{\lambda}_{\sigma_{(r)}}\right)^{\omega_r}}{\prod_{r=1}^{g}\left(1 + \widetilde{\lambda}_{\sigma_{(r)}}\right) + \prod_{r=1}^{g}\left(1 + \widetilde{\lambda}_{\sigma_{(r)}}\right)} \end{pmatrix}, \\[6mm] \begin{pmatrix} \begin{bmatrix} \dfrac{2\prod_{r=1}^{g}\left(\widetilde{c}_{\sigma_{(r)}}^{-}\right)^{\omega_r}}{\prod_{r=1}^{g}\left(2 - \widetilde{c}_{\sigma_{(r)}}^{-}\right)^{\omega_r} + \prod_{r=1}^{g}\left(\widetilde{c}_{\sigma_{(r)}}^{-}\right)^{\omega_r}}, \\[4mm] \dfrac{2\prod_{r=1}^{g}\left(\widetilde{c}_{\sigma_{(r)}}^{+}\right)^{\omega_r}}{\prod_{r=1}^{g}\left(2 - \widetilde{c}_{\sigma_{(r)}}^{+}\right)^{\omega_r} + \prod_{r=1}^{g}\left(\widetilde{c}_{\sigma_{(r)}}^{+}\right)^{\omega_r}} \end{bmatrix}, \\[4mm] \dfrac{2\prod_{r=1}^{g}\left(\widetilde{\widetilde{\psi}}_{\sigma_{(r)}}^{+}\right)^{\omega_r}}{\prod_{r=1}^{g}\left(2 - \widetilde{\widetilde{\psi}}_{\sigma_{(r)}}^{+}\right)^{\omega_r} + \prod_{r=1}^{g}\left(2 - \widetilde{\widetilde{\psi}}_{\sigma_{(r)}}^{+}\right)^{\omega_r}} \end{pmatrix}, \\[6mm] \begin{pmatrix} \begin{bmatrix} \dfrac{2\prod_{r=1}^{g}\left(\widetilde{b}_{\sigma_{(r)}}^{-}\right)^{\omega_r}}{\prod_{r=1}^{g}\left(2 - \widetilde{b}_{\sigma_{(r)}}^{-}\right)^{\omega_r} + \prod_{r=1}^{g}\left(\widetilde{b}_{\sigma_{(r)}}^{-}\right)^{\omega_r}}, \\[4mm] \dfrac{2\prod_{r=1}^{g}\left(\widetilde{b}_{\sigma_{(r)}}^{+}\right)^{\omega_r}}{\prod_{r=1}^{g}\left(2 - \widetilde{b}_{\sigma_{(r)}}^{+}\right)^{\omega_r} + \prod_{r=1}^{g}\left(\widetilde{b}_{\sigma_{(r)}}^{+}\right)^{\omega_r}} \end{bmatrix}, \\[4mm] \dfrac{2\prod_{r=1}^{g}\left(\widetilde{\widetilde{\delta}}_{\sigma_{(r)}}^{+}\right)^{\omega_r}}{\prod_{r=1}^{g} 2 - \left(\widetilde{\widetilde{\delta}}_{\sigma_{(r)}}^{+}\right)^{\omega_r} + \prod_{r=1}^{g}\left(\widetilde{\widetilde{\delta}}_{\sigma_{(r)}}^{+}\right)^{\omega_r}} \end{pmatrix} \end{matrix} \right\}. \tag{50}
$$

Proposition 4. *Suppose that* $P_r = \langle a_{P_r}, c_{P_r}, b_{P_r} \rangle$ *($r = 1, 2, 3, \ldots, g$) is the set of PCFVs in $\breve{T}$ and $\omega = (\omega_1, \omega_2, \omega_3, \ldots, \omega_g)^T$ are the weight vector of P_r with $\sum_{r=1}^{g} \omega_r = 1$ and $\omega_r \in [0, 1]$; then, the coming properties are initiated.*

Idempotency Property. If all $P_r = \langle a_{P_r}, c_{P_r}, b_{P_r} \rangle$ *($r = 1, 2, 3, \ldots, g$) are equal, that is, $P_r = P$, then*

$$\text{PCFHHA}_\omega(P_1, P_2, P_3, \ldots, P_g) = P. \tag{51}$$

Boundedness Property. For every ω,

$$P^- \leq \text{PCFHHA}_\omega(P_1, P_2, P_3, \ldots, P_g) \leq P^+, \tag{52}$$

where

$$P^+ = \left\{ \begin{array}{l} \left(\left[\min a^-_{\sigma_{(r)}}, \max a^+_{\sigma_{(r)}} \right], \max \breve{\lambda}_{\sigma_{(r)}} \right), \\ \left(\left[\max c^-_{\sigma_{(r)}}, \min c^+_{\sigma_{(r)}} \right], \min \breve{\psi}_{\sigma_{(r)}} \right), \\ \left(\left[\max b^-_{\sigma_{(r)}}, \min b^+_{\sigma_{(r)}} \right], \min \breve{\delta}_{\sigma_{(r)}} \right) \end{array} \right\},$$

$$P^- = \left\{ \begin{array}{l} \left(\left[\min a^-_{\sigma_{(r)}}, \max a^+_{\sigma_{(r)}} \right], \min \breve{\lambda}_{\sigma_{(r)}} \right), \\ \left(\left[\max c^-_{\sigma_{(r)}}, \min c^+_{\sigma_{(r)}} \right], \max \breve{\psi}_{\sigma_{(r)}} \right), \\ \left(\left[\max b^-_{\sigma_{(r)}}, \min b^+_{\sigma_{(r)}} \right], \max \breve{\delta}_{\sigma_{(r)}} \right) \end{array} \right\}. \tag{53}$$

Monotonicity Property. Let

$$P_r^* = \left\{ \left(\langle \left[\tilde{a}^{*-}_{\sigma_{(r)}}, \tilde{a}^{*+}_{\sigma_{(r)}} \right], \tilde{\breve{\lambda}}^*_{\sigma_{(r)}} \rangle, \langle \left[\tilde{c}^{*-}_{\sigma_{(r)}}, \tilde{c}^{*+}_{\sigma_{(r)}} \right], \tilde{\breve{\psi}}^*_{\sigma_{(r)}} \rangle, \langle \left[\tilde{b}^{*-}_{\sigma_{(r)}}, \tilde{b}^{*+}_{\sigma_{(r)}} \right], \tilde{\breve{\delta}}^*_{\sigma_{(r)}} \rangle \right) \right\}, \tag{54}$$

where ($r = 1, 2, 3, \ldots, g$) is a group of PCFNs if

$$\begin{aligned} \left[\tilde{a}^-_{\sigma_{(r)}}, \tilde{a}^+_{\sigma_{(r)}} \right] &\leq \left[\tilde{a}^{*-}_{\sigma_{(r)}}, \tilde{a}^{*+}_{\sigma_{(r)}} \right], \tilde{\breve{\lambda}}_{\sigma_{(r)}} \leq \tilde{\breve{\lambda}}^*_{\sigma_{(r)}}, \\ \left[\tilde{c}^{*-}_{\sigma_{(r)}}, \tilde{c}^{*+}_{\sigma_{(r)}} \right] &\leq \left[\tilde{c}^-_{\sigma_{(r)}}, \tilde{c}^+_{\sigma_{(r)}} \right], \tilde{\breve{\psi}}^*_{\sigma_{(r)}} \leq \tilde{\breve{\psi}}_{\sigma_{(r)}}, \\ \left[\tilde{b}^{*-}_{\sigma_{(r)}}, \tilde{b}^{*+}_{\sigma_{(r)}} \right] &\leq \left[\tilde{b}^-_{\sigma_{(r)}}, \tilde{b}^+_{\sigma_{(r)}} \right], \tilde{\breve{\delta}}^*_{\sigma_{(r)}} \leq \tilde{\breve{\delta}}_{\sigma_{(r)}}. \end{aligned} \tag{55}$$

Then,

$$\text{PCFHHA}_{w,\omega}(P_1, P_2, P_3, \ldots, P_g) \leq \text{PCFHHA}_{w,\omega}(P_1^*, P_2^*, P_3^*, \ldots, P_g^*). \tag{56}$$

Theorem 4. *The PCFHWA operator is a special case of the PCFHHA operator.*

Proof. Suppose $\omega = (1/g, 1/g, 1/g, \ldots, 1/g)^T$; then,

$$\begin{aligned} \text{PCFHHA}_{w,\omega}(P_1, P_2, P_3, \ldots, P_g) &= \omega_1 \tilde{P}_{\sigma_{(1)}} \oplus \omega_2 \tilde{P}_{\sigma_{(2)}} \oplus, \ldots, \oplus \omega_g \tilde{P}_{\sigma_{(g)}}, \\ &= \frac{1}{g} \left(\tilde{P}_{\sigma_{(1)}} \oplus \tilde{P}_{\sigma_{(2)}} \oplus, \ldots, \tilde{P}_{\sigma_{(g)}} \right) \\ &= \omega_1 P_\sigma \oplus \omega_2 P_\sigma \oplus, \ldots, \omega_g P_{\sigma_{(g)}} \\ &= \text{PCFHWA}_\omega(P_1, P_2, P_3, \ldots, P_g). \end{aligned} \tag{57}$$

Hence, it is proved.   □

Theorem 5. *The PCFHOWA operator is a special case of the PCFHHA operator.*

Proof. Suppose $\omega = (1/g, 1/g, 1/g, \ldots, 1/g)^T$, so $\tilde{P}_{\sigma_{(r)}} = P_{\sigma_{(r)}}$ ($r = 1, 2, 3, \ldots, g$); thus,

$$\mathrm{PCFHHA}_{w,\omega}\left(P_1, P_2, P_3, \ldots, P_g\right) = \omega_1 \widetilde{P}_{\sigma_{(1)}} \oplus \omega_2 \widetilde{P}_{\sigma_{(2)}} \oplus, \ldots, \oplus \omega_g \widetilde{P}_{\sigma_{(g)}}$$

$$= \omega_1 P_{\sigma_{(1)}} \oplus \omega_2 P_{\sigma_{(2)}} \oplus, \ldots, \omega_g P_{\sigma_{(g)}} \tag{58}$$

$$= \mathrm{PCFHOWA}_{\omega}\left(P_1, P_2, P_3, \ldots, P_g\right).$$

Hence, the result is proved.   □

5. MAGDM Methods on the Basis of Planned Operators

In this section, picture cubic fuzzy Hamacher weighted aggregation (PCFHWA) operators are utilized to MAGDM algorithm. Consider there are **u** alternatives $\widetilde{\varrho} = \{\widetilde{\varrho}_1, \widetilde{\varrho}_2, \ldots, \widetilde{\varrho}_u\}$ and **v** attributes $\widetilde{\Gamma} = \{\widetilde{\Gamma}_1, \widetilde{\Gamma}_2, \ldots, \widetilde{\Gamma}_v\}$ with weight vector $\omega = \{\omega_1, \omega_2, \ldots, \omega_v\}$ such that $\sum_{h=1}^{v} \omega_h = 1$ and $\omega_h \in [0, 1]$. To evaluate the accomplishment of the alternatives $\widetilde{\varrho}_x$ $(x = 1, 2, \ldots, u)$ based on attributes $\widetilde{\Gamma}_h$, the experts have to give only the statistics about the alternative $\widetilde{\varrho}_x$, fulfilling the attributes but also about the alternative $\widetilde{\varrho}_x$ and not fulfilling the attributes $\widetilde{\Gamma}_h$ $(h = 1, 2, \ldots, v)$. Suppose that the rating of the alternatives $\widetilde{\varrho}_x$ based on the criteria $\widetilde{\Gamma}_h$ provided by the experts in the form of PCFNs in $\check{T}$: $P_{xh} = \langle a_{xh}, b_{xh}, c_{xh} \rangle$ $(x = 1, 2, \ldots, u; h = 1, 2, \ldots, v)$. Suppose a_{xh} represent the degree of alternatives $\widetilde{\varrho}_x$ that satisfying the criteria $\widetilde{\Gamma}_h$, c_{xh} represents the degree of alternatives $\widetilde{\varrho}_x$ that are neutral, and b_{xh} represent the degree of alternatives $\widetilde{\varrho}_x$ that not satisfying the criteria $\widetilde{\Gamma}_h$, such that $a_{xh} = \langle [a_{xh}^-, a_{xh}^+], \breve{\lambda}_{xh} \rangle 1/2$, $c_{xh} = \langle [c_{xh}^-, c_{xh}^+], \breve{\psi}_{xh} \rangle$, and $b_{xh} = \langle [b_{xh}^-, b_{xh}^+], \delta_{xh} \rangle$, under the condition $[a_{xh}^-, a_{xh}^+], [c_{xh}^-, c_{xh}^+], [b_{xh}^-, b_{xh}^+] \subset [0, 1]$ and $\lambda_{xh} : \check{T} \longrightarrow [0, 1]$, $\psi_{xh} : \check{T} \longrightarrow [0, 1]$, and $\delta_{xh} : \check{T} \longrightarrow [0, 1]$, subject to $0 \le \sup[a_{xh}^-, a_{xh}^+] + \sup[c_{xh}^-, c_{xh}^+] + \sup[b_{xh}^-, b_{xh}^+] \le 1$ and $0 \le \lambda_{xh} + \psi_{xh} + \delta_{xh} \le 1$ $(x = 1, 2, \ldots, u; h = 1, 2, \ldots, v)$. Consequently, a MAGDM problem can be shortly given in a PCF decision matrix $M = (P_{xh})_{u \times v} = (\langle a_{xh}, c_{xh}, b_{xh} \rangle)_{u \times v}(x = 1, 2, \ldots, u; h = 1, 2, \ldots, v)$. Further steps which are involved in the MAGDM method are given below.

5.1. Main Algorithm
Start.

Step 1: construct PCF decision matrix $M = (P_{xh})_{u \times v} = (\langle a_{xh}, c_{xh}, b_{xh} \rangle)_{u \times v}(x = 1, 2, \ldots, u; h = 1, 2, \ldots, v)$. The attribute is usually classified as benefit and cost attributes. Of course, it is unnecessary of normalizing the rating values if all attributes be the identical types. The values of the cost attributes can be transformed into the values of benefit attributes by the following formula, when M contains the two cost and benefits attributes:

$$s_{xh} = \langle a_{xh}, b_{xh}, c_{xh} \rangle = \begin{cases} q_{xh} \text{ for benefit criteria,} \\ q_{xh}^c \text{ for cost criteria,} \end{cases} \tag{59}$$

where the complement of q_{xh} is q_{xh}^c. Consequently, we obtained a normalized PCF decision matrix denoted by M^u and is assigned as

$$M^u = s_{xh} = \left(\langle a_{xh}, b_{ij}, c_{xh} \rangle\right)_{u \times v} \tag{60}$$

$$(x = 1, 2, \ldots, u; h = 1, 2, \ldots, v).$$

Next, we will apply the PCFHWA, PCFHOWA, and PCFHHA operators to MCGDM, moreover consist of the coming steps.

Step 2: utilize planned operators to calculate PCFNs Px $(x = 1, 2, \ldots, u)$ for the alternatives $\widetilde{\varrho}_x$. This is the established operators to maintain the overall collective choice values Px $(x = 1, 2, \ldots, u)$ for the alternatives $\widetilde{\varrho}_x$, where $\omega = \{\omega_1, \omega_2, \ldots, \omega_v\}$ is the weight vector of the attributes.

Step 3: utilizing the score function formula of PCFNs, we calculate the score functions $S(P_x)$ $(x = 1, 2, \ldots, u)$ of P_x to rank the alternatives $\widetilde{\varrho}_x$. When the two score functions $S(P_s)$ and $S(P_e)$ are equal, we need their accuracy function $A(P_s)$ and $S(P_e)$; then, we rank the alternative based on accuracy degree.

Step 4: rank the alternatives $\widetilde{\varrho}_x$ $(x = 1, 2, \ldots, u)$ for choosing a suitable one.

End.

6. Application

Suppose that $\{\widetilde{\varrho}_1, \widetilde{\varrho}_2, \widetilde{\varrho}_3\}$ are three SHPPs from power plant category. The generation capacity of these three SHPPs is 25 MW, to be located at different geographical sites in Pakistan. Three decision makers have been appointed to select the most suitable plant for beginning the construction activity (adopted from [48]), on the basis of four criteria such that

$$\begin{aligned} &\widetilde{\Gamma}_1 : \text{approachability,} \\ &\widetilde{\Gamma}_2 : \text{socioeconomic climate,} \\ &\widetilde{\Gamma}_3 : \text{constructability,} \\ &\widetilde{\Gamma}_4 : \text{technical feasilibility.} \end{aligned} \tag{61}$$

Utilizing attributes' weighting vector $(0.35, 0.3, 0.21, 0.14)^T$ and the decision makers' weighting $(0.4, 0.35, 0.25)^T$, three experts present the information in the form of evaluation matrices, as shown in Table 1–3.

6.1. By PCFHWA Operator

Step 5: the experts' decision is given in Tables 1–3. On this spot, it is unnecessary of normalization because all the attributes are given as beneficial attributes.

Suppose $k = 2$ and $\omega = (0.4, 0.35, 0.25)^T$ as a weight vector of experts; using PCFHWA operator, we have collected the information stated by the three experts in Tables 1
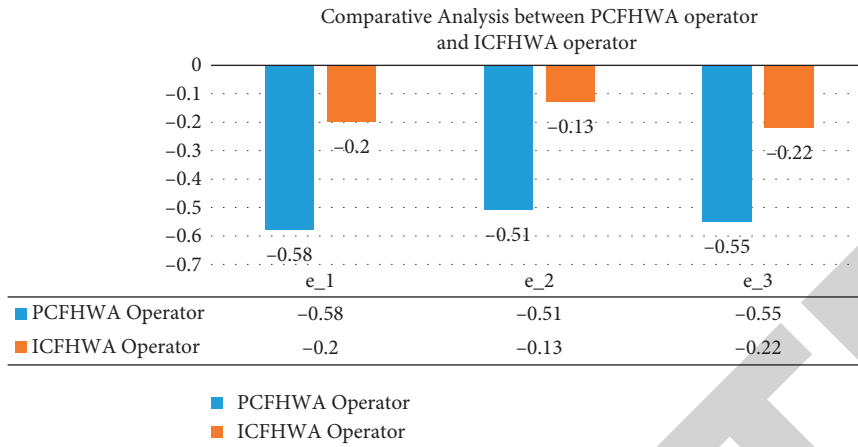
Figure 1: Comparative study between PCFHWA operator and ICFHWA operator and ranking of the alternatives.
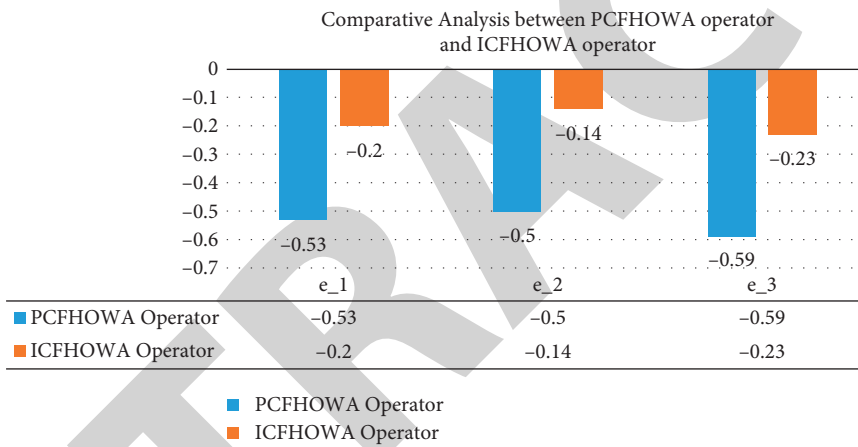
Figure 2: Comparative study between PCFHOWA operator and ICFHOWA operator and ranking of the alternatives.
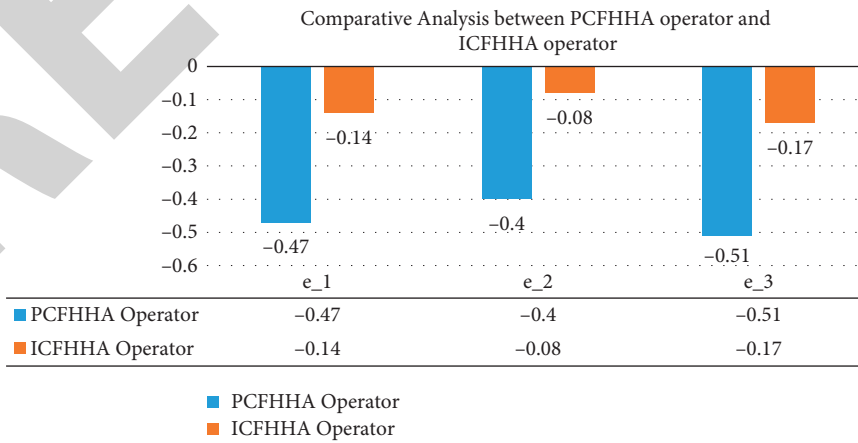
Figure 3: Comparative study between PCFHHA operator and ICFHHA operator and ranking of the alternatives.

TABLE 1: First experts' information.

Supp.	$\widetilde{\Gamma}_1$	$\widetilde{\Gamma}_2$	$\widetilde{\Gamma}_3$	$\widetilde{\Gamma}_4$
$\widetilde{\varrho}_1$	$\begin{pmatrix} ([0.1,0.12],0.12), \\ ([0.1,0.2],0.5), \\ ([0.2,0.3],0.2) \end{pmatrix}$	$\begin{pmatrix} \begin{pmatrix} ([0.3,0.31],0.1), \\ ([0.1,0.3],0.3), \\ ([0.1,0.3],0.1) \end{pmatrix} \end{pmatrix}$	$\begin{pmatrix} ([0.2,0.21],0.21), \\ ([0.1,0.4],0.2), \\ ([0.1,0.2],0.2) \end{pmatrix}$	$\begin{pmatrix} ([0.1,0.14],0.14), \\ ([0.1,0.3],0.3), \\ ([0.1,0.2],0.4) \end{pmatrix}$
$\widetilde{\varrho}_2$	$\begin{pmatrix} ([0.2,0.22],0.21), \\ ([0.2,0.21],0.25), \\ ([0.1,0.2],0.15) \end{pmatrix}$	$\begin{pmatrix} ([0.3,0.31],0.31), \\ ([0.2,0.3],0.3), \\ ([0.1,0.16],0.2) \end{pmatrix}$	$\begin{pmatrix} ([0.2,0.201],0.21), \\ ([0.3,0.4],0.31), \\ ([0.1,0.2],0.22) \end{pmatrix}$	$\begin{pmatrix} ([0.1,0.201],0.22), \\ ([0.1,0.24],0.3), \\ ([0.1,0.12],0.13) \end{pmatrix}$
$\widetilde{\varrho}_3$	$\begin{pmatrix} ([0.1,0.104],0.14), \\ ([0.1,0.4],0.2), \\ ([0.1,0.2],0.2) \end{pmatrix}$	$\begin{pmatrix} ([0.2,0.22],0.21), \\ ([0.2,0.3],0.22), \\ ([0.2,0.3],0.31) \end{pmatrix}$	$\begin{pmatrix} ([0.1,0.102],0.12), \\ ([0.1,0.3],0.1), \\ ([0.1,0.2],0.31) \end{pmatrix}$	$\begin{pmatrix} ([0.2,0.201],0.21), \\ ([0.2,0.3],0.4), \\ ([0.1,0.2],0.4) \end{pmatrix}$

TABLE 2: Second experts' information.

Supp.	$\widetilde{\Gamma}_1$	$\widetilde{\Gamma}_2$	$\widetilde{\Gamma}_3$	$\widetilde{\Gamma}_4$
$\widetilde{\varrho}_1$	$\begin{pmatrix} ([0.1,0.13]0.13), \\ ([0.1,0.2],0.3), \\ ([0.1,0.2],0.1) \end{pmatrix}$	$\begin{pmatrix} ([0.1,0.11],0.11), \\ ([0.2,0.3],0.4), \\ ([0.2,0.3],0.2) \end{pmatrix}$	$\begin{pmatrix} ([0.1,0.11],0.11), \\ ([0.1,0.2],0.4), \\ ([0.2,0.3],0.4) \end{pmatrix}$	$\begin{pmatrix} ([0.1,0.12],0.12), \\ ([0.1,0.21],0.2), \\ ([0.2,0.4],0.21) \end{pmatrix}$
$\widetilde{\varrho}_2$	$\begin{pmatrix} ([0.2,0.201],0.201), \\ ([0.2,0.25],0.25), \\ ([0.1,0.2],0.21) \end{pmatrix}$	$\begin{pmatrix} ([0.2,0.201],0.201), \\ ([0.1,0.2],0.2), \\ ([0.2,0.22],0.3) \end{pmatrix}$	$\begin{pmatrix} ([0.2,0.22],0.22), \\ ([0.3,0.31],0.32), \\ ([0.1,0.2],0.23) \end{pmatrix}$	$\begin{pmatrix} ([0.102,0.23],0.21), \\ ([0.2,0.21],0.24), \\ ([0.1,0.11],0.14) \end{pmatrix}$
$\widetilde{\varrho}_3$	$\begin{pmatrix} ([0.1,0.103],0.12), \\ ([0.1,0.3],0.3), \\ ([0.1,0.2],0.5) \end{pmatrix}$	$\begin{pmatrix} ([0.1,0.103],0.11), \\ ([0.1,0.2],0.3), \\ ([0.1,0.2],0.3) \end{pmatrix}$	$\begin{pmatrix} ([0.1,0.103],0.103), \\ ([0.1,0.3],0.31), \\ ([0.2,0.3],0.21) \end{pmatrix}$	$\begin{pmatrix} ([0.1,0.105],0.102), \\ ([0.2,0.3],0.21), \\ ([0.1,0.2],0.3) \end{pmatrix}$

TABLE 3: Third experts' information.

Supp.	$\widetilde{\Gamma}_1$	$\widetilde{\Gamma}_2$	$\widetilde{\Gamma}_3$	$\widetilde{\Gamma}_4$
$\widetilde{\varrho}_1$	$\begin{pmatrix} ([0.2,0.22],0.22), \\ ([0.3,0.4],0.1), \\ ([0.1,0.2],0.2) \end{pmatrix}$	$\begin{pmatrix} ([0.2,0.21],0.21), \\ ([0.1,0.3],0.1), \\ ([0.1,0.2],0.1) \end{pmatrix}$	$\begin{pmatrix} ([0.1,0.12],0.12), \\ ([0.1,0.2],0.1), \\ ([0.2,0.21],0.2) \end{pmatrix}$	$\begin{pmatrix} ([0.1,0.13],0.13), \\ ([0.1,0.2],0.2), \\ ([0.1,0.2],0.21) \end{pmatrix}$
$\widetilde{\varrho}_2$	$\begin{pmatrix} ([0.1,0.101],0.102), \\ ([0.1,0.2],0.15), \\ ([0.1,0.5],0.2) \end{pmatrix}$	$\begin{pmatrix} ([0.1,0.101],0.101), \\ ([0.2,0.3],0.25), \\ ([0.1,0.15],0.3) \end{pmatrix}$	$\begin{pmatrix} ([0.1,0.2],0.21), \\ ([0.1,0.2],0.23), \\ ([0.1,0.2],0.2) \end{pmatrix}$	$\begin{pmatrix} ([0.1,0.2],0.105), \\ ([0.2,0.3],0.3), \\ ([0.2,0.21],0.31) \end{pmatrix}$
$\widetilde{\varrho}_3$	$\begin{pmatrix} ([0.1,0.13],0.11), \\ ([0.2,0.4],0.21), \\ ([0.1,0.3],0.21) \end{pmatrix}$	$\begin{pmatrix} ([0.1,0.105],0.102), \\ ([0.1,0.2],0.3), \\ ([0.2,0.3],0.31) \end{pmatrix}$	$\begin{pmatrix} ([0.2,0.3],0.201), \\ ([0.2,0.4],0.3), \\ ([0.2,0.3],0.22) \end{pmatrix}$	$\begin{pmatrix} ([0.1,0.104],0.11), \\ ([0.1,0.2],0.15), \\ ([0.1,0.3],0.3) \end{pmatrix}$

to 3 on the basis of different importance of all the experts given in Table 4.

Step 6: let $k = 2$; again, using PCFHWA operator and utilizing aggregated report in Table 4 with weight vector $(0.35, 0.3, 0.21, 0.14^T)$, we obtain the collective PCFNs for alternatives $\{\widetilde{\varrho}_1, \widetilde{\varrho}_2, \widetilde{\varrho}_3\}$:

$$\widetilde{\varrho}_1 = (([0.1,0.16],0.14), ([0.3,0.4],0.4), ([0.3,0.4],0.3)),$$
$$\widetilde{\varrho}_2 = (([0.18,0.22],0.21), ([0.33,0.4],0.4), ([0.3,0.35],0.36)), \tag{62}$$
$$\widetilde{\varrho}_3 = (([0.101,0.2],0.14), ([0.3,0.4],0.4), ([0.3,0.4],0.4)).$$

TABLE 4: Collected information by PCFHWA operator.

Supp.	$\widetilde{\Gamma}_1$	$\widetilde{\Gamma}_2$	$\widetilde{\Gamma}_3$	$\widetilde{\Gamma}_4$
$\widetilde{\varrho}_1$	$\begin{pmatrix} ([0.1, 0.14], 0.14), \\ ([0.2, 0.3], 0.3), \\ ([0.2, 0.3], 0.2) \end{pmatrix}$	$\begin{pmatrix} ([0.2, 0.21], 0.13), \\ ([0.2, 0.4], 0.3), \\ ([0.2, 0.3], 0.2) \end{pmatrix}$	$\begin{pmatrix} ([0.1, 0.14], 0.14), \\ ([0.2, 0.3], 0.3), \\ ([0.2, 0.3], 0.3) \end{pmatrix}$	$\begin{pmatrix} ([0.1, 0.13], 0.13), \\ ([0.2, 0.3], 0.3), \\ ([0.2, 0.3], 0.3) \end{pmatrix}$
$\widetilde{\varrho}_2$	$\begin{pmatrix} ([0.18, 0.2], 0.18), \\ ([0.3, 0.31], 0.305), \\ ([0.2, 0.3], 0.3) \end{pmatrix}$	$\begin{pmatrix} ([0.2, 0.22], 0.23), \\ ([0.2, 0.3], 0.3), \\ ([0.2, 0.26], 0.3) \end{pmatrix}$	$\begin{pmatrix} ([0.2, 0.21], 0.21), \\ ([0.3, 0.4], 0.4), \\ ([0.2, 0.3], 0.3) \end{pmatrix}$	$\begin{pmatrix} ([0.1, 0.21], 0.19), \\ ([0.2, 0.3], 0.4), \\ ([0.2, 0.21], 0.2) \end{pmatrix}$
$\widetilde{\varrho}_3$	$\begin{pmatrix} ([0.1, 0.11], 0.13), \\ ([0.2, 0.4], 0.3), \\ ([0.2, 0.3], 0.4) \end{pmatrix}$	$\begin{pmatrix} ([0.1, 0.15], 0.15), \\ ([0.2, 0.3], 0.3), \\ ([0.2, 0.3], 0.4) \end{pmatrix}$	$\begin{pmatrix} ([0.1, 0.15], 0.13), \\ ([0.2, 0.4], 0.3), \\ ([0.2, 0.3], 0.3) \end{pmatrix}$	$\begin{pmatrix} ([0.1, 0.15], 0.15), \\ ([0.3, 0.4], 0.3), \\ ([0.2, 0.3], 0.3) \end{pmatrix}$

Abbreviation: PCFHWA, picture cubic fuzzy Hamacher weighted averaging

Step 7: utilizing score function formula of PCFNs, calculate $S(\widetilde{\varrho}_1), S(\widetilde{\varrho}_2)$, and $S(\widetilde{\varrho}_3)$:

$$S(\widetilde{\varrho}_1) = -0.5667,$$
$$S(\widetilde{\varrho}_2) = -0.5100, \tag{63}$$
$$S(\widetilde{\varrho}_3) = -0.5527.$$

Step 8: rank the alternatives:

$$\widetilde{\varrho}_2 > \widetilde{\varrho}_3 > \widetilde{\varrho}_1. \tag{64}$$

Rank all the alternatives to select the good alternative is $\widetilde{\varrho}_2$.

6.2. By PCFHOWA Operator

Step 9: the collected information stated by three experts with respect to different importance three experts is given in Table 4.

Step 10: let $k = 2$, and using PCFHOWA operator and utilizing the aggregated information in Table 4, with weight vector $(0.35, 0.3, 0.21, 0.14)^T$, we obtain the collective PCFNs for the alternatives $\{\widetilde{\varrho}_1, \widetilde{\varrho}_2, \widetilde{\varrho}_3\}$, which are given below:

$$\widetilde{\varrho}_{\sigma_{(1)}} = (([0.14, 0.17], 0.14), ([0.29, 0.4], 0.38), ([0.29, 0.38], 0.31)),$$
$$\widetilde{\varrho}_{\sigma_{(2)}} = (([0.17, 0.2], 0.21), ([0.31, 0.38], 0.41), ([0.29, 0.34], 0.35)), \tag{65}$$
$$\widetilde{\varrho}_{\sigma_{(3)}} = (([0.101, 0.15], 0.14), ([0.3, 0.4], 0.38), ([0.29, 0.38], 0.41)).$$

Step 11: utilizing score function formula of PCFNs, calculate $S(\widetilde{\varrho}_1), S(\widetilde{\varrho}_2)$, and $S(\widetilde{\varrho}_3)$:

$$S(\widetilde{\varrho}_1) = -0.5333,$$
$$S(\widetilde{\varrho}_2) = -0.5000, \tag{66}$$
$$S(\widetilde{\varrho}_3) = -0.5897.$$

Step 12: rank the alternatives:

$$\widetilde{\varrho}_2 > \widetilde{\varrho}_1 > \widetilde{\varrho}_3. \tag{67}$$

Rank all the alternatives to select the good alternative is $\widetilde{\varrho}_2$.

6.3. By PCFHHWA Operator.
The experts have presented their decision in Tables 1–3. Utilize the formula $\widetilde{P}_r = \mathrm{uw}P_r = \langle ([\widetilde{a}_r^-, \widetilde{a}_r^+], \widetilde{\lambda}_r), ([\widetilde{c}_r^-, \widetilde{c}_r^+], \widetilde{\psi}_r), ([\widetilde{b}_r^-, \widetilde{b}_r^+], \widetilde{\delta}_r) \rangle$ $(r = 1, 2, \ldots, u)$ to the information given in Tables 1–3, taking weight vector $w = (0.4, 0.35, 0.25)^T$.

The aggregated information by utilizing the PCFHHA operator with taking weight vector $(0.45, 0.3, 0.25)$, given by three experts w.r.t the varied importance of the experts, is presented in Table 5.

Step 14: again using PCFHHA operator, having $\bar{\omega} = (0.35, 0.3, 0.21, 0.14)$, as a weight vector, we get collective PCFNs of the alternatives as given below:

Table 6: Once more weight multiplied to Table 5.

Supp.	$\widetilde{\Gamma}_1$	$\widetilde{\Gamma}_2$	$\widetilde{\Gamma}_3$	$\widetilde{\Gamma}_4$
$\widetilde{\varrho}_1$	$\begin{pmatrix}([0.14,0.18],0.18),\\([0.12,0.2],0.3),\\([0.14,0.23],0.15)\end{pmatrix}$	$\begin{pmatrix}([0.24,0.25],0.13),\\([0.18,0.36],0.33),\\([0.18,0.3],0.18)\end{pmatrix}$	$\begin{pmatrix}([0.16,0.17],0.17),\\([0.15,0.35],0.28),\\([0.2,0.29],0.31)\end{pmatrix}$	$\begin{pmatrix}([0.1,0.11],0.1),\\([0.24,0.42],0.4),\\([0.27,0.41],0.5)\end{pmatrix}$
$\widetilde{\varrho}_2$	$\begin{pmatrix}([0.23,0.24],0.27),\\([0.17,0.2],0.22),\\([0.09,0.21],0.16)\end{pmatrix}$	$\begin{pmatrix}([0.25,0.25],0.25),\\([0.22,0.33],0.32),\\([0.18,0.24],0.3)\end{pmatrix}$	$\begin{pmatrix}([0.19,0.21],0.22),\\([0.32,0.38],0.36),\\([0.15,0.26],0.28)\end{pmatrix}$	$\begin{pmatrix}([0.09,0.18],0.16),\\([0.29,0.4],0.44),\\([0.26,0.27],0.31)\end{pmatrix}$
$\widetilde{\varrho}_3$	$\begin{pmatrix}([0.13,0.13],0.18),\\([0.11,0.33],0.21),\\([0.09,0.19],0.24)\end{pmatrix}$	$\begin{pmatrix}([0.16,0.17],0.17),\\([0.21,0.31],0.32),\\([0.22,0.33],0.36)\end{pmatrix}$	$\begin{pmatrix}([0.12,0.14],0.13),\\([0.17,0.36],0.23),\\([0.2,0.3],0.32)\end{pmatrix}$	$\begin{pmatrix}([0.13,0.13],0.14),\\([0.33,0.44],0.44),\\([0.24,0.37],0.4)\end{pmatrix}$

Table 5: Calculated experts' information by PCFHHA operator.

Supp.	$\widetilde{\Gamma}_1$	$\widetilde{\Gamma}_2$	$\widetilde{\Gamma}_3$	$\widetilde{\Gamma}_4$
$\widetilde{\varrho}_1$	$\begin{pmatrix}([0.12,0.15],0.15),\\([0.18,0.28],0.38),\\([0.21,0.31],0.22)\end{pmatrix}$	$\begin{pmatrix}([0.24,0.25],0.13),\\([0.18,0.36],0.33),\\([0.18,0.3],0.18)\end{pmatrix}$	$\begin{pmatrix}([0.16,0.17],0.17),\\([0.15,0.35],0.28),\\([0.2,0.29],0.31)\end{pmatrix}$	$\begin{pmatrix}([0.12,0.14],0.14),\\([0.15,0.32],0.31),\\([0.18,0.31],0.43)\end{pmatrix}$
$\widetilde{\varrho}_2$	$\begin{pmatrix}([0.19,0.2],0.2),\\([0.24,0.28],0.3),\\([0.15,0.29],0.23)\end{pmatrix}$	$\begin{pmatrix}([0.25,0.25],0.25),\\([0.22,0.33],0.32),\\([0.18,0.24],0.3)\end{pmatrix}$	$\begin{pmatrix}([0.19,0.21],0.22),\\([0.32,0.38],0.36),\\([0.15,0.26],0.28)\end{pmatrix}$	$\begin{pmatrix}([0.11,0.22],0.2),\\([0.2,0.3],0.34),\\([0.17,0.18],0.21)\end{pmatrix}$
$\widetilde{\varrho}_3$	$\begin{pmatrix}([0.11,0.11],0.14),\\([0.17,0.41],0.29),\\([0.15,0.27],0.32)\end{pmatrix}$	$\begin{pmatrix}([0.16,0.17],0.17),\\([0.21,0.31],0.32),\\([0.22,0.33],0.36)\end{pmatrix}$	$\begin{pmatrix}([0.12,0.14],0.13),\\([0.17,0.36],0.23),\\([0.2,0.3],0.32)\end{pmatrix}$	$\begin{pmatrix}([0.16,0.16],0.17),\\([0.24,0.34],0.34),\\([0.15,0.27],0.3)\end{pmatrix}$

Abbreviation: PCFHHA, picture cubic fuzzy Hamacher hybrid averaging

$$\widetilde{\varrho}_{\sigma_{(1)}} = (([0.17,0.19],0.15),([0.23,0.37],0.39),([0.26,0.37],0.3)),$$
$$\widetilde{\varrho}_{\sigma_{(2)}} = (([0.21,0.24],0.25),([0.31,0.37],0.37),([0.22,0.32],0.32)), \qquad (68)$$
$$\widetilde{\varrho}_{\sigma_{(3)}} = (([0.14,0.14],0.16),([0.25,0.41],0.34),([0.24,0.35],0.38)).$$

Step 15: utilizing score function formula of PCFNs, calculate the score functions of $\widetilde{\varrho}_1, \widetilde{\varrho}_2,$ and $\widetilde{\varrho}_3$:

$$S(\widetilde{\varrho}_1) = -0.4700,$$
$$S(\widetilde{\varrho}_2) = -0.4033, \qquad (69)$$
$$S(\widetilde{\varrho}_3) = -0.5100.$$

Step 16: rank the alternatives:

$$\widetilde{\varrho}_2 > \widetilde{\varrho}_1 > \widetilde{\varrho}_3. \qquad (70)$$

Step 13: utilize the formula $\widetilde{P}_r = uw\widetilde{\varrho}_r = \langle ([\widetilde{a}_r^-, \widetilde{a}_r^+], \lambda_r), ([\widetilde{c}_r^-, \widetilde{c}_r^+], \psi_r), ([\widetilde{b}_r^-, \widetilde{b}_r^+], \delta_r) \rangle$ $(r = 1, 2, \ldots, u)$ to the data given in Table 5, taking weight vector $w = (0.3, 0.25, 0.25, 0.2)^T$ of $\widetilde{\varrho}_r$; the result is presented in Table 6.

Rank all the alternatives to select the good alternative is $\widetilde{\Phi}_2$. By this ranking, we obtain $\widetilde{\varrho}_2$ is the best choice for construction company.

6.4. Comparative Analysis.
To verify the superiority of our planned PCF Hamacher weighted aggregation operators, we conduct a comparative analysis of the planned operators with intuitionistic cubic fuzzy Hamacher aggregation operators [48]. The score values $(\widetilde{\varrho}_r \;\; (r = 1, 2, 3))$ and rating order of the alternatives are compiled in Table 7.

From Table 7, we see that the most good alternative is $\widetilde{\varrho}_2$. Obviously, the picture cubic fuzzy Hamacher aggregation operators are more accurate and more stable. Because in any unit composed of membership, neutral and nonmembership functions are defined in PCFS. The membership function is represented as CFN is likewise neutral and nonmembership functions are represented in the same style, but each variable composed of membership and nonmembership functions is expressed in the intuitionist cubic fuzzy set. The function of membership is expressed by the CFN and the nonmembership function is defined in the same way. In case we suppose the discussed example, PCFS is the very modern set, so it is not desirable for existing intuitionistic cubic fuzzy Hamacher aggregation operators to solve the data involved

Table 7: Observation table.

)Operators.	$S(\bar{\varrho}_1)$	$S(\bar{\varrho}_2)$	$S(\bar{\varrho}_3)$	Ranking order
ICFHWA operator [48]	−0.20	−0.13	−0.22	$\bar{\varrho}_2 > \bar{\varrho}_1 > \bar{\varrho}_3$
ICFHOWA operator [48]	−0.20	−0.14	−0.23	$\bar{\varrho}_2 > \bar{\varrho}_1 > \bar{\varrho}_3$
ICFHHA operator [48]	−0.14	−0.08	−0.17	$\bar{\varrho}_2 > \bar{\varrho}_1 > \bar{\varrho}_3$
PCFHWA operator	−0.58	−0.51	−0.55	$\bar{\varrho}_2 > \bar{\varrho}_3 > \bar{\varrho}_1$
PCFHOWA operator	−0.53	−0.50	−0.59	$\bar{\varrho}_2 > \bar{\varrho}_1 > \bar{\varrho}_3$
PCFHHA operator	−0.47	−0.40	−0.51	$\bar{\varrho}_2 > \bar{\varrho}_1 > \bar{\varrho}_3$

in the discussed numerical problem, which indicate the existing intuitionistic cubic fuzzy Hamacher aggregation operators have limited approach. So, our planned operators are most reliable for such types of problem.

Although picture fuzzy set theory has been trailed to handle MADM problems in various fields, some circumstances in real-world picture fuzzy sets are not appropriate. So, we employed picture cubic fuzzy sets in those cases, which are extension of intuitionistic fuzzy sets and picture fuzzy sets; therefore, PCFS is almost always superior than the IFS and PFS.

In some cases, the PFS is unable to handle an issue that the PCFS can; for example, if a DM provides information on positive, neutral, and negative degree of membership in an interval and as a single value, this type of issue is only handled with PCFS. PCFS, in particular, is better at dealing with ambiguous problems. We present a technique for making decisions in complicated real-life scenarios using picture cubic fuzzy information.

Preexisting structures such as fuzzy sets, intuitionistic fuzzy sets, cubic sets, and picture fuzzy sets cannot address the numerical example provided in this study. So, our suggested technique is a generalization of the existent structure of fuzzy sets in order to better deal with real-world decision-making challenges.

7. Discussion and Conclusion

In the literature, there have been several research related to Hamacher aggregation operators, but in 2020, Muneeza et al. introduced the notion of intuitionistic cubic fuzzy set (ICFS) and also introduced intuitionistic cubic fuzzy Hamacher weighted aggregation operators. ICFS is a new generalization of intuitionistic fuzzy set. We still have not seen, to date, any Hamacher weighted aggregation operators-based research for intelligence fusion under the picture cubic fuzzy set (PCFS) framework. Thus, it is essential to give attention to this subject. Inspired by ICFS, we concentrate our attention upon this concept in order to expand the Hamacher aggregation operators to aggregate picture cubic fuzzy data and their activity in multiple attribute decision-making problems.

The main purpose in this study is to present some Hamacher weighted aggregation operators under picture cubic fuzzy environment, i.e., PCFHWA operator, PCFHOWA operator, and PCFHHA operator, and applied them to MAGDM problems. Basically, SHPP locations' selection is MAGDMP problem, where the attributes' value is in the form of PCFNs. Firstly, we have established picture cubic fuzzy set, introduced score degree, and accuracy function formula for the comparison of PCFNs. The motivation of Hamacher operators also defined a number of PCF Hamacher aggregation operators. Furthermore, we discussed few properties of planned operators, such as monotonicity, boundedness, and idempotency, and demonstrated relationship among abovementioned planned operators. We have defined new MAGDM algorithm by utilizing these planned operators with PCFVs. To verify the superiority of these planned operators, we conduct a comparison analysis of these planned operators with intuitionistic cubic fuzzy Hamacher aggregation operators.

In future picture cubic fuzzy context, we may further study different types of averaging operators and apply them to realistic decision-making situations, taking advantage of the enhanced simulation capacity of picture cubic fuzzy sets.

Furthermore, numerous sectors, such as medical diagnostic, pattern recognition, weather forecasting, sustainable energy planning decision-making, robotics, and informatics can made significant methodological improvements of picture cubic fuzzy sets in future.

We expect that the convergence of these main climate-centric research fields will provide significant growth and opportunity to better comprehend our world.

Abbreviations

FS:	Fuzzy set
μ_R:	Membership degree for fuzzy set
IVIFS:	Interval-valued intuitionistic fuzzy set
$[\mu_R^-(\dot{t}), \mu_R^+(\dot{t})]$:	Membership function for IVIFS
$[\nu_R^-(\dot{t}), \nu_R^+(\dot{t})]$:	Nonmembership function for IVIFS
CFS:	Cubic fuzzy set
ICFS:	Intuitionistic cubic fuzzy set
$\breve{\lambda}$:	Degree of membership for ICFS
δ:	Degree of nonmembership for ICFS
$\langle [a^-, a^+], \breve{\lambda} \rangle$:	Exact degree of membership for ICFS
$\langle [b^-, b^+], \delta \rangle$:	Exact degree of nonmembership for ICFS
HOs:	Hamacher operations
PCFS:	Picture cubic fuzzy set
S:	Score function
A:	Accuracy function.

Appendix

A. Proof of Theorem 1

Proof. By the method of mathematical induction, the authors will prove this theorem.

(i) When $r = 1$ and $n = 1$, based *HOs* on PCFVs, we obtain the following result as

$$\mathrm{PCFHWA}_{\hat{\omega}}\left(P_1\right)$$

$$= \left\{ \left(\begin{bmatrix} \dfrac{1 + (d-1)a^- - (1-a^-)}{1 + (d-1)a^- + (d-1)(1-a^-)}, \\[4mm] \dfrac{1 + (d-1)a^+ - (1-a^+)}{1 + (d-1)a^+ + (d-1)(1-a^+)} \end{bmatrix}, \\[4mm] \dfrac{1 + (d-1)\breve{\lambda} - (1-\breve{\lambda})}{1 + (d-1)\breve{\lambda} + (d-1)(1-\breve{\lambda})} \right), \\[6mm] \left(\begin{bmatrix} \dfrac{d(c^-)}{1 + (d-1)(1-c^-) + (d-1)(c^-)}, \\[4mm] \dfrac{d(c^+)}{1 + (d-1)(1-c^+) + (d-1)(c^+)} \end{bmatrix}, \\[4mm] \dfrac{d(\breve{\psi})}{1 + (d-1)(1-\breve{\psi}) + (d-1)(\breve{\psi})} \right), \\[6mm] \left(\begin{bmatrix} \dfrac{d(b^-)}{1 + (d-1)(1-b^-) + (d-1)(b^-)}, \\[4mm] \dfrac{d(b^+)}{1 + (d-1)(1-b^+) + (d-1)(b^+)} \end{bmatrix}, \\[4mm] \dfrac{d(\breve{\delta})}{1 + (d-1)(1-\breve{\delta}) + (d-1)(\breve{\delta})} \right) \right\}. \tag{A.1}$$

Hence, equation (14) is true, for $r = 1$.

(ii) Let equation (14) is true, for $g = n$; on the basis, from equation (14), we obtain

$$\text{PCFHWA}_{\varpi}\left(P_1, P_2, P_3, \ldots, P_n\right)$$

$$
= \left\{
\begin{pmatrix}
\left[\dfrac{\prod_{r=1}^{n}\left(1+(d-1)a_r^-\right)^{\varpi_r} - \prod_{r=1}^{n}\left(1-a_r^-\right)^{\varpi_r}}{\prod_{r=1}^{n}\left(1+(d-1)a_r^-\right)^{\varpi_r} - \prod_{r=1}^{n}\left(1-a_r^-\right)^{\varpi_r}}, \right. \\[2em]
\left. \dfrac{\prod_{r=1}^{n}\left(1+(d-1)a_r^+\right)^{\varpi_r} - \prod_{r=1}^{n}\left(1-a_r^+\right)^{\varpi_r}}{\prod_{r=1}^{n}\left(1+(d-1)a_r^+\right)^{\varpi_r} - \prod_{r=1}^{n}\left(1-a_r^+\right)^{\varpi_r}} \right], \\[2em]
\dfrac{\prod_{r=1}^{n}\left(1+(d-1)\breve{\lambda}_r\right)^{\varpi_r} - \prod_{r=1}^{n}\left(1-\breve{\lambda}_r\right)^{\varpi_r}}{\prod_{r=1}^{n}\left(1+(d-1)\breve{\lambda}_r\right)^{\varpi_r} - \prod_{r=1}^{n}\left(1-\breve{\lambda}_r\right)^{\varpi_r}}
\end{pmatrix},
\right.
$$

$$
\begin{pmatrix}
\left[d\,\dfrac{\prod_{r=1}^{n}\left(c_r^-\right)^{\varpi_r}}{\prod_{r=1}^{n}\left(1+(d-1)\left(1-c_r^-\right)\right)^{\varpi_r} + (d-1)\prod_{r=1}^{n}\left(c_r^-\right)^{\varpi_r}}, \right. \\[2em]
\left. d\,\dfrac{\prod_{r=1}^{n}\left(c_r^+\right)^{\varpi_r}}{\prod_{r=1}^{n}\left(1+(d-1)\left(1-c_r^+\right)\right)^{\varpi_r} + (d-1)\prod_{r=1}^{n}\left(c_r^+\right)^{\varpi_r}} \right], \\[2em]
d\,\dfrac{\prod_{r=1}^{n}\left(\breve{\psi}_r\right)^{\varpi_r}}{\prod_{r=1}^{n}\left(1+(d-1)\left(1-\breve{\psi}_r\right)\right)^{\varpi_r} + (d-1)\prod_{r=1}^{n}\left(\breve{\psi}_r\right)^{\varpi_r}}
\end{pmatrix},
\tag{A.2}
$$

$$
\left.
\begin{pmatrix}
\left[\dfrac{\prod_{r=1}^{n}\left(b_r^-\right)^{\varpi_r}}{\prod_{r=1}^{n}\left(1+(d-1)\left(1-b_r^-\right)\right)^{\varpi_r} + (d-1)\prod_{r=1}^{n}\left(b_r^-\right)^{\varpi_r}}, \right. \\[2em]
\left. \dfrac{\prod_{r=1}^{n}\left(b_r^+\right)^{\varpi_r}}{\prod_{r=1}^{n}\left(1+(d-1)\left(1-b_r^-\right)\right)^{\varpi_r} + (d-1)\prod_{r=1}^{n}\left(b_r^+\right)^{\varpi_r}} \right], \\[2em]
d\,\dfrac{\prod_{r=1}^{n}\left(\left(\breve{\delta}_r\right)\right)^{\varpi_r}}{\prod_{r=1}^{n}\left(1+(d-1)\left(\left(\breve{\delta}_r\right)\right)\right)^{\varpi_r} + (d-1)\prod_{r=1}^{n}\left(\left(\breve{\delta}_r\right)\right)^{\varpi_r}}
\end{pmatrix}
\right\}.
$$

Now, for $g = n + 1$, we have

$$\text{PCFHWA}_\varpi \left(P_1, P_2, P_3, \ldots, P_n, P_{n+1} \right) = \oplus_{r=1}^{n} \varpi_r P_r \oplus \varpi_{n+1} P_{n+1}$$

$$
= \left\{ \begin{array}{l}
\left(\begin{bmatrix} \dfrac{\prod_{r=1}^{n} \left(1 + (d-1)a_r^-\right)^{\varpi_r} - \prod_{r=1}^{n} \left(1 - a_r^-\right)^{\varpi_r}}{\prod_{r=1}^{n} \left(1 + (d-1)a_r^-\right)^{\varpi_r} - \prod_{r=1}^{n} \left(1 - a_r^-\right)^{\varpi_r}}, \\[20pt] \dfrac{\prod_{r=1}^{n} \left(1 + (d-1)a_r^+\right)^{\varpi_r} - \prod_{r=1}^{n} \left(1 - a_r^+\right)^{\varpi_r}}{\prod_{r=1}^{n} \left(1 + (d-1)a_r^+\right)^{\varpi_r} - \prod_{r=1}^{n} \left(1 - a_r^+\right)^{\varpi_r}} \end{bmatrix}, \\[40pt] \dfrac{\prod_{r=1}^{n} \left(1 + (d-1)\breve{\lambda}_r\right)^{\varpi_r} - \prod_{r=1}^{n} \left(1 - \breve{\lambda}_r\right)^{\varpi_r}}{\prod_{r=1}^{n} \left(1 + (d-1)\breve{\lambda}_r\right)^{\varpi_r} - \prod_{r=1}^{n} \left(1 - \breve{\lambda}_r\right)^{\varpi_r}} \end{array} \right), \\[80pt]

\left(\begin{bmatrix} d\,\dfrac{\prod_{r=1}^{n} \left(c_r^-\right)^{\varpi_r}}{\prod_{r=1}^{n} \left(1 + (d-1)\left(1 - c_r^-\right)\right)^{\varpi_r} + (d-1)\prod_{r=1}^{n} \left(c_r^-\right)^{\varpi_r}}, \\[30pt] d\,\dfrac{\prod_{r=1}^{n} \left(c_r^+\right)^{\varpi_r}}{\prod_{r=1}^{n} \left(1 + (d-1)\left(1 - c_r^+\right)\right)^{\varpi_r} + (d-1)\prod_{r=1}^{n} \left(c_r^+\right)^{\varpi_r}} \end{bmatrix}, \\[40pt] d\,\dfrac{\prod_{r=1}^{n} \left(\breve{\psi}_r\right)^{\varpi_r}}{\prod_{r=1}^{n} \left(1 + (d-1)\left(1 - \breve{\psi}_r\right)\right)^{\varpi_r} + (d-1)\prod_{r=1}^{n} \left(\breve{\psi}_r\right)^{\varpi_r}} \end{array} \right), \\[80pt]

\left(\begin{bmatrix} \dfrac{\prod_{r=1}^{n} \left(b_r^-\right)^{\varpi_r}}{\prod_{r=1}^{n} \left(1 + (d-1)\left(1 - b_r^-\right)\right)^{\varpi_r} + (d-1)\prod_{r=1}^{n} \left(b_r^-\right)^{\varpi_r}}, \\[30pt] \dfrac{\prod_{r=1}^{n} \left(b_r^+\right)^{\varpi_r}}{\prod_{r=1}^{n} \left(1 + (d-1)\left(1 - b_r^-\right)\right)^{\varpi_r} + (d-1)\prod_{r=1}^{n} \left(b_r^+\right)^{\varpi_r}} \end{bmatrix}, \\[40pt] d\,\dfrac{\prod_{r=1}^{n} \left(\left(\breve{\delta}_r\right)\right)^{\varpi_r}}{\prod_{r=1}^{n} \left(1 + (d-1)\left(\left(\breve{\delta}_r\right)\right)\right)^{\varpi_r} + (d-1)\prod_{r=1}^{n} \left(\left(\breve{\delta}_r\right)\right)^{\varpi_r}} \end{array} \right)
\end{array} \right\}
$$

$$
\left\{
\begin{array}{l}
\left(
\begin{bmatrix}
\dfrac{1+(d-1)a^- - (1-a^-)}{1+(d-1)a^- + (d-1)(1-a^-)}, \\[3ex]
\dfrac{1+(d-1)a^+ - (1-a^+)}{1+(d-1)a^+ + (d-1)(1-a^+)}
\end{bmatrix}, \\[5ex]
\dfrac{1+(d-1)\breve{\lambda} - (1-\breve{\lambda})}{1+(d-1)\breve{\lambda} + (d-1)(1-\breve{\lambda})}
\end{array}
\right) \\[8ex]
\oplus
\left(
\begin{array}{l}
\begin{bmatrix}
\dfrac{d(c_{n+1}^-)^{n+1}}{1+(d-1)(1-c_{n+1}^-)^{n+1} + (d-1)(c_{n+1}^-)^{n+1}}, \\[3ex]
\dfrac{d(c_{n+1}^+)^{n+1}}{1+(d-1)(1-(c_{n+1}^+))^{n+1} + (d-1)(c_{n+1}^+)^{n+1}}
\end{bmatrix}, \\[5ex]
\dfrac{d\left(\breve{\psi}_{n+1}^+\right)^{n+1}}{1+(d-1)\left(1-\breve{\psi}_{n+1}^+\right)^{n+1} + (d-1)\left(\breve{\psi}_{n+1}^+\right)^{n+1}}
\end{array}
\right), \\[8ex]
\left(
\begin{array}{l}
\begin{bmatrix}
\dfrac{d(b_{n+1}^-)^{n+1}}{1+(d-1)(1-b_{n+1}^-)^{n+1} + (d-1)(b_{n+1}^-)^{n+1}}, \\[3ex]
\dfrac{d(b_{n+1}^+)^{n+1}}{1+(d-1)(1-b_{n+1}^+)^{n+1} + (d-1)(b_{n+1}^+)^{n+1}}
\end{bmatrix}, \\[5ex]
\left(\dfrac{d\left(\breve{\delta}_{n+1}\right)^{n+1}}{1+(d-1)\left(1-\breve{\delta}_{n+1}\right)^{n+1} + (d-1)\left(\breve{\delta}_{n+1}\right)^{n+1}}\right)
\end{array}
\right)
\end{array}
\right\}.
\tag{A.3}
$$

$$
\begin{aligned}
&\left\{ \left(\begin{bmatrix} \dfrac{\prod_{r=1}^{n+1}\left(1+(d-1)a_r^-\right)^{\textcircled{\scriptsize w}_r}-\prod_{r=1}^{n+1}\left(1-a_r^-\right)^{\textcircled{\scriptsize w}_r}}{\prod_{r=1}^{n+1}\left(1+(d-1)a_r^-\right)^{\textcircled{\scriptsize w}_r}-\prod_{r=1}^{n+1}\left(1-a_r^-\right)^{\textcircled{\scriptsize w}_r}}, \\[6mm] \dfrac{\prod_{r=1}^{n+1}\left(1+(d-1)a_r^+\right)^{\textcircled{\scriptsize w}_r}-\prod_{r=1}^{n+1}\left(1-a_r^+\right)^{\textcircled{\scriptsize w}_r}}{\prod_{r=1}^{n+1}\left(1+(d-1)a_r^+\right)^{\textcircled{\scriptsize w}_r}-\prod_{r=1}^{n+1}\left(1-a_r^+\right)^{\textcircled{\scriptsize w}_r}} \end{bmatrix}, \\[6mm] \dfrac{\prod_{r=1}^{n+1}\left(1+(d-1)\breve{\lambda}_r\right)^{\textcircled{\scriptsize w}_r}-\prod_{r=1}^{n+1}\left(1-\breve{\lambda}_r\right)^{\textcircled{\scriptsize w}_r}}{\prod_{r=1}^{n+1}\left(1+(d-1)\breve{\lambda}_r\right)^{\textcircled{\scriptsize w}_r}-\prod_{r=1}^{n+1}\left(1-\breve{\lambda}_r\right)^{\textcircled{\scriptsize w}_r}} \end{matrix} \right), \right. \\[10mm]
&\left(\begin{bmatrix} d\,\dfrac{\prod_{r=1}^{n+1}\left(c_r^-\right)^{\textcircled{\scriptsize w}_r}}{\prod_{r=1}^{n+1}\left(1+(d-1)\left(1-c_r^-\right)\right)^{\textcircled{\scriptsize w}_r}+(d-1)\prod_{r=1}^{n+1}\left(c_r^-\right)^{\textcircled{\scriptsize w}_r}}, \\[6mm] d\,\dfrac{\prod_{r=1}^{n+1}\left(c_r^+\right)^{\textcircled{\scriptsize w}_r}}{\prod_{r=1}^{n+1}\left(1+(d-1)\left(1-c_r^+\right)\right)^{\textcircled{\scriptsize w}_r}+(d-1)\prod_{r=1}^{n+1}\left(c_r^+\right)^{\textcircled{\scriptsize w}_r}} \end{bmatrix}, \\[6mm] d\,\dfrac{\prod_{r=1}^{n+1}\left(\breve{\psi}_r\right)^{\textcircled{\scriptsize w}_r}}{\prod_{r=1}^{n+1}\left(1+(d-1)\left(1-\breve{\psi}_r\right)\right)^{\textcircled{\scriptsize w}_r}+(d-1)\prod_{r=1}^{n+1}\left(\breve{\psi}_r\right)^{\textcircled{\scriptsize w}_r}} \end{matrix} \right), \\[10mm]
&\left. \left(\begin{bmatrix} \dfrac{\prod_{r=1}^{n+1}\left(b_r^-\right)^{\textcircled{\scriptsize w}_r}}{\prod_{r=1}^{n+1}\left(1+(d-1)\left(1-b_r^-\right)\right)^{\textcircled{\scriptsize w}_r}+(d-1)\prod_{r=1}^{n+1}\left(b_r^-\right)^{\textcircled{\scriptsize w}_r}}, \\[6mm] \dfrac{\prod_{r=1}^{n+1}\left(b_r^+\right)^{\textcircled{\scriptsize w}_r}}{\prod_{r=1}^{n+1}\left(1+(d-1)\left(1-b_r^-\right)\right)^{\textcircled{\scriptsize w}_r}+(d-1)\prod_{r=1}^{n+1}\left(b_r^+\right)^{\textcircled{\scriptsize w}_r}} \end{bmatrix}, \\[6mm] d\,\dfrac{\prod_{r=1}^{n+1}\left(\left(\breve{\delta}_r\right)\right)^{\textcircled{\scriptsize w}_r}}{\prod_{r=1}^{n+1}\left(1+(d-1)\left(\left(\breve{\delta}_r\right)\right)\right)^{\textcircled{\scriptsize w}_r}+(d-1)\prod_{r=1}^{n+1}\left(\left(\breve{\delta}_r\right)\right)^{\textcircled{\scriptsize w}_r}} \end{matrix} \right) \right\}.
\end{aligned}
\tag{A.4}
$$

Thus, equation (14) is true, for $r = n + 1$. By the method of mathematical induction, (*i*) to (*ii*), the authors conclude that equation (14) is true for each-and-every values of r. □

B. Proof of Proposition 2 (Idempotency)

Since, for all r, $P_r = P$, that is, $a_r^- = a^-$, $a_r^+ = a^+$, $c_r^- = c^-$, $c_r^+ = c^+$, $b_r^- = b^-$, $b_r^+ = b^+$, $\breve{\lambda}_r = \breve{\lambda}$, $\breve{\psi}_r = \breve{\psi}$, and $\delta_r = \delta$,

$$\text{PCFHWA}_{\omega}\left(P_1, P_2, P_3, \ldots, P_g\right)$$

$$= \left\{ \begin{array}{l} \left(\begin{array}{c} \left[\dfrac{\prod_{r=1}^{g}\left(1+(d-1)a_r^-\right)^{\omega_r} - \prod_{r=1}^{g}\left(1-a_r^-\right)^{\omega_r}}{\prod_{r=1}^{g}\left(1+(d-1)a_r^-\right)^{\omega_r} - \prod_{r=1}^{g}\left(1-a_r^-\right)^{\omega_r}}, \\ \\ \dfrac{\prod_{r=1}^{g}\left(1+(d-1)a_r^+\right)^{\omega_r} - \prod_{r=1}^{g}\left(1-a_r^+\right)^{\omega_r}}{\prod_{r=1}^{g}\left(1+(d-1)a_r^+\right)^{\omega_r} - \prod_{r=1}^{g}\left(1-a_r^+\right)^{\omega_r}} \end{array} \right], \\ \\ \dfrac{\prod_{r=1}^{g}\left(1+(d-1)\breve{\lambda}_r\right)^{\omega_r} - \prod_{r=1}^{g}\left(1-\breve{\lambda}_r\right)^{\omega_r}}{\prod_{r=1}^{g}\left(1+(d-1)\breve{\lambda}_r\right)^{\omega_r} - \prod_{r=1}^{g}\left(1-\breve{\lambda}_r\right)^{\omega_r}} \end{array} \right), \\ \\ \left(\begin{array}{c} \left[d\dfrac{\prod_{r=1}^{g}\left(c_r^-\right)^{\omega_r}}{\prod_{r=1}^{g}\left(1+(d-1)(1-c_r^-)\right)^{\omega_r} + (d-1)\prod_{r=1}^{g}\left(c_r^-\right)^{\omega_r}}, \\ \\ d\dfrac{\prod_{r=1}^{g}\left(c_r^+\right)^{\omega_r}}{\prod_{r=1}^{g}\left(1+(d-1)(1-c_r^+)\right)^{\omega_r} + (d-1)\prod_{r=1}^{g}\left(c_r^+\right)^{\omega_r}} \end{array} \right], \\ \\ d\dfrac{\prod_{r=1}^{n+1}\left(\breve{\psi}_r\right)^{\omega_r}}{\prod_{r=1}^{g}\left(1+(d-1)(1-\breve{\psi}_r)\right)^{\omega_r} + (d-1)\prod_{r=1}^{g}\left(\breve{\psi}_r\right)^{\omega_r}} \end{array} \right), \\ \\ \left(\begin{array}{c} \left[\dfrac{\prod_{r=1}^{g}\left(b_r^-\right)^{\omega_r}}{\prod_{r=1}^{g}\left(1+(d-1)(1-b_r^-)\right)^{\omega_r} + (d-1)\prod_{r=1}^{g}\left(b_r^-\right)^{\omega_r}}, \\ \\ \dfrac{\prod_{r=1}^{n+1}\left(b_r^+\right)^{\omega_r}}{\prod_{r=1}^{g}\left(1+(d-1)(1-b_r^-)\right)^{\omega_r} + (d-1)\prod_{r=1}^{g}\left(b_r^+\right)^{\omega_r}} \end{array} \right], \\ \\ d\dfrac{\prod_{r=1}^{g}\left(\left(\breve{\delta}_r\right)\right)^{\omega_r}}{\prod_{r=1}^{g}\left(1+(d-1)\left(\left(\breve{\delta}_r\right)\right)\right)^{\omega_r} + (d-1)\prod_{r=1}^{g}\left(\left(\breve{\delta}_r\right)\right)^{\omega_r}} \end{array} \right) \end{array} \right\}$$

$$(B.1)$$

$\mathrm{PCFHWA}_\omega\left(P_1\right)$

$$= \left\{ \begin{array}{l} \left(\left[\dfrac{1+(d-1)a^- - (1-a^-)}{1+(d-1)a^- + (d-1)(1-a^-)}, \right. \right. \\ \left. \qquad \dfrac{1+(d-1)a^+ - (1-a^+)}{1+(d-1)a^+ + (d-1)(1-a^+)} \right], \\ \left. \qquad \dfrac{1+(d-1)\breve{\lambda} - (1-\breve{\lambda})}{1+(d-1)\breve{\lambda} + (d-1)(1-\breve{\lambda})} \right), \\[4mm] \left(\left[\dfrac{d(c^-)}{1+(d-1)(1-c^-)+(d-1)(c^-)}, \right. \right. \\ \left. \qquad \dfrac{d(c^+)}{1+(d-1)(1-c^+)+(d-1)(c^+)} \right], \\ \left. \qquad \dfrac{d(\breve{\psi})}{1+(d-1)(1-\breve{\psi})+(d-1)(\breve{\psi})} \right), \\[4mm] \left(\left[\dfrac{d(b^-)}{1+(d-1)(1-b^-)+(d-1)(b^-)}, \right. \right. \\ \left. \qquad \dfrac{d(b^+)}{1+(d-1)(1-b^+)+(d-1)(b^+)} \right], \\ \left. \qquad \dfrac{d(\breve{\delta})}{1+(d-1)(1-\breve{\delta})+(d-1)(\breve{\delta})} \right) \end{array} \right\}.$$

$$= \left\{ \left([a^-,a^+],\breve{\lambda}\right), \left([c^-,c^+],\breve{\psi}\right), \left([b^-,b^+],\breve{\delta}\right) \right\}$$

$$= P$$

$$(\mathrm{B.2})$$

Hence, it is proved.

C. Proof of Proposition 2 (Monotonicity)

$$
\mathrm{PCFHWA}_{\Omega}\left(P_1, P_2, P_3, \ldots, P_g\right)
$$

$$
= \left\{ \begin{array}{l}
\left(\begin{bmatrix} \dfrac{\prod_{r=1}^{g}\left(1+(d-1)a_r^-\right)^{\Omega_r} - \prod_{r=1}^{g}\left(1-a_r^-\right)^{\Omega_r}}{\prod_{r=1}^{g}\left(1+(d-1)a_r^-\right)^{\Omega_r} - \prod_{r=1}^{g}\left(1-a_r^-\right)^{\Omega_r}}, \\[4ex]
\dfrac{\prod_{r=1}^{g}\left(1+(d-1)a_r^+\right)^{\Omega_r} - \prod_{r=1}^{g}\left(1-a_r^+\right)^{\Omega_r}}{\prod_{r=1}^{g}\left(1+(d-1)a_r^+\right)^{\Omega_r} - \prod_{r=1}^{g}\left(1-a_r^+\right)^{\Omega_r}} \end{bmatrix}, \\[8ex]
\dfrac{\prod_{r=1}^{g}\left(1+(d-1)\breve{\lambda}_r\right)^{\Omega_r} - \prod_{r=1}^{g}\left(1-\breve{\lambda}_r\right)^{\Omega_r}}{\prod_{r=1}^{g}\left(1+(d-1)\breve{\lambda}_r\right)^{\Omega_r} - \prod_{r=1}^{g}\left(1-\breve{\lambda}_r\right)^{\Omega_r}} \end{array} \right),
$$
$$
\left(\begin{bmatrix} d\,\dfrac{\prod_{r=1}^{g}\left(c_r^-\right)^{\Omega_r}}{\prod_{r=1}^{g}\left(1+(d-1)\left(1-c_r^-\right)\right)^{\Omega_r}+(d-1)\prod_{r=1}^{g}\left(c_r^-\right)^{\Omega_r}}, \\[6ex]
d\,\dfrac{\prod_{r=1}^{g}\left(c_r^+\right)^{\Omega_r}}{\prod_{r=1}^{g}\left(1+(d-1)\left(1-c_r^+\right)\right)^{\Omega_r}+(d-1)\prod_{r=1}^{g}\left(c_r^+\right)^{\Omega_r}} \end{bmatrix}, \\[8ex]
d\,\dfrac{\prod_{r=1}^{n+1}\left(\breve{\psi}_r\right)^{\Omega_r}}{\prod_{r=1}^{g}\left(1+(d-1)\left(1-\breve{\psi}_r\right)\right)^{\Omega_r}+(d-1)\prod_{r=1}^{g}\left(\breve{\psi}_r\right)^{\Omega_r}} \end{array} \right),
$$
$$
\left(\begin{bmatrix} \dfrac{\prod_{r=1}^{g}\left(b_r^-\right)^{\Omega_r}}{\prod_{r=1}^{g}\left(1+(d-1)\left(1-b_r^-\right)\right)^{\Omega_r}+(d-1)\prod_{r=1}^{g}\left(b_r^-\right)^{\Omega_r}}, \\[6ex]
\dfrac{\prod_{r=1}^{n+1}\left(b_r^+\right)^{\Omega_r}}{\prod_{r=1}^{g}\left(1+(d-1)\left(1-b_r^-\right)\right)^{\Omega_r}+(d-1)\prod_{r=1}^{g}\left(b_r^+\right)^{\Omega_r}} \end{bmatrix}, \\[8ex]
d\,\dfrac{\prod_{r=1}^{g}\left(\left(\breve{\delta}_r\right)\right)^{\Omega_r}}{\prod_{r=1}^{g}\left(1+(d-1)\left(\left(\breve{\delta}_r\right)\right)\right)^{\Omega_r}+(d-1)\prod_{r=1}^{g}\left(\left(\breve{\delta}_r\right)\right)^{\Omega_r}} \end{array} \right)
\end{array} \right\}
$$

(C.1)

as

$$\frac{\prod_{r=1}^{g}\left(1+(d-1)a_r^-\right)^{\varpi_r}-\prod_{r=1}^{g}\left(1-a_r^-\right)^{\varpi_r}}{\prod_{r=1}^{g}\left(1+(d-1)a_r^-\right)^{\varpi_r}-\prod_{r=1}^{g}\left(1-a_r^-\right)^{\varpi_r}},$$

$$\geq\frac{\prod_{r=1}^{g}\left(1+(d-1)a_r^{*-}\right)^{\varpi_r}-\prod_{r=1}^{g}\left(1-a_r^{*-}\right)^{\varpi_r}}{\prod_{r=1}^{g}\left(1+(d-1)a_r^{*-}\right)^{\varpi_r}-\prod_{r=1}^{g}\left(1-a_r^{*-}\right)^{\varpi_r}},$$

$$\frac{\prod_{r=1}^{g}\left(1+(d-1)a_r^{*+}\right)^{\varpi_r}-\prod_{r=1}^{g}\left(1-a_r^{*+}\right)^{\varpi_r}}{\prod_{r=1}^{g}\left(1+(d-1)a_r^{*+}\right)^{\varpi_r}-\prod_{r=1}^{g}\left(1-a_r^{*+}\right)^{\varpi_r}},$$

$$\frac{\prod_{r=1}^{g}\left(1+(d-1)a_r^+\right)^{\varpi_r}-\prod_{r=1}^{g}\left(1-a_r^+\right)^{\varpi_r}}{\prod_{r=1}^{g}\left(1+(d-1)a_r^+\right)^{\varpi_r}-\prod_{r=1}^{g}\left(1-a_r^+\right)^{\varpi_r}},$$

$$\Rightarrow\left[\frac{\prod_{r=1}^{g}\left(1+(d-1)a_r^-\right)^{\varpi_r}-\prod_{r=1}^{g}\left(1-a_r^-\right)^{\varpi_r}}{\prod_{r=1}^{g}\left(1+(d-1)a_r^-\right)^{\varpi_r}-\prod_{r=1}^{g}\left(1-a_r^-\right)^{\varpi_r}},\right.$$
$$\left.\frac{\prod_{r=1}^{g}\left(1+(d-1)a_r^+\right)^{\varpi_r}-\prod_{r=1}^{g}\left(1-a_r^+\right)^{\varpi_r}}{\prod_{r=1}^{g}\left(1+(d-1)a_r^+\right)^{\varpi_r}-\prod_{r=1}^{g}\left(1-a_r^+\right)^{\varpi_r}}\right]$$

$$\leq\left[\frac{\prod_{r=1}^{g}\left(1+(d-1)a_r^{*-}\right)^{\varpi_r}-\prod_{r=1}^{g}\left(1-a_r^{*-}\right)^{\varpi_r}}{\prod_{r=1}^{g}\left(1+(d-1)a_r^{*-}\right)^{\varpi_r}-\prod_{r=1}^{g}\left(1-a_r^{*-}\right)^{\varpi_r}},\right.$$
$$\left.\frac{\prod_{r=1}^{g}\left(1+(d-1)a_r^{*+}\right)^{\varpi_r}-\prod_{r=1}^{g}\left(1-a_r^{*+}\right)^{\varpi_r}}{\prod_{r=1}^{g}\left(1+(d-1)a_r^{*+}\right)^{\varpi_r}-\prod_{r=1}^{g}\left(1-a_r^{*+}\right)^{\varpi_r}}\right].$$

$$(C.2)$$

Now,

$$\Rightarrow \left[\frac{d \prod_{r=1}^{g} \left(c_r^{*^-} \right)^{\varpi_r}}{\prod_{r=1}^{g} \left(1 + (d-1)\left(1 - c_r^{*^-} \right) \right)^{\varpi_r} + (d-1) \prod_{r=1}^{g} \left(c_r^{*^-} \right)^{\varpi_r}}, \right.$$

$$\left. \frac{d \prod_{r=1}^{g} \left(c_r^{*^+} \right)^{\varpi_r}}{\prod_{r=1}^{g} \left(1 + (d-1)\left(1 - c_r^{*^+} \right) \right)^{\varpi_r} + (d-1) \prod_{r=1}^{g} \left(c_r^{*^+} \right)^{\varpi_r}} \right]$$

$$\leq \left[\frac{d \prod_{r=1}^{g} \left(c_r^{*^-} \right)^{\varpi_r}}{\prod_{r=1}^{g} \left(1 + (d-1)\left(1 - c_r^{*^-} \right) \right)^{\varpi_r} + (d-1) \prod_{r=1}^{g} \left(c_r^{*^-} \right)^{\varpi_r}}, \right.$$

$$\left. \frac{d \prod_{r=1}^{g} \left(c_r^{*^+} \right)^{\varpi_r}}{\prod_{r=1}^{g} \left(1 + (d-1)\left(1 - c_r^{*^+} \right) \right)^{\varpi_r} + (d-1) \prod_{r=1}^{g} \left(c_r^{*^+} \right)^{\varpi_r}} \right], \qquad (C.3)$$

$$\Rightarrow \left[\frac{d \prod_{r=1}^{g} \left(b_r^{*^-} \right)^{\varpi_r}}{\prod_{r=1}^{g} \left(1 + (d-1)\left(1 - b_r^{*^-} \right) \right)^{\varpi_r} + (d-1) \prod_{r=1}^{g} \left(b_r^{*^-} \right)^{\varpi_r}}, \right.$$

$$\left. \frac{d \prod_{r=1}^{g} \left(b_r^{*^+} \right)^{\varpi_r}}{\prod_{r=1}^{g} \left(1 + (d-1)\left(1 - b_r^{*^+} \right) \right)^{\varpi_r} + (d-1) \prod_{r=1}^{g} \left(b_r^{*^+} \right)^{\varpi_r}} \right]$$

$$\leq \left[\frac{d \prod_{r=1}^{g} \left(b_r^{*^-} \right)^{\varpi_r}}{\prod_{r=1}^{g} \left(1 + (d-1)\left(1 - b_r^{*^-} \right) \right)^{\varpi_r} + (d-1) \prod_{r=1}^{g} \left(b_r^{*^-} \right)^{\varpi_r}}, \right.$$

$$\left. \frac{d \prod_{r=1}^{g} \left(b_r^{*^+} \right)^{\varpi_r}}{\prod_{r=1}^{g} \left(1 + (d-1)\left(1 - b_r^{*^+} \right) \right)^{\varpi_r} + (d-1) \prod_{r=1}^{g} \left(b_r^{*^+} \right)^{\varpi_r}} \right],$$

$$\breve{\lambda}_r \leq \breve{\lambda}_r^*,$$

$$\frac{\prod_{r=1}^{g} \left(1 + (d-1)\breve{\lambda}_r \right)^{\varpi_r} - \prod_{r=1}^{g} \left(1 - \breve{\lambda}_r \right)^{\varpi_r}}{\prod_{r=1}^{g} \left(1 + (d-1)\breve{\lambda}_r^* \right)^{\varpi_r} + (d-1) \prod_{r=1}^{g} \left(1 - \breve{\lambda}_r^* \right)^{\varpi_r}}$$

$$\leq \frac{\prod_{r=1}^{g} \left(1 + (d-1)\breve{\lambda}_r \right)^{\varpi_r} - \prod_{r=1}^{g} \left(1 - \breve{\lambda}_r \right)^{\varpi_r}}{\prod_{r=1}^{g} \left(1 + (d-1)\breve{\lambda}_r^* \right)^{\varpi_r} + (d-1) \prod_{r=1}^{g} \left(1 - \breve{\lambda}_r^* \right)^{\varpi_r}}, \qquad (C.4)$$

$$\breve{\delta}_r^* \leq \breve{\delta}_r,$$

and

$$\breve{\psi}_r^* \leq \breve{\psi}_r,$$

$$\frac{d \prod_{r=1}^{g} \left(\breve{\psi}_r \right)^{\varpi_r}}{\prod_{r=1}^{g} \left(1 + (d-1)\left(1 - \breve{\psi}_r \right) \right)^{\varpi_r} + (d-1) \prod_{r=1}^{g} \left(\breve{\psi}_r \right)^{\varpi_r}}$$

$$\leq \frac{d \prod_{r=1}^{g} \left(\breve{\psi}_r \right)^{\varpi_r}}{\prod_{r=1}^{g} \left(1 + (d-1)\left(1 - \breve{\psi}_r \right) \right)^{\varpi_r} + (d-1) \prod_{r=1}^{g} \left(\breve{\psi}_r \right)^{\varpi_r}}. \qquad (C.5)$$

Also,

$$d \frac{\prod_{r=1}^{g} \left(\breve{\delta}_r^* \right)^{\varpi_r}}{\prod_{r=1}^{g} 1 + (d-1)\left(1 - \breve{\delta}_r^* \right)^{\varpi_r} + (d-1) \prod_{r=1}^{g} \left(\breve{\delta}_r^* \right)^{\varpi_r}},$$

$$\leq \frac{d \prod_{r=1}^{g} \left(\breve{\delta}_r \right)^{\varpi_r}}{\prod_{r=1}^{g} \left(1 + (d-1)\left(1 - \breve{\delta}_r \right) \right)^{\varpi_r} + (d-1) \prod_{r=1}^{g} \left(\breve{\delta}_r \right)^{\varpi_r}}. \qquad (C.6)$$

Equations (15) to (24) imply

$\mathrm{PCFHWA}_\omega\big(P_1, P_2, P_3, \ldots, P_g\big)$

$$
= \left\{
\begin{array}{l}
\left(
\begin{array}{l}
\left[
\begin{array}{l}
\dfrac{\prod_{r=1}^{g}\left(1+(d-1)a_r^-\right)^{\omega_r} - \prod_{r=1}^{g}\left(1-a_r^-\right)^{\omega_r}}{\prod_{r=1}^{g}\left(1+(d-1)a_r^-\right)^{\omega_r} - \prod_{r=1}^{g}\left(1-a_r^-\right)^{\omega_r}}, \\[4mm]
\dfrac{\prod_{r=1}^{g}\left(1+(d-1)a_r^+\right)^{\omega_r} - \prod_{r=1}^{g}\left(1-a_r^+\right)^{\omega_r}}{\prod_{r=1}^{g}\left(1+(d-1)a_r^+\right)^{\omega_r} - \prod_{r=1}^{g}\left(1-a_r^+\right)^{\omega_r}}
\end{array}
\right], \\[10mm]
\dfrac{\prod_{r=1}^{g}\left(1+(d-1)\breve{\lambda}_r\right)^{\omega_r} - \prod_{r=1}^{g}\left(1-\breve{\lambda}_r\right)^{\omega_r}}{\prod_{r=1}^{g}\left(1+(d-1)\breve{\lambda}_r\right)^{\omega_r} - \prod_{r=1}^{g}\left(1-\breve{\lambda}_r\right)^{\omega_r}}
\end{array}
\right), \\[20mm]

\left(
\begin{array}{l}
\left[
\begin{array}{l}
d\,\dfrac{\prod_{r=1}^{g}\left(c_r^-\right)^{\omega_r}}{\prod_{r=1}^{g}\left(1+(d-1)\left(1-c_r^-\right)\right)^{\omega_r} + (d-1)\prod_{r=1}^{g}\left(c_r^-\right)^{\omega_r}}, \\[6mm]
d\,\dfrac{\prod_{r=1}^{g}\left(c_r^+\right)^{\omega_r}}{\prod_{r=1}^{g}\left(1+(d-1)\left(1-c_r^+\right)\right)^{\omega_r} + (d-1)\prod_{r=1}^{g}\left(c_r^+\right)^{\omega_r}}
\end{array}
\right], \\[10mm]
d\,\dfrac{\prod_{r=1}^{n+1}\left(\breve{\psi}_r\right)^{\omega_r}}{\prod_{r=1}^{g}\left(1+(d-1)\left(1-\breve{\psi}_r\right)\right)^{\omega_r} + (d-1)\prod_{r=1}^{g}\left(\breve{\psi}_r\right)^{\omega_r}}
\end{array}
\right), \\[20mm]

\left(
\begin{array}{l}
\left[
\begin{array}{l}
\dfrac{\prod_{r=1}^{g}\left(b_r^-\right)^{\omega_r}}{\prod_{r=1}^{g}\left(1+(d-1)\left(1-b_r^-\right)\right)^{\omega_r} + (d-1)\prod_{r=1}^{g}\left(b_r^-\right)^{\omega_r}}, \\[6mm]
\dfrac{\prod_{r=1}^{n+1}\left(b_r^+\right)^{\omega_r}}{\prod_{r=1}^{g}\left(1+(d-1)\left(1-b_r^-\right)\right)^{\omega_r} + (d-1)\prod_{r=1}^{g}\left(b_r^+\right)^{\omega_r}}
\end{array}
\right], \\[10mm]
d\,\dfrac{\prod_{r=1}^{g}\left(\left(\breve{\delta}_r\right)\right)^{\omega_r}}{\prod_{r=1}^{g}\left(1+(d-1)\left(\left(\breve{\delta}_r\right)\right)\right)^{\omega_r} + (d-1)\prod_{r=1}^{g}\left(\left(\breve{\delta}_r\right)\right)^{\omega_r}}
\end{array}
\right)
\end{array}
\right\}
$$

$$\text{(C.7)}$$

$$\leq \left\{ \left(\left[\frac{\prod_{r=1}^{g}\left(1+(d-1)a_r^{*-}\right)^{\omega_r} - \prod_{r=1}^{g}\left(1-a_r^{*-}\right)^{\omega_r}}{\prod_{r=1}^{g}\left(1+(d-1)a_r^{*-}\right)^{\omega_r} + (d-1)\prod_{r=1}^{g}\left(1-a_r^{*-}\right)^{\omega_r}}, \frac{\prod_{r=1}^{g}\left(1+(d-1)a_r^{*+}\right)^{\omega_r} - \prod_{r=1}^{g}\left(1-a_r^{*+}\right)^{\omega_r}}{\prod_{r=1}^{g}\left(1+(d-1)a_r^{*+}\right)^{\omega_r} + (d-1)\prod_{r=1}^{g}\left(1-a_r^{*+}\right)^{\omega_r}} \right], \frac{\prod_{r=1}^{g}\left(1+(d-1)\breve{\lambda}_r^{*}\right)^{\omega_r} - \prod_{r=1}^{g}\left(1-\breve{\lambda}_r^{*}\right)^{\omega_r}}{\prod_{r=1}^{g}\left(1+(d-1)\breve{\lambda}_r^{*}\right)^{\omega_r} + (d-1)\prod_{r=1}^{g}\left(1-\breve{\lambda}_r^{*}\right)^{\omega_r}} \right), \right.$$

$$\left(\left[\frac{d\prod_{r=1}^{g}\left(c_r^{*-}\right)^{\omega_r}}{\prod_{r=1}^{g}\left(1+(d-1)\left(1-c_r^{*-}\right)\right)^{\omega_r} + (d-1)\prod_{r=1}^{g}\left(c_r^{*-}\right)^{\omega_r}}, \frac{d\prod_{r=1}^{g}\left(c_r^{*+}\right)^{\omega_r}}{\prod_{r=1}^{g}\left(1+(d-1)\left(1-c_r^{*+}\right)\right)^{\omega_r} + (d-1)\prod_{r=1}^{g}\left(c_r^{*+}\right)^{\omega_r}} \right], \frac{d\prod_{r=1}^{g}\left(\breve{\psi}_r^{*}\right)^{\omega_r}}{\prod_{r=1}^{g}\left(1+(d-1)\left(1-\breve{\psi}_r^{*}\right)\right)^{\omega_r} + (d-1)\prod_{r=1}^{g}\left(\breve{\psi}_r^{*}\right)^{\omega_r}} \right),$$

$$\left. \left(\left[\frac{d\prod_{r=1}^{g}\left(b_r^{*-}\right)^{\omega_r}}{\prod_{r=1}^{g}\left(1+(d-1)\left(1-cb_r^{*-}\right)\right)^{\omega_r} + (d-1)\prod_{r=1}^{g}\left(b_r^{*-}\right)^{\omega_r}}, \frac{d\prod_{r=1}^{g}\left(b_r^{*+}\right)^{\omega_r}}{\prod_{r=1}^{g}\left(1+(d-1)\left(1-cb_r^{*+}\right)\right)^{\omega_r} + (d-1)\prod_{r=1}^{g}\left(b_r^{*+}\right)^{\omega_r}} \right], \frac{d\prod_{r=1}^{g}\left(\breve{\delta}_r^{*}\right)^{\omega_r}}{\prod_{r=1}^{g}\left(1+(d-1)\left(1-\breve{\delta}_r^{*}\right)\right)^{\omega_r} + (d-1)\prod_{r=1}^{g}\left(\breve{\delta}_r^{*}\right)^{\omega_r}} \right) \right\}. \tag{C.8}$$

The authors get our required inequality:

$$\mathrm{PCFHWA}_\omega\left(P_1, P_2, \ldots, P_g\right) \leq \mathrm{PCFHWA}_\omega\left(P_1^*, P_2^*, \ldots, P_g^*\right) \tag{C.9}$$

Data Availability

No data were used to support the study.

Conflicts of Interest

The authors declare that they have no conflicts of interest.

Acknowledgments

References

[1] A. Contreras, M. Serrano, R. Acosta, and J. rez, "The importance of geological and geophysical exploration costs in the construction of hydroelectric dams comparative examples in Mexico," *International Journal of Research and Reviews in Applied Sciences*, vol. 12, no. 3, pp. 438–448, 2012.

[2] A. KarimiAzari, N. Mousavi, S. F. Mousavi, and S. Hosseini, "Risk assessment model selection in construction industry," *Expert Systems with Applications*, vol. 38, no. 8, pp. 9105–9111, 2011.

[3] Y. Q. Chen, J. Y. Liu, B. Li, and B. Lin, "Project delivery system selection of construction projects in China," *Expert Systems with Applications*, vol. 38, no. 5, pp. 5456–5462, 2011.

[4] J. Chen and J. Ye, "Some single-valued neutrosophic Dombi weighted aggregation operators for multiple attribute decision-making," *Symmetry*, vol. 9, no. 6, p. 82, 2017.

[5] A. Fahmi, S. Abdullah, F. Amin, N. Siddiqui, and A. Ali, "Aggregation operators on triangular cubic fuzzy numbers and its application to multi-criteria decision making problems," *Journal of Intelligent and Fuzzy Systems*, vol. 33, no. 6, pp. 3323–3337, 2017.

[6] A. Fahmi, S. Abdullah, F. Amin, A. Ali, and W. A. Khan, "Some geometric operators with triangular cubic linguistic hesitant fuzzy number and their application in group decision-making," *Journal of Intelligent and Fuzzy Systems*, vol. 35, no. 2, pp. 2485–2499, 2018.

[7] A. Fahmi, A. Saleem, F. Amin, and A. J. P. U. J. M. Ali, "Weighted average rating (war) method for solving group decision making problem using triangular cubic fuzzy hybrid aggregation (tcfha)," *Punjab University Journal of Mathematics*, vol. 50, no. 1, pp. 23–34, 2018.

[8] A. Fahmi, F. Amin, S. Abdullah, and A. Ali, "Cubic fuzzy Einstein aggregation operators and its application to decision-making," *International Journal of Systems Science*, vol. 49, no. 11, pp. 2385–2397, 2018.

[9] F. Amin, A. Fahmi, S. Abdullah, A. Ali, R. Ahmad, and F. Ghani, "Triangular cubic linguistic hesitant fuzzy aggregation operators and their application in group decision making," *Journal of Intelligent and Fuzzy Systems*, vol. 34, no. 4, pp. 2401–2416, 2018.

[10] A. Fahmi, S. Abdullah, and F. Amin, "Expected values of aggregation operators on cubic trapezoidal fuzzy number and its application to multi-criteria decision making problems," *Journal of New Theory*, vol. 22, pp. 51–65, 2018.

[11] X. He, "Typhoon disaster assessment based on Dombi hesitant fuzzy information aggregation operators," *Natural Hazards*, vol. 90, no. 3, pp. 1153–1175, 2018.

[12] C. Jana, T. Senapati, M. Pal, and R. R. Yager, "Picture fuzzy Dombi aggregation operators: application to MADM process," *Applied Soft Computing*, vol. 74, pp. 99–109, 2019.

[13] G. Kaur and H. Garg, "Generalized cubic intuitionistic fuzzy aggregation operators using t-norm operations and their applications to group decision-making process," *Arabian Journal for Science and Engineering*, vol. 44, no. 3, pp. 2775–2794, 2019.

[14] P. Liu and P. Wang, "Some improved linguistic intuitionistic fuzzy aggregation operators and their applications to multiple-attribute decision making," *International Journal of Information Technology and Decision Making*, vol. 16, no. 03, pp. 817–850, 2017.

[15] M. Amiri, M. Hashemi-Tabatabaei, M. Ghahremanloo, M. Keshavarz-Ghorabaee, E. K. Zavadskas, and A. Banaitis, "A new fuzzy BWM approach for evaluating and selecting a sustainable supplier in supply chain management," *The International Journal of Sustainable Development and World Ecology*, vol. 28, no. 2, pp. 125–142, 2021.

[16] H. Garg, "Generalized intuitionistic fuzzy interactive geometric interaction operators using Einstein t-norm and t-conorm and their application to decision making," *Computers & Industrial Engineering*, vol. 101, pp. 53–69, 2016.

[17] H. Garg, "Generalized intuitionistic fuzzy multiplicative interactive geometric operators and their application to multiple criteria decision making," *International Journal of Machine Learning and Cybernetics*, vol. 7, no. 6, pp. 1075–1092, 2016.

[18] M. Khan and A. Saleem, "Akhtar zeb and abdul majid. "CUCBIC AGGREGATION OPERATORS"," *International Journal of Computer Science and Information Security*, vol. 14, no. 8, p. 670, 2016.

[19] P. Liu, "Some Hamacher aggregation operators based on the interval-valued intuitionistic fuzzy numbers and their application to group decision making," *IEEE Transactions on Fuzzy Systems*, vol. 22, no. 1, pp. 83–97, 2014.

[20] C. Liang, S. Zhao, and J. Zhang, "Multi-criteria group decision making method based on generalized intuitionistic trapezoidal fuzzy prioritized aggregation operators," *International Journal of Machine Learning and Cybernetics*, vol. 8, no. 2, pp. 597–610, 2017.

[21] P. Liu, J. Liu, and S.-M. Chen, "Some intuitionistic fuzzy Dombi Bonferroni mean operators and their application to multi-attribute group decision making," *Journal of the Operational Research Society*, vol. 69, no. 1, pp. 1–24, 2017.

[22] T. Mahmood, F. Mehmood, and Q. Khan, "Cubic hesitant fuzzy sets and their applications to multi criteria decision making," *International Journal of Algebra and Statistics*, vol. 5, no. 1, pp. 19–51, 2016.

[23] Ganie, Abdul Haseeb, and S. Singh, "A picture fuzzy similarity measure based on direct operations and novel multi-attribute decision-making method," *Neural Computing & Applications*, vol. 33, no. 15, pp. 1–21, 2021.

[24] L. Shi and J. Ye, "Dombi aggregation operators of neutrosophic cubic sets for multiple attribute decision-making," *Algorithms*, vol. 11, no. 3, p. 29, 2018.

[25] W. Ullah, I. Muhammad, A. Khan, and M. Khan, "Multiple attribute decision making problem using GRA method with incomplete weight information based on picture hesitant fuzzy setting," *International Journal of Intelligent Systems*, vol. 1-24, 2020.

[26] M. Luo and H. Long, "Picture fuzzy geometric aggregation operators based on a trapezoidal fuzzy number and its application," *Symmetry*, vol. 13, no. 1, p. 119, 2021.

[27] G, ndo, F. K.. du, D.. Szabolcs, S. Moslem, and S. Aydin, Evaluating public transport service quality using picture fuzzy analytic hierarchy process and linear assignment model," *Applied Soft Computing*, vol. 100, Article ID 106920, 2021.

[28] M. Qiyas, M. A. Khan, S. Khan, and S. Abdullah, "Concept of Yager operators with the picture fuzzy set environment and its application to emergency program selection," *International Journal of Intelligent Computing and Cybernetics*, 2020.

[29] A. H Ganie, S. Singh, and P. K. Bhatia, "Some new correlation coefficients of picture fuzzy sets with applications," *Neural Computing & Applications*, vol. 32, no. 16, pp. 1–17, 2020.

[30] L. A. Zadeh, "Fuzzy sets," *Information and Control*, vol. 8, no. 3, pp. 338–353, 1965.

[31] M. J.. Khan, P. Kumam, D.. Wejdan, W. Kumam, and Z. Shah, "Bi-parametric distance and similarity measures of picture fuzzy sets and their applications in medical diagnosis," *Egyptian Informatics Journal*, 2020.

[32] N. X. Thao, "Similarity measures of picture fuzzy sets based on entropy and their application in MCDM," *Pattern Analysis & Applications*, vol. 23, no. 3, pp. 1203–1213, 2020.

[33] E. Egrioglu, E. Bas, U. Yolcu, and M. Y. Chen, "Picture fuzzy time series: defining, modeling and creating a new forecasting method," *Engineering Applications of Artificial Intelligence*, vol. 88, Article ID 103367, 2020.

[34] M. Akram, "Ayesha Bashir and Harish Garg. "Decision-making model under complex picture fuzzy Hamacher aggregation operators," *Computational and Applied Mathematics*, vol. 39, no. 3, pp. 1–38, 2020.

[35] C.. Wang, X. Zhou, H. Tu, and S. Tao, "Some geometric aggregation operators based on picture fuzzy sets and their

WILEY | Hindawi

Retraction

Retracted: Face Security Authentication System Based on Deep Learning and Homomorphic Encryption

Security and Communication Networks

This article has been retracted by Hindawi following an investigation undertaken by the publisher [1]. This investigation has uncovered evidence of one or more of the following indicators of systematic manipulation of the publication process:

(1) Discrepancies in scope

(2) Discrepancies in the description of the research reported

(3) Discrepancies between the availability of data and the research described

(4) Inappropriate citations

(5) Incoherent, meaningless and/or irrelevant content included in the article

(6) Peer-review manipulation

The presence of these indicators undermines our confidence in the integrity of the article's content and we cannot, therefore, vouch for its reliability. Please note that this notice is intended solely to alert readers that the content of this article is unreliable. We have not investigated whether authors were aware of or involved in the systematic manipulation of the publication process.

Wiley and Hindawi regrets that the usual quality checks did not identify these issues before publication and have since put additional measures in place to safeguard research integrity.

We wish to credit our own Research Integrity and Research Publishing teams and anonymous and named external researchers and research integrity experts for contributing to this investigation.

The corresponding author, as the representative of all authors, has been given the opportunity to register their agreement or disagreement to this retraction. We have kept a record of any response received.

References

[1] D. Sun, H. Huang, D. Zheng, H. Hu, C. Bi, and R. Wang, "Face Security Authentication System Based on Deep Learning and Homomorphic Encryption," *Security and Communication Networks*, vol. 2022, Article ID 7752292, 8 pages, 2022.

WILEY | Hindawi

Research Article

Face Security Authentication System Based on Deep Learning and Homomorphic Encryption

Dechao Sun [ID],[1] **Hong Huang** [ID],[1] **Dongsong Zheng** [ID],[2] **Haoliang Hu** [ID],[1] **Chunyue Bi** [ID],[1] **and Renfang Wang** [ID][1]

[1]*College of Big Data and Software Engineering, Zhejiang Wanli University, Ningbo, China*
[2]*School of Data Science and Artificial Intelligence, Wenzhou University of Technology, Wenzhou, China*

Correspondence should be addressed to Dongsong Zheng; jsj_zds@126.com and Haoliang Hu; huhaoliang79@163.com

The development of deep learning technology has promoted the wide application of face recognition in many scenarios such as mobile payment and social media, but the security of user data is facing great challenges. To protect the privacy of users, face authentication cannot be operated in plaintext. To solve this problem, a face feature ciphertext authentication scheme based on homomorphic encryption is proposed. First, the face image feature extraction is completed based on a deep learning model. Second, the face features are packaged into ciphertext by using homomorphic encryption and batch processing technology, and the face feature ciphertext is saved in the database of the cloud server. Third, combined with automorphism mapping and Hamming distance, a face feature ciphertext recognition method is designed, which can complete face recognition in the case of ciphertext. Finally, the integrity and consistency of face feature ciphertext recognition results before and after decryption are guaranteed by the one-time MAC authentication method. The whole framework can finish identity recognition without decrypting face feature coding, and the homomorphic ciphertext of face feature coding is saved in the database, so there is no risk of face feature coding leakage. Experiments show that the system has met the requirements of real application scenarios.

1. Introduction

In recent years, with the continuous development of artificial intelligence technology with deep learning as the core, the face recognition system has been widely used in mobile payment, social media, and many other scenes. The wide application of this technology also makes it easy to become the target of malicious attacks. If facial features are directly stored in the database in plaintext, the risk of disclosure of registered users' biometric privacy will be greatly increased, which will seriously affect the security of the authentication system. Therefore, as an authentication system, it is particularly important to develop a solution with stronger protections for biometric data.

The privacy protection of biometric data has always been a research hotspot in academic research. To solve this problem, researchers have proposed many solutions based on different technologies. Belguechi et al. [1, 2] proposed to convert characteristic data into random data by using a hash function or password. This method is practical in performance, but if the user password is broken, it is no longer secure. Fuzzy vault-based approaches [3, 4] bind the user's biometrics with secret information to generate real points and produce the vault by adding a large number of hash points. It can encrypt the biometric template while protecting the biometric information, so it has been widely used [5]. However, due to the invariance of biometrics, it is easy for attackers to obtain real points from the biometric-based fuzzy vault, resulting in the permanent loss of biometric templates.

Fontaine and Galand [6] proposed a homomorphic encryption scheme that can compare and calculate on the ciphertext. This scheme greatly improves the security of data, but due to the use of multiparty computing it needs interactive computing between multiple parties, which reduces the efficiency of computing. Another scheme uses the Paillier

homomorphic encryption system, but the scheme requires that the participants must be honest and credible, and the scheme is limited to a face recognition system [7].

A fully homomorphic encryption (FHE) system supports the arbitrary operation of ciphertext without decryption [8]. This special property makes FHE have a wide range of theoretical and practical applications. An IBM researcher Craig Gentry [9] proposed the first FHE scheme based on bootstrapping technology on an ideal lattice. Although this scheme cannot meet the practical feasibility, it opens a new chapter in the research of homomorphic cryptography. Dijk et al. [10] proposed DGHV algorithm based on integer ring. This algorithm constructs a homomorphic encryption scheme according to the difficulty of approximating GCD (great common divisor) [11], which is transformed into a homomorphic public-key encryption algorithm through simple transformation and then transformed into a fully homomorphic encryption scheme by bootstrap technology. The scheme is simpler than Gentry's ideal lattice scheme, but the operation efficiency is still not high and the storage space of the key still needs to be large. On this basis, Brakerski and others proposed a homomorphic BGV encryption scheme based on integer ring module switching technology, which greatly reduces the storage space of the key and significantly speeds up the operation efficiency [12]. Ducas and Micciancio proposed a new method of homomorphic computing bit [13] operation, which improved the efficiency of calculation to a certain extent. Xiang et al. [14] proposed the privacy protection online face authentication scheme in an outsourcing scenario based on the FHE scheme, which avoids the decryption process with large computational consumption in the homomorphic encryption algorithm. Although there is a great improvement in efficiency, there is still much room for improvement.

FHE-based schemes often require high computational overhead, which is not applicable in some scenarios with high real-time requirements or resource constraints. To address the limitation of the computational complexity, Vishnu et al. [15] proposed a scheme based on FFE, which uses batch processing and dimension reduction methods to decrease the computational complexity, and this achieved good performance. However, in this scheme, the ciphertext authentication result is sent to the client for decryption and is not returned to the server. Therefore, it lacks the verification of the calculation result and cannot be applied to the cloud server scenario.

Therefore, to prevent the client data from being tampered with and further improve the computational efficiency of the whole system, a fully homomorphic encrypted face recognition scheme based on Fan–Vercauteren (FV) scheme is proposed. It does not use trusted hardware and adopts one-time MAC authentication, which well protects the user's face feature template and completes the corresponding face authentication.

In summary, the following contributions are made in this paper: (1) a face recognition security system is designed based on the FHE scheme, batching technology, and Hamming distance (HD) calculation, which greatly improves the efficiency and flexibility of calculation; (2) the one-time MAC authentication method is directly utilized on the server, removing the trusted center for authentication. This scheme ensures the integrity and consistency of face feature ciphertext recognition results before and after decryption; and (3) improved face recognition technology and dimension reduction methods are used to further decrease the computational complexity.

2. Materials and Methods

2.1. FV Fully Homomorphic Encryption Algorithm. The FV scheme in this study is based on the ring $R = Z[x]/(x^n + 1)$. The elements in R are polynomials with integral coefficients of degree less than n, and n is always a power of 2. Let λ be the security level, q the ciphertext module, and t the plaintext module. ω is the base for decomposing the integer coefficients, and $\ell = \lfloor \log_\omega d \rfloor$ means decomposing the integer d into ℓ parts [12]. The algorithm is as follows:

(1) GenKey (λ)

An element $s \leftarrow R_2$ is randomly and evenly selected as the private key in R_2, and then $a_1 \leftarrow R_q$ is randomly and evenly selected in R_q. Meanwhile, an error $e \leftarrow \chi$ is randomly selected from Gaussian distribution χ, and $a_0 = -(a_1 s + e) \bmod q$ is calculated. The output is a private key and public key $(s_k, p_k) = (s, (a_0, a_1))$.

(2) EvKeyGen (s_k, ω)

Let $i \in \{0, \dots \ell\}$ randomly and evenly select the element $a_i \leftarrow R_q$ in R_q, and randomly select the error $e_i \leftarrow \chi$ with Gaussian distribution χ, and output the calculated public key $ev_k = ((-(a_i s + e_i) + \omega^i s_2) \bmod q, a_i)$.

(3) Encrypt (pk, m)

To encrypt the message $m \in R_t$, an element $u \leftarrow R_2$ is randomly and evenly selected from R_2, and the error $e_1, e_2 \leftarrow \chi$ is randomly selected from Gaussian distribution χ. According to the public key, $pk = (a_0, a_1)$, $c_0 = (\Delta m + a_0 u + e_1) \bmod q$, and $c_1 = (a_1 u + e_2) \bmod q$ are calculated, and the ciphertext $c_t = (c_0, c_1)$ is output.

(4) Decrypt (s_k, c_t)

According to the ciphertext $t = (c_0, c_1)$, using the private key $s_k = s$, $m' = ((t/q \times (c_0 + c_1 s)) \bmod q) \bmod t$ is calculated.

(5) Add (c_{t0}, c_{t1})

Input the two ciphertexts c_{t0}, c_{t1}, and output the sum of $c_{t0} + c_{t1}$ by calculating $(c_{t0}[0] + c_{t1}[0], c_{t0}[1] + c_{t1}[1])$.

(6) Mul (c_{t0}, c_{t1})

Input c_{t0}, c_{t1}, and output the product $c_{t0} \times c_{t1}$ of the two ciphertexts by calculating as follows: $c_0 = [t/q(ct_0[0]ct_1[0])]_q$, $c_1 = [t/q(ct_0[0]ct_1[1] + ct_0[1]ct_1[0])]_q$, $c_2 = [t/q(ct_0[1]ct_1[1])]_q$, $c_2 = \sum_{j=0}^{l} c_2^{(j)} w^j$.

Then calculate: $c_0' = c_0 + \sum_{j=1}^{l} a_0[j][0]c_2^j$, $c_1' = c_1 + \sum_{j=1}^{l} a_1[j][1]c_2^j$.

Finally, (c_0', c_1') is the product of the two ciphertexts $c_{t0} \times c_{t1}$.

2.2. Batch Processing and Automorphism Mapping.

The main bottleneck of encrypted face matching is the number of homomorphic multiplications needed to calculate face similarity. To improve the processing efficiency, batch processing technology is used in this study, which utilizes Chinese remainder theorem (CRT) and single instruction multiple data (SIMD) [9, 16], n numbers can be packed into a plaintext polynomial, and the operation on this polynomial is the same as on n numbers in plaintext slot. It is conditional to use batch processing: the plaintext module t is prime, $t = 1 (\mathrm{mod}\ 2n)$. Under this condition: $\zeta \in Z_t$ makes $\zeta^{2n} = 1 (\mathrm{mod}\ t)$, and $\forall m, 0 < m < 2n$, there is $\zeta^m \neq 1 (\mathrm{mod}\ t)$. It is called the $2n$-th primitive unit root of the module t. So we have

$$x^n + 1 = (x - \zeta)(x - \zeta^3)\ldots(x - \zeta^{2n-1})(\mathrm{mod}\ t). \quad (1)$$

According to the Chinese remainder theorem, a ring can be decomposed into two parts:

$$R_t = \frac{Z_t[x]}{(x^n + 1)} = \frac{Z_t[x]}{\prod_{i=0}^{n-1}(x - \zeta^{2i+1})} \overset{CRT}{\cong} \prod_{i=0}^{n-1} \frac{Z_t[x]}{(x - \zeta^{2i+1})} \cong \prod_{i=0}^{n-1} Z_t[\zeta^{2i+1}] \cong \prod_{i=0}^{n-1} Z_t. \quad (2)$$

All above isomorphisms are over rings, which means that both sides of the equation keep the structure of addition and multiplication. The rightmost $\prod_{i=0}^{n-1} Z_t$ can be expressed as $Z_t \times Z_t \times \ldots \times Z_t$. As a result, the addition of the two vectors on the right is actually to perform the same operation of n corresponding elements. Based on additive homomorphism, the corresponding left is only one addition of two polynomials on R_t. Similarly, multiplication is homomorphic. Let $g_i = \zeta^{2i+1}$, we can get the unpacking:

$$R_t \longrightarrow \sum_{i=0}^{n-1} Z_t, q(k) \longrightarrow [q(k_0)q(k_1),\ldots,q(k_{n-1})]. \quad (3)$$

In the same way, the opposite operation is also called packing. Automorphism is a method that can replace the plaintext corresponding to each plaintext slot. If the plaintext is $q(k)$, the corresponding plaintext with each plaintext slot is $q(k_0), q(k_1), \ldots, q(k_{n-1})$. When Frobenius automorphism mapping is used, we can make $q(k) \longrightarrow q(k^{2^i})$ move i plaintext slots circularly. When $i = 2$, for instance, the plaintext slot of $m(\alpha)$ circularly moves two steps, and the corresponding plaintext becomes $q(k_2), q(k_3), \ldots, q(k_{n-1}), q(k_0), q(k_1)$ [17]. Therefore, we can use batch processing technology and automorphism mapping to make the plaintext move circularly in the ciphertext environment.

2.3. Facial Feature Coding.

Facial feature representation is an important part of homomorphic face security authentication. The face recognition algorithm based on deep learning has achieved very high recognition accuracy with the support of the powerful computing and storage capacity of the server. However, due to the limitation of hardware resources and the lack of computing and storage capacity, these excellent models cannot achieve good results when transplanted to the mobile terminal. To apply the face security recognition model based on deep learning to the mobile terminal and make it more widely used in real-life scenes, this paper proposes a method of combining the lightweight network MobileNet and the high-precision face recognition model FaceNet [18, 19] and uses the lightweight network as the basic network of FaceNet model as well as softmax loss and center loss as comprehensive loss functions for training [20].

2.3.1. Face Feature Extraction Model.

FaceNet [18] is one of the most excellent algorithms for face recognition at present. It does not need face alignment and other preprocessing operations on the image and directly learns the feature representation from the original pixel value. Its model structure is shown in Figure 1, and FaceNet uses the inception model as the basic network model and achieves very good results. However, this network model has a deep network level, many parameters, and a large model, so it cannot achieve ideal results when transplanted to the mobile device. MobileNet is a lightweight network using deep separable convolution. Depth separable convolution decomposes the standard convolution into depth convolution and point convolution, which play the role of filtering and linear combination, respectively, and reduce the number of parameters and calculations. To reduce the model parameters, this paper uses MobileNet instead of the inception model as the basic network of FaceNet.

2.3.2. Loss Function.

The innovation of FaceNet is to remove softmax, the last classification layer of the network structure, and uses the triple loss as the loss function, which can achieve very good results. However, the choice of tuples has a great impact on the model. A good choice of tuples can converge quickly. On the contrary, it is difficult to converge and cannot achieve the ideal effect. Therefore, it is often difficult to use the triple loss for training. In this paper, softmax loss function-weighted and center loss function-weighted training are used to make the feature distance between similar classes closer and the feature distance between different classes longer, to learn more distinguishing and generalization features.

The formula of center loss (LC), where x_i represents the feature, before the full connection layer, and y_i represents the center of the category, is as follows:
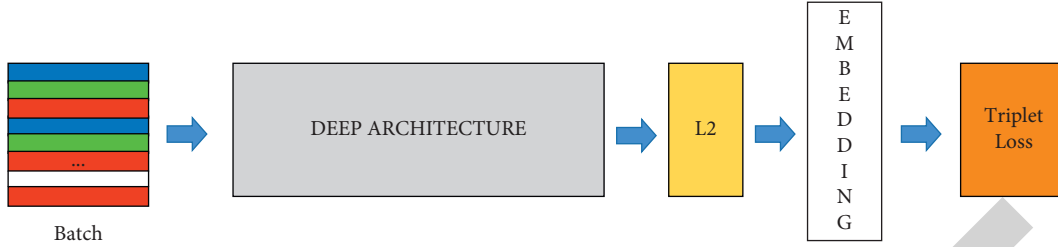
Figure 1: Network structure of FaceNet.

$$LC = \frac{1}{N} \sum_{i=1}^{N} \left| x_i - c_{y_i} \right|_2^2. \tag{4}$$

The gradient of LC and the update formula of the category center c_{y_i} are as follows:

$$\frac{\partial L\,C}{\partial x_i} = x_i - c_{y_i},$$

$$\Delta c_j = \frac{\sum i = 1_m \delta(y_i = y).(c_j - x_i)}{1 + \sum_{i=1}^{m} \delta(y_i = j)}. \tag{5}$$

When using softmax loss (LS) and center loss as the total loss for training, the parameter λ is used to control the ratio of two. The total loss function is shown in the following equation:

$$L_{total} = LS + \lambda LC = -\sum_{i=1}^{m} \log \frac{e^{W_{y_i}^T + b_{y_i}}}{\sum_{j=1}^{n} e^{W_j^i x_i + b_j}} + \frac{\lambda}{2} \sum_{i=1}^{m} \left\| x_i - c_{y_i} \right\|_2^2. \tag{6}$$

2.4. MAC Authentication Research.

After computing the HD of the ciphertext, the cloud server sends the result to the client that will decrypt the plaintext and return the result to the cloud server. There is a security problem, which is how to ensure that the result received by the cloud server is the decryption result of the ciphertext transmitted to the user. To solve this security problem, message authentication code (MAC) is used.

The MAC generally uses cryptographic hash functions such as MD5 and SHA-1 to confirm that the message comes from the specified sender and has not been tampered with [21, 22]. However, this paper needs to verify the binary data decrypted by the front end on the cloud server. Therefore, we develop a one-time MAC authentication algorithm, that is, the cipher generated by the message authentication code can only be used once. The specific scheme description is given below:

MkGen (Z_J): let the message key $m_k = (r_0, r_1)$ and r_0 and r_1 be randomly selected from Z_J, where Z_J is composed of J-bit integers

MacGen (m_k, m): authentication code of the message m be calculated through $m_c = m \times r_0 + r_1$

Verification (m_k, m, m_c): verify whether m is equal to $(m_c - r_0)/r_1$ by inputting a key m_k, message m, and message authentication code m_c, and output authentication result $b \in \{0, 1\}$. If b is 1, the authentication succeeds, and message m has not tampered with; otherwise, the authentication fails and the message x has tampered with.

2.5. Ciphertext Recognition Method.

The face recognition method in this study compares the encoded face feature templates by calculating HD. It takes the number of different corresponding bits on two feature codes as the distance between them [23]. The smaller the distance, the better the matching of the two templates.

Suppose $A = (a_1, a_2, \ldots, a_n)$ and $B = (b_1, b_2, \ldots, b_n)$ denote two binary vectors of length n, as the initial template. HD can be obtained by calculating the sum of XORs of two vectors, that is:

$$\text{Ham}(A, B) = \sum_{i=1}^{n} a_i \oplus b_i. \tag{7}$$

To prevent the user's biometric information from being leaked in the identity authentication service, we use the characteristics of homomorphic encryption technology to design a recognition method based on the facial ciphertext. First, this paper aims to test the homomorphism performance by converting XORs into a combination of multiplication and subtraction while calculating HD. Second, because the FHE method is based on ring R, it is necessary to encode the facial feature template into integer polynomial. In this paper, the feature extracted from the face image based on the deep learning method is a binary vector with length n calculating the HD between two face image features requires at least N times of multiplication. However, the multiplication time between face feature ciphertexts after homomorphic encryption is very long, which will increase the computational complexity of the system.

Therefore, we develop batch processing technology to package the binary vector with length n into a polynomial, only one subtraction and one multiplication can complete the XOR calculation of the vector. At the same time, using the characteristics of automorphism mapping, the sum of elements in the homomorphic ciphertext slot can be calculated by only $\log 2^n$ shifts and $\log 2^n$ additions, that is, HD of ciphertext can be calculated. Assume the vector $I = (2, 6, 3, 7)$, and its corresponding homomorphic ciphertext is $I' = (I_1, I_2, I_3, I_4)$. Because the length of the slot is four, operations of $\log 2^4$ shifts and $\log 2^4$ additions are needed, here $(I_1, I_2) = (2^0, 2^1)$. Figure 2 shows the illustration.
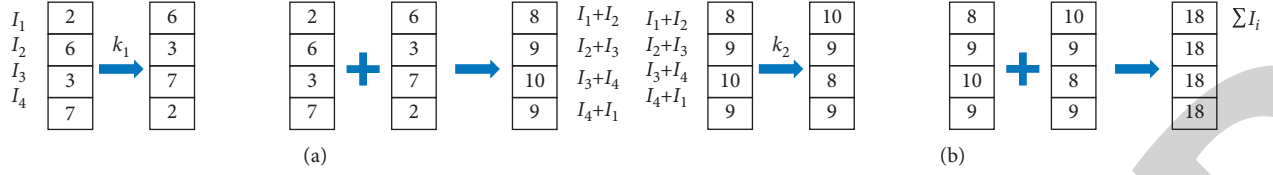
FIGURE 2: Illustration for homomorphic ciphertext slot element summation operation. (a) First shift and addition operation in homomorphic encryption slot. (b) Second shift and addition operation in homomorphic encryption slot.

To sum up, the face recognition method mainly includes the following steps:

Step 1. The binary features A and B of two face images are packaged into plaintext polynomials: BP_A and $BP_B \in R_t$, $(BP_A, BP_B) \leftarrow (Compose(A), Compose(B))$.

Step 2. The plaintext polynomials BP_A and BP_B are encrypted by homomorphism, and the ciphertext polynomials are output: ct_A and $ct_B \in R_q \times R_q$, $(ct_A, ct_B) \leftarrow (Encry(A), Encry(B))$

Step 3. ct_A and ct_B are sent to the cloud server S: $(ct_A, ct_B) \longrightarrow [S]$:

Step 4. Calculate the HD between ct_A and ct_B: $Ham(ct_A, ct_B) = \sum_{i=1}^{n}(ct_A - ct_B)^2$.

2.6. Ciphertext Feature Authentication Protocol. In this study, we use homomorphic encryption to encrypt the biometric template and store the ciphertext, then measure the similarity by calculating HD between the two ciphertext features, and finally authenticate by one-time MAC authentication. The overall authentication protocol of the system is shown in Figure 3. The overall protocol includes two parts: registration and authentication.

2.6.1. Registration. At this stage, the user extracts feature vectors from many face images and encrypts them. The specific processing process is as follows: (1) the private key and public key (sk, pk) are generated using the GenKey algorithm; (2) n face images of a registered user are acquired, and the face feature vector Fea is extracted with our method based on deep learning, and n represents the number of samples of registered users; (3) the Fea is packaged into polynomial BP_{Fea} through batch processing technology; (4) BP_{Fea} is encrypted and ciphertext ct_{Fea} is generated using pk, and (5) the ciphertext ct_{Fea} and identity label U_{lab} of the registered user are sent to the server. The public key pk, the ciphertext ct_{Fea}, and identity label U_{lab} are stored in the database.

2.6.2. Authentication. During this stage, user face authentication is completed through the following process: (1) the current user's facial image is captured, and the facial feature is extracted and represented as y; (2) y is packaged into polynomial BP_y through batch processing technology; (3)

1.[U]	$(sk, pk) \leftarrow KeyGen(\lambda)$
	$ct_{Fea} \leftarrow Encrypt(BP_{Fea} \leftarrow Package(Fea))$
2.[U→S]	(U_{id}, ct_{Fea})
3.[U←S]	Data stroage
4.[U]	$ct_y \leftarrow Encrypt(BP_y \leftarrow Package(y))$
5.[U→S]	(U_{id}, ct_y)
6.[S]	$Ct_d = Ham(ct_{Fea}, ct_y)$
	$mk \leftarrow MKGen(Z_I)$
	$Ct_T \leftarrow MACGen(mk, ct_d)$
7.[U←S]	(Ct_d, Ct_T)
8.[U]	$d \leftarrow Decompose(BP_d \leftarrow Decrypt(Ct_d))$
	$T \leftarrow Decompose(BP_T \leftarrow Decrypt(Ct_T))$
9.[U→S]	(d, T)
10.[S]	$b \leftarrow Verification(mk, d, T)$
11.[U←S]	$B \in \{0, 1\}$
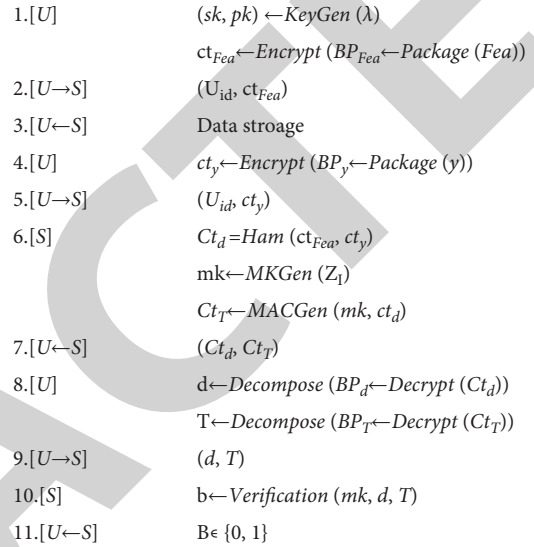
FIGURE 3: Ciphertext feature authentication protocol diagram.

BP_y is encrypted, and the ciphertext ct_y is generated; (4) then, the authentication request (U_{id}, ct_y) is transmitted to the server; (5) HD Ct_d between ciphertext ct_{Fea} and ct_y is calculated (equation (7)); (6) the server randomly selects (r_0, r_1) from the Z_I, outputs the message key $mk = (r_0, r_1)$, and calculates the message authentication code ct_T of the HD by $ct_T = ct_d \times r_0 + r_1$, (7) the server sends (ct_d, ct_T) to the client; (8) on the client, (ct_d, ct_T) is decrypted using the private key sk; (9) the decryption result is unpacked to generate the plaintext (d, T); (10) (d, T) is sent to the server; (11) on the server, the authentication result b is output and it is sent to the client by verifying whether d is equal to $(T - r_0)/r_1$; and (12) when the received data is equal to one, the authentication result is not tampered; otherwise, the result is modified.

3. Experiments

To verify the effectiveness of the face encryption scheme based on FHE in this paper, our scheme adopts browser/server mode. The front end mainly uses our improved FaceNet-Mobile deep learning model to extract users' facial features and provide users with registration service. The server has rich processing resources and sufficient storage capacity and can calculate the distance of the face feature vector under ciphertext to provide homomorphic operation and authentication services.

Table 1: Face recognition accuracy.

Data set	Method	FaceNet + Mobi 128-D			Origin FaceNet 128-D			PCA FaceNet 64-D		
		0.01%	0.1%	1%	0.01%	0.1%	1%	0.01%	0.1%	1%
LFW	No FHE	82.62	93.47	97.25	84.12	94.62	98.67	84.01	94.56	98.75
	FHE (2.5×10^{-3})	83.48	93.38	97.25	84.09	94.62	98.67	84.01	94.56	98.72
	FHE (1.0×10^{-2})	81.65	93.42	97.16	83.90	94.60	98.65	83.94	94.62	98.72
	FHE (1.0×10^{-1})	77.72	91.37	97.21	79.12	92.39	98.36	78.16	92.86	98.40
IJB-A	No FHE	21.15	43.87	68.32	23.32	45.76	70.72	20.15	45.97	73.69
	FHE (2.5×10^{-3})	21.12	43.94	68.27	23.26	45.80	70.68	20.06	46.02	73.60
	FHE (1.0×10^{-2})	20.91	42.78	68.15	22.67	45.69	70.23	19.78	45.93	73.70
	FHE (1.0×10^{-1})	18.67	41.53	67.26	19.61	41.98	69.01	17.48	43.80	72.08
IJB-B	No FHE	24.36	47.06	72.61	25.80	48.26	74.51	24.70	47.83	74.61
	FHE (2.5×10^{-3})	24.52	46.97	72.59	25.77	48.27	74.46	24.67	47.86	74.59
	FHE (1.0×10^{-2})	24.42	46.96	72.61	25.69	48.20	74.39	24.68	47.80	74.59
	FHE (1.0×10^{-1})	22.68	45.18	71.70	23.68	46.01	72.56	22.52	45.67	73.08
CASIA	No FHE	68.12	82.50	91.16	70.87	84.67	93.25	70.85	84.68	93.40
	FHE (2.5×10^{-3})	68.12	82.50	91.16	70.87	84.67	93.25	70.83	84.71	93.41
	FHE (1.0×10^{-2})	68.09	82.47	91.12	70.85	84.66	93.23	70.89	84.70	93.37
	FHE (1.0×10^{-1})	68.07	82.45	91.09	70.80	84.65	93.21	70.86	84.68	93.36

3.1. Development Environment. This system uses Python Flash Web framework to implement B/S architecture, Intel Core i7-6700HQ processor, and the Python Tensorflow module to realize face detection, face alignment, and face feature vector extraction under deep learning. The homomorphic encryption algorithm library uses the SEAL library, which does not need external dependencies and is easily compiled under many different development tools. Presently, the encryption operations supported in SEAL library include negation, addition, accumulation, subtraction, multiplication, cumulative multiplication, power square, ciphertext plus plaintext, and ciphertext plus plaintext. The front end and back end of the web are realized by the Python web module and MySQL database. It mainly realizes the functions of user file upload, calling camera to take photos in real time, user ciphertext feature vector database management, face comparison result, ciphertext decryption display, and so on.

3.2. Computing Performance Analysis. In this scheme, FHE needs to encode the face features into integers before operation. Therefore, three different quantization schemes are designed for the coding of face eigenvalues, with coding accuracies of 0.1, 0.01, and 0.025. Two models—our Face-Net-Mobile and origin FaceNet [18]—are used for face matching tests on benchmark data sets (LFW [24], IJB-A [25], IJB-B [26], and CASIA [27]). The experimental result evaluation takes the unencrypted face feature matching performance as the benchmark. Table 1 provides a list of the correct acceptance rate when the false acceptance rates are 0.01%, 0.1%, and 1.0%. We can observe that when the coding accuracy is 0.0025, its accuracy can reach the level of unencrypted face features. At the same time, it can be seen from Table 1 that the accuracy of our model trained with softmax loss and center loss using the lightweight network as the basic network is slightly lower than that of the original network, but the complexity is greatly reduced.

The complexity of the model is analyzed from the aspects of calculation amount and model size. Table 2 shows the experimental results. The model size refers to the size after saving the model as a PB file. According to Table 2, the model based on MobileNet proposed in this paper reduces the number of parameters by three times compared with the original FaceNet model and the improved model based on conception ResNet v1. Similarly, the model size is greatly reduced to meet the operation requirements of the mobile terminal. Therefore, while providing face template protection, preventing information leakage, and protecting user privacy, the matching based on homomorphic face can achieve the performance of matching with the original facial features. Finally, the experimental results also show that, even after using the dimension reduction method of classical PCA, its performance is the same as the original high-dimensional face features, but the matching efficiency of the homomorphic faces is improved.

3.3. Parameter Optimization. Using the SEAL library for homomorphic encryption will produce some noise, and with the improvement of security level, the noise of ciphertext will also increase. If the total noise is greater than the threshold, the system cannot decrypt correctly. So, we must first ensure that the ciphertext can be decrypted successfully and then consider improving the security level of authentication.

For encrypting binary data with a length of 1024 bits, according to the homomorphic encryption principle, the transformed polynomial degree m must be greater than 1024. Yet if the value of m is too large, the calculation time of ciphertext will be very long. To solve this, this paper studies the partition of a 1024-bit binary vector. The minimum $\log_2 q$ is given in Table 3 under the completion of ciphertext HD calculation at different intervals.

Table 3 shows the reduction of ciphertext module after segmentation is small; therefore, this method cannot remarkably improve the system's efficiency and security. At

Table 2: Comparison of model complexity.

Model	Number of parameters (Million)	Model size (MB)
FaceNet (MobileNet)	1.25	4.1
FaceNet (origin)	6.47	59
FaceNet (Inception V1)	6.47	89

Table 3: Comparison of $(m, \log_2^q)$ values under a different number of segments.

Subsection	m	$(\log_2^q)_{\min}$
8	128	63
4	256	65
2	512	66
1	1024	67

Table 4: Comparison of $(n, \log_2^q)$ values under 80 bit security level.

n	$(\log_2^q)_{\max}$
1024	47.2
2048	95.4
4096	192
8192	391.1
16384	799.2

the same time, Table 4 gives the maximum value of $\log_2 q$ for $n = 1024, 2048, 4096, 8192, 16384$ in the case of 80-bit security level [22]. Based on the data in Table 3 and Table 4, the parameters $m = 2048$ and $q = 2^{76} - 2^{22} + 1$ are selected. At this time, the noise growth of the ciphertext after completing the HD calculation does not exceed the upper limit of noise while the safety level is above 80 bits.

3.4. Safety Analysis. The system mainly includes three possible attack sources: (1) front end, (2) communication channel, and (3) cloud server. Our B/S architecture ensures the higher security of the front end because the location of its facial feature template and private key cannot be fixed, which makes it more difficult for attackers to obtain these data; if the attacker wants to edit the front-end authentication results, the one-time MAC authentication used in this paper can well avoid this problem. In the communication channel, the attacker can only get the facial feature data based on FHE. So, network attackers could not utilize the intercepted data to decode the facial feature code before encryption. The database of the cloud server stores the user's fully homomorphic encrypted feature template data and user label data. If the attacker cannot get the private key, the server is also secure.

4. Conclusion

Aiming at the problem that sensitive data are easy to be leaked in the face authentication system, this paper proposes a safe and efficient privacy protection face authentication scheme. The system combines homomorphic encryption technology with improved face recognition technology, which ensures the security and integrity of the user face feature template and keeps the accuracy of the feature comparison of ciphertext. From the performance, we can see that the fully homomorphic encryption does not have a great influence on the matching of face feature templates. After our optimization, the computation time of the ciphertext feature vector is greatly reduced. This efficiency can be used in practice, which provides a good guide for the practice of homomorphism. However, in the complex application scenario, further research and optimization are needed.

Data Availability

Readers can access our data on the findings by sending an email to the corresponding author.

Conflicts of Interest

The authors declare that they have no conflicts of interest.

Acknowledgments

References

[1] R. Belguechi, E. Cherrier, and V. Alimi, "An overview on privacy preserving biometrics," *Recent Application in Biometrics. Croatia*, , pp. 65–84, InTech, 2014.

[2] N. K. Ratha, J. H. Connell, and R. M. Bolle, "Enhancing security and privacy in biometrics-based authentication systems," *IBM Systems Journal*, vol. 40, no. 3, pp. 614–634, 2001.

[3] A. Juels and M. Sudan, "A fuzzy vault scheme," *Designs, Codes and Cryptography*, vol. 38, no. 2, pp. 237–257, 2006.

[4] S. Zeng, J. Zhou, C. Zhang, and J. M. Merigó, "Intuitionistic fuzzy social network hybrid MCDM model for an assessment of digital reforms of manufacturing industry in China," *Technological Forecasting and Social Change*, vol. 176, p. 121435, 2022.

[5] M. Wattenberg and M. Wattenberg, "A fuzzy commitment scheme," in *Proceedings of the ACM. Conference on Computer and Communications Security*, pp. 28–36, Kent Ridge Digital Labs Singapore, Singapore, November, 1999.

[6] C. Fontaine and F. Galand, "A survey of homomorphic encryption for nonspecialists," *EURASIP Journal on Information Security*, vol. 15, p. 2007, 2007.

[7] Z. Erkin, M. Franz, J. Guajardo, S. Katzenbeisser, I. Lagendijk, and T. Toft, "Privacy-preserving face recognition," *Privacy Enhancing Technologies*, vol. 5672, pp. 235–253, 2009.

WILEY | Hindawi

Retraction

Retracted: Fixed Point of Rational Contractions and Its Application for Secure Dynamic Routing in Wireless Sensor Networks

Security and Communication Networks

This article has been retracted by Hindawi following an investigation undertaken by the publisher [1]. This investigation has uncovered evidence of one or more of the following indicators of systematic manipulation of the publication process:

(1) Discrepancies in scope

(2) Discrepancies in the description of the research reported

(3) Discrepancies between the availability of data and the research described

(4) Inappropriate citations

(5) Incoherent, meaningless and/or irrelevant content included in the article

(6) Peer-review manipulation

The presence of these indicators undermines our confidence in the integrity of the article's content and we cannot, therefore, vouch for its reliability. Please note that this notice is intended solely to alert readers that the content of this article is unreliable. We have not investigated whether authors were aware of or involved in the systematic manipulation of the publication process.

Wiley and Hindawi regrets that the usual quality checks did not identify these issues before publication and have since put additional measures in place to safeguard research integrity.

We wish to credit our own Research Integrity and Research Publishing teams and anonymous and named external researchers and research integrity experts for contributing to this investigation.

The corresponding author, as the representative of all authors, has been given the opportunity to register their agreement or disagreement to this retraction. We have kept a record of any response received.

References

[1] A. Asif, E. Savas, H. AlSalman, M. Arshad, A. Gumaei, and A. Rehman, "Fixed Point of Rational Contractions and Its Application for Secure Dynamic Routing in Wireless Sensor Networks," *Security and Communication Networks*, vol. 2021, Article ID 9939546, 10 pages, 2021.

WILEY | Hindawi

Research Article

Fixed Point of Rational Contractions and Its Application for Secure Dynamic Routing in Wireless Sensor Networks

Awais Asif,[1] Ekrem Savas,[2] Hussain AlSalman [ID],[3] Muahammad Arshad,[1] Abdu Gumaei [ID],[4] and Abdul Rehman[5]

[1]*Department of Math and Stats, International Islamic University Islamabad, Islamabad 44000, Pakistan*
[2]*Department of Mathematics, Usak University, Amkara, Turkey*
[3]*Department of Computer Science, College of Computer and Information Sciences, King Saud University, Riyadh 11543, Saudi Arabia*
[4]*Computer Science Department, Faculty of Applied Sciences, Taiz University, Taiz 6803, Yemen*
[5]*Department of Computer Science and, Kyungpook National University, Daegu 41566, Republic of Korea*

Correspondence should be addressed to Abdu Gumaei; abdugumaei@gmail.com

Security is one of the major concerns for data communication over wireless sensor networks (WSNs). Dynamic routing algorithms can provide small similarity paths of data delivery between two consecutive transmitted packets, improving data security without adding extra information or control messages. This article illustrates the iteration of the fixed point (FP) of rational contractions and generalized Banach contractions (BC) in the setting of *F*-metric space (F-MS). It also describes an FP of the said mappings, while restricting the imposition of the contraction only to a subset of the F-MS, the closed ball, rather than executing it on the entire F-MS. The results have been verified and supported by concise examples. Further, the application of the functional equation proved results with randomization is given to find a solution for secure dynamic routing of data transmission in WSNs. The application is a tool to analyze and model a network structure in which sensors can be deployed with high security and low risk in a greater region (sensor field), thus boosting the accuracy.

1. Introduction and Preliminaries

The idea of metric space is extended and generalized by many authors in different ways (see [1–8]). Getting motivation from Wardowski's *F*-contraction, an interesting generalization was put forwarded by Jleli [8], which he named as *F*-metric space (F-MS). He proved fixed point results of Banach contractions (BC) in the frame of F-MS and defined the topological properties in the new given setting. Following this conception, various authors (see [8–13]) furthered this idea by presenting their fixed point (FP) models in F-MS, and a new and more discussion was initiated on the topic.

In continuation to this, our paper focuses on the advancement of the said F-MS, and we prove certain FP and typical FP results in F-MS. Also, following the concept of the closed ball in generalized metric spaces (for discussion on closed ball, see [13–17]), we will present both FP and typical

FP results for rational contractions and Banach contractions, which are imposed only on a subset that is closed ball for the whole F-MS. With the help of examples, the difference between locally contractive and globally contractive mappings and their outcomes will be explained.

Section 1 of this manuscript defines the basic notions and definitions that will be used or referred to in our paper. Section 2 of the article is dedicated to the Banach as well rational contractions and its investigation for FP in F-MS, while Section 3 of the paper revises the same results for the structure of the closed ball. Section 4 presents the application of our results. The role of the functional equation in solving many real-world problems is inevitable. Besides the application discussed in the abstract, the functional equation approach may be executed to construct the algorithm that finds the solution point in no more than steps equal to N−1 for a network having *N* nodes (see [18]). Also, the functional equations enable multistage decision-making and

lead to water security sustainability evaluation (see [19]). Therefore, the importance and contribution of our work are not limited to what we have discussed in this Section 4 of our article. It can apply to stochastic processes, economics, classical mechanics, dynamic programming, computer graphics, game theory, neural networks, artificial intelligence, fuzzy set theory, decision theory, digital image processing, multivalued logic, and many other fields. At last, the work done in this paper is concluded in the Conclusion section. Following are related and relevant to the main study of our work.

Definition 1 (see [8]). Suppose G is a family of mappings $g: (0, +\infty) \longrightarrow R$ with the following constraints:

(F1) g be a nondecreasing mapping, i.e., $0 < q < s \Longrightarrow g(q) \leq g(s)$

(F2) For every sequence $u_n \subset (0, +\infty)$, we have

$$\lim_{n \longrightarrow \infty} u_n = 0 \Longleftrightarrow \lim_{n \longrightarrow \infty} g(u_n) = -\infty. \quad (1)$$

Definition 2 (see [8]). Suppose a set $E \neq \varnothing$ and a map $d: E \times E \longrightarrow [0, \infty)$. as well as suppose there is some $(g, \sigma) \in tGn \times q[0, +\infty)$ in which

Distance (d1) $(q, s) \in E \times E$, $d(q, s) = 0 \Longleftrightarrow q = s$ and $(q, s) \in E \times E$, $d(q, s) = d(s, q)$

Distance (d2) $(q, s) \in E \times E$, $d(q, s) = d(s, q)$

Distance (d3) For each $(q, s) \in E \times E$, and for all $N \ni \prime N \prime \geq 2$, as well as for each $(u_i)_{i=1}^n \subset E$ with $(u_1, u_{N_\prime}) = (q, s)$, we have

$$(q, s) > 0 \Longrightarrow g(d(q, s)) \leq g\left(\sum_{i=1}^{N'-1} d(u_i, u_{i+1})\right) + \sigma. \quad (2)$$

Then, (E, d) is called an F-metric space (F-MS)

Example 1 (see [8]). Let $E = N$ and $d: E \times E \longrightarrow (0, \infty)$ be given as

$$d(q, s) = \begin{cases} (q - s)^2 \, if \, (q, s) \in [0, 3] \times [0, 3], \\ |q - s| \, if \, (q, s) \notin [0, 3] \times [0, 3]. \end{cases} \quad (3)$$

For each $(q, s) \in E \times E$, then d is an F-metric space (F-MS).

Example 2 (see [8]). Assuming $E = N$ and distance (d): $E \times E \longrightarrow (0, \infty)$ is given as

$$d(q, s) = \begin{cases} 0, & if \, q = s, \\ e^{|q - s|}, & if \, q \neq s. \end{cases} \quad (4)$$

For each $(q, s) \in E \times E$, then d is an F-metric space (F-MS).

Definition 3 (see [8]). Let $(q_n) \in E$. If

(i) $\lim_{n \longrightarrow \infty} d(q_n, q) = 0$ for some $q \in E$, at this point (q_n) will be F-convergent to q

(ii) $\lim_{n,m \longrightarrow \infty} d(q_n, q_m) = 0$, then the sequence (q_n) F-Cauchy

(iii) (E, d) is said to be F-complete if for every $(q_n) \subset E \Longrightarrow (q_n)$

Definition 4 (see [8]). Let (E, d) an F-metric space (F-MS). A set $O \subset E$ is an F-metric open (F-MO) if and only if for each $q \in O$, there is a number $\sigma > 0$ provided that $B(q, \sigma) \subset O$, and

$$B(q, \sigma) = \{s \in E: d(q, s) < \sigma\}. \quad (5)$$

While a subset C from the set E is an F-metric closed (F-MC) whenever E or C is an F-open.

Definition 5 (see [8]). Let $\phi \neq B \subset E$, and distance (d) be an F-metric space (F-MS); then, the subsequent rules are equivalent:

(i) B is an F-MC

(ii) For every $(q_n) \subset B$, we have

$$\lim_{n \longrightarrow \infty} d(q_n, q) = 0, \, q \in E \Longrightarrow q \in B. \quad (6)$$

For convenience, we write only E rather than (E, d) for an F-MS. For a complete F-MS, we will write CF-MS.

Theorem 1 (see [8]). *Let h be a self-mapping on a CF-MS E and $k \in (0, 1)$ such that*

$$d(h(q), h(s)) \leq k \, d(q, s), \, (q, s) \in E \times E. \quad (7)$$

Then, $h q^* = q^*$ for a unique $q^* \in E$. Further, for any $q_0 \in E$, the sequence $(q_n) \subset E$ defined by $q_{n+1} = h(q_n)$, $n \in N$, is F-convergent to q^*.

Theorem 2 (see [8]). *Let (E, d) is a complete MS and h is a self-mapping on E such that*

$$d(h(q), h(s)) \leq \alpha \, d(q, s) + \beta \, d(q, h(s)) + \gamma \, d(q, h(s)). \quad (8)$$

For all q and $s \in E$, where α, β, and γ are nonnegative numbers satisfying $\alpha + \beta/1 - \gamma < 1$, then h has a unique fixed point in E.

Lemma 1 (see [8]). *Let $(B(W), \| \cdot \|)$ be a Banach space and distance (d) is stated by*

$$d(J, h) = ||J - h|| = \max_{q \in W} |J(q) - h(q)|, J, h \in B(W). \quad (9)$$

Then, $(B(W), \| \cdot \|)$ will be an F-MS.

2. Fixed Points of Generalized Contractions in $F - MS$

This portion of the article illustrates FP and typical FP results of rational type and Banach type contraction in the setting of F-MS. The results have been explained with the help of

concise examples, and some essential corollaries are developed.

Theorem 3. *Assume* $(g, \alpha) \in \mathcal{G} \times (0, \infty)$ *and* (A, d) *is a CF-MS, and suppose* $S, T: A \longrightarrow A$ *be self-mappings such that*

$$d(Ss, Ty) \leq \lambda \, d(s, y). \tag{10}$$

For $\lambda \in [0, \infty)$ and for all $(s, y) \in A \times A$, then there exists a single typical FP of the mappings S and T in A.

Proof. Pick an arbitrary element s_0 and iterate a sequence (s_n) as

$$\begin{aligned} Ss_{2x} &= s_{2x+1}, \\ Ts_{2x+1} &= s_{2x+2}, \\ x &= 0, 1, 2, \dots. \end{aligned} \tag{11}$$

From (12) and (13), we obtain

$$d(s_{2x+1}, s_{2x+2}) = d(Ss_{2x}, Ts_{2x+1}) \leq \lambda \, d(s_{2x}, s_{2x+1}). \tag{12}$$

This implies

$$d(s_{2x+1}, s_{2x+2}) < \lambda \, d(s_{2x}, s_{2x+1}). \tag{13}$$

Similarly,

$$d(s_{2x}, s_{2x+1}) = d(Ss_{2x-1}, Ts_{2x}) \leq \lambda \, d(s_{2x-1}, s_{2x}), \tag{14}$$

i.e.,

$$d(s_{2x}, s_{2x+1}) \leq \lambda \, d(s_{2x-1}, s_{2x}). \tag{15}$$

Generalizing this as follows:

$$d(s_n, s_{n+1}) < \lambda \, d(s_{n-1}, s_n) \text{ for all } n \epsilon \mathbb{N}, \tag{16}$$

which yields

$$\begin{aligned} d(s_n, s_{n+1}) &< \lambda \, d(s_{n-1}, s_n) < \lambda^2 d(s_{n-2}, s_{n-1}) \\ &< \cdots < \lambda^n d(s_0, s_1), n \in \mathbb{N}. \end{aligned} \tag{17}$$

Using (16), we can write

$$\begin{aligned} \sum_{k=n}^{m-1} d(s_k, s_{k+1}) &= d(s_n, s_{n+1}) + d(s_{n+1}, s_{n+2}) + \cdots + d(s_{m-1}, s_m) \\ &< \lambda^n \left[1 + \lambda + \lambda^2 + \cdots + \lambda^{m-n-1} \right] d(s_0, s_1) \\ &\leq \frac{\lambda^n}{1 - \lambda} d(s_0, s_1), \quad m > n. \end{aligned} \tag{18}$$

i.e.,

$$\sum_{k=n}^{m-1} d(s_k, s_{k+1}) \leq \frac{\lambda^n}{1 - \lambda} d(s_0, s_1), \quad m > n. \tag{19}$$

Since $\lim_{n \longrightarrow \infty} \lambda^n / 1 - \lambda d(s_0, s_1) = 0$, for any $\delta > 0$, there are some $n' \in \mathbb{N}$ in which

$$0 < \frac{\lambda^n}{1 - \lambda} d(s_0, s_1) < \delta, \tag{20}$$

$$n \geq n'.$$

Further, suppose $(g, \alpha) \in tGn \times q[0, \infty)$ meets (d3) and $\epsilon > 0$ is fixed. By $(F2)$, there exists some $\delta > 0$ where

$$0 < l < \delta \Longrightarrow g(l) < g(\epsilon) - \alpha. \tag{21}$$

By (20) and (21), we write

$$g\left(\sum_{k=n}^{m-1} d(s_k, s_{k+1}) \right) \leq g\left(\frac{\lambda^n}{1 - \lambda} d(s_0, s_1) \right) \tag{22}$$

$$< g(\epsilon) - \alpha, m > n \geq n'.$$

By (d3) and the above equation, we can get

$$d(s_n, s_m) > 0, m > n > n' \Longrightarrow g(d(s_n, s_m)) < g(\epsilon). \tag{23}$$

This shows

$$d(s_n, s_m) < \epsilon, \, m > n \geq n'. \tag{24}$$

Thus, it proved that the sequence (s_n) is F-Cauchy in A. Now, as (A, d) is F-complete, so there must be some element c^* in A and (s_n) converges to c^* i.e.,

$$\lim_{n \longrightarrow \infty} d(s_n, c^*) = 0. \tag{25}$$

Next, we show that c^* is the FP of S. For this,

$$d(Sc^*, s_{2x+2}) = d(Sc^*, Ts_{2x+1}) \leq \lambda \, d(c^*, s_{2x+1}). \tag{26}$$

If limit $x \longrightarrow \infty$, we obtain

$$d(Sc^*, c^*) \leq \lambda . d(c^*, c^*). \tag{27}$$

Thus, $d(Sc^*, c^*) = 0$, i.e., $Sc^* = c^*$.
Similarly, we obtain $Tc^* = c^*$. Hence, $Tc^* = Sc^* = c^*$.
Uniqueness: let c^{**} is also a typical FP of S and T, and $c^* \neq c^{**}$. Then,

$$d(c^*, c^{**}) = d(Sc^*, Tc^{**}) \leq \lambda \, d(c^*, c^{**}), \tag{28}$$

which is a contradiction. Thus, $c^* = c^{**}$.
Taking $S = T$, the following outcome is achieved. $\quad \square$

Corollary 1. *Suppose* $(g, \alpha) \in tGn \times q[0, \infty)$ *and* (A, d) *is an F-complete F-MS and* $S: A \longrightarrow A$ *is a self-mapping such that*

$$d(Ss, Sy) \leq \lambda \, d(s, y). \tag{29}$$

For $\lambda \in (0, \infty)$ and each $(s, y) \in A \times A$, then there exists a single FP of the mappings S in A.

Theorem 4. *Assume* $(g, \alpha) \in tGn \times q[0, \infty)$, (A, d) *is a CF-MS, and* $S, T: A \longrightarrow A$ *are self-maps such that*

$$d(Ss, Ty) \leq \alpha \, d(s, y) + \beta. \frac{(p + d(s, Ss)).d(y, Ty)}{(p + d(s, y))}$$
$$+ \gamma [d(s, Ss) + d(y, Ty)]. \tag{30}$$

For $\alpha, \beta, \gamma,$ and $p \in (0, \infty)$ such that $(\alpha + \gamma)/(1 - \beta - \gamma) < 1$ and for all $(s, y) \in A \times A$, then there exists a single typical FP of the mappings S and T in A.

Proof. Choose an arbitrary element s_0 and iterate a sequence (s_n) as

$$Ss_{2x} = s_{2x+1},$$
$$Ts_{2x+1} = s_{2x+2}; \quad x = 0, 1, 2, \ldots. \tag{31}$$

From (30) and (31), we obtain

$$d(s_{2x+1}, s_{2x+2}) = d(Ss_{2x}, Ts_{2x+1}) \leq \alpha \, d(s_{2x}, s_{2x+1}) + \beta. \frac{(p + d(s_{2x}, Ss_{2x})).d(s_{2x+1}, Ts_{2x+1})}{(p + d(s_{2x}, s_{2x+1}))} + \gamma [d(s_{2x}, Ss_{2x}) + d(s_{2x+1}, Ts_{2x+1})]$$

$$= \alpha \, d(s_{2x}, s_{2x+1}) + \beta. \frac{(p + d(s_{2x}, s_{2x+1})).d(s_{2x+1}, s_{2x+2})}{(p + d(s_{2x}, s_{2x+1}))} + \gamma [d(s_{2x}, s_{2x+1}) + d(s_{2x+1}, s_{2x+2})]$$

$$= \alpha \, d(s_{2x}, s_{2x+1}) + \beta \, d(s_{2x+1}, s_{2x+2}) + \gamma [d(s_{2x}, s_{2x+1}) + d(s_{2x+1}, s_{2x+2})]$$

$$= (\alpha + \gamma) d(s_{2x}, s_{2x+1}) + (\beta + \gamma) d(s_{2x+1}, s_{2x+2}), \tag{32}$$

or

$$(1 - \beta - \gamma) d(S_{2x+1}, S_{2x+2}) \leq (\alpha + \gamma)(S_{2x+1}, S_{2x+2}), \tag{33}$$

which implies that

$$d(s_{2x+1}, s_{2x+2}) \leq \frac{(\alpha + \gamma)}{(1 - \beta - \gamma)} d(s_{2x}, s_{2x+1})$$

$$= \lambda \, d(s_{2x}, s_{2x+1}) \, say \, \frac{(\alpha + \gamma)}{(1 - \beta - \gamma)} = \lambda. \tag{34}$$

Similarly,

$$d(s_{2x}, s_{2x+1}) \leq \lambda \, d(s_{2x-1}, s_{2x}). \tag{35}$$

Continuing the same way, we obtain

$$d(s_n, s_{n+1}) < \lambda \, d(s_{n-1}, s_n). \tag{36}$$

For all $n \in \mathbb{N}$, it yields

$$d(s_n, s_{n+1}) < \lambda \, d(s_{n-1}, s_n) < \lambda^2 d(s_{n-2}, s_{n-1})$$
$$< \cdots < \lambda^n d(s_0, s_1), \, n \in \mathbb{N}. \tag{37}$$

Using (37), we can write

$$\sum_{k=n}^{m-1} d(s_k, s_{k+1}) = d(s_n, s_{n+1}) + d(s_{n+1}, s_{n+2}) + \cdots + d(s_{m-1}, s_m)$$

$$< \lambda^n [1 + \lambda + \lambda^2 + \cdots + \lambda^{m-n-1}] d(s_0, s_1)$$

$$\leq \frac{\lambda^n}{1 - \lambda} d(s_0, s_1), \quad m > n. \tag{38}$$

i.e.,

$$\sum_{k=n}^{m-1} d(s_k, s_{k+1}) \leq \frac{\lambda^n}{1 - \lambda} d(s_0, s_1), \quad m > n. \tag{39}$$

Since $\lim_{n \to \infty} \lambda^n / 1 - \lambda \, d(s_0, s_1) = 0$, for any $\delta > 0$, there exists some $n' \in \mathbb{N}$ such that

$$0 < \frac{\lambda^n}{1 - \lambda} d(s_0, s_1) < \delta \quad n \geq n'. \tag{40}$$

Further, suppose $(g, \alpha) \in \mathcal{G} \times [0, \infty)$ satisfies (d3), and $\epsilon > 0$ is fixed. By (F2), there is some $\delta > 0$ such that

$$0 < l < \delta \Longrightarrow g(l) < g(\epsilon) - \alpha. \tag{41}$$

By (40) and (41), we write

$$g\left(\sum_{k=n}^{m-1} d(s_k, s_{k+1})\right) \leq g\left(\frac{\lambda^n}{1 - \lambda} d(s_0, s_1)\right) \tag{42}$$

$$< g(\epsilon) - \alpha m > n \geq n'.$$

By (d3) and the above equation, we obtain

$$d(s_n, s_m) > 0, \quad m > n > n' \Longrightarrow g(d(s_n, s_m)) < g(\epsilon). \tag{43}$$

This shows

$$d(s_n, s_m) < \epsilon, \quad m > n \geq n'. \tag{44}$$

Thus, it proved that the sequence (s_n) is F-Cauchy in A. Now, as (A, d) is F-complete, so there must be some element c^* in A and (s_n) converges to c^* i.e.,

$$\lim_{n \to \infty} d(s_n, c^*) = 0. \tag{45}$$

Next, we show that c^* is the FP of S:

$$d(Sc^*, s_{2x+2}) = d(Sc^*, Ts_{2x+1}) \le \alpha \, d(c^*, s_{2x+1}) + \beta.\frac{(p + d(c^*, Sc^*)).d(s_{2x+1}, Ts_{2x+1})}{(p + d(c^*, s_{2x+1}))} + \gamma[d(c^*, Sc^*) + d(s_{2x+1}, Ts_{2x+1})]$$

$$= \alpha \, d(c^*, s_{2x+1}) + \beta.\frac{(p + d(c^*, s_{2x+1})).d(s_{2x+1}, s_{2x+2})}{(p + d(c^*, s_{2x+1}))} + \gamma[d(c^*, s_{2x+1}) + d(s_{2x+1}, s_{2x+2})].$$

$$(46)$$

Applying limit $n \longrightarrow \infty$, we obtain

$$d(Sc^*, c^*) \le \alpha.d(c^*, c^*). \qquad (47)$$

Hence, $d(Sc^*, c^*) = 0$, i.e., $Sc^* = c^*$.

Similarly, we obtain $Tc^* = c^*$. Hence, $Tc^* = Sc^* = c^*$.

Uniqueness: if there is another distinct typical FP c^{**} S and T, then

$$d(c^*, c^{**}) = d(Sc^*, Tc^{**}) \le \alpha \, d(c^*, c^{**}) + \beta.\frac{(p + d(c^*, Sc^*)).d(c^{**}, Tc^{**})}{(p + d(c^*, c^{**}))} + \gamma[d(c^*, Sc^*) + d(c^{**}, Tc^{**})]$$

$$= \alpha \, d(c^*, c^{**}) + \beta.\frac{(p + d(c^*, c^*)).d(c^{**}, c^{**})}{(p + d(c^*, c^{**}))} + \gamma[d(c^*, c^*) + d(c^{**}, c^{**})].$$

$$(48)$$

Thus, $(1 - \alpha)d(c^*, c^{**}) \le d(c^*, c^{**})$, and this implies that $d(c^*, c^{**})$, i.e., $c^* = c^{**}$. □

Example 3. Suppose $A = A_x\{6x + 2/3, x \in N\}$, $d(A_x, A_k) = \begin{cases} 0 & \text{if } A_x = A_k \\ e^{|A_x - A_k|} & \text{if } A_x \ne A_k \end{cases}$, $g(A_x) = -1/\sqrt{A_x}$, and $S, T: A \longrightarrow A$ are defined by

$$TA_x = \begin{cases} A_1, & \text{if } x = 1, 2 \\ A_{x-1}, & \text{if } x > 2, \end{cases}$$

$$SA_x = \begin{cases} A_1, & \text{if } x = 1, \\ A_2, & \text{if } x = 2, \\ A_{x-2}, & \text{if } x > 4. \end{cases} \qquad (49)$$

One can easily verify that d is an F-metric and g satisfies $(F1) - (F2)$. Suppose $x \ne k$, $\alpha = e^{-1/2}$, and $\beta = \gamma = 0$; then,

$$d(SA_x, TA_k) = e^{|A_{x-2} - A_{k-1}|} = e^{|2(x-k)-2|} < e^{-\frac{1}{2}}.e^{|2(x-k)|} = \alpha \, d(A_x, A_k)$$

$$(50)$$

$$< \alpha \, d(A_x, A_k) + \beta.\frac{(p + d(A_x, SA_x)).d(A_k, TA_k)}{(p + d(A_x, A_k))} + \gamma\{d(A_k, SA_k) + d(A_x, TA_x)\}.$$

Hence, inequality (30) holds. Clearly, A_1 is the only typical FP of S and T.

3. Fixed Points of Rational Type Contractions (RTC) on Metric Closed (F-MC) Ball

In this section of the manuscript, we explore similar results in the domain of an metric closed (F-MC) ball rather than in the whole F-MS. We will show that the FP of the above

contraction can be iterated even if the contractive condition is imposed only on the metric closed (*F*-MC) ball. The example in this section gives a comparative analysis of the results in this section to those in the previous section.

Definition 6. Let (A, d) be a CF-MS and $S, T: A \longrightarrow A$ be self-mappings. Suppose for α, β, γ, and $p \in (0, \infty)$ with $(\alpha + \gamma)/(1 - \beta - \gamma) < 1$; then, the map T is called an RTC on $B(s_0, \mu) \subseteq A$ if

$$d(Ss, Ty) \le \alpha \, d(s, y) + \beta \frac{(p + d(s, Ss)).d(y, Ty)}{(p + d(s, y))}$$
$$+ \gamma[d(s, Ss) + d(y, Ty)], \tag{51}$$

for each $(s, y) \in B(s_0, \mu) \subseteq A$.

Theorem 5. *Assume $(g, \alpha) \in \mathscr{G} \times [0, \infty)$, (A, d) is a CF-MS, and T be an RTC on $B(s_0, \mu)$. Suppose for some $s_0 \in A$ and $\mu > 0$, and the next conditions can hold:*

(a) $B(s_0, \mu)$ is an F-MC

(b) $d(s_0, s_1) \le (1 - \lambda)\mu$, for $s_1 \in A$ and $\lambda = (\alpha + \gamma)/(1 - \beta - \gamma)$

(c) There exist $0 < \epsilon < \mu$ such as $g((1 - \lambda^{k+1})\mu) \le g(\epsilon) - \alpha$, where $k \in \mathbb{N}$

Then, there exists a single typical FP of the mappings S and T in $B(s_0, \mu)$.

Proof: Choose an arbitrary element s_0 and iterate a sequence (s_n) as

$$T(s_{2x}) = s_{2x+1},$$
$$S(s_{2x+1}) = s_{2x+2}, \tag{52}$$
$$x = 0, 1, 2, \ldots.$$

Before proceeding to our proof, first we show that s_n is in $B(s_0, \mu)$ for every $n \in \mathbb{N}$. We do this by mathematical induction. Using (b), we write

$$d(s_0, s_1) < \mu \tag{53}$$

Hence, $s_1 \in B(s_0, \mu)$. Let $s_2, \ldots, s_k \in B(s_0, \mu)$ for some $k \in \mathbb{N}$. Next, if $s_{2x+1} \le s_k$, then by (51), we can write

$$d(s_{2x}, s_{2x+1}) = d(Ss_{2x-1}, Ts_{2x}) \le \alpha \, d(s_{2x-1}, s_{2x}) + \beta. \frac{(p + d(s_{2x-1}, Ss_{2x-1})).d(s_{2x}, Ts_{2x})}{(p + d(s_{2x-1}, s_{2x}))} + \gamma[d(s_{2x-1}, Ss_{2x-1}) + d(s_{2x}, Ts_{2x})]$$

$$= \alpha \, d(s_{2x-1}, s_{2x}) + \beta. \frac{(p + d(s_{2x-1}, s_{2x})).d(s_{2x}, s_{2x+1})}{(p + d(s_{2x-1}, s_{2x}))} + \gamma[d(s_{2x-1}, s_{2x}) + d(s_{2x}, s_{2x+1})]$$

$$= \alpha \, d(s_{2x-1}, s_{2x}) + \beta.d(s_{2x}, s_{2x+1}) + \gamma[d(s_{2x-1}, s_{2x}) + d(s_{2x}, s_{2x+1})]$$

$$= (\alpha + \gamma)d(s_{2x-1}, s_{2x}) + (\beta + \gamma)d(s_{2x}, s_{2x+1}), \tag{54}$$

or

$$(1 - \beta - \gamma)d(s_{2x}, s_{2x+1}) \le (\alpha + \gamma)d(s_{2x-1}, s_{2x}), \tag{55}$$

which implies that

$$d(s_{2x}, s_{2x+1}) \le \frac{(\alpha + \gamma)}{(1 - \beta - \gamma)} d(s_{2x-1}, s_{2x})$$
$$= \lambda \, d(s_{2x-1}, s_{2x}) \, say \, \frac{(\alpha + \gamma)}{(1 - \beta - \gamma)} = \lambda. \tag{56}$$

Similarly,

$$d(s_{2x-1}, s_{2x}) \le \lambda \, d(s_{2x-2}, s_{2x-1}). \tag{57}$$

Similarly, if $s_{2x} \le s_k$,

$$d(s_{2x-1}, s_{2x}) < \frac{(\alpha + \gamma)}{(1 - \beta - \gamma)} d(s_{2x-2}, s_{2x-1})$$
$$= \lambda \, d(s_{2x-2}, s_{2x-1}). \tag{58}$$

Therefore, from inequality (55) and (56), we write

$$d(s_{2x}, s_{2x+1}) < \lambda \, d(s_{2x-1}, s_{2x}) < \ldots < \lambda^{2x} d(s_0, s_1), \tag{59}$$

and

$$d(s_{2x-1}, s_{2x}) < \lambda \, d(s_{2x-2}, s_{2x-1}) < \cdots < \lambda^{2x-1} d(s_0, s_1). \tag{60}$$

From (59) and (60), we write

$$d(s_k, s_{k+1}) \le \lambda^k d(s_0, s_1) \text{ for some } k \varepsilon N. \tag{61}$$

Now, using (61), we have

$$g\left(d\left(s_0, s_{k+1}\right)\right) \le g\left(\sum_{i=1}^{k+1} d\left(s_{i-1}, s_i\right)\right) + \alpha = g\left(d\left(s_0, s_1\right) + \cdots + d\left(s_k, s_{k+1}\right)\right) + \alpha$$

$$\le g\left[\left(1 + \lambda + \lambda^2 + \cdots + \lambda^k\right)d\left(s_0, s_1\right)\right] + \alpha = g\left[\frac{1 - \lambda^{k+1}}{1 - \lambda}\, d\left(s_0, s_1\right)\right] + \alpha.$$

(62)

By (b) and (c), we can write

$$g\left(d\left(s_0, s_{k+1}\right)\right) \le g\left(\left(1 - \lambda^{k+1}\right)\mu\right) + \alpha \le g(\epsilon) < g(\mu). \quad (63)$$

Hence, by (F1), we deduce that

$$s_{k+1} \in B\left(s_0, \mu\right). \quad (64)$$

Thus, $s_n \in B\left(s_0, \mu\right)$ for all $n \in \mathbb{N}$. By (30), we have the following equations:

$$d\left(s_{2i+1}, s_{2i+2}\right) = d\left(Ss_{2i}, Ts_{2i+1}\right) \le \alpha\, d\left(s_{2i}, s_{2i+1}\right) + \beta.\frac{\left(p + d\left(s_{2i}, Ss_{2i}\right)\right).d\left(s_{2i+1}, Ts_{2i+1}\right)}{\left(p + d\left(s_{2i}, s_{2i+1}\right)\right)} + \gamma\left[d\left(s_{2i}, Ss_{2i}\right) + d\left(s_{2i+1}, Ts_{2i+1}\right)\right]$$

$$= \alpha\, d\left(s_{2i}, s_{2i+1}\right) + \beta.\frac{\left(p + d\left(s_{2i}, s_{2i+1}\right)\right).d\left(s_{2i+1}, s_{2i+2}\right)}{\left(p + d\left(s_{2i}, s_{2i+1}\right)\right)} + \gamma\left[d\left(s_{2i}, s_{2i+1}\right) + d\left(s_{2i+1}, s_{2i+2}\right)\right].$$

(65)

Now, proceeding in a similar way as in Theorem 4 and using (a), we find that (s_n) converges to some c^* in $B\left(s_0, \mu\right)$. Also, we prove c^* as the single common FP of S and T by following the method of Theorem 4.

Put $\alpha = 0$ in Theorem 5, and the following results are given. □

Corollary 2. *Assume* $(g, \alpha) \in \mathcal{G} \times [0, \infty)$, (A, d) *is an F-complete F-MS,* $S, T: A \longrightarrow A$ *are self-mappings, and* $\beta/(1 - \alpha - \beta)$ *with* $\alpha, \beta, p \in (0, \infty)$. *Let, for* $s_0 \in A$ *and* $\mu > 0$, *the following conditions hold:*

(i) $B\left(s_0, \mu\right) \subseteq A$ *is F-closed*

(ii) $d\left(Ss, Ty\right) \le \alpha. (p + d\left(s, Ss\right)).d\left(y, Ty\right)/(p + d\left(s, y\right)) + \beta\left[d\left(s, Ss\right) + d\left(y, Ty\right)\right]$, *for all* s *and* $y \in B\left(s_0, \mu\right)$

(iii) $d\left(s_0, s_1\right) \le (1 - \lambda)\mu$, *for* $s_1 \in A$ *and* $\lambda = \beta/(1 - \alpha - \beta)$

(iv) *There exists* $0 < \epsilon < \mu$ *such as* $g\left((1 - \lambda^{k+1})\mu\right) \le g(\epsilon) - \alpha$, *where* $k \in \mathbb{N}$.

Then, there exists a single typical FP of the mappings S and T in $B\left(s_0, \mu\right)$.

If we take $S = T$ in Theorem 5, the following results are developed.

Corollary 3. *Let* $(g, \alpha) \in \mathcal{G} \times [0, \infty)$, (A, d) *is an F-complete F-MS, and* $T: A \longrightarrow A$ *is a self-mapping, and assume that* $(\alpha + \gamma)/(1 - \beta - \gamma)$ *with* α, β, γ, *and* $p \in (0, \infty)$. *Assume that, for* $s_0 \in A$ *and* $\mu > 0$, *the following conditions hold:*

(i) $B\left(s_0, \mu\right) \subseteq A$ *is F-closed*

(ii) $d\left(Ts, Ty\right) \le \alpha\, d(s, y) + \beta. (p + d\left(s, Ts\right)).d\left(y, Ty\right)/(p + d\left(s, y\right)) + \gamma\left[d\left(s, Ts\right) + d\left(y, Ty\right)\right]$, *for every* s *and* $y \in B\left(s_0, \mu\right)$

(iii) $d\left(s_0, s_1\right) \le (1 - \lambda)\mu$, *for* $s_1 \in A$ *and* $\lambda = (\alpha + \gamma)/(1 - \beta - \gamma)$

(iv) *There exist* $0 < \epsilon < \mu$ *such as* $g\left((1 - \lambda^{k+1})\mu\right) \le g(\epsilon) - \alpha$, *where* $k \in \mathbb{N}$

Then, there is a single FP of the mapping T in $B\left(s_0, \mu\right)$.

Example 4. Let $A = [0, \infty)$ and $g(s) = -1/\sqrt{s}$. Define $T: A \longrightarrow A$ by

$$Ts = \begin{cases} \dfrac{s}{3}, & \text{if } s \in [0, 2], \\[2mm] s^3, & \text{if } s \in (2, \infty), \end{cases} \quad (66)$$

and define $d\beta\, y$:

$$d(s, y) = \begin{cases} (s - y)^2, & \text{if } (s, y) \in [0, 2] \times [0, 2], \\ |s - y|, & \text{if } (s, y) \notin [0, 2] \times [0, 2]. \end{cases} \quad (67)$$

Observe that d is an F-metric space (F-MS) and the mapping g fulfills (F1)-(F2). Choose $s_0 = \mu = 1$; then, $B\left(s_0, \mu\right) = [0, 2]$. Notice that $B\left(s_0, \mu\right)$ is $\mathcal{F}$-closed, so condition (a) of Corollary 2 is fulfilled. Next, if $\alpha = 3/4$ and $\beta = \gamma = 0$, then $\lambda = \alpha$ and

$$d\left(s_0, s_1\right) = d\left(s_0, Ts_0\right) = \left(\frac{1}{2} - \frac{1}{6}\right)^2 = \frac{1}{9} < \left(1 - \frac{3}{4}\right).1 = (1 - \lambda)\mu. \quad (68)$$

Thus, condition (b) is obeyed. Further, as the function g is increasing and $\lambda < 1$, therefore, for every $k \in \mathbb{N}$, we can

$$d(Ts, Ty) = \left(\frac{s}{3} - \frac{y}{3}\right)^2 = \frac{1}{9}(s-y)^2 < \frac{3}{4}(s-y)^2 = \alpha \, d(s,y)$$
$$= \alpha \, d(s,y) + \beta.\frac{(p+d(s,Ts)).d(y,Ty)}{(p+d(s,y))} + \gamma[d(s,Ts) + d(y,Ty)]. \tag{69}$$

Hence, (d) holds for all $(s,y) \in B(s_0,\mu) \times B(s_0,\mu)$. But, if $(s,y) \notin B(s_0,\mu) \times B(s_0,\mu)$ e.g., $s = 3$ and $y = 4$, then

$$d(Ts, Ty) = \left|3^3 - 4^3\right| > \frac{3}{4}|(3-4)| = (\alpha \, d(s,y)) = (\alpha \, d(s,y)) + \beta.\frac{(p+d(s,Ts)).d(y,Ty)}{(p+d(s,y))} + \gamma[d(s,Ts) + d(y,Ty)]. \tag{70}$$

Hence, it is now verified that the condition (b) holds true only for and not on the whole space A. Finally, $0 \in B(s_0,\mu)$ is the FP of T.

4. Application

This section assures a solution for dynamic programming (DP) by using the fixed point technique. Thus, in turn, it renders a solution to dynamic routing with randomization for secure wireless sensor networks.

A DP is two states process: a state space (SS) and a decision space (DC). One can further divide SS into (a) initial state, (b) transitional state, and (c) action state. On the contrary, DS comprises the procedure and steps adopted to iterate the solution of the particular problem. Such algorithms are mainly used in computer programming and optimization.

There used to be hundreds or thousands of sensor nodes in a wireless sensor. They sometimes communicate among themselves and sometimes directly to a base station. If there are more sensors in a network, they can sense a large region with more considerable accuracy, minimizing the risk. The sensor nodes are often dispersed on a broader sensor field, where they share the quality data/information.

All such sensor nodes tend to gather and route the data back to the base station or to among themselves. Sending the traffic of a network can be done by the process of routing. For a high communication capacity, efficient tools are needed to select a network that can respond sharply to changes in the communication link. For this purpose, many algorithms have already been developed for routing protocols in a network.

Bellman [20], in 1958, using the approach of functional equations, designed an algorithm that converges in $N - 1$ (or lesser) iterations to perform dynamic routing with randomization in a sensor network of N nodes and supporting its security in terms of data transmission. One can formulate

locate some $\epsilon < \mu$ and $\alpha \in [0, \infty)$ such that $g((1-\lambda^{k+1})\mu) = g(\epsilon) - \alpha$ is satisfied. i.e., condition (c) is obeyed.

Now, when $(s,y) \in B(s_0,\mu) \times B(s_0,\mu)$, then

the problem of DP in the structure of a function equation as follows:

$$p(s) = \max_{t \in T}\{F(s,t) + f_1(s,t,p(\eta(s,t)))\} \text{ for } s \in S. \tag{71}$$

$$x(s) = \max_{t \in T}\{F(s,t) + f_2(s,t,p(\eta(s,t)))\} \text{ for } s \in S, \tag{72}$$

where Y and Z are Banach spaces such as $S \subseteq Y$ and $T \subseteq Z$, and

$$\eta: S \times T \longrightarrow S,$$
$$F: S \times T \longrightarrow R, \tag{73}$$
$$f_1, f_2: S \times T \times R \longrightarrow R.$$

Suppose S and T are the DS and SS, respectively. We tend to investigate a similar solution point occurrence for both (71) and (72). Let us represent the family of real-valued bounded mappings on S by $W(S)$. Suppose an arbitrary element $j \in W(S)$, and $\|j\| = \max_{s \in S}|j(s)|$. Then, $(W(S), \|.\|)$ is Banach space endowed with d defined as

$$d(j,k) = \max_{s \in S}|j(s) - k(s)|. \tag{74}$$

Suppose the below speculations hold:

(C1): F, f_1, and f_2 are bounded.

(C2): For $s \in S$ and $j \in W(S)$, define $Q, Z: W(S) \longrightarrow W(S)$ by

$$Qj(u) = \max_{t \in T}\{F(s,t) + f_1(s,t,j(\eta(s,t)))\} \text{ for } s \in S,$$
$$Zj(u) = \max_{t \in T}\{F(s,t) + f_2(s,t,j(\eta(s,t)))\} \text{ for } s \in S. \tag{75}$$

Observe that the mappings F, f_1, and f_2 are all bounded.

(C3): For $(s, t) \in S \times T$, j and $k \in W(S)$ and $l \in S$, and we write

$$\left| f_1(s, t, j(l)) - f_1(s, t, k(l)) \right| \le M(j, k), \quad (76)$$

where

$$M(j, k) = \alpha\, d(j, k) + \beta \frac{(p + d(j, Qj)).d(k, Zk)}{(p + d(j, k))} \\ + \gamma (d(j, Qj) + d(k, Zk)), \quad (77)$$

for α, β, and $\gamma \in [0, \infty)$ and $\alpha + 2\beta + 2\gamma < 1$.

Now, we develop the following theorem.

Theorem 6. *Suppose conditions (C1)-(C3) hold; then, at most one identical bounded solution for both (71) and (72).*

Proof: By Lemma 1, it is evident that $(W(S), d)$ is an F-complete F-MS. d is defined by (74), and from (C1), we deduce that S and T are self-mappings on $W(S)$. Let ω be an arbitrary positive number and j_1 and $j_2 \in W(S)$. Take $s \in S$ and t_1 and $t_2 \in T$ such as

$$Qj_x < F(s, t_x) + f_1\left(s, t_x, j_x(\eta(s, t_x))\right) + \omega, \quad (78)$$

$$Zj_x < F(s, t_x) + f_2\left(s, t_x, j_x(\eta(s, t_x))\right) + \omega, \quad (79)$$

and

$$Qj_1 \ge F(s, t_2) + f_1\left(s, t_2, j_1(\eta(s, t_2))\right), \quad (80)$$

$$Zj_2 \ge F(s, t_1) + f_1\left(s, t, j_2(\eta(s, t_1))\right). \quad (81)$$

Then, using (78) and (81), we obtain

$$Qj_1(s) - Zj_2(s) < f_1\left(s, t_1, j_1(\eta(s, t_1))\right) - f_1\left(s, t_1, j_2(\eta(s, t_1))\right) + \omega \\ \le \left| f_1\left(s, t_1, j_1(\eta(s, t_1))\right) - f_1\left(s, t_1, j_2(\eta(s, t_1))\right) \right| + \omega \le M(j_1(s), j_2(s)) + \omega. \quad (82)$$

Also, from (78) and (79), we get

$$Zj_2(s) - Qj_1(s) < M(j_1(s), j_2(s)) + \omega. \quad (83)$$

Merging the above two inequalities, we write

$$\left| Qj_1(s) - Zj_2(s) \right| < M(j_1(s), j_2(s)) + \omega, \quad (84)$$

for all $\omega > 0$. Thus,

$$d(Qj_1(s), Zj_2(s)) \le M(j_1(s), j_2(s)), \quad (85)$$

i.e.,

$$d(Sj_1, Tj_2) \le M(j_1, j_2), \quad (86)$$

for every $s \in S$. All the requirements of Theorem 4 are fulfilled. Therefore, using Theorem 4, S and T have a unique bounded and standard solution for equations (70) and (71). □

5. Conclusion

This research work has highlighted the essentialness and usefulness of the newly-introduced F-MS by establishing interesting FP theorems of some contractions. It is obtained that the FP and typical FP of a contractive mapping is beneficial even if the contraction condition is not imposed on the whole F-MS and is shrunk only to a closed ball inside it. The two different examples are indeed a comparative analysis of the outcome of assessing the contraction locally and globally. Few practical corollaries have been developed from the proven results. We will extend this idea to the frame of fuzzy metric space and picture fuzzy metric space in the future. The effects will be investigated in the mentioned setting, and its application in multistage optimization will be discussed. Finally, there is a discussion on the applications side for development and establishing a single solution of the functional equation, which leads to a dynamic routing with randomization and improving data security tasks in a wireless sensor network.

Data Availability

Data sharing is not applicable to this article as no data set were generated during this study.

Conflicts of Interest

The authors declare that there are no conflicts of interest regarding the publication of this paper.

Authors' Contributions

The authors have equally contributed to this research work.

Acknowledgments

References

[1] A. Branciari, "A fixed point theorem of Banach-Caccioppoli type on a class of generalized metric spaces," *Publ. Math. Debr.* vol. 57, pp. 31–37, 2000.

[2] S. Czerwik, "Contraction mappings in b-metric spaces," *Acta Mathematica et Informatica Universitatis Ostraviensis*, vol. 1, no. 1, pp. 5–11, 1993.

[3] R. Fagin, R. Kumar, and D. Sivakumar, "Comparing top k lists," *SIAM Journal on Discrete Mathematics*, vol. 17, no. 1, pp. 134–160, 2003.

WILEY | Hindawi

Retraction

Retracted: A Systematic Analysis of Regression Test Case Selection: A Multi-Criteria-Based Approach

Security and Communication Networks

This article has been retracted by Hindawi following an investigation undertaken by the publisher [1]. This investigation has uncovered evidence of one or more of the following indicators of systematic manipulation of the publication process:

(1) Discrepancies in scope

(2) Discrepancies in the description of the research reported

(3) Discrepancies between the availability of data and the research described

(4) Inappropriate citations

(5) Incoherent, meaningless and/or irrelevant content included in the article

(6) Peer-review manipulation

The presence of these indicators undermines our confidence in the integrity of the article's content and we cannot, therefore, vouch for its reliability. Please note that this notice is intended solely to alert readers that the content of this article is unreliable. We have not investigated whether authors were aware of or involved in the systematic manipulation of the publication process.

Wiley and Hindawi regrets that the usual quality checks did not identify these issues before publication and have since put additional measures in place to safeguard research integrity.

We wish to credit our own Research Integrity and Research Publishing teams and anonymous and named external researchers and research integrity experts for contributing to this investigation.

The corresponding author, as the representative of all authors, has been given the opportunity to register their agreement or disagreement to this retraction. We have kept a record of any response received.

References

[1] M. Rehan, N. Senan, M. Aamir et al., "A Systematic Analysis of Regression Test Case Selection: A Multi-Criteria-Based Approach," *Security and Communication Networks*, vol. 2021, Article ID 5834807, 11 pages, 2021.

WILEY | Hindawi

Research Article

A Systematic Analysis of Regression Test Case Selection: A Multi-Criteria-Based Approach

Muhammad Rehan ,[1] **Norhalina Senan** ,[1] **Muhammad Aamir** ,[2] **Ali Samad** ,[3] **Mujtaba Husnain** ,[3] **Noraini Ibrahim** ,[1] **Sikandar Ali** ,[4] and **Hizbullah Khatak** [5]

[1]*Faculty of Computer Science and Information Technology, University Tun Hussein Onn Malaysia (UTHM), Johor 8000, Malaysia*
[2]*School of Electronics, Computing and Mathematics, University of Derby, Derby 01332, UK*
[3]*Faculty of Computing, The Islamia University of Bahawalpur, Bahawalpur, 63100, Pakistan*
[4]*Department of Computer Science and Technology, China University of Petroleum-Beijing, Beijing 102249, China*
[5]*Department of Information Technology, Hazara University Mansehra, Khyber Pakhtunkhwa, Pakistan*

Correspondence should be addressed to Muhammad Aamir; m.aamir@derby.ac.uk and Sikandar Ali; sikandar@cup.edu.cn

Received 14 July 2021; Accepted 21 August 2021; Published 22 September 2021

Academic Editor: Kifayat Ullah

In applied software engineering, the algorithms for selecting the appropriate test cases are used to perform regression testing. The key objective of this activity is to make sure that modification in the system under test (SUT) has no impact on the overall functioning of the updated software. It is concluded from the literature that the efficacy of the test case selection solely depends on the following metrics, namely, the execution cost of the test case, the lines of the code covered in unit time also known as the code coverage, the ability to capture the potential faults, and the code modifications. Furthermore, it is also observed that the approaches for the regression testing developed so far generated results by focusing on one or two parameters. In this paper, our key objectives are twofold: one is to explore the importance of the role of each metric in detail. The secondary objective is to study the combined effect of these metrics in test case selection task that is capable of achieving more than one objective. In this paper, a detailed and comprehensive review of the work related to regression testing is provided in a very distinct and principled way. This survey will be useful for the researchers contributing to the field of regression testing. It is noteworthy that our systematic literature review (SLR) included the noteworthy work published from 2007 to 2020. Our study observed that about 52 relevant studies focused on all of the four metrics to perform their respective tasks. The results also revealed that about 30% of the different categories of regression test case reported the results using metaheuristic regression test selection (RTS). Similarly, about 31% of the literature reported results using the generic regression test case selection techniques. Most of the researchers focus on the datasets, namely, Software-Artefact Infrastructure Repository (SIR), JodaTime, TreeDataStructure, and Apache Software Foundation. For validation purpose, following parameters were focused, namely, the inclusiveness, precision, recall, and retest-all.

1. Introduction

The cost associated with the regression testing can be curtailed by the in-depth analysis for finding the optimal solutions of the three processes, namely, the regression test selection (RTS), regression test prioritization (RTP), and the regression test reduction (RTR) [1–4]. The process of RTS deals with selecting a set of test cases from a repository of test suites that are capable enough of performing the regression test [5–7]. Similarly, the RTP is the study of rearranging the test cases in the test suite with higher priority based on the ability of capturing faults in minimum time, cost, and effort. Furthermore, the test cases are chosen from the categories like re-usable test cases, change affecting test cases, fault affecting test cases, and redundant test cases. On the other hand, the removal of redundant test cases that failed to capture the maximum faults is known as the RTR process [8, 9].

Figure 1 shows the details of related 2776 articles retrieved from Web of Science. Similarly, Figure 1(a) depicts the articles published in the period 2007–2020 on software testing in general and test selection in specific. More than 900 articles were published in 2018, which indicates research on the software regression testing in applied software engineering field. Figure 1(b) shows the 2007–2020 citation trends for articles on various approaches used in software testing while Figure 2 represents the global distribution of studies on artificial intelligence (AI) applications in software regression testing. This research has spread across the globe, especially active in the United States, China, Germany, Japan, India, Australia, and several European countries. The conventional approaches used in RTS comprised of the following three components, namely, the test case selection model, the selection parameters, and the selection adequacy measures, as shown in Figure 1. The original target program Prog, its modified version *Prog'*, and test suite *TS* having test cases are given as inputs to the first component of the system. The test case selection model tries to identify the change in the code in the modified version *Prog'*. Besides, it also retrieves other relevant and important information like the code coverage, number of faults detected, and the total execution time of the test case. On completion, the model may select the test cases from TS and move it to *TS'* (a subset of TS) on the basis of the computations performed in the model. These computations play a key role in estimating the effectiveness of the algorithms used for the selection of appropriate test cases. It is worthy to note that we deduced the idea of writing such an article from a noteworthy work reported in [10].

It is pertinent to mention that these computations can be used in a twofold way in the RTS process; the first is to observe the performance and then select a set of appropriate test cases based on some selection criteria, and second these calculations play a significant role in evaluating the efficacy of RTS by comparing with other approaches. It is of significant importance that to organize these four metrics, namely, cost, coverage, fault detection, and code modifications, we have to analyze the dependencies with respect to each other. The key issues in this regard are discussed as under; the first issue is to choose the suitable and apposite type of these measures, like the subtypes of the coverage-based information, the types of the potential faults, and the degree of severity. The critical issue that we try to resolve is to acquire and explore the model that is closely related to the RTS that helps in justifying including these four parameters for the selection of test cases on the basis of their efficacy and adequacy scale. Furthermore, we also try to explore and identify the set of techniques that are capable of producing the efficient and acceptable results based on these effective measures. The primary objective of this paper is to explore the test case selection methods that perform solely on these metrics and work as an effective contributor. The second objective our study is to assess the current state-of-the-art regression test case selection frameworks and techniques developed so far and to identify the available datasets and algorithms for the solution of test case selection problems.

The paper is further organized as follows. In Section 2, the methodology adopted in this paper is discussed in detail by including the source of data and the framework adopted for analysis. In Section 3 and Section 4, we discussed the various indicators on the basis of which we analyzed the bibliographic data related to test case selection, namely, the co-cited reference network, burst references, co-occurrence keyword network, burst keywords, and dual-map overlay network. For this purpose, we make use of the information visualization software VOSviewer [11]. It is pertinent to mention that this program is equally applicable in both focusing on the structural and fundamental variations in regression testing and identifying the new trends in software testing domain. The paper is concluded in Section 5 followed by Section 6 in which the limitations and future work are given.

2. Review Methodology

In this section, we will discuss the methods that we used to retrieve the related articles. In this review, we collected the noteworthy articles from a number of databases associated with Web of Science (WoS). The WoS platform is sufficient enough to provide and explore a number of useful links that are related to the search query and criteria that the researcher may use for collecting the data. Furthermore, the repository of the research articles offers a variety of search criteria to search the items with complete bibliographic information, previous versions of the article, the reference data that are cited according to the current article, and the links to full texts. The WoS repository is different from other sources in a way that it adds about 20,000 articles along with an average of 500, 000 cited references every other week.

Furthermore, in this survey, we focused to include the related literature as much as possible. To perform this task, we first quantified the compactness of the retrieved articles by using a number of combinations of the relevant keywords. Furthermore, we also tried to verify manually the articles retrieved from the WoS. We applied the following query to search (QtS) and retrieved the related articles.

QtS = "(Regression Testing OR Test case selection OR Test case Prioritization OR Test Case Reduction) AND (Multi-level OR Multi-criteria OR Multi-purpose OR multi-dimensional OR multi-directional)".

It is clear that our search query has two parts: (1) regression testing related terms and (2) multi-criteria-based related terms. The query uses 9 keywords that cover most of the fields of software regression testing and test case selection. The key purpose of the query is to search the articles that reported the results on test case selection while considering multiple criteria at the same time. The bibliographic metadata of each paper contain the following information: the title of the article, list of authors indicating the corresponding author, its abstract, the keywords, digital object identifier (DOI), journal (or conference) name, and references. It is noteworthy that our systematic review is solely based on the articles retrieved through Science Citation Index Expanded (SCIE) dataset. The dataset contains about 2776 records which is about 31% of the literature reported in the domain of regression testing.
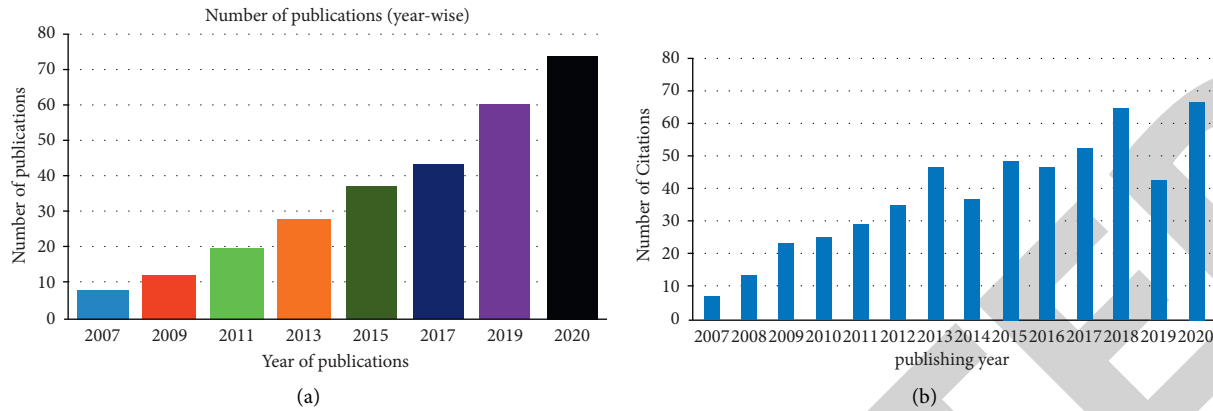
Figure 1: Trend in research on software regression testing in applied software engineering: (a) published articles each year; (b) article citations each year.

Figure 2: The heatmap for studies on AI applications in software regression testing indicating the regions that are highly active in this domain.

2.1. Scientometric Analysis. With the rapid growth in the literature published in a number of domains, the visualization tools were made efficient enough to process the publications' metadata for better understanding. The relevant terms are depicted in Table 1.

The most widely used software for mapping the scientific literature, namely, the CiteSpace V [12], is one of the tools that is capable enough of generating a number of mappings like the network representing the references that were found co-cited in the literature, the frequency of the keywords appeared, and so on using dual-map overlay network. Furthermore, it is also helpful in identifying the changes and modifications in the hotspots by computing the cluster size from the associated network to determine foremost and frontier topics. This task is performed by calculating the annual publications published on average using its cluster. Furthermore, we also make use of the VOSviewer [11] to perform the analysis at co-authorship level. The VOSviewer is one of the software tools to construct the visualization of the bibliometric or citation-based graph models. The VOSviewer is equally applicable in text mining related tasks for the same purpose mentioned above.

The analysis of these network visualizations produced useful findings and observations about the emerging trends in software test case selection using different approaches while focusing on multiple criteria. Furthermore, a disciplined framework is adopted to perform functions on the dual-map overlays to ascertain the target hotspots with the recent trends in the field of software testing.

3. Scientometric Analysis and Visualization for Detecting the Emerging Trends, Structural Changes, and Future Work in Software Test Case Selection

The contributors in the scientometric analysis concluded that the network-based mapping containing the links representing the co-citations among the document pairs is capable enough to reveal the research focus and knowledge base of a domain [13–15].

TABLE 1: Basic terms and their explanation along with the respective purposes.

Terms	Explanation	Usage
Burst references	This term depicts the number of citations of a specific research document in a specific time. The higher the value of burst references, the higher the impact of that document.	It is used to show the concern level of research communities working in the same domain
Hotspots	It gives information about the number of times a specific research document is visited	It is useful in identifying references and the keywords that appeared in most of the research articles
Centrality	This term refers to the availability of the document either located in some center of the repository or some other location	This assists in finding the relevant research articles in the neighborhood of the visualization graph (or network)
Modularity	This term is related to the overall structure of the visualization network	This information is used to identify and extract the minimum set of the related articles in the network (i.e., clique in a graph)
Co-cited references	It represents the situation when two different research items were cited in a single document	It helps in finding the set of significant research articles along with the recent trends
Co-occurrence keywords	If two relevant keywords appear simultaneously in a single document	This information is helpful in identifying the significant and focused keywords
Silhouette value	This term depicts how much similar a research document is to its cluster neighbors	Its value is in [−1, 1] that refers to the degree of associativity of the research articles within a cluster
Mutual information (MI)	This refers to the information about the two different clusters	It is computed as the similarity measure of two or more clusters in a network

The graph of the network representing a model of co-cited references to extract the research on the application of test case selection can be generated by importing all the 2776 research documents to CiteSpace V. The parameters are tuned to the following values. We retrieved the related documents published in the time span of 2007–2020. Furthermore, we used the switch of "Setup per slice" for each paper included in our scientometrics analysis. If the switch is set to 100, it means that top 100 papers will be selected for visualization in the coreference tree that was mostly cited. It means that if we enter a value of 50, then CiteSpace will select the 50 most cited or occurred items from each slice to construct a network, depending on the node types we selected in the previous step. Similarly, if we selected multiple node types, then these nodes will be ranked by the number of times they appeared in the records for each slice. It is pertinent to mention that the overall structure of the resulting network is not too large to be pruned; therefore, there is no need of pruning the graph. The generated results showed that, in Figures 3–5, the co-cited references network generated by 10, 237 cited documents (from 2776 citing documents) created about 527 nodes with mutual connections of 1587 connections. It is pertinent to mention that from the publications retrieved between 2007 and 2020, a total of 18 clusters were displayed by removing the small-sized clusters. These clusters were produced by fixing the vertex index to 2.75.

The nodes in the graph depict the co-cited references while the node size represents the number of items that were cited, i.e., the larger the node size is, the higher will be the number of that item cited. As a result, this node affects significantly the impact factor of the journal in which it is published. The large-sized circles of the nodes depict the burst reference that is ultimately reflecting the research hotspots in different intervals of time. The edges in the network are the co-citation links, whereas the different colors of the links are reflecting the first ever and the latest citations. It is concluded from Figures 3–5 that the research in the field of test case selection in software engineering attracted a number of researchers from different academic and research institutes globally. Furthermore, it also depicts that the research in this field has not been performed without involving the other methodologies from the domains.

For example, the edges are observed between the cluster "test selection" and "effective test case selection" depicting that the domain of test selection can be improvised in an effective way using the algorithms of machine learning and artificial intelligence. Some smaller node values like "the regression test case," "test case selection method," and "adaptive random testing" are of key importance while searching the research articles of the same kind. Furthermore, these small clusters are most likely to be the hot topics in near future in the domain of software testing.

In Table 2, the complete information about the 6 large clusters depicting the studies in software testing in software engineering is given. The clusters are numbered in the clockwise direction as depicted in Figure 3. As mentioned earlier, the cluster size reflects the number of references that ultimately refers to its hotspot status, whereas the measurement of cluster similarity is computed by the mutual information (MI) that is shared among the clusters. The average number of publications is shown by the time span on year scaling, representing that the papers that were published recently will appear on the front, indicating the emerging trends in the cluster.

It is depicted from Table 2 that the clusters such as "test selection, 2011," "data mining, 2011," "quality-aware test case prioritization, 2017," and "continuous integration, 2020," are concluded as the key hotspots in the software testing related research using different approaches including artificial intelligence (AI) and machine learning (ML) in the field of applied software engineering. Furthermore, it is also observed that the recent trends that were exercised in the field of software
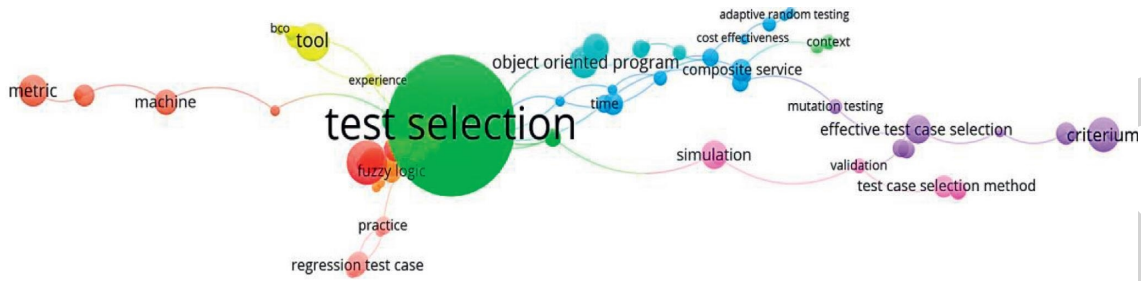
Figure 3: The reference network representing the references that were co-cited in the field of test case selection in applied software engineering.

Table 2: Basic terms and their explanation along with the respective purposes.

Cluster	Silhouette	Frequently occurred terms (FQTs)	Size	Mean (year)	Mutual information (MI)	Frequently occurred terms depicted as a likelihood ratio $p = 1.04^{-4}$
1	0.634	Regression testing, software testing, test case selection	67	2011	Effective testing, regression cycles	Genetic algorithm
2	0.748	Test suite, software testing	63	2012	Software development life cycle, software quality assurance	Swarm intelligence
3	0.897	Quality-aware test case prioritization	75	2017	Maximizing coverage	Weighted source code
4	0.715	Risk-based testing	54	2020	Software modification information	Method invocation relationship
5	0.530	Multiple testing criteria	68	2018	Cost-cognizant average percentage	Pareto-optimal clonal selection algorithm
6	0.472	Continuous integration	71	2020	Test case selection	Machine learning

testing are "multiple testing criteria, 2018," "risk-based testing, 2020," and "cost-cognizant, 2020."

In last 3 years, the research community showed significant interest in adopting the machine learning concepts like k-mean clustering, regression analysis, and decision trees in predicting dynamically the type of research methodology used in the retrieved documents. This type of research is found in "continuous integration, 2020," article.

The variance in the trends of the changing patterns of the research associated with software testing is observed throughout the years proving that the structural changes emerged as a continuous trend in applied software engineering with the emergence of artificial intelligence algorithms.

3.1. Burst References as an Indicator. The increasing number of citations of a specific research object represents its dynamic properties that eventually reflect the reputation of the journal in which it is published. This characteristic property is also referred to as "burst references," as mentioned in Table 1. It helps the research community to diverge their attention towards the concerned research articles based on their respective burst reference graph.

In order to have close tabs on the recent and important research areas specific to some domain, we make use of tracing process to track the timely progress trends in burst references. This activity assists in finding the duration of the burst intensities in a specific time duration to extract the prominent features that play a key role in assigning the ranks to the research objects. In Figure 6, we depict the structural and operational modifications that appeared constantly with the intervention of AI-assisted algorithms in software testing process. It is also observed that the AI-related algorithms and framework played a key role in generating effective results in software regression testing since 2013. It is concluded from the literature that the most of the researchers showed interest in using modern algorithms of machine learning (ML) in 2013 and 2014 while dealing with high dimensional data since the conventional approaches failed to extract the key features from the huge data. The experiments showed that ML- and AI-based models outperformed the conventional approaches while performing software testing at the unit level. The top 8 research objects with significant burst reference values are shown in Figure 6, which depicts the results in some self-explanatory way in capturing the research hotspots and evolutionary trends in the recent studies of AI applications in software testing.

It is evident from Figure 6 that the quality of these research objects solely depends on the data mining and machine learning techniques of AI in applied software engineering that attracted a number of researchers since 2014. Among these research articles, last two articles were ranked on top in late 2019 and early 2020. The authors of these articles also recommend use of Weka and Python libraries to perform a comprehensive and disciplined series of experiments using machine learning procedures to pre-process and then classify the test case on the basis of the criteria set by the practitioners. These tools are also capable of rapid application development and comparing the results with state-of-the art approaches working on new datasets.

4. Role of Co-Occurrence Keyword Network and Burst Keywords

It is a common observation that the two keywords are considered as potentially important and relevant if they appear in some document concurrently in the same order. A network that represents the co-occurrence keywords or potentially important indicating terms is capable of showing the emergent and importance of the important and key terms in a research area. Moreover, this network also assists in indicating the hotspots and the recent trends in a specific domain [18, 19]. Figure 7 depicts the time zone mapping of the co-occurrence network for the recent noteworthy work in software testing.

In Figure 7, the co-occurrence network depicts 271 key terms represented by the nodes with more than 1800 links showing powerfully build connections among the keywords that were mostly used in the articles published between 2007 and 2020. The size of the nodes indicates how frequent the term appeared while the edges are the links of co-occurrence, variation in the line colors depicts the pioneer connection, and thickness of the link corresponds to the co-occurrence strength. Figure 7 also indicates that hotspots in the recent studies including AI in the domain of software engineering in the time interval of 2009–2020 involve the following terms: "test-suite selection," "test-case selection," "test-case ordering," "software testing," "test case prioritization," "test-case reduction," "k-means clustering," "machine learning models," "unit-testing," "regression-testing," "high-dimensional data," "fault detection," "code coverage," "execution cost," "pattern matching," and "mutation testing."

4.1. Overlay Network in Dual Mapping as Indicator. Two other important mappings are also drawn in overlay mode in CiteSpace V that bridges the gap between the maps generated by the program (aka as overlay) with the map depicting the basic knowledge known as base layer. The base layer is associated with the information of some publishing discipline listed in the Journal Citation Reports (JCR). It helps in detecting the changes in the journal metrics time to time in a very disciplined and comprehensive way.

In Figure 8, a base mapping network is shown that is generated using the information provided by the publication(s) in a specific journal having higher number of citations. CiteSpace is capable enough to support visualization of these mappings via the same interface. The number of articles published in a specific journal is mentioned in front of each journal name. The edges among the journals and the academic discipline with different colors show the information about cite-in and cite-out occurrence. In summary, Figure 8 signifies the key disciplines and significant journals among the researchers that are working in the domain of software testing using a number of approaches including ML and AI.

4.2. Most Trending Disciplines and Key Journals. Figure 8 shows that the journal "IEEE Transactions on Software Engineering" making a red cluster (in the middle of the network) is one of the significant journals that covered the most trending disciplines in the field of software testing. In addition, the following studies and science disciplines also played a key role in the related studies: "web services, computer networks, atomic rules, and web-based software." In summary, it is concluded that AI-based algorithms play a key role along with other approaches while performing the software testing at the unit level. Furthermore, these algorithms provide an in-depth picture of the software testing using the statistical and applied mathematical models that also helped in increasing citation of the journal (or the article).

4.3. Country Implications. In Figure 9, a country collaboration network is drawn showing the collaborating countries between 2007 and 2020 in software testing. It is obvious that only three countries around the world are contributing more than 90% from rest of the world. Among these, USA is at the top with 764 publications so far. It is one of the interesting facts that a number of other regions and countries contribute in a relatively very low percentile.

4.4. Author Contribution. One of the key metrics in designing a comprehensive systematic review is exploiting the co-authorship information among the retrieved literature related to some specific domain. The same type of co-authorship network in this field is depicted in Figure 10 that is generated by using VOSviewer. It is observed that the minimum number of publications out of a total 12,405 authors, only 695 publications satisfied the abovementioned criteria.

The analysis at cluster level of the co-author map detects that there are 12 clusters with variant colors. The most important cluster, "Chen Tsong Yueh," is shown in sea-green on the left, showing 54 published articles with 267 citations and link strength of 109. The second most important cluster "Cai Kai-Yuan" is shown in light green with 54 articles with 124 citations and link strength of 37. The authors with higher degrees of centrality are more central in the network structure and tend to have a greater capacity to influence others. The co-authorship analysis indicates that most of the authors of papers on software testing are densely connected with each other in terms of collaboration and citations.
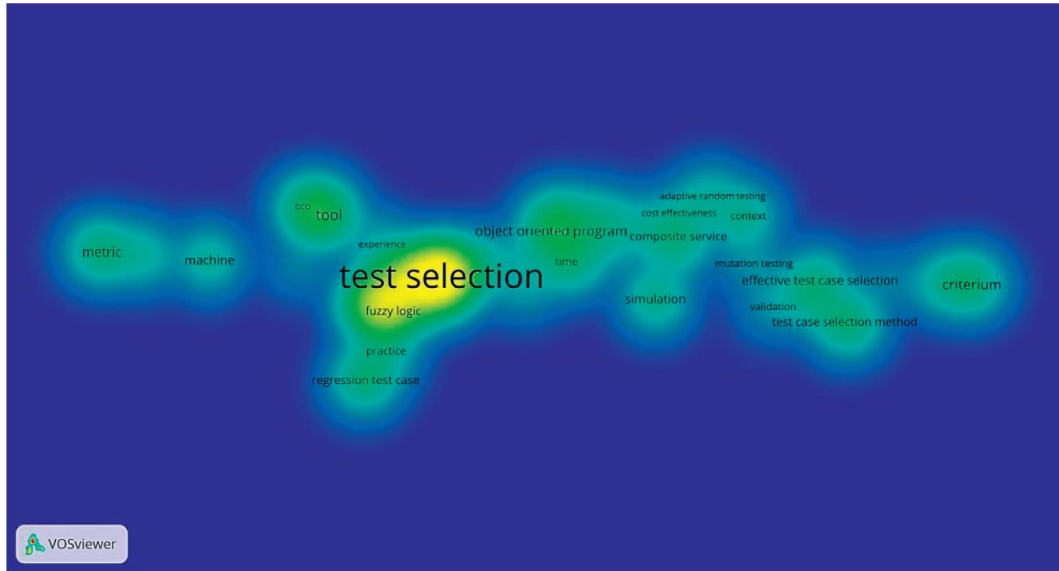
FIGURE 4: The equivalent density visualization graph representing that the most frequently appeared term is the "test selection."
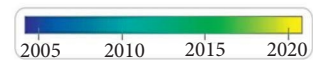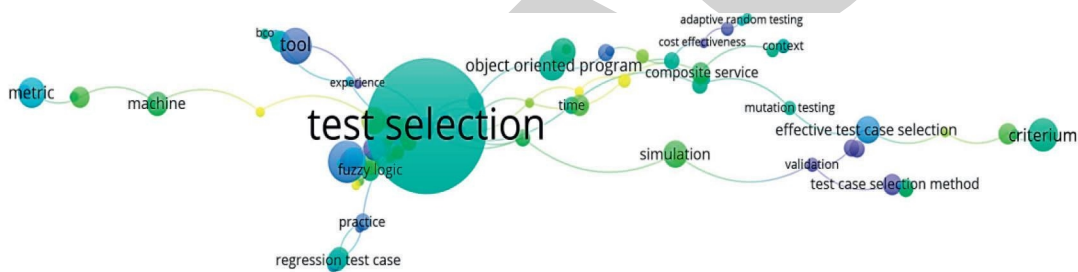
FIGURE 5: Overlay analysis of the published articles related with the test case selection, depicting the spatial data with the attribute data.

Top 8 References with the Strongest Citation Bursts

References	Year	Strength	Begin	End	2016-2019
Yoo S, 2012, Software Testing Verification and Reliability, V22, P67, DOI 10.1002/stv.430, DOI	2012	18.86	2016	2017	
Mirarab S, 2012, IEEE Transactions on Software Engineering, V38, P936, DOI 10.1109/tse.2011.56, DOI	2012	2.86	2016	2017	
Harman M, 2012, ACM Computing Surveys, V45, P11, DOI 10.1145/2379776.2379787, DOI	2012	2.2	2016	2017	
Catal C, 2012, Software Quality Journal, V21, P445, DOI 10.1007/s11219-012-9181-z, DOI	2012	2.2	2016	2017	
Johansen MF, 2012, Proceedings ...... n - SPLC 12-Volume 1, V0,P46, DOI	2012	2.2	2016	2017	
Marijan D, 2013, 2013 IEEE Int ...... Software Maintenance, V0, P540, DOI	2013	2.98	2017	2019	
Gotlieb A, 2014, Proceedings o ...... nalysis-ISSTA 2014, VO, P171, DOI	2014	1.73	2017	2019	
Hao D, 2014, ACM Transaction on Software Engineering and Methodology, V24, P1, DOI 10.1145/2685614, DOI	2014	1.63	2017	2019	

FIGURE 6: Top 8 research objects having the significant burst values. The red line depicts the total burst time while the dark blue line represents the publication time.
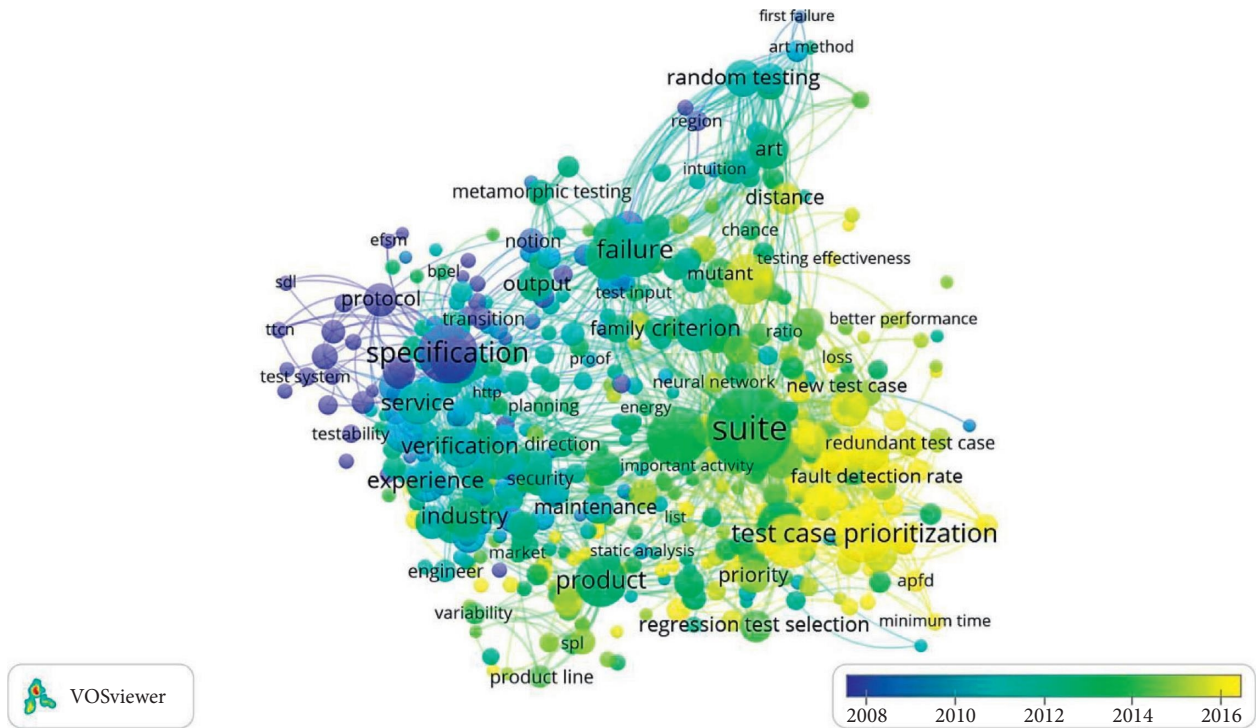
FIGURE 7: Mapping of co-occurrences of keywords used in the studies of software testing. The nodes in the mapping depict the keywords.
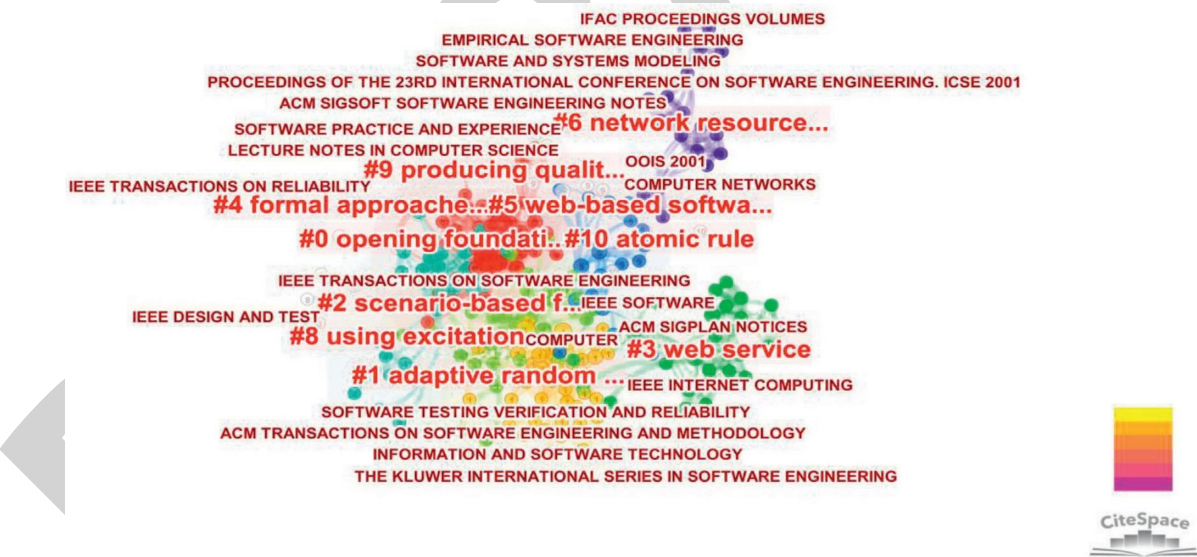
FIGURE 8: A dual-map overlay network showing both the citing journals and the cited journals in the domain of software regression testing.

The application of both the classical and AI-based approaches in software regression testing attracted a number of research communities globally; specifically, the institutes from the United States, China, and India emerged as the growing and prominent institutes compared to other regions. Figure 9 depicts that USA is prominent among other regions and is densely connected to other countries in the research on regression testing in applied software engineering with the largest number of publications with 654 articles. In continental terms, the Asian research institutes dominate the research in software regression testing. Similarly, the figure shows that "IEEE Transactions on Software Engineering" is among one of the top research journals with a total of 649 published articles related to regression testing.

The retrieved data from the WoS platform depicts that the number of published and cited papers on regression testing grew rapidly in recent years. As mentioned earlier,
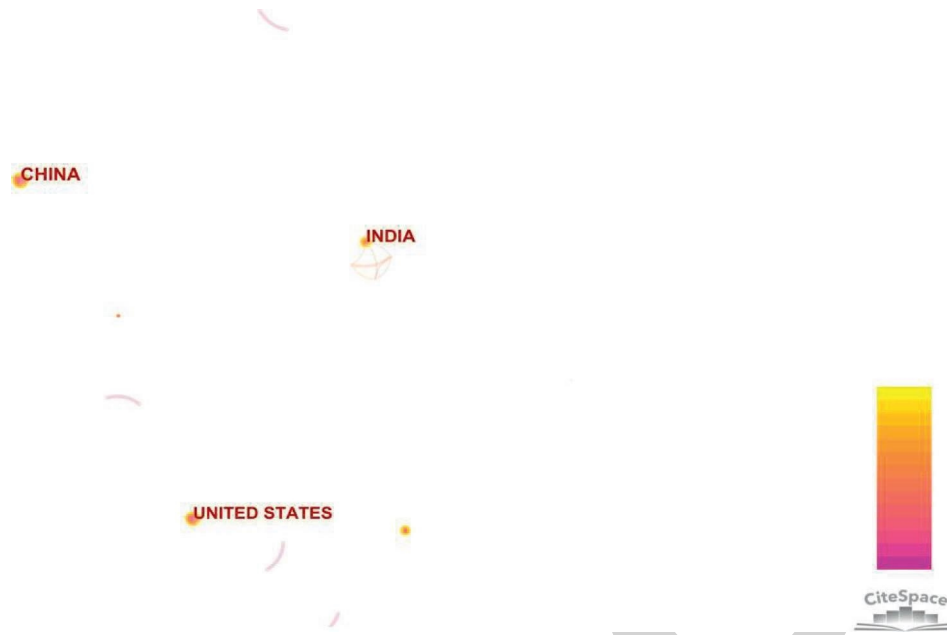
FIGURE 9: A knowledge panorama of studies on software testing using different approaches.
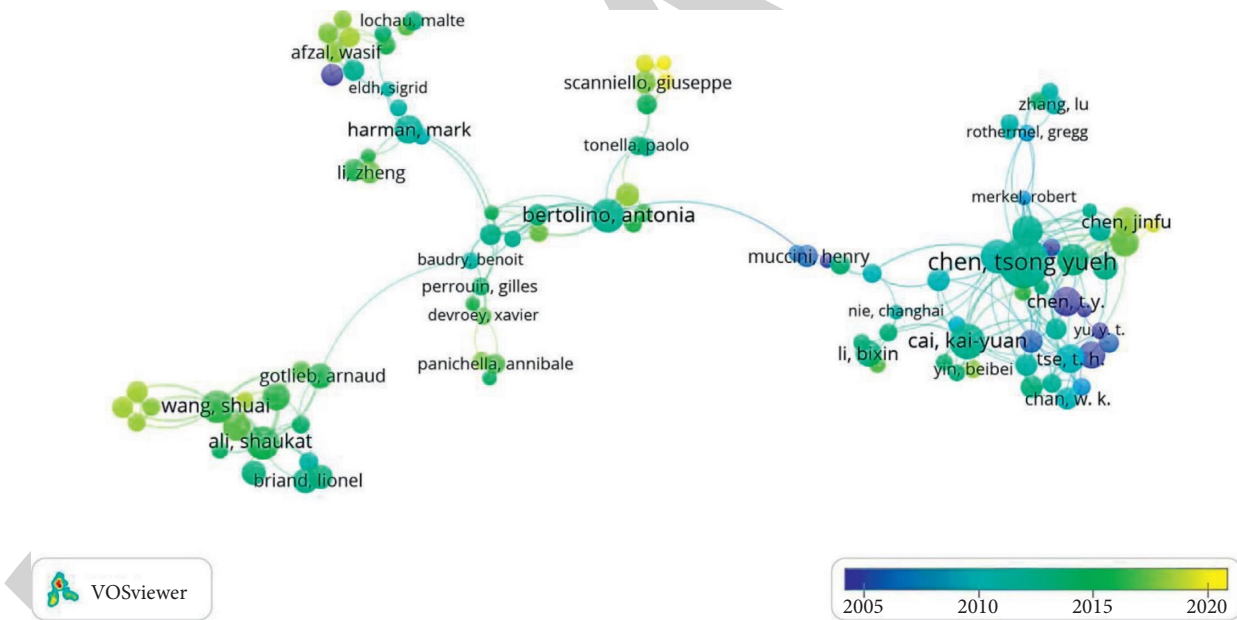
FIGURE 10: The co-authorship network.

USA-based institutes are heavily connected in terms of both journals and collaboration. The journal Information and Software Technology is ranked second, with 604 articles, and it is distributed globally including 17 countries including France and the Netherlands. Regarding the authorship, Figure 10 shows that Chen Tsong Yueh is one of the authors who is highly active in collaborative research activities.

It is noteworthy that according to the Journal Citation Report (JCR) published in 2020 that the authors of the articles discussed in our paper produced the research articles with a ratio of 0.56 in 2017 to 2019, while the productivity rates of the research articles from the same authors were 0.43, 0.35, and 0.28, respectively, in 2007–2008, 2001–2011, and 2012–2013, respectively.

4.5. Revolutionary Changes in Regression Testing with the Intervention of AI-Based Approaches.
The following indicative points show the changes in the basic structure that emerged with the advent of AI-based approaches in regression testing:

(1) According to the indicating reference provided by the co-cited reference network in Table 1, the initial research in regression testing mainly focused on the

basic metrics including the code coverage and execution time of the individual test case that solely depends on the data provided by the previously executed processes. In recent years, amid the impacts of machine learning and deep network, the research in regression testing gave rise to a next new level representing the new aspect of the testing process by considering the training data. The thematic patterns in the scientific literature differ over time indicating the structural changes in the field since the AI-based algorithms behave differently than the conventional approaches.

(2) In Figure 7, the time zone map of the co-occurrence keyword network indicates that from 2007 to 2010, most of the literature of both the conventional and AI-based approaches in software regression testing was reflected in the following keywords: "system," "regression testing," "unit testing," "model checking," "machine learning," "classification," and "k-means clustering."

(3) The timeline map of the co-occurrence keyword network (see Figure 7) shows the structural changes in the field of regression testing in software engineering. It is clear that the "test-case prioritization" was researched earliest and "specification" was the starting point. Moreover, the "failure" hotspot "metamorphic testing" promoted the emergence of "artificial neural networks." The divergent directions of the curves of "computational cost" and "genetic algorithms" show that it gave birth to today's research on intelligent regression testing.

5. Conclusions and Discussion

In this paper, the noteworthy contribution in the field of software testing is visualized by considering different aspects of the research like co-cited reference network analysis, co-occurrence keyword network analysis, burst reference analysis, and so on. Furthermore, the recent hotspots and evolving developments in regression testing using conventional and modern AI approaches are recognized in a very disciplined and comprehensive way. Moreover, the involvement of the global research community is also highlighted.

In the literature reviewed in this article, it is observed that most of the selection methods focus their tabs on the application of some specific software domain that limits our effort in retrieving any significant evidence to analyze and assess the superiority and dominancy of one method over the other. Some relevant topics for future works are (1) to evaluate the selection methods and metrics surveyed in different contexts to prove their effectiveness, efficiency, applicability, and scalability; (2) to develop selection methodologies that can be extended to different software domains; and (3) to develop frameworks or tools to support the test case selection. Furthermore, while analyzing the empirical results generated in the experiment reported in the literature, it is concluded that most of the work was performed in software developed by the researchers and classified by them as small. Analysis and validation of results in test case selection experiments are still limited. Despite the availability of important sources, such as SIR and the Free Software Foundation, it is necessary to expand the experiments in terms of size, application (e.g., industrial use), and software complexity, as replicating studies using different test suites may reveal different patterns of effectiveness and efficiency as well as help prove the viability and applicability of the proposed selection methods.

6. Limitations and Future Work

Although the WoS core collection was chosen as the study's data source, we may have missed some important research publications on AI and conventional approaches in the software regression analysis and testing. To ensure high data quality, this study selected only articles from the SCIE database that may also have led us to omit some important research results (e.g., books, Ph.D. theses, and SSCI database).

Furthermore, the "Top 100 per slice" was set as the standard for data extraction using CiteSpace V that may have some different effect on the analyses when compared to some other slice value. In the future, we will perform a detailed analysis of studies on some genetic and deep learning applications in validation and verification of the developed software before launching or handing over to the clients. Furthermore, we also plan to use a latent Dirichlet allocation (LDA) model for text clustering in the future. We plan to extend the analysis by running correlations between number of citations with respect to the number of primary studies and quality measures of secondary studies. We may even be able to build a regression model to predict citations to secondary studies.

Data Availability

The data used to support the findings of this study are available from the corresponding author upon request.

Conflicts of Interest

The authors declare that they have no conflicts of interest.

References

[1] J. Anderson, S. Salem, and H. Do, "Improving the effectiveness of test suite through mining histor- ical data," in *Proceedings of the 11th Working Conference on Mining Software Repositories*, Hyderabad, India, May 2014.

[2] A. Celik, M. Vasic, A. Milicevic, and M. Gligoric, "Regression test selection across jvm bound- aries," in *Proceedings of the*

Retraction

Retracted: Some Novel Geometric Aggregation Operators of Spherical Cubic Fuzzy Information with Application

Security and Communication Networks

This article has been retracted by Hindawi following an investigation undertaken by the publisher [1]. This investigation has uncovered evidence of one or more of the following indicators of systematic manipulation of the publication process:

(1) Discrepancies in scope

(2) Discrepancies in the description of the research reported

(3) Discrepancies between the availability of data and the research described

(4) Inappropriate citations

(5) Incoherent, meaningless and/or irrelevant content included in the article

(6) Peer-review manipulation

The presence of these indicators undermines our confidence in the integrity of the article's content and we cannot, therefore, vouch for its reliability. Please note that this notice is intended solely to alert readers that the content of this article is unreliable. We have not investigated whether authors were aware of or involved in the systematic manipulation of the publication process.

Wiley and Hindawi regrets that the usual quality checks did not identify these issues before publication and have since put additional measures in place to safeguard research integrity.

We wish to credit our own Research Integrity and Research Publishing teams and anonymous and named external researchers and research integrity experts for contributing to this investigation.

The corresponding author, as the representative of all authors, has been given the opportunity to register their agreement or disagreement to this retraction. We have kept a record of any response received.

References

[1] Z. Ullah, H. Bashir, R. Anjum et al., "Some Novel Geometric Aggregation Operators of Spherical Cubic Fuzzy Information with Application," *Security and Communication Networks*, vol. 2021, Article ID 3774353, 14 pages, 2021.

WILEY | Hindawi

Research Article

Some Novel Geometric Aggregation Operators of Spherical Cubic Fuzzy Information with Application

Zafar Ullah [1], **Huma Bashir** [2], **Rukhshanda Anjum**, [3] **Mabrook Al-Rakhami** [4], **Suheer Al-Hadhrami** [5], **and Abdul Ghaffar** [6]

¹Department of Mathematics, Division of Science and Technology, University of Education, Lahore, Pakistan
²Departemant of Basic Sciences, UCET, Bahauddin Zakariya University, Multan, Pakistan
³Deaprtament of Mathematics and Statistics, University of Lahore, Lahore, Pakistan
⁴STC's Artificial Intelligence Chair, Department of Information Systems, College of Computer and Information Sciences, King Saud University, Riyadh 11543, Saudi Arabia
⁵Computer Engineering Department, Engineering College, Hadhramout University, Hadhramout, Yemen
⁶Department of Mathematics, Ghazi University, DG Khan 32200, Pakistan

Correspondence should be addressed to Mabrook Al-Rakhami; malrakhami@ksu.edu.sa and Suheer Al-Hadhrami; s.alhadhrami1@gmail.com

Technology is quickly evolving and becoming part of our lives. Life has become better and easier due to the technologies. Although it has lots of benefits, it also brings serious risks and threats, known as cyberattacks, which are neutralized by cybersecurities. Since spherical fuzzy sets (SFSs) and interval-valued SFS (IVSFS) are an excellent tool in coping with uncertainty and fuzziness, the current study discusses the idea of spherical cubic FSs (SCFSs). These sets are characterized by three mappings known as membership degree, neutral degree, and nonmembership degree. Each of these degrees is spherical cubic fuzzy numbers (SCFNs) such that the summation of their squares does not exceed one. The score function and accuracy function are presented for the comparison of SCFNs. Moreover, the spherical cubic fuzzy weighted geometric (SCFWG) operators and SCF ordered weighted geometric (SCFOWG) operators are established for determining the distance between two SCFNs. Furthermore, some operational rules of the proposed operators are analyzed and multiattribute decision-making (MADM) approach based on these operators is presented. These methods are applied to make the best decision on the basis of risks factors as a numerical illustration. Additionally, the comparison of the proposed method with the existing methods is carried out; since the proposed methods and operators are the generalizations of existing methods, they provide more general, exact, and accurate results. Finally, for the legitimacy, practicality, and usefulness of the decision-making processes, a detailed illustration is given.

1. Introduction

Multiple-attribute decision-making (MADM) means that, from the restricted alternatives set according to multiple attribute, the best alternative is selected that could be called cognitive processing. MADM is a key subdivision of the theory of decision-making (DM), commonly used in human activities [1]. The fuzzy knowledge usually is of two forms: qualitative and quantitative. The quantitative fuzzy knowledge is determined by fuzzy set (FS) [2], intuitionistic FS (IFS) [3], Pythagorean FS (PyFS) [4], and so forth. Zadeh's

FS theory was utilized to characterize fuzzy quantitative knowledge comprising of only membership degree. In light of this, Atanassov proposed IFS, consisting of two degrees, namely, membership and nonmembership. The summation of two grades should be less than or equal to one in an IFS. However, the two degrees often do not fulfill the constraints, but the sum of their squares does. Yager et al. [5] laid down the PyFS, which contains that the square sum of both the degrees is less than or equal to 1. In certain cases, the PyFSs will convey the details more effectively than the IFSs. For instance, if the membership, representing the support of an

expert, is 0.8 and nonmembership representing the opposition, is 0.6, then surely, this information cannot be represented by IFS, but it can be effectively described by PyFS.

Now, the IFS and PyFS do not provide a satisfactory result, since the neutral degree calculates the real-world problems independently. In order to handle this situation, Cuong and Kreinovich [6] originated the notion of a picture fuzzy set (PFS). A PFS is able to use three indexes, namely, membership degree $\check{P}(x)$, neutral degree $\check{I}(x)$, and nonmembership degree $\check{N}(x)$ on condition that $0 \leq \check{P}(x) + \check{I}(x) + \check{N}(x) \leq 1$. Of course, PFSs are more appropriate for managing the fuzziness and ambiguity than IFS or PyFS. Garg [7] presented the picture fuzzy weighted average operator (PFWAO) and picture fuzzy ordered weighted averaging aggregation operators. Since the last few decades, several researchers have investigated PyFS and have successfully applied it to a wide range of fields such as strategic decision-making, decision-making qualities, and design recognition [8–11]. In real life, we often have a lot of problems which cannot be solved with PFS; for instance, $\check{P}(x) + \check{I}(x) + \check{N}(x) > 1$. In these conditions, PFS cannot produce an acceptable result. To make this clear, an example is given: to support and to oppose the extent of an alternative membership, they are, respectively, 1/5, 3/5, and 3/5. This is based on their number exceeding 1 and not being presented for PFS. In light of these conditions, a generalization of PFS is introduced as the concept of spherical fuzzy sets (SFSs). The degrees of membership, neutral, and nonmembership in an SFS has the following condition:

$$0 \leq \overset{\vee}{P}^2(x) + \check{I}^2(x) + \check{N}^2(x) \leq 1. \tag{1}$$

In PyFS, Peng and Yang [12] introduced some new properties that are division, subtraction, and other important characteristics. The authors addressed the superiority and dependence ranking methodologies in the Pythagorean fuzzy setting to clarify the multiattribute decision-making problems. We et al. [13] implemented a maximizing variance protocol in order to clarify decisions based on Pythagorean fuzzy interval conditions. Garg [14] presented the IVPyF average (IVPyFWA) and IVPyF geometric (IVPFWG) and provided a concept of the new precision function based on PyF's interval-evaluated setting. Liang et al. [10] proposed the concepts of the medium and weighted PyF geometric Bonferroni mean (WPFGBM) operator. Many researchers proposed the idea of IVSF and its applications in DM problems [15–17]. Ayaz et al. [18] introduced the idea of SCFSs and applied it to the problems of multiattribute decision-making.

Many researchers presented the various applications of SFSs, IVSFSs. Kutlu Gündoğdu and Kahraman [19] presented the new approach of SFSs by using the TOPSIS methodology. Gündoğdu [20] presented the principals of SFSs and their applications in DM theory. Zeng et al. [21] gave the new concept by defining the probabilistic interactive aggregation operator of T-SFSs and their applications in solar cell selection. Liu et al. [22] gave the concept of multiattribute decision-making approach for Baiyao's R&D

project selection problem. Mathew et al. [23] presented the novel approach under SFSs for the selection of advanced manufacturing system. Gong et al. [24] gave a new approach of spherical distance for IFSs and its applications in DM. Kutlu Gundogdu and Kahraman [25] presented the WASPAS extension with spherical fuzzy sets. After that, Gundogdu and Kahraman [26] gave a new concept and related the TOPSIS methods to IVSFSs. Zeng et al. [27] introduced the TOPSIS methodology with covering-based SF rough set model for MADM. Liu et al. [28] gave a linguistic SFSs approach with applications for evaluation of shared bicycles in China. In 2019, Kutlu Gundogdu and Kahraman [29] showed a novel approach of VIKOR method using the SFSs and their applications in selection of warehouse site. We et al. [30] presented the similarity measures of SFSs based on cosine function. After that, in 2020, Khan et al. [31] introduced a new approach and related the distance and similarity measures for SFSs and their application in selection of mega project selection. Shishavan et al. [32] extended the idea of similarity measure in the environment of SF information. Recently, Mahmood et al. [33] further enhanced the idea of similarity measure and discussed it applications in pattern recognition and medical diagnosis.

The objectives of this paper include the following: (1) to determine an SCFS, (2) to define SCFNs and the associated operating identity; (3) to propose comparison functions for score, accuracy, or certainty; (4) to propose SCF geometric aggregation operators and some discussion on their properties.

Convincing accretion is one of the commanding tools of decision-making. The values are normalized by the collection operators. Additionally, these operators represent a wide range of data values. The weighted geometric aggregation operators are used for the position values of the required weight. The problems arise whenever the load segments of the weight vectors comprise segments that have a vital difference in parts of the weight vectors. This issue inspired proposing the idea of spherical cubic geometric aggregation operators. Henceforth, we present the notion of spherical cubic geometric aggregation operators. Moreover, the target of the DM techniques is to select the best choice among the available choices. In certain situations, the available choices are arranged in order to select the most suitable choice. These circumstances motivated presenting a method for the ranking of the available choices. We aim to combine the Einstein product and introduce the concepts of SCF Einstein weighted averaging (SCFEWA) operator, SCF Einstein ordered weighted averaging (SCFEOWA) operator, SCF Einstein weighted geometric (SCFEWG) operator, SCF Einstein ordered weighted geometric (SCFEOWG) operator, and some more generalized operators in MADM processes.

This article describes the concept of the SCFS, which is the extension of IVSF based on the constraints of the fact that the square sum of the supremum of its degrees of membership is less than one. Here, the concept of the SCFS is introduced, that is, the generalization of the IVSFS. We analyze certain SCFS properties. For comparison of SCFNs, the score and degree of deviation are described. The distance

between SCFNs is defined. SCFS states that the square of the supremacy to its membership is less than or equal to 1. Based on this information, aggregation operators are, for example, SCF weighted geometric (SCFWG), SCF ordered weighted geometric (SCFOWG), and SCF hybrid weighted geometric (SCFHWG). In addition, the proposed operators are utilized in problems of decision-making where experts give their preferences in the SCF details to illustrate the practicality of the new method and its efficiency.

The remaining of the paper is organized as follows: Section 2 presents some basic definitions and important properties. Section 3 proposes some geometric aggregation operators for SCFNs and their properties. Section 4 applies the spherical cubic geometric aggregation operators for MADM process. Section 5 presents the numerical illustration for the application and the final section concludes the study.

2. Preliminaries

This section presents a few elementary definitions with their key properties.

Definition 1 (see [2]). Supposing $\widehat{T}$ be a universal set, the fuzzy set (FS) $\widetilde{F}$ formulates as follows:

$$\widetilde{F} = \left\{ \left\langle \widehat{t}, \widetilde{\mu}_{\widetilde{F}}(\widehat{t}) \right\rangle | \widehat{t} \in \widehat{T} \right\}, \tag{2}$$

where $\widetilde{\mu}_{\widetilde{F}}: \widehat{T} \longrightarrow [0,1]$ is the membership degree of $\widehat{t} \in \widehat{T}$.

Definition 2 (see [3]). Supposing $\widehat{T}$ be a universal set, the fuzzy set (FS) $\widetilde{I}$ formulates as follows:

$$\widetilde{I} = \left\{ \left\langle \widehat{t}, \widetilde{\mu}_{\widetilde{I}}(\widehat{t}), \widetilde{\vartheta}_{\widetilde{I}}(\widehat{t}) \right\rangle | \widehat{t} \in \widehat{T} \right\}, \tag{3}$$

where $\widetilde{\mu}_{\widetilde{I}}: \widehat{T} \longrightarrow [0,1]$ is the membership degree and $\widetilde{\vartheta}_{\widetilde{I}}: \widehat{T} \longrightarrow [0,1]$ is the nonmembership degree of $\widehat{t} \in \widehat{T}$, under the specified condition

$$0 \le \widetilde{\mu}_{\widetilde{I}} + \widetilde{\vartheta}_{\widetilde{I}} \le 1. \tag{4}$$

Definition 3 (see [18]). Suppose $\widehat{T}$ be a universal set. A cubic set (CS) $\widetilde{C}$ formulates as follows:

$$\widetilde{C} = \left\{ \left\langle \widehat{t}, \widetilde{\mu}_{\widetilde{C}}(\widehat{t}), \widetilde{\vartheta}_{\widetilde{C}}(\widehat{t}) \right\rangle | \widehat{t} \in \widehat{T} \right\}, \tag{5}$$

where $\widetilde{\mu}_{\widetilde{C}}$ is an IVFS in $\widehat{T}$ and $\widetilde{\vartheta}_{\widetilde{C}}$ is a simple FS.

Definition 4 (see [18]). Supposing $\widehat{T}$ be a universal set, then a spherical fuzzy set (SFS) $\widetilde{Q}$ is of the following form:

$$\widetilde{Q} = \left\{ \left\langle \widehat{t}, \widetilde{\mu}_{\widetilde{Q}}(\widehat{t}), \widetilde{\eta}_{\widetilde{Q}}(\widehat{t}), \widetilde{\vartheta}_{\widetilde{Q}}(\widehat{t}) \right\rangle | \widehat{t} \in \widehat{T} \right\}, \tag{6}$$

where $\widetilde{\mu}_{\widetilde{Q}}: \widehat{T} \longrightarrow [0,1]$ is the membership degree, $\widetilde{\eta}_{\widetilde{Q}}: \widehat{T} \longrightarrow [0,1]$ is the neutral degree, and $\widetilde{\vartheta}_{\widetilde{Q}}: \widehat{T} \longrightarrow [0,1]$ is the nonmembership degree of $\widehat{t} \in \widehat{T}$, under the specified condition:

$$0 \le \left(\widetilde{\mu}_{\widetilde{Q}}\right)^2 + \left(\widetilde{\eta}_{\widetilde{Q}}\right)^2 + \left(\widetilde{\vartheta}_{\widetilde{Q}}\right)^2 \le 1. \tag{7}$$

The indeterminacy degree for SFS $\widetilde{Q}$ is defined as follows:

$$\widetilde{\pi}_{\widetilde{Q}} = \sqrt{1 - \left(\widetilde{\mu}_{\widetilde{Q}}\right)^2 - \left(\widetilde{\eta}_{\widetilde{Q}}\right)^2 - \left(\widetilde{\vartheta}_{\widetilde{Q}}\right)^2}. \tag{8}$$

For uncomplicatedness, we represent the SFN as $\widetilde{Q} = \Gamma_{\widetilde{Q}}, \Upsilon_{\widetilde{Q}}, \Lambda_{\widetilde{Q}}$.

Definition 5 (see [26]). Supposing $\widehat{T}$ be a universal set, an interval-valued SFS (IVSFS) $\widetilde{A}_{\widetilde{Q}}$ is defined as follows:

$$\widetilde{A}_{\widetilde{Q}} = \left\{ \left\langle \widehat{t}, \left(\left[\widetilde{\mu}^L_{A_{\widetilde{Q}}}(\widehat{t}), \widetilde{\mu}^U_{A_{\widetilde{Q}}}(\widehat{t}) \right], \left[\widetilde{\eta}^L_{A_{\widetilde{Q}}}(\widehat{t}), \widetilde{\eta}^U_{A_{\widetilde{Q}}}(\widehat{t}) \right], \left[\widetilde{\vartheta}^L_{A_{\widetilde{Q}}}(\widehat{t}), \widetilde{\vartheta}^U_{A_{\widetilde{Q}}}(\widehat{t}) \right] \right) \right\rangle | \widehat{t} \in \widehat{T} \right\}, \tag{9}$$

where $0 \le \widetilde{\mu}^L_{A_{\widetilde{Q}}}(\widehat{t}) \le \widetilde{\mu}^U_{A_{\widetilde{Q}}}(\widehat{t}) \le 1$, $0 \le \widetilde{\eta}^L_{A_{\widetilde{Q}}}(\widehat{t}) \le \widetilde{\eta}^U_{A_{\widetilde{Q}}}(\widehat{t}) \le 1$, $0 \le \widetilde{\vartheta}^L_{A_{\widetilde{Q}}}(\widehat{t}) \le \widetilde{\vartheta}^U_{A_{\widetilde{Q}}}(\widehat{t})) \le 1$, and $0 \le (\widetilde{\mu}^U_{A_{\widetilde{Q}}}(\widehat{t}))^2 + (\widetilde{\eta}^U_{A_{\widetilde{Q}}}(\widehat{t}))^2 + (\widetilde{\vartheta}^U_{A_{\widetilde{Q}}}(\widehat{t}))^2 \le 1$. If $\widetilde{\mu}^L_{A_{\widetilde{Q}}}(\widehat{t}) = \widetilde{\mu}^U_{A_{\widetilde{Q}}}(\widehat{t})$, $\widetilde{\eta}^L_{A_{\widetilde{Q}}}(\widehat{t}) = \widetilde{\eta}^U_{A_{\widetilde{Q}}}(\widehat{t})$, $\widetilde{\vartheta}^L_{A_{\widetilde{Q}}}(\widehat{t}) = \widetilde{\vartheta}^U_{A_{\widetilde{Q}}}(\widehat{t})$, then IVSFS reduces to SFS.

$$\text{Score}\left(\widetilde{A}_{\widetilde{Q}}\right) = \frac{1}{2} \left(\left(\widetilde{\mu}^L_{A_{\widetilde{Q}}}(\widehat{t})\right)^2 + \left(\widetilde{\mu}^U_{A_{\widetilde{Q}}}(\widehat{t})\right)^2 - \left(\widetilde{\eta}^L_{A_{\widetilde{Q}}}(\widehat{t})\right)^2 - \left(\widetilde{\eta}^U_{A_{\widetilde{Q}}}(\widehat{t})\right)^2 - \left(\widetilde{\vartheta}^L_{A_{\widetilde{Q}}}(\widehat{t})\right)^2 - \left(\widetilde{\vartheta}^U_{A_{\widetilde{Q}}}(\widehat{t})\right)^2 \right), \tag{10}$$

where score $(\widetilde{A}_{\widetilde{Q}}) \in [-1,1]$.

Definition 6 (see 27). Let $\widetilde{A}_{\widetilde{Q}} = ([\widetilde{\mu}^L_{A_{\widetilde{Q}}}(\widehat{t}), \widetilde{\mu}^U_{A_{\widetilde{Q}}}(\widehat{t})], [\widetilde{\eta}^L_{A_{\widetilde{Q}}}(\widehat{t}), \widetilde{\eta}^U_{A_{\widetilde{Q}}}(\widehat{t})], [\widetilde{\vartheta}^L_{A_{\widetilde{Q}}}(\widehat{t}), \widetilde{\vartheta}^U_{A_{\widetilde{Q}}}(\widehat{t})])$ be IVSFS, the score function of $\widetilde{A}_{\widetilde{Q}}$ can be described in the following way:

Definition 7 (see 27). Let $\widetilde{A}_{\widetilde{Q}} = ([\widetilde{\mu}^L_{A_{\widetilde{Q}}}(\widehat{t}), \widetilde{\mu}^U_{A_{\widetilde{Q}}}(\widehat{t})], [\widetilde{\eta}^L_{A_{\widetilde{Q}}}(\widehat{t}), \widetilde{\eta}^U_{A_{\widetilde{Q}}}(\widehat{t})], [\widetilde{\vartheta}^L_{A_{\widetilde{Q}}}(\widehat{t}), \widetilde{\vartheta}^U_{A_{\widetilde{Q}}}(\widehat{t})])$ be IVSFS, the accuracy function of $\widetilde{A}_{\widetilde{Q}}$ can be described in the following way:

$$\text{accuracy}\left(\widetilde{A}_{\widetilde{Q}}\right) = \frac{1}{2}\left(\left(\widetilde{\mu}^{L}_{A_{\widetilde{Q}}}(\hat{t})\right)^2 + \left(\widetilde{\mu}^{U}_{A_{\widetilde{Q}}}(\hat{t})\right)^2 + \left(\widetilde{\eta}^{L}_{A_{\widetilde{Q}}}(\hat{t})\right)^2 \right.$$
$$\left. + \left(\widetilde{\eta}^{U}_{A_{\widetilde{Q}}}(\hat{t})\right)^2 + \left(\widetilde{\vartheta}^{L}_{A_{\widetilde{Q}}}(\hat{t})\right)^2 + \left(\widetilde{\vartheta}^{U}_{A_{\widetilde{Q}}}(\hat{t})\right)(\hat{t})^2 \right), \tag{11}$$

where accuracy $\left(\widetilde{A}_{\widetilde{Q}}\right) \in [0, 1]$.

Definition 8 (see [27]). Let $\widetilde{A}_{\widetilde{Q}_1} = ([\widetilde{\mu}^{L}_{A_{\widetilde{Q}_1}}(\hat{t}), \widetilde{\mu}^{U}_{A_{\widetilde{Q}_1}}(\hat{t})], [\widetilde{\eta}^{L}_{A_{\widetilde{Q}_1}}(\hat{t}), \widetilde{\eta}^{U}_{A_{\widetilde{Q}_1}}(\hat{t})], [\widetilde{\vartheta}^{L}_{A_{\widetilde{Q}_1}}(\hat{t}), \widetilde{\vartheta}^{U}_{A_{\widetilde{Q}_1}}(\hat{t})])$ and $\widetilde{A}_{\widetilde{Q}_2} = ([\widetilde{\mu}^{L}_{A_{\widetilde{Q}_2}}(\hat{t}), \widetilde{\mu}^{U}_{A_{\widetilde{Q}_2}}(\hat{t})], [\widetilde{\eta}^{L}_{A_{\widetilde{Q}_2}}(\hat{t}), \widetilde{\eta}^{U}_{A_{\widetilde{Q}_2}}(\hat{t})], [\widetilde{\vartheta}^{L}_{A_{\widetilde{Q}_2}}(\hat{t}), \widetilde{\vartheta}^{U}_{A_{\widetilde{Q}_2}}(\hat{t})])$ be two IVSFNs; then,

$$S\left(\widetilde{A}_{\widetilde{Q}_1}\right) = \text{Score}\left(\widetilde{A}_{\widetilde{Q}_1}\right)$$
$$= \frac{1}{2}\left(\left(\widetilde{\mu}^{L}_{A_{\widetilde{Q}_1}}(\hat{t})\right)^2 + \left(\widetilde{\mu}^{U}_{A_{\widetilde{Q}_1}}(\hat{t})\right)^2 - \left(\widetilde{\eta}^{L}_{A_{\widetilde{Q}_1}}(\hat{t})\right)^2 - \left(\widetilde{\eta}^{U}_{A_{\widetilde{Q}_1}}(\hat{t})\right)^2 - \left(\widetilde{\vartheta}^{L}_{A_{\widetilde{Q}_1}}(\hat{t})\right)^2 - \left(\widetilde{\vartheta}^{U}_{A_{\widetilde{Q}_1}}(\hat{t})\right)^2 \right),$$
$$S\left(\widetilde{A}_{\widetilde{Q}_2}\right) = \text{Score}\left(\widetilde{A}_{\widetilde{Q}_2}\right)$$
$$= \frac{1}{2}\left(\left(\widetilde{\mu}^{L}_{A_{\widetilde{Q}_2}}(\hat{t})\right)^2 + \left(\widetilde{\mu}^{U}_{A_{\widetilde{Q}_2}}(\hat{t})\right)^2 - \left(\widetilde{\eta}^{L}_{A_{\widetilde{Q}_2}}(\hat{t})\right)^2 - \left(\widetilde{\eta}^{U}_{A_{\widetilde{Q}_2}}(\hat{t})\right)^2 - \left(\widetilde{\vartheta}^{L}_{A_{\widetilde{Q}_2}}(\hat{t})\right)^2 - \left(\widetilde{\vartheta}^{U}_{A_{\widetilde{Q}_2}}(\hat{t})\right)^2 \right), \tag{12}$$

are the score functions of $\widetilde{A}_{\widetilde{Q}_1}$ and $\widetilde{A}_{\widetilde{Q}_2}$, respectively. And

$$H\left(\widetilde{A}_{\widetilde{Q}_1}\right) = \text{accuracy}\left(\widetilde{A}_{\widetilde{Q}_1}\right)$$
$$= \frac{1}{2}\left(\left(\widetilde{\mu}^{L}_{A_{\widetilde{Q}_1}}(\hat{t})\right)^2 + \left(\widetilde{\mu}^{U}_{A_{\widetilde{Q}_1}}(\hat{t})\right)^2 + \left(\widetilde{\eta}^{L}_{A_{\widetilde{Q}_1}}(\hat{t})\right)^2 + \left(\widetilde{\eta}^{U}_{A_{\widetilde{Q}_1}}(\hat{t})\right)^2 + \left(\widetilde{\vartheta}^{L}_{A_{\widetilde{Q}_1}}(\hat{t})\right)^2 + \left(\widetilde{\vartheta}^{U}_{A_{\widetilde{Q}_1}}(\hat{t})\right)^2 \right),$$
$$H\left(\widetilde{A}_{\widetilde{Q}_2}\right) = \text{accuracy}\left(\widetilde{A}_{\widetilde{Q}_2}\right)$$
$$== \frac{1}{2}\left(\left(\widetilde{\mu}^{L}_{A_{\widetilde{Q}_2}}(\hat{t})\right)^2 + \left(\widetilde{\mu}^{U}_{A_{\widetilde{Q}_2}}(\hat{t})\right)^2 + \left(\widetilde{\eta}^{L}_{A_{\widetilde{Q}_2}}(\hat{t})\right)^2 + \left(\widetilde{\eta}^{U}_{A_{\widetilde{Q}_2}}(\hat{t})\right)^2 + \left(\widetilde{\vartheta}^{L}_{A_{\widetilde{Q}_2}}(\hat{t})\right)^2 + \left(\widetilde{\vartheta}^{U}_{A_{\widetilde{Q}_2}}(\hat{t})\right)^2 \right), \tag{13}$$

are the accuracy functions of $\widetilde{A}_{\widetilde{Q}_1}$ and $\widetilde{A}_{\widetilde{Q}_2}$, respectively. Then, we have the following properties:

(1) If $S(\widetilde{A}_{\widetilde{Q}_1}) < S(\widetilde{A}_{\widetilde{Q}_2})$, then $\widetilde{A}_{\widetilde{Q}_1} < \widetilde{A}_{\widetilde{Q}_2}$,
(2) If $S(\widetilde{A}_{\widetilde{Q}_1}) > S(\widetilde{A}_{\widetilde{Q}_2})$, then $\widetilde{A}_{\widetilde{Q}_1} > \widetilde{A}_{\widetilde{Q}_2}$,
(3) If $S(\widetilde{A}_{\widetilde{Q}_1}) = S(\widetilde{A}_{\widetilde{Q}_2})$, then we have

    (a) If $H(\widetilde{A}_{\widetilde{Q}_1}) < H(\widetilde{A}_{\widetilde{Q}_2})$, then $\widetilde{A}_{\widetilde{Q}_1} < \widetilde{A}_{\widetilde{Q}_2}$,
    (b) If $H(\widetilde{A}_{\widetilde{Q}_1}) > H(\widetilde{A}_{\widetilde{Q}_2})$, then $\widetilde{A}_{\widetilde{Q}_1} > \widetilde{A}_{\widetilde{Q}_2}$,
    (c) If $H(\widetilde{A}_{\widetilde{Q}_1}) = H(\widetilde{A}_{\widetilde{Q}_2})$, then $\widetilde{A}_{\widetilde{Q}_1} = \widetilde{A}_{\widetilde{Q}_2}$.

Definition 9 (see [27]). Let $\widetilde{A}_{\widetilde{Q}_1} = ([\widetilde{\mu}^{L}_{A_{\widetilde{Q}_1}}(\hat{t}), \widetilde{\mu}^{U}_{A_{\widetilde{Q}_1}}(\hat{t})], [\widetilde{\eta}^{L}_{A_{\widetilde{Q}_1}}(\hat{t}), \widetilde{\eta}^{U}_{A_{\widetilde{Q}_1}}(\hat{t})], [\widetilde{\vartheta}^{L}_{A_{\widetilde{Q}_1}}(\hat{t}), \widetilde{\vartheta}^{U}_{A_{\widetilde{Q}_1}}(\hat{t})])$ and $\widetilde{A}_{\widetilde{Q}_2} = ([\widetilde{\mu}^{L}_{A_{\widetilde{Q}_2}}(\hat{t}), \widetilde{\mu}^{U}_{A_{\widetilde{Q}_2}}(\hat{t})], [\widetilde{\eta}^{L}_{A_{\widetilde{Q}_2}}(\hat{t}), \widetilde{\eta}^{U}_{A_{\widetilde{Q}_2}}(\hat{t})], [\widetilde{\vartheta}^{L}_{A_{\widetilde{Q}_2}}(\hat{t}), \widetilde{\vartheta}^{U}_{A_{\widetilde{Q}_2}}(\hat{t})])$ be two IVSFNs; then,

(1) $\widetilde{\lambda}\widetilde{A}_{\widetilde{Q}_1} =$
$$\left(\begin{array}{c} \left[\sqrt{(\widetilde{\mu}^{L}_{A_{\widetilde{Q}_1}}(\hat{t}))^2 + (\widetilde{\mu}^{L}_{A_{\widetilde{Q}_2}}(\hat{t}))^2 - (\widetilde{\mu}^{L}_{A_{\widetilde{Q}_1}}(\hat{t}))^2(\widetilde{\mu}^{L}_{A_{\widetilde{Q}_2}}(\hat{t}))^2}, \sqrt{(\widetilde{\mu}^{U}_{A_{\widetilde{Q}_1}}(\hat{t}))^2 + (\widetilde{\mu}^{U}_{A_{\widetilde{Q}_2}}(\hat{t}))^2 - (\widetilde{\mu}^{U}_{A_{\widetilde{Q}_1}}(\hat{t}))^2(\widetilde{\mu}^{U}_{A_{\widetilde{Q}_2}}(\hat{t}))^2} \right], \\ [\widetilde{\eta}^{L}_{A_{\widetilde{Q}_1}}(\hat{t}) \cdot \widetilde{\eta}^{L}_{A_{\widetilde{Q}_2}}(\hat{t}), \widetilde{\eta}^{U}_{A_{\widetilde{Q}_1}}(\hat{t}) \cdot \widetilde{\eta}^{U}_{A_{\widetilde{Q}_2}}(\hat{t})], \\ \left[\sqrt{(1-(\widetilde{\mu}^{L}_{A_{\widetilde{Q}_1}}(\hat{t}))^2)(\widetilde{\vartheta}^{L}_{A_{\widetilde{Q}_2}}(\hat{t}))^2 + (1-(\widetilde{\mu}^{L}_{A_{\widetilde{Q}_2}}(\hat{t}))^2)(\widetilde{\vartheta}^{L}_{A_{\widetilde{Q}_1}}(\hat{t}))^2 - (\widetilde{\vartheta}^{L}_{A_{\widetilde{Q}_1}}(\hat{t}))^2(\widetilde{\vartheta}^{L}_{A_{\widetilde{Q}_2}}(\hat{t}))^2}}, \\ \sqrt{(1-(\widetilde{\mu}^{U}_{A_{\widetilde{Q}_2}}(\hat{t}))^2)(\widetilde{\vartheta}^{U}_{A_{\widetilde{Q}_1}}(\hat{t}))^2 + (1-(\widetilde{\mu}^{U}_{A_{\widetilde{Q}_1}}(\hat{t}))^2)(\widetilde{\vartheta}^{U}_{A_{\widetilde{Q}_2}}(\hat{t}))^2 - (\widetilde{\vartheta}^{U}_{A_{\widetilde{Q}_1}}(\hat{t}))^2(\widetilde{\vartheta}^{U}_{A_{\widetilde{Q}_2}}(\hat{t}))^2}\right] \end{array}\right)$$

(2) $[\widetilde{\mu}^{L}_{A_{\widetilde{Q}_1}}(\hat{t}) \cdot \widetilde{\mu}^{L}_{A_{\widetilde{Q}_2}}(\hat{t}), \widetilde{\mu}^{U}_{A_{\widetilde{Q}_1}}(\hat{t}) \cdot \widetilde{\mu}^{U}_{A_{\widetilde{Q}_2}}(\hat{t})]$
$$\left[\sqrt{(\widetilde{\eta}^{L}_{A_{\widetilde{Q}_1}}(\hat{t}))^2 + (\widetilde{\eta}^{L}_{A_{\widetilde{Q}_2}}(\hat{t}))^2 - (\widetilde{\eta}^{L}_{A_{\widetilde{Q}_1}}(\hat{t}))^2(\widetilde{\eta}^{L}_{A_{\widetilde{Q}_2}}(\hat{t}))^2}, \sqrt{(\widetilde{\eta}^{U}_{A_{\widetilde{Q}_1}}(\hat{t}))^2 + (\widetilde{\eta}^{U}_{A_{\widetilde{Q}_2}}(\hat{t}))^2 - (\widetilde{\eta}^{U}_{A_{\widetilde{Q}_1}}(\hat{t}))^2(\widetilde{\eta}^{U}_{A_{\widetilde{Q}_2}}(\hat{t}))^2} \right]$$
$[\widetilde{\mu}^{L}_{A_{\widetilde{Q}_1}}(\hat{t}) \cdot \widetilde{\mu}^{L}_{A_{\widetilde{Q}_2}}(\hat{t}), \widetilde{\mu}^{U}_{A_{\widetilde{Q}_1}}(\hat{t}) \cdot \widetilde{\mu}^{U}_{A_{\widetilde{Q}_2}}(\hat{t})]$
$$\left[\sqrt{(1-(\widetilde{\eta}^{L}_{A_{\widetilde{Q}_1}}(\hat{t}))^2)(\widetilde{\eta}^{L}_{A_{\widetilde{Q}_2}}(\hat{t}))^2 + (1-(\widetilde{\eta}^{L}_{A_{\widetilde{Q}_2}}(\hat{t}))^2)(\widetilde{\eta}^{L}_{A_{\widetilde{Q}_1}}(\hat{t}))^2 - (\widetilde{\vartheta}^{L}_{A_{\widetilde{Q}_1}}(\hat{t}))^2(\widetilde{\vartheta}^{L}_{A_{\widetilde{Q}_2}}(\hat{t}))^2}, \\ \sqrt{(1-(\widetilde{\eta}^{U}_{A_{\widetilde{Q}_1}}(\hat{t}))^2)(\widetilde{\eta}^{U}_{A_{\widetilde{Q}_2}}(\hat{t}))^2 + (1-(\widetilde{\eta}^{U}_{A_{\widetilde{Q}_2}}(\hat{t}))^2)(\widetilde{\eta}^{U}_{A_{\widetilde{Q}_1}}(\hat{t}))^2 - (\widetilde{\vartheta}^{U}_{A_{\widetilde{Q}_1}}(\hat{t}))^2(\widetilde{\vartheta}^{U}_{A_{\widetilde{Q}_2}}(\hat{t}))^2}\right]$$

(3) $\widetilde{\lambda}\widetilde{A}_{\widetilde{Q}_1} =$
$$\left(\begin{array}{c} [\sqrt{1-(1-(\widetilde{\mu}^{L}_{A_{\widetilde{Q}_1}}(\hat{t}))^2)^{\widetilde{\lambda}}}, \sqrt{1-(1-(\widetilde{\mu}^{U}_{A_{\widetilde{Q}_1}}(\hat{t}))^2)^{\widetilde{\lambda}}}], [(\widetilde{\eta}^{L}_{A_{\widetilde{Q}_1}}(\hat{t}))^{\widetilde{\lambda}}, (\widetilde{\eta}^{U}_{A_{\widetilde{Q}_1}}(\hat{t}))^{\widetilde{\lambda}}], \\ \left[\sqrt{(1-(\widetilde{\mu}^{L}_{A_{\widetilde{Q}_1}}(\hat{t}))^2)^{\widetilde{\lambda}} - (1-(\widetilde{\mu}^{L}_{A_{\widetilde{Q}_1}}(\hat{t}))^2 - (\widetilde{\vartheta}^{L}_{A_{\widetilde{Q}_1}}(\hat{t}))^2)^{\widetilde{\lambda}}}, \\ \sqrt{(1-(\widetilde{\mu}^{U}_{A_{\widetilde{Q}_1}}(\hat{t}))^2)^{\widetilde{\lambda}} - (1-(\widetilde{\mu}^{U}_{A_{\widetilde{Q}_1}}(\hat{t}))^2 - (\widetilde{\vartheta}^{U}_{A_{\widetilde{Q}_1}}(\hat{t}))^2)^{\widetilde{\lambda}}}\right] \end{array}\right)$$

$$(4)\ \widetilde{A}^{\widetilde{\lambda}}_{\widetilde{Q}_1} = \begin{pmatrix} [(\widetilde{\mu}^L_{\widetilde{A}_{Q_1}}(\hat{t})^{\widetilde{\lambda}}, (\widetilde{\mu}^U_{\widetilde{A}_{Q_1}}(\hat{t})^{\widetilde{\lambda}}] \\ [\sqrt{1-(1-(\widetilde{\eta}^L_{\widetilde{A}_{Q_1}}(\hat{t})^2)^{\widetilde{\lambda}}}, \sqrt{1-(1-(\widetilde{\eta}^U_{\widetilde{A}_{Q_1}}(\hat{t})^2)^{\widetilde{\lambda}}}], [(\widetilde{\eta}^L_{\widetilde{A}_{Q_1}}(\hat{t})^{\widetilde{\lambda}}, (\widetilde{\eta}^U_{\widetilde{A}_{Q_1}}(\hat{t})^{\widetilde{\lambda}}], \\ \left[\sqrt{(1-(\widetilde{\eta}^L_{\widetilde{A}_{Q_1}}(\hat{t})^2)^{\widetilde{\lambda}}-(1-(\widetilde{\eta}^L_{\widetilde{A}_{Q_1}}(\hat{t})^2-(\widetilde{\vartheta}^L_{\widetilde{A}_{Q_1}}(\hat{t})^2)^{\widetilde{\lambda}}}, \\ \sqrt{(1-(\widetilde{\eta}^U_{\widetilde{A}_{Q_1}}(\hat{t})^2)^{\widetilde{\lambda}}-(1-(\widetilde{\eta}^U_{\widetilde{A}_{Q_1}}(\hat{t})^2-(\widetilde{\vartheta}^U_{\widetilde{A}_{Q_1}}(\hat{t})^2)^{\widetilde{\lambda}}} \right] \end{pmatrix}.$$

Definition 10 (see [27]). Let $\widetilde{A}_{\widetilde{Q}_1} = ([\widetilde{\mu}^L_{\widetilde{A}_{Q_1}}(\hat{t}), \widetilde{\mu}^U_{\widetilde{A}_{Q_1}}(\hat{t})],$ $[\widetilde{\eta}^L_{\widetilde{A}_{Q_1}}(\hat{t}), \widetilde{\eta}^U_{\widetilde{A}_{Q_1}}(\hat{t})],\ [\widetilde{\vartheta}^L_{\widetilde{A}_{Q_1}}(\hat{t}), \widetilde{\vartheta}^U_{\widetilde{A}_{Q_1}}(\hat{t})](\hat{t}))$ and $\widetilde{A}_{\widetilde{Q}_2} = ([\widetilde{\mu}^L_{\widetilde{A}_{Q_2}}$

$(\hat{t}), \widetilde{\mu}^U_{\widetilde{A}_{Q_2}}(\hat{t})], [\widetilde{\eta}^L_{\widetilde{A}_{Q_2}}(\hat{t}), \widetilde{\eta}^U_{\widetilde{A}_{Q_2}}(\hat{t})], [\widetilde{\vartheta}^L_{\widetilde{A}_{Q_2}}(\hat{t}), \widetilde{\vartheta}^U_{\widetilde{A}_{Q_2}}(\hat{t})])$ be the set comprised of IVSFNs; then, IVSF weighted geometric (IVSFWG) operator is defined as follows:

$$\text{IVSFWG}\left(\widetilde{A}_{\widetilde{Q}_1}, \widetilde{A}_{\widetilde{Q}_2}, \ldots, \widetilde{A}_{\widetilde{Q}_N}\right) = \begin{pmatrix} \left[\prod_{i=1}^{n}\left(\widetilde{\mu}^L_{\widetilde{A}_{Q_1}}(\hat{t})\right)^{\omega i}, \prod_{i=1}^{n}\left(\widetilde{\mu}^U_{\widetilde{A}_{Q_1}}(\hat{t})\right)^{\omega i}, \right] \\ \left[\sqrt{1-\prod_{i=1}^{n}\left(1-\left(\widetilde{\eta}^L_{\widetilde{A}_{Q_1}}(\hat{t})^2\right)\right)^{\omega i}}, \sqrt{1-\prod_{i=1}^{n}\left(1-\left(\widetilde{\eta}^U_{\widetilde{A}_{Q_1}}(\hat{t})^2\right)\right)^{\omega i}} \right], \left[\left(\widetilde{\eta}^L_{\widetilde{A}_{Q_1}}(\hat{t})\right)^{\widetilde{\lambda}}, \left(\widetilde{\eta}^U_{\widetilde{A}_{Q_1}}(\hat{t})\right)^{\widetilde{\lambda}}\right], \\ \left[\sqrt{\prod_{i=1}^{n}\left(1-\left(\widetilde{\eta}^L_{\widetilde{A}_{Q_1}}(\hat{t})^2\right)\right)^{\omega i} - \prod_{i=1}^{n}\left(1-\left(\widetilde{\eta}^L_{\widetilde{A}_{Q_1}}(\hat{t})^2\right)-\left(\widetilde{\vartheta}^L_{\widetilde{A}_{Q_1}}(\hat{t})^2\right)\right)^{\omega i}}, \right. \\ \left. \sqrt{\prod_{i=1}^{n}\left(1-\left(\widetilde{\eta}^U_{\widetilde{A}_{Q_1}}(\hat{t})^2\right)\right)^{\omega i} - \prod_{i=1}^{n}\left(1-\left(\widetilde{\eta}^U_{\widetilde{A}_{Q_1}}(\hat{t})^2\right)-\left(\widetilde{\vartheta}^U_{\widetilde{A}_{Q_1}}(\hat{t})^2\right)\right)^{\omega i}}, \right] \end{pmatrix} \tag{14}$$

where $\omega = (\omega_1, \omega_2, \ldots, \omega_n)^T$ represent the weight vector of $\widetilde{A}_{\widetilde{Q}_i}$ $(i = 1, 2, \ldots, n)$ and $0 \le \omega_i \le 1, \sum_{i=1}^{n} \omega_i = 1$.

Definition 11 (see [18]). Supposing $\widehat{T}$ a universal set, then a spherical cubic FS (SCFS) $\widetilde{Q}_{\widetilde{C}}$ is defined as follows:

$$\widetilde{Q}_{\widetilde{C}} = \left\{ \left\langle \hat{t}, \Gamma_{\widetilde{Q}_C}(\hat{t}), \Upsilon_{\widetilde{Q}_C}(\hat{t}), \Lambda_{\widetilde{Q}_C}(\hat{t}) \right\rangle \mid \hat{t} \in \widehat{T} \right\}, \tag{15}$$

where $\Gamma_{\widetilde{Q}_C}(\hat{t}) = [a^-_{\widetilde{Q}_C}, a^{\pm}_{\widetilde{Q}_C}], \widetilde{\mu}_{\widetilde{Q}_C}$ represents the membership function, $\Upsilon_{\widetilde{Q}_C}(\hat{t}) = [n^-_{\widetilde{Q}_C}, n^{\pm}_{\widetilde{Q}_C}], \widetilde{\eta}_{\widetilde{Q}_C}$ represents the neutral degree, and $\Lambda_{\widetilde{Q}_C}(\hat{t}) = [b^-_{\widetilde{Q}_C}, b^{\pm}_{\widetilde{Q}_C}], \widetilde{\vartheta}_{\widetilde{Q}_C}$ represents the non-membership function, in which $\widetilde{\mu}_{\widetilde{Q}_C}: \widehat{T} \longrightarrow [0, 1], \widetilde{\eta}_{\widetilde{Q}_C}:$

$\widehat{T} \longrightarrow [0, 1]$, and $\widetilde{\vartheta}_{\widetilde{Q}_C}: \widehat{T} \longrightarrow [0, 1], \hat{t} \in \widehat{T}$, under the specified condition:

$$0 \le \left(\sup\left[a^-_{\widetilde{Q}_C}, a^{\pm}_{\widetilde{Q}_C} \right] \right)^2 + \left(\sup\left[n^-_{\widetilde{Q}_C}, n^{\pm}_{\widetilde{Q}_C} \right] \right)^2$$
$$+ \left(\sup\left[b^-_{\widetilde{Q}_C}, b^{\pm}_{\widetilde{Q}_C} \right] \right)^2 \le 1, \tag{16}$$
$$0 \le \left(\widetilde{\mu}_{\widetilde{Q}_C} \right)^2 + \left(\widetilde{\eta}_{\widetilde{Q}_C} \right)^2 + \left(\widetilde{\vartheta}_{\widetilde{Q}_C} \right)^2 \le 1.$$

The indeterminacy degree for (SCFS) $\widetilde{Q}_{\widetilde{C}}$ is defined as follows:

$$\widetilde{\pi}_{\widetilde{Q}} = \left\langle \left| \begin{array}{c} \sqrt{1 - \left(\sup\left[a^-_{\widetilde{Q}_C}, a^{\pm}_{\widetilde{Q}_C} \right] \right)^2 - \left(\sup\left[n^-_{\widetilde{Q}_C}, n^{\pm}_{\widetilde{Q}_C} \right] \right)^2 - \left(\sup\left[b^-_{\widetilde{Q}_C}, b^{\pm}_{\widetilde{Q}_C} \right] \right)^2}, \\ \sqrt{1 - \left(\widetilde{\mu}_{\widetilde{Q}_C} \right)^2 - \left(\widetilde{\eta}_{\widetilde{Q}_C} \right)^2 - \left(\widetilde{\vartheta}_{\widetilde{Q}_C} \right)^2} \end{array} \right. \right\rangle. \tag{17}$$

For simplicity, we represent the spherical number (SCFN) as $\widetilde{Q}_{\widetilde{C}} = \Gamma_{\widetilde{Q}_C}, \Upsilon_{\widetilde{Q}_C}, \Lambda_{\widetilde{Q}_C}$.

Definition 12 (see [19]). Let $\widetilde{Q}_{\widetilde{C}} = \left\{ \left\langle [a^-_{\widetilde{Q}_C}, a^{\pm}_{\widetilde{Q}_C}], \widetilde{\mu}_{\widetilde{Q}_C} \right\rangle, \left[n^-_{\widetilde{Q}_C}, n^{\pm}_{\widetilde{Q}_C} \right], \widetilde{\eta}_{\widetilde{Q}_C}, \left\langle \left[b^-_{\widetilde{Q}_C}, b^{\pm}_{\widetilde{Q}_C} \right], \widetilde{\vartheta}_{\widetilde{Q}_C} \right\rangle \right\}$ be SCFS; then, the score function of $\widetilde{Q}_{\widetilde{C}}$ is defined as follows:

$$\text{Score}\left(\tilde{Q}_{\tilde{C}}\right) = \frac{1}{9}\left(\left(a_{\tilde{Q}_{\tilde{C}}}^{-} + a_{\tilde{Q}_{\tilde{C}}}^{+} + \tilde{\mu}_{\tilde{Q}_{\tilde{C}}}\right)^2 + \left(n_{\tilde{Q}_{\tilde{C}}}^{-} + n_{\tilde{Q}_{\tilde{C}}}^{+} + \tilde{\eta}_{\tilde{Q}_{\tilde{C}}}\right)^2 - \left(b_{\tilde{Q}_{\tilde{C}}}^{-} + b_{\tilde{Q}_{\tilde{C}}}^{+} + \tilde{\vartheta}_{\tilde{Q}_{\tilde{C}}}\right)^2\right), \tag{18}$$

where Score $(\tilde{Q}_{\tilde{C}}) \in [-1, 1]$.

Definition 13 (see [19]). Supposing $\tilde{Q}_{\tilde{C}} = \left\{ \left\langle \left[a_{\tilde{Q}_{\tilde{C}}}^{-}, a_{\tilde{Q}_{\tilde{C}}}^{+}\right], \tilde{\mu}_{\tilde{Q}_{\tilde{C}}} \right\rangle, \left\langle \left[n_{\tilde{Q}_{\tilde{C}}}^{-}, n_{\tilde{Q}_{\tilde{C}}}^{+}\right], \tilde{\eta}_{\tilde{Q}_{\tilde{C}}} \right\rangle, \left\langle \left[b_{\tilde{Q}_{\tilde{C}}}^{-}, b_{\tilde{Q}_{\tilde{C}}}^{+}\right], \tilde{\vartheta}_{\tilde{Q}_{\tilde{C}}} \right\rangle \right\}$ be SCFS, then the accuracy function of $\tilde{Q}_{\tilde{C}}$ is defined as follows:

$$\begin{aligned} \text{accuracy}\left(\tilde{Q}_{\tilde{C}}\right) = \frac{1}{9}\left(\left(a_{\tilde{Q}_{\tilde{C}}}^{-} + a_{\tilde{Q}_{\tilde{C}}}^{+} + \tilde{\mu}_{\tilde{Q}_{\tilde{C}}}\right)^2 \right. \\ \left. + \left(n_{\tilde{Q}_{\tilde{C}}}^{-} + n_{\tilde{Q}_{\tilde{C}}}^{+} + \tilde{\eta}_{\tilde{Q}_{\tilde{C}}}\right)^2 + \left(b_{\tilde{Q}_{\tilde{C}}}^{-} + b_{\tilde{Q}_{\tilde{C}}}^{+} + \tilde{\vartheta}_{\tilde{Q}_{\tilde{C}}}\right)^2\right), \end{aligned} \tag{19}$$

where accuracy $(\tilde{Q}_{\tilde{C}}) \in [0, 1]$.

Definition 14 (see [19]). Let $\tilde{Q}_{\tilde{C}_1} = \Gamma_{\tilde{Q}_{\tilde{C}_1}}, \Upsilon_{\tilde{Q}_{\tilde{C}_1}}, \Lambda_{\tilde{Q}_{\tilde{C}_1}}$ and $\tilde{Q}_{\tilde{C}_2} = \Gamma_{\tilde{Q}_{\tilde{C}_2}}, \Upsilon_{\tilde{Q}_{\tilde{C}_2}}, \Lambda_{\tilde{Q}_{\tilde{C}_2}}$ be two SCFNs; then, we have the following:

(1) If score $(\tilde{Q}_{\tilde{C}_1}) <$ score $(\tilde{Q}_{\tilde{C}_2})$, then $\tilde{Q}_{\tilde{C}_1} < \tilde{Q}_{\tilde{C}_2}$,

(2) If score $(\tilde{Q}_{\tilde{C}_1}) >$ score $(\tilde{Q}_{\tilde{C}_2})$, then $\tilde{Q}_{\tilde{C}_1} > \tilde{Q}_{\tilde{C}_2}$,

(3) If score $(\tilde{Q}_{\tilde{C}_1}) =$ score $(\tilde{Q}_{\tilde{C}_2})$, then

   (a) If accuracy $(\tilde{Q}_{\tilde{C}_1}) <$ accuracy $(\tilde{Q}_{\tilde{C}_2})$, then

   (b) If accuracy $(\tilde{Q}_{\tilde{C}_1}) >$ accuracy $(\tilde{Q}_{\tilde{C}_2})$, then i $\tilde{Q}_{\tilde{C}_1} > \tilde{Q}_{\tilde{C}_2}$,

   (c) If accuracy $(\tilde{Q}_{\tilde{C}_1}) =$ accuracy $(\tilde{Q}_{\tilde{C}_2})$, then $\tilde{Q}_{\tilde{C}_1} = \tilde{Q}_{\tilde{C}_2}$.

Definition 15 (see [19]). Let $\tilde{Q}_{\tilde{C}_1} = \Gamma_{\tilde{Q}_{\tilde{C}_1}}, \Upsilon_{\tilde{Q}_{\tilde{C}_1}}, \Lambda_{\tilde{Q}_{\tilde{C}_1}}$ and $\tilde{Q}_{\tilde{C}_2} = \Gamma_{\tilde{Q}_{\tilde{C}_2}}, \Upsilon_{\tilde{Q}_{\tilde{C}_2}}, \Lambda_{\tilde{Q}_{\tilde{C}_2}}$ be two SCFNs; then, the distance function among $\tilde{Q}_{\tilde{C}_2}$ and $\tilde{Q}_{\tilde{C}_2}$ is defined as follows:

$$\tilde{D}\left(\tilde{Q}_{\tilde{C}_1}, \tilde{Q}_{\tilde{C}_2}\right) = \frac{1}{9}\left[\begin{array}{l} \left|\left(a_{\tilde{Q}_{\tilde{C}_1}}^{-}\right)^2 - \left(a_{\tilde{Q}_{\tilde{C}_2}}^{-}\right)^2\right| + \left|\left(a_{\tilde{Q}_{\tilde{C}_1}}^{+}\right)^2 - \left(a_{\tilde{Q}_{\tilde{C}_2}}^{+}\right)^2\right| + \left|\left(\tilde{\mu}_{\tilde{Q}_{\tilde{C}_1}}\right)^2 - \left(\tilde{\mu}_{\tilde{Q}_{\tilde{C}_2}}\right)^2\right| + \\ \left|\left(n_{\tilde{Q}_{\tilde{C}_1}}^{-}\right)^2 - \left(n_{\tilde{Q}_{\tilde{C}_2}}^{-}\right)^2\right| + \left|\left(n_{\tilde{Q}_{\tilde{C}_1}}^{+}\right)^2 - \left(n_{\tilde{Q}_{\tilde{C}_2}}^{+}\right)^2\right| + \left|\left(\tilde{\eta}_{\tilde{Q}_{\tilde{C}_1}}\right)^2 - \left(\tilde{\eta}_{\tilde{Q}_{\tilde{C}_2}}\right)^2\right| + \\ \left|\left(b_{\tilde{Q}_{\tilde{C}_1}}^{-}\right)^2 - \left(b_{\tilde{Q}_{\tilde{C}_2}}^{-}\right)^2\right| + \left|\left(b_{\tilde{Q}_{\tilde{C}_1}}^{+}\right)^2 - \left(b_{\tilde{Q}_{\tilde{C}_2}}^{+}\right)^2\right| + \left|\left(\tilde{\vartheta}_{\tilde{Q}_{\tilde{C}_1}}\right)^2 - \left(\tilde{\vartheta}_{\tilde{Q}_{\tilde{C}_2}}\right)^2\right| \end{array} \right]. \tag{20}$$

Definition 16 (see [19]). Let $\tilde{Q}_{\tilde{C}_1} = \Gamma_{\tilde{Q}_{\tilde{C}_1}}, \Upsilon_{\tilde{Q}_{\tilde{C}_1}}, \Lambda_{\tilde{Q}_{\tilde{C}_1}}$ and $\tilde{Q}_{\tilde{C}_2} = \Gamma_{\tilde{Q}_{\tilde{C}_2}}, \Upsilon_{\tilde{Q}_{\tilde{C}_2}}, \Lambda_{\tilde{Q}_{\tilde{C}_2}}$ be two spherical cubic fuzzy numbers; then, the below operational laws hold:

(1) $\tilde{Q}_{\tilde{C}_1} \oplus \tilde{Q}_{\tilde{C}_2} =$
$$\left\{ \begin{array}{l} \left(\left[\sqrt{(a_{\tilde{Q}_{\tilde{C}_1}}^{-})^2 + (a_{\tilde{Q}_{\tilde{C}_2}}^{-})^2 - (a_{\tilde{Q}_{\tilde{C}_1}}^{-})^2(a_{\tilde{Q}_{\tilde{C}_2}}^{-})^2},\right.\right. \\ \left.\sqrt{(a_{\tilde{Q}_{\tilde{C}_1}}^{+})^2 + (a_{\tilde{Q}_{\tilde{C}_2}}^{+})^2 - (a_{\tilde{Q}_{\tilde{C}_1}}^{+})^2(a_{\tilde{Q}_{\tilde{C}_2}}^{+})^2}\right], \\ \left.\sqrt{(\tilde{\mu}_{\tilde{Q}_{\tilde{C}_1}})^2 + (\tilde{\mu}_{\tilde{Q}_{\tilde{C}_2}})^2 - (\tilde{\mu}_{\tilde{Q}_{\tilde{C}_1}})^2(\tilde{\mu}_{\tilde{Q}_{\tilde{C}_2}})^2}\right), \\ \left([n_{\tilde{Q}_{\tilde{C}_1}}^{-}.n_{\tilde{Q}_{\tilde{C}_2}}^{-}, n_{\tilde{Q}_{\tilde{C}_1}}^{+}.n_{\tilde{Q}_{\tilde{C}_2}}^{+}], \tilde{\eta}_{\tilde{Q}_{\tilde{C}_1}}.\tilde{\eta}_{\tilde{Q}_{\tilde{C}_2}}\right), \\ \left([b_{\tilde{Q}_{\tilde{C}_1}}^{-}.b_{\tilde{Q}_{\tilde{C}_2}}^{-}, b_{\tilde{Q}_{\tilde{C}_1}}^{+}.b_{\tilde{Q}_{\tilde{C}_2}}^{+}], \tilde{\vartheta}_{\tilde{Q}_{\tilde{C}_1}}.\tilde{\vartheta}_{\tilde{Q}_{\tilde{C}_2}}\right) \end{array} \right\};$$

(2) $\tilde{Q}_{\tilde{C}_1} \otimes \tilde{Q}_{\tilde{C}_2} =$
$$\left\{ \begin{array}{l} \left([a_{\tilde{Q}_{\tilde{C}_1}}^{-}.a_{\tilde{Q}_{\tilde{C}_2}}^{-}, a_{\tilde{Q}_{\tilde{C}_1}}^{+}.a_{\tilde{Q}_{\tilde{C}_2}}^{+}], \tilde{\mu}_{\tilde{Q}_{\tilde{C}_1}}.\tilde{\mu}_{\tilde{Q}_{\tilde{C}_2}}\right), \left([n_{\tilde{Q}_{\tilde{C}_1}}^{-}.n_{\tilde{Q}_{\tilde{C}_2}}^{-}, n_{\tilde{Q}_{\tilde{C}_1}}^{+}.n_{\tilde{Q}_{\tilde{C}_2}}^{+}], \tilde{\eta}_{\tilde{Q}_{\tilde{C}_1}}.\tilde{\eta}_{\tilde{Q}_{\tilde{C}_2}}\right) \\ \left(\left[\sqrt{(b_{\tilde{Q}_{\tilde{C}_1}}^{-})^2 + (b_{\tilde{Q}_{\tilde{C}_2}}^{-})^2 - (b_{\tilde{Q}_{\tilde{C}_1}}^{-})^2(b_{\tilde{Q}_{\tilde{C}_2}}^{-})^2},\right.\right. \\ \left.\sqrt{(b_{\tilde{Q}_{\tilde{C}_1}}^{+})^2 + (b_{\tilde{Q}_{\tilde{C}_2}}^{+})^2 - (b_{\tilde{Q}_{\tilde{C}_1}}^{+})^2(b_{\tilde{Q}_{\tilde{C}_2}}^{+})^2}\right], \\ \left.\sqrt{(\tilde{\vartheta}_{\tilde{Q}_{\tilde{C}_1}})^2 + (\tilde{\vartheta}_{\tilde{Q}_{\tilde{C}_2}})^2 - (\tilde{\vartheta}_{\tilde{Q}_{\tilde{C}_1}})^2(\tilde{\vartheta}_{\tilde{Q}_{\tilde{C}_2}})^2}\right), \end{array} \right\};$$

(3) $\tau.\tilde{Q}_{\tilde{C}_1} =$
$$\left\{ \begin{array}{l} \left(\left[\sqrt{1 - (1 - (a_{\tilde{Q}_{\tilde{C}_1}}^{-})^2)^\tau}, \sqrt{1 - (1 - (a_{\tilde{Q}_{\tilde{C}_1}}^{+})^2)^\tau}\right], \right. \\ \left.\sqrt{1 - (1 - (\tilde{\mu}_{\tilde{Q}_{\tilde{C}_1}})^2)^\tau}\right), \left([(n_{\tilde{Q}_{\tilde{C}_1}}^{-})^\tau, (n_{\tilde{Q}_{\tilde{C}_1}}^{+})^\tau], (\tilde{\eta}_{\tilde{Q}_{\tilde{C}_1}})^\tau\right), \\ \left([(b_{\tilde{Q}_{\tilde{C}_1}}^{-})^\tau, (b_{\tilde{Q}_{\tilde{C}_1}}^{+})^\tau], (\tilde{\vartheta}_{\tilde{Q}_{\tilde{C}_1}})^\tau\right) \end{array} \right\};$$

(4) $\tilde{Q}_{\tilde{C}_1}^{\tau} =$
$$\left\{ \begin{array}{l} \left([(a_{\tilde{Q}_{\tilde{C}_1}}^{-})^\tau, (a_{\tilde{Q}_{\tilde{C}_1}}^{+})^\tau], (\tilde{\mu}_{\tilde{Q}_{\tilde{C}_1}})^\tau\right), \\ \left([(n_{\tilde{Q}_{\tilde{C}_1}}^{-})^\tau, (n_{\tilde{Q}_{\tilde{C}_1}}^{+})^\tau], (\tilde{\eta}_{\tilde{Q}_{\tilde{C}_1}})^\tau\right) \\ \left(\left[\sqrt{1 - (1 - (b_{\tilde{Q}_{\tilde{C}_1}}^{-})^2)^\tau}, \sqrt{1 - (1 - (b_{\tilde{Q}_{\tilde{C}_1}}^{+})^2)^\tau}\right], \right. \\ \left.\sqrt{1 - (1 - (\tilde{\vartheta}_{\tilde{Q}_{\tilde{C}_1}})^2)^\tau}\right) \end{array} \right\}.$$

3. Spherical Cubic Fuzzy Geometric Aggregation Operators

This section proposes a few geometric aggregation operators for spherical cubic fuzzy numbers and discusses their properties.

$$\text{SCFWG}\left(\tilde{Q}_{\widetilde{C_1}}, \tilde{Q}_{\widetilde{C_2}}, \tilde{Q}_{\widetilde{C_3}}, \ldots, \tilde{Q}_{\widetilde{C_n}}\right) = \left(\tilde{Q}_{\widetilde{C_1}}\right)^{\omega_1} \otimes \left(\tilde{Q}_{\widetilde{C_2}}\right)^{\omega_2} \otimes, \ldots, \left(\tilde{Q}_{\widetilde{C_n}}\right)^{\omega_n},$$ (21)

where $\omega = (\omega_1, \omega_2, \ldots, \omega_n)^T$ is the weight vector of $\tilde{Q}_{\widetilde{C_i}}$, with $0 \le \omega_i \le 1$ and $\sum_{i=1}^n \omega_i = 1$.

Definition 17. Let $\tilde{Q}_{\widetilde{C_i}} = \Gamma_{\widetilde{Q}_{\widetilde{C_i}}}, \Upsilon_{\widetilde{Q}_{\widetilde{C_i}}}, \Lambda_{\widetilde{Q}_{\widetilde{C_i}}}$ $(i = 1, 2, 3, \ldots, n)$ be a collection of SCFNs; then, SCF weighted geometric (SCFWG) operator is a mapping SCFWG: $\text{SCFN}^n \longrightarrow \text{SCFN}$ defined as follows:

Theorem 1. Let $\tilde{Q}_{\widetilde{C_i}} = \Gamma_{\widetilde{Q}_{\widetilde{C_i}}}, \Upsilon_{\widetilde{Q}_{\widetilde{C_i}}}, \Lambda_{\widetilde{Q}_{\widetilde{C_i}}}$ $(i = 1, 2, 3, \ldots, n)$ be a collection of SCFNs, and let $\omega = (\omega_1, \omega_2, \ldots, \omega_n)^T$ be the weight vector of $\tilde{Q}_{\widetilde{C_i}}$, with $0 \le \omega_i \le 1$ and $\sum_{i=1}^n \omega_i = 1$. Then, the aggregation of SCFWG operator is also an SCFN:

$$\text{SCFWG}\left(\tilde{Q}_{\widetilde{C_1}}, \tilde{Q}_{\widetilde{C_2}}, \ldots, \tilde{Q}_{\widetilde{C_n}}\right) = \left\{ \begin{array}{c} \left(\left[\prod_{i=1}^n \left(a_{\widetilde{Q}_{\widetilde{C_i}}}^-\right)^{\omega_i}, \prod_{i=1}^n \left(a_{\widetilde{Q}_{\widetilde{C_i}}}^+\right)^{\omega_i}\right], \prod_{i=1}^n \left(\tilde{\mu}_{\widetilde{Q}_{\widetilde{C_i}}}\right)^{\omega_i}\right), \\ \left(\left[\prod_{i=1}^n \left(n_{\widetilde{Q}_{\widetilde{C_i}}}^-\right)^{\omega_i}, \prod_{i=1}^n \left(n_{\widetilde{Q}_{\widetilde{C_i}}}^+\right)^{\omega_i}\right], \prod_{i=1}^n \left(\tilde{\eta}_{\widetilde{Q}_{\widetilde{C_i}}}\right)^{\omega_i}\right), \\ \left(\left[\sqrt{1 - \prod_{i=1}^n \left(1 - \left(b_{\widetilde{Q}_{\widetilde{C_i}}}^-\right)^2\right)^{\omega_i}}, \sqrt{1 - \prod_{i=1}^n \left(1 - \left(b_{\widetilde{Q}_{\widetilde{C_i}}}^+\right)^2\right)^{\omega_i}}\right], \sqrt{1 - \prod_{i=1}^n \left(1 - \left(\tilde{\vartheta}_{\widetilde{Q}_{\widetilde{C_i}}}\right)^2\right)^{\omega_i}}\right), \end{array} \right\}.$$ (22)

Proof. Proof of the theorem follows from theorem [7] of [18]. □

3.1. Properties. Let $\tilde{Q}_{\widetilde{C_i}} = \Gamma_{\widetilde{Q}_{\widetilde{C_i}}}, \Upsilon_{\widetilde{Q}_{\widetilde{C_i}}}, \Lambda_{\widetilde{Q}_{\widetilde{C_i}}}$ $(i = 1, 2, 3 \ldots, n)$ be a set comprising of SCFNs, and the weight vector of $\tilde{Q}_{\widetilde{C_i}}$ is $\omega = (\omega_1, \omega_2, \ldots, \omega_n)^T$ with $0 \le \omega_i \le 1$ and $\sum_{i=1}^n \omega_i = 1$ Then, there are some properties that the SCFWG operator has clearly fulfilled.

3.1.1. Idempotency. If all $\tilde{Q}_{\widetilde{C_i}}$ are identical, that is, $\tilde{Q}_{\widetilde{C_i}} = \tilde{Q}_{\widetilde{C}}$, then

$$\text{SCFWG}\left(\tilde{Q}_{\widetilde{C_1}}, \tilde{Q}_{\widetilde{C_2}}, \tilde{Q}_{\widetilde{C_3}}, \ldots, \tilde{Q}_{\widetilde{C_n}}\right) = \tilde{Q}_{\widetilde{C}}.$$ (23)

3.1.2. Boundary.

$$\tilde{Q}_{\widetilde{C}(\min)} \le \text{SCFWG}\left(\tilde{Q}_{\widetilde{C_1}}, \tilde{Q}_{\widetilde{C_2}}, \tilde{Q}_{\widetilde{C_3}}, \ldots, \tilde{Q}_{\widetilde{C_n}}\right) \le \tilde{Q}_{\widetilde{C}(\max)},$$ (24)

where

$$\tilde{Q}_{\widetilde{C}(\min)} = \left(\min \Gamma_{\widetilde{Q}_{\widetilde{C_i}}}, \min \Upsilon_{\widetilde{Q}_{\widetilde{C_i}}}, \max \Lambda_{\widetilde{Q}_{\widetilde{C_i}}}\right),$$
$$\tilde{Q}_{\widetilde{C}(\max)} = \left(\max \Gamma_{\widetilde{Q}_{\widetilde{C_i}}}, \min \Upsilon_{\widetilde{Q}_{\widetilde{C_i}}}, \min \Lambda_{\widetilde{Q}_{\widetilde{C_i}}}\right).$$ (25)

3.1.3. Monotonicity. Let $\tilde{Q}_{\widetilde{C_i}} = \Gamma_{\widetilde{Q}_{\widetilde{C_i}}}, \Upsilon_{\widetilde{Q}_{\widetilde{C_i}}}, \Lambda_{\widetilde{Q}_{\widetilde{C_i}}}$ and $\tilde{Q}_{\widetilde{C_i}}^* = \Gamma_{\widetilde{Q}_{\widetilde{C_i}}}^*, \Upsilon_{\widetilde{C_i}}^*, \Lambda_{\widetilde{C_i}}^*$ $(i = 1, 2, \ldots, n)$ be collections of SCFNs; if $\tilde{Q}_{\widetilde{C_i}} \subseteq \tilde{Q}_{\widetilde{C_i}}^*$ for all, then

$$\text{SCFWG}\left(\tilde{Q}_{\widetilde{C_1}}, \tilde{Q}_{\widetilde{C_2}}, \tilde{Q}_{\widetilde{C_3}}, \ldots, \tilde{Q}_{\widetilde{C_n}}\right)$$
$$\subseteq \text{SCFWG}\left(\tilde{Q}_{\widetilde{C_1}}^*, \tilde{Q}_{\widetilde{C_2}}^*, \tilde{Q}_{\widetilde{C_3}}^*, \ldots, \tilde{Q}_{\widetilde{C_n}}^*\right).$$ (26)

Definition 18. Let $\tilde{Q}_{\widetilde{C_i}} = \Gamma_{\widetilde{Q}_{\widetilde{C_i}}}, \Upsilon_{\widetilde{Q}_{\widetilde{C_i}}}, \Lambda_{\widetilde{Q}_{\widetilde{C_i}}}$ $(i = 1, 2, 3, \ldots, n)$ be a set comprising of SCFNs; then, SCF ordered weighted

$$\text{SCFHOWG}\left(\tilde{Q}_{\widetilde{C_1}}, \tilde{Q}_{\widetilde{C_2}}, \ldots, \tilde{Q}_{\widetilde{C_n}}\right) = \left\{ \begin{array}{c} \left(\left[\prod_{i=1}^{n}\left(a_{Q_{\sigma\left(\widetilde{C_i}\right)}}^{-}\right)^{\varpi_i}, \prod_{i=1}^{n}\left(a_{Q_{\sigma\left(\widetilde{C_i}\right)}}^{+}\right)^{\varpi_i}\right], \prod_{i=1}^{n}\left(\tilde{\mu}_{Q_{\sigma\left(\widetilde{C_i}\right)}}\right)^{\varpi_i}\right), \\[12pt] \left(\left[\prod_{i=1}^{n}\left(n_{Q_{\sigma\left(\widetilde{C_i}\right)}}^{-}\right)^{\varpi_i}, \prod_{i=1}^{n}\left(n_{Q_{\sigma\left(\widetilde{C_i}\right)}}^{+}\right)^{\varpi_i}\right], \prod_{i=1}^{n}\left(\tilde{\eta}_{Q_{\sigma\left(\widetilde{C_i}\right)}}\right)^{\varpi_i}\right), \\[12pt] \left(\left[\sqrt{1-\prod_{i=1}^{n}\left(1-\left(b_{Q_{\sigma\left(\widetilde{C_i}\right)}}^{-}\right)^2\right)^{\varpi_i}}, \sqrt{1-\prod_{i=1}^{n}\left(1-\left(b_{Q_{\sigma\left(\widetilde{C_i}\right)}}^{+}\right)^2\right)^{\varpi_i}}\right], \sqrt{1-\prod_{i=1}^{n}\left(1-\left(\tilde{\vartheta}_{Q_{\sigma\left(\widetilde{C_i}\right)}}\right)^2\right)^{\varpi_i}}\right), \end{array} \right\}.$$

$$\tag{34}$$

Proof. Proof of the theorem follows from theorem [9] of [18].

3.3. Properties.
Let $\tilde{Q}_{\widetilde{C_i}} = \Gamma_{\tilde{Q}_{\widetilde{C_i}}}, \Upsilon_{\tilde{Q}_{\widetilde{C_i}}}, \Lambda_{\tilde{Q}_{\widetilde{C_i}}}$ $(i = 1, 2, 3, \ldots, n)$ be a set comprised of SCFNs, and the weight vector of $\tilde{Q}_{\widetilde{C_i}}$ is $\varpi = (\varpi_1, \varpi_2, \ldots, \varpi_n)^T$ with $0 \le \varpi_i \le 1$ and $\sum_{i=1}^{n} \varpi_i = 1$. Then, there are some properties that the SCFHOWG operator has clearly fulfilled.

3.3.1. Idempotency.
If all $\tilde{Q}_{\widetilde{C_i}}$ are identical, that is, $\tilde{Q}_{\widetilde{C_i}} = \tilde{Q}_{\widetilde{C}}$, then

$$\text{SCFHOWG}\left(\tilde{Q}_{\widetilde{C_1}}, \tilde{Q}_{\widetilde{C_2}}, \tilde{Q}_{\widetilde{C_3}}, \ldots, \tilde{Q}_{\widetilde{C_n}}\right) = \tilde{Q}_{\widetilde{C}}. \tag{35}$$

3.3.2. Boundary.

$$\tilde{Q}_{\widetilde{C}(\min)} \le \text{SCFHOWG}\left(\tilde{Q}_{\widetilde{C_1}}, \tilde{Q}_{\widetilde{C_2}}, \tilde{Q}_{\widetilde{C_3}}, \ldots, \tilde{Q}_{\widetilde{C_n}}\right) \le \tilde{Q}_{\widetilde{C}(\max)}, \tag{36}$$

where

$$\begin{aligned} \tilde{Q}_{\widetilde{C}(\min)} &= \left(\min \sigma_{\tilde{Q}_{\widetilde{C_i}}}, \min \beta_{\tilde{Q}_{\widetilde{C_i}}}, \max \gamma_{\tilde{Q}_{\widetilde{C_i}}}\right), \\ \tilde{Q}_{\widetilde{C}(\max)} &= \left(\max \sigma_{\tilde{Q}_{\widetilde{C_i}}}, \min \beta_{\tilde{Q}_{\widetilde{C_i}}}, \min \gamma_{\tilde{Q}_{\widetilde{C_i}}}\right). \end{aligned} \tag{37}$$

3.3.3. Monotonicity.
Let $\tilde{Q}_{\widetilde{C_i}} = \Gamma_{\tilde{Q}_{\widetilde{C_i}}}, \Upsilon_{\tilde{Q}_{\widetilde{C_i}}}, \Lambda_{\tilde{Q}_{\widetilde{C_i}}}$ and $\tilde{Q}_{\widetilde{C_i}}^* = \Gamma_{\tilde{Q}_{\widetilde{C_i}}}^*, \Upsilon_{\tilde{C_i}}^*, \Lambda_{\tilde{C_i}}^*$ $(i = 1, 2, \ldots, n)$ be collections of SCFNs; if $\tilde{Q}_{\widetilde{C_i}} \subseteq \tilde{Q}_{\widetilde{C_i}}^*$ for all i, then

$$\begin{aligned} &\text{SCFHOWG}\left(\tilde{Q}_{\widetilde{C_1}}, \tilde{Q}_{\widetilde{C_2}}, \tilde{Q}_{\widetilde{C_3}}, \ldots, \tilde{Q}_{\widetilde{C_n}}\right) \\ &\subseteq \text{SCFHOWG}\left(\tilde{Q}_{\widetilde{C_1}}^*, \tilde{Q}_{\widetilde{C_2}}^*, \tilde{Q}_{\widetilde{C_3}}^*, \ldots, \tilde{Q}_{\widetilde{C_n}}^*\right). \end{aligned} \tag{38}$$

4. Application for MADM Based on Spherical Cubic Fuzzy Geometric Aggregation Operators

This section utilizes the SCF geometric aggregation operators for the MADM process. Suppose we have n choices $\hat{Y} = \{\hat{y}_1, \hat{y}_2, \ldots, \hat{y}_n\}$ and m criteria $\hat{A} = \{\hat{A}_1, \hat{A}_2, \hat{A}_3, \ldots, \hat{A}_m\}$ to be determined with weight vector $\varpi = (\varpi_1, \varpi_2, \ldots, \varpi_n)^T$ with $0 \le \varpi_j \le 1$ and $\sum_{j=1}^{n} \varpi_j = 1$. In order to assess the proficiency of the alternative $\hat{y}_i$ according to $\hat{A}_j$ criteria, the decision-maker must not simply provide the details where $\hat{y}_i$ fulfills the criteria $\hat{A}_j$, but the alternative $\hat{y}_i$ does not fulfill the criteria $\hat{A}_j$ or the alternative $\hat{y}_i$ remains unchanged. These three components can be defined by $\Gamma_{\tilde{Q}_{\widetilde{C}}}, \Upsilon_{\tilde{Q}_{\widetilde{C}}}, \Lambda_{\tilde{Q}_{\widetilde{C}}}$ where $\Gamma_{\tilde{Q}_{\widetilde{C}}} = [a_{\tilde{Q}_{\widetilde{C}}}^{-}, a_{\tilde{Q}_{\widetilde{C}}}^{+}], \tilde{\mu}_{\tilde{Q}_{\widetilde{C}}}$ represent the degree where the alternative $\hat{y}_i$ fulfills the criteria $\hat{A}_j$ and $\Upsilon = [n_{\tilde{Q}_{\widetilde{C}}}^{-}, n_{\tilde{Q}_{\widetilde{C}}}^{+}], \tilde{\eta}_{\tilde{Q}_{\widetilde{C}}}$ represents the degree where the alternative $\hat{y}_i$ remains unchanged and $\Lambda_{\tilde{Q}_{\widetilde{C}}} = [b_{\tilde{Q}_{\widetilde{C}}}^{-}, b_{\tilde{Q}_{\widetilde{C}}}^{+}], \tilde{\vartheta}_{\tilde{Q}_{\widetilde{C}}}$ represents the degree where the alternative $\hat{y}_i$ does not fulfill the criteria $\hat{A}_j$; then, the efficiency of $\hat{y}_i$ under the criteria $\hat{A}_j$ can be defined by SCFN, $\tilde{Q}_{\widetilde{C}} = ([a_{\tilde{Q}_{\widetilde{C}}}^{-}, a_{\tilde{Q}_{\widetilde{C}}}^{+}], \tilde{\mu}_{\tilde{Q}_{\widetilde{C}}}, [n_{\tilde{Q}_{\widetilde{C}}}^{-}, n_{\tilde{Q}_{\widetilde{C}}}^{+}], \tilde{\eta}_{\tilde{Q}_{\widetilde{C}}}, [b_{\tilde{Q}_{\widetilde{C}}}^{-}, b_{\tilde{Q}_{\widetilde{C}}}^{+}], \tilde{\vartheta}_{\tilde{Q}_{\widetilde{C}}})$ with the specified condition $0 \le (\sup[a_{\tilde{Q}_{\widetilde{C}}}^{-}, a_{\tilde{Q}_{\widetilde{C}}}^{+}])^2 + (\sup[a_{\tilde{Q}_{\widetilde{C}}}^{-}, a_{\tilde{Q}_{\widetilde{C}}}^{+}])^2 + (\sup[b_{\tilde{Q}_{\widetilde{C}}}^{-}, b_{\tilde{Q}_{\widetilde{C}}}^{+}])^2 \le$ and $0 \le (\tilde{\mu}_{\tilde{Q}_{\widetilde{C}}})^2 + (\tilde{\eta}_{\tilde{Q}_{\widetilde{C}}})^2 + (\tilde{\vartheta}_{\tilde{Q}_{\widetilde{C}}})^2 \le 1$. The following steps are specified to obtain the ranking of the alternatives.

Table 1: First spherical cubic fuzzy decision matrix.

	$\widehat{A}_1$	$\widehat{A}_2$	$\widehat{A}_3$	$\widehat{A}_4$
$\widehat{y}_1$	$\left(\begin{array}{c}\langle[.1,.2],.3,\rangle\\ \langle[.4,.5],.4,\rangle\\ \langle[.1,.3],.1\rangle\end{array}\right)$	$\left(\begin{array}{c}\langle[.1,.3],.3,\rangle\\ \langle[.1,.4],.3,\rangle\\ \langle[.1,.3],.1\rangle\end{array}\right)$	$\left(\begin{array}{c}\langle[.3,.5],.3,\rangle\\ \langle[.1,.5],.5,\rangle\\ \langle[.1,.3],.1\rangle\end{array}\right)$	$\left(\begin{array}{c}\langle[.1,.4],.4,\rangle\\ \langle[.1,.4],.2,\rangle\\ \langle[.3,.5],.5\rangle\end{array}\right)$
$\widehat{y}_2$	$\left(\begin{array}{c}\langle[.2,.4],.1,\rangle\\ \langle[.1,.4],.3,\rangle\\ \langle[.1,.5],.6\rangle\end{array}\right)$	$\left(\begin{array}{c}\langle[.3,.6],.5,\rangle\\ \langle[.1,.2],.2,\rangle\\ \langle[.1,.4],.2\rangle\end{array}\right)$	$\left(\begin{array}{c}\langle[.1,.2],.1,\rangle\\ \langle[.1,.4],.2,\rangle\\ \langle[.1,.3],.3\rangle\end{array}\right)$	$\left(\begin{array}{c}\langle[.3,.5],.5,\rangle\\ \langle[.1,.4],.5,\rangle\\ \langle[.1,.4],.4\rangle\end{array}\right)$
$\widehat{y}_3$	$\left(\begin{array}{c}\langle[.1,.2],.1,\rangle\\ \langle[.1,.4],.2,\rangle\\ \langle[.3,.6],.5\rangle\end{array}\right)$	$\left(\begin{array}{c}\langle[.2,.5],.5,\rangle\\ \langle[.4,.5],.2,\rangle\\ \langle[.2,.3],.1\rangle\end{array}\right)$	$\left(\begin{array}{c}\langle[.2,.4],.1,\rangle\\ \langle[.1,.4],.3,\rangle\\ \langle[.2,.4],.7\rangle\end{array}\right)$	$\left(\begin{array}{c}\langle[.1,.2],.2,\rangle\\ \langle[.1,.3],.4,\rangle\\ \langle[.3,.4],.4\rangle\end{array}\right)$
$\widehat{y}_4$	$\left(\begin{array}{c}\langle[.1,.2],.3,\rangle\\ \langle[.1,.3],.7,\rangle\\ \langle[.1,.5],.2\rangle\end{array}\right)$	$\left(\begin{array}{c}\langle[.1,.1],.3,\rangle\\ \langle[.2,.4],.6,\rangle\\ \langle[.3,.7],.2\rangle\end{array}\right)$	$\left(\begin{array}{c}\langle[.4,.5],.8,\rangle\\ \langle[.1,.2],.2,\rangle\\ \langle[.1,.2],.1\rangle\end{array}\right)$	$\left(\begin{array}{c}\langle[.1,.2],.1,\rangle\\ \langle[.1,.1],.3,\rangle\\ \langle[.2,.3],.6\rangle\end{array}\right)$

Table 2: Second spherical cubic fuzzy decision matrix.

	$\widehat{A}_1$	$\widehat{A}_2$	$\widehat{A}_3$	$\widehat{A}_4$
$\widehat{y}_1$	$\left(\begin{array}{c}\langle[.1,.2],.5,\rangle\\ \langle[.4,.4],.2,\rangle\\ \langle[.2,.3],.5\rangle\end{array}\right)$	$\left(\begin{array}{c}\langle[.1,.3],.2,\rangle\\ \langle[.1,.4],.1,\rangle\\ \langle[.1,.4],.3\rangle\end{array}\right)$	$\left(\begin{array}{c}\langle[.1,.5],.6,\rangle\\ \langle[.2,.3],.1,\rangle\\ \langle[.1,.3],.2\rangle\end{array}\right)$	$\left(\begin{array}{c}\langle[.1,.2],.5,\rangle\\ \langle[.3,.6],.5,\rangle\\ \langle[.1,.4],.2\rangle\end{array}\right)$
$\widehat{y}_2$	$\left(\begin{array}{c}\langle[.1,.4],.3,\rangle\\ \langle[.1,.3],.4,\rangle\\ \langle[.1,.7],.6\rangle\end{array}\right)$	$\left(\begin{array}{c}\langle[.1,.4],.2,\rangle\\ \langle[.1,.2],.1,\rangle\\ \langle[.3,.7],.2\rangle\end{array}\right)$	$\left(\begin{array}{c}\langle[.1,.3],.2,\rangle\\ \langle[.2,.4],.5,\rangle\\ \langle[.1,.5],.3\rangle\end{array}\right)$	$\left(\begin{array}{c}\langle[.1,.6],.2,\rangle\\ \langle[.1,.2],.6,\rangle\\ \langle[.2,.5],.2\rangle\end{array}\right)$
$\widehat{y}_3$	$\left(\begin{array}{c}\langle[.2,.1],.3,\rangle\\ \langle[.1,.5],.5,\rangle\\ \langle[.1,.3],.2\rangle\end{array}\right)$	$\left(\begin{array}{c}\langle[.2,.4],.5,\rangle\\ \langle[.6,.7],.1,\rangle\\ \langle[.1,.2],.5\rangle\end{array}\right)$	$\left(\begin{array}{c}\langle[.1,.3],.2,\rangle\\ \langle[.1,.5],.5,\rangle\\ \langle[.1,.2],.3\rangle\end{array}\right)$	$\left(\begin{array}{c}\langle[.1,.3],.2,\rangle\\ \langle[.1,.4],.5,\rangle\\ \langle[.1,.4],.5\rangle\end{array}\right)$
$\widehat{y}_4$	$\left(\begin{array}{c}\langle[.2,.4],.3,\rangle\\ \langle[.4,.5],.3,\rangle\\ \langle[.2,.4],.2\rangle\end{array}\right)$	$\left(\begin{array}{c}\langle[.6,.7],.5,\rangle\\ \langle[.1,.1],.2,\rangle\\ \langle[.1,.4],.3\rangle\end{array}\right)$	$\left(\begin{array}{c}\langle[.1,.4],.2,\rangle\\ \langle[.3,.2],.7,\rangle\\ \langle[.2,.6],.4\rangle\end{array}\right)$	$\left(\begin{array}{c}\langle[.1,.3],.2,\rangle\\ \langle[.1,.2],.3,\rangle\\ \langle[.3,.7],.2\rangle\end{array}\right)$

Table 3: Third spherical cubic fuzzy decision matrix.

	$\widehat{A}_1$	$\widehat{A}_2$	$\widehat{A}_3$	$\widehat{A}_4$
$\widehat{y}_1$	$\left(\begin{array}{c}\langle[.1,.3],.2,\rangle\\ \langle[.1,.2],.3,\rangle\\ \langle[.2,.1],.5\rangle\end{array}\right)$	$\left(\begin{array}{c}\langle[.1,.2],.1,\rangle\\ \langle[.2,.4],.2,\rangle\\ \langle[.2,.3],.5\rangle\end{array}\right)$	$\left(\begin{array}{c}\langle[.3,.5],.6,\rangle\\ \langle[.1,.3],.1,\rangle\\ \langle[.1,.3],.2\rangle\end{array}\right)$	$\left(\begin{array}{c}\langle[.1,.2],.5,\rangle\\ \langle[.2,.4],.2,\rangle\\ \langle[.3,.6],.5\rangle\end{array}\right)$
$\widehat{y}_2$	$\left(\begin{array}{c}\langle[.1,.2],.3,\rangle\\ \langle[.1,.2],.3,\rangle\\ \langle[.2,.4],.1\rangle\end{array}\right)$	$\left(\begin{array}{c}\langle[.1,.3],.2,\rangle\\ \langle[.1,.4],.3,\rangle\\ \langle[.3,.6],.2\rangle\end{array}\right)$	$\left(\begin{array}{c}\langle[.1,.2],.1,\rangle\\ \langle[.1,.2],.1,\rangle\\ \langle[.4,.5],.3\rangle\end{array}\right)$	$\left(\begin{array}{c}\langle[.2,.3],.1,\rangle\\ \langle[.3,.4],.5,\rangle\\ \langle[.1,.2],.1\rangle\end{array}\right)$
$\widehat{y}_3$	$\left(\begin{array}{c}\langle[.1,.5],.3,\rangle\\ \langle[.2,.3],.1,\rangle\\ \langle[.1,.2],.5\rangle\end{array}\right)$	$\left(\begin{array}{c}\langle[.4,.3],.1,\rangle\\ \langle[.2,.4],.5,\rangle\\ \langle[.2,.3],.2\rangle\end{array}\right)$	$\left(\begin{array}{c}\langle[.4,.3],.6,\rangle\\ \langle[.1,.4],.1,\rangle\\ \langle[.5,.6],.4\rangle\end{array}\right)$	$\left(\begin{array}{c}\langle[.1,.4],.2,\rangle\\ \langle[.3,.4],.1,\rangle\\ \langle[.1,.3],.2\rangle\end{array}\right)$
$\widehat{y}_4$	$\left(\begin{array}{c}\langle[.1,.2],.4,\rangle\\ \langle[.4,.5],.2,\rangle\\ \langle[.2,.3],.2\rangle\end{array}\right)$	$\left(\begin{array}{c}\langle[.1,.2],.4,\rangle\\ \langle[.5,.7],.1,\rangle\\ \langle[.1,.3],.2\rangle\end{array}\right)$	$\left(\begin{array}{c}\langle[.1,.5],.2,\rangle\\ \langle[.2,.3],.5,\rangle\\ \langle[.1,.2],.4\rangle\end{array}\right)$	$\left(\begin{array}{c}\langle[.1,.3],.2,\rangle\\ \langle[.1,.2],.3,\rangle\\ \langle[.1,.2],.3\rangle\end{array}\right)$

Step 1: Firstly, we make a spherical cubic fuzzy matrix:

$$D_{\widetilde{N}} = \left(\left\langle\left[a_{\widetilde{Q}_C^-}, a_{\widetilde{Q}_C}^+\right], \widetilde{\mu}_{\widetilde{Q}_C}\right\rangle, \left\langle\left[n_{\widetilde{Q}_C^-}, n_{\widetilde{Q}_C}^\pm\right], \widetilde{\eta}_{\widetilde{Q}_C}\right\rangle, \left\langle\left[b_{\widetilde{Q}_C}^-, b_{\widetilde{Q}_C}^\pm\right], \widetilde{\vartheta}_{\widetilde{Q}_C}\right\rangle\right)_{m \times n}. \tag{39}$$

Table 4: Spherical cubic fuzzy weighted geometric aggregation information of decision-makers.

	$\widehat{A}_1$	$\widehat{A}_2$	$\widehat{A}_3$	$\widehat{A}_4$
$\widehat{y}_1$	$\begin{pmatrix} \langle[.10,.22],.33,\rangle \\ \langle[.16,.36],.28,\rangle \\ \langle[.17,.27],.42\rangle \end{pmatrix}$	$\begin{pmatrix} \langle[.10,.27],.19,\rangle \\ \langle[.12,.40],.17,\rangle \\ \langle[.13,.34],.33\rangle \end{pmatrix}$	$\begin{pmatrix} \langle[.19,.50],.47,\rangle \\ \langle[.13,.36],.18,\rangle \\ \langle[.10,.30],.17\rangle \end{pmatrix}$	$\begin{pmatrix} \langle[.10,.25],.46,\rangle \\ \langle[.18,.47],.29,\rangle \\ \langle[.24,.50],.41\rangle \end{pmatrix}$
$\widehat{y}_2$	$\begin{pmatrix} \langle[.13,.34],.20,\rangle \\ \langle[.10,.30],.34,\rangle \\ \langle[.13,.58],.54\rangle \end{pmatrix}$	$\begin{pmatrix} \langle[.15,.43],.28,\rangle \\ \langle[.10,.24],.17,\rangle \\ \langle[.25,.60],.20\rangle \end{pmatrix}$	$\begin{pmatrix} \langle[.10,.24],.13,\rangle \\ \langle[.13,.34],.24\rangle, \\ \langle[.22,.44],.30\rangle \end{pmatrix}$	$\begin{pmatrix} \langle[.17,.47],.23,\rangle \\ \langle[.13,.30],.45,\rangle \\ \langle[.15,.41],.28\rangle \end{pmatrix}$
$\widehat{y}_3$	$\begin{pmatrix} \langle[.13,.19],.20,\rangle \\ \langle[.12,.41],.24,\rangle \\ \langle[.20,.43],.41\rangle \end{pmatrix}$	$\begin{pmatrix} \langle[.24,.40],.33,\rangle \\ \langle[.40,.54],.19,\rangle \\ \langle[.17,.27],.35\rangle \end{pmatrix}$	$\begin{pmatrix} \langle[.18,.33],.21,\rangle \\ \langle[.10,.44],.28,\rangle \\ \langle[.29,.41],.52\rangle \end{pmatrix}$	$\begin{pmatrix} \langle[.10,.28],.20,\rangle \\ \langle[.13,.36],.31,\rangle \\ \langle[.20,.38],.41\rangle \end{pmatrix}$
$\widehat{y}_4$	$\begin{pmatrix} \langle[.13,.26],.32,\rangle \\ \langle[.25,.42],.36,\rangle \\ \langle[.17,.42],.20\rangle \end{pmatrix}$	$\begin{pmatrix} \langle[.20,.26],.40,\rangle \\ \langle[.19,.26],.25,\rangle \\ \langle[.20,.53],.25\rangle \end{pmatrix}$	$\begin{pmatrix} \langle[.16,.46],.32,\rangle \\ \langle[.18,.22],.42,\rangle \\ \langle[.15,.43],.33\rangle \end{pmatrix}$	$\begin{pmatrix} \langle[.10,.26],.16,\rangle \\ \langle[.10,.16],.30,\rangle \\ \langle[.23,.52],.42\rangle \end{pmatrix}$

Table 5: SCF ordered weighted geometric aggregation information of decision-makers.

	$\widehat{A}_1$	$\widehat{A}_2$	$\widehat{A}_3$	$\widehat{A}_4$
$\widehat{y}_1$	$\begin{pmatrix} \langle[.19,.45],.62,\rangle \\ \langle[.26,.58],.46,\rangle \\ \langle[.20,.44],.30\rangle \end{pmatrix}$	$\begin{pmatrix} \langle[.17,.40],.42,\rangle \\ \langle[.28,.49],.31,\rangle \\ \langle[.23,.40],.39\rangle \end{pmatrix}$	$\begin{pmatrix} \langle[.15,.36],.33,\rangle \\ \langle[.13,.44],.36,\rangle \\ \langle[.20,.38],.51\rangle \end{pmatrix}$	$\begin{pmatrix} \langle[.13,.40],.43,\rangle \\ \langle[.16,.50],.26,\rangle \\ \langle[.32,.60],.54\rangle \end{pmatrix}$
$\widehat{y}_2$	$\begin{pmatrix} \langle[.25,.51],.33,\rangle \\ \langle[.14,.34],.50,\rangle \\ \langle[.15,.46],.27\rangle \end{pmatrix}$	$\begin{pmatrix} \langle[.16,.49],.38,\rangle \\ \langle[.16,.50],.50,\rangle \\ \langle[.29,.56],.39\rangle \end{pmatrix}$	$\begin{pmatrix} \langle[.10,.40],.26,\rangle \\ \langle[.17,.36],.40\rangle, \\ \langle[.20,.58],.48\rangle \end{pmatrix}$	$\begin{pmatrix} \langle[.23,.47],.24,\rangle \\ \langle[.13,.32],.21,\rangle \\ \langle[.34,.64],.51\rangle \end{pmatrix}$
$\widehat{y}_3$	$\begin{pmatrix} \langle[.30,.50],.46,\rangle \\ \langle[.50,.64],.30,\rangle \\ \langle[.21,.36],.51\rangle \end{pmatrix}$	$\begin{pmatrix} \langle[.26,.50],.26,\rangle \\ \langle[.20,.51],.40,\rangle \\ \langle[.21,.39],.62\rangle \end{pmatrix}$	$\begin{pmatrix} \langle[.13,.29],.27,\rangle \\ \langle[.24,.50],.43,\rangle \\ \langle[.26,.47],.44\rangle \end{pmatrix}$	$\begin{pmatrix} \langle[.10,.28],.20,\rangle \\ \langle[.13,.36],.31,\rangle \\ \langle[.20,.38],.41\rangle \end{pmatrix}$
$\widehat{y}_4$	$\begin{pmatrix} \langle[.13,.26],.32,\rangle \\ \langle[.25,.42],.36,\rangle \\ \langle[.17,.42],.20\rangle \end{pmatrix}$	$\begin{pmatrix} \langle[.20,.26],.40,\rangle \\ \langle[.19,.26],.25,\rangle \\ \langle[.20,.53],.25\rangle \end{pmatrix}$	$\begin{pmatrix} \langle[.10,.32],.30,\rangle \\ \langle[.29,.48],.60,\rangle \\ \langle[.34,.70],.42\rangle \end{pmatrix}$	$\begin{pmatrix} \langle[.24,.36],.19,\rangle \\ \langle[.10,.24],.42,\rangle \\ \langle[.35,.61],.52\rangle \end{pmatrix}$

Table 6: Rowwise aggregated (SCFDWG) decision-makers.

$\widehat{y}_1$	$(\langle[.16,.11],.25\rangle, \langle[.20,.29],.31\rangle, \langle[.19,.41],.35\rangle)$
$\widehat{y}_2$	$(\langle[.21,.38],.31\rangle, \langle[.17,.20],.33\rangle, \langle[.19,.49],.31\rangle)$
$\widehat{y}_3$	$(\langle[.18,.19],.26\rangle, \langle[.24,.21],.28\rangle, \langle[.22,.38],.43\rangle)$
$\widehat{y}_4$	$(\langle[.19,.13],.25\rangle, \langle[.19,.18],.18\rangle, \langle[.20,.49],.35\rangle)$

If there are two types of criteria, for instance, cost-benefit criteria, the SC decision matrix could be transformed into a normalized one:

$$\widetilde{\alpha}_{\widetilde{Q}_{C_{ij}}} = \begin{cases} \widetilde{Q}_{\widetilde{C}_{ij}} \text{ if the benefit } - \text{ type attribute} \\ \widetilde{Q}_{\widetilde{C}_{ij}}^c \text{ if the cost } - \text{ type attribute} \end{cases}, \quad (40)$$

where $\widetilde{Q}_{\widetilde{C}_{ij}}^c$ represents the complement of $\widetilde{Q}_{\widetilde{C}_{ij}}$ if every parameter is of the same form as they are not necessary to normalize the decision matrix.

Step 2: To obtain an SCFN $\widetilde{Q}_{\widetilde{C}_i}$ ($i = 1, 2, \ldots, n$), use the suggested aggregation operators for the alternatives $\widehat{y}_i$. To be precise, the established operators stem the

$\widetilde{Q}_{\widetilde{C}_i}$ ($i = 1, 2, 3, \ldots, n$) of alternative $\widehat{y}_i$ where the weighted vector for the criteria is $\varpi = (\varpi_1, \varpi_2, \ldots, \varpi_n)^T$.

Step 3: Determine the scores, score $(\widetilde{Q}_{\widetilde{C}_i})$ ($i = 1, 2, 3, \ldots, n$), and the degree of accuracy $(\widetilde{Q}_{\widetilde{C}_i})$ of each $\widetilde{Q}_{\widetilde{C}_i}$.

Step 4: The best alternative is selected by the ranking of all the alternatives.

5. Numerical Illustration

Suppose an investment group wants to spend money on the best option (alternative). A board with four possibilities options (alternative) for investing money: $\{\widehat{y}_1, \widehat{y}_2, \widehat{y}_3, \widehat{y}_4\}$.

TABLE 7: Rowwise aggregated (SCFDOWG) decision-makers.

$\widehat{y}_1$	$(\langle[.16,.11],.25\rangle,\langle[.20,.29],.31\rangle,\langle[.19,.41],.35\rangle)$
$\widehat{y}_2$	$(\langle[.21,.38],.31\rangle,\langle[.17,.20],.33\rangle,\langle[.19,.49],.31\rangle)$
$\widehat{y}_3$	$(\langle[.18,.19],.26\rangle,\langle[.24,.21],.28\rangle,\langle[.22,.38],.43\rangle)$
$\widehat{y}_4$	$(\langle[.19,.13],.25\rangle,\langle[.19,.18],.18\rangle,\langle[.20,.49],.35\rangle)$

TABLE 8: Ranking criteria of alternatives.

Operator	$\widetilde{Q}_{\widetilde{C}_i}(\widehat{A}_1)$	$\widetilde{Q}_{\widetilde{C}_i}(\widehat{A}_2)$	$\widetilde{Q}_{\widetilde{C}_i}(\widehat{A}_3)$	$\widetilde{Q}_{\widetilde{C}_i}(\widehat{A}_4)$	Ranking
SCFWG	0.06	0.02	0.04	0.01	$\widehat{A}_1 > \widehat{A}_3 > \widehat{A}_2 > \widehat{A}_4$
SCFOWG	0.11	0.07	0.08	0.03	$\widehat{A}_1 > \widehat{A}_3 > \widehat{A}_2 > \widehat{A}_4$
SCFHWG	0.05	0.02	0.04	0.01	$\widehat{A}_1 > \widehat{A}_3 > A_2 > \widehat{A}_4$

TABLE 9: Comparison analysis using spherical fuzzy sets.

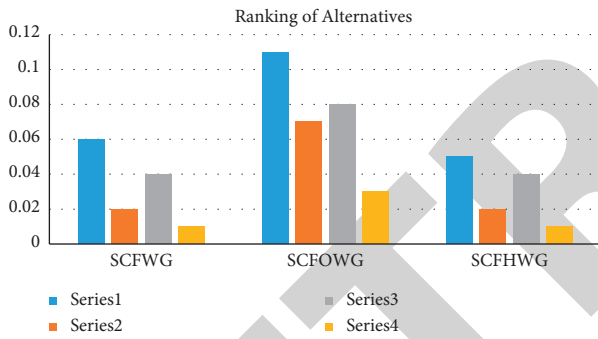| Operator	$\widetilde{Q}_{\widetilde{C}_i}(\widehat{A}_1)$	$\widetilde{Q}_{\widetilde{C}_i}(\widehat{A}_2)$	$\widetilde{Q}_{\widetilde{C}_i}(\widehat{A}_3)$	$\widetilde{Q}_{\widetilde{C}_i}(\widehat{A}_4)$	Ranking
SFWG	0.08	0.07	0.02	0.05	$\widehat{A}_1 > \widehat{A}_2 > \widehat{A}_4 > \widehat{A}_2$
SFOWG	0.02	0.03	0.05	0.01	$\widehat{A}_3 > \widehat{A}_2 > \widehat{A}_1 > \widehat{A}_4$
SFHWG	0.06	0.09	0.03	0.02	$\widehat{A}_2 > A_1 > A_3 > \widehat{A}_2$

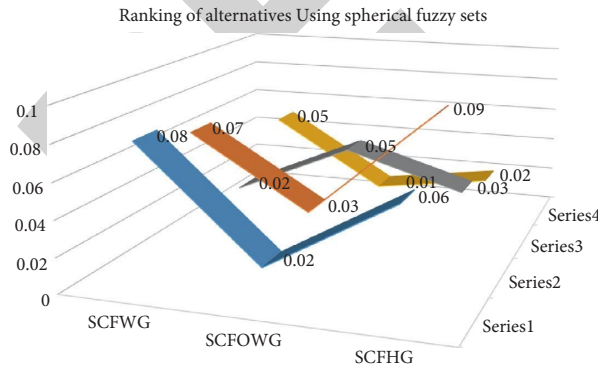FIGURE 1: Ranking of alternatives using SCFSs.

FIGURE 2: Ranking of alternatives using spherical fuzzy sets.

$\widehat{y}_1$ is a vehicle manufacturer, $\widehat{y}_2$ a food company, $\widehat{y}_3$ a washing machine company, and $\widehat{y}_4$ a television company. Four criteria, including a risk analysis $(\widehat{A}_1)$, a growth and development analysis $(\widehat{A}_2)$, a social impact analysis $(\widehat{A}_3)$, and an environment impact analysis $(\widehat{A}_4)$, are taken into account. $\varpi = (0.1, 0.2, 0.25, 0.45)^T$ is the $\widehat{A}_j$ criterion weight vector $(j = 1, 2, \ldots, n)$. A three-decision-maker committee explores four possible alternatives $\widehat{y}_i (i = 1, 2, 3, 4)$ in the four $\widehat{A}_j (j = 1, 2, 3, 4)$ criteria above. Then, the ranking is needed to assess the investment company $\{\widehat{y}_1, \widehat{y}_2, \widehat{y}_3, \widehat{y}_4\}$. The following matrices represent these experts in the form of spherical cubic fuzzy numbers:

Step 1. The decision-makers make their decisions given in Table3 1–3.

Step 2. Using the SCFWG aggregation operator, we get the collection of SCFN for $\widehat{y}_i$ alternative given in Table 4. Table 5 contains the decision-makers' SCF ordered weighted geometric (SCFOWG) aggregation information. And the rowwise aggregated (SCFDWG) decision-makers are given in Table 6. In Table 7, the rowwise aggregation of (SCFOWG) operators is given.

Step 3. Using equation (22) to determine the scores of $\widetilde{Q}_{\widetilde{C}_i} (i = 1, 2, 3, \ldots, n)$, the ranking criteria of alternatives using the spherical cubic geometric aggregation operators are given in Table 8.

Step 4. The scores are arranged in a descending order. Choose the highest alternative. Figure 1 represents the graphical representation of alternative by using the spherical cubic geometric aggregation operators. By using the proposed aggregation operator, the ranking of the four possible alternatives achieved is more accurate in comparison with Table 9. The best choice for these operators is $\widehat{A}_1$. These approaches are ideal for addressing circumstances in which the inputs, viewpoints, and the interaction of experts and criteria may be considered which are more likely to handle such problems. Figure 2 shows the graphical representation

of alternative by using the spherical geometric aggregation operators.

6. Conclusion

In this paper, we have discussed the spherical cubic fuzzy set (SCFS) which is the generalization of the interval-valued SFS (IVSFS). Some operational laws of SCFS were presented. For the comparison of SCFNs, we have established accuracy and score functions. We also described SCF distances between SCFNs. Further, we proposed various aggregation operators in the SCF environment, SCFWG, SCFOWG, and SCFHWG operators.

Some interesting properties such as idempotency, boundary, and monotonicity were also discussed. Furthermore, a relationship was formed among the proposed operators. Additionally, we suggested a MADM to demonstrate the prominence and the strength of the proposed operators. Moreover, by applying the developed aggregation operators, we explained the problems of decision-making. A numerical illustration is presented to indicate an alternative way of addressing the decision-making process more effectively by using the proposed operators. Finally, we compared the practicality, efficiency, and validity of the new approach with existing operators.

We would combine other SCFS approaches such as Einstein product and introduce the concept of SCF Einstein weighted averaging (SCFEWA) operator, SCF Einstein ordered weighted averaging (SCFEOWA) operator, SCF Einstein weighted geometric (SCFEWG) operator, SCF Einstein ordered weighted geometric (SCFEOWG) operator, and some more generalized operators in MADM processes.

Data Availability

No data were used to support the study.

Conflicts of Interest

The authors declare no conflicts of interest about the publication of the research article.

Acknowledgments

References

[1] S.-M. Chen and J.-M. Tan, "Handling multicriteria fuzzy decision-making problems based on vague set theory," *Fuzzy Sets and Systems*, vol. 67, no. 2, pp. 163–172, 1994.

[2] L. A. Zadeh, "Fuzzy sets," *Information and Control*, vol. 8, no. 3, pp. 332–83, 1965.

[3] K. T. Atanassov, *Intuitionistic Fuzzy Sets*, Physica-Verlag hd, Heidelberg, Germany, pp. 1–137, 1999.

[4] R. R. Yager, "Properties and applications of pythagorean fuzzy sets," in *Imprecision and Uncertainty in Information Representation and Processing*, pp. 119–136, Springer, Berlin, Germany, 2016.

[5] R. R. Yager, J. Kacprzyk, and G. Beliakov, Eds., *Recent Developments in the Ordered Weighted Averaging Operators: Theory and Practice*, Springer, Vol. 265, Berlin, Germany, 2011.

[6] B. C. Cuong and V. Kreinovich, "Picture fuzzy sets-a new concept for computational intelligence problems," in *Proceedings of the 2013 3rd World Congress on Information and Communication Technologies (WICT 2013)*, pp. 1–6, IEEE, Hainan, China, December 2013.

[7] H. Garg, "Some picture fuzzy aggregation operators and their applications to multicriteria decision-making," *Arabian Journal for Science and Engineering*, vol. 42, no. 12, pp. 5275–5290, 2017.

[8] H. Garg, "A novel accuracy function under interval-valued pythagorean fuzzy environment for solving multicriteria decision making problem," *Journal of Intelligent and Fuzzy Systems*, vol. 31, no. 1, pp. 529–540, 2016.

[9] X. Gou, Z. Xu, and P. Ren, "The properties of continuous pythagorean fuzzy information," *International Journal of Intelligent Systems*, vol. 31, no. 5, pp. 401–424, 2016.

[10] W. Liang, T. Zhang, and M. Liu, "The maţimizing deviation method based on interval-valued pythagorean fuzzy weighted aggregating operator for multiple criteria group decision analysis," *Discrete Dynamics in Nature and Society*, vol. 2015, Article ID 746572, 15 pages, 2015.

[11] D. Liang, Z. Xu, and A. P. Darko, "Projection model for fusing the information of pythagorean fuzzy multicriteria group decision making based on geometric Bonferroni mean," *International Journal of Intelligent Systems*, vol. 32, no. 9, pp. 966–987, 2017.

[12] X. Peng and Y. Yang, "Some results for pythagorean fuzzy sets," *International Journal of Intelligent Systems*, vol. 30, no. 11, pp. 1133–1160, 2015.

[13] M. Wei, T. Tang, and Y. Wei, "Pythagorean hesitant fuzzy hamacher aggregation operators and their application to multiple attribute decision making," *International Journal of Intelligent Systems*, vol. 33, no. 6, pp. 1197–1233, 2018.

[14] H. Garg, *Special Issue on "Pythagorean Fuzzy Set and its Eţtensions in Decision-Making Process*, Springer, Berlin, Germany, 2019.

[15] F. K. Gündoğdu and C. Kahraman, "Spherical fuzzy sets and decision making applications," in *Proceedings of the International Conference on Intelligent and Fuzzy Systems*, pp. 979–987, Istanbul, Turkey, July 2019.

[16] T. Mahmood, K. Ullah, Q. Khan, and N. Jan, "An approach toward decision-making and medical diagnosis problems using the concept of spherical fuzzy sets," *Neural Computing & Applications*, vol. 31, no. 11, pp. 7041–7053, 2019.

[17] K. Ullah, H. Garg, T. Mahmood, N. Jan, and Z. Ali, "Correlation coefficients for t-spherical fuzzy sets and their applications in clustering and multi-attribute decision making," *Soft Computing*, vol. 24, no. 3, pp. 1647–1659, 2020.

[18] T. Ayaz, M. M. Al-Shomrani, S. Abdullah, and A. Hussain, "Evaluation of enterprise production based on spherical cubic hamacher aggregation operators," *Mathematics*, vol. 8, no. 10, p. 1761, 2020.

[19] F. Kutlu Gündoğdu and C. Kahraman, "Spherical fuzzy sets and spherical fuzzy TOPSIS method," *Journal of Intelligent & Fuzzy Systems*, vol. 36, no. 1, pp. 337–352, 2019.

[20] F. K. Gündoğdu, "Principals of spherical fuzzy sets," in *Proceedings of the International Conference on Intelligent and Fuzzy Systems*, pp. 15–23, Istanbul, Turkey, July 2019.

WILEY | Hindawi

Retraction

Retracted: Cross-Border E-Commerce Supply Chain Risk Evaluation with FUZZY-ISM Model

Security and Communication Networks

This article has been retracted by Hindawi following an investigation undertaken by the publisher [1]. This investigation has uncovered evidence of one or more of the following indicators of systematic manipulation of the publication process:

(1) Discrepancies in scope

(2) Discrepancies in the description of the research reported

(3) Discrepancies between the availability of data and the research described

(4) Inappropriate citations

(5) Incoherent, meaningless and/or irrelevant content included in the article

(6) Peer-review manipulation

The presence of these indicators undermines our confidence in the integrity of the article's content and we cannot, therefore, vouch for its reliability. Please note that this notice is intended solely to alert readers that the content of this article is unreliable. We have not investigated whether authors were aware of or involved in the systematic manipulation of the publication process.

Wiley and Hindawi regrets that the usual quality checks did not identify these issues before publication and have since put additional measures in place to safeguard research integrity.

We wish to credit our own Research Integrity and Research Publishing teams and anonymous and named external researchers and research integrity experts for contributing to this investigation.

The corresponding author, as the representative of all authors, has been given the opportunity to register their agreement or disagreement to this retraction. We have kept a record of any response received.

References

[1] Z. Fang and Q. Wang, "Cross-Border E-Commerce Supply Chain Risk Evaluation with FUZZY-ISM Model," *Security and Communication Networks*, vol. 2021, Article ID 5155524, 14 pages, 2021.

WILEY | Hindawi

Research Article

Cross-Border E-Commerce Supply Chain Risk Evaluation with FUZZY-ISM Model

Zhiqi Fang [ID] **and Qifeng Wang** [ID]

Logistics and E-Commerce College, Zhejiang Wanli University, Ningbo, China

Correspondence should be addressed to Qifeng Wang; wqf2000@zwu.edu.cn

As a main new business model of Internet plus foreign trade, cross-border e-commerce has become an important way and breakthrough for China creating new foreign trade requirements in Internet economy. Cross-border supply chain management is one of the most important supports for cross-border e-commerce. Compared with domestic e-commerce, the supply chain of cross-border e-commerce faces more risks. In order to effectively identify and avoid the operational risks in the cross-border e-commerce supply chain, this article firstly analyzes the cross-border e-commerce supply chain risks from the operation process of the cross-border e-commerce supply chain. The risks include product selection management risks, cross-border transaction risks, and customs clearance risks that exist in the operation of cross-border e-commerce. Secondly, the cross-border e-commerce supply chain risk evaluation index system is established based on the risk elements. Finally, the risk evaluation is carried out through the FUZZY-ISM evaluation method, and the internal connection of each risk factor and the risk generation mechanism are revealed through structural model analysis, which provides a theoretical reference for cross-border e-commerce enterprise supply chain risk management.

1. Introduction

With the rise of Internet economy, traditional international trade has begun to transform to cross-border e-commerce, and cross-border e-commerce business has a breakthrough development [1]. Cross-border e-commerce is a business process in which both transaction parties in different countries or regions use the Internet as the transaction media to transport goods out of the country with the help of postal logistics or express logistics to achieve the purpose of the transaction [2]. China's cross-border e-commerce exports totaled 1.12 trillion RMB in 2021, an increase of 40.1% year-on-year growth. Cross-border e-commerce has become an important form of international trade in China [3].

Cross-border e-commerce supply chain management plays a critical role in the process of cross-border e-commerce business transactions. It promotes the business progress of cross-border transactions through the integration of resource, collaborating operation, supply and demand matching, and sharing business benefit [4]. Cross-border supply chain management can help e-commerce enterprises guarantee the normal production and sales effectively and reduce the cost of each sector in business transactions [5]. The cross-border e-commerce supply chain management has become the core competitiveness for the cross-border e-commerce enterprises.

In recent years, more and more black swans occur in international trading fields, such as Sino-US trade frictions, which have brought the risk of disruption to the cross-border e-commerce supply chain [6, 7]. At the same time, some unexpected irresistible force factors, such as the COVID-19 outbreak in early 2020 and the blockage of the Suez Canal, have also led to the interruption of the cross-border supply chain [8]. Therefore, more and more scholars have found that there are many problems and risks in the cross-border e-commerce supply chain under the current international trade environment. Such as unstable international transportation, tariff issues, trade barriers, and

other factors make cross-border e-commerce supply chains more complicated and unstable than traditional supply chains [9]. Secondly, risk factors such as the market environment (natural disasters, terrorist events, crisis events, etc.) [10] will also cause the paralysis and interruption of these cross-border supply chains, causing huge losses [11]. Therefore, how to effectively identify and evaluate the risks in the operation of the cross-border e-commerce supply chain and provide solutions to the risks has important theoretical and practical value for cross-border e-commerce. Presently, most former studies on cross-border e-commerce supply chain risks are based on qualitative analysis, such as Mensah et al.'s [12] qualitative methods to study the integration of cultural dimensions, such as power distance, collectivism, uncertainty avoidance, masculinity, and long-term orientation into UTAUT, and examined the comparative impact of cultural dimensions on the adoption of cross-border e-commerce by Chinese and Russian citizens. However, the quantitative analysis of the internal relationship between risk factors is still scarce, and most of the risks are ambiguous. To evaluate the supply chain risks for cross-border e-commerce enterprises under uncertain international business environment, this paper adopts Fuzzy Interpretative Structural Modeling (FUZZY-ISM) to construct an evaluation model for cross-border e-commerce supply chain risk management [13, 14]. The empirical analysis is carried out to explore the mechanism of the influencing factors of cross-border e-commerce supply chain risk as well as the mutual relationship between various factors, so as to provide theoretical guidance for cross-border e-commerce enterprises' supply chain risk management.

The paper is organized as follows. Section 2 summarizes the current research status of supply chain risk evaluation. Section 3 presents the method of the cross-border e-commerce supply chain risk evaluation process based on FUZZY-ISM. Section 4 presents the operation process of the cross-border e-commerce supply chain to provide a theoretical basis for subsequent risk identification. Section 5 identifies the risk factors of the cross-border e-commerce supply chain and establishes the risk evaluation index system. Section 6 conducts empirical analysis through calculation examples. Section 7 concludes.

2. Review of Literatures

As an important study issues in supply chain management, many valuable research results have been achieved in supply chain risk management fields. Christopher and Rutherford [15] provided that supply chain risk is "the risk from the original supplier to the final product delivery with product, material, and information flow." Ponomarov and Holcomb [16] presented that the goal of supply chain risk management is to develop adaptability, prepare for unexpected events, respond to supply chain interruptions, and recover from them. Fahimnia [17] put forward that supply chain risk management is the process of managing the risk of information, materials, and products flowing from suppliers to end users. Cucchiella and Gastaldi [18] used real options to reduce corporate risk and studied risk management in the supply chain. In order to protect the company from risks caused by various uncertain factors, a personalized theoretical framework suitable for the company has been formulated so that it can choose feasible methods to reduce corporate risks. Um and Han [19] explored the relationships amongst global supply chain risks, supply chain resilience, and mitigating strategies through theoretically hypothesis and empirical study. The results provide practical implications for managing uncertain events and offering theoretical insight for future research in supply chain resilience. Ritchie and Brindley [20] studied supply chain risk performance and management and provided a reference framework for the future development of enterprises. The framework helps to provide a classification of risk drivers and integrates supply chain performance and risk dimensions. Giannakis and Louis [21] proposed a multiagent-based decision support system design framework in order to prevent and manage the risk interruption of the manufacturing supply chain. The framework focuses on the demand-driven supply chain, rather than the forecast-driven supply chain.

The evaluation methods of supply chain risk are also widely studied. Fazli et al. [22] identified the main risks and the crude oil supply chain through the decision-making trial and evaluation laboratory (DEMATEL) method to determine the correlation between risks and use the network analysis (ANP) method to assess the importance of each risk and determine the best response strategy. Rajesh [23] used a decision support model to incorporate an amalgamation of grey theory, and the layered analytic network process (ANP) has been employed for quantifying various resilient strategies for risk mitigation. The proposed model was also applied in a practical setting with the case study of an electronics manufacturing company. Song [24] evaluated the risk by text mining and fuzzy rule reasoning, which can assess the risk of cross-border e-commerce supply chain quantitatively and semi-automatically and also can evaluate the related risk factors. The output of the cross-border e-commerce supply chain is summarized to obtain the overall risk of the cross-border e-commerce supply chain, so as to improve the efficiency and accuracy of the risk assessment of the cross-border e-commerce supply chain. Soni et al. [25] established a supply chain elasticity measurement model based on graph theory and used the model to consider the main driving factors of elasticity and the relationship between them and measure elasticity through a single value. Similar to the above evaluation method, Tan et al. [26] proposed a conceptual model of the supply chain network to quantify the structural redundancy of supply chain risk management. Min [27] used block chain technology to enhance the resilience of the supply chain to avoid the supply chain risks. In addition, some research studies are more inclined to empirical research on supply chain risk management. For example, Donadoni et al. [28] used data from the sixth edition of the International Manufacturing Strategy Survey to study the relationship between product complexity, supply chain disruption, and performance. Research results show that product complexity increases the probability of supply chain disruption. Ceryno et al. [29] investigated the

performance of the automotive industry in three supply chains in Brazil, determined the main risks in the automotive supply chain, provided an initial risk profile for the Brazilian automotive industry, and by analyzing the real-life risks in different supply chains, determined the main risks that the supply chain may expose, as a way to help the supply chain start the supply chain risk management process.

In summary, risk management, as an important part of supply chain management, plays a vital role in maintaining the sustainability of the supply chain [30]. The current market competition is a more direct competition between supply chains, especially the global supply chain competition has become a consensus [31]. However, the current supply chain risk evaluation and management are mainly concentrated in the manufacturing supply chain or the domestic supply chain field, and there are relatively few studies on the supply chain risk management issues of the cross-border e-commerce industry. Compared with domestic supply chains, cross-border e-commerce supply chains involve more risk factors, and the relationships among risk factors are complicated. Therefore, this paper adopts the fuzzy interpretation structure model to build the evaluation model of cross-border e-commerce supply chain risk management and conducts empirical analysis to explore the internal connection and mechanism of each risk factor of cross-border e-commerce supply chain risk, so as to provide advises for cross-border e-commerce enterprises to manage the supply chain risks.

3. Methodology

This section presents the methodology applied in this research. We provide the cross-border e-commerce supply chain risk evaluation method framework, which is shown in Figure 1.

The cross-border e-commerce supply chain risk evaluation method is based on ISM method, fuzzy sets theory, and FUZZY-ISM method. Firstly, the FUZZY-ISM method will be studied. Secondly, the operation process of the cross-border e-commerce supply chain is analyzed and summarized through field investigation and literature analysis. Thirdly, combined with the relevant literature of cross-border e-commerce supply chain risk management, the actual operation process of cross-border e-commerce is analyzed, and the questionnaire survey method and expert interview method are used to further screen out the key influencing factors of the cross-border e-commerce supply chain and establish the risk evaluation index system of cross-border e-commerce. Finally, through the example analysis, the risk factors of cross-border e-commerce are evaluated and ranked, and the results are analyzed and summarized.

In the rest of this section, we will present the Fuzzy-ISM model and its establishment process based on the induction of basic theory of ISM and fuzzy sets.

3.1. ISM. There are many risk factors in the cross-border e-commerce supply chain, and the relationship between the various influencing factors is intricate, and the explanatory

structure model, proposed by Warfeldt in 1973, is a static analysis method used to analyze the complex relationship between multiple factors. It uses an incidence matrix to analyze the overall structure of a project's complex risk system, uses a directed graph to describe the relationship between the elements in the system, extracts and analyzes the structural relationship of the elements by calculating the reachability matrix between the elements, and obtains the relationship between the elements. Through the transfer and hierarchical structure, a multilevel ladder model of the analysis object is finally constructed [13]. Lim et al. [32] used the ISM method to identify the driving forces and dependencies of sustainable supply chain management in the context of knowledge management, so as to improve the performance of textile enterprises in Vietnam. The research results show that learning organization, information, knowledge sharing, collaboration knowledge creation, information technology, and knowledge storage are the main driving and dependent forces. Dubey et al. [33] used the TISM model to identify the barriers of green supply chain management (GSCM). Wu et al. [34] used the Integrated Interpretive Structure Model (ISM) and Bayesian Network (BN) methods for risk assessment and used ISM to clearly specify the engineering risk factor relationships expressed in the causal relationship diagram and formed the structure of BN. The subjective judgment of experts is transformed into prior probability and conditional probability set and embedded in BN. The results show that the balance sheet can provide clear risk information for better project management.

3.2. Fuzzy Sets. However, it is not enough to only consider whether there are influences between systems. In the cross-border e-commerce supply chain risk, both the natural environment risk and the economic environment risk will have an impact on the risk of logistics interruption, but in contrast, the former will have greater influencing factors. And, in most business scenario, the influencing factors are inaccuracy and vague. The fuzzy theory was proposed by Zadeh to solve the inaccuracy and vague issue, and the fuzzy theory is widely used in quality management and risk management [35]. Presently, the fuzzy theory is widely extended to solve more complicated problems. Mahmood et al. [36] presented the concept of complex hesitant FSs (CHFSs) and applied to pattern recognition and medical diagnosis. Chen et al. [37] used a fuzzy evaluation method based on life cycle assessment and cost-benefit analysis to achieve a comprehensive quantitative evaluation of the environmental and economic benefits of anaerobic digestion technology. In order to solve uncertain and unpredictable information in real-life problems, Mahmood et al. [38] proposed the complex dual hesitant fuzzy set (CDHFS) and applied to the environment of pattern recognition and medical diagnosis to assess the capability and feasibility of the interpreted measures.

3.3. FUZZY-ISM. In the FUZZY-ISM model, different values of α will generate different interpretation structure models, which are superior to the ISM model in terms of flexibility and
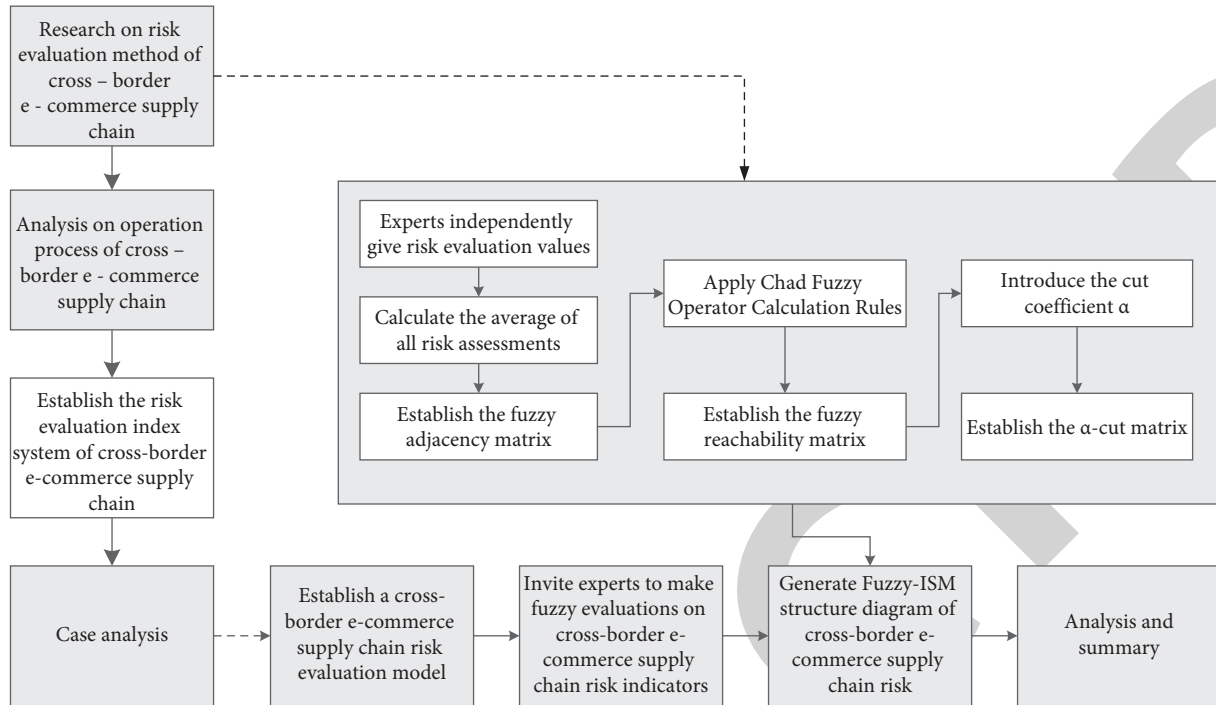
Figure 1: Cross-border e-commerce supply chain risk evaluation method framework based on the FUZZY-ISM model.

are more suitable for the diagnosis of complex system problems [14]. Therefore, this article introduces fuzzy theory to improve the ISM structure model and establishes the FUZZY-ISM model for risk factors of the cross-border e-commerce supply chain, which can conduct a more in-depth and intuitive analysis of risk factors and reveal the internal connections and risk generation of various risk factors and their mechanisms. At the same time, for the convenience of research, the weak influence relationship is weakened and omitted. The model establishment process is as follows:

Step 1: establish the relationship between risk factors through expert data

Step 2: establish a fuzzy adjacency matrix

Step 3: use the Chad fuzzy operator in the fuzzy matrix [39] calculation rules to calculate the fuzzy reachability matrix from the fuzzy adjacency matrix

Step 4: introduce the intercept coefficient α to transform it into a reachable matrix of 0 to 1, and obtain the α intercept matrix

Step 5: generate the FUZZY-ISM structure diagram

Step 6: analysis of risk assessment results

4. Operation Process of Cross-Border E-Commerce Supply Chain

The cross-border e-commerce enterprises sell the goods to abroad customers via the cross-border e-commerce platform, such as Amazon, eBay, and Wish. The cross-border supply chain is the core support for cross-border e-commerce transaction. The operation process of the cross-border e-commerce supply chain is shown in Figure 2.

Firstly, the cross-border e-commerce enterprises conduct product selection management through their own production or purchase from upstream suppliers or manufacturers. They can pick up the goods themselves or distribute them by manufacturers and publish and trade the company's product information on cross-border e-commerce platforms. After the cross-border e-commerce enterprise receives the goods, confirm whether the quality of the goods meets the receiving requirements and confirm the payment to the manufacturer or supplier after receiving the goods. After the goods are in warehouse, they will be sorted and packaged. After that, they will be transported to the exit customs through third-party logistics, and the procedures of application for customs declaration, customs inspection, tariff payment, release, export tax rebate, etc., are carried out. Then, the goods will be transported to the destination country by sea, air, land, or international multimodal transport. After arriving in the destination country, the consignee or the entrusted customs declaration company will apply to the customs of the destination country for customs clearance. After customs inspection, customs duties, value-added tax, and other taxes will be paid, and the goods will be shipped to overseas warehouses and put on shelves. And, cross-border e-commerce platform operators can provide cross-border e-commerce companies with corresponding cross-border service capabilities, such as installation and commissioning of products, technical guidance, data analysis, and related policy services. Overseas buyers can place orders online through cross-border e-commerce trading platforms such as Amazon and eBay. Domestic cross-border e-commerce companies received the orders and released them to the overseas warehouse. The overseas warehouse management system automatically
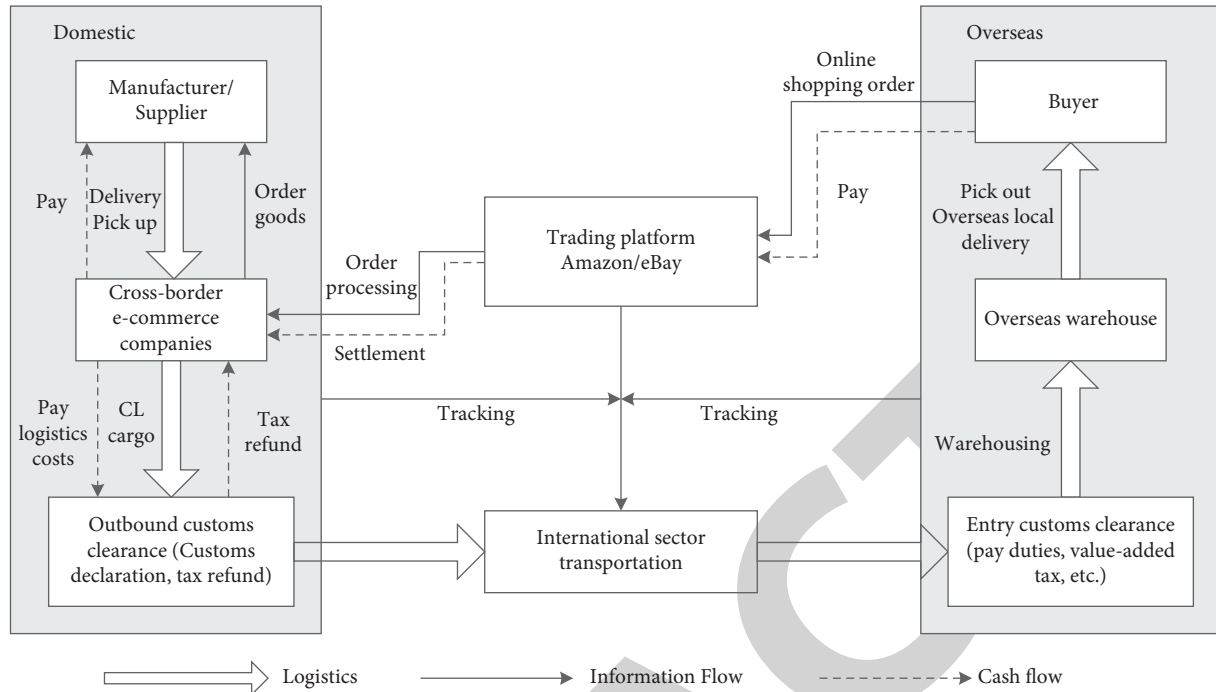
Figure 2: Operation process of the cross-border e-commerce supply chain.

obtains order information, and the goods will be sorted, packed, and then distributed to the customer via local postal or express delivery. In order to ensure the normal operation of the entire operation process of the cross-border e-commerce supply chain, the system will track the real-time information of logistics, information flow, and capital flow throughout the process.

Compared with traditional trade, cross-border e-commerce supply chains face different consumers. The consumers faced by traditional traders are mostly manufacturers, so the supply chain of traditional trade mainly plays a role in the transportation of goods from sellers to buyers, with relatively simple functions and simple structure. Cross-border e-commerce not only faces corporate customers but also faces consumers. The cross-border e-commerce supply chain is the way that cross-border e-commerce uses the cross-border supply chain to manage the entire cross-border e-commerce transaction activities, which means cross-border e-commerce is a special form of supply chain in the context of e-commerce. It is a modern form of supply chain under the background of cross-border e-commerce, advocating the concept of resource integration, coordinated operation, matching of supply and demand, and benefit sharing [4] including the entire online electronic transaction, online and offline cross-border payments, and cross-border logistics distribution and transportation.

Therefore, in the supply chain of cross-border e-commerce, multiple cross-border links such as cross-border payment and cross-border logistics are not only added but also laws and regulations, network information security, cultural backgrounds of different countries, and consumption must also be considered in the operation process. The risk factors faced by the cross-border e-commerce supply chain are higher than that of the traditional trade supply chain.

5. Construction of Risk Evaluation Index System for Cross-Border E-Commerce Supply Chain

Gomez-Herrera et al. [40] examined consumer data in the EU market and analyzed the factors affecting the development of cross-border e-commerce, such as cost advantages, online payment, and logistics models, and recommended that the state should actively provide convenience for enterprises in terms of planning, supervision, and customs clearance. Van Heel et al. [41] studied cross-border e-commerce export trade and found that there are obstacles in customs clearance, logistics, and supervision. Shi et al. [42] conducted a data-driven analysis and research on Chinese fashion retailers and found that the risks affecting the cross-border e-commerce supply chain of enterprises include online marketing risks, cross-border e-payment risks, e-customs clearance risks, cross-border logistics risks, and credit risk. Nuruzzaman and Weber [43] have employed the qualitative research methods to identify some key issues such as supply chain facility, inventory management, and legal obstacles with today's supply chain performance of international e-commerce. To analyse the risks in the cross-border e-commerce supply chain under unexpected environment, this paper analyzes the relevant literature and the actual operation process of the cross-border e-commerce supply chain through the analysis of the operation process of the cross-border e-commerce supply chain and the literature analysis method, selects the risk factors of the cross-border

e-commerce supply chain from the literature, and then adopts the questionnaire survey method and expert interview method to provide the key influencing factors of the cross-border e-commerce supply chain. However, with the environmental issues such as the Sino-US trade conflict and the outbreak of the new crown epidemic, the logistics interruption caused by the supply chain failure and the failure of funds to return to the circulation also need to attract the attention of cross-border e-commerce companies. Therefore, this article finally classifies risk factors into 5 categories, including product selection management risk, cross-border transaction risk, customs clearance risk, logistics risk, and environmental risk. Finally, 5 first-level indicators and 16 second-level indicators are formed, and the risk evaluation index system is established. The results are shown in Table 1.

5.1. Product Selection Management Risk Including Product Quality Risk, Product Delivery Risk, and Intellectual Property Disputes Risk. When cross-border e-commerce companies purchase goods, they will buy shoddy goods, which will cause the risk of not being able to continue to sell. In addition, if the product is not communicated or tracked in time after the product is purchased, the product cannot be delivered and there is a risk. However, companies do not have a strong awareness of intellectual property rights and do not know much about overseas laws. Infringements occur from time to time. Infringed persons use e-commerce platforms to carry out phishing law enforcement and freeze the accounts of companies or clear their accounts.

5.2. Cross-Border Transaction Risks Including Credit Risk, Information Risk, and Capital Settlement Risk. Selling goods online is prone to dishonesty. The credit risk is particularly prominent in cross-border transactions. The subjects that cause the risk include domestic sellers, overseas buyers, and third-party payment platforms. In the online world, there are also information security issues, and its own security risks are prone to information and data leakage issues, such as seller data and buyer information. The settlement of funds is entirely dependent on third-party payment platforms. If cross-border payment channels are not smooth and cross-border e-commerce foreign exchange settlement problems occur, corporate funds will not be able to withdraw, resulting in cross-border e-commerce companies operating difficulties.

5.3. Customs Clearance Risk Including Customs Clearance Risk, Declaration Risk, and Taxation Risk. In the process of cross-border e-commerce transactions, all commodities entering and leaving the country need to be supervised by the customs. After the basic steps of declaration, inspection, taxation, and release are completed, customs clearance is completed. However, goods at different customs locations may have slow customs clearance efficiency or noncustoms clearance. In addition, some cross-border e-commerce companies have special circumstances such as high market value of goods. In order to reduce the tariffs, cross-border e-

commerce enterprise uses the fictitious information, such as fictitious weights of goods and fictitious prices. After the customs finds it, the goods will be intercepted and returned, and the logistics timeliness will not be guaranteed. In the tax collection process, risks mainly come from tax system risks, tax source supervision risks, and tax law enforcement risks.

5.4. Logistics Risk Including Logistics Timeliness Risk, Logistics Information Risk, Logistics Damage Risk, and Logistics Interruption Risk. At present, cross-border e-commerce logistics includes five modes, including traditional transnational logistics, postal parcel, special line express, overseas warehouse, and multimodal transport. Cross-border logistics transportation takes a long time and long distances, increasing the links of customs clearance, commodity inspection, tax refund and foreign exchange settlement, overseas warehousing, etc., which greatly increases the risks of cross-border logistics and also puts forward high requirements for its efficiency and service quality. The risk of cross-border statute of limitations lies in the low cross-border efficiency and the increasing differences in the national conditions of countries in cross-border transactions, which make cross-border logistics work impossible to carry out efficiently. In addition, errors in logistics information, difficulty in real-time tracking, and damage to goods during transportation may also occur. And, with the Sino-US trade conflict and the outbreak of the new crown epidemic, it will lead to the supply chain breakage and logistics interrupted.

5.5. Environmental Risks Including Natural Environmental Risks, Economic Environmental Risks, and Industrial Policy Environmental Risks. The environmental risk of the cross-border e-commerce supply chain refers to the risk of cross-border e-commerce enterprises caused by the uncertainty of the external environment. Natural disasters, environmental issues, disease outbreaks, and other risks may suddenly occur in the natural environment, such as the outbreak of the COVID-19 outbreak in early 2020 and the earthquake in Japan. Economic environment risks will have large fluctuations in the market economy and real-time changes in exchange rates and interest rates, such as the Sino-US trade war. The cross-border e-commerce industry has changed greatly, and national economic policies are constantly changing. Fluctuations in market demand and changes in the market scale will affect the economic benefits of enterprises. The faster the development, the fiercer of the competition in the cross-border trade fields, there will be certain risks for cross-border e-commerce companies.

6. Case Analysis

The COVID-19 epidemic has caused a huge impact on the cross-border e-commerce supply chain. Due to lack of awareness of supply chain risk management, many cross-border e-commerce enterprises have experienced supply chain disruptions or even business failures. In order to effectively identify the risk factors of the COVID-19 epidemic

Table 1: Risk evaluation index system of the cross-border e-commerce supply chain.

First-level indicator	Second-level indicator	Description of risk indicator
Product selection management risk [4, 5, 12, 40, 42–44]	Product quality risk C1	During the product selection process, the actual product cannot be seen, and the product can only be understood through the pictures, evaluations, introductions, and videos on the website; some speculative merchants who only pursue short-term benefits pretend to be shoddy and display high-quality products online; the products are actually fake and inferior, and the actual goods are completely different from the description
	Product delivery risk C2	After the products are purchased, the materials or products provided by the supplier may not be delivered on time, which may cause the delay or interruption of the domestic logistics of the supply chain
	Intellectual property disputes risk C3	Sometimes, the companies do not have a strong awareness of intellectual property rights and do not know much about overseas laws; infringed persons use e-commerce platforms to carry out phishing law enforcement, freeze the accounts of companies or clear their accounts, and put companies in a difficult position
Cross-border transaction risk [1, 5, 40, 42–44]	Credit risk C4	Transaction credit risk refers to the fact that cross-border e-commerce companies do not understand foreign consumers in the online transaction process, and it is difficult to grasp the transaction motives of foreign consumers, and transactions that violate the principle of good faith are likely to occur; dishonest behaviors cause "abortion" of transactions and bring losses to cross-border e-commerce companies
	Information risk C5	Information risk includes domestic supplier information risk and cyber security information risk
	Capital settlement risk C6	In the field of cross-border e-commerce, international payments are basically monopolized by international credit organizations and international payment companies, and their payment procedures are relatively expensive; most payment tools in China are not recognized by overseas users; cross-border payment channels are not smooth, cross-border e-commerce foreign exchange settlement is prone to problems, and corporate funds cannot be withdrawn, resulting in cross-border e-commerce companies operating difficulties
Customs clearance risk [9, 40–42, 44, 45]	Customs clearance risk C7	Includes customs clearance efficiency and cargo clearance rate; different customs locations have different customs clearance requirements, and goods may have slow customs clearance efficiency or noncustoms clearance
	Customs declaration risk C8	Some cross-border e-commerce companies have special circumstances such as high market value of goods; in order to reduce tariffs, false declarations of goods and goods weight, virtual logistics prices, virtual consignees and consignees, or split declarations
	Taxation risk C9	Taxation risks include tax system risks, tax source supervision risks, and tax enforcement risks
Logistics risk [1, 4, 8, 9, 12, 40–45]	Logistics timeliness risk C10	Cross-border logistics transportation takes a long time and long distances; due to transportation delays, customs clearance delays, delivery delays, etc., the logistics timeliness will be affected, and customers will not be able to sign for a long time, affecting corporate reputation and payment
	Logistics information risk C11	In the process of cross-border logistics information transmission, information errors may occur or it is difficult to achieve real-time tracking
	Logistics damage risk C12	In the process of cross-border transportation of cross-border goods, the goods are damaged or lost, which prevents the goods from reaching overseas consumers in a timely and safe manner
	Logistics interruption risk C13	Due to force majeure and other reasons, such as wars and epidemics, there is a risk of interruption of cross-border logistics and transportation

TABLE 1: Continued.

First-level indicator	Second-level indicator	Description of risk indicator
Environmental risk [1, 4, 6–8, 10–12, 41, 44, 46]	Natural environment risk C14	Natural disasters, environmental issues, disease outbreaks, and other risks may suddenly occur in the natural environment, such as the outbreak of the COVID-19 outbreak in early 2020 and the earthquake in Japan
	Economic environment risk C15	Economic environment risks will have large fluctuations in the market economy and real-time changes in exchange rates and interest rates, such as the Sino-US trade conflict
	Industry policy environmental risks C16	The cross-border e-commerce industry has changed greatly, and national economic policies are constantly changing; fluctuations in market demand and changes in the market scale will affect the economic benefits of enterprises; the faster the development, the fierce the competition in the industry and unpredictable the development prospects of the industry, and there will be certain risks for cross-border e-commerce companies

on the cross-border e-commerce supply chain and conduct an objective evaluation, this article takes Ningbo cross-border comprehensive zone e-commerce enterprises as an example. Since Ningbo was approved as the second batch of comprehensive pilot zone for cross-border e-commerce by the state in January 2016, cross-border e-commerce has achieved rapid development. In 2019, the scale of cross-border e-commerce transactions in the city reached 128.2 billion RMB, accounting for 13.98% of the city's total foreign trade import and export, upto 374.4% compared with 2016, and 328.9 percentage points higher than the growth rate of foreign trade in the same period.

Based on the risk evaluation indicators and methods in the previous section, this section will take the e-commerce enterprise in the Ningbo comprehensive pilot zone as an example. Based on the establishment of a cross-border e-commerce supply chain risk factor index system, the risk factor evaluation research method based on the FUZZY-ISM model is used for quantitative evaluation.

Step 1: *Establish the Fuzzy Adjacency Matrix.*

Through the design of questionnaires and via online and offline surveys, a 16×16 matrix was set up to confirm and score the interrelationships of cross-border e-commerce supply chain risk factors and take the average value as the final degree of influence between the two factors. The fuzzy relationship between various risk factors is analyzed, and the fuzzy adjacency matrix A of cross-border e-commerce supply chain risk factors is generated (see in Figure 3).

In this matrix, the cross-border e-commerce supply chain risk is regarded as a system, which includes 16 components such as $C_i (i = 1, 2, \ldots, 16)$ and builds a 16×16 adjacency matrix on this basis $A = [C_{ij}]_{16 \times 16}$. When constructing this adjacency matrix, the logical relationship between the two influencing factors is represented by C_{ij}, $0 \le C_{ij} \le 1$. In addition, the direct relationship between factor i and factor j, that is, the cell on the diagonal is recorded as 0.

Step 2: *Calculate the Reachable Matrix.*

After obtaining the fuzzy adjacency matrix, calculate the sum $A + I$ of A and the identity matrix I and use the Chad fuzzy operator calculation rules in the fuzzy matrix to perform matrix $A + I$ power operation on a certain integer n until the following formula holds:

$$M = (A + I)^{n+1} = (A + I)^n \ne (A + I)^{n-1} \tag{1}$$
$$\ne \cdots \ne (A + I)^2 \ne (A + I).$$

Use MATLAB to calculate the order of matrix convergence. When $n = 6$, the matrix converges, and the reachable matrix M is obtained (see in Figure 4).

Step 3: *α-Cut Matrix.*

Since the fuzzy reachable matrix cannot be decomposed into domains and interstages, the cut-off coefficient α is introduced to transform it into a reachable matrix of 0~1. Because the value of α is different, different 0~1 reachable matrices will be generated. For the convenience of research, the intermediate threshold $\alpha = 0.5$ is adopted, and the horizontal intercept matrix $M_{\alpha=0.5}$ can be obtained as (see in Figure 5):

$$\alpha_{xij} = \begin{cases} 1, & x_{ij} \ge 0.5 = \alpha, \\ 0, & x_{ij} \le 0.5 = \alpha. \end{cases} \tag{2}$$

Step 4: *Divide the Hierarchical Relationship of Each Factor.*

(1) According to the reachability matrix, the reachability set $R(C_i)$ and the antecedent set $A(C_i)$ of each influencing factor can be determined first. The reachable set $R(C_i)$ refers to the set of all reachable factors starting from C_i, that is, the set of all the column factors with a score of 1 in the row of the factor C_i in the reachable matrix; the antecedent set $A(C_i)$ refers to all possible reach. The set of factors of C_i can be the set of all the row factors with a score of 1 in the column of factor C_i in the matrix [47].

(2) According to the obtained reachable set $R(C_i)$ and antecedent set $A(C_i)$ of each influencing factor, find

$$A =$$

	C_1	C_2	C_3	C_4	C_5	C_6	C_7	C_8	C_9	C_{10}	C_{11}	C_{12}	C_{13}	C_{14}	C_{15}	C_{16}
C_1	0	0.3	0.8	0	0	0.5	0.5	0.5	0	0	0	0	0	0	0	0
C_2	0	0	0	0	0	0.5	0	0	0	0.5	0	0	0	0	0	0
C_3	0	0	0	0	0	0.9	0.7	0.4	0	0.5	0	0	0	0	0	0.6
C_4	0	0	0	0	0	0.9	0.5	0	0	0	0	0	0	0	0	0.5
C_5	0	0.1	0	0.1	0	0.7	0	0	0	0	0.7	0	0	0	0	0.1
C_6	0	0	0	0	0	0	0	0	0	0	0	0	0	0	0	0.3
C_7	0	0	0.5	0	0	0.5	0	0	0	0.5	0	0	0.2	0	0	0
C_8	0.5	0	0.5	0	0	0.5	0.5	0	0	0.2	0	0	0	0	0	0
C_9	0	0	0	0	0	0.5	0	0	0	0	0	0	0	0	0	0.5
C_{10}	0	0.5	0	0.1	0	0.7	0	0	0	0	0	0	0	0	0	0
C_{11}	0	0	0	0.5	0	0.5	0	0	0	0	0	0	0	0	0	0
C_{12}	0.5	0.2	0	0	0	0.5	0	0	0	0.5	0	0	0	0	0	0
C_{13}	0	0.5	0	0.5	0	0.8	0	0	0	0.9	0	0	0	0	0	0
C_{14}	0	0.2	0	0	0	0.5	0	0	0.2	0.5	0	0.5	0.8	0	0.3	0.5
C_{15}	0	0	0	0	0	0.5	0	0	0	0	0	0	0.6	0	0	0.1
C_{16}	0	0	0.5	0	0	0.5	0	0	0.3	0	0	0	0	0	0	0

FIGURE 3: Adjacency matrix of the FISM model for cross-border e-commerce supply chain risk.

	C_1	C_2	C_3	C_4	C_5	C_6	C_7	C_8	C_9	C_{10}	C_{11}	C_{12}	C_{13}	C_{14}	C_{15}	C_{16}
C_1	1	0.5	0.8	0.2	0	0.8	0.7	0.5	0.3	0.5	0	0	0.2	0	0	0.6
C_2	0.3	1	0.3	0.2	0	0.5	0.3	0.3	0.3	0.5	0	0	0.2	0	0	0.3
C_3	0.4	0.5	1	0.2	0	0.9	0.7	0.4	0.3	0.5	0	0	0.2	0	0	0.6
C_4	0.4	0.5	0.5	1	0	0.9	0.5	0.4	0.3	0.5	0	0	0.2	0	0	0.5
C_5	0.4	0.5	0.5	0.5	1	0.7	0.5	0.4	0.3	0.5	0.7	0	0.2	0	0	0.5
C_6	0.3	0.3	0.3	0.2	0	1	0.3	0.3	0.3	0.3	0	0	0.2	0	0	0.3
C_7	0.4	0.5	0.5	0.2	0	0.5	1	0.4	0.3	0.5	0	0	0.2	0	0	0.5
C_8	0.5	0.5	0.5	0.2	0	0.5	0.5	1	0.3	0.5	0	0	0.2	0	0	0.5
C_9	0.4	0.5	0.4	0.2	0	0.5	0.4	0.4	1	0.5	0	0	0.2	0	0	0.5
C_{10}	0.3	0.5	0.3	0.2	0	0.7	0.3	0.3	0.3	1	0	0	0.2	0	0	0.3
C_{11}	0.4	0.5	0.5	0.5	0	0.5	0.5	0.4	0.3	0.5	1	0	0.2	0	0	0.5
C_{12}	0.5	0.5	0.5	0.2	0	0.5	0.5	0.5	0.3	0.5	0	1	0.2	0	0	0.5
C_{13}	0.4	0.5	0.5	0.5	0	0.8	0.5	0.4	0.3	0.9	0	0	1	0	0	0.5
C_{14}	0.5	0.5	0.5	0.5	0	0.8	0.5	0.5	0.3	0.8	0	0.5	0.8	1	0.3	0.5
C_{15}	0.4	0.5	0.5	0.5	0	0.6	0.5	0.4	0.3	0.6	0	0	0.6	0	1	0.5
C_{16}	0.4	0.4	0.5	0.2	0	0.5	0.5	0.4	0.3	0.4	0	0	0.2	0	0	1

FIGURE 4: Reachability matrix of the FISM model for cross-border e-commerce supply chain risk.

the intersection of them to get the intersection set I (C_i). The results are shown in Table 2.

(3) Calculate the top factor set: when the reachable set is equal to the intersection, the factor in the reachable set is the top-most set of factors, and the top-most set of factors is thus determined $L_1 = \{C_6\}$.

(4) The same influencing factors at the intersection set C (C_i) and reachable set R (C_i) are classified as the same influencing factor level. Then, remove the crossed-out factors to get a new matrix, and then, follow step 2 to determine the second-level factor set of the new matrix. The 16 cross-border

	C_1	C_2	C_3	C_4	C_5	C_6	C_7	C_8	C_9	C_{10}	C_{11}	C_{12}	C_{13}	C_{14}	C_{15}	C_{16}
C_1	1	1	1	0	0	1	1	1	0	1	0	0	0	0	0	1
C_2	0	1	0	0	0	1	0	0	0	1	0	0	0	0	0	0
C_3	0	1	1	0	0	1	1	0	0	1	0	0	0	0	0	1
C_4	0	1	1	1	0	1	1	0	0	1	0	0	0	0	0	1
C_5	0	1	1	1	1	1	1	0	0	1	1	0	0	0	0	1
C_6	0	0	0	0	0	1	0	0	0	0	0	0	0	0	0	0
C_7	0	1	1	0	0	1	1	0	0	1	0	0	0	0	0	1
C_8	1	1	1	0	0	1	1	1	0	1	0	0	0	0	0	1
C_9	0	1	0	0	0	1	0	0	1	1	0	0	0	0	0	1
C_{10}	0	1	0	0	0	1	0	0	0	1	0	0	0	0	0	0
C_{11}	0	1	1	1	0	1	1	0	0	0	1	0	0	0	0	1
C_{12}	1	1	1	0	0	1	1	1	0	1	0	1	0	0	0	1
C_{13}	0	1	1	1	0	1	1	0	0	1	0	0	1	0	0	1
C_{14}	1	1	1	1	0	1	1	1	0	1	0	1	1	1	0	1
C_{15}	0	1	1	1	0	1	1	0	0	1	0	0	1	0	1	1
C_{16}	0	0	1	0	0	1	1	0	0	0	0	0	0	0	0	1

Figure 5: α-cut matrix of the FISM model for cross-border e-commerce supply chain risk.

Table 2: Reachable set, antecedent set, and intersection set.

Element C_i	Reachable set $R\ (C_i)$	Antecedent set $A\ (C_i)$	Intersection set $I\ (C_i)$
1	1, 2, 3, 6, 7, 8, 10, 16	1, 8, 12, 14	1, 8
2	2, 6, 10	1, 2, 3, 4, 5, 7, 8, 9, 10, 11, 12, 13, 14, 15	2, 10
3	2, 3, 6, 7, 10, 16	1, 3, 4, 5, 7, 8, 9, 11, 12, 13, 14, 15, 16	3, 7, 16
4	2, 3, 4, 6, 7, 10, 16	4, 5, 7, 8, 9, 11, 12, 13, 14, 15, 16	4, 7, 16
5	2, 3, 4, 5, 6, 7, 10, 11, 16	5	5
6	6	1, 2, 3, 4, 5, 6, 7, 8, 9, 10, 11, 12, 13, 14, 15, 16	6
7	2, 3, 6, 7, 10, 16	1, 3, 4, 5, 7, 8, 9, 11, 12, 13, 14, 15, 16	3, 7, 16
8	1, 2, 3, 6, 7, 8, 10, 16	1, 8, 12, 14	1, 8
9	2, 6, 9, 10, 16	9	9
10	2, 6, 10	1, 2, 3, 4, 5, 7, 8, 9, 10, 12, 13, 14, 15	2, 10
11	2, 3, 4, 6, 7, 11, 16	5, 11	11
12	1, 2, 3, 6, 7, 8, 10, 12, 16	12	12
13	2, 3, 4, 6, 7, 10, 13, 16	13, 14, 15	13
14	1, 2, 3, 4, 6, 7, 8, 10, 12, 13, 14, 16	14	14
15	2, 3, 4, 6, 7, 10, 13, 15, 16	15	15
16	3, 6, 7, 16	1, 3, 4, 5, 7, 8, 9, 11, 12, 13, 14, 15, 16	3, 7, 16

e-commerce supply chain risk factors are divided into 6 levels in turn, namely, $L = \{L_1, L_2, L_3, L_4, L_5, L_6\}$, and the results are shown in Table 3.

(5) Drawing of the structural model: according to the above calculation and analysis, the reachable matrix M is divided into 5 levels, and the first-level node $L_1 = \{C_6\}$ of cross-border e-commerce supply chain risk factors, the second-level node $L_2 = \{C_2, C_{10}, C_{16}\}$, the third-level node $L_3 = \{C_3, C_7, C_9\}$, the fourth-level node $L_4 = \{C_1, C_4, C_8\}$, the fifth-level node $L_5 = \{C_{11}, C_{12}, C_{13}\}$, and the sixth-level node $L_6 = \{C_5, C_{14}, C_{15}\}$. Sort the risk factors according to the hierarchical results, and draw a multilayer

hierarchical structure diagram (see Figure 6), which intuitively reflects the logical relationship, transmission path, and interaction mechanism between the risk factors of the cross-border e-commerce supply chain.

Step 5: Analysis of Risk Factors' Results.

According to Figure 6, the risk factors of the cross-border e-commerce supply chain are a 6-level hierarchical structure.

(1) The first-level factor is the risk of capital settlement. As a surface risk factor, the inability of funds to settle foreign exchange is the most direct risk factor

TABLE 3: Results of the hierarchical structure of risk factors in cross-border e-commerce supply chains.

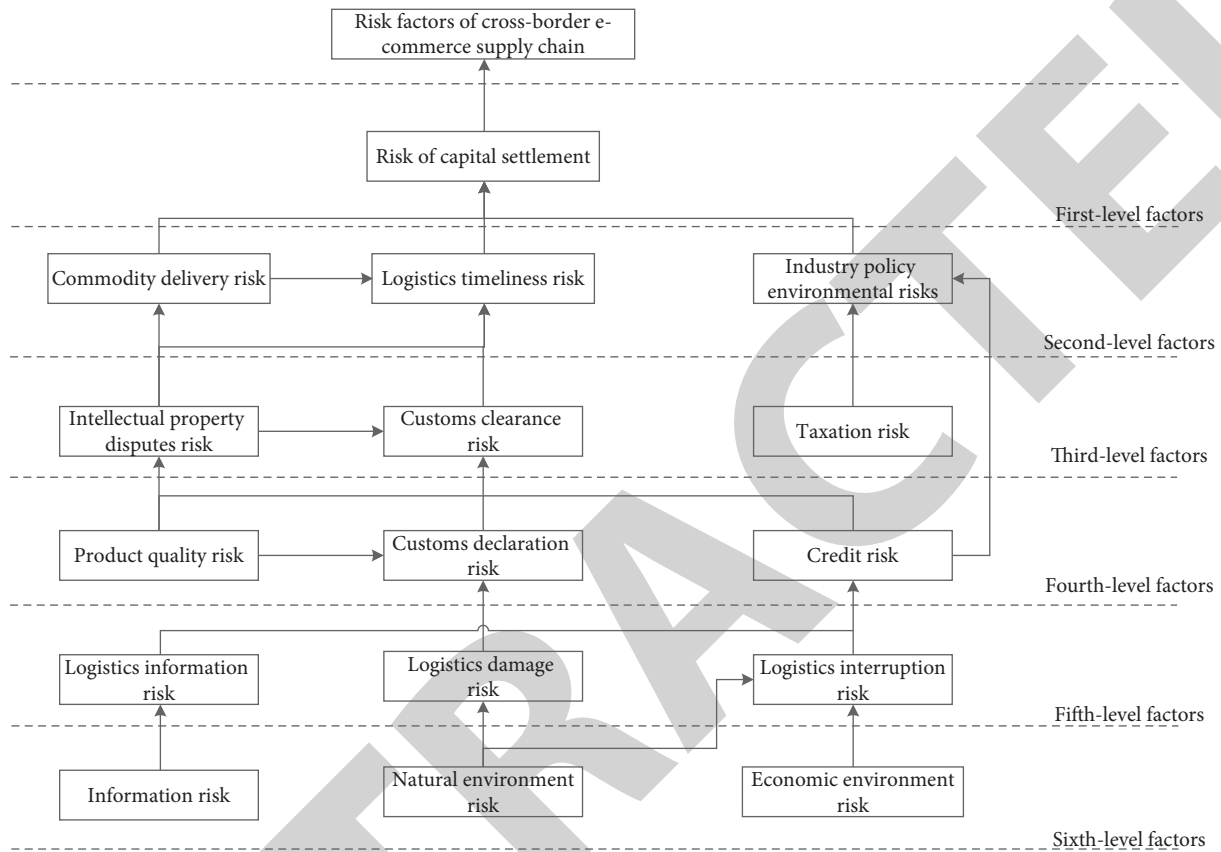| Level	1	2	3	4	5	6
Node C_i	6	2, 10, 16	3, 7, 9	1, 4, 8	11, 12, 13	5, 14, 15

FIGURE 6: Cross-border e-commerce supply chain risk factors' FUZZY-ISM multilevel hierarchical diagram.

affecting the operation of cross-border logistics enterprises. The risk of capital settlement is also affected by the second-level factors of commodity delivery risk, logistics timeliness risk, and industry environment risk. The reason is that whether the goods are in domestic logistics or international logistics, if they cannot be delivered and the logistics timeliness cannot be guaranteed, buyers cannot sign for them, and cross-border e-commerce sellers cannot receive payment back. And, if the development of cross-border industries and policies are not controlled in time, it will also pose risks to foreign exchange settlement. In cross-border e-commerce foreign exchange settlement transactions, international payments are basically monopolized by foreign payment companies such as PayPal, which is unstable and affects cross-border e-commerce companies.

(2) The second-level factors are middle-level factors, including commodity delivery risks, logistics timeliness risks, and industry policy environmental risks. Industry policy environmental risks are

affected by intellectual property disputes, taxation risks, credit risks, and economic environment risks. Cross-border e-commerce companies do not have a strong sense of intellectual property rights, and infringements occur from time to time. Once intellectual property disputes arise, corporate payment accounts such as PayPal will be frozen, cleared, and even their stores will be closed. International taxation policies, domestic and foreign trade policies, language barriers, and other political, geographic, and cultural constraints, as well as seller credit constraints, will all have a certain impact on industry development and policies. Commodity delivery risk is affected by commodity quality risk. The risk of logistics timeliness will be directly affected by the risk of customs clearance. If there is a problem in the customs clearance of the goods, the logistics efficiency will not be guaranteed, and the goods will take a long time to transport.

(3) The third-level factors are the risk of property rights' disputes, customs clearance risks, and

taxation risks. The risk of customs clearance will be affected by the risk of commodity declaration and property rights' disputes. When the commodity is cleared, if the commodity declaration is not consistent, the goods and the weight of the goods are falsely reported, fictitious goods information and fictitious consignee or consignor. After the customs finds it, the goods will be intercepted and returned, and if the goods are infringing, they will be directly detained, which will have a great impact on customs clearance. The risk of property rights' disputes will also be affected by product quality risks. If a product has quality or infringement, property rights' disputes will occur, which will bring a heavy blow to cross-border e-commerce companies.

(4) The fourth-level factors are product quality risk, declaration risk, and credit risk. Credit risk will be affected by the risk of logistics interruption, and credit risk plays an important role in the process of risk, directly affecting the upper-level customs clearance risk. At the same time, credit risk is bound to restrict the industry policy environment, which means that credit risk is directly affected by logistics disruption. Credit risks include controllable and uncontrollable risks. The controllable part includes the credit of cross-border e-commerce companies, such as guaranteeing not to sell infringing goods and counterfeit and shoddy goods, and uncontrollable risks include foreign buyer credit and third-party payment platforms.

(5) The fifth-level factors are logistics information risk, logistics loss risk, and logistics interruption risk. The risk of logistics loss and logistics interruption will be affected by natural environmental risks. Such as the Sino-US trade conflict, the outbreak of the new crown epidemic, earthquakes, and tsunamis, there are situations such as logistics interruption, damage to the transportation process of goods, and depressed economic environment. The logistics information risk will also be affected by the information risk. Security issues arising from online transactions and untimely supervision will lead to errors in logistics information or failure to track in real time, which will affect cross-border e-commerce companies.

(6) The sixth-level factors are information risk, natural environment risk, and economic environment risk. This risk is at the bottom of the model, is an input element of the risk system, has an impact on other risk factors, and is the fundamental cause of cross-border e-commerce supply chain risks. We need to make adequate preparations in the face of different natural environments and timely maintain and supervise the systems and software used by the company to ensure that corporate information, data, and buyer information are not leaked. When faced with different situations, make corresponding strategy.

7. Conclusions

The unexpected events, such as COVID-19 and the Suez Canal blockage, caused the cross-border supply chains disrupted and made the cross-border e-commerce companies face many risks in business operation. How to evaluate the supply chain risks and take measures to avoid the cross-border e-commerce supply chain risks becomes an important issue for the cross-border e-commerce enterprises. Based on studying the operation process of the cross-border e-commerce supply chain, this article pointed out that the cross-border supply chain risk factors involved were divided into five aspects and creatively added the product selection management risk analysis, and more in the past studies focused on the risk of cross-border transaction risk, customs clearance risk, logistics risk, and environmental risk, and these four aspects rarely consider the enterprise when picking product management which will also produce risk. Secondly, this paper provided the relationship between risk factors, through the FUZZY-ISM model, while the ISM model only considers whether there is influence between risks, it cannot determine the degree of influence between risk factors and provides a theoretical basis for further study of the logical level. Finally, the FUZZY-ISM model is used to rank the 16 risk factors. However, most of the previous studies focus on the relationship between risk factors and supply chain risk management and rarely consider the mechanism of action between risk factors. In this paper, the FUZZY-ISM model revealed the mechanism of action among risk factors, revealed the relationship between risk factors, and provided theoretical support for the supply chain risk management of cross-border e-commerce enterprises.

For future research, according to different types and cross-border e-commerce enterprise operation patterns, we will establish a more comprehensive supply chain risk index system and provide corresponding suggestions.

Data Availability

The data used to support the findings of the study are available from the corresponding author upon request.

Conflicts of Interest

The authors declare that there are no conflicts of interest regarding the publication of this paper.

Acknowledgments

References

[1] Y. Wang, F. Jia, T. Schoenherr, Y. Gong, and L. Chen, "Cross-border e-commerce firms as supply chain integrators: the management of three flows," *Industrial Marketing Management*, vol. 89, pp. 72–88, 2020.

[2] W. Xue, D. Li, and Y. Pei, "The development and current of cross-border E-commerce," in *Proceedings of the WHICEB 2016 Proceedings*, vol. 53, pp. 131–138, Wuhan, China, June 2016.

[3] Penny, *Cross-border E-Commerce Industry Data Analysis: In 2020, China's Total Import and export Volume of Cross-Border E-Commerce Reached 1.69 Trillion Yuan*, https://www.iimedia.cn/c1061/78795.html, 2021.

[4] X. Liu, Z. Dou, and W. Yang, "Research on influencing factors of cross border E-commerce supply chain resilience based on integrated fuzzy DEMATEL-ISM," *IEEE Access*, vol. 9, pp. 36140–36153, 2021.

[5] Z. Liu and Z. Li, "A blockchain-based framework of cross-border e-commerce supply chain," *International Journal of Information Management*, vol. 52, pp. 1–18, 2020.

[6] A. Lukin, "The US-China trade war and China's strategic future," *Survival*, vol. 61, no. 1, pp. 23–50, 2019.

[7] T. P. Velavan and C. G. Meyer, "The COVID-19 epidemic," *Tropical Medicine and International Health*, vol. 25, no. 3, pp. 278–280, 2020.

[8] K. Lawrence, *When "Just-In-Time" Falls Short: Examining the Effects of the Suez Canal Blockage*, SAGE Business Cases Originals, London, UK, 2021.

[9] G. H. Gessner and C. R. Snodgrass, "Designing e-commerce cross-border distribution networks for small and medium-size enterprises incorporating Canadian and U.S. trade incentive programs," *Research in Transportation Business & Management*, vol. 16, pp. 84–94, 2015.

[10] B. Rabta, C. Wankmüller, and G. Reiner, "A drone fleet model for last-mile distribution in disaster relief operations," *International Journal of Disaster Risk Reduction*, vol. 28, pp. 107–112, 2018.

[11] G. A. Lopez, "Terrorism in Latin America," *The Politics of Terrorism*, CRC Press, Boca Raton, FL, USA, pp. 497–524, 2020.

[12] I. K. Mensah, G. Zeng, and C. Luo, "The impact of national culture dimensions on the adoption of cross-border E-commerce," *International Journal of Information Systems in the Service Sector*, vol. 12, no. 4, pp. 91–112, 2020.

[13] A. P. Sage, *Interpretive Structural Modelling: Methodology for Large Scale Systems*, pp. 91–164, McGraw-Hill, New York, NY, USA, 1977.

[14] R. K. Ragade, "Fuzzy sets in communication systems and in consensus formation systems," *Cybernetics and Systems*, vol. 6, no. 1-2, pp. 21–38, 1976.

[15] M. Christopher and C. Rutherford, "Creating supply chain resilience through agile six sigma," *Critical Eye*, vol. 7, no. 1, pp. 24–28, 2004.

[16] S. Y. Ponomarov and M. C. Holcomb, "Understanding the concept of supply chain resilience," *International Journal of Logistics Management*, vol. 20, no. 1, pp. 124–143, 2009.

[17] B. Fahimnia, C. S. Tang, H. Davarzani, and J. Sarkis, "Quantitative models for managing supply chain risks: a review," *European Journal of Operational Research*, vol. 247, no. 1, pp. 1–15, 2015.

[18] F. Cucchiella and M. Gastaldi, "Risk management in supply chain: a real option approach," *Journal of Manufacturing Technology Management*, vol. 17, no. 6, pp. 700–720, 2006.

[19] J. Um and N. Han, "Understanding the relationships between global supply chain risk and supply chain resilience: the role of mitigating strategies," *Supply Chain Management: International Journal*, vol. 26, no. 2, pp. 240–255, 2020.

[20] B. Ritchie and C. Brindley, "Supply chain risk management and performance," *International Journal of Operations and Production Management*, vol. 27, no. 3, pp. 303–322, 2007.

[21] M. Giannakis and M. Louis, "A multi-agent based framework for supply chain risk management," *Journal of Purchasing and Supply Management*, vol. 17, no. 1, pp. 23–31, 2011.

[22] S. Fazli, R. Kiani Mavi, and M. Vosooghidizaji, "Crude oil supply chain risk management with DEMATEL–ANP," *Operational Research*, vol. 15, no. 3, pp. 453–480, 2015.

[23] R. Rajesh, "A grey-layered ANP based decision support model for analyzing strategies of resilience in electronic supply chains," *Engineering Applications of Artificial Intelligence*, vol. 87, pp. 1–18, 2020.

[24] B. Song, W. Yan, and T. Zhang, "Cross-border e-commerce commodity risk assessment using text mining and fuzzy rule-based reasoning," *Advanced Engineering Informatics*, vol. 40, pp. 69–80, 2019.

[25] U. Soni, V. Jain, and S. Kumar, "Measuring supply chain resilience using a deterministic modeling approach," *Computers and Industrial Engineering*, vol. 74, pp. 11–25, 2014.

[26] W. J. Tan, A. N. Zhang, and W. Cai, "A graph-based model to measure structural redundancy for supply chain resilience," *International Journal of Production Research*, vol. 57, no. 20, pp. 6385–6404, 2019.

[27] H. Min, "Blockchain technology for enhancing supply chain resilience," *Business Horizons*, vol. 62, no. 1, pp. 35–45, 2019.

[28] M. Donadoni, F. Caniato, and R. Cagliano, "Linking product complexity, disruption and performance: the moderating role of supply chain resilience," *Supply Chain Forum: International Journal*, vol. 19, no. 4, pp. 300–310, 2018.

[29] P. S. Ceryno, L. F. Scavarda, and K. Klingebiel, "Supply chain risk: empirical research in the automotive industry," *Journal of Risk Research*, vol. 18, no. 9, pp. 1145–1164, 2015.

[30] R. Rostamzadeh, M. K. Ghorabaee, K. Govindan, A. Esmaeili, and H. B. K. Nobar, "Evaluation of sustainable supply chain risk management using an integrated fuzzy TOPSIS- CRITIC approach," *Journal of Cleaner Production*, vol. 175, pp. 651–669, 2018.

[31] CY. Chu, K. Park, and G. E. Kremer, "A global supply chain risk management framework: an application of text-mining to identify region-specific supply chain risks," *Advanced Engineering Informatics*, vol. 45, pp. 1–17, 2020.

[32] M. K. Lim, M.-L. Tseng, K. H. Tan, and T. D. Bui, "Knowledge management in sustainable supply chain management: improving performance through an interpretive structural modelling approach," *Journal of Cleaner Production*, vol. 162, pp. 806–816, 2017.

[33] R. Dubey, A. Gunasekaran, S. F. Wamba, and S. Bag, "Building theory of green supply chain management using total interpretive structural modeling (TISM)," *IFAC-PapersOnLine*, vol. 48, no. 3, pp. 1688–1694, 2015.

[34] W.-S Wu, C.-F. Yang, J.-C. Chang, P.-A. Château, and Y.-C. Chang, "Risk assessment by integrating interpretive structural modeling and Bayesian network, case of offshore pipeline project," *Reliability Engineering & System Safety*, vol. 142, pp. 515–524, 2015.

[35] L. A. Zadeh, "Fuzzy sets," *Information and Control*, vol. 8, no. 3, pp. 338–353, 1965.

[36] T. Mahmood, U. Ur Rehman, Z. Ali, and T. Mahmood, "Hybrid vector similarity measures based on complex hesitant

WILEY | Hindawi

Retraction

Retracted: An IoT-Based Water Level Detection System Enabling Fuzzy Logic Control and Optical Fiber Sensor

Security and Communication Networks

This article has been retracted by Hindawi following an investigation undertaken by the publisher [1]. This investigation has uncovered evidence of one or more of the following indicators of systematic manipulation of the publication process:

(1) Discrepancies in scope

(2) Discrepancies in the description of the research reported

(3) Discrepancies between the availability of data and the research described

(4) Inappropriate citations

(5) Incoherent, meaningless and/or irrelevant content included in the article

(6) Manipulated or compromised peer review

The presence of these indicators undermines our confidence in the integrity of the article's content and we cannot, therefore, vouch for its reliability. Please note that this notice is intended solely to alert readers that the content of this article is unreliable. We have not investigated whether authors were aware of or involved in the systematic manipulation of the publication process.

Wiley and Hindawi regrets that the usual quality checks did not identify these issues before publication and have since put additional measures in place to safeguard research integrity.

We wish to credit our own Research Integrity and Research Publishing teams and anonymous and named external researchers and research integrity experts for contributing to this investigation.

The corresponding author, as the representative of all authors, has been given the opportunity to register their agreement or disagreement to this retraction. We have kept a record of any response received.

References

[1] Y. Zheng, G. Dhiman, A. Sharma, A. Sharma, and M. A. Shah, "An IoT-Based Water Level Detection System Enabling Fuzzy Logic Control and Optical Fiber Sensor," *Security and Communication Networks*, vol. 2021, Article ID 4229013, 11 pages, 2021.

WILEY | Hindawi

Research Article

An IoT-Based Water Level Detection System Enabling Fuzzy Logic Control and Optical Fiber Sensor

Yani Zheng ,[1] Gaurav Dhiman ,[2] Ashutosh Sharma ,[3] Amit Sharma,[4] and Mohd Asif Shah [5]

[1]*College of Mathematics and Information Science, Xianyang Normal University, Xianyang, Shaanxi 712000, China*
[2]*Government Bikram College of Commerce, Patiala, Punjab, India*
[3]*Institute of Computer Technology and Information Security, Southern Federal University, Rostov-on-Don, Russia*
[4]*Chitkara University, Chandigarh, India*
[5]*Bakhtar University, Kabul, Afghanistan*

Correspondence should be addressed to Yani Zheng; yanizheng31@outlook.com and Mohd Asif Shah; ohaasif@bakhtar.edu.af

The usage of wireless sensors has become widespread for the collection of data for various Internet of Things (IoT) products. Specific wireless sensors use optical fiber technology as transmission media and lightwave signals as carriers, showing the advantages of antielectromagnetic interference, high sensitivity, and strong reliability. Hence, their application in IoT systems becomes a research hotspot. In this article, multiple optical fiber sensors are constructed as an IoT detection system, and a Transmission Control Protocol (TCP)/Internet Protocol (IP) communication stack is used for the sensor module. Furthermore, design of gateway module, data server, and monitoring module is established in order to run the data server in the Windows system and communicate across the network segments. Furthermore, the optical fiber sensor is connected to the development board with WiFi, meanwhile considering the optical fiber wireless network's congestion problem. The fuzzy logic concept is introduced from the perspective of cache occupancy, and a fiber sensor's network congestion control algorithm is proposed. In the experiment, the IoT detection system with multiple optical fiber sensors is used for water level detection, and the sensor's real-time data detected by the User Interface (UI) are consistent with the feedback results. The proposed method is also compared with the SenTCP algorithm and the CODA algorithm, and it was observed that the proposed network congestion control algorithm based on the fuzzy logic can improve network throughput and reduce the network data packet loss.

1. Introduction

With the development of information technologies such as personal computer (PC), Internet, and mobile Internet in the current information technology era, a new information technology era represented by the Internet of Things (IoT) [1–3] comes. The IoT [4, 5] concept was proposed by the International Telecommunication Union (ITU) in 2005. This technology regards mobile devices such as mobile phones, pads, or smartwatches as networks to control them remotely in smart homes. A typical IoT-based system using the fuzzy approach is depicted in Figure 1.

High-performance sensors are required for signal sending and receiving to realize the interconnection of everything and the links among devices. The sensors need to have strong anti-interference and remote-control supporting abilities. An optical fiber sensor [6–8] is a high-performance sensor contributing to the network connection among devices. The optical fiber as its medium allows this sensor to form a new optical technology with lasers and semiconductor detectors. As society develops, optical fiber sensing technology with optical fiber as the transmission medium has been affirmed and welcomed in many fields [9–11]. The optical fiber sensor emits light from the light source into the optical fiber, and the optical signals are
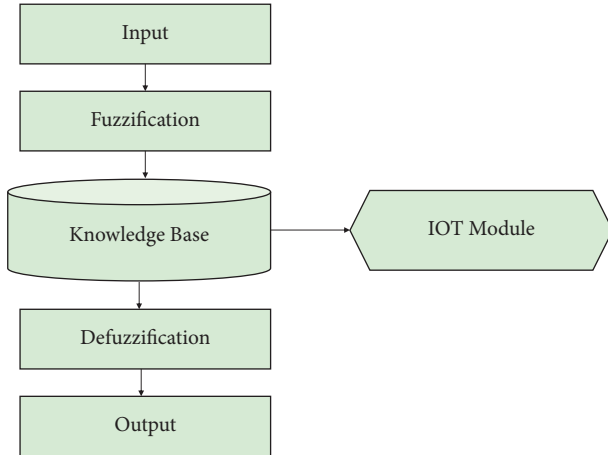
FIGURE 1: A typical IoT-based system using the fuzzy approach.

transmitted to the modulator in the optical fiber. The modulated lightwave and the parameter to be measured interact to change the signals' optical properties. The modulated lightwave signals are detected by a photoelectric detector and uploaded to the demodulation processing module, realizing remote detection.

Optical fiber sensors are categorized into functional optical fiber sensors (FFSs) and nonfunctional optical fiber sensors (NFFSs) according to whether the optical fiber is a sensitive element for signal sensing [12–14]. The FFSs' optical fiber can sense the measured signals and transmit optical signals [15–17]. The optical fibers in FFSs are continuous, and their characteristics make FFSs sensitive elements. With optical fibers as their transmission medium, NFFSs transmit signals in remote or harsh environments. NFFSs' output and incident fibers are discontinuous, and the modulators among them are unique sensitive elements. The more light is received, the more it is conducive to the terminal signal processing. More light coupled devices are required [18–20] because optical fibers are primarily used in optical signal transmission. Therefore, communication fibers or multimode fibers are appropriate for NFFSs.

There are various articles which utilize different wireless sensor-based methodologies along with fuzzy logics for mitigating the risk of detection in various scenarios. Ali et al. [21] presented an assessment model for decision making using the fuzzy logical approach to meet the software testing criteria for the cloud-based approach. The authors in [21] presented a wireless sensor-based methodology for false alarm warning reduction in case of smart home application system. Saeed et al. [22] proposed a multisensor-based mechanism for data fusion enabling artificial intelligence (AI) and wearable sensor network for controlling the home appliances working and positioning. A microcontroller based fuzzy logic technology is introduced by Chou et al. [23] for the detection of fire in case of automobiles. This technology utilizes the temperature, smoke, and flame sensors. Olivares-Mercado et al. [24] utilize an early detection methodology using the smoke sensor for the detection of fire events. Park et al. [25] used the multifunctionality of AI framework along with adaptive

fuzzy-based methodology to detect the early fire events. Further various other present techniques use the fuzzy-based methods for the navigation of robots [26], monitoring of healthcare [27], controlling the air conditions [28], identification of flood susceptibility [29], and many more. Recently, the success rate of IoT for smart systems has equipped its usage along with fuzzy logic for achieving better accuracy and high efficiency rates.

This article contributes in building a multiple optical fiber sensor-based IoT detection system for water level detection. It uses a Transmission Control Protocol (TCP)/ Internet Protocol (IP) communication protocol stack for sensor module along with gateway module, data server, and monitoring module design for establishing the data server in the Windows system to communicate across the network segments [30, 31]. The data server end is connected to the Ethernet with the gateway program implementing protocol conversion, and the optical fiber sensor is connected to the development board with WiFi, considering the optical fiber wireless network's congestion problem. The fuzzy logic concept is introduced is this article from the perspective of cache occupancy and a fiber sensor's network congestion control algorithm is proposed. In the experiment, a monitoring terminal analyzes the optical fiber sensor's data collection, and a network congestion algorithm is introduced to test the algorithm's network performance in cache occupancy and cache changes.

The rest of this article is organized as follows: Section 2 presents the overall design of the IoT detection system followed by the design and implementation of the detection system in Section 3. Section 4 depicts the fuzzy logic control method for network congestion, and the test results analysis is presented in Section 5. Section 6 reveals the concluding remarks along with the future research directions.

2. Overall Design of the IoT Detection System

This section provides the basics of the fuzzy set along with the system architecture of the IoT detection system. The detection system's architecture is introduced, and then each module is elaborated, including the sensor, gateway, data server, and monitoring terminal. The sensor module includes a WeMos D1 circuit board and an optical fiber sensor.

2.1. Basics of Fuzzy Sets.
The fuzzy sets are considered as the extension of the classical set, and this can be better interpreted using the varying degrees of membership function. The fuzzy logic builds a connection between the qualitative and quantitative modelling using input-output mapping. The fuzzy logic control system should have at least one component with fuzzy representation of knowledge. The fuzzy sets used to represent this information are the noncrisp sets with a specific membership function. Its representation is provided in the following equation:

$$\widetilde{X} = \left\{ \left(y, \mu_{\widetilde{X}} \left(y \right) \right) | y \in U \right\}, \tag{1}$$

where the fuzzy set is represented by $\widetilde{X}$ indicating the information U which can be arranged as a fuzzy pair set with

$\mu_{\widetilde{X}}(y)$ indicating the degree of membership of y which ranges from 0 to 1.

For the discrete information representation, the fuzzy set is indicated in equation (2), whereas the continued representation provides the fuzzy illustration in equation (3).

$$\widetilde{X} = \left\{ \frac{\left(\mu_{\widetilde{X}}(y_1)\right)}{y_1} + \frac{\left(\mu_{\widetilde{X}}(y_2)\right)}{y_2} + \frac{\left(\mu_{\widetilde{X}}(y_3)\right)}{y_3} + \cdots \right\}, \quad (2)$$

$$\widetilde{X} = \left\{ \int \frac{\left(\mu_{\widetilde{X}}(y)\right)}{y} \right\}. \quad (3)$$

These basic assumptions are considered for the experimentation in this article.

2.2. System Architecture.

The detection system includes the sensor, gateway, a data server, and a monitoring terminal. The sensor includes an optical fiber sensor and a WeMos D1 development board. Figure 2 shows the system architecture.

In Figure 2, a data server connects multiple monitoring terminals and gateways, a gateway connects multiple WeMos D1 development boards, and a WeMos D1 development board connects an optical fiber sensor. The monitoring terminal and data server run in the Windows system, and the gateway runs in the Debian-Raspbian system. The monitoring terminal, data server, and gateway are connected through the network for Socket communication. The WeMos D1 development board is connected to the network through WiFi and to the gateway through socket communication.

2.3. Other Modules in the Detection System.

The sensor is composed of a WeMos D1 development board and optical fiber sensor. Figure 3 shows the multiple leads between the sensor and the development board. When the optical fiber sensor is energized, it can obtain the surrounding environment's real-time data based on its principles. The leads between the sensor and the development boards include a power line, a ground line, and multiple data lines.

The data server connects the monitoring terminal and the gateway. Assuming that the monitoring terminal and the gateway are in the same local network, the monitoring terminal is connected to the gateway through the gateway IP address and port number for communication. Otherwise, the monitoring terminal cannot access through the internal network address and port number where the gateway is located. The PC in the local network cannot communicate directly through the internal network IP address. Figure 4 shows that a data server can forward the messages for cross-network segment communication between the PC and the internal network IP address.

Figure 4 includes the monitoring module, the monitoring-terminal message processing module, and a gateway message processing module. The monitoring module monitors data transceiving of the gateway and the monitoring terminal. The data server filters the received messages and starts the corresponding message processing thread. The
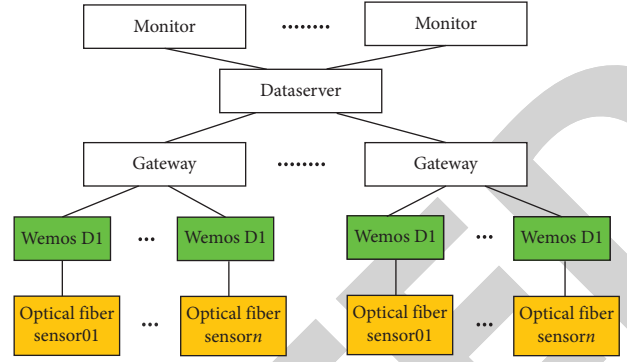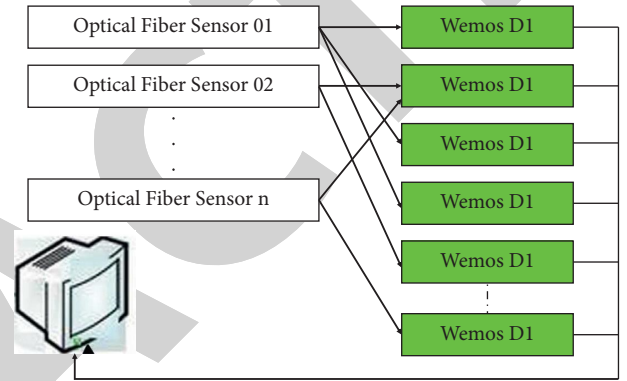

Figure 2: System architecture.

Figure 3: Sensor data paths.

monitoring message processing module receives messages sent by the monitoring terminals and sends corresponding processing commands. It takes out the messages from the message queue and analyzes and processes them. The gateway message processing module arranges the gateway's messages into message queues and starts the corresponding threads for analysis and processing.

3. Detailed Design and Implementation of the Detection System

The detection system designed herein includes the optical fiber sensor and the gateway. The sensor includes the WeMos development board and the optical fiber sensor module. The gateway includes the program's design and implementation.

3.1. Design and Implementation of the Optical Fiber Sensor.

The optical fiber sensor's design enables the WeMos D1 development board to collect data from the optical fiber sensor and transmit the acquired data to the gateway via WiFi. The hardware includes the sensor and WeMos D1 development board, and the software includes the Arduino program. Figure 5 shows the partial circuit of the WeMos D1 development board.

The development board includes six power pins, one analog input pin, and eleven digital input/output pins with the analog input pin number represented by A0 and the
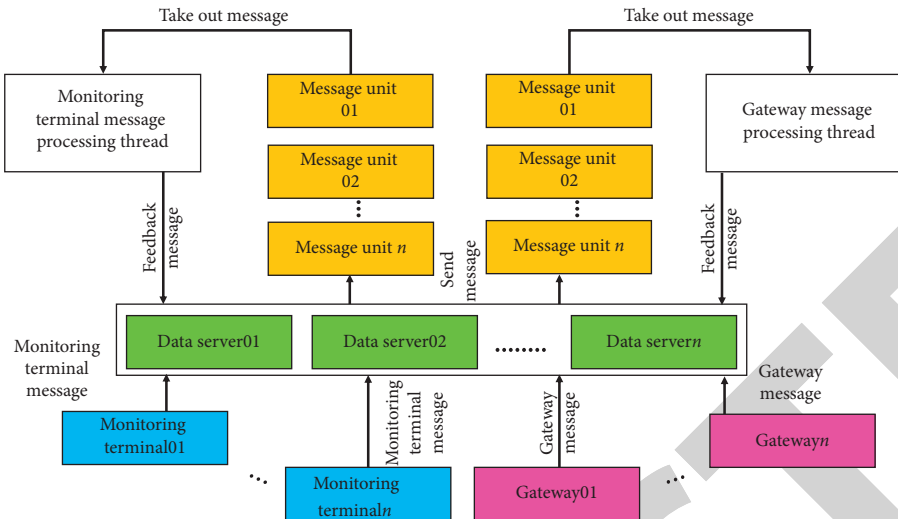
FIGURE 4: The data server's processing.

digital input and output number D0~D10. The development board's digital signal pin D0 represents the serial signal pin RX, and the digital signal pin D1 represents the serial signal pin TX. The development board's digital signal pin D2 can be connected to the LED to display the analysis results.

The fiber optic sensor module adopted herein includes laser, fiber coupler, optical circulator, fiber optic cable, and photodetector. The laser wavelength is 1550 nm, the working current is 40 mA, the output power is 50 mW, and the photodetector's wavelength range is 800 nm~1700 nm with a bandwidth of 3 dB. The optical fiber coupler can divide the optical signal from one optical fiber to multiple optical components for optical signal power distribution or combination. An optical fiber coupler of 1550 nm, 3 dB, and 1×2 is adopted. An optical circulator makes the optical signal transmitted in the ports' order. Figure 6 shows an optical circulator with 1550 nm, 0.6 dB insertion loss, and 46 dB optical isolation bandwidth. The optical fiber sensor module designed is used for water level measurement, adjusting the circuit length according to the water depth and the measurement's analog quantity.

In a software development environment of Arduino IDE v1.8.5, the WeMos D1 development board adopts the ESP8266EX chip. The native Arduino IDE does not support development on the ESP8266, so an open-source library that supports ESP8266 in the Arduino IDE is necessary. After the program is written, the development board's ESP8266EX chip can be connected to WiFi and the target host port by a socket for network communication.

A TCP connection between the ESP8266EX chip and the gateway is established on the development board to communicate between the client and the gateway. Figure 7 shows the design of the corresponding program development process based on the class and interface functions.

After the Arduino program is completed, the sensor and WeMos D1 development board are connected. When the development board is energized, the optical fiber sensor is energized by the power and ground pins and transmits data to the WeMos D1 development board, which runs in Flash programs and sends the collected optical fiber signals to the gateway.

3.2. Design and Implementation of the Gateway Programs.
The sensor has a unique ID in the data architecture herein, and sensor information is represented by a structure that includes a type field, an ID field, a sensor data field, a sensor connection status field, and a sensor communication sentence field. Different sensors have different IP addresses. A static IP address is configured on the router. After the gateway accepts the development board's connection, the development board can be distinguished based on the IP address.

With the gateway's connection to multiple optical fiber sensors, the socket is set in a nonblocking state, connecting to the sensor efficiently. During program development, with the local monitoring, the gateway cannot establish the monitoring if the corresponding network address is configured on the Raspberry Pi, so the monitoring address needs to be modified. The wired or the wireless network addresses' modification realizes the connection between the gateway and the optical fiber sensor.

The gateway program's parameters can be set in the form of IP address + port number; that is, after the target host runs the data server program, the gateway connects the data server. When the gateway sends messages to the data server continuously, the transmission efficiency is significantly reduced with the gateway's socket in the blocking mode. Therefore, the gateway's socket needs to be set in the nonblocking mode.

The data processed by the gateway come from the data server and the optical fiber sensor. The interactive messages of the gateway and the data server include the gateway information response messages, the polling feedback messages, and the sensor data feedback messages. In message processing, message types need to be distinguished. The message types include the gateway request messages sent by the monitoring terminal to the data server, the gateway
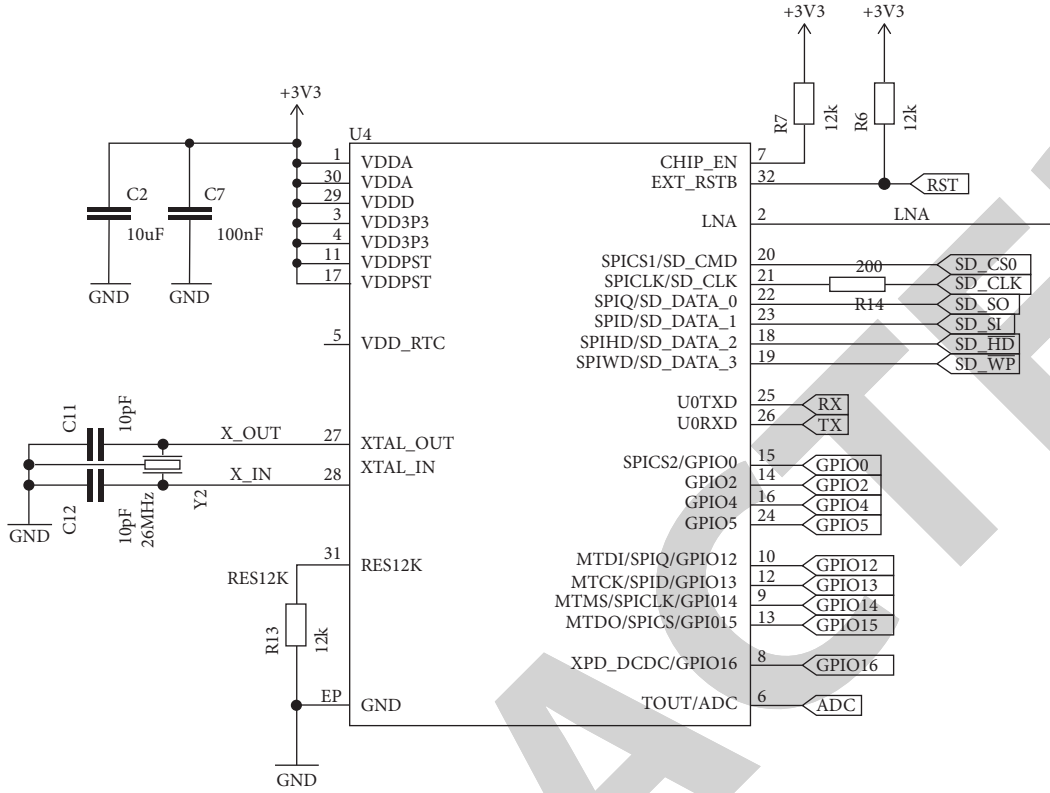
Figure 5: The partial circuit in the WeMos D1 development board.

response messages sent by the gateway to the data server, the sensor request messages sent by the monitoring terminal to the gateway, the sensor response messages sent by the gateway to the monitoring terminal, the polling messages sent by the gateway to the monitoring terminal, and the sensor data messages sent by the sensor to the gateway.

4. Fuzzy Logic Control Method for Network Congestion

When detecting network congestion, the fuzzy logic reasoning process [32, 33] is adopted. The network's cache occupancy state and cache usage state are analyzed in the IoT detection system based on fiber optic sensors. Cache usage state indicates the congestion variation trend and the degree. This parameter is defined as the ratio of the local data service time to the adjacent data packets' time interval. When cache occupancy is used for reasoning, the congestion usage state parameters [34, 35] are also used, and the network congestion is obtained by combining the two indicators.

Fuzzy logic is used for congestion detection in the IoT network with optical fiber sensors, and hop-by-hop realizes the traversal process. Figure 8 shows the specific algorithm implementation's three parts.

In Figure 9, when network congestion occurs at node B, the fuzzy logic-based congestion control algorithm is executed to increase the data transmission rate and reduce the possible signal access in the contention window, thus

reducing other nodes' possible signal occupation. Meanwhile, the nodes near B process the received data control frame.

The fuzzy logic process includes data fuzzing and data logical derivation. The data fuzzing adopts the Mamdani model, a dual-input and single-output model, which supports two variables as input, namely, cache occupancy rate and cache usage rate. The output parameter is the network congestion degree (FCD).

Fuzzy Inference System (FIS) calculates a value when the cache occupancy rate and cache queue changes are input to the FIS. The first input parameter involves the current buffer size and total buffer size, and the second local data's average packet sending time (T_{local}) and the average time interval between two adjacent data packets (T_{adjacent}). The following equation shows the second input parameter's calculation:

$$CT = \min\left\{\frac{T_{\text{local}}}{T_{\text{adjacent}}}\right\}. \tag{4}$$

In equation (4), CT represents the cache queue's variation trend, and CT < 6. The corresponding parameters T_{local} and T_{adjacent} are obtained by optical fiber sensors' numerical analysis in the network. When N data packets arrive, T_{adjacent} is updated periodically. The following equation shows the parameter's calculation:

$$T_{\text{adjacent}} = 1 - W_{\text{adjacent}} * T_{\text{adjacent}} + W_{\text{adjacent}} * \frac{T_N}{N}. \tag{5}$$
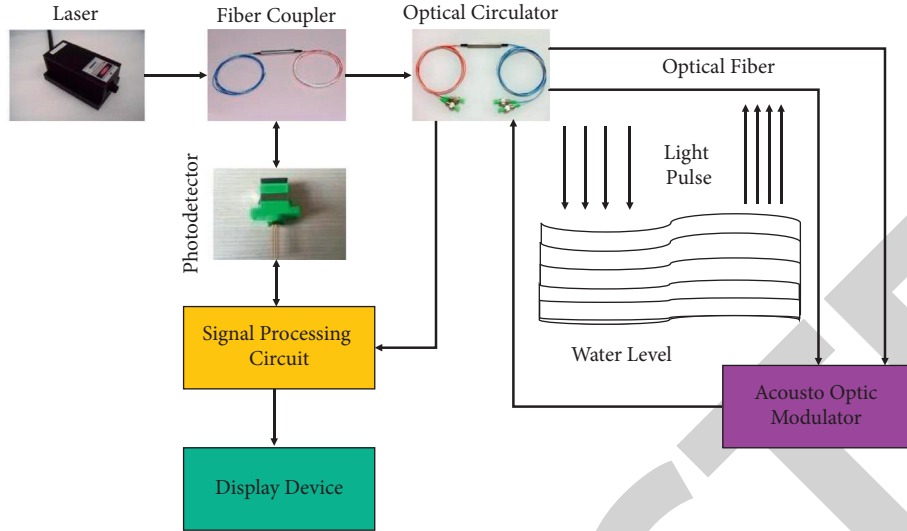
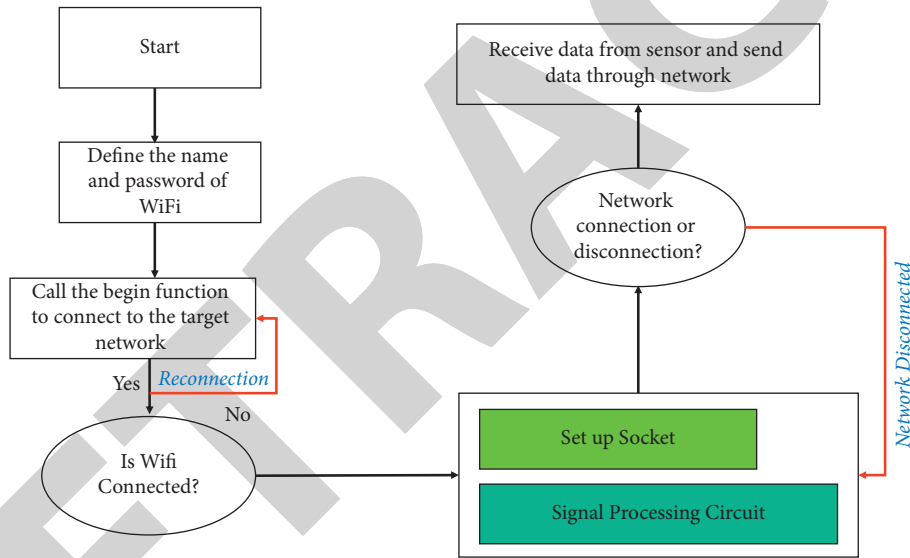FIGURE 6: The architecture of the fiber optic sensor module.

FIGURE 7: The development board's program development process.

In equation (5), W_{adjacent} represents a variable between 0 and 1, and T_N represents the transmitted data packet's serial number. A membership function (MF) is introduced to express the congestion status. The higher the cache occupancy rate, the greater the congestion degree among the nodes. Figure 10 shows the MFs of the cache occupancy rate and the cache queue's variation trend.

In Figure 10(a), {MS, S, K, H, MH} represent very small, small, medium, high, and very high cache occupancy, respectively. In Figure 10(b), {HL, ML, LL, VHL} represent high-low, medium-low, low-low, and very high-low cache usage trends, respectively. FCD's membership degree output is categorized into minimum, maximum, or average value according to membership rules. Equation (6) shows the congestion referring to the average congestion value in multiple possible conditions.

$$C(i) = \frac{\sum_{u=1}^{e} X_u \cdot h(X_u)}{\sum_{u=1}^{e} h(X_u)}. \tag{6}$$

In equation (6), X_u represents the occurrence probability of the uth congestion value with the value range in [0, 1]. The congestion detection mechanism comprehensively considers the cache occupancy rate and cache variation trends. Table 1 shows the congestion rules based on fuzzy logic.

5. Test Results and Analysis

An IoT detection system with multiple optical fiber sensors includes the sensor, gateway, data server, and monitoring terminal. The sensor includes the WeMos D1 development board and optical fiber sensor module. The PC adopts Arduino IDE v1.8.5 for program development. The sensor
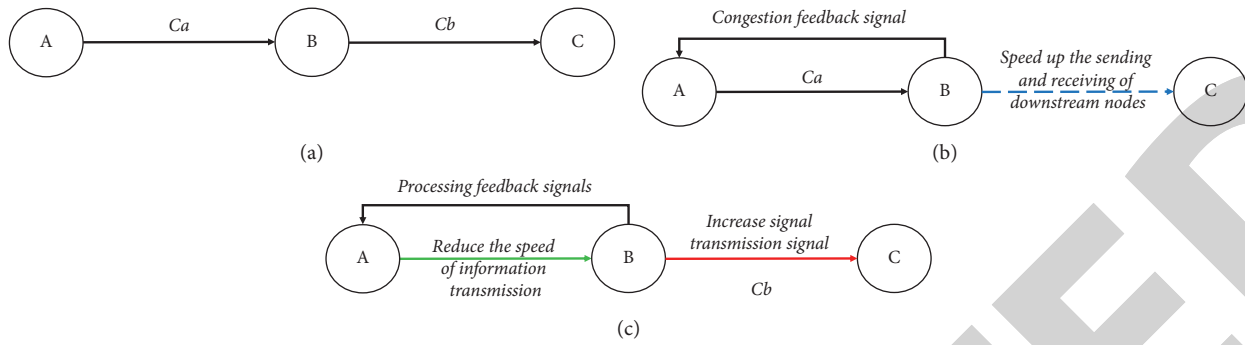
Figure 8: The congestion control method based on fuzzy logic. (a) Congestion detection, (b) feedback signal transmission and local congestion processing, and (c) feedback signal processing.
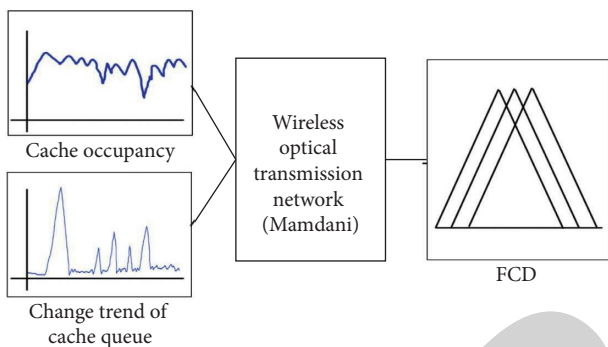

Figure 9: Fuzzy logic's derivation.

programs are developed by VC++ and MFC framework. The gateway runs on the Raspberry 3b+'s Raspbian system, and the programs are developed by C++, compiled by the makefile. The data server and monitoring terminal programs are developed by VS2015 and MFC framework.

In the system running, the data server programs are executed on the host with an address of 10.192.168.96 in the first step. Figure 11(a) shows the operation result. The data server starts monitoring the connection requests from the gateway and the monitoring terminal. The executable files are obtained by compiling the Make commands on the above host, namely, gateway. The default data server's connection port is set to run the command/gateway 10.192.168.96 and change the gateway-data server's connection port. Meanwhile, Figure 11(b) shows that the gateway information can be seen by checking the data server program's real-time status.

With the optical fiber sensor connected to the WeMos D1 development board and Arduino program compiled by the PC uploaded to the development board, the development board sends the sensor data through WiFi when the board is energized. Targeted at water level measurement with analog data in the experiment, the sensor output line is connected to the development board's A0 pin. Figure 12 shows part of the gateway's running after the development board's energization and connection to the gateway.

In Figure 12, the gateway is connected to the host at 10.192.168.96. The sensor starts to analyze the water level data and actively informs the gateway of its location

information. Here, the optical fiber sensor's default type is 1, meaning water level measurement usage. The sensor's ID is 100 with the location name "Eric Johnson 501." Data represent real-time data, that is, the current data value measured by the sensor.

In Figure 13, the monitoring terminal feeds back the current sensor status and data collected by the monitoring terminal and gateway in real time. Multiple optional items are set, including data server, gateway, alarm, and early warning. According to different water level values, different warning levels are displayed. With any option clicked, the corresponding information is displayed in the middle of the displayed page.

In water level detection depicted in Figure 14, the Sensor Operation subwindow displays the water level's real-time curve values, including the solid-line section and dashed-line section representing the water level's dynamic and stable changing sections, respectively.

When the gateway is connected to multiple optical fiber sensors, each sensor is polled to determine an early warning. A WeMos D1 development board is adopted in the system design, so a virtual sensor connection program is needed to achieve multiple connections. Figure 15 shows that ten fiber optic sensors are connected with IDs from 101 to 110. Multiple connection threads are started here for multiple fiber optic sensors' data transmission to the gateway with connection time limits because only the fiber optic sensor with the ID of 100 keeps a constant connection to the gateway.

The network topology in Figure 16 is adopted in IoT's congestion control with multiple optical fiber sensors. The topology involves 15 nodes, and the transmission distance between nodes is limited to 200 m. With a detection radius of 650 m, each hop-by-hop data packet's length is set to 1500 bits.

The SenTCP algorithm [36, 37] and CODA algorithm [38, 39] are introduced for network congestion performance comparison. In Figures 17 and 18, the network packet loss and network throughput are compared. When the network data packets are sent and received in the proposed IoT with optical fiber sensors, the packet loss is reduced, with an average packet loss of 40 packets/s. However, those of the SenTCP algorithm and the CODA algorithm are over 100 packets/s. The proposed congestion control algorithm achieves a throughput of 180 packets/s, significantly better
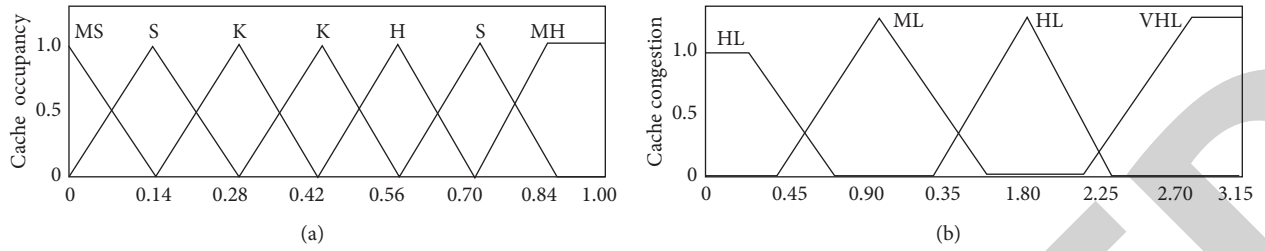
Figure 10: (a) Cache occupancy MF. (b) Cache congestion MF.

Table 1: Congestion rules based on fuzzy logic.

Cache occupancy rate	Cache variation trend	Congestion
MS	VL	LL
MS	L	LL
S	VL	LL
S	M	LM
K	M	MM
K	H	MH
H	M	MH
H	H	HH
MH	L	MH
MH	M	HH
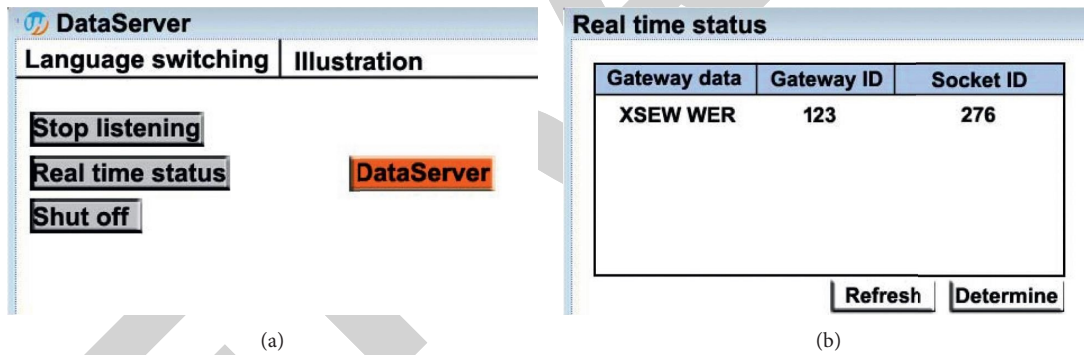
Figure 11: (a) The data server's operation interface. (b) The data server's gateway information.

Figure 12: Gateway-fiber sensor information.

Figure 13: The monitoring terminal's main program interface.
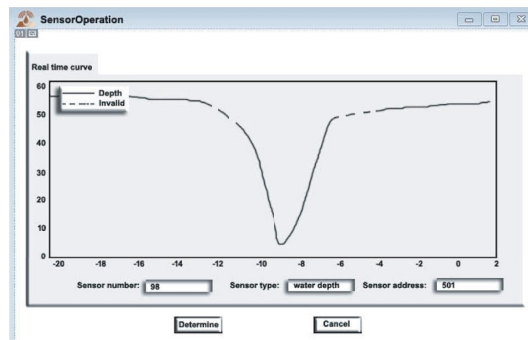
Figure 14: The real-time monitoring of water level measurement based on IoT detection.

Figure 15: The gateway's connection to 13 optical fiber sensors.

Figure 16: The IoT network topology.

Figure 17: Network packet losses of different congestion control algorithms.

Figure 18: Network throughputs of different congestion control algorithms.

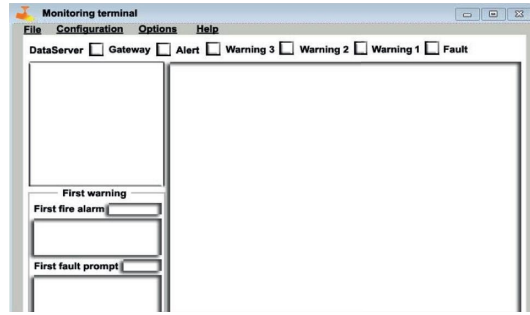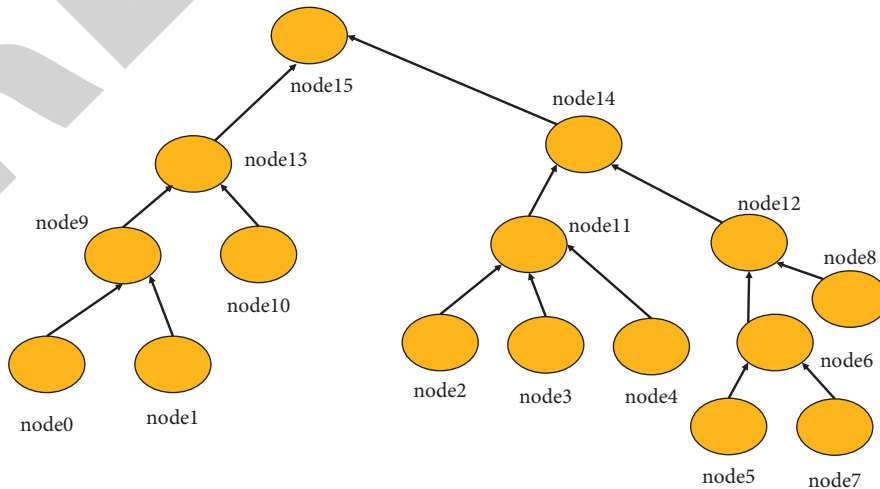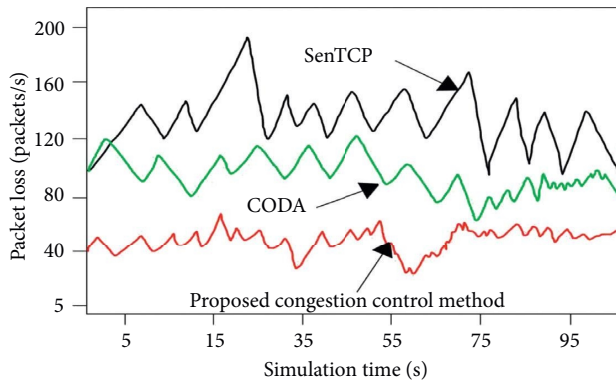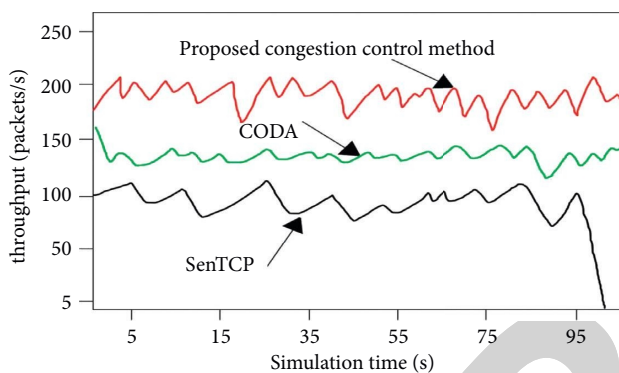than introducing the SenTCP algorithm and CODA algorithm.

6. Conclusion

This article designed a multiple optical fiber sensor-based IoT detection system for water level detection based on optical fiber sensors' characteristics. A network congestion control method is proposed based on the fuzzy logic principles. The Transmission Control Protocol (TCP)/Internet Protocol (IP) communication protocol stack is used for sensor module, gateway module, data server, and monitoring module design for establishing the data server in the Windows system for communicate across the network segments. The experimental analysis opens the data server for detection first and after the gateway program's running, the WeMos D1 development board is connected to the fiber sensor. The regular operation of the curve drawing, water level alarm, and multisensor connection indicates that the proposed IoT detection system is effective. It is revealed that the fuzzy logic-based network congestion control method performs better than other traditional network congestion control methods, such as SenTCP and CODA, in network operation. Further, the future research directions indicates that the combination of fuzzy, multiple optical fiber sensor, and IoT detection methodology can be applied for the detection in various other domains of detection and transmission.

References

[1] J. Gubbi, R. Buyya, S. Marusic, and M. Palaniswami, "Internet of things (IoT): a vision, architectural elements, and future directions," *Future Generation Computer Systems*, vol. 29, no. 7, pp. 1645–1660, 2013.

[2] C. Perera, A. Zaslavsky, P. Christen, and D. Georgakopoulos, "Context aware computing for the internet of things: a survey," *IEEE Communications Surveys & Tutorials*, vol. 16, no. 1, pp. 414–454, 2014.

[3] C. Perera, A. Zaslavsky, P. Christen, and D. Georgakopoulos, "Sensing as a service model for smart cities supported by internet of things," *Transactions on Emerging Telecommunications Technologies*, vol. 25, no. 1, pp. 81–93, 2014.

[4] V. Pande, C. Marlecha, and S. Kayte, "A review-fog computing and its role in the internet of things," *International Journal of Engineering Research in Africa*, vol. 6, no. 10, pp. 2248–96227, 2016.

[5] L. Yancong, Y. Jiachen, L. Zhihan, W. Wei, and S. Houbing, "A self-assessment stereo capture model applicable to the internet of things," *Sensors*, vol. 15, no. 8, pp. 20925–20944, 2015.

[6] M. A. Soto and L. Thévenaz, "Modeling and evaluating the performance of brillouin distributed optical fiber sensors," *Optics Express*, vol. 21, no. 25, pp. 31347–31366, 2013.

[7] C. Elosúa, I. Vidondo, F. J. Arregui et al., "Lossy mode resonance optical fiber sensor to detect organic vapors," *Sensors and Actuators B: Chemical*, vol. 187, pp. 65–71, 2013.

[8] W. C. Wong, C. C. Chan, P. Hu et al., "Miniature ph optical fiber sensor based on waist-enlarged bitaper and mode excitation," *Sensors and Actuators B: Chemical*, vol. 191, pp. 579–585, 2014.

[9] A. G. Mignani, I. R. Matias, and R. O. Claus, "Special issue on optical fiber sensors," *Journal of Display Technology*, vol. 41, no. 2, pp. 111–116, 2003.

[10] Q. Li, G. Li, G. Wang, F. Ansari, and Q. Liu, "Elasto-plastic bonding of embedded optical fiber sensors in concrete," *Journal of Engineering Mechanics*, vol. 128, no. 4, pp. 471–478, 2015.

[11] I. García, "Optical fiber sensors for aircraft structural health monitoring," *Sensors*, vol. 15, no. 7, pp. 15494–15519, 2015.

[12] B. Bao, L. Melo, B. Davies, H. Fadaei, D. Sinton, and P. Wild, "Detecting supercritical co2 in brine at sequestration pressure with an optical fiber sensor," *Environmental ence & Technology*, vol. 47, no. 1, pp. 306–313, 2013.

[13] L. Mescia and F. Prudenzano, "Advances on optical fiber sensors," *Fibers*, vol. 2, no. 1, pp. 1–23, 2013.

Retraction

Retracted: Hybrid Structures Applied to Subalgebras of BCH-Algebras

Security and Communication Networks

This article has been retracted by Hindawi following an investigation undertaken by the publisher [1]. This investigation has uncovered evidence of one or more of the following indicators of systematic manipulation of the publication process:

(1) Discrepancies in scope

(2) Discrepancies in the description of the research reported

(3) Discrepancies between the availability of data and the research described

(4) Inappropriate citations

(5) Incoherent, meaningless and/or irrelevant content included in the article

(6) Peer-review manipulation

The presence of these indicators undermines our confidence in the integrity of the article's content and we cannot, therefore, vouch for its reliability. Please note that this notice is intended solely to alert readers that the content of this article is unreliable. We have not investigated whether authors were aware of or involved in the systematic manipulation of the publication process.

Wiley and Hindawi regrets that the usual quality checks did not identify these issues before publication and have since put additional measures in place to safeguard research integrity.

We wish to credit our own Research Integrity and Research Publishing teams and anonymous and named external researchers and research integrity experts for contributing to this investigation.

The corresponding author, as the representative of all authors, has been given the opportunity to register their agreement or disagreement to this retraction. We have kept a record of any response received.

References

[1] G. Muhiuddin, D. Al-Kadi, W. Khan, and C. Jana, "Hybrid Structures Applied to Subalgebras of BCH-Algebras," *Security and Communication Networks*, vol. 2021, Article ID 8960437, 8 pages, 2021.

WILEY | Hindawi

Research Article

Hybrid Structures Applied to Subalgebras of BCH-Algebras

G. Muhiuddin [ID],[1] D. Al-Kadi [ID],[2] W.A. Khan,[3] and C. Jana[4]

[1]*Department of Mathematics, University of Tabuk, Tabuk 71491, Saudi Arabia*
[2]*Department of Mathematics and Statistic, College of Science, Taif University, P.O. Box 11099, Taif 21944, Saudi Arabia*
[3]*Department of Mathematics and Natural Sciences, Prince Mohammad Bin Fahd University, P.O. Box 1664,
 Al Khobar 31952, Saudi Arabia*
[4]*Department of Applied Mathematics with Oceanology and Computer Programming, Vidyasagar University,
 Midnapore 721102, India*

Correspondence should be addressed to G. Muhiuddin; chishtygm@gmail.com

Received 17 April 2021; Accepted 4 July 2021; Published 16 July 2021

Academic Editor: Kifayat Ullah

The algebraic structures have many applications in coding theory, cryptography, and security networks. In this paper, the notion
of hybrid subalgebras of BCH-algebras is introduced and related properties are investigated. Moreover, some characterizations of
hybrid subalgebras of BCH-algebras are given. Furthermore, we state and prove some theorems in hybrid subalgebras of
BCH-algebras. The homomorphic images and inverse images of fuzzy BCH-subalgebras are studied and discussed.

1. Introduction

The notions of BCK/BCI-algebras were initiated by Imai
and Iséki in 1966. A number of research papers have been
produced on the theory of BCK/BCI-algebras. Hu and Li
[1, 2] introduced the notion of a BCH-algebra as a gen-
eralization of BCK/BCI-algebras and subsequently gave
examples of proper BCH-algebras and studied some
properties. Certain other properties of BCH-algebras have
been studied by Ahmad [3], Dudek and Thomys [4],
Chaudhry [5], Roh et al. [6, 7], Chaudhry et al. [8], and Dar
et al. [9], and Smarandache structure has been applied to
BCH-algebra [10].

Fuzzy sets, which were introduced in the 1960s by Zadeh
[11], have been developed considerably by many research
studies. Molodtsov introduced the concept of soft set [12]
and pointed out several directions for its applications (for
more details, see [12–15]). This concept was applied to BCH-
algebras introducing soft BCH-algebras which were studied
in [16]. Moreover, the fuzzy set theoretical approach to
BCH-algebras was extensively investigated by many re-
searchers on different aspects. For example, fuzzy *n*-fold
ideals [17], fuzzy closed ideals and fuzzy filters [18], filters

based on bipolar-valued fuzzy sets [19], and cubic sub-
algebras [20].

Jun et al. [21] combined the concepts of fuzzy sets and
soft sets, introduced the notion of hybrid structure in a set of
parameters over an initial universe set, and investigated
several properties. They also introduced the concepts of
hybrid linear space, hybrid subalgebra, and hybrid field.
Moreover, hybrid structure applications have been studied
in semigroups (see [22–25] and references there in), and
recently, hybrid ideals of BCK = BCI-algebras were studied
in [26–29]. For more important terminologies, the readers
are referred to [30–36].

In the present paper, we present an application of fuzzy
set theory to an algebraic structure called, BCH-algebra. As
we know it algebraic structures play a prominent role in
mathematics with wide ranging applications in many
disciplines such as theoretical physics, computer sciences,
control engineering, information sciences, coding theory,
topological spaces, and the like. This provides sufficient
motivation to researchers to review various concepts and
results from the realm of abstract algebra in the broader
framework of fuzzy setting. The objective of this study is to
introduce the concept of hybrid subalgebras of BCH-

algebras. The notion of hybrid subalgebras of BCH-algebras is defined, and related properties are investigated. This paper is organized as follows: in Section 2, we recall some definitions related to the subject. In Section 3, the concepts and operations of hybrid subalgebras of BCH-algebras are introduced and their properties are discussed in detail. Furthermore, some properties of hybrid subalgebras of BCH-algebras under homomorphisms are explored.

2. Preliminaries

This section begins with the following definitions and properties that will be needed in the sequel.

An algebra $(L, *, 0)$ of type $(2, 0)$ is called a BCH-algebra [1] if it satisfies the following axioms, for all $q, l, n \in L$:

(1) $q * q = 0$,
(2) $q * l = 0$ and $l * q = 0$ imply $q = l$,
(3) $(q * l) * n = (q * n) * l$.

Any BCH-algebra L satisfies the following axioms:

(i) $q * 0 = q$,
(ii) $(q * (q * l)) * l = 0$,
(iii) $0 * (q * l) = (0 * q) * (0 * l)$,
(iv) $0 * (0 * (0 * q)) = 0 * q$,
(v) $q \leq l$ implies $0 * q = 0 * l$,

for all $q, l, n \in L$ [8].

A nonempty subset S of a BCH-algebra L is called a subalgebra of L if $q * l \in S$, for all $q, l \in S$.

We now review some fuzzy logic concepts as follows.

Let L be the collection of objects denoted generally by q. Then, a fuzzy set [11] A in L is defined as $A = \{\langle q, \mu_A \infty(q) \rangle : q \in L\}$ where $\mu_A(q)$ is called the membership degree of q in A and $0 \leq \mu_A(q) \leq 1$.

Furthermore, we collect some basic notions and results on hybrid structures due to Jun et al. [21]. Let I be the unit interval, L be a set of parameters, and $\mathbb{P}(U)$ be the power set of an initial universe set U.

Definition 1 (see [21]). A hybrid structure in L over U is a mapping:

$$\widetilde{h}_\eta := (\widetilde{h}; \eta): L \longrightarrow \mathbb{P}(U) \times I; q \mapsto (\widetilde{h}(q); \eta(q)), \quad (1)$$

where $\widetilde{h}: L \longrightarrow \mathbb{P}(U)$ and $\eta: L \longrightarrow I$ are mappings.

Definition 2 (see [21]). For hybrid structures $\widetilde{h}_\eta$ and $\widetilde{g}_\mu$ in L over U, the hybrid intersection denoted by $\widetilde{h}_\eta \Cap \widetilde{g}_\mu$ is a hybrid structure:

$$\widetilde{h}_\eta \Cap \widetilde{g}_\mu: L \longrightarrow \mathbb{P}(U) \times I, q \mapsto ((\widetilde{h} \widetilde{\cap} \widetilde{g})(q), (\eta \vee \mu)(q)), \quad (2)$$

where

$$\widetilde{h} \widetilde{\cap} \widetilde{g}: L \longrightarrow \mathbb{P}(U), q \mapsto \widetilde{h}(q) \cap \widetilde{g}(q), \eta \vee \mu: L \longrightarrow I, q \mapsto \vee \{\eta(q), \eta(q)\}. \quad (3)$$

Definition 3 (see [21]). Let L be a BCK/BCI-algebra. For a hybrid structure $\widetilde{h}_\eta$ in L over U, $\widetilde{h}_\eta$ is said to be a hybrid subalgebra of L if the following statements are valid:

$$(\forall q, l \in L) \begin{pmatrix} \widetilde{h}(q * l) \supseteq \widetilde{h}(q) \cap \widetilde{h}(l), \\ \eta(q * l) \leq \vee \{\eta(q), \eta(l)\} \end{pmatrix}. \quad (4)$$

Lemma 1 (see [21]). *Every hybrid subalgebra $\widetilde{h}_\eta$ of a BCK/BCI-algebra L over U satisfies*

$$(\forall q \in L) (\widetilde{h}(0) \supseteq \widetilde{h}(q), \eta(0) \leq \eta(q)). \quad (5)$$

3. Hybrid Subalgebras of BCH-Algebras

In this section, we obtain our main results. Throughout our discussion, L will denote a BCH-algebra unless otherwise mentioned.

Definition 4. Let L be a BCH-algebra. A hybrid structure $\widetilde{h}_\eta = (\widetilde{h}; \eta)$ in L over U is called a hybrid subalgebra of L over U if the following assertions are valid:

$$(\forall q, l \in L) \begin{pmatrix} \widetilde{h}(q * l) \supseteq \widetilde{h}(q) \cap \widetilde{h}(l), \\ \eta(q * l) \leq \vee \{\eta(q), \eta(l)\} \end{pmatrix}. \quad (6)$$

Let us illustrate this definition using the following example.

Example 1. Let the initial universe be the set $U = \{u_1, u_2, u_3, u_4, u_5\}$ and $L = \{0, l_1, l_2, l_3, l_4\}$ be a BCH-algebra with the Cayley table (Table 1).

Let $\widetilde{h}_\eta = (\widetilde{h}; \eta)$ be a hybrid structure in L over U which is given in Table 2.

It can be easily verified that $\widetilde{h}_\eta$ is a hybrid subalgebra of L over U.

Proposition 1. *Every hybrid subalgebra $\widetilde{h}_\eta = (\widetilde{h}; \eta)$ in L over U satisfies the following assertions:*

$$(\forall q \in L) (\widetilde{h}(q) \subseteq \widetilde{h}(0), \eta(q) \geq \eta(0)). \quad (7)$$

Proof. For all $q \in L$, we have $\widetilde{h}(0) = \widetilde{h}(q * q) \supseteq \widetilde{h}(q) \cap \widetilde{h}(q) = \widetilde{h}(q)$ and $\eta(0) = \eta(q * q) \leq \vee \{\eta(q), \eta(q)\} = \eta(q)$. $\square$

Proposition 2. *Let $\widetilde{h}_\eta = (\widetilde{h}; \eta)$ be a hybrid subalgebra in L over U. Then, the following assertions are equivalent:*

(1) $(\forall q, l \in L) (\widetilde{h}(q * l) \supseteq \widetilde{h}(l), \eta(q * l) \leq \eta(q))$.
(2) $(\forall q \in L) (\widetilde{h}(0) = \widetilde{h}(q), \eta(0) = \eta(q))$.

Proof. If we take $l = 0$ in (1), then $\widetilde{h}(q) \supseteq \widetilde{h}(0)$ and $\eta(q) \leq \eta(0)$ for all $q \in L$. Combining this and Proposition 1, we have $(\widetilde{h}(0) = \widetilde{h}(q), \eta(0) = \eta(q))$ for all $q \in L$.

Conversely, assume that (2) is valid. Then,

Table 1: Cayley table of the binary operation $*$.

$*$	0	l_1	l_2	l_3	l_4
0	0	0	l_4	l_3	l_2
l_1	l_1	0	l_4	l_3	l_2
l_2	l_2	l_2	0	l_4	l_3
l_3	l_3	l_3	l_2	0	l_4
l_4	l_4	l_4	l_3	l_2	0

Table 2: Table representation of the hybrid structure $\widetilde{h}_\eta$.

L	$\widetilde{h}$	η
0	U	0.3
l_1	$\{u_1, u_2, u_3, u_4\}$	0.3
l_2	$\{u_3, u_4\}$	0.9
l_3	$\{u_3, u_4\}$	0.9
l_4	$\{u_3, u_4\}$	0.9

$$\widetilde{h}(l) = \widetilde{h}(0) \cap \widetilde{h}(l) = \widetilde{h}(q) \cap \widetilde{h}(l) \subseteq \widetilde{h}(q * l),$$
$$\eta(l) = \vee\{\eta(0), \eta(l)\} = \vee\{\eta(q), \eta(l)\} \geq \eta(q * l), \quad (8)$$

for all $q, l \in L$. $\qquad \square$

Proposition 3. Let $\widetilde{h}_\eta = (\widetilde{h}; \eta)$ be a hybrid subalgebra in L over U. Then, for all $q \in L$, $\widetilde{h}(q) \subseteq \widetilde{h}(0 * q)$ and $\eta(q) \geq \eta(0 * q)$.

Proof. Let $q \in L$. Then,

$$
\begin{aligned}
\widetilde{h}(0 * q) &\supseteq \widetilde{h}(0) \cap \widetilde{h}(q) \\
&= \widetilde{h}(q * q) \cap \widetilde{h}(q) \\
&\supseteq (\widetilde{h}(q) \cap \widetilde{h}(q)) \cap \widetilde{h}(q) \\
&= \widetilde{h}(q), \\
\eta(0 * q) &\leq \vee\{\eta(0), \eta(q)\} \\
&= \vee\{\eta(q * q), \eta(q)\} \\
&\leq \vee\{\vee\{\eta(q), \eta(q)\}, \eta(q)\} \\
&= \eta(q).
\end{aligned}
\quad (9)
$$

This completes the proof. $\qquad \square$

For any hybrid structure $\widetilde{h}_\eta = (\widetilde{h}; \eta)$ in L over U, we consider two level sets:

$$
\begin{aligned}
\widetilde{h}_\eta(\alpha) &:= \{q \in L | \alpha \subseteq \widetilde{h}(q)\}, \\
\widetilde{h}_\eta(t) &:= \{q \in L | \eta(q) \leq t\},
\end{aligned}
\quad (10)
$$

where $\alpha \in \mathbb{P}(U)$ and $t \in I$.

Theorem 1. Let L be a BCH-algebra. For a hybrid structure $\widetilde{h}_\eta = (\widetilde{h}; \eta)$ in L over U, the following are equivalent:

(1) $\widetilde{h}_\eta$ is a hybrid subalgebra of L over U.

(2) For any $\alpha \in \mathbb{P}(U)$ and $t \in I$, the nonempty sets $\widetilde{h}_\eta(\alpha)$ and $\widetilde{h}_\eta(t)$ are subalgebras of L.

Proof

(1) $\Longrightarrow$ (2). Suppose that $\widetilde{h}_\eta$ is a hybrid subalgebra of L. Let $q, l \in \widetilde{h}_\eta(\alpha)$. Then, $\alpha \subseteq \widetilde{h}(q)$ and $\alpha \subseteq \widetilde{h}(l)$. It follows that $\alpha \subseteq \widetilde{h}(q) \cap \widetilde{h}(l) \subseteq \widetilde{h}(q * l)$ and so $q * l \in \widetilde{h}_\eta(\alpha)$. Hence, $\widetilde{h}_\eta(\alpha)$ is a subalgebra of L. Also, let $q, l \in \widetilde{h}_\eta(t)$. Then, $\eta(q) \leq t$ and $\eta(l) \leq t$. It follows that $\eta(q * l) \leq \vee\{\eta(q), \eta(l)\} \leq t$ and so $q * l \in \widetilde{h}_\eta(t)$. Hence, $\widetilde{h}_\eta(t)$ is a subalgebras of L.

(2) $\Longrightarrow$ (1). Let for any $\alpha \in \mathbb{P}(U)$ and $t \in I$, the nonempty sets $\widetilde{h}_\eta(\alpha)$ and $\widetilde{h}_\eta(t)$ are subalgebras of L. For contradiction, let $q_0, l_0 \in L$ such that $\widetilde{h}(q_0 * l_0) \subset \widetilde{h}(q_0) \cap \widetilde{h}(l_0)$. Let $\widetilde{h}(q_0) = \beta_1, \widetilde{h}(l_0) = \beta_2$ and $\widetilde{h}(q_0 * l_0) = \alpha$. Then, $\alpha \subset \beta_1 \cap \beta_2$. Let us consider $\alpha_1 | \widetilde{h}(q_0 * l_0) \subset \alpha_1 \subset \widetilde{h}(q_0) \cap \widetilde{h}(l_0)$. We get that $\widetilde{h}(q_0 * l_0) = \alpha \subset \alpha_1 \subset \beta_1 \cap \beta_2$, and so $q_0 * l_0 \notin \widetilde{h}_\eta(\alpha)$ which is a contradiction. Thus, $\widetilde{h}(q * l) \supseteq \widetilde{h}(q) \cap \widetilde{h}(l)$ for all $q, l \in L$. Also, let $q_0, l_0 \in L$ such that $\eta(q_0 * l_0) > \vee\{\eta(q_0), \eta(l_0)\}$. Let $\eta(q_0) = \eta_1, \eta(l_0) = \eta_2$ and $\eta(q_0 * l_0) = t$. Then, $t > \vee\{\eta_1, \eta_2\}$. Let us consider $t_1 | \eta(q_0 * l_0) > t_1 > \vee\{\eta(q_0), \eta(l_0)\}$. We get that $t > t_1 > \vee\{\eta_1, \eta_2\}$. Hence, $\vee\{\eta_1, \eta_2\} < t_1 < t = \eta(q_0 * l_0)$, and so $q_0 * l_0 \notin \widetilde{h}_\eta(t)$ which is a contradiction. Thus, $\eta(q * l) \leq \vee\{\eta(q), \eta(l)\}$ for all $q, l \in L$. Hence, $\widetilde{h}_\eta$ is a hybrid subalgebra of L. $\qquad \square$

Next, we define $H_{\widetilde{h}} = \{q \in L | \widetilde{h}(q) = \widetilde{h}(0)\}$ and $H_\eta = \{q \in L | \eta(q) = \eta(0)\}$. These two sets are also subalgebras of a BCH-algebra L over U.

Proposition 4. Let $\widetilde{h}_\eta = (\widetilde{h}; \eta)$ be a hybrid subalgebra in L over U. Then, the sets $H_{\widetilde{h}}$ and H_η are subalgebras of L over U.

Proof. Let $q, l \in H_{\widetilde{h}}$. Then, $\widetilde{h}(q) = \widetilde{h}(0) = \widetilde{h}(l)$ and so $\widetilde{h}(q * l) \supseteq \widetilde{h}(q) \cap \widetilde{h}(l) = \widetilde{h}(0)$. By using Proposition 1, we know that $\widetilde{h}(q * l) = \widetilde{h}(0)$. Consequently, $q * l \in H_{\widetilde{h}}$.

Let $q, l \in I_\eta$. Then, $\eta(q) = \eta(0) = \eta(l)$ and so $\eta(q * l) \leq \vee\{\eta(q), \eta(l)\} = \eta(0)$. Again by Proposition 1, we know that $\eta(q * l) = \eta(0)$ or equivalently $q * l \in H_\eta$.

Hence, the sets $H_{\widetilde{h}}$ and H_η are subalgebras of L over U. $\qquad \square$

Proposition 5. Let $\widetilde{h}_\eta = (\widetilde{h}; \eta)$ be a hybrid structure in L over U where $\widetilde{h}: L \longrightarrow \mathbb{P}(U)$ and $\eta: L \longrightarrow I$ are mappings given by

$$q \mapsto \begin{cases} \alpha_1, & \text{if } 0 * (0 * q) = q, \\ \alpha_2, & \text{otherwise}, \end{cases} \qquad \text{such that } \alpha_1 \subset \alpha_2 \in \mathbb{P}(U)$$

$$q \mapsto \begin{cases} t_1, & \text{if } 0 * (0 * q) = q, \\ t_2, & \text{otherwise}, \end{cases} \qquad \text{such that } t_1 < t_2 \in I, \tag{11}$$

for $q \in L$. Then, $\widetilde{h}_\eta$ is a hybrid subalgebra of L.

Proof. Let $q, l \in L$. If $0 * (0 * q) = q$ and $0 * (0 * l) = l$, then $\widetilde{h}(q) = \widetilde{h}(l) = \alpha_1, \eta(q) = \eta(l) = t_1$. Since, $(q * l) * (0 * 0 * (q * l))) = 0$ (using condition (3), property (iv), and property (ii)) and $(0 * 0 * (q * l)) * (q * l) = 0$ (using property (iii) and condition (1)). This implies that $(q * l) = (0 * 0 * (q * l))$, by condition (2). Thus, $\widetilde{h}(q * l) = \alpha_1 = \widetilde{h}(q) \cap \widetilde{h}(l)$ and $\eta(q * l) = t_1 = \vee\{\eta(q), \eta(l)\}$. If

$0 * (0 * q) \neq q$ or $0 * (0 * l) \neq l$, then $\widetilde{h}(q) = \alpha_2$ or $\widetilde{h}(l) = \alpha_2$ and $\eta(q) = t_2$ or $\eta(l) = t_2$. Then, $\widetilde{h}(q * l) \supseteq \alpha_2 = \widetilde{h}(q) \cap \widetilde{h}(l)$ and $\eta(q * l) \leq t_2 = \vee\{\eta(q), \eta(l)\}$. Thus, $\widetilde{h}_\eta$ is a hybrid subalgebra. $\square$

Proposition 6. *Let $\varnothing \neq Q \subseteq L$ and let $\widetilde{h}_\eta = (\widetilde{h}; \eta)$ be a hybrid structure of L over U where $\widetilde{h}: L \longrightarrow \mathbb{P}(U)$ and $\eta: L \longrightarrow I$ are mappings given by*

$$q \mapsto \begin{cases} \alpha_1, & \text{if } q * m = (0 * m) * (0 * q), \\ \alpha_2, & \text{otherwise}, \end{cases} \qquad \text{such that } \alpha_1 \subset \alpha_2 \in \mathbb{P}(U),$$

$$q \mapsto \begin{cases} t_1, & \text{if } q * m = (0 * m) * (0 * q), \\ t_2, & \text{otherwise}, \end{cases} \qquad \text{such that } t_1 < t_2 \in I, \tag{12}$$

for $q \in L, m \in Q$. Then, $\widetilde{h}_\eta$ is a hybrid subalgebra of L.

Proof. Let $q, l \in L$. If there exists $m \in Q$ such that $q * m = (0 * m) * (0 * q)$ and $l * m = (0 * m) * (0 * l)$, then $\widetilde{h}(q) = \widetilde{h}(l) = \alpha_1, \eta(q) = \eta(l) = t_1$. Using condition (3), property (ii), and property (iii), we have $(q * l) * m = (0 * m) * (0 * (q * l))$. If there exists $m \in Q$ such that either $q * m \neq (0 * m) * (0 * q)$ or $l * m \neq (0 * m) * (0 * l)$, then $\widetilde{h}(q) = \alpha_2$ or $\widetilde{h}(l) = \alpha_2$ and $\eta(q) = t_2$ or $\eta(l) = t_2$. It follows that $\widetilde{h}(q * l) \supseteq \alpha_2 = \widetilde{h}(q) \cap \widetilde{h}(l)$ and $\eta(q * l) \leq t_2 = \vee\{\eta(q), \eta(l)\}$. Therefore, $\widetilde{h}_\eta$ is a hybrid subalgebra of L. $\square$

Conversely, suppose that $\widetilde{g}_\mu$ is a subalgebra of L. Let $q, l \in L$. Consider the following two cases:

Case (i): if $q, l \in \widetilde{g}_\mu$, then $q * l \in \widetilde{g}_\mu$. Thus, $\widetilde{h}(q * l) = \alpha = \widetilde{h}(q) \cap \widetilde{h}(l)$ and $\eta(q * l) = \gamma = \vee\{\eta(q), \eta(l)\}$.

Case (ii): if $q \notin \widetilde{g}_\mu$ or $l \notin \widetilde{g}_\mu$, then $\widetilde{h}(q * l) \supseteq \beta = \widetilde{h}(q) \cap \widetilde{h}(l)$ and $\eta(q * l) \leq \delta = \vee\{\eta(q), \eta(l)\}$.

Hence, $\widetilde{h}_\eta$ is a hybrid subalgebra of L.
Also, $H_{\widetilde{h}} = \{q \in L: \widetilde{h}(q) = \widetilde{h}(0)\} = \{q \in L: \widetilde{h}(q) = \alpha\} = \widetilde{g}_\mu$ and $H_\eta = \{q \in L: \eta(q) = \eta(0)\} = \{q \in L: \eta(q) = \gamma\} = \widetilde{g}_\mu$. $\square$

Proposition 7. *Let $\widetilde{g}_\mu = (\widetilde{g}; \mu)$ be a nonempty subset in L over U and $\widetilde{h}_\eta = (\widetilde{h}; \eta)$ be a hybrid structure of L over U defined by*

$$\widetilde{h}(q) := \begin{cases} \alpha, & \text{if } q \in \widetilde{g}_\mu, \\ \beta, & \text{otherwise}, \end{cases}$$

$$\eta(q) := \begin{cases} \gamma, & \text{if } q \in \widetilde{g}_\mu, \\ \delta, & \text{otherwise}, \end{cases} \tag{13}$$

for all $\alpha, \beta \in \mathbb{P}(U)$ and $\gamma, \delta \in [0, 1]$. Then, $\widetilde{h}_\eta$ is a hybrid subalgebra of L over U if and only if $\widetilde{g}_\mu$ is a subalgebra of L over U. Moreover, $H_{\widetilde{h}} = \widetilde{g}_\mu = H_\eta$.

Proof. Let $\widetilde{h}_\eta$ be a hybrid subalgebra of a *BCH*-algebra L over U. Let $q, l \in L$ such that $q, l \in \widetilde{g}_\mu$. Then, we have $\widetilde{h}(q * l) \supseteq \widetilde{h}(q) \cap \widetilde{h}(l) = \alpha \cap \alpha = \alpha$ and $\eta(q * l) \leq \vee\{\eta(q), \eta(l)\} = \vee\{\gamma, \gamma\}$. Hence, we have proved that $q * l \in \widetilde{g}_\mu$. Thus, $\widetilde{g}_\mu$ is indeed a subalgebra of L.

Proposition 8. *Let $\widetilde{h}_\eta = (\widetilde{h}; \eta)$ be a hybrid subalgebra in L over U. Then, the set $\Omega := \{q * l \in L | \widetilde{h}(q * l) \cap \alpha \neq \varnothing, \eta(q * l) \leq t\}$ is a subalgebra in L over U, for $\varnothing \neq \alpha \in \mathbb{P}(U), t \in I$.*

Proof. Let $q, l \in L$ such that $q, l \in \Omega$. Thus, $\widetilde{h}(q) \cap \alpha \neq \varnothing, \widetilde{h}(l) \cap \alpha \neq \varnothing$ and $\eta(q) \leq t, \eta(l) \leq t$. It follows that $(\widetilde{h}(q) \cap \alpha) \cap (\widetilde{h}(l) \cap \alpha) = (\widetilde{h}(q) \cap \widetilde{h}(l)) \cap \alpha \subseteq \widetilde{h}(q * l) \cap \alpha \neq \varnothing$ and $\eta(q * l) \leq \vee\{\eta(q), \eta(l)\} \leq t$. Thus, $q * l \in \Omega$ and so Ω is a subalgebra in L. $\square$

Proposition 9. *Let $\widetilde{h}_\eta = (\widetilde{h}; \eta)$ be a hybrid structure in L over U. Then, $\widetilde{h}_\eta$ is a hybrid subalgebra of L over U if and only if for $\alpha \in \mathbb{P}(U), t \in I$, and the sets $\widetilde{h}_\eta(\alpha) := \{q * l \in L | \widetilde{h}(q * l) \supseteq \alpha\}$ and $\widetilde{h}_\eta(t) := \{q * l \in L | \eta(q * l) \leq t\}$ are subalgebras in L.*

Proof. "$\Rightarrow$". Let $\widetilde{h}_\eta = (\widetilde{h}; \eta)$ be a hybrid subalgebra in a BCH-algebra L over U and consider the sets $\widetilde{h}_\eta(\alpha) := \{q \in L | \widetilde{h}(q) \supseteq \alpha\}$ and $\widetilde{h}_\eta(t) := \{q \in L | \eta(q) \leq t\}$. Now,

let $q, l \in L$ such that $q, l \in \widetilde{h}_\eta(\alpha)$ and $q, l \in \widetilde{h}_\eta(t)$. Thus, $\widetilde{h}(q) \supseteq \alpha, \widetilde{h}(l) \supseteq \alpha$ and $\eta(q) \leq t, \eta(l) \leq t$. Then, from (3), we have $\widetilde{h}(q * l) \supseteq \widetilde{h}(q) \cap \widetilde{h}(l) \supseteq \alpha$ and $\eta(q * l) \leq \vee\{\eta(q), \eta(l)\} \leq t$. That is, $\widetilde{h}(q * l) \supseteq \alpha$ and $\eta(q * l) \leq t$ and so $q * l \in \widetilde{h}_\eta(\alpha)$ and $q * l \in \widetilde{h}_\eta(t)$. Hence, $\widetilde{h}_\eta(\alpha)$ and $\widetilde{h}_\eta(t)$ are subalgebras in L.

"$\Leftarrow$". For $\alpha \in \mathbb{P}(U)$, $t \in I$, let $\widetilde{h}_\eta(\alpha) := \{q * l \in L | \widetilde{h}(q * l) \supseteq \alpha\}$ and $\widetilde{h}_\eta(t) := \{q * l \in L | \eta(q * l) \leq t\}$ be subalgebras in L. Let $q \in L$ such that $\widetilde{h}(q) = \alpha$ and $\eta(q) = t$. Suppose for contradiction that

$$\widetilde{h}(q * l) \subset \widetilde{h}(q) \cap \widetilde{h}(l),$$
$$\eta(q * l) > \vee\{\eta(q), \eta(l)\}. \tag{14}$$

Take α and t such that

$$\widetilde{h}(q * l) \subset \alpha \subset \widetilde{h}(q) \cap \widetilde{h}(l),$$
$$\eta(q * l) > t > \vee\{\eta(q), \eta(l)\}. \tag{15}$$

This means that both $\widetilde{h}_\eta(\alpha)$ and $\widetilde{h}_\eta(t)$ are not subalgebras which contradicts the assumption. Thus, $\widetilde{h}(q * l) \supseteq \widetilde{h}(q) \cap \widetilde{h}(l)$ and $\eta(q * l) \leq \vee\{\eta(q), \eta(l)\}$. Hence, $\widetilde{h}_\eta$ is a hybrid subalgebra of L. □

For any hybrid structure $\widetilde{h}_\eta$ in L over U, let $\widetilde{h}_\eta^* := (\widetilde{h}^*; \eta^*)$ be a hybrid structure in L over U defined by

$$\widetilde{h}^*: L \longrightarrow \mathbb{P}(U), q \mapsto \begin{cases} \widetilde{h}(q), & \text{if } q \in \widetilde{h}_\eta(\alpha), \\ \beta, & \text{otherwise,} \end{cases}$$
$$\eta^*: L \longrightarrow I, q \mapsto \begin{cases} \eta(q), & \text{if } q \in \widetilde{h}_\eta(s), \\ t, & \text{otherwise,} \end{cases} \tag{16}$$

where $\alpha, \beta \in \mathbb{P}(U)$ and $s, t \in I$ with $\beta \subsetneq \widetilde{h}(q)$ and $t > \eta(q)$.

Proposition 10. *Let L be a BCH-algebra. If $\widetilde{h}_\eta$ is a hybrid subalgebra in L over U, then so is $\widetilde{h}_\eta^*$.*

Proof. Assume that $\widetilde{h}_\eta$ is a hybrid subalgebra of a BCH-algebra L over U. Then, $\widetilde{h}_\eta(\alpha)$ and $\widetilde{h}_\eta(t)$ are subalgebras of L for all $\alpha \in \mathbb{P}(U)$ and $t \in I$ provided that they are nonempty by Proposition 9. Let $q, l \in L$. If $q, l \in \widetilde{h}_\eta(\alpha)$, then $q * l \in \widetilde{h}_\eta(\alpha)$. Thus,

$$\widetilde{h^*}(q * l) = \widetilde{h}(q * l) \supseteq \widetilde{h}(q) \cap \widetilde{h}(l) = \widetilde{h}^*(q) \cap \widetilde{h}^*(l). \tag{17}$$

If $q \notin \widetilde{h}_\eta(\alpha)$ or $l \notin \widetilde{h}_\eta(\alpha)$, then $\widetilde{h}^*(q) = \beta$ or $\widetilde{h}^*(l) = \beta$. Hence,

$$\widetilde{h}^*(q * l) \supseteq \beta = \widetilde{h}^*(q) \cap \widetilde{h}^*(l). \tag{18}$$

Now, if $q, l \in \widetilde{h}_\eta(s)$, then $q * l \in \widetilde{h}_\eta(s)$. Thus,

$$\eta^*(q * l) = \eta(q * l) \leq \vee\{\eta(q), \eta(l)\} = \vee\{\eta^*(q), \eta^*(l)\}. \tag{19}$$

If $q \notin \widetilde{h}_\eta(s)$ or $l \notin \widetilde{h}_\eta(s)$, then $\eta^*(q) = t$ or $\eta^*(l) = t$. Hence,

$$\eta^*(q * l) \leq t = \vee\{\eta^*(q), \eta^*(l)\}. \tag{20}$$

Therefore, $\widetilde{h}_\eta^*$ is a hybrid subalgebra of L over U.

Table 3: Cayley table of the binary operation $*$.

$*$	0	l_1	l_2	l_3
0	0	l_1	l_2	l_3
l_1	l_1	0	l_3	l_2
l_2	l_2	l_3	0	l_1
l_3	l_3	l_2	l_1	0

The converse of Proposition 10 may not true in general.

Example 2. Let $L = \{0, l_1, l_2, l_3\}$ be a *BCH*-algebra with the Cayley table (Table 3) and $U = \{u_1, u_2, u_3, u_4, u_5, u_6, u_7, u_8, u_9\}$ be an initial universe set.

Let $\widetilde{h}_\eta = (\widetilde{h}; \eta)$ be a hybrid structure in L over U which is given in Table 4. Let $\widetilde{h}_\eta(\alpha) = \widetilde{h}_\eta(s) = \{0, l_1\}$, where $\alpha = \{u_1, u_3, u_5, u_7, u_9\}$ and $s = 0.6$. Define the hybrid structure $\widetilde{h}_\eta^* := (\widetilde{h}^*; \eta^*)$ by Table 5.

It can be easily verified that $\widetilde{h}_\eta^*$ is a hybrid subalgebra of L. Moreover, $\widetilde{h}_\eta$ is not hybrid subalgebra of L as $\widetilde{h}(l_1 * l_2) = \widetilde{h}(l_3) = \{u_7\} \not\supseteq \{u_5\} = \widetilde{h}(l_1) \cap \widetilde{h}(l_2) = \{u_1, u_3, u_5, u_7, u_9\} \cap \{u_2, u_5, u_8\}$.

Proposition 11. *If $\widetilde{h}_\eta = (\widetilde{h}; \eta)$ and $\widetilde{g}_\mu = (\widetilde{g}; \mu)$ are two hybrid subalgebras in L over U, then the hybrid intersection $\widetilde{h}_\eta \Cap \widetilde{g}_\mu$ is also a hybrid subalgebra of L.*

Proof. Let $q, l \in L$. Then,

$$\begin{aligned}
(\widetilde{h} \widetilde{\cap} \widetilde{g})(q * l) &= \widetilde{h}(q * l) \cap \widetilde{g}(q * l) \\
&\supseteq (\widetilde{h}(q) \cap \widetilde{h}(l)) \cap (\widetilde{g}(q) \cap \widetilde{g}(l)) \\
&= (\widetilde{h}(q) \cap \widetilde{g}(q)) \cap (\widetilde{h}(l) \cap \widetilde{g}(l)) \\
&= (\widetilde{h} \widetilde{\cap} \widetilde{g})(q) \cap (\widetilde{h} \widetilde{\cap} \widetilde{g})(l), \\
(\eta \vee \mu)(q * l) &= \vee\{\eta(q * l), \mu(q * l)\} \\
&\leq \vee\{\vee\{\eta(q), \eta(l)\}, \vee\{\mu(q), \mu(l)\}\} \\
&= \vee\{\vee\{\eta(q), \mu(q)\}, \vee\{\eta(q), \mu(l)\}\} \\
&= \vee\{(\eta \vee \mu)(q), (\eta \vee \mu)(l)\}.
\end{aligned} \tag{21}$$

Consequently, $\widetilde{h}_\eta \Cap \widetilde{g}_\mu$ is a hybrid subalgebra of L. □

Definition 5. Let $\widetilde{h}_\eta = (\widetilde{h}; \eta)$ be a hybrid structure of a BCH-algebra L over U. Then, the "power-m" operation on a hybrid structure of a BCH-algebra L over U is defined as follows:

$$\widetilde{h}_\eta^m := (\widetilde{h}^m; \eta^m), \tag{22}$$

where m is any nonnegative integer.

Proposition 12. *If $\widetilde{h}_\eta = (\widetilde{h}; \eta)$ is a hybrid subalgebra in L over U, then $\widetilde{h}_\eta^m$ is a hybrid subalgebra in L over U.*

Proof. Let $\widetilde{h}_\eta = (\widetilde{h}; \eta)$ be a hybrid subalgebra in a BCH-algebra L over U and let $q \in L$. Then,

Table 4: Table representation of the hybrid structure $\widetilde{h}_\eta$.

L	$\widetilde{h}$	η
0	U	0.5
l_1	$\{u_1, u_3, u_5, u_7, u_9\}$	0.6
l_2	$\{u_2, u_5, u_8\}$	0.8
l_3	$\{u_7\}$	0.8

Table 5: Table representation of the hybrid structure $\widetilde{h}_\eta^*$.

L	$\widetilde{h}^*$	η^*
0	U	0.5
l_1	$\{u_1, u_3, u_5, u_7, u_9\}$	0.6
l_2	$\varnothing$	0.9
l_3	$\varnothing$	0.9

$$
\begin{aligned}
\widetilde{h}^m(0) &= [\widetilde{h}(0)]^m \\
&= [\widetilde{h}(q*q)]^m \\
&\supseteq [\widetilde{h}(q) \cap \widetilde{h}(q)]^m \\
&= \widetilde{h}(q)^m \cap \widetilde{h}(q)^m \\
&= \widetilde{h}^m(q) \cap \widetilde{h}^m(q) \\
&= \widetilde{h}^m(q), \\
\eta^m(0) &= [\eta(0)]^m \\
&= [\eta(q*q)]^m \\
&\leq \vee\{\eta(q), \eta(q)\}^m \\
&= \vee\{\eta(q)^m, \eta(q)^m\} \\
&= \vee\{\eta^m(q), \eta^m(q)\} \\
&= \eta^m(q).
\end{aligned}
\tag{23}
$$

Let $q, l \in L$. Then,

$$
\begin{aligned}
\widetilde{h}^m(q*l) &= [\widetilde{h}(q*l)]^m \\
&\supseteq \{\widetilde{h}(q) \cap \widetilde{h}(l)\}^m \\
&= \widetilde{h}(q)^m \cap \widetilde{h}(l)^m \\
&= \widetilde{h}^m(q) \cap \widetilde{h}^m(l) \\
\eta^m(q*l) &= [\eta(q*l)]^m \\
&\leq \vee\{\eta(q), \eta(l)\}^m \\
&= \vee\{\eta(q)^m, \eta(l)^m\} \\
&= \vee\{\eta^m(q), \eta^m(l)\}.
\end{aligned}
\tag{24}
$$

Hence, $\widetilde{h}_\eta^m$ is a hybrid subalgebra of L. $\qquad\square$

Definition 6. Let $\widetilde{h}_\eta = (\widetilde{h}; \eta)$ be a hybrid structure of a BCH-algebra L over U. Then, the "ρ-multiply" operation on a hybrid structure of a *BCH*-algebra L over U is defined as

$$
\rho\widetilde{h}_\eta := (\rho\widetilde{h}, \rho\eta),
\tag{25}
$$

where ρ is any nonnegative integer.

Proposition 13. *If $\widetilde{h}_\eta = (\widetilde{h}; \eta)$ is a hybrid subalgebra in L over U, then $\rho\widetilde{h}_\eta$ is a hybrid subalgebra of L over U.*

Proof. Let $\widetilde{h}_\eta = (\widetilde{h}; \eta)$ be a hybrid subalgebra of a BCH-algebra L over U and let ρ be any nonnegative integer. Then, for any $q \in L$, we have

$$
\begin{aligned}
\rho\widetilde{h}(0) &= \rho\widetilde{h}(q*q) \\
&\supseteq \rho[\widetilde{h}(q) \cap \widetilde{h}(q)] \\
&= \rho\widetilde{h}(q) \cap \rho\widetilde{h}(q) \\
&= \rho\widetilde{h}(q), \\
\rho\eta(0) &= \rho\eta(q*q) \\
&\leq \rho\vee\{\eta(q), \eta(q)\} \\
&= \vee\{\rho\eta(q), \rho\eta(q)\} \\
&= \rho\eta(q).
\end{aligned}
\tag{26}
$$

Let $q, l \in L$. Then,

$$
\begin{aligned}
\rho\widetilde{h}(q*l) &\supseteq \rho[\widetilde{h}(q) \cap \widetilde{h}(l)] \\
&= \rho\widetilde{h}(q) \cap \rho\widetilde{h}(l), \\
\rho\eta(q*l) &\leq \rho\vee\{\eta(q), \eta(l)\} \\
&= \vee\{\rho\eta(q), \rho\eta(l)\}.
\end{aligned}
\tag{27}
$$

Hence, $\rho\widetilde{h}_\eta$ is a hybrid subalgebra of L over U. $\qquad\square$

Let φ be a mapping from the set L into the set Q. Let $\widetilde{g}_\mu$ be a hybrid structure of a BCH-algebra L over U. Then, the preimage of $\widetilde{g}_\mu$ is defined as $\varphi^{-1}(\widetilde{g}_\mu) = (\varphi^{-1}(\widetilde{g}), \varphi^{-1}(\mu))$ in L with the membership function and nonmembership function given by $\varphi^{-1}(\widetilde{g})(q) = \widetilde{g}(\varphi(q))$ and $\varphi^{-1}(\mu)(q) = \mu(\varphi(q))$. It can be shown that $\varphi^{-1}(\widetilde{g}_\mu)$ is a hybrid structure of a BCH-algebra L over U.

Definition 7. A mapping $\varphi: L \longrightarrow Q$ is called a homomorphism of a BCH-algebra if $\varphi(q*l) = \varphi(q)*\varphi(l)$, for all $q, l \in L$. Note that if $\varphi: L \longrightarrow Q$ is a homomorphism of a *BCH*-algebra, then $\varphi(0) = 0$.

Proposition 14. *Let $\varphi: L \longrightarrow Q$ be a homomorphism of BCH-algebras. If $\widetilde{g}_\mu = (\widetilde{g}, \mu)$ is a hybrid subalgebra of a BCH-algebra Q over U, then the preimage $\varphi^{-1}(\widetilde{g}_\mu) = (\varphi^{-1}(\widetilde{g}), \varphi^{-1}(\mu))$ of $\widetilde{g}_\mu$ under φ is a hybrid subalgebra of a BCH-algebra L over U.*

Proof. Assume that $\widetilde{g}_{\mu} = (\widetilde{g}; \mu)$ is a hybrid subalgebra of a BCH-algebra Q over U and let $q, l \in L$. Then,

$$
\begin{aligned}
\varphi^{-1}(\widetilde{g})(q * l) &= \widetilde{g}(\varphi(q * l)) \\
&= \widetilde{g}(\varphi(q) * \varphi(l)) \\
&\supseteq \widetilde{g}(\varphi(q)) \cap \widetilde{g}(\varphi(l)) \\
&= \varphi^{-1}(\widetilde{g})(q) \cap \varphi^{-1}(\widetilde{g})(l), \\
\varphi^{-1}(\mu)(q * l) &= \mu(\varphi(q * l)) \\
&= \mu(\varphi(q) * \varphi(l)) \\
&\leq \vee\{\mu(\varphi(q)), \mu(\varphi(l))\} \\
&= \vee\{\varphi^{-1}(\mu)(q), \varphi^{-1}(\mu)(l)\}.
\end{aligned}
\tag{28}
$$

Therefore, $\varphi^{-1}(\widetilde{g}_{\mu}) = (\varphi^{-1}(\widetilde{g}), \varphi^{-1}(\mu))$ is a hybrid subalgebra of L. $\qquad\square$

4. Conclusion

The present work is devoted to the study of hybrid subalgebras of BCH-algebras introduced, and related properties are investigated. Furthermore, some characterizations of hybrid subalgebras of BCH-algebras are given. Also, we stated and proved some theorems in hybrid subalgebras of BCH-algebras. Finally, the homomorphic images and inverse images of fuzzy BCH-subalgebras are studied and discussed. To extend these results, one can further study these notions on different algebras such as rings, hemirings, BL-algebras, MTL-algebras, R0-algebras, MV-algebras, EQ-algebras, d-algebras, Q-algebras, and lattice implication algebras. Some important issues for future work are as follows: (1) to develop strategies for obtaining more valuable results and (2) to apply these notions and results for studying related notions in other algebraic (hybrid) structures.

Data Availability

No data were used to support the study.

Conflicts of Interest

The authors declare that they have no conflicts of interest.

Acknowledgments

References

[1] Q. P. Hu and X. Li, "On BCH-algebras," *Mathematics Seminar Notes*, vol. 11, no. 2, pp. 313–320, 1983.

[2] Q. P. Hu and X. Li, "On proper BCH-algebras," *Mathematica Japonica*, vol. 30, no. 4, pp. 659–661, 1985.

[3] B. Ahmad, "Forthcoming conferences," *Water Research*, vol. 24, no. 6, pp. 801–804, 1990.

[4] W. A. Dudek and J. Thomys, "On decompositions of BCH-algebras," *Mathematica Japonica*, vol. 35, no. 6, pp. 1131–1138, 1990.

[5] M. A. Chaudhry, "On BCH-algebras," *Mathematica Japonica*, vol. 36, no. 4, pp. 665–676, 1991.

[6] E. H. Roh, S. Y. Kim, and Y. B. Jun, "On a problem in BCH-algebras," *Mathematica Japonica*, vol. 52, pp. 279–283, 2000.

[7] E. H. Roh, Y. B. Jun, and Q. Zhang, "Special subset in BCH-algebras," *Far East Journal of Mathematical Sciences*, vol. 3, pp. 723–729, 2001.

[8] M. A. Chaudhry and H. Fakhar-Ud-Din, "On some classes of BCH-algebras," *International Journal of Mathematics and Mathematical Sciences*, vol. 25, no. 3, pp. 205–211, 2001.

[9] K. H. Dar and M. Akram, "On endomorphisms of BCH-algebras," *The Annals of the University of Craiova—Mathematics and Computer Science series*, vol. 33, pp. 227–234, 2006.

[10] A. Borumand Saeid and A. Namdar, "Smarandache BCH-algebras," *World Applied Sciences Journal*, vol. 7, pp. 77–83, 2009.

[11] L. A. Zadeh, "Fuzzy sets," *Information and Control*, vol. 8, no. 3, pp. 338–353, 1965.

[12] D. Molodtsov, "Soft set theory-First results," *Computers & Mathematics with Applications*, vol. 37, no. 4-5, pp. 19–31, 1999.

[13] D. A. Molodtsov, "The description of a dependence with the help of soft sets," *Journal of Computer and Systems Sciences International*, vol. 40, no. 6, pp. 977–984, 2001.

[14] D. A. Molodtsov, *The Theory of Soft Sets*, URSS Publishers, Moscow, Russia, 2004, in Russian.

[15] D. A. Molodtsov, V. Yu. Leonov, and D. V. Kovkov, "Soft sets technique and its application," *Nechetkie Sistemy i Myagkie Vychisleniya*, vol. 1, no. 1, pp. 8–39, 2006.

[16] O. Kazanci, S. Yilmaz, and S. Yamak, "Soft sets and soft BCH-algebras," *Hacettepe Journal of Mathematics and Statistics*, vol. 39, no. 2, pp. 205–217, 2010.

[17] A. Borumand Saeid, A. Namdar, and M. K. Rafsanjani, "Fuzzy n-fold ideals in BCH-algebras," *Neural Computing & Applications*, vol. 19, no. 5, pp. 775–783, 2010.

[18] Y. B. Jun, "Fuzzy closed ideals and fuzzy filters in BCH-algebras," *Journal of Fuzzy Mathematics*, vol. 7, no. 2, pp. 435–444, 1999.

[19] Y. B. Jun and C. H. Park, "Filters of BCH-algebras based on bipolar-valued fuzzy sets," *International Mathematical Forum*, vol. 4, no. 13, pp. 631–643, 2009.

[20] T. Senapati and K. P. Shum, "Cubic subalgebras of BCH-algebras," *Annals of Communications in Mathematics*, vol. 1, no. 1, pp. 65–73, 2018.

[21] Y. Jun, S.-Z. Song, and S. Kim, "Length-fuzzy subalgebras in BCK/BCI-algebras," *Mathematics*, vol. 6, no. 1, pp. 11–25, 2018.

[22] S. Anis, M. Khan, and Y. B. Jun, "Hybrid ideals in semigroups," *Cogent Mathematics*, vol. 4, no. 1, Article ID 1352117, 12 pages, 2017.

[23] B. Elavarasan and Y. B. Jun, "Regularity of semigroups in terms of hybrid ideals and hybrid bi-ideals," *Kragujevac Journal of Mathematics*, vol. 46, no. 6, pp. 857–864, 2022.

[24] B. Elavarasan, K. Porselvi, and Y. B. Jun, "Hybrid generalized bi-ideals in semigroups," *International Journal of Mathematics and Computer Science*, vol. 14, no. 3, pp. 601–612, 2019.

[25] B. Elavarasan, G. Muhiuddin, K. Porselvi, and Y. B. Jun, "Hybrid structures applied to ideals in near-rings," *Complex & Intelligent Systems*, vol. 7, no. 3, pp. 1489–1498, 2021.

[26] K.-T. Kang, S.-Z. Song, E. H. Roh, and Y. B. Jun, "Hybrid ideals of BCK/BCI-algebras," *Axioms*, vol. 9, no. 3, p. 85, 2020.

[27] G. Muhiuddin, D. Al-Kadi, and A. Mahboob, "Ideal theory of BCK/BCI-algebras based on hybrid structures," *The Journal of*

Retraction

Retracted: The Segmentation of Road Scenes Based on Improved ESPNet Model

Security and Communication Networks

This article has been retracted by Hindawi following an investigation undertaken by the publisher [1]. This investigation has uncovered evidence of one or more of the following indicators of systematic manipulation of the publication process:

(1) Discrepancies in scope

(2) Discrepancies in the description of the research reported

(3) Discrepancies between the availability of data and the research described

(4) Inappropriate citations

(5) Incoherent, meaningless and/or irrelevant content included in the article

(6) Peer-review manipulation

The presence of these indicators undermines our confidence in the integrity of the article's content and we cannot, therefore, vouch for its reliability. Please note that this notice is intended solely to alert readers that the content of this article is unreliable. We have not investigated whether authors were aware of or involved in the systematic manipulation of the publication process.

Wiley and Hindawi regrets that the usual quality checks did not identify these issues before publication and have since put additional measures in place to safeguard research integrity.

We wish to credit our own Research Integrity and Research Publishing teams and anonymous and named external researchers and research integrity experts for contributing to this investigation.

The corresponding author, as the representative of all authors, has been given the opportunity to register their agreement or disagreement to this retraction. We have kept a record of any response received.

References

[1] R. Jin, T. Yu, X. Han, and Y. Liu, "The Segmentation of Road Scenes Based on Improved ESPNet Model," *Security and Communication Networks*, vol. 2021, Article ID 1681952, 11 pages, 2021.

WILEY | Hindawi

Research Article

The Segmentation of Road Scenes Based on Improved ESPNet Model

Ran Jin [ID], Tongrui Yu, Xiaozhen Han [ID], and Yunpeng Liu

College of Big Data and Software Engineering, Zhejiang Wanli University, Ningbo 315100, China

Correspondence should be addressed to Ran Jin; ran.jin@163.com and Xiaozhen Han; 170748822@qq.com

Image segmentation is an important research in image processing and machine vision in which automated driving can be seen the main application scene of image segmentation algorithms. Due to the many constraints of power supply and communication in in-vehicle systems, the vast majority of current image segmentation algorithms are implemented based on the deep learning model. Despite the ultrahigh segmentation accuracy, the problem of mesh artifacts and segmentation being too severe is obvious, and the high cost, computational, and power consumption devices required are difficult to apply in real-world scenarios. It is the focus of this paper to construct a road scene segmentation model with simple structure and no need of large computing power under the premise of certain accuracy. In this paper, the ESPNet (Efficient Spatial Pyramid of Dilated Convolutions for Semantic Segmentation) model is introduced in detail. On this basis, an improved ESPNet model is proposed based on ESPNet. Firstly, the network structure of the ESPNet model is optimized, and then, the model is optimized by using a small amount of weakly labeled and unlabeled scene sample data. Finally, the new model is applied to video image segmentation based on dash cam. It is verified on Cityscape, PASCAL VOC 2012, and other datasets that the algorithm proposed in this paper is faster, and the amount of parameters required is less than 1% of other algorithms, so it is suitable for mobile terminals.

1. Introduction

In recent years, CNN (Convolutional Neural Network) has made great progress in tasks such as image classification and object detection. The most important first step in these tasks is to predict the classification of each pixel in an image, and by segmenting the original image, researchers hopefully achieved accurate identification of what part of the image each pixel belongs to. It is very critical as the first step in computer vision applications. Some traditional methods, such as the Otsu (Maximum Between-Class Variance) method has been used with some success. The FCN (Full Convolutional Network) proposed by Long et al. [1] in 2015 opens up new avenues for image segmentation. The method trains an end-to-end network that uses a convolutional layer instead of an inner layer in a traditional network and can accept image input of any size. Based on the FCN, Chen et al. [2] added conditional random fields to further fine-grained optimization of the FCN model to improve the effect of

image segmentation of the boundaries, as the result of achieving 71.6% IOU (Intersection over Union) at the PASCAL VOC 2012 dataset. To address the accuracy problem of image edge information segmentation, Zheng et al. [3] suggested embedding CRF (Conditional Random Fields) as a Recurrent Neural Network (RNN) in FCNs. The average IOU of the PASCAL VOC 2012 dataset increased to 74.7% in the CRF-RNN (Conditional Random Fields-Recurrent Neural Networks) model. To address the problem of overfitting of small samples, the DenseNet (Densely Connected Convolutional Network) model of FCN can achieve the required accuracy without prior training and reduce the number of parameter to 1/10 of the original model, which has a broad application prospect in tasks such as automatic driving, medical images, and satellite images.

The remaining parts of this paper are organized as follows. In Section 2, we first review the ESPNet algorithm and model evaluation criteria. In Section 3, we provide some related work. Section 4 presents an improved ESPNet model.

Then, experiments are conducted in Section 5. Finally, the paper is concluded in Section 6.

2. Preliminaries

2.1. ESPNet. The ESPNet was introduced by Mehta et al. [4] in 2018, where a semantic segmentation network architecture featuring fast calculation and excellent effect of segmentation is presented in detail. ESPNet can be as fast as it achieves processing speeds of 112 frames per second on the GPU and up to 9 frames per second on edge devices. It is faster than the most well-known lightweight networks such as the MobileNet (Efficient Convolutional Neural Networks for Mobile Vision), ENet (a deep neural network architecture for real-time semantic segmentation), and ShuffleNet (an extremely efficient convolutional neural network for mobile) [5, 6], among others. With a loss of only 8% classification accuracy in the control model, ESPNet is only 1/180th as fast as its model parameters and 22 times faster than the best PSPNet (Pyramid Scene Parsing Network) architecture of the time. The design idea of convolutional factor decomposition is used in many deep CNN structures, such as Inception, ResNext (Residual Neural Network), Xception [7, 8], and others. Based on the basic idea of convolutional factor decomposition, the authors introduced a convolutional module called effective space pyramid in ESPNet which makes the network architecture fast, low power, and low latency, making it ideal for deployment in resource-constrained edge devices.

The basic network architecture of ESPNet is shown in Figure 1. In the model, the number of channels is reduced by point convolution and then sent to the convolution pyramid of the cavity. A larger receptive field is obtained by expanding convolution of different proportions, and feature fusion is carried out at the same time. Therefore, the number of parameters is very small. When the number of channels is reduced, the parameters of each expansion convolution are very few. The concatenation strategy is quite different from the ordinary method of feature fusion by expanding convolution. In order to avoid gridding artifacts [9], strategy of adding step by step is adopted. The main architecture of the ESPNet design is shown in Figure 1. The lightweight code-decoding network architecture is shown in Figure 2.

ESPNet can achieve an accuracy of 60.3% on the Cityscapes Dataset. Currently, for the application of deep convolutional neural networks in semantic segmentation tasks, the main means of model lightening include convolutional factor decomposition, network compression, low-bit networks, and sparse CNN [10–12]. Convolutional factor decomposition reduces the complexity of convolutional operations by breaking them down into several steps. ESPNet divides the convolutional layer in the network into point convolution and spatial pyramid-based dilated convolution based on the means of convolutional factor decomposition.

The dilated convolution means that holes are injected into the standard convolution operation to increase the size of the receptive field of the convolutional layer. Compared to conventional convolution operations, dilated convolution increases the hyperparameter of the dilation rate. This hyperparameter represents the number of intervals between kernels. The pairing of standard and dilated convolution operations is shown in Figure 3.

The main purpose of using dilated convolution is to solve the problem that the small object information in the image cannot be reconstructed due to the application of a large number of pooling layers in traditional deep CNN, thus affecting the resolution of the semantic segmentation model.

2.2. Model Evaluation Criteria

2.2.1. Accuracy. The accuracy of scene segmentation directly affects the safety performance of driving. The calculations are based on the following four criteria to provide a more comprehensive assurance of accuracy. The main evaluation criteria are shown in equations (1)–(4). These are the various forms of pixel accuracy evaluation. Pixel accuracy (PA) is the most intuitive calculation method for evaluating image segmentation algorithms, and its purpose is to represent the ratio of total pixels in the image of a pixel station with a correct prediction, calculated by the following formula:

$$PA = \frac{\sum_{i=0}^{k} P_{it}}{\sum_{i=0}^{k} \sum_{j=0}^{k} P_{ij}}. \tag{1}$$

Definition 1: mean pixel accuracy (MPA); calculating the ratio of the total number of correct pixels in each category to the total number of pixels in each category firstly, and then, finding the mean value of each category's PA, which is calculated as follows:

$$MPA = \frac{1}{k+1} \sum_{i=0}^{k} \frac{p_{ii}}{\sum_{j=0}^{k} p_{ij}}. \tag{2}$$

Definition 2: mean intersection over union (MIOU) [13]; calculating the intersection and union ratio to measure the advantages and disadvantages of the algorithm, it is one of the important evaluation indexes in the semantic segmentation model. Here, the intersection and union ratio is the ratio of overlap between the standard labeling of the dataset and the predicted segmentation. It is the calculation of the ratio between TP and TP + FN + FP. The MIOU is first calculated based on each category, and then, its mean value is calculated. The formula is as follows:

$$MIoU = \frac{1}{k+1} \sum_{i=0}^{k} \frac{p_{ii}}{\sum_{j=0}^{k} p_{ij} + \sum_{j=0}^{k} p_{ji} - P_{it}}. \tag{3}$$

Definition 3: frequency weighted intersection over union (FWIOU) [14]; assigning different weighting factors for each classification according to the
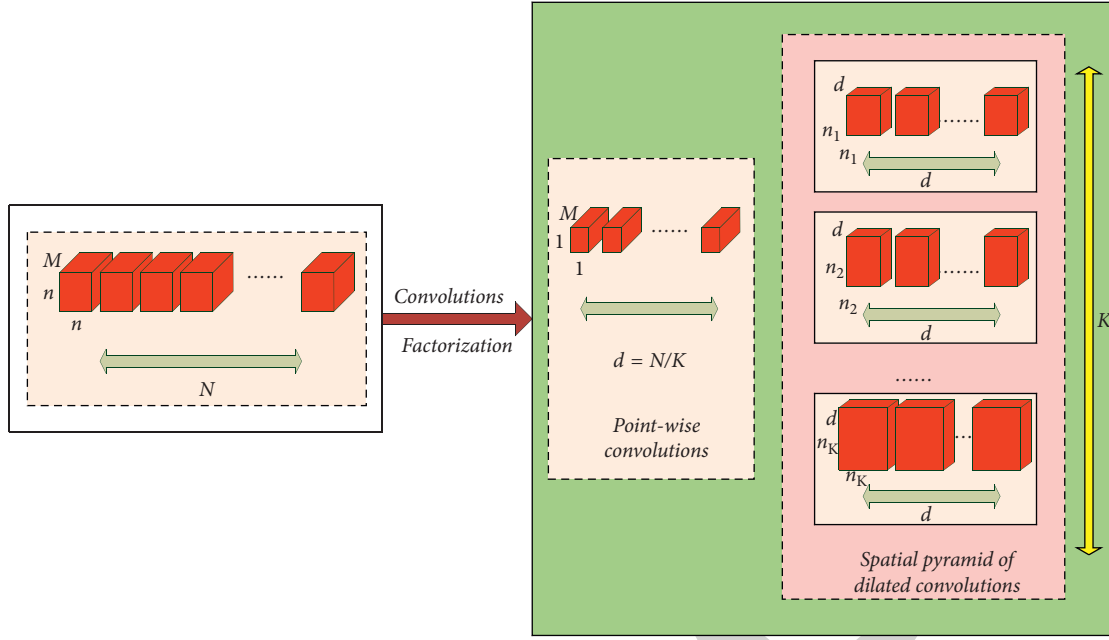
Figure 1: Basic network architecture of ESPNet.
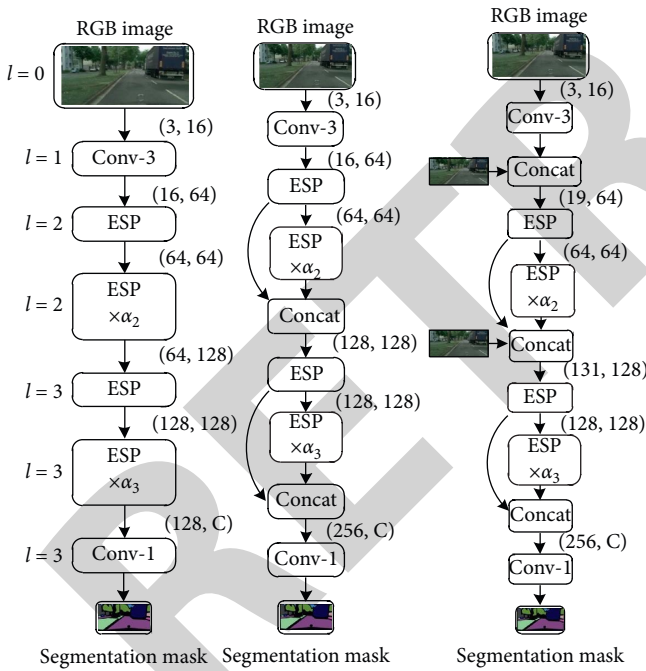
Figure 2: Main architecture of ESPNet.

frequency of each classification, it is an improved version of MIOU. The formula is as follows:

$$
\text{FWIoU} = \frac{1}{\sum_{i=0}^{k} \sum_{j=0}^{k} p_{ij}} \sum_{i=0}^{k} \frac{\sum_{j=0}^{k} p_{ij} p_{ii}}{\sum_{j=0}^{k} p_{ji} - P_{ii}}, \quad (4)
$$

where P_{ij} is the total number of pixels that belong to class i but are predicted to be class j and k indicates the total number of categories.

2.2.2. Latency. Latency represents the time of a CNN processing a single image and is usually evaluated by the number of frames processed per second. The latency rate is an important reference index for intelligent driving. Therefore, this paper adopts a distributed computing method to deal with the real-time image recognition analysis of roads, with the advantage of being able to label massive data to perform an optimal solution. It is calculated as follows:

$$
\min_{\theta \in \vartheta} \sum_{1}^{S} \frac{1}{N} \sum_{1}^{N} L\left(f_{\theta}^{s}(x_{i}^{s}), y_{i}^{s}\right) + \lambda \text{Reg}\left(f_{\theta}^{s}\right), \quad (5)
$$

where S is the number of replicas of the model to be optimized, i.e., the number of replicas of the model improved by the ESPNet model in this paper.

Network parameters represent the number of parameters to be learned in the neural network. The network size indicates the amount of storage space required to store the network. Sensitivity to GPU frequency is important for evaluating the computational power of the model. This is usually expressed as the ratio of the rate of change in execution time and the rate of change in GPU frequency. The higher this ratio, the better the ability of that deep learning application to utilize the GPU. Resource utilization refers to the ability to use a combination of CPU and GPU resources when running on an edge device [15]. In fact, edge computing devices such as the Jetson TX2 and the CPU and GPU share storage space.

3. Related Works

Many scholars have carried out useful research on image segmentation [16–27]. Zhao et al. [16] introduced horizontal crossover search (HCS) and vertical crossover search (VCS)

FIGURE 3: Conventional convolution on the left and dilated convolution on the right.

into the ACOR and improved the selection mechanism of the original ACOR to form an improved algorithm (CCACO) for the first time. Liu et al. [17] proposed a novel structure to fuse image and LiDAR point cloud in an end-to-end semantic segmentation network, in which the fusion is perfor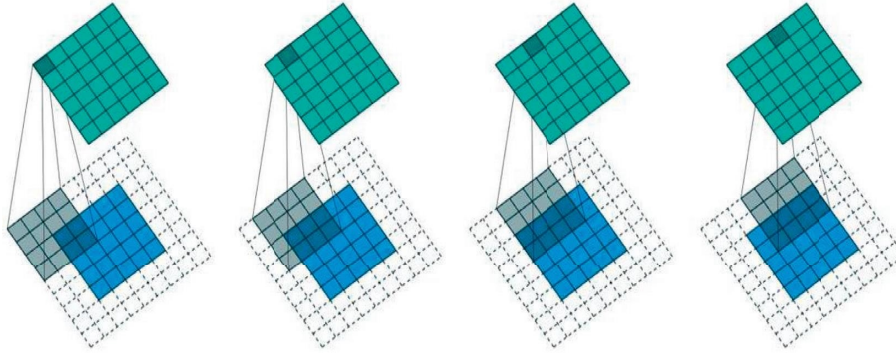med at the decoder stage instead of at, more commonly, the encoder stage. Ji et al. [18] proposed a new architecture of feature aggregation, which is designed to deal with the problem that the information of each convolutional layer cannot be used reasonably and the shallow layer information is lost in the process of transmission. Reis et al. [19] took advantage of the learned model in a deep architecture, by extracting side outputs at different layers of the network for the task of image segmentation. Parajuli et al. [20] performed pixel-wise segmentation to classify each pixel as road or nonroad based on color and depth features in a larger neighborhood context and described a cost-effective, modular, deep convolution network design. In order to improve the effect of image segmentation, directly at the deficiency of single seed point and fixed threshold of traditional region growing algorithm, a seed selection method based on the gray level of two-dimensional histogram and local variance is proposed, and the dynamic threshold is used to change the region growing rule [21]. Badrinarayanan et al. [22] presented a novel and practical deep fully convolutional neural network architecture for semantic pixel-wise segmentation termed SegNet. Akagic et al. [23] proposed an efficient unsupervised vision-based method for pothole detection without the process of training and filtering. Zhang et al. [24] adapted the multidimensional Haar-like features as well as the AdaBoost algorithm, to implement training of the cascade classifier, which will achieve the reliable vehicle detection.

In the past two years, some scholars have carried out useful research based on ESPNet [13–15, 28]. Kim and Heo [13] proposed ESCNet based on ESPNet architecture which is one of the state-of-the-art real-time semantic segmentation network that can be easily deployed on edge devices. Nuechterlein and Sachin [14] extended ESPNet, a fast and efficient network designed for vanilla 2D semantic segmentation, to challenging 3D data in the medical imaging domain.

4. Improvements Based on the ESPNet Model

In this section, we improve ESPNet, describe the core module that builds it, and compare the improved ESP module with similar CNN modules, such as Inception, ResNet, MobileNet, and ShuffleNet.

ESPNet is a decomposed form of convolution based on the Efficient Spatial Pyramid (ESP) module. It decomposes the standard convolution into spatial pyramids of point and unfolded convolution. The point convolution in the ESP module uses $1 * 1$ convolution to map high-dimensional features to low-dimensional space. The spatial pyramid of extended convolution resamples these low-dimensional feature maps simultaneously using K and $N * N$ extended convolution kernels. The expansion rate of each convolutional core is $2K - 1$ ($K = F1$). Based on this decomposition, the number of parameters and memory required for the ESP module is greatly reduced, while preserving a large effective receive domain $(n - 1) \, 2K - 1$. The pyramidal convolution operation is called a spatial expansion convolution pyramid.

Designed for fast semantic segmentation of high-resolution images with limited resource, ESPNet is efficient in terms of computational memory and power consumption and is 22 times faster than PSPNet [28] on the GPU, with 180 times smaller files and only 8% accuracy loss. ESPNet is validated on the Cityscapes, PASCAL VOC 2012, and other datasets and outperformed all current efficient CNN networks such as MobileNet, ShuffleNet, and ENet in both standard metrics and newly introduced performance metrics (measuring the efficiency of edge devices) under the same memory and compute conditions. ESPNet is fast, small, low power, and low latency to ensure a network with segmentation accuracy. The improved ESPNet model follows the principle based on convolution factor decomposition, as shown in Figure 4, and can be easily adopted to resource-constrained end devices based on the ESP module.

On the basis of extended convolution, the ASPP (Atrous Spatial Pyramid Pooling) module is introduced to realize multiscale information collection, and image level feature information is integrated in the existing ASPP module. ASPP uses four different expansion rates of extended convolution to capture multiscale information in parallel on the
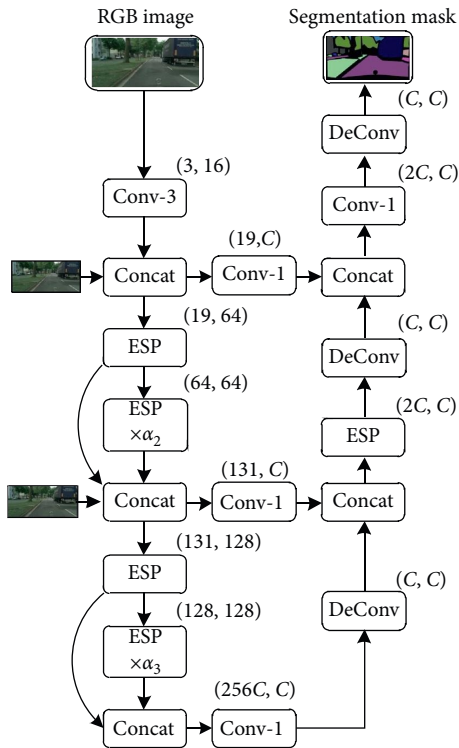
Figure 4: Basic structure of the improved model.

top-level feature responses of the backbone. The improved ASPP module gives the neurons a larger receptive field. The Pyramid Pooling Module (PPM) is introduced into the proposed ESPNet in DeepLab-v3 (Semantic Image Segmentation with Deep Convolutional Nets, Atrous Convolution, and Fully Connected CRFs). Thus, in aggregating the contextual semantic information of different regions, a better segmentation is obtained. The basic structure and working principle of the improved ESPNet model are shown in Figures 4 and 5.

It is well known that irrational use of void convolution can lead to mesh artifacts, and ESPNet's use of stacked convolutional structures with large void ratios is also easy to form artifacts [29]. This paper uses HFF (Hierarchical Feature Fusion) to enrich the use of void convolution and effectively reduce the formation of artifacts. The minimum $(n_1 * n_1)$ feature map of the hole kernel is directly output, and the hole kernel $(n_2 * n_2)$ feature map is output as a residual with the previous output. The summation is used as the output. Subsequent feature maps are similar to this operation to obtain fused features with different void rates, which are then stitched together and later form residuals with the original input. In summary, HFF ensures the quality of the output through the restriction of residuals in a way that stitches together different layers of feature maps, preserving local details and global semantic features. The HFF structure allows the use of large void-rate convolution kernels, speeding up the extraction of semantic features. The decoder is similar to UNet (Convolutional Networks for Biomedical Image Segmentation), which uses layer-by-layer up-sampling, hopping connection, and restoring detailed

information. Because of the fusion method of residual calculation, we use the PreLU activation function and finally connect softmax for network training.

4.1. Activate Function Module. In this paper, scene segmentation experiments are conducted using a variety of different activation functions based on ESPNet to investigate which type of activation function can lead to better network performance improvement for CNN. In this section, pairs of functions of different forms of Maxout, Tanh, ReLU, ELU, and PreLU are used as activation functions for neural networks [30, 31], respectively, while extensive comparative experiments are conducted. The experiments on activation function selection are performed on the PASCAL VOC 2012 dataset. Based on the variation in segmentation accuracy observed in this paper, the advantages and disadvantages of different activation functions throughout the training process were deeply studied.

An intuitive idea is to apply softmax to each weight [32], such that all weights are normalized to a probability with values ranging from 0 to 1, indicating the importance of each input. However, as shown in our previous studies, the additional softmax results in a significant slowdown in the GPU hardware. In order to minimize the cost of the additional delay, we further propose a fast fusion method. The formula is shown in the following equation:

$$O = \sum_i \frac{e^{w_i}}{\sum_j e^{w_j}} \cdot I_i. \tag{6}$$

4.2. Pooling Module. Figure 6 explains the principle of the pooling approach with the aim of analyzing the impact of different pooling approaches on the performance of this paper's scene segmentation network. In this paper, three approaches, average pooling, max pooling, and random sampling pooling [33], are investigated in depth, and comparative experiments are conducted.

Different pooling layers in ESPNet are used to compare and analyze the average pooling (Mean), max pooling (Max), and random pooling (Stoh) on the network performance with three different pooling layer structures. Figure 6 shows the change of accuracy during the iteration of ESPNet with different pooling layers. The x-axis edge is the number of iterations, and the y-axis represents the accuracy [34, 35]. To more clearly compare the training of the network under the three pooling layers, Figure 7 shows only the change in accuracy during the beginning rounds of iteration. In this paper, various pooling methods are further analyzed, and local pixel maxima are often extracted as feature points in traditional image features such as textures and gradients because these local extreme points are better able to describe the edge information of the image.

The function of the maximization operation is that whenever a feature is extracted in any quadrant, it is retained in the maximized pooled output. So what the maximization operation actually does is that if a feature is extracted in the
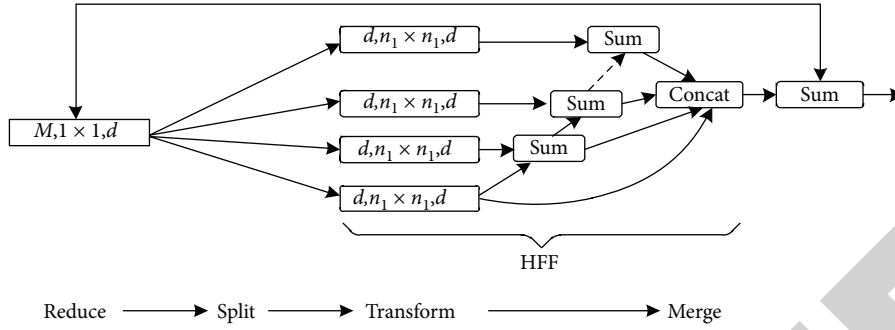
FIGURE 5: Schematic diagram of the improved model.
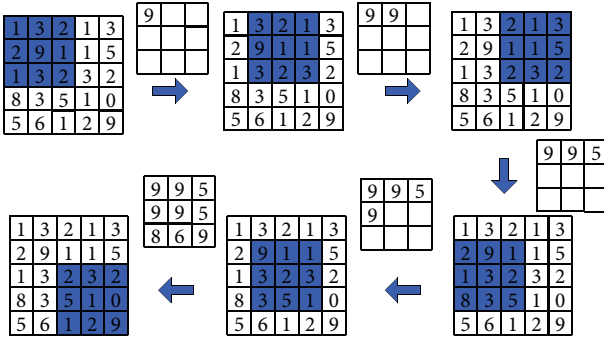
FIGURE 6: Pooling layer basic mode diagram.
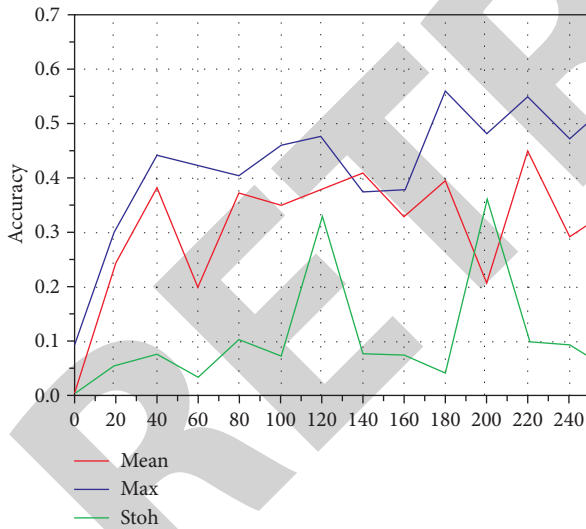
FIGURE 7: Comparison of basic approaches to pooling layers.

filter, then the maximum value is preserved. If this feature is not extracted, it may not exist in the upper right quadrant, and the maximum value of it is still small, which is an intuitive understanding of max pooling.

It can be seen that when there are several examples of superparameters and the input is a $5 * 5$ matrix, we use max pooling. The filter parameter is $3 * 3$, i.e., f is 3, the step is 1, i.e., s is 1, and the output matrix is $3 * 3$. The same formula for calculating the output size of the convolutional layer

described earlier also applies to the max pooling, as shown in the following equation:

$$S = n + 2p - f s + 1. \qquad (7)$$

In Section 5, all experiments are conducted on the PASCAL VOC 2012 dataset. To search for a more suitable semantic segmentation for urban road scenarios, we studied the accuracy of the proposed model for image segmentation and the influence of various pooling methods on the model.

5. Experimental Classification Results and Analysis

5.1. Common Dataset.

> *PASCAL VOC 2012 Dataset.* This set contains 20 object categories, and the training sample contains 11,530 images. This includes 27,450 regions of interest for labeled object types and 6,929 semantic segmentation regions.

> *Cityscapes Dataset.* This set is derived from a large number of video sequences recorded from streets in different cities, covering the 50 cities in spring, summer, and autumn, mainly in Germany and neighbouring countries. By using camera systems and postprocessing that represent the current state-of-the-art in the automotive field, a total of 5,000 images with high quality pixel-level labeled fine images and 20,000 additional images with coarse labels were obtained.

5.2. Experimental Environment.
Considering that the scene objects are mainly partitioned within the city, their driving speed and equipment costs are limited, so the experimental equipment in this paper hardware and software are matched to ensure low latency and high efficiency while avoiding the use of costly equipment. Therefore, the experimental environment setup is shown in Table 1.

5.3. Experimental Results on the Cityscapes Dataset.
Figure 8 describes the experimental results on the Cityscapes Dataset.

TABLE 1: Experimental environment configuration table.

CPU	Intel core i5-6200K
RAM	16G
Operating system	Ubuntu 16.04
Display card (computer)	GTX 1080Ti
PyTorch	1.2.0
Python	3.7.1
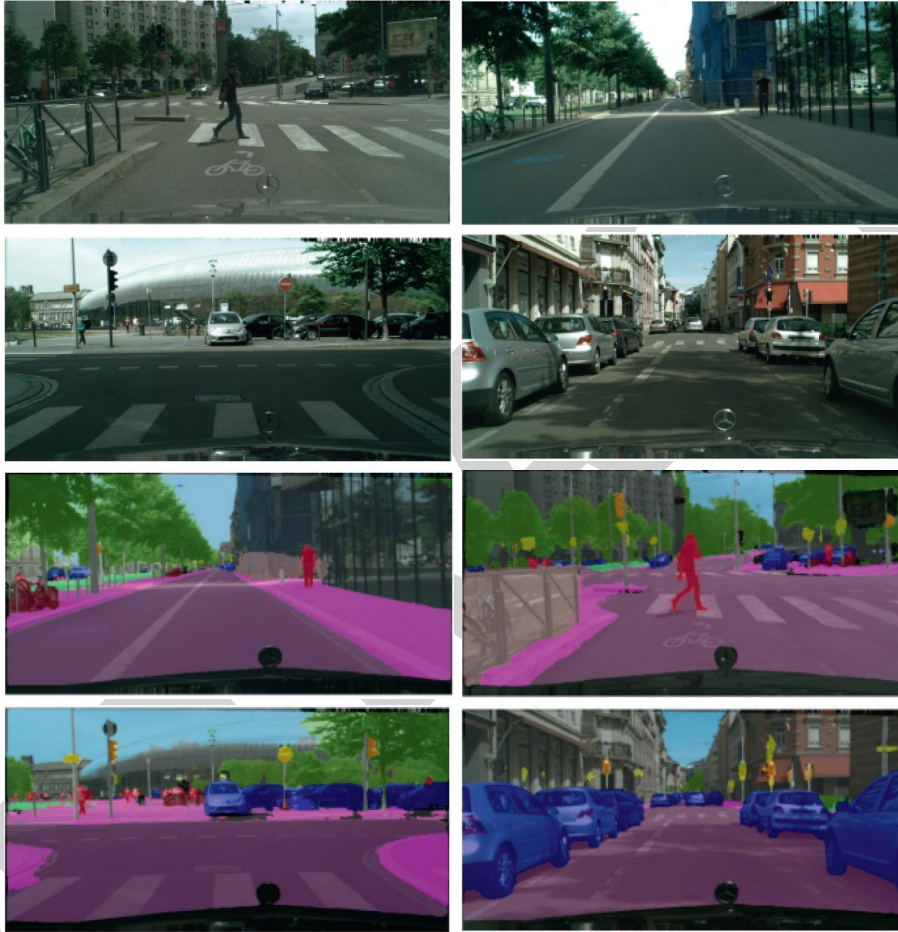
FIGURE 8: Plot of Cityscapes experimental segmentation results.

5.4. Experimental Results on the PASCAL VOC 2012 Dataset.

Since most data of the PASCAL VOC 2012 dataset is not obtained from the camera loaded on the vehicle, it is moderately effective when using the proposed model in this paper for identification. The data and results of this experiment are shown in Table 2 and Figure 9, respectively. The upper part of the results is the original image, and the lower part is the segmentation result. Although the data segmentation results are missing compared to the Cityscapes Dataset, the overall object segmentation is basically correct.

For the characteristics of more pedestrians and vehicles on the road, this paper adjusts the type distribution of PASCAL VOC 2012 dataset to ensure the maximum number of pedestrian and vehicle data and appropriately reduces other type of data, so as to obtain more targeted experimental results to illustrate the segmentation effect of the model on the urban road scene.

5.5. Experimental Results on Self-Selected Data.

This section shows the segmentation results of the road scene segmentation model designed in this paper in a continuous video. Two frames with an interval of about 1 second are extracted for illustration. The results are shown in Figure 10. It can be seen that the network designed in this paper has high accuracy and generalization ability in road segmentation and can identify the existence of obstacles on the road ahead in good prospects for application on road obstacle prediction for driving assistance.

Table 2: Experiment data table of PASCAL VOC 2012.

	Training set		Test set		Training set 1		Test set 1	
	Images	Object	Images	Object	Images	Object	Images	Object
Aeroplane	112	151	126	155	238	306	204	285
Bicycle	116	176	127	177	243	353	239	337
Bus	97	115	89	114	186	229	174	213
Car	376	625	337	625	713	1250	721	1201
Horse	139	182	148	180	287	362	274	348
Motorbike	120	167	125	172	245	339	222	325
Person	1025	2358	983	2332	2008	4690	2007	4528
Total	1985	3774	1935	3755	3920	7529	3841	7237
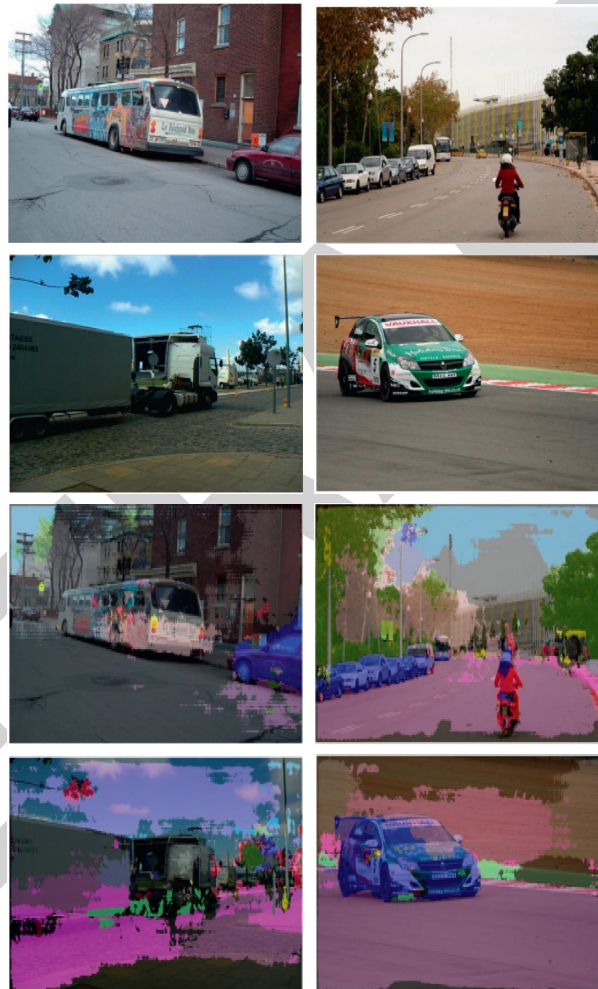
Figure 9: Experimental segmentation result graph of PASCAL VOC 2012.

5.6. Test of Different Activation Function. In this paper, different activation functions are used in ESPNet to test the effect of different activation functions on the training results. The activation functions tested are Maxout, Tanh, ReLU, ELU, and PReLU. In this paper, we document the changes in the training sample segmentation accuracy metric during the iterative process, and the experimental results are shown in Figure 11 with the *x*-axis of the figure indicating the number of iterations and the *y*-axis indicating the accuracy.

In terms of final accuracy, better experimental results were obtained using ESPNet with ELU and PReLU. However, throughout the iterations, the ELU model fluctuates sharply several times during the iterations, and the accuracy of the ascension process is slow. In contrast, the accuracy of the PReLU model improves rapidly to near the peak during iteration, and there are some fluctuations after that; the whole iterative process always maintains the highest accuracy level in the same period.

FIGURE 10: Comparison of two frames of self-selected data.
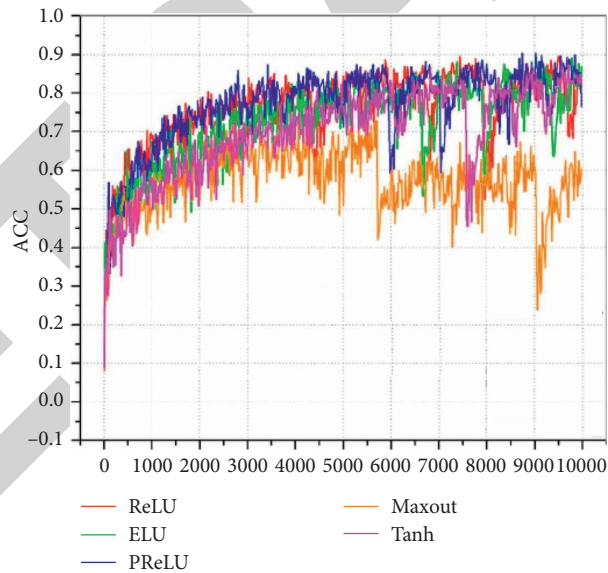
FIGURE 11: Comparison of experimental results for activation functions.

5.7. Comparison of Approaches to Pooling Layers. Edge segmentation is important for semantic segmentation, especially in semantic segmentation oriented towards road scene understanding. This paper argues that the reason why max pooling can achieve better segmentation is related to its ability to preserve better boundary information. The experimental results are shown in Figure 7, indicating that the model with the max pooling layer (MAX) exhibits better segmentation results.

5.8. Comparison of the Proposed Model and Common Models. Provided with the same memory and calculation condition, performance of the proposed model is superior to some efficient convolutional neural networks under the standard metrics and introduced performance metrics, with the test results given in Table 3.

Referring to Table 3, the amount of parameters involved in the paper is very small, and the recognition and segmentation are fast.

TABLE 3: Comparison of experimental results.

	This paper	SegNet	RefineNet	DeepLab	PSPNet	LRR	Dilation-8	FCN-8s
Params	0.364	29.5	42.6	44.04	65.7	48	141.13	134.5
MIOU	80.01	59.10	82.40	79.70	85.40	79.30	75.30	67.20

Note: parameter unit: millions; velocity unit: frames per second (fps).

6. Conclusions

Image segmentation consists of creating partitions within an image into meaningful areas and objects. It can be used in scene understanding and recognition, in fields such as biology, medicine, robotics, and satellite imaging, amongst others. This paper focuses on ESPNet as the underlying network structure and proposed an improved ESPNet model based on ESPNet to optimize the segmental results of road scenes. The proposed model in this paper is verified on Cityscape, PASCAL VOC 2012, and other datasets. Under the same memory and computing conditions, its performance is better than some efficient convolutional neural networks in the standard metrics and the newly introduced performance metrics. In the processing of high-resolution images, it has the characteristics of fast, small size, low power consumption, and low delay and ensures the segmentation accuracy. Although the proposed method in this paper has achieved good experimental results, there is also the problem of high accuracy that cannot achieve nonreal-time performance. The main reason may be the fuzziness and unclear boundary semantics caused by less parameters in the aspect of pooling layer and HFF feature fusion.

Data Availability

The experimental datasets used in this work are publicly available, and the bundled data and code of this work are available from the corresponding author upon request.

Conflicts of Interest

The authors declare that they have no conflicts of interest.

Acknowledgments

References

[1] J. Long, E. Shelhamer, and T. Darrell, "Fully convolutional networks for semantic segmentation," 2014, https://arxiv.org/abs/1411.4038.

[2] L.-C. Chen, J. Barron, G. Papandreou et al., "Semantic image segmentation with task-specific edge detection using CNNs and a discriminatively trained domain transform," 2015, https://arxiv.org/abs/1511.03328.

[3] S. Zheng, S. Jayasumana, B. Romera-Paredes et al., "Conditional random fields as recurrent neural networks," in *Proceedings of the IEEE International Conference on Computer Vision*, Santiago, Chile, December 2015.

[4] S. Mehta, M. Rastegari, A. Caspi et al., "ESPNet: efficient spatial pyramid of dilated convolutions for semantic segmentation," 2018, https://arxiv.org/abs/1803.06815.

[5] M. Siam, M. Gamal, M. Abdel-Razek et al., "Rtseg: real-time semantic segmentation comparative study," in *Proceedings of the 25th IEEE International Conference on Image Processing (ICIP)*, Athens, Greece, October 2018.

[6] X. Zhang, X. Zhou, M. Lin et al., "Shufflenet: an extremely efficient convolutional neural network for mobile devices," in *Proceedings of the IEEE Conference on Computer Vision and Pattern Recognition*, Salt Lake City, UT, USA, June 2018.

[7] F. Chollet, "Xception: deep learning with depthwise separable convolutions," in *Proceedings of the IEEE Conference on Computer Vision and Pattern Recognition*, Honolulu, HI, USA, July 2017.

[8] A. Rosebrock, *ImageNet: VGGNet, ResNet, Inception, and Xception with Keras*, Springer, Berlin, Germany, 2017.

[9] L. Gómez-Chova, R. Zurita-Milla, and L. Alonso, "Gridding artifacts on medium-resolution satellite image time series: MERIS case study," *IEEE Transactions on Geoscience and Remote Sensing*, vol. 49, no. 7, pp. 2601–2611, 2011.

[10] K. Ullrich, E. Meeds, and M. Welling, "Soft weight-sharing for neural network compression," in *Proceedings of the International Conference on Representation Learning (ICLR)*, Toulon, France, April 2017.

[11] R. Gong, X. Liu, S. Jiang et al., "Differentiable soft quantization: bridging full-precision and low-bit neural networks," in *Proceedings of the IEEE International Conference on Computer Vision*, Seoul, South Korea, 2019.

[12] H. Zhou, J. Alvarez, and F. Porikli, "Less is more: towards compact cnns," in *Proceedings of the European Conference on Computer Vision*, Amsterdam, Netherlands, October 2016.

[13] J. Kim and Y. S. Heo, "Efficient semantic segmentation using spatio-channel dilated convolutions," *IEEE Access*, vol. 7, pp. 154239–154252, 2018.

[14] N. Nuechterlein and M. Sachin, "3D-ESPNet with pyramidal refinement for volumetric brain tumor image segmentation," *Lecture Notes in Computer Science*, vol. 11384, pp. 245–253, 2018.

[15] D. Franklin, "Nvidia jetson TX2 delivers twice the intelligence to the edge," 2017, https://developer.nvidia.com/blog/jetson-tx2-delivers-twice-intelligence-edge/.

[16] D. Zhao, L. Liu, F. Yu et al., "Ant colony optimization with horizontal and vertical crossover search: fundamental visions for multi-threshold image segmentation," *Expert Systems with Applications*, vol. 167, pp. 1–45, 2021.

[17] H. Liu, Y. Yao, Z. Sun et al., "Road segmentation with image-LiDAR data fusion in deep neural network," *Multimedia Tools and Applications*, vol. 79, no. 47-48, pp. 35503–35518, 2020.

WILEY | Hindawi

Retraction

Retracted: Analysis of Economic Relationship Using the Concept of Complex Pythagorean Fuzzy Information

Security and Communication Networks

This article has been retracted by Hindawi following an investigation undertaken by the publisher [1]. This investigation has uncovered evidence of one or more of the following indicators of systematic manipulation of the publication process:

(1) Discrepancies in scope

(2) Discrepancies in the description of the research reported

(3) Discrepancies between the availability of data and the research described

(4) Inappropriate citations

(5) Incoherent, meaningless and/or irrelevant content included in the article

(6) Manipulated or compromised peer review

The presence of these indicators undermines our confidence in the integrity of the article's content and we cannot, therefore, vouch for its reliability. Please note that this notice is intended solely to alert readers that the content of this article is unreliable. We have not investigated whether authors were aware of or involved in the systematic manipulation of the publication process.

Wiley and Hindawi regrets that the usual quality checks did not identify these issues before publication and have since put additional measures in place to safeguard research integrity.

We wish to credit our own Research Integrity and Research Publishing teams and anonymous and named external researchers and research integrity experts for contributing to this investigation.

The corresponding author, as the representative of all authors, has been given the opportunity to register their agreement or disagreement to this retraction. We have kept a record of any response received.

References

[1] N. Jan, S. U. Rehman, A. Nasir, H. Aydi, and S. U. Khan, "Analysis of Economic Relationship Using the Concept of Complex Pythagorean Fuzzy Information," *Security and Communication Networks*, vol. 2021, Article ID 4513992, 12 pages, 2021.

WILEY | Hindawi

Research Article

Analysis of Economic Relationship Using the Concept of Complex Pythagorean Fuzzy Information

Naeem Jan [ID],[1] **Saif Ur Rehman** [ID],[1] **Abdul Nasir,**[1] **Hassen Aydi** [ID],[2,3,4] **and Sami Ullah Khan** [ID][1]

[1]*Department of Mathematics, Gomal University, Dera Ismail Khan 29050, Pakistan*
[2]*Université de Sousse, Institut Supérieur d'Informatique et des Techniques de Communication, H. Sousse 4000, Tunisia*
[3]*Department of Mathematics and Applied Mathematics, Sefako Makgatho Health Sciences University, Ga-Rankuwa, South Africa*
[4]*China Medical University Hospital, China Medical University, Taichung 40402, Taiwan*

Correspondence should be addressed to Hassen Aydi; hassen.aydi@isima.rnu.tn

Fuzzy set theory and fuzzy logics are the powerful mathematical tools to model the imprecision and vagueness. In this research, the novel concept of complex Pythagorean fuzzy relation (CPFR) is introduced. Furthermore, the types of CPFRs are explained with appropriate examples such as CPF composite relation, CPF equivalence relation, CPF order relation, and CPF equivalence classes. Moreover, numerous results and interesting properties of CPFRs are discussed in detail. Furthermore, the impacts of economic parameters over each other are studied through the proposed concepts of CPFRs. In addition, the application also discusses the effects of economic parameters of one country over the other countries' economic parameters.

1. Introduction

In 1965, Zadeh [1] initiated the concepts of fuzzy sets (FSs). A FS is characterized by a mapping whose range is the unit interval [0, 1]. This mapping is called a degree of membership. Zadeh's FS theory is used to model imprecise information and vagueness. Later in 1986, Atanassov [2] introduced the notion of intuitionistic fuzzy sets (IFSs). An IFS is a collection of objects characterized by a pair of mappings whose values range are between 0 and 1. These mappings represent the degree of membership and the degree of nonmembership of the object. Moreover, the sum of both the degrees of membership and nonmembership in an IFS must not exceed 1. This limitation persuaded Yager [3] to introduce a modified version of IFS, called a Pythagorean fuzzy set (PFS). Like IFSs, PFSs also consist of the degree of membership and the degree of nonmembership that attain values from the unit interval [0, 1] provided that the sum of squares of both the degrees does not exceed 1. Deschrijver and Kerre [4] wrote on the relationships

between some extensions of FS theory. Maiers and Sherif [5] proposed the applications of FS theory. Klir [6] worked on FS interpolation of possibility theory. De et al. [7, 8] discussed some operations on IFSs and provided an application of IFSs in medical diagnosis. Szmidt and Kacprzyk [9] measured distance between IFSs. Peng et al. [10, 11] conceived some results for PFSs and provided an application.

Ramot et al. [12] initiated the concept of complex fuzzy sets (CFSs). A CFS is characterized by the degree of membership that is a complex valued mapping, whose range is a unit circle in the complex plane. Since a complex number is a combination of real and imaginary numbers, the degree of membership is expressed in the polar form as $\eta_{\mathbb{C}}(\hbar)e^{\xi_{\mathbb{C}}(\hbar)2\pi i}$, where $\eta_{\mathbb{C}}(\hbar)$ and $\xi_{\mathbb{C}}(\hbar)$ are the real numbers from the unit interval. $\eta_{\mathbb{C}}(\hbar)$ is known as the amplitude term and $\xi_{\mathbb{C}}(\hbar)$ is known as the phase term. Therefore, a CFS is capable to model problems having a periodic nature. Alkouri and Salleh [13] introduced the concept of complex intuitionistic fuzzy sets (CIFSs). These sets comprise of a pair of complex valued degrees of membership and degree of

nonmembership. Both the degrees attain values from a unit circle in a complex plane provided that their sum also lied within the unit circle. In other words, the sum of amplitude terms lies in the unit interval, and the sum of both the phase terms also lies in [0, 1]. Ullah et al. [14] amended the concept of CIFSs and provided the notion of complex Pythagorean fuzzy set (CPFS). These sets also discuss the complex valued degrees of membership and nonmembership provided that both the degrees and the sum of their squares lie within the unit circle of complex plane. Yazdanbakhsh and Dick [15] carried out a systematic review of CFSs and logics. Tamir et al. [16, 17] provided the axiomatic theory of CF logics and the applications of CFS and CF logics. Rani and Garg [18] proposed the distance measures between CIFSs and applied them to decision-making processes. Ngan et al. [19] represented CIFS by quaternion numbers and applied them to decision-making. Yaqoob et al. [20] applied the concept of IFSs to cellular network provider companies. Dick et al. [21] wrote on Pythagorean and CFS operations. Ma et al. [22] worked on the group decision-making framework by CPF information, and Bi et al. [23] introduced the CF arithmetic aggregation operators.

The set relations have various applications in mathematics, engineering, social sciences, and many other fields. Klir and Folger [24] defined the crisp relations (CRs). Several types of relations, such as inverse relation, reflexive relation, symmetric relation, transitive relation, composite relation, and equivalence relation, are defined. Mendel [25] initiated the theory of fuzzy relations (FRs). The plus point of FRs is that these relations indicate the grade of the relationship by the degree of membership. Burillo et al. [26] instigated the notion of intuitionistic fuzzy relations (IFRs). These relations not only discuss the degree of membership of the relationship but also deliberate the degree of nonmembership. Bhattacharya and Mukherjee [27] discussed the FRs and fuzzy groups. Yeh and Bang [28] presented the FRs and fuzzy graphs and applied these notions in clustering analysis. Blin [29] proposed FRs in group decision theory. Deschrijver and Kerre [30] worked on the composition of IFRs. Bustince and Burillo [31] gave structures on IFRs. Bustince [32] constructed the IFRs with predetermined properties, and Naz et al. [33] came up with a novel approach to decision-making with PF information. Alshammari et al. [34] presented the topological structure of CPFSs, and Dinakaran [35] analyzed the online food delivery industries using PFRs and composition.

This article proposes a novel concept of complex Pythagorean fuzzy relation (CPFR). The CPFRs consider the degrees of membership and nonmembership of any relation between the elements of CPFSs. Moreover, the complex nature of the relation allows to model problems with phase changes, such as periodicity. Although IFRs also cover both the degrees of membership as well as nonmembership, but they restrict the choice of numbers that could be assigned to the members of sets. For example, we cannot assign the membership degree $0.7e^{0.5}$ when the degree of nonmembership is $0.4e^{0.6}$ because the sum of amplitude terms exceeds 1, i.e., $0.7 + 0.4 = 1.1$. The same applies for the phase terms that their sum must not exceed 1. But, the advantage of

proposed structure is that it eases these constraints by some modifications. It expands the choice of numbers to be assigned as the degrees. Furthermore, the types of CPFRs are explained with appropriate examples. Some of the types include CPF irreflexive relations, CPF antisymmetric relations, CPF equivalence relations, CPF order relations, and CPF equivalence classes. Additionally, some unique and interesting properties and results are achieved. Finally, in the support of the proposed work, an application is provided that helps in the investigation of quality of relationships among different economic indicators and the impacts that each economic parameter has on the other rest of the economic parameters. These concepts can be stretched to other frameworks of the fuzzy set theory which will give rise to many interesting structures. The range of applications of these complex natured structures might be so vast, since they can deal with problems that have multiple dimensions. In future, we would be looking to apply these notions to study the security and communication networks.

The study is arranged in the following way: Section 1 presents the introduction and the literature review. Section 2 reviews some of the predefined concepts that are used in current study. In Section 3, the complex Pythagorean fuzzy relations (CPFRs) and their types are discussed along with examples. Additionally, some results of the proposed relations have also been proved. The Section 4 proposes an application of CPFRs and its types for the investigation of direct and indirect effects of economic factors of one country on other countries. Finally, in Section 5, the research work is concluded.

2. Preliminaries

This section enlightens some related prerequisites such as fuzzy set (FS), complex fuzzy set (CFS), intuitionistic fuzzy set (IFS), complex intuitionistic fuzzy set (CIFS), Pythagorean fuzzy set (PFS), and complex Pythagorean fuzzy set (CPFS). Moreover, the Cartesian product and relations in above sets are also described with some examples.

Definition 1 (see [1]). Let $\ddot{\mathscr{B}}$ be a universal set. Then, a set $\ddot{\mathbb{H}}$ on $\mathscr{B}$ is said to be an FS if it is of the form

$$\ddot{\mathbb{H}} = \left\{ \hbar_1, m(\hbar_1) | \hbar_1 \in \ddot{\mathscr{B}} \right\}, \tag{1}$$

where $m(\hbar_1)$ is a fuzzy valued mapping, i.e., $m: \ddot{\mathscr{B}} \longrightarrow [0, 1]$ and symbolizes the membership degree of the FS $\ddot{\mathbb{H}}$.

Definition 2 (see [12]). Let $\ddot{\mathscr{B}}$ be a universal set. Then, a set $\ddot{\mathbb{H}}$ on $\mathscr{B}$ is said to be CFS if it is of the form

$$\ddot{\mathbb{H}} = \left\{ \hbar_1, m_{\ddot{\mathbb{H}}_c}(\hbar_1) | \hbar_1 \in \ddot{\mathscr{B}} \right\}, \tag{2}$$

where $m_{\ddot{\mathbb{H}}_c}(\hbar_1)$ is a complex valued mapping which symbolizes the membership degree of the CFS $\ddot{\mathbb{H}}$. This mapping $m_{\ddot{\mathbb{H}}_c}(\hbar_1)$ is defined as

$$m_{\ddot{\mathbb{H}}_c} : \ddot{\mathscr{B}} \longrightarrow \{\Upsilon | \Upsilon \in \mathbb{C}, |\Upsilon| \leq 1\}, \qquad (3)$$

where $\mathbb{C}$ is the set of complex numbers, thus

$$\Upsilon(\hbar_1) = \alpha + i\beta, \qquad (4)$$

or

$$\Upsilon(\hbar_1) = \eta_{\mathbb{C}}(\hbar_1) e^{\xi_{\mathbb{C}}(\hbar_1) 2\pi i}, \quad \text{where } \eta_{\mathbb{C}}(\hbar_1), \xi_{\mathbb{C}}(\hbar_1) \in [0, 1]. \qquad (5)$$

Definition 3 (see [16]). Let $\ddot{\mathbb{H}} = \left\{ \hbar_j, m_{\ddot{\mathbb{H}}_C}(\hbar_j) | \hbar_j \in \ddot{\mathscr{B}} \right\}$ and $\ddot{\mathbb{K}} = \left\{ \hbar_k, m_{\ddot{\mathbb{K}}_C}(\hbar_k) | \hbar_k \in \ddot{\mathscr{B}} \right\}$, $j, k \in \mathbb{N}$, be two CFS on the universal set $\ddot{\mathscr{B}}$ with the membership degrees symbolized by the complex valued mappings $m_{\ddot{\mathbb{H}}_C}$ and $m_{\ddot{\mathbb{K}}_C}$, respectively. Then, the Cartesian product of $\ddot{\mathbb{H}}$ and $\ddot{\mathbb{K}}$ is denoted and defined as

$$\ddot{\mathbb{H}} \times \ddot{\mathbb{K}} = \left\{ (\hbar_j, \hbar_k), m_{(\ddot{\mathbb{H}} \times \ddot{\mathbb{K}})_C}(\hbar_j, \hbar_k), | \hbar_j \in \ddot{\mathbb{H}}, \hbar_k \in \ddot{\mathbb{K}} \right\}, \quad (6)$$

where the mapping $m_{(\ddot{\mathbb{H}} \times \ddot{\mathbb{K}})_C} : \ddot{\mathbb{H}} \times \ddot{\mathbb{K}} \longrightarrow \{\Upsilon | \Upsilon \in \mathbb{C}, |\Upsilon| \leq 1\}$ symbolizes the membership degree of the product $\ddot{\mathbb{H}} \times \ddot{\mathbb{K}}$ and is defined as

$$m_{(\ddot{\mathbb{H}} \times \ddot{\mathbb{K}})_C}(\hbar_j, \hbar_k) \leq \min \left\{ m_{\ddot{\mathbb{H}}_C}(\hbar_j), m_{\ddot{\mathbb{K}}_C}(\hbar_k) \right\}. \qquad (7)$$

Since $m_{(\ddot{\mathbb{H}} \times \ddot{\mathbb{K}})_C}$ is a complex valued mapping, one writes

$$\Upsilon(\hbar_j, \hbar_k) = \alpha_{jk} + i\beta_{jk}, \qquad (8)$$

or

$$\Upsilon(\hbar_j, \hbar_k) = \eta_{(\ddot{\mathbb{H}} \times \ddot{\mathbb{K}})_C}(\hbar_j, \hbar_k) e^{\xi_{(\ddot{\mathbb{H}} \times \ddot{\mathbb{K}})_C}(\hbar_j, \hbar_k) 2\pi i}$$
$$= \min \left\{ \eta_{\ddot{\mathbb{H}}_C}(\hbar_j), \eta_{\ddot{\mathbb{K}}_C}(\hbar_k) \right\} e^{\min \left\{ \xi_{\ddot{\mathbb{H}}_C}(\hbar_j), \xi_{\ddot{\mathbb{K}}_C}(\hbar_k) \right\} 2\pi i}, \qquad (9)$$

where $\eta_{(\ddot{\mathbb{H}} \times \ddot{\mathbb{K}})_C}(\hbar_j, \hbar_k), \xi_{(\ddot{\mathbb{H}} \times \ddot{\mathbb{K}})_C}(\hbar_j, \hbar_k) \in [0, 1]$.

Definition 4 (see [16]). Let $\ddot{\mathbb{H}} = \left\{ \hbar_j, m_{\ddot{\mathbb{H}}_C}(\hbar_j) | \hbar_j \in \ddot{\mathscr{B}} \right\}$ and $\ddot{\mathbb{K}} = \left\{ \hbar_k, m_{\ddot{\mathbb{K}}_C}(\hbar_k) | \hbar_k \in \ddot{\mathscr{B}} \right\}$ be two CFSs on $\ddot{\mathscr{B}}$. Then, a fuzzy relation (FR) $\mathbb{R}$ is any subset of the product $\ddot{\mathbb{H}} \times \ddot{\mathbb{K}}$. It is denoted and defined as

$$\mathbb{R} = \left\{ (\hbar_j, \hbar_k), m_{\mathbb{R}_C}(\hbar_j, \hbar_k) | (\hbar_j, \hbar_k) \in \ddot{\mathbb{H}} \times \ddot{\mathbb{K}} \right\}, \qquad (10)$$

where $m_{\mathbb{R}_C}(\hbar_j, \hbar_k)$ symbolizes the membership degree of FR $\mathbb{R}$ and

$$m_{\mathbb{R}_C}(\hbar_j, \hbar_k) = m_{(\ddot{\mathbb{H}} \times \ddot{\mathbb{K}})_C}(\hbar_j, \hbar_k). \qquad (11)$$

Example 1. Consider a CFS $\ddot{\mathbb{H}}$ on $\ddot{\mathscr{B}}$.

$$\ddot{\mathbb{H}} = \left\{ (\hbar_1, 0.8 e^{(0.5)2\pi i}), (\hbar_2, 0.3 e^{(0.6)2\pi i}), (\hbar_3, 0 e^{(1)2\pi i}) \right\}. \qquad (12)$$

The Cartesian product $\ddot{\mathbb{H}} \times \ddot{\mathbb{H}}$ is

$$\ddot{\mathbb{H}} \times \ddot{\mathbb{H}} = \left\{ \begin{array}{l} ((\hbar_1, \hbar_1) 0.8 e^{(0.5)2\pi i}), ((\hbar_1, \hbar_2) 0.3 e^{(0.5)2\pi i}), ((\hbar_1, \hbar_3) 0 e^{(0.5)2\pi i}), \\ ((\hbar_2, \hbar_1) 0.3 e^{(0.5)2\pi i}), ((\hbar_2, \hbar_2) 0.3 e^{(0.6)2\pi i}), ((\hbar_2, \hbar_3) 0 e^{(0.6)2\pi i}), \\ ((\hbar_3, \hbar_1) 0 e^{(0.5)2\pi i}), ((\hbar_3, \hbar_2) 0 e^{(0.6)2\pi i}), ((\hbar_3, \hbar_3) 0 e^{(1)2\pi i}), \end{array} \right\}. \qquad (13)$$

The CFR $\mathbb{R}$ is

$$\mathbb{R} = \left\{ ((\hbar_1, \hbar_1) 0.8 e^{(0.5)2\pi i}), ((\hbar_1, \hbar_2) 0.3 e^{(0.5)2\pi i}), ((\hbar_2, \hbar_3) 0 e^{(0.6)2\pi i}), ((\hbar_3, \hbar_1) 0 e^{(0.5)2\pi i}) \right\}. \qquad (14)$$

Definition 5 (see [2]). Let $\ddot{\mathscr{B}}$ be a universal set. Then, a set $\ddot{\mathbb{H}}$ on $\ddot{\mathscr{B}}$ is said to be an IFS if it is of the form

$$\ddot{\mathbb{H}} = \left\{ \hbar_1, m(\hbar_1), n(\hbar_1) | \hbar_1 \in \ddot{\mathscr{B}} \right\}, \qquad (15)$$

provided that $m(\hbar_1) + n(\hbar_1) \in [0, 1]$, where $m(\hbar_1)$ and $n(\hbar_1)$ are the fuzzy valued mappings which symbolize the membership and nonmembership degrees of the IFS $\ddot{\mathbb{H}}$, respectively.

Definition 6 (see [13]). Let $\ddot{\mathscr{B}}$ be a universal set. Then, a set $\ddot{\mathbb{H}}$ on $\ddot{\mathscr{B}}$ is said to be a CIFS if it is of the form

$$\ddot{\mathbb{H}} = \left\{ \hbar_1, m_{\ddot{\mathbb{H}}_C}(\hbar_1), n_{\ddot{\mathbb{H}}_C}(\hbar_1) | \hbar_1 \in \ddot{\mathscr{B}} \right\}, \qquad (16)$$

where $m_{\ddot{\mathbb{H}}_C}$ and $n_{\ddot{\mathbb{H}}_C}$ are the complex valued mappings which represent the membership degree and nonmembership degree of CIFS $\ddot{\mathbb{H}}$, respectively. These mappings are defined as

$$m_{\ddot{\mathbb{H}}_C} : \ddot{\mathscr{B}} \longrightarrow \{\Upsilon_1 | \Upsilon_1 \in \mathbb{C}, |\Upsilon_1| \le 1\},$$
$$n_{\ddot{\mathbb{H}}_C} : \ddot{\mathscr{B}} \longrightarrow \{\Upsilon_2 | \Upsilon_2 \in \mathbb{C}, |\Upsilon_2| \le 1\}, \qquad (17)$$

where $\mathbb{C}$ is the set of complex numbers. Thus,

$$\Upsilon_1(\hbar_1) = \alpha_1 + i\beta_1,$$
$$\Upsilon_2(\hbar_1) = \alpha_2 + i\beta_2, \qquad (18)$$

provided that $(|\Upsilon_1(\hbar_1)|^2 + |\Upsilon_2(\hbar_1)|^2) \in [0,1]$ or

$$\Upsilon_1(\hbar_1) = \eta_{1\ddot{\mathbb{H}}_C}(\hbar_1)e^{\xi_{1\ddot{\mathbb{H}}_C}(\hbar_1)2\pi i},$$
$$\Upsilon_2(\hbar_1) = \eta_{2\ddot{\mathbb{H}}_C}(\hbar_1)e^{\xi_{2\ddot{\mathbb{H}}_C}(\hbar_1)2\pi i}, \qquad (19)$$

where $\eta_{1\ddot{\mathbb{H}}_C}(\hbar_1), \eta_{2\ddot{\mathbb{H}}_C}(\hbar_1), \xi_{1\ddot{\mathbb{H}}_C}(\hbar_1), \xi_{2\ddot{\mathbb{H}}_C}(\hbar_1) \in [0,1]$, provided that $((\eta_{1\ddot{\mathbb{H}}_C}(\hbar_1))^2 + (\eta_{2\ddot{\mathbb{H}}_C}(\hbar_1))^2) \in [0,1]$ and $((\xi_{1\ddot{\mathbb{H}}_C}(\hbar_1))^2 + (\xi_{2\ddot{\mathbb{H}}_C}(\hbar_1))^2) \in [0,1]$.

Definition 7. ([3]). Let $\ddot{\mathscr{B}}$ be a universal set. Then, a set $\ddot{\mathbb{H}}$ on $\ddot{\mathscr{B}}$ is said to be a Pythagorean fuzzy set (PFS) if it is of the form

$$\ddot{\mathbb{H}} = \{\hbar_1, m(\hbar_1), n(\hbar_1) | \hbar_1 \in \ddot{\mathscr{B}}\}, \qquad (20)$$

provided that $(m^2(\hbar_1) + n^2(\hbar_1)) \in [0,1]$, where $m(\hbar_1)$ and $n(\hbar_1)$ are the fuzzy valued mappings which symbolize the membership and nonmembership degrees of the PFS $\ddot{\mathbb{H}}$, respectively.

Definition 8 (see [14]). Let $\ddot{\mathscr{B}}$ be a universal set. Then, a set $\ddot{\mathbb{H}}$ on $\ddot{\mathscr{B}}$ is said to be a CPFS if it is of the form

$$\ddot{\mathbb{H}} = \{\hbar_1, m_{\ddot{\mathbb{H}}_C}(\hbar_1), n_{\ddot{\mathbb{H}}_C}(\hbar_1) | \hbar_1 \in \ddot{\mathscr{B}}\}, \qquad (21)$$

where $m_{\ddot{\mathbb{H}}_C}(\hbar_1)$ and $n_{\ddot{\mathbb{H}}_C}(\hbar_1)$ are the complex valued mappings which symbolize the membership degree and nonmembership degree of CPFS $\ddot{\mathbb{H}}$, respectively. These mappings are defined as

$$m_{\ddot{\mathbb{H}}_C} : \ddot{\mathscr{B}} \longrightarrow \{\Upsilon_1 | \Upsilon_1 \in \mathbb{C}, |\Upsilon_1| \le 1\},$$
$$n_{\ddot{\mathbb{H}}_C} : \ddot{\mathscr{B}} \longrightarrow \{\Upsilon_2 | \Upsilon_2 \in \mathbb{C}, |\Upsilon_2| \le 1\}, \qquad (22)$$

where $\mathbb{C}$ is the set of complex numbers. Thus,

$$\Upsilon_1(\hbar_1) = \alpha_1 + i\beta_1,$$
$$\Upsilon_2(\hbar_1) = \alpha_2 + i\beta_2, \qquad (23)$$

provided that $(|\Upsilon_1(\hbar_1)|^2 + |\Upsilon_2(\hbar_1)|^2) \in [0,1]$ or

$$\Upsilon_1(\hbar_1) = \eta_{1\ddot{\mathbb{H}}_C}(\hbar_1)e^{\xi_{1\ddot{\mathbb{H}}_C}(\hbar_1)2\pi i},$$
$$\Upsilon_2(\hbar_1) = \eta_{2\ddot{\mathbb{H}}_C}(\hbar_1)e^{\xi_{2\ddot{\mathbb{H}}_C}(\hbar_1)2\pi i}, \qquad (24)$$

where $\eta_{1\ddot{\mathbb{H}}_C}(\hbar_1), \eta_{2\ddot{\mathbb{H}}_C}(\hbar_1), \xi_{1\ddot{\mathbb{H}}_C}(\hbar_1), \xi_{2\ddot{\mathbb{H}}_C}(\hbar_1) \in [0,1]$, provided that $((\eta_{1\ddot{\mathbb{H}}_C}(\hbar_1))^2 + (\eta_{2\ddot{\mathbb{H}}_C}(\hbar_1))^2) \in [0,1]$ and $((\xi_{1\ddot{\mathbb{H}}_C}(\hbar_1))^2 + (\xi_{2\ddot{\mathbb{H}}_C}(\hbar_1))^2) \in [0,1]$.

3. Main Results

Definition 9. The Cartesian product of the CPFSs $\ddot{\mathbb{H}} = \{\hbar_j, m_{\ddot{\mathbb{H}}_C}(\hbar_j), n_{\ddot{\mathbb{H}}_C}(\hbar_j) | \hbar_j \in \ddot{\mathscr{B}}\}$ and $\mathbb{K} = \{\hbar_k, m_{\ddot{\mathbb{K}}_C}(\hbar_k), n_{\ddot{\mathbb{K}}_C}(\hbar_k) | \hbar_k \in \ddot{\mathscr{B}}\}$, $j, k \in \mathbb{N}$ is defined by

$$\ddot{\mathbb{H}} \times \ddot{\mathbb{K}} = \{(\hbar_j, \hbar_k), m_{(\ddot{\mathbb{H}} \times \ddot{\mathbb{K}})_C}(\hbar_j, \hbar_k), n_{(\ddot{\mathbb{H}} \times \ddot{\mathbb{K}})_C}(\hbar_j, \hbar_k) | \hbar_i \in \ddot{\mathbb{H}}, \hbar_k \in \ddot{\mathbb{K}}\}. \qquad (25)$$

The mappings $m_{(\ddot{\mathbb{H}} \times \ddot{\mathbb{K}})_C} : \ddot{\mathscr{B}} \longrightarrow \{\Upsilon_m | \Upsilon_m \in \mathbb{C}, |\Upsilon_m| \le 1\}$ and $n_{(\ddot{\mathbb{H}} \times \ddot{\mathbb{K}})_C} : \ddot{\mathscr{B}} \longrightarrow \{\Upsilon_n | \Upsilon_n \in \mathbb{C}, |\Upsilon_n| \le 1\}$ represent the degrees of membership and nonmembership $\mathbb{H} \times \mathbb{K}$ and is defined as $m_{(\ddot{\mathbb{H}} \times \ddot{\mathbb{K}})_C}(\hbar_j, \hbar_k) = \min\{m_{\ddot{\mathbb{H}}_C}(\hbar_j), m_{\ddot{\mathbb{K}}_C}(\hbar_k)\}$ and $n_{(\ddot{\mathbb{H}} \times \ddot{\mathbb{K}})_C}(\hbar_j, \hbar_k) = \max\{n_{\ddot{\mathbb{H}}_C}(\hbar_j), n_{\ddot{\mathbb{K}}_C}(\hbar_k)\}$. Moreover, the complex numbers Υ_n and Υ_m for $\mathbb{H} \times \mathbb{K}$ can be defined as

$$\Upsilon_m(\hbar_j, \hbar_k) = \eta_{(\ddot{\mathbb{H}} \times \ddot{\mathbb{K}})_m}(\hbar_j, \hbar_k)e^{\xi_{(\ddot{\mathbb{H}} \times \ddot{\mathbb{K}})_m}(\hbar_j, \hbar_k)2\pi i} = \min\{\eta_{\ddot{\mathbb{H}}_m}(\hbar_j), \eta_{\ddot{\mathbb{K}}_m}(\hbar_k)\}e^{\min\{\xi_{\ddot{\mathbb{H}}_m}(\hbar_j), \xi_{\ddot{\mathbb{K}}_m}(\hbar_k)\}2\pi i},$$
$$\Upsilon_n(\hbar_j, \hbar_k) = \eta_{(\ddot{\mathbb{H}} \times \ddot{\mathbb{K}})_n}(\hbar_j, \hbar_k)e^{\xi_{(\ddot{\mathbb{H}} \times \ddot{\mathbb{K}})_n}(\hbar_j, \hbar_k)2\pi i} = \max\{\eta_{\ddot{\mathbb{H}}_n}(\hbar_j), \eta_{\ddot{\mathbb{K}}_n}(\hbar_k)\}e^{\max\{\xi_{\ddot{\mathbb{H}}_n}(\hbar_j), \xi_{\ddot{\mathbb{K}}_n}(\hbar_k)\}2\pi i}, \qquad (26)$$

with the conditions

$$0 \le \left(\eta_{(\ddot{\mathbb{H}} \times \ddot{\mathbb{K}})_m}(\hbar_j, \hbar_k)\right)^2 + \left(\eta_{(\ddot{\mathbb{H}} \times \ddot{\mathbb{K}})_n}(\hbar_j, \hbar_k)\right)^2 \le 1,$$
$$0 \le \left(\xi_{(\ddot{\mathbb{H}} \times \ddot{\mathbb{K}})_m}(\hbar_j, \hbar_k)\right)^2 + \left(\xi_{(\ddot{\mathbb{H}} \times \ddot{\mathbb{K}})_n}(\hbar_j, \hbar_k)\right)^2 \le 1. \qquad (27)$$

Definition 10. A complex Pythagorean fuzzy relation (CPFR) denoted by $\mathbb{R}$ is a nonempty subset of $\ddot{\mathbb{H}} \times \ddot{\mathbb{K}}$, where $\ddot{\mathbb{H}}$ and $\ddot{\mathbb{K}}$ are the CPFSs.

Example 2. Take the CPFS,

$$\ddot{\mathbb{H}} = \left\{ \begin{array}{l} \left(\hbar_1, 0.6e^{(0.5)2\pi i}, 0.7e^{(0.6)2\pi i} \right), \\ \left(\hbar_2, 0.7e^{(0.6)2\pi i}, 0.5e^{(0.7)2\pi i} \right) \end{array} \right\}. \tag{28}$$

Now, find $\ddot{\mathbb{H}} \times \ddot{\mathbb{H}}$. We have

$$\ddot{\mathbb{H}} \times \ddot{\mathbb{H}} = \left\{ \begin{array}{l} \left((\hbar_1, \hbar_1), 0.6e^{(0.5)2\pi i}, 0.7e^{(0.6)2\pi i} \right), \left((\hbar_1, \hbar_2), 0.5e^{(0.5)2\pi i}, 0.5e^{(0.6)2\pi i} \right), \\ \left((\hbar_2, \hbar_1), 0.5e^{(0.5)2\pi i}, 0.6e^{(0.5)2\pi i} \right), \left((\hbar_2, \hbar_2), 0.7e^{(0.6)2\pi i}, 0.5e^{(0.7)2\pi i} \right) \end{array} \right\}. \tag{29}$$

The CPR is

$$\ddot{\mathbb{R}} = \left\{ \left((\hbar_1, \hbar_2), 0.5e^{(0.5)2\pi i}, 0.5e^{(0.6)2\pi i} \right), \left((\hbar_2, \hbar_2), 0.7e^{(0.6)2\pi i}, 0.5e^{(0.7)2\pi i} \right) \right\}. \tag{30}$$

Definition 11. The inverse of the CPFR $\ddot{\mathbb{R}}^{-1}$ of the CPFR $\ddot{\mathbb{R}} = \left\{ (\hbar_j, \hbar_k), m_{\ddot{\mathbb{R}}_C}(\hbar_j, \hbar_k), n_{\ddot{\mathbb{R}}_C}(\hbar_j, \hbar_k) | (\hbar_j, \hbar_k) \in \ddot{\mathbb{R}} \right\}$ is $\ddot{\mathbb{R}}^{-1} = \left\{ (\hbar_k, \hbar_j), m_{\ddot{\mathbb{R}}_C}(\hbar_k, \hbar_j), n_{\ddot{\mathbb{R}}_C}(\hbar_k, \hbar_j) | (\hbar_k, \hbar_j) \in \ddot{\mathbb{R}} \right\}$.

Example 3. Let the CPFR $\ddot{\mathbb{R}}$ from (29),

$$\ddot{\mathbb{R}}_1 = \left\{ \left((\hbar_1, \hbar_2), 0.5e^{(0.5)2\pi i}, 0.5e^{(0.6)2\pi i} \right), \left((\hbar_2, \hbar_1), 0.5e^{(0.5)2\pi i}, 0.6e^{(0.5)2\pi i} \right) \right\}, \tag{31}$$

where $\ddot{\mathbb{R}}_1 \subset \ddot{\mathbb{R}}$. Now, the inverse of $\ddot{\mathbb{R}}_1$ is

$$\ddot{\mathbb{R}}_1^{-1} = \left\{ \left((\hbar_2, \hbar_1), 0.5e^{(0.5)2\pi i}, 0.5e^{(0.6)2\pi i} \right), \left((\hbar_1, \hbar_2), 0.5e^{(0.5)2\pi i}, 0.6e^{(0.5)2\pi i} \right) \right\}. \tag{32}$$

Definition 12. The CPFR $\ddot{\mathbb{R}}_2$ is called a CPF reflexive relation if

$$\forall \left(\hbar_1, m_{\ddot{\mathbb{H}}_C}(\hbar_1), n_{\ddot{\mathbb{H}}_C}(\hbar_1) \right) \in \ddot{\mathbb{H}} \Rightarrow \left((\hbar_1, \hbar_1), m_{\ddot{\mathbb{H}}_C}(\hbar_1, \hbar_1), n_{\ddot{\mathbb{H}}_C}(\hbar_1, \hbar_1) \right) \in \ddot{\mathbb{R}}_2, \tag{33}$$

while the CPFR $\ddot{\mathbb{R}}_3$ is an irreflexive relation if $((\hbar_1, \hbar_1), m_{\ddot{\mathbb{H}}_C}(\hbar_1, \hbar_1), n_{\ddot{\mathbb{H}}_C}(\hbar_1, \hbar_1)) \notin \ddot{\mathbb{R}}_3$.

Example 4. From Example 2, in (29), the following relations $\ddot{\mathbb{R}}_2$ and $\ddot{\mathbb{R}}_3$ are CPF reflexive relation and irreflexive relation, respectively:

$$\ddot{\mathbb{R}}_2 = \left\{ \left((\hbar_1, \hbar_1), 0.6e^{(0.5)2\pi i}, 0.7e^{(0.6)2\pi i} \right), \left((\hbar_2, \hbar_2), 0.7e^{(0.6)2\pi i}, 0.5e^{(0.7)2\pi i} \right) \right\},$$
$$\ddot{\mathbb{R}}_3 = \left\{ \left((\hbar_1, \hbar_2), 0.5e^{(0.5)2\pi i}, 0.5e^{(0.6)2\pi i} \right), \left((\hbar_2, \hbar_1), 0.5e^{(0.5)2\pi i}, 0.6e^{(0.5)2\pi i} \right) \right\}. \tag{34}$$

Definition 13. A CPFR $\ddot{\mathbb{R}}$ is called a CPF symmetric relation if

$$\forall\left((\hbar_1,\hbar_2),m_{\ddot{\mathbb{R}}_C}(\hbar_1,\hbar_2),n_{\ddot{\mathbb{R}}_C}(\hbar_1,\hbar_2)\right)\in\ddot{\mathbb{R}}\Rightarrow\left((\hbar_2,\hbar_1),m_{\ddot{\mathbb{R}}_C}(\hbar_2,\hbar_1),n_{\ddot{\mathbb{R}}_C}(\hbar_2,\hbar_1)\right)\in\ddot{\mathbb{R}}. \tag{35}$$

A CPFR $\ddot{\mathbb{R}}_1$ is called a CPF asymmetric relation if

$$\forall\left((\hbar_1,\hbar_2),m_{\ddot{\mathbb{R}}_C}(\hbar_1,\hbar_2),n_{\ddot{\mathbb{R}}_C}(\hbar_1,\hbar_2)\right)\in\ddot{\mathbb{R}}_1\Rightarrow\left((\hbar_2,\hbar_1),m_{\ddot{\mathbb{R}}_C}(\hbar_2,\hbar_1),n_{\ddot{\mathbb{R}}_C}(\hbar_2,\hbar_1)\right)\notin\ddot{\mathbb{R}}_1. \tag{36}$$

A CPFR $\ddot{\mathbb{R}}_2$ is called a CPF antisymmetric relation if

$$\begin{aligned}&\left((\hbar_1,\hbar_2),m_{\ddot{\mathbb{R}}_C}(\hbar_1,\hbar_2),n_{\ddot{\mathbb{R}}_C}(\hbar_1,\hbar_2)\right)\in\ddot{\mathbb{R}}_2,\\&\left((\hbar_2,\hbar_1),m_{\ddot{\mathbb{R}}_C}(\hbar_2,\hbar_1),n_{\ddot{\mathbb{R}}_C}(\hbar_2,\hbar_1)\right)\in\ddot{\mathbb{R}}_2\\&\Rightarrow\left((\hbar_1,\hbar_2),m_{\ddot{\mathbb{R}}_C}(\hbar_1,\hbar_2),n_{\ddot{\mathbb{R}}_C}(\hbar_1,\hbar_2)\right)\\&=\left((\hbar_2,\hbar_1),m_{\ddot{\mathbb{R}}_C}(\hbar_2,\hbar_1),n_{\ddot{\mathbb{R}}_C}(\hbar_2,\hbar_1)\right).\end{aligned} \tag{37}$$

Example 5. The following CPF relations $\ddot{\mathbb{R}}_1$, $\ddot{\mathbb{R}}_2$, and $\ddot{\mathbb{R}}_3$ are CPF symmetric relation, CPF asymmetric relation, and CPF antisymmetric relation, respectively:

$$\begin{aligned}\ddot{\mathbb{R}}_1 &= \left\{\left((\hbar_1,\hbar_2),0.5e^{(0.7)2\pi i},0.6e^{(0.5)2\pi i}\right),\left((\hbar_2,\hbar_1),0.5e^{(0.7)2\pi i},0.6e^{(0.5)2\pi i}\right)\right\},\\\ddot{\mathbb{R}}_2 &= \left\{\left((\hbar_1,\hbar_2),0.6e^{(0.5)2\pi i},0.7e^{(0.6)2\pi i}\right),\left((\hbar_1,\hbar_3),0.7e^{(0.6)2\pi i},0.6e^{(0.5)2\pi i}\right)\right\},\\\ddot{\mathbb{R}}_3 &= \left\{\left((\hbar_3,\hbar_1),0.4e^{(0.5)2\pi i},0.9e^{(0.7)2\pi i}\right),\left((\hbar_3,\hbar_3),0.8e^{(0.6)2\pi i},0.4e^{(0.7)2\pi i}\right)\right\}.\end{aligned} \tag{38}$$

Theorem 1. *A CPFR $\ddot{\mathbb{R}}$ is a symmetric relation iff $\ddot{\mathbb{R}}=\ddot{\mathbb{R}}^{-1}$.*

Proof. Let $\ddot{\mathbb{R}}=\ddot{\mathbb{R}}^{-1}$, then we have

$$\left((\hbar_1,\hbar_2),m_{\ddot{\mathbb{R}}_C}(\hbar_1,\hbar_2),n_{\ddot{\mathbb{R}}_C}(\hbar_1,\hbar_2)\right)\in\ddot{\mathbb{R}}\Rightarrow\left((\hbar_2,\hbar_1),m_{\ddot{\mathbb{R}}_C}(\hbar_2,\hbar_1),n_{\ddot{\mathbb{R}}_C}(\hbar_2,\hbar_1)\right)\in\ddot{\mathbb{R}}^{-1}. \tag{39}$$

Since $\ddot{\mathbb{R}}=\ddot{\mathbb{R}}^{-1}$, one writes

$$\left((\hbar_2,\hbar_1),m_{\ddot{\mathbb{R}}_C}(\hbar_2,\hbar_1),n_{\ddot{\mathbb{R}}_C}(\hbar_2,\hbar_1)\right)\in\ddot{\mathbb{R}}. \tag{40}$$

Hence proved that $\ddot{\mathbb{R}}$ is a CPF symmetric relation. Conversely, assume that $\ddot{\mathbb{R}}$ is a CPF symmetric relation. Then,

$$\begin{aligned}&\left((\hbar_1,\hbar_2),m_{\ddot{\mathbb{R}}_C}(\hbar_1,\hbar_2),n_{\ddot{\mathbb{R}}_C}(\hbar_1,\hbar_2)\right)\\&\in\ddot{\mathbb{R}}\Rightarrow\left((\hbar_2,\hbar_1),m_{\ddot{\mathbb{R}}_C}(\hbar_2,\hbar_1),n_{\ddot{\mathbb{R}}_C}(\hbar_2,\hbar_1)\right)\in\ddot{\mathbb{R}}.\end{aligned} \tag{41}$$

But, if

$$\begin{aligned}&\left((\hbar_1,\hbar_2),m_{\ddot{\mathbb{R}}_C}(\hbar_1,\hbar_2),n_{\ddot{\mathbb{R}}_C}(\hbar_1,\hbar_2)\right)\\&\in\ddot{\mathbb{R}}\Rightarrow\left((\hbar_2,\hbar_1),m_{\ddot{\mathbb{R}}_C}(\hbar_2,\hbar_1),n_{\ddot{\mathbb{R}}_C}(\hbar_2,\hbar_1)\right)\in\ddot{\mathbb{R}}^{-1},\end{aligned} \tag{42}$$

this implies that $\ddot{\mathbb{R}}=\ddot{\mathbb{R}}^{-1}$.   □

Theorem 2. *Let $\ddot{\mathbb{R}}_1$ and $\ddot{\mathbb{R}}_2$ are CPF symmetric relations, then their intersection, i.e, $\ddot{\mathbb{R}}_1\cap\ddot{\mathbb{R}}_2$ is also a CPF symmetric relation.*

Proof. Assume that $\ddot{\mathbb{R}}_1$ and $\ddot{\mathbb{R}}_2$ are two CPFR symmetric relations on CPFS $\mathbb{H}$. Then, from the definition of CPFR,

$\ddot{\mathbb{R}}_1 \subseteq \ddot{\mathbb{H}} \times \ddot{\mathbb{H}}$ and $\ddot{\mathbb{R}}_2 \subseteq \ddot{\mathbb{H}} \times \ddot{\mathbb{H}} \Rightarrow \ddot{\mathbb{R}}_1 \cap \ddot{\mathbb{R}}_2 \subseteq \ddot{\mathbb{H}} \times \ddot{\mathbb{H}} \Rightarrow \ddot{\mathbb{R}}_1 \cap \ddot{\mathbb{R}}_2$ is CPR on $\ddot{\mathbb{H}}$. Now, assume that

$$\left((\hbar_2, \hbar_1), m_{\ddot{\mathbb{R}}_C}(\hbar_2, \hbar_1), n_{\ddot{\mathbb{R}}_C}(\hbar_2, \hbar_1) \right) \in \ddot{\mathbb{R}}_1 \cap \ddot{\mathbb{R}}_2$$

$$\Rightarrow \left((\hbar_2, \hbar_1), m_{\ddot{\mathbb{R}}_C}(\hbar_2, \hbar_1), n_{\ddot{\mathbb{R}}_C}(\hbar_2, \hbar_1) \right) \in \ddot{\mathbb{R}}_1 \text{ and} \quad (43)$$

$$\left((\hbar_2, \hbar_1), m_{\ddot{\mathbb{R}}_C}(\hbar_2, \hbar_1), n_{\ddot{\mathbb{R}}_C}(\hbar_2, \hbar_1) \right) \in \ddot{\mathbb{R}}_2.$$

Since, $\ddot{\mathbb{R}}_1$ and $\ddot{\mathbb{R}}_2$ are CPF symmetric relations. Therefore,

$$\left((\hbar_1, \hbar_2), m_{\ddot{\mathbb{R}}_C}(\hbar_1, \hbar_2), n_{\ddot{\mathbb{R}}_C}(\hbar_1, \hbar_2) \right) \in \ddot{\mathbb{R}}_1,$$

$$\left((\hbar_1, \hbar_2), m_{\ddot{\mathbb{R}}_C}(\hbar_1, \hbar_2), n_{\ddot{\mathbb{R}}_C}(\hbar_1, \hbar_2) \right) \in \ddot{\mathbb{R}}_2 \quad (44)$$

$$\Rightarrow \left((\hbar_1, \hbar_2), m_{\ddot{\mathbb{R}}_C}(\hbar_1, \hbar_2), n_{\ddot{\mathbb{R}}_C}(\hbar_1, \hbar_2) \right) \in \ddot{\mathbb{R}}_1 \cap \ddot{\mathbb{R}}_2. \qquad \square$$

Definition 14. A CPFR $\ddot{\mathbb{R}}$ is called a CPF transitive relation if

$$\left((\hbar_1, \hbar_2), m_{\ddot{\mathbb{R}}_C}(\hbar_1, \hbar_2), n_{\ddot{\mathbb{R}}_C}(\hbar_1, \hbar_2) \right) \in \ddot{\mathbb{R}},$$

$$\left((\hbar_2, \hbar_3), m_{\ddot{\mathbb{R}}_C}(\hbar_2, \hbar_3), n_{\ddot{\mathbb{R}}_C}(\hbar_2, \hbar_3) \right) \in \ddot{\mathbb{R}}, \quad (45)$$

this implies that

$$\left((\hbar_1, \hbar_3), m_{\ddot{\mathbb{R}}_C}(\hbar_1, \hbar_3), n_{\ddot{\mathbb{R}}_C}(\hbar_1, \hbar_3) \right) \in \ddot{\mathbb{R}}. \quad (46)$$

Example 6. A CPFR $\ddot{\mathbb{R}}$ is a CPF transitive relation if

$$\ddot{\mathbb{R}} = \left\{ \begin{array}{l} \left((\hbar_1, \hbar_2), 0.6e^{(0.5)2\pi i}, 0.4e^{(0.7)2\pi i} \right), \\ \left((\hbar_2, \hbar_3), 0.5e^{(0.8)2\pi i}, 0.6e^{(0.3)2\pi i} \right), \\ \left((\hbar_1, \hbar_3), 0.7e^{(0.4)2\pi i}, 0.5e^{(0.6)2\pi i} \right) \end{array} \right\}. \quad (47)$$

Definition 15. A CPF composite relation $\ddot{\mathbb{R}}_1 \circ \ddot{\mathbb{R}}_2$ combines the CPFRs $\ddot{\mathbb{R}}_1$ and $\ddot{\mathbb{R}}_2$ as for

$$\left((\hbar_1, \hbar_2), m_{\ddot{\mathbb{R}}_C}(\hbar_1, \hbar_2), n_{\ddot{\mathbb{R}}_C}(\hbar_1, \hbar_2) \right) \in \ddot{\mathbb{R}}_1,$$

$$\left((\hbar_2, \hbar_3), m_{\ddot{\mathbb{R}}_C}(\hbar_2, \hbar_3), n_{\ddot{\mathbb{R}}_C}(\hbar_2, \hbar_3) \right) \in \ddot{\mathbb{R}}_2, \quad (48)$$

this implies that

$$\left((\hbar_1, \hbar_3), m_{\ddot{\mathbb{R}}_C}(\hbar_1, \hbar_3), n_{\ddot{\mathbb{R}}_C}(\hbar_1, \hbar_3) \right) \in \ddot{\mathbb{R}}_1 \circ \ddot{\mathbb{R}}_2. \quad (49)$$

Theorem 3. *A CPFR $\ddot{\mathbb{R}}$ is a transitive relation iff $\ddot{\mathbb{R}} \circ \ddot{\mathbb{R}} \subseteq \ddot{\mathbb{R}}$.*

Proof. Assume that $\ddot{\mathbb{R}}$ is a CPF transitive relation, then for

$$\left((\hbar_1, \hbar_2), m_{\ddot{\mathbb{R}}_C}(\hbar_1, \hbar_2), n_{\ddot{\mathbb{R}}_C}(\hbar_1, \hbar_2) \right) \in \ddot{\mathbb{R}},$$

$$\left((\hbar_2, \hbar_3), m_{\ddot{\mathbb{R}}_C}(\hbar_2, \hbar_3), n_{\ddot{\mathbb{R}}_C}(\hbar_2, \hbar_3) \right) \in \ddot{\mathbb{R}}, \quad (50)$$

one has

$$\left((\hbar_1, \hbar_3), m_{\ddot{\mathbb{R}}_C}(\hbar_1, \hbar_3), n_{\ddot{\mathbb{R}}_C}(\hbar_1, \hbar_3) \right) \in \ddot{\mathbb{R}}. \quad (51)$$

But,

$$\left((\hbar_1, \hbar_3), m_{\ddot{\mathbb{R}}_C}(\hbar_1, \hbar_3), n_{\ddot{\mathbb{R}}_C}(\hbar_1, \hbar_3) \right) \in \ddot{\mathbb{R}} \circ \ddot{\mathbb{R}}. \quad (52)$$

Hence, $\ddot{\mathbb{R}} \circ \ddot{\mathbb{R}} \subseteq \ddot{\mathbb{R}}$
Conversely assume that $\ddot{\mathbb{R}} \circ \ddot{\mathbb{R}} \subseteq \ddot{\mathbb{R}}$, then for

$$\left((\hbar_1, \hbar_2), m_{\ddot{\mathbb{R}}_C}(\hbar_1, \hbar_2), n_{\ddot{\mathbb{R}}_C}(\hbar_1, \hbar_2) \right) \in \ddot{\mathbb{R}},$$

$$\left((\hbar_2, \hbar_3), m_{\ddot{\mathbb{R}}_C}(\hbar_2, \hbar_3), n_{\ddot{\mathbb{R}}_C}(\hbar_2, \hbar_3) \right) \in \ddot{\mathbb{R}}, \quad (53)$$

one has

$$\left((\hbar_1, \hbar_3), m_{\ddot{\mathbb{R}}_C}(\hbar_1, \hbar_3), n_{\ddot{\mathbb{R}}_C}(\hbar_1, \hbar_3) \right) \in \ddot{\mathbb{R}} \circ \ddot{\mathbb{R}}. \quad (54)$$

But, $\ddot{\mathbb{R}} \circ \ddot{\mathbb{R}} \subseteq \ddot{\mathbb{R}}$; this implies that

$$\left((\hbar_1, \hbar_3), m_{\ddot{\mathbb{R}}_C}(\hbar_1, \hbar_3), n_{\ddot{\mathbb{R}}_C}(\hbar_1, \hbar_3) \right) \in \ddot{\mathbb{R}}. \quad (55)$$

Hence, it is proved that $\ddot{\mathbb{R}}$ is a CPF transitive relation. $\qquad \square$

Definition 16. A CPFR $\ddot{\mathbb{R}}_1$ is called a CPF equivalence relation, if $\ddot{\mathbb{R}}_1$ satisfies the properties of a CPF reflexive relation, a CPF symmetric relation, and a CPF transitive relation. While, a CPFR $\ddot{\mathbb{R}}_2$ is called a CPF-order relation if $\ddot{\mathbb{R}}_2$ satisfies the properties a CPF reflexive relation, a CPF antisymmetric relation, and a CPF transitive relation.

Theorem 4. *A CPF equivalence relation implies that $\ddot{\mathbb{R}} \circ \ddot{\mathbb{R}} = \ddot{\mathbb{R}}$.*

Proof. We know that a CPF equivalence relation $\ddot{\mathbb{R}}$ is also a CPF transitive relation, so in view of Theorem 3,

$$\ddot{\mathbb{R}} \times \ddot{\mathbb{R}} \subseteq \ddot{\mathbb{R}}. \quad (56)$$

We assume that

$$\left((\hbar_1, \hbar_2), m_{\ddot{\mathbb{R}}_C}(\hbar_1, \hbar_2), n_{\ddot{\mathbb{R}}_C}(\hbar_1, \hbar_2) \right) \in \ddot{\mathbb{R}}. \quad (57)$$

As $\ddot{\mathbb{R}}$ is an equivalence relation and verifies the axioms of a CPF symmetric relation and CPF is a transitive relation,

$$\left((\hbar_2, \hbar_1), m_{\ddot{\mathbb{R}}_C}(\hbar_2, \hbar_1), n_{\ddot{\mathbb{R}}_C}(\hbar_2, \hbar_1) \right) \in \ddot{\mathbb{R}}. \quad (58)$$

In view of (57) and (58), we have that $((\hbar_1, \hbar_1), m_{\ddot{\mathbb{R}}_C}(\hbar_1, \hbar_1), n_{\ddot{\mathbb{R}}_C}(\hbar_1, \hbar_1)) \in \ddot{\mathbb{R}}$. By using the concept of a CPF composite relation, we have

$$\left((\hbar_1, \hbar_1), m_{\ddot{\mathbb{R}}_C}(\hbar_1, \hbar_1), n_{\ddot{\mathbb{R}}_C}(\hbar_1, \hbar_1) \right) \in \ddot{\mathbb{R}} \circ \ddot{\mathbb{R}}. \quad (59)$$

Now, from (57) and (59), we get that

$$\ddot{\mathbb{R}} \subseteq \ddot{\mathbb{R}} \times \ddot{\mathbb{R}}. \quad (60)$$

Hence, from (56) and (60), we get that $\ddot{\mathbb{R}} \circ \ddot{\mathbb{R}} = \ddot{\mathbb{R}}$. □

Theorem 5. *The inverse CPFR $\ddot{\mathbb{R}}^{-1}$ of a CPF order relation is also a CPF-order relation.*

Proof. The inverse CPFR $\ddot{\mathbb{R}}^{-1}$ of a CPF-order relation is also a CPF-order relation, if $\ddot{\mathbb{R}}^{-1}$ verifies the following three properties of a CPF-order relation:

(P_1) $\forall \hbar_1 \in \ddot{\mathbb{H}}$, $((\hbar_1, \hbar_1), m_{\ddot{\mathbb{H}}_C}(\hbar_1, \hbar_1), n_{\ddot{\mathbb{H}}_C}(\hbar_1, \hbar_1)) \in \ddot{\mathbb{R}}$. Since $\ddot{\mathbb{R}}$ is a CPyF reflexive relation, $\Rightarrow ((\hbar_1, \hbar_1), m_{\ddot{\mathbb{H}}_C}(\hbar_1, \hbar_1), n_{\ddot{\mathbb{H}}_C}(\hbar_1, \hbar_1)) \in \ddot{\mathbb{R}}^{-1}$.
Hence, $\ddot{\mathbb{R}}^{-1}$ is a CPF reflexive relation

(P_2) Let $((\hbar_1, \hbar_2), m_{\ddot{\mathbb{R}}_C}(\hbar_1, \hbar_2), n_{\ddot{\mathbb{R}}_C}(\hbar_1, \hbar_2)) \in \ddot{\mathbb{R}}$ and $((\hbar_2, \hbar_1), m_{\ddot{\mathbb{R}}_C}(\hbar_2, \hbar_1), n_{\ddot{\mathbb{R}}_C}(\hbar_2, \hbar_1)) \in \ddot{\mathbb{R}}$, $\Rightarrow ((\hbar_2, \hbar_1), m_{\ddot{\mathbb{R}}_C}(\hbar_2, \hbar_1), n_{\ddot{\mathbb{R}}_C}(\hbar_2, \hbar_1)) \in \ddot{\mathbb{R}}^{-1}$ and $((\hbar_1, \hbar_2), m_{\ddot{\mathbb{R}}_C}(\hbar_1, \hbar_2), n_{\ddot{\mathbb{R}}_C}(\hbar_1, \hbar_2)) \in \ddot{\mathbb{R}}^{-1}$.

Since $\ddot{\mathbb{R}}$ is a CPF antisymmetric relation, one gets

$$\left((\hbar_1, \hbar_2), m_{\ddot{\mathbb{R}}_C}(\hbar_1, \hbar_2), n_{\ddot{\mathbb{R}}_C}(\hbar_1, \hbar_2)\right) \\ = \left((\hbar_2, \hbar_1), m_{\ddot{\mathbb{R}}_C}(\hbar_2, \hbar_1), n_{\ddot{\mathbb{R}}_C}(\hbar_2, \hbar_1)\right). \tag{61}$$

Hence, $\ddot{\mathbb{R}}^{-1}$ is a CPF antisymmetric relation

(P_3) Assume that $((\hbar_1, \hbar_2), m_{\ddot{\mathbb{R}}_C}(\hbar_1, \hbar_2), n_{\ddot{\mathbb{R}}_C}(\hbar_1, \hbar_2)) \in \ddot{\mathbb{R}}$ and $((\hbar_2, \hbar_3), m_{\ddot{\mathbb{R}}_C}(\hbar_2, \hbar_3), n_{\ddot{\mathbb{R}}_C}(\hbar_2, \hbar_3)) \in \ddot{\mathbb{R}}, \Rightarrow ((\hbar_2, \hbar_1), m_{\ddot{\mathbb{R}}_C}(\hbar_2, \hbar_1), n_{\ddot{\mathbb{R}}_C}(\hbar_2, \hbar_1)) \in \ddot{\mathbb{R}}^{-1}$ and $((\hbar_3, \hbar_2), m_{\ddot{\mathbb{R}}_C}(\hbar_3, \hbar_2), n_{\ddot{\mathbb{R}}_C}(\hbar_3, \hbar_2)) \in \ddot{\mathbb{R}}^{-1}$

Since $\ddot{\mathbb{R}}$ is a CPF transitive relation,

$$\left((\hbar_1, \hbar_3), m_{\ddot{\mathbb{R}}_C}(\hbar_1, \hbar_3), n_{\ddot{\mathbb{R}}_C}(\hbar_1, \hbar_3)\right) \in \ddot{\mathbb{R}} \\ \Rightarrow \left((\hbar_3, \hbar_1), m_{\ddot{\mathbb{R}}_C}(\hbar_3, \hbar_1), n_{\ddot{\mathbb{R}}_C}(\hbar_3, \hbar_1)\right) \in \ddot{\mathbb{R}}^{-1}. \tag{62}$$

Hence, $\ddot{\mathbb{R}}^{-1}$ is a CPF transitive relation.
Thus, from (P_1), (P_2), and (P_3), $\ddot{\mathbb{R}}^{-1}$ is also a CPF-order relation. □

Definition 17. For a CPF equivalence relation $\ddot{\mathbb{R}}$, $(\hbar_1, m_{\ddot{\mathbb{H}}_C}(\hbar_1), n_{\ddot{\mathbb{H}}_C}(\hbar_1))$, the equivalence class of $\hbar_1$ modulo $\ddot{\mathbb{R}}$, is $\ddot{\mathbb{R}}^{\hbar_1} = \left\{ (\hbar_2, m_{\ddot{\mathbb{H}}_C}(\hbar_2), n_{\ddot{\mathbb{H}}_C}(\hbar_2)) | ((\hbar_2, \hbar_1), m_{\ddot{\mathbb{R}}_C}(\hbar_2, \hbar_1), n_{\ddot{\mathbb{R}}_C}(\hbar_2, \hbar_1)) \in \ddot{\mathbb{R}} \right\}$.

Example 7. Let the CPF equivalence relation

$$\ddot{\mathbb{R}} = \left\{ \begin{array}{l} \left((\hbar_1, \hbar_1), 0.6e^{(0.5)2\pi i}, 0.5e^{(0.7)2\pi i}\right), \left((\hbar_1, \hbar_2), 0.5e^{(0.6)2\pi i}, 0.5e^{(0.7)2\pi i}\right), \\ \left((\hbar_2, \hbar_1), 0.5e^{(0.4)2\pi i}, 0.6e^{(0.6)2\pi i}\right), \left((\hbar_2, \hbar_2), 0.7e^{(0.6)2\pi i}, 0.4e^{(0.5)2\pi i}\right) \end{array} \right\}. \tag{63}$$

Now, the equivalence classes of a CPF relation are

$$\ddot{\mathbb{R}}^{\hbar_1} = \ddot{\mathbb{R}}^{\hbar_2} = \left\{ \left(\hbar_1, 0.6e^{(0.5)2\pi i}, 0.5e^{(0.7)2\pi i}\right), \left(\hbar_2, 0.7e^{(0.6)2\pi i}, 0.4e^{(0.5)2\pi i}\right) \right\}. \tag{64}$$

Theorem 6. *For a CPF equivalence relation $\ddot{\mathbb{R}}$, $((\hbar_1, \hbar_2), m_{\ddot{\mathbb{R}}_C}(\hbar_1, \hbar_2), n_{\ddot{\mathbb{R}}_C}(\hbar_1, \hbar_2)) \in \ddot{\mathbb{R}}$ iff $\ddot{\mathbb{R}}^{\hbar_1} = \ddot{\mathbb{R}}^{\hbar_2}$.*

Proof. Assume that $\ddot{\mathbb{R}}^{\hbar_1} = \ddot{\mathbb{R}}^{\hbar_2}$, then for $\hbar_3 \in \ddot{\mathscr{B}}$,

$$\left(\hbar_3, m_{\ddot{\mathbb{H}}_C}(\hbar_3), n_{\ddot{\mathbb{H}}_C}(\hbar_3)\right) \in \ddot{\mathbb{R}}^{\hbar_1} \\ \Rightarrow \left((\hbar_3, \hbar_1), m_{\ddot{\mathbb{R}}_C}(\hbar_3, \hbar_1), n_{\ddot{\mathbb{R}}_C}(\hbar_3, \hbar_1)\right) \in \ddot{\mathbb{R}}. \tag{65}$$

Since $\ddot{\mathbb{R}}$ is symmetric, one writes

$$\left((\hbar_1, \hbar_3), m_{\ddot{\mathbb{R}}_C}(\hbar_1, \hbar_3), n_{\ddot{\mathbb{R}}_C}(\hbar_1, \hbar_3)\right) \in \ddot{\mathbb{R}}. \tag{66}$$

Hence, $\ddot{\mathbb{R}}$ is a CPF symmetric relation. Similarly,

$$\left(\hbar_3, m_{\ddot{\mathbb{H}}_C}(\hbar_3), n_{\ddot{\mathbb{H}}_C}(\hbar_3)\right) \in \ddot{\mathbb{R}}^{\hbar_2} \\ \Rightarrow \left((\hbar_3, \hbar_2), m_{\ddot{\mathbb{R}}_C}(\hbar_3, \hbar_2), n_{\ddot{\mathbb{R}}_C}(\hbar_3, \hbar_2)\right) \in \ddot{\mathbb{R}}, \tag{67}$$

since $\ddot{\mathbb{R}}$ is transitive,

$$\Rightarrow \left((\hbar_1, \hbar_2), m_{\ddot{\mathbb{R}}_C}(\hbar_1, \hbar_2), n_{\ddot{\mathbb{R}}_C}(\hbar_1, \hbar_2)\right) \in \ddot{\mathbb{R}}. \tag{68}$$

Hence, $\ddot{\mathbb{R}}$ is a CPF transitive relation.
Conversely assume that $((\hbar_1, \hbar_2), m_{\ddot{\mathbb{R}}_C}(\hbar_1, \hbar_2), n_{\ddot{\mathbb{R}}_C}(\hbar_1, \hbar_2)) \in \ddot{\mathbb{R}}$ and $(\hbar_3, m_{\ddot{\mathbb{H}}_C}(\hbar_3), n_{\ddot{\mathbb{H}}_C}(\hbar_3)) \in \ddot{\mathbb{R}}^{\hbar_1}$, then

$$\left((\hbar_3, \hbar_1), m_{\ddot{\mathbb{R}}_C}(\hbar_3, \hbar_1), n_{\ddot{\mathbb{R}}_C}(\hbar_3, \hbar_1)\right) \in \ddot{\mathbb{R}}. \tag{69}$$

Thus,

$$\left((\hbar_3, \hbar_1), m_{\ddot{\mathbb{R}}_C}(\hbar_3, \hbar_1), n_{\ddot{\mathbb{R}}_C}(\hbar_3, \hbar_1)\right) \in \ddot{\mathbb{R}} \text{ and} \\ \left((\hbar_1, \hbar_2), m_{\ddot{\mathbb{R}}_C}(\hbar_1, \hbar_2), n_{\ddot{\mathbb{R}}_C}(\hbar_1, \hbar_2)\right) \in \ddot{\mathbb{R}} \\ \Rightarrow \left((\hbar_3, \hbar_2), m_{\ddot{\mathbb{R}}_C}(\hbar_3, \hbar_2), n_{\ddot{\mathbb{R}}_C}(\hbar_3, \hbar_2)\right) \in \ddot{\mathbb{R}}, \tag{70}$$

as $\ddot{\mathbb{R}}$ is a CPF transitive relation.

$$\left(\hbar_3, m_{\ddot{\mathbb{H}}_C}(\hbar_3), n_{\ddot{\mathbb{H}}_C}(\hbar_3)\right) \in \ddot{\mathbb{R}}^{\hbar_2}. \tag{71}$$

Hence, we get that

$$\ddot{\mathbb{R}}^{\hbar_1} \subseteq \ddot{\mathbb{R}}^{\hbar_2}. \tag{72}$$

Similarly, we assume that $((\hbar_1, \hbar_2), m_{\ddot{\mathbb{R}}_C}(\hbar_1, \hbar_2), n_{\ddot{\mathbb{R}}_C}(\hbar_1, \hbar_2)) \in \ddot{\mathbb{R}}$ and $(\hbar_3, m_{\ddot{\mathbb{H}}_C}(\hbar_3), n_{\ddot{\mathbb{H}}_C}(\hbar_3)) \in \ddot{\mathbb{R}}^{\hbar_2}$, then

$$\left((\hbar_3, \hbar_2), m_{\ddot{\mathbb{R}}_C}(\hbar_3, \hbar_2), n_{\ddot{\mathbb{R}}_C}(\hbar_3, \hbar_2) \right) \in \ddot{\mathbb{R}}. \tag{73}$$

Since $((\hbar_1, \hbar_2), m_{\ddot{\mathbb{R}}_C}(\hbar_1, \hbar_2), n_{\ddot{\mathbb{R}}_C}(\hbar_1, \hbar_2)) \in \ddot{\mathbb{R}}$, one writes $((\hbar_2, \hbar_1), m_{\ddot{\mathbb{R}}_C}(\hbar_2, \hbar_1), n_{\ddot{\mathbb{R}}_C}(\hbar_2, \hbar_1)) \in \ddot{\mathbb{R}}$, as $\ddot{\mathbb{R}}$ is a CPF symmetric relation. Now, we have

$$\left((\hbar_3, \hbar_2), m_{\ddot{\mathbb{R}}_C}(\hbar_3, \hbar_2), n_{\ddot{\mathbb{R}}_C}(\hbar_3, \hbar_2) \right) \in \ddot{\mathbb{R}},$$
$$\left((\hbar_2, \hbar_1), m_{\ddot{\mathbb{R}}_C}(\hbar_2, \hbar_1), n_{\ddot{\mathbb{R}}_C}(\hbar_2, \hbar_1) \right) \in \ddot{\mathbb{R}} \tag{74}$$
$$\Rightarrow \left((\hbar_3, \hbar_1), m_{\ddot{\mathbb{R}}_C}(\hbar_3, \hbar_1), n_{\ddot{\mathbb{R}}_C}(\hbar_3, \hbar_1) \right) \in \ddot{\mathbb{R}},$$

as $\Rightarrow ((\hbar_3, \hbar_1), m_{\ddot{\mathbb{R}}_C}(\hbar_3, \hbar_1), n_{\ddot{\mathbb{R}}_C}(\hbar_3, \hbar_1)) \in \ddot{\mathbb{R}}$ is a CPF transitive relation. This implies that

$$\left(\hbar_3, m_{\ddot{\mathbb{H}}_C}(\hbar_3), n_{\ddot{\mathbb{H}}_C}(\hbar_3) \right) \in \ddot{\mathbb{R}}^{\hbar_1}. \tag{75}$$

Hence,

$$\ddot{\mathbb{R}}^{\hbar_2} \subseteq \ddot{\mathbb{R}}^{\hbar_1}. \tag{76}$$

Now, from (72) and (76), we get that $\ddot{\mathbb{R}}^{\hbar_2} = \ddot{\mathbb{R}}^{\hbar_1}$. □

4. Application

In the section, an application of the proposed concepts is presented, which discusses the relationships among different economic indicators. Moreover, it also specifies the level of positive and negative impacts of one parameter on the others with respect to time phase.

Figure 1 demonstrates the algorithm and the procedure used in the application. The flow chart describes the stepwise progression for the investigation of quality of relationships between any two economic indicators. Initially, the economic parameters or indicators to be studied are collected. After that, the Cartesian product is found to achieve all the possible relations, which proves to be helpful in learning the relationships and the level of impacts of one parameter over the others. Next, different types and properties of CPFRs can be utilized to find out the unknown and indirect relationships. Last, the experiment is concluded by reading the complex Pythagorean fuzzy information, such that the first element in the pair of relation affects the second element. The amplitude term represents the level of effectiveness, and the phase term refers to the time phase. The degree of membership characterizes the positive effects, while the degree of nonmembership characterizes the negative effects of one parameter over the others.

Consider the set $\mathbb{H} = \{$Import, export, GDP, industry, agriculture, employment$\}$ of a country's economic indicators. The goal is to find out the impacts of each indicator over the other with respect to time. Note that, in this experiment, the unit of time is taken to be a year. Hence, a CPFS $\ddot{\mathbb{H}}$ is induced from the set $\mathbb{H}$ as

$$\ddot{\mathbb{H}} = \left\{ \begin{array}{l} \left(\text{Import}, 0.3e^{(0.5)2\pi i}, 0.6e^{(0.5)2\pi i} \right), \left(\text{export}, 0.8e^{(0.5)2\pi i}, 0.2e^{(0.75)2\pi i} \right), \\ \left(\text{industry}, 0.7e^{(0.5)2\pi i}, 0.4e^{(0.25)2\pi i} \right), \left(\text{agriculture}, 0.7e^{(0.25)2\pi i}, 0.5e^{(0.75)2\pi i} \right), \\ \left(\text{employment}, 0.9e^{(0.25)2\pi i}, 0.3e^{(0.75)2\pi i} \right) \end{array} \right\}. \tag{77}$$
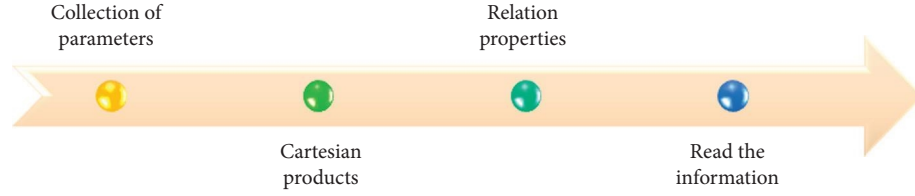
Figure 1: Flowchart of the method used in the application.

The investigation of relationships among the economic indicators tempts to find out the Cartesian product of $\ddot{\mathbb{H}} \times \ddot{\mathbb{H}}$. Hence,

$$\ddot{\mathbb{H}} \times \ddot{\mathbb{H}} = \left\{ \begin{array}{l} \left(\text{Import, import}, 0.3e^{(0.5)2\pi i}, 0.6e^{(0.5)2\pi i}\right), \left(\text{import, export}, 0.3e^{(0.5)2\pi i}, 0.6e^{(0.75)2\pi i}\right), \\ \left(\text{import, industry}, 0.3e^{(0.5)2\pi i}, 0.6e^{(0.5)2\pi i}\right), \left(\text{import, agriculture}, 0.3e^{(0.25)2\pi i}, 0.6e^{(0.75)2\pi i}\right), \\ \left(\text{import, employment}, 0.3e^{(0.25)2\pi i}, 0.6e^{(0.75)2\pi i}\right), \left(\text{export, import}, 0.3e^{(0.5)2\pi i}, 0.6e^{(0.75)2\pi i}\right), \\ \left(\text{export, export}, 0.8e^{(0.5)2\pi i}, 0.2e^{(0.75)2\pi i}\right), \left(\text{export, industry}, 0.7e^{(0.5)2\pi i}, 0.4e^{(0.75)2\pi i}\right), \\ \left(\text{export, agriculture}, 0.7e^{(0.25)2\pi i}, 0.5e^{(0.75)2\pi i}\right), \left(\text{export, employment}, 0.8e^{(0.25)2\pi i}, 0.3e^{(0.75)2\pi i}\right) \\ \left(\text{industry, import}, 0.3e^{(0.5)2\pi i}, 0.6e^{(0.5)2\pi i}\right), \left(\text{industry, export}, 0.7e^{(0.5)2\pi i}, 0.4e^{(0.75)2\pi i}\right) \\ \left(\text{industry, industry}, 0.7e^{(0.5)2\pi i}, 0.4e^{(0.25)2\pi i}\right), \left(\text{industry, agriculture}, 0.7e^{(0.25)2\pi i}, 0.5e^{(0.75)2\pi i}\right) \\ \left(\text{industry, employment}, 0.7e^{(0.25)2\pi i}, 0.4e^{(0.25)2\pi i}\right), \left(\text{agriculture, import}, 0.3e^{(0.25)2\pi i}, 0.6e^{(0.75)2\pi i}\right) \\ \left(\text{agriculture, export}, 0.7e^{(0.25)2\pi i}, 0.5e^{(0.75)2\pi i}\right), \left(\text{agriculture, industry}, 0.7e^{(0.25)2\pi i}, 0.5e^{(0.75)2\pi i}\right) \\ \left(\text{agriculture, agriculture}, 0.7e^{(0.25)2\pi i}, 0.5e^{(0.75)2\pi i}\right), \left(\text{agriculture, employment}, 0.3e^{(0.5)2\pi i}, 0.6e^{(0.5)2\pi i}\right) \\ \left(\text{employment, import}, 0.3e^{(0.25)2\pi i}, 0.6e^{(0.75)2\pi i}\right), \left(\text{employment, export}, 0.8e^{(0.25)2\pi i}, 0.3e^{(0.75)2\pi i}\right) \\ \left(\text{employment, industry}, 0.7e^{(0.25)2\pi i}, 0.4e^{(0.25)2\pi i}\right), \left(\text{employment, agriculture}, 0.7e^{(0.25)2\pi i}, 0.3e^{(0.75)2\pi i}\right) \\ \left(\text{employment, employment}, 0.9e^{(0.25)2\pi i}, 0.3e^{(0.75)2\pi i}\right) \end{array} \right\}. \tag{78}$$

Each element of the Cartesian product given by equation (78) describes the magnitude of impacts of one factor over the other. For instance, (industry, export, $0.7e^{(0.5)2\pi i}, 0.4e^{(0.75)2\pi i}$) conveys that the degree of good impacts of the industry on the export of the country is 0.7 with respect to a year. Since, the imaginary part represents the time phase, so $(0.5)2 = 1$ year. In addition, the degree of bad impacts is 0.4 with respect to one and a half year. Likewise, (agriculture, industry, $0.7e^{(0.25)2\pi i}, 0.5e^{(0.75)2\pi i}$) expresses that the degree of good and positive impacts of the agriculture over the industry of a country is 0.7 with respect to half a year, and the degree of bad and negative impacts is 0.5 with respect to one and a half year.

Suppose that the impacts of export on industry and the impacts of industry on employment are known, but the impacts of export over employment are not known. These unknown impacts can be easily found by using the complex Pythagorean fuzzy transitive relations because the Cartesian product is an equivalence relation.

Moreover, multiple sets of economic indicators of different countries can be considered, and the indirect impacts of one country's economy over the other countries' can be found using the CPF composite relations.

Consider three different countries: Pakistan (P), China (C), and Iran (I). The aim is to relate their economies through some economic parameters. Henceforth following are the three $\mathbb{C}P_y$ FSs,

TABLE 1: The CPyF composition relation $\ddot{\mathbb{R}}$.

$\ddot{\mathbb{R}} = \ddot{\mathbb{R}}_1 \circ \ddot{\mathbb{R}}_2$	Trade (I)	Employment (I)
Trade (P)	$0.6e^{(0.25)2\pi i}, 0.5e^{(0.5)2\pi i}$	$0.7e^{(0.5)2\pi i}, 0.5e^{(0.75)2\pi i}$
Agriculture (P)	$0.6e^{(0.25)2\pi i}, 0.3e^{(0.5)2\pi i}$	$0.7e^{(0.5)2\pi i}, 0.3e^{(0.75)2\pi i}$

$$
\begin{aligned}
P &= \left\{ \left(\text{Trade}, 0.7e^{(0.5)2\pi i}, 0.5e^{(0.5)2\pi i}\right), \left(\text{agriculture}, 0.8e^{(0.75)2\pi i}, 0.3e^{(0.5)2\pi i}\right) \right\}, \\
C &= \left\{ \left(\text{Industry}, 0.8e^{(0.5)2\pi i}, 0.5e^{(0.5)2\pi i}\right), \left(\text{agriculture}, 0.5e^{(0.75)2\pi i}, 0.6e^{(0.25)2\pi i}\right) \right\}, \\
I &= \left\{ \left(\text{Trade}, 0.6e^{(0.25)2\pi i}, 0.5e^{(0.5)2\pi i}\right), \left(\text{employment}, 0.7e^{(0.5)2\pi i}, 0.5e^{(0.75)2\pi i}\right) \right\}.
\end{aligned}
\tag{79}
$$

The CPFR $\ddot{\mathbb{R}}_1$ between the set P and C is found to be

$$
\ddot{\mathbb{R}}_1 = P \times C = \left\{
\begin{array}{l}
\left((\text{Trade, industry}), 0.7e^{(0.5)2\pi i}, 0.5e^{(0.5)2\pi i}\right), \\
\left((\text{trade, agriculture}), 0.5e^{(0.5)2\pi i}, 0.6e^{(0.5)2\pi i}\right), \\
\left((\text{agriculture, industry}), 0.8e^{(0.5)2\pi i}, 0.5e^{(0.5)2\pi i}\right), \\
\left((\text{agriculture, agriculture}), 0.5e^{(0.75)2\pi i}, 0.6e^{(0.5)2\pi i}\right)
\end{array}
\right\}.
\tag{80}
$$

The CPFR $\ddot{\mathbb{R}}_2$ between the sets C and I is found to be

$$
\ddot{\mathbb{R}}_2 = C \times I = \left\{
\begin{array}{l}
\left((\text{Industry, trade}), 0.6e^{(0.25)2\pi i}, 0.5e^{(0.5)2\pi i}\right), \\
\left((\text{industry, employment}), 0.7e^{(0.5)2\pi i}, 0.5e^{(0.75)2\pi i}\right), \\
\left((\text{agriculture, trade}), 0.5e^{(0.25)2\pi i}, 0.6e^{(0.5)2\pi i}\right), \\
\left((\text{agriculture, employment}), 0.5e^{(0.5)2\pi i}, 0.6e^{(0.75)2\pi i}\right)
\end{array}
\right\}.
\tag{81}
$$

Now, by using the CPF composition relation $\ddot{\mathbb{R}}$, the indirect relation between the sets P and I are found as given in Table 1. Trade (I) and employment (I) are the parameters of Iran, while trade (P) and agriculture (P) are the parameters of Pakistan.

5. Conclusion

In this study, the novel concept of complex Pythagorean fuzzy relation (CPFR) is defined. Additionally, the types of CPFRs are described with suitable examples. Some of the types are a CPF irreflexive relation, a CPF inverse relation, a CPF asymmetric relation, a CPF composite relation, a CPF equivalence relation, a CPF order relation, and a CPF equivalence class. Furthermore, some useful and interesting properties and results of CPFRs are elaborated in detail. Moreover, an application of the proposed method is presented that discusses the impacts of economic parameters of a country over each other. Furthermore, the application also explains the effects of economic parameters of one country over the economic parameters of the other countries. The introduced concepts can be extended to other generalizations of fuzzy sets which will produce very interesting structures. These novel structures might have a rich variety of applications in sciences, technology, and economics.

Data Availability

No data were used to support this study.

Conflicts of Interest

The authors declare that they have no conflicts of interest.

References

[1] L. A. Zadeh, "Fuzzy sets," *Information and Control*, vol. 8, no. 3, pp. 338–353, 1965.

[2] K. T. Atanassov, "Intuitionistic fuzzy sets," *Fuzzy Sets and Systems*, vol. 20, no. 1, pp. 87–96, 1986.

[3] R. R. Yager, "Pythagorean fuzzy subsets," in *Proceedings of the 2013 Joint IFSA World Congress and NAFIPS Annual Meeting (IFSA/NAFIPS)*, pp. 57–61, IEEE, Edmonton, Canada, June 2013.

[4] G. Deschrijver and E. E. Kerre, "On the relationship between some extensions of fuzzy set theory," *Fuzzy Sets and Systems*, vol. 133, no. 2, pp. 227–235, 2003.

[5] J. Maiers and Y. S. Sherif, "Applications of fuzzy set theory," *IEEE Transactions on Systems, Man, and Cybernetics*, vol. SMC-15, no. 1, pp. 175–189, 1985.

[6] G. J. Klir, "On fuzzy-set interpretation of possibility theory," *Fuzzy Sets and Systems*, vol. 108, no. 3, pp. 263–273, 1999.

[7] S. K. De, R. Biswas, and A. R. Roy, "Some operations on intuitionistic fuzzy sets," *Fuzzy Sets and Systems*, vol. 114, no. 3, pp. 477–484, 2000.

[8] S. K. De, R. Biswas, and A. R. Roy, "An application of intuitionistic fuzzy sets in medical diagnosis," *Fuzzy Sets and Systems*, vol. 117, no. 2, pp. 209–213, 2001.

[9] E. Szmidt and J. Kacprzyk, "Distances between intuitionistic fuzzy sets," *Fuzzy Sets and Systems*, vol. 114, no. 3, pp. 505–518, 2000.

[10] X. Peng and Y. Yang, "Some results for Pythagorean fuzzy sets," *International Journal of Intelligent Systems*, vol. 30, no. 11, pp. 1133–1160, 2015.

[11] X. Peng, H. Yuan, and Y. Yang, "Pythagorean fuzzy information measures and their applications," *International Journal of Intelligent Systems*, vol. 32, no. 10, pp. 991–1029, 2017.

[12] D. Ramot, R. Milo, M. Friedman, and A. Kandel, "Complex fuzzy sets," *IEEE Transactions on Fuzzy Systems*, vol. 10, no. 2, pp. 171–186, 2002.

WILEY | Hindawi

Retraction

Retracted: More General Form of Interval-Valued Fuzzy Ideals of BCK/BCI-Algebras

Security and Communication Networks

This article has been retracted by Hindawi following an investigation undertaken by the publisher [1]. This investigation has uncovered evidence of one or more of the following indicators of systematic manipulation of the publication process:

(1) Discrepancies in scope

(2) Discrepancies in the description of the research reported

(3) Discrepancies between the availability of data and the research described

(4) Inappropriate citations

(5) Incoherent, meaningless and/or irrelevant content included in the article

(6) Manipulated or compromised peer review

The presence of these indicators undermines our confidence in the integrity of the article's content and we cannot, therefore, vouch for its reliability. Please note that this notice is intended solely to alert readers that the content of this article is unreliable. We have not investigated whether authors were aware of or involved in the systematic manipulation of the publication process.

Wiley and Hindawi regrets that the usual quality checks did not identify these issues before publication and have since put additional measures in place to safeguard research integrity.

We wish to credit our own Research Integrity and Research Publishing teams and anonymous and named external researchers and research integrity experts for contributing to this investigation.

The corresponding author, as the representative of all authors, has been given the opportunity to register their agreement or disagreement to this retraction. We have kept a record of any response received.

References

[1] G. Muhiuddin, D. Al-Kadi, and A. Mahboob, "More General Form of Interval-Valued Fuzzy Ideals of BCK/BCI-Algebras," *Security and Communication Networks*, vol. 2021, Article ID 9930467, 10 pages, 2021.

WILEY | Hindawi

Research Article

More General Form of Interval-Valued Fuzzy Ideals of BCK/BCI-Algebras

G. Muhiuddin ,[1] D. Al-Kadi,[2] and A. Mahboob[3]

[1]*Department of Mathematics, University of Tabuk, Tabuk 71491, Saudi Arabia*
[2]*Department of Mathematics and Statistic, College of Science, Taif University, P. O. Box 11099, Taif 21944, Saudi Arabia*
[3]*Department of Mathematics, Madanapalle Institute of Technology & Science, Madanapalle-517325, India*

Correspondence should be addressed to G. Muhiuddin; chishtygm@gmail.com

The concepts of interval-valued $(\in, \in \vee (\widetilde{\kappa^*}, q_{\widetilde{\kappa}}))$-fuzzy subalgebras, interval-valued $(\in, \in \vee (\widetilde{\kappa^*}, q_{\widetilde{\kappa}}))$-fuzzy ideals, and interval-valued $(\in \vee (\widetilde{\kappa^*}, q_{\widetilde{\kappa}}), \in \vee (\widetilde{\kappa^*}, q_{\widetilde{\kappa}}))$-fuzzy ideals are introduced, and related properties are studied. Many examples are given in support of these new notions. Furthermore, interval-valued $(\in, \in \vee (\widetilde{\kappa^*}, q_{\widetilde{\kappa}}))$-fuzzy commutative ideals are defined, and some important properties are discussed. For a BCK-algebra X, it is proved that every interval-valued $(\in, \in \vee (\widetilde{\kappa^*}, q_{\widetilde{\kappa}}))$-fuzzy commutative ideal of BCK-algebra X is an interval-valued $(\in, \in \vee (\widetilde{\kappa^*}, q_{\widetilde{\kappa}}))$-fuzzy ideal of X, but the converse need not be true, in general, and then a counterexample is constructed.

1. Introduction

As an extension of fuzzy sets, Zadeh defined fuzzy sets with an interval-valued membership function proposing the concept of interval-valued fuzzy sets. This concept has been studied from various points of view in different algebraic structures as BCK-algebras and some of its generalization (see, for example, [1–5]), groups (see for example, [6–10]), and rings (see, for example, [11–13]). Moreover, as novel approaches in decision-making, theoretical models were introduced based on (fuzzy) soft sets in [14–19]. In BCK/BCI-algebras and other related algebraic structures, different kinds of related concepts were investigated in various ways (see, for example, [20–33]). Jun [34] studied interval-valued fuzzy ideals in BCI-algebras. Zhan et al. [35, 36] studied $(\in, \in \vee q)$-fuzzy ideals of BCI-algebras. The concept of "quasi-coincidence" of an interval-valued fuzzy point together with "belongingness" within an interval-valued fuzzy set was used in the studies made by Ma et al. in [37, 38] where they discussed properties of some types of $(\in, \in \vee q)$-interval-valued fuzzy ideals of BCI-algebras.

It is natural to introduce the general form of the existing interval-valued fuzzy ideals of BCK/BCI-algebras. For this purpose, we first recall in Section 2 some elementary notions used in the sequel. Then, in Section 3, we introduce the concepts: interval-valued $(\in, \in \vee (\widetilde{\kappa^*}, q_{\widetilde{\kappa}}))$-fuzzy subalgebras, interval-valued $(\in, \in \vee (\widetilde{\kappa^*}, q_{\widetilde{\kappa}}))$-fuzzy ideals, interval-valued $(\in, \in \vee q)$-fuzzy ideals, and interval-valued $(\in \vee (\widetilde{\kappa^*}, q_{\widetilde{\kappa}}), \in \vee (\widetilde{\kappa^*}, q_{\widetilde{\kappa}}))$-fuzzy ideals, and related properties are studied. In Section 4, interval-valued $(\in, \in \vee (\widetilde{\kappa^*}, q_{\widetilde{\kappa}}))$-fuzzy commutative ideals are introduced, some properties are studied, and their relation with interval-valued $(\in, \in \vee (\widetilde{\kappa^*}, q_{\widetilde{\kappa}}))$-fuzzy ideals is investigated.

2. Preliminaries

An algebra $X = (X; *, 0)$ of type $(2, 0)$ is a BCI-algebra if for all $v, p, \hbar \in X$,

(1) $((v * p) * (v * \hbar)) * (\hbar * p) = 0$
(2) $(v * (v * p)) * p = 0$
(3) $v * v = 0$
(4) $v * p = 0$ and $p * v = 0 \Rightarrow v = p$

If X satisfies (1)–(4) and (5) $0 * v = 0$, then X is a BCK-algebra.

Any BCK/BCI-algebra X satisfies

(1) $v * 0 = v$

(2) $(v * p) * \hbar = (v * \hbar) * p$

From now on, let X be a BCK/BCI-algebra unless otherwise specified.

We define a partially ordered set $(X, \leq)$, where $v \leq \kappa \Leftrightarrow v * p = 0$.

A nonempty subset P of X is said to be a subalgebra of X if $\hbar * v \in P$ for all $\hbar, v \in P$.

A nonempty subset I of X is said to be an ideal of X if

(I_1) $0 \in I$

(I_2) $\forall \hbar, v \in I, \hbar * v \in I$, and $v \in I \Rightarrow \hbar \in I$

By an interval number $\tilde{a}$, we mean an interval, denoted by $[a^-, a^+]$, where $0 \leq a^- \leq a^+ \leq 1$. The set of all interval numbers is denoted by $D[0, 1]$. In whatever follows, the interval $[a, a]$ is identified by the number $a \in [0, 1]$. For the interval numbers $\tilde{a}_i = [a_i^-, a_i^+]$ and $\tilde{b}_i = [b_i^-, b_i^+] \in D[0, 1], i \in I$, we define

$$\min\{\tilde{a}_i, \tilde{b}_i\} = [\min(a_i^-, b_i^-), \min(a_i^+, b_i^+)],$$
$$\max\{\tilde{a}_i, \tilde{b}_i\} = [\max(a_i^-, b_i^-), \max(a_i^+, b_i^+)],$$
$$\tilde{a}_1 \leq \tilde{a}_2 \Leftrightarrow a_1^- \leq a_2^- \text{ and } a_1^+ \leq a_2^+,$$
$$\tilde{a}_1 = \tilde{a}_2 \Leftrightarrow a_1^- = a_2^- \text{ and } a_1^+ = a_2^+, \quad (1)$$
$$\kappa \tilde{a} = [\kappa a^-, \kappa a^+], \quad \text{whenever } 0 \leq \kappa \leq 1,$$
$$\tilde{\kappa}^* = [\kappa^{*-}, \kappa^{*+}], \quad \text{whenever } 0 < \kappa^* \leq 1.$$

A mapping $\tilde{\mathcal{U}}: X \longrightarrow D[0, 1]$ is called an interval-valued fuzzy subset (briefly, IVFS) of X, where $\tilde{\mathcal{U}}(x) = [\tilde{\mathcal{U}}^-(x), \tilde{\mathcal{U}}^+(x)]$ for all $x \in X$, $\tilde{\mathcal{U}}^-$ and $\tilde{\mathcal{U}}^+$ are fuzzy sets of X with $\tilde{\mathcal{U}}^-(x) \leq \tilde{\mathcal{U}}^+(x)$ for all $x \in X$.

3. Interval-Valued $(\in, \in \vee (\tilde{\kappa}^*, q_{\tilde{\kappa}}))$-Fuzzy Ideals

Definition 1. Let $a \in X$ and $\tilde{\ell} \in D(0, 1]$. An interval-valued ordered fuzzy point (briefly, IVOFP) $a_{\tilde{\ell}}$ of X is defined as:

$$a_{\tilde{\ell}}(x) = \begin{cases} \tilde{\ell}, & \text{if } x \in (a], \\ [0, 0], & \text{if } x \notin (a], \end{cases} \quad (2)$$

for all $x \in X$.

Clearly, $a_{\tilde{\ell}}$ is an IVFS of X. For any IVFS $\tilde{\mathcal{U}}$ of X, we denote $a_{\tilde{\ell}} \subseteq \tilde{\mathcal{U}}$ as $a_{\tilde{\ell}} \in \tilde{\mathcal{U}}$ in the sequel. So, $a_{\tilde{\ell}} \in \tilde{\mathcal{U}} \Leftrightarrow \tilde{\mathcal{U}}(a) \geq \tilde{\ell}$.

Definition 2. Let $\hbar_{\tilde{l}}$ be an IVOFP of X and $\tilde{\kappa}^* \in D(0, 1]$. Then, $\hbar_{\tilde{l}}$ is called $(\tilde{\kappa}^*, q)$-quasi-coincident with an IVFS $\tilde{\mathcal{U}}$ of X, represented as $\hbar_{\tilde{l}}(\tilde{\kappa}^*, q)\tilde{\mathcal{U}}$, if $\tilde{\mathcal{U}}(\hbar) + \tilde{l} > \tilde{\kappa}^*$.

Assume $[0, 0] \leq \tilde{\kappa} < \tilde{\kappa}^* \leq [1, 1]$. For an IVOFP $\hbar_{\tilde{\ell}}$, we write

(1) $\hbar_{\tilde{\ell}}(\tilde{\kappa}^*, q_{\tilde{\kappa}})\tilde{\mathcal{U}}$ if $\tilde{\mathcal{U}}(\hbar) + \tilde{\ell} + \tilde{\kappa} > \tilde{\kappa}^*$

(2) $\hbar_{\tilde{\ell}} \in \vee (\tilde{\kappa}^*, q_{\tilde{\kappa}})\tilde{\mathcal{U}}$ if $\hbar_{\tilde{\ell}} \in \tilde{\mathcal{U}}$ or $\hbar_{\tilde{\ell}}(\tilde{\kappa}^*, q_{\tilde{\kappa}})\tilde{\mathcal{U}}$

(3) $\hbar_{\tilde{\ell}} \overline{\alpha} \tilde{\mathcal{U}}$ if $\hbar_{\tilde{\ell}} \alpha \tilde{\mathcal{U}}$ does not hold for $\alpha \in \{(\tilde{\kappa}^*, q_{\tilde{\kappa}}), \in \vee (\tilde{\kappa}^*, q_{\tilde{\kappa}})\}$

Definition 3. An IVFS $\tilde{\mathcal{U}}$ of X is called an interval-valued $(\in, \in \vee (\tilde{\kappa}^*, q_{\tilde{\kappa}}))$-fuzzy subalgebra (in short, IV $(\in, \in \vee (\tilde{\kappa}^*, q_{\tilde{\kappa}}))$-FS) of X if $\hbar_{\tilde{\ell}} \in \tilde{\mathcal{U}}$ and $v_{\tilde{j}} \in \tilde{\mathcal{U}}$ imply $(\hbar * v)_{\min\{\tilde{\ell}, \tilde{j}\}} \in \vee (\tilde{\kappa}^*, q_{\tilde{\kappa}})\tilde{\mathcal{U}}$ for all $\tilde{\ell}, \tilde{j} \in {}^j D(0, 1]$ and $\hbar, v \in X$.

Theorem 1. *An IVFS $\tilde{\mathcal{U}}$ of X is an IV $(\in, \in \vee (\tilde{\kappa}^*, q_{\tilde{\kappa}}))$-FS of $X \Leftrightarrow$*

$$\tilde{\mathcal{U}}(\hbar * v) \geq \min\left\{\tilde{\mathcal{U}}(\hbar), \tilde{\mathcal{U}}(v), \left[\frac{\kappa^{*-} - \kappa^-}{2}, \frac{\kappa^{*+} - \kappa^+}{2}\right]\right\},$$
$$(3)$$

for all $\hbar, v \in X$.

Proof. $(\Rightarrow)$ On the contrary, suppose that $\tilde{\mathcal{U}}(\hbar * v) < \min\{\tilde{\mathcal{U}}(\hbar), \tilde{\mathcal{U}}(v), [((\kappa^{*-} - \kappa^-)/2), ((\kappa^{*+} - \kappa^+)/2)]\}$, for some $\hbar, v \in X$. Choose $\omega \in D(0, 1]$ such that

$$\tilde{\mathcal{U}}(\hbar * v) < \omega \leq \min\left\{\tilde{\mathcal{U}}(\hbar), \tilde{\mathcal{U}}(v), \left[\frac{\kappa^{*-} - \kappa^-}{2}, \frac{\kappa^{*+} - \kappa^+}{2}\right]\right\}.$$
$$(4)$$

Then, $\hbar_\omega \in \tilde{\mathcal{U}}$ and $v_\omega \in \tilde{\mathcal{U}}$, but $(\hbar * v)_\omega \overline{\in \vee (\tilde{\kappa}^*, q_{\tilde{\kappa}})}\tilde{\mathcal{U}}$, which is impossible. Hence, $\tilde{\mathcal{U}}(\hbar * v) \geq \min\{\tilde{\mathcal{U}}(\hbar), \tilde{\mathcal{U}}(v), [((\kappa^{*-} - \kappa^-)/2), ((\kappa^{*+} - \kappa^+)/2)]\}$.

$(\Leftarrow)$ Assume that $\tilde{\mathcal{U}}(\hbar * v) \geq \min\{\tilde{\mathcal{U}}(\hbar), \tilde{\mathcal{U}}(v), [((\kappa^{*-} - \kappa^-)/2), ((\kappa^{*+} - \kappa^+)/2)]\}$ for all $\hbar, v \in X$. Let $\hbar_{\tilde{\ell}} \in \tilde{\mathcal{U}}$ and $v_{\tilde{j}} \in \tilde{\mathcal{U}}$ for all $\tilde{\ell}, \tilde{j} \in D(0, 1]$. Then, $\tilde{\mathcal{U}}(\hbar) \geq \tilde{\ell}$ and $\tilde{\mathcal{U}}(v) \geq \tilde{j}$. So, $\tilde{\mathcal{U}}(\hbar * v) \geq \min\{\tilde{\mathcal{U}}(\hbar), \tilde{\mathcal{U}}(v), [((\kappa^{*-} - \kappa^-)/2), ((\kappa^{*+} - \kappa^+)/2)]\} \geq \min\{\tilde{\ell}, \tilde{j}, [((\kappa^{*-} - \kappa^-)/2), ((\kappa^{*+} - \kappa^+)/2)]\}$. If $\min\{\tilde{\ell}, \tilde{j}\} \leq [((\kappa^{*-} - \kappa^-)/2), ((\kappa^{*+} - \kappa^+)/2)]$, then $\tilde{\mathcal{U}}(\hbar * v) \geq \min\{\tilde{\ell}, \tilde{j}\}$ implies that $(\hbar * v)_{\min\{\tilde{\ell}, j\}} \in \tilde{\mathcal{U}}$. If $\min\{\tilde{\ell}, \tilde{j}\} > [((\kappa^{*-} - \kappa^-)/2), ((\kappa^{*+} - \kappa^+)/2)]$, then $\tilde{\mathcal{U}}(\hbar * v) \geq [((\kappa^{*-} - \kappa^-)/2), ((\kappa^{*+} - \kappa^+)/2)]$. So, $\tilde{\mathcal{U}}(\hbar * v) + \min\{\tilde{\ell}, \tilde{j}\} > [((\kappa^{*-} - \kappa^-)/2), ((\kappa^{*+} - \kappa^+)/2)] + [((\kappa^{*-} - \kappa^-)/2), ((\kappa^{*+} - \kappa^+)/2)] = [\kappa^{*-} - \kappa^-, \kappa^{*+} - \kappa^+]$ implies that $(\hbar * v)_{\min\{\tilde{\ell}, j\}}(\tilde{\kappa}^*, q_{\tilde{\kappa}})\tilde{\mathcal{U}}$. Hence, $(\hbar * v)_{\min\{\tilde{\ell}, j\}} \in \vee (\tilde{\kappa}^*, q_{\tilde{\kappa}})\tilde{\mathcal{U}}$. Therefore, $\tilde{\mathcal{U}}$ is an IV $(\in, \in \vee (\tilde{\kappa}^*, q_{\tilde{\kappa}}))$-FS of X. □

Definition 4. An IVFS $\tilde{\mathcal{U}}$ of X is called an interval-valued $(\in, \in \vee (\tilde{\kappa}^*, q_{\tilde{\kappa}}))$-fuzzy ideal (in short, IV $(\in, \in \vee (\tilde{\kappa}^*, q_{\tilde{\kappa}}))$-FI) of X if

(1) $\hbar_{\tilde{\ell}} \in \tilde{\mathcal{U}}$ implies $0_{\tilde{\ell}} \in \vee (\tilde{\kappa}^*, q_{\tilde{\kappa}})\tilde{\mathcal{U}}$

(2) $(\hbar * v)_{\tilde{\ell}} \in \tilde{\mathcal{U}}$ and $v_{\tilde{j}} \in \tilde{\mathcal{U}}$ imply $\hbar_{\min\{\tilde{\ell}, j\}} \in \vee (\tilde{\kappa}^*, q_{\tilde{\kappa}})\tilde{\mathcal{U}}$

for all $\hbar, v \in X$ and $\tilde{\ell}, \tilde{j} \in D(0, 1]$.

Example 1. Consider a BCI-algebra $X = \{0, 1, 2, 3\}$ with the binary operation $*$ as defined in Table 1.

Define $\tilde{\mathcal{U}}: X \longrightarrow D[0, 1]$ by

$$\tilde{\mathcal{U}}(\hbar) = \begin{cases} [0.9, 1], & \text{if } \hbar = 0, \\ [0.3, 0.4], & \text{if } \hbar \in \{1, 2, 3\}. \end{cases} \quad (5)$$

TABLE 1: Cayley Table of the binary operation*.

*	0	1	2	3
0	0	0	0	3
1	1	0	0	3
2	2	2	0	3
3	3	3	3	0

TABLE 2: Cayley Table of the binary operation*.

*	0	1	2	3	4
0	0	0	0	0	0
1	1	0	1	0	1
2	2	2	0	2	0
3	3	1	3	0	3
4	4	4	2	4	0

Choose $\widetilde{\kappa}^* = [0.2, 0.3]$ and $\widetilde{\kappa} = [0.1, 0.2]$. Then, with direct computation, we find that $\widetilde{\mathcal{U}}$ is an IV $(\in, \in \vee(\widetilde{\kappa}^*, q_{\widetilde{\kappa}}))$-FI of X.

Definition 5. An IVFS $\widetilde{\mathcal{U}}$ of X is called an interval-valued $(\in, \in \vee q)$-fuzzy ideal (in short, IV $(\in, \in \vee q)$-FI) of X if

(1) $\hbar_{\widetilde{\ell}} \in \widetilde{\mathcal{U}}$ implies $0_{\widetilde{\ell}} \in \vee q \widetilde{\mathcal{U}}$

(2) $(\hbar * v)_{\widetilde{\ell}} \in \widetilde{\mathcal{U}}$ and $v_{\widetilde{j}} \in \widetilde{\mathcal{U}}$ imply $\hbar_{\min\{\widetilde{\ell}, \widetilde{j}\}} \in \vee q \widetilde{\mathcal{U}}$

for all $\hbar, v \in X$ and $\widetilde{\ell}, \widetilde{j} \in D(0, 1]$.

Theorem 2. *In X, every IV $(\in, \in \vee q)$-FI is an IV $(\in, \in \vee(\widetilde{\kappa}^*, q_{\widetilde{\kappa}}))$-FI.*

Proof. Let $\widetilde{\mathcal{U}}$ be any IV $(\in, \in \vee q)$-FI of X. Take any $\hbar_{\widetilde{\ell}} \in \widetilde{\mathcal{U}}$ for $\hbar \in X$ and $\widetilde{\ell} \in D(0, 1]$. Then, by hypothesis, $0_{\widetilde{\ell}} \in \vee q \widetilde{\mathcal{U}}$. It follows that $\widetilde{\mathcal{U}}(0) \geq \widetilde{\ell}$ or $\widetilde{\mathcal{U}}(0) + \widetilde{\ell} \geq [1, 1]$, and so, $\widetilde{\mathcal{U}}(0) \geq \widetilde{\ell}$ or $\widetilde{\mathcal{U}}(0) + \widetilde{\kappa} + \widetilde{\ell} \geq \widetilde{\kappa}^*$. Therefore, $0_{\widetilde{\ell}} \in \vee(\widetilde{\kappa}^*, q_{\widetilde{\kappa}})\widetilde{\mathcal{U}}$. Next, let $(\hbar * v)_{\widetilde{\ell}} \in \widetilde{\mathcal{U}}$ and $v_{\widetilde{j}} \in \widetilde{\mathcal{U}}$. So, $\hbar_{\min\{\widetilde{\ell}, \widetilde{j}\}} \in \vee q \widetilde{\mathcal{U}}$ implies $\widetilde{\mathcal{U}}(\hbar) \geq \min\{\widetilde{\ell}, \widetilde{j}\}$ or $\widetilde{\mathcal{U}}(\hbar) + \min\{\widetilde{\ell}, \widetilde{j}\} > [1, 1]$. Therefore, $\widetilde{\mathcal{U}}(\hbar) \geq \min\{\widetilde{\ell}, \widetilde{j}\}$ or $\widetilde{\mathcal{U}}(\hbar) + \widetilde{\kappa} + \min\{\widetilde{\ell}, \widetilde{j}\} > \widetilde{\kappa}^*$. Thus, $\hbar_{\widetilde{\ell}} \in \vee(\widetilde{\kappa}^*, q_{\widetilde{\kappa}})\widetilde{\mathcal{U}}$. Hence, $\widetilde{\mathcal{U}}$ is an IV $(\in, \in \vee(\widetilde{\kappa}^*, q_{\widetilde{\kappa}}))$-FI of X. □

Example 2. Consider a BCK-algebra $X = \{0, 1, 2, 3, 4\}$ with the binary operation $*$ as defined in Table 2.

Define $\widetilde{\mathcal{U}}: X \longrightarrow D[0, 1]$ by

$$\widetilde{\mathcal{U}}(\hbar) = \begin{cases} [0.4, 0.5], & \text{if } \hbar = 0, \\ [0.2, 0.3], & \text{if } \hbar \in \{1, 2\}, \\ [0.5, 0.6], & \text{if } \hbar = 3, \\ [0.1, 0.2], & \text{if } \hbar = 4. \end{cases} \tag{6}$$

Choose $\widetilde{\kappa}^* = [0.2, 0.3]$ and $\widetilde{\kappa} = [0.1, 0.2]$. Then, $\widetilde{\mathcal{U}}$ is an IV $(\in, \in \vee(\widetilde{\kappa}^*, q_{\widetilde{\kappa}}))$-FI of X but is not an IV $(\in, \in \vee q)$-FI of X as $2_{\widetilde{\ell}=[0.6,0.6]} = (4 * 2)_{\widetilde{\ell}=[0.6,0.6]} \in \widetilde{\mathcal{U}}$ and $2_{\widetilde{j}=[0.6,0.6]} \in \widetilde{\mathcal{U}}$ but $4_{\min\{\widetilde{\ell}, \widetilde{j}\}=[0.6,0.6]} \overline{\in \vee q} \widetilde{\mathcal{U}}$.

Definition 6. An IVFS $\widetilde{\mathcal{U}}$ of X is called an interval-valued $(\in \vee(\widetilde{\kappa}^*, q_{\widetilde{\kappa}}), \in \vee(\widetilde{\kappa}^*, q_{\widetilde{\kappa}}))$-fuzzy ideal (in short, IV $(\in \vee(\widetilde{\kappa}^*, q_{\widetilde{\kappa}}), \in \vee(\widetilde{\kappa}^*, q_{\widetilde{\kappa}}))$-FI) of X if

(1) $\hbar_{\widetilde{\ell}} \in \vee(\widetilde{\kappa}^*, q_{\widetilde{\kappa}})\widetilde{\mathcal{U}}$ implies $0_{\widetilde{\ell}} \in \vee(\widetilde{\kappa}^*, q_{\widetilde{\kappa}})\widetilde{\mathcal{U}}$

(2) $(\hbar * v)_{\widetilde{\ell}} \in \vee(\widetilde{\kappa}^*, q_{\widetilde{\kappa}})\widetilde{\mathcal{U}}$ and $v_{\widetilde{j}} \in \vee(\widetilde{\kappa}^*, q_{\widetilde{\kappa}})\widetilde{\mathcal{U}}$ imply $\hbar_{\min\{\widetilde{\ell}, \widetilde{j}\}} \in \vee(\widetilde{\kappa}^*, q_{\widetilde{\kappa}})\widetilde{\mathcal{U}}$

for all $\hbar, v \in X$ and $\widetilde{\ell}, \widetilde{j} \in D(0, 1]$.

Theorem 3. *In X, every IV $(\in \vee(\widetilde{\kappa}^*, q_{\widetilde{\kappa}}), \in \vee(\widetilde{\kappa}^*, q_{\widetilde{\kappa}}))$-FI is an IV $(\in, \in \vee(\widetilde{\kappa}^*, q_{\widetilde{\kappa}}))$-FI.*

Proof. Let $\widetilde{\mathcal{U}}$ be any IV $(\in \vee(\widetilde{\kappa}^*, q_{\widetilde{\kappa}}), \in \vee(\widetilde{\kappa}^*, q_{\widetilde{\kappa}}))$-FI of X. Take any $\hbar_{\widetilde{\ell}} \in \widetilde{\mathcal{U}}$ for $\hbar \in X$ and $\widetilde{\ell} \in D(0, 1]$. Then, $\hbar_{\widetilde{\ell}} \in \vee(\widetilde{\kappa}^*, q_{\widetilde{\kappa}})\widetilde{\mathcal{U}}$. So, by hypothesis, $0_{\widetilde{\ell}} \in \vee(\widetilde{\kappa}^*, q_{\widetilde{\kappa}})\widetilde{\mathcal{U}}$. Suppose that $(\hbar * \ell)_{\widetilde{\ell}} \in \widetilde{\mathcal{U}}$ and $\ell_{\widetilde{j}} \in \widetilde{\mathcal{U}}$. Then, $(\hbar * \ell)_{\widetilde{\ell}} \in \vee(\widetilde{\kappa}^*, q_{\widetilde{\kappa}})\widetilde{\mathcal{U}}$ and $\ell_{\widetilde{j}} \in \vee(\widetilde{\kappa}^*, q_{\widetilde{\kappa}})\widetilde{\mathcal{U}}$. Therefore, by hypothesis, $\hbar_{\min\{\widetilde{\ell}, \widetilde{j}\}} \in \vee(\widetilde{\kappa}^*, q_{\widetilde{\kappa}})\widetilde{\mathcal{U}}$. Hence, $\widetilde{\mathcal{U}}$ is an IV $(\in, \in \vee(\widetilde{\kappa}^*, q_{\widetilde{\kappa}}))$-FI of X. □

Example 3. Consider a BCK-algebra of Example 2. Define $\widetilde{\mathcal{U}}: X \longrightarrow D[0, 1]$ by

$$\widetilde{\mathcal{U}}(\hbar) = \begin{cases} [0.4, 0.5], & \text{if } \hbar = 0, \\ [0.6, 0.7], & \text{if } \hbar \in \{1, 3\}, \\ [0.1, 0.2], & \text{if } \hbar = \{2, 4\}. \end{cases} \tag{7}$$

Choose $\widetilde{\kappa} = [0, 0]$ and $\widetilde{\kappa}^* = [0.7, 0.9]$. Then, $\widetilde{\mathcal{U}}$ is an IV $(\in, \in \vee(\widetilde{\kappa}^*, q_{\widetilde{\kappa}}))$-FI of X but is not an IV $(\in \vee(\widetilde{\kappa}^*, q_{\widetilde{\kappa}}), \in \vee(\widetilde{\kappa}^*, q_{\widetilde{\kappa}}))$-FI of X as $2_{\widetilde{\ell}=[0.95,0.95]} = (2 * 1)_{\widetilde{\ell}=[0.95,0.95]} \in \vee(\widetilde{\kappa}^*, q_{\widetilde{\kappa}})\widetilde{\mathcal{U}}$ and $1_{\widetilde{j}=[0.5,0.6]} \in \vee(\widetilde{\kappa}^*, q_{\widetilde{\kappa}})\widetilde{\mathcal{U}}$ but $2_{\min\{\widetilde{\ell}, \widetilde{j}\}=[0.5,0.6]} \overline{\in \vee(\widetilde{\kappa}^*, q_{\widetilde{\kappa}})}\widetilde{\mathcal{U}}$.

Lemma 1. *Let $\widetilde{\mathcal{U}}$ be an IVFS of X. Then, $\hbar_{\widetilde{\ell}} \in \widetilde{\mathcal{U}}$ implies $0_{\widetilde{\ell}} \in \vee (\widetilde{\kappa}^*, q_{\widetilde{\kappa}})\widetilde{\mathcal{U}} \Leftrightarrow \forall \hbar \in X, \widetilde{\mathcal{U}}(0) \geq \min\{\widetilde{\mathcal{U}}(\hbar), [((\kappa^{*-} - \kappa^-)/2), ((\kappa^{*+} - \kappa^+)/2)]\}$.*

Proof. ($\Rightarrow$) On the contrary, suppose that, for some $\hbar \in X$, $\widetilde{\mathcal{U}}(0) < \min\{\widetilde{\mathcal{U}}(\hbar), [((\kappa^{*-} - \kappa^-)/2), ((\kappa^{*+} - \kappa^+)/2)]\}$. Take $\widetilde{\ell} \in D(0, ((\kappa^* - k)/2)]$ such that

$$\widetilde{\mathcal{U}}(0) < \widetilde{\ell} \leq \min\left\{\widetilde{\mathcal{U}}(\hbar), \left[\frac{\kappa^{*-} - \kappa^-}{2}, \frac{\kappa^{*+} - \kappa^+}{2}\right]\right\}. \tag{8}$$

Then, $\hbar_{\widetilde{\ell}} \in \widetilde{\mathcal{U}}$, but $0_{\widetilde{\ell}} \overline{\in \vee(\widetilde{\kappa}^*, q_{\widetilde{\kappa}})}\widetilde{\mathcal{U}}$, a contradiction. Hence, $\widetilde{\mathcal{U}}(0) \geq \min\{\widetilde{\mathcal{U}}(\hbar), [((\kappa^{*-} - \kappa^-)/2), ((\kappa^{*+} - \kappa^+)/2)]\}$.
($\Leftarrow$) Let $\hbar \in X$ such that $\hbar_{\widetilde{\ell}} \in \widetilde{\mathcal{U}}$. Then, $\widetilde{\mathcal{U}}(\hbar) \geq \widetilde{\ell}$. So,

$$\begin{aligned} \widetilde{\mathcal{U}}(0) &\geq \min\left\{\widetilde{\mathcal{U}}(\hbar), \left[\frac{\kappa^{*-} - \kappa^-}{2}, \frac{\kappa^{*+} - \kappa^+}{2}\right]\right\} \\ &\geq \min\left\{\widetilde{\ell}, \left[\frac{\kappa^{*-} - \kappa^-}{2}, \frac{\kappa^{*+} - \kappa^+}{2}\right]\right\}. \end{aligned} \tag{9}$$

Now, if $\widetilde{\ell} \leq [((\kappa^{*-} - \kappa^-)/2), ((\kappa^{*+} - \kappa^+)/2)]$, then $\widetilde{\mathcal{U}}(0) \geq \widetilde{\ell}$. Therefore, $0_{\widetilde{\ell}} \in \widetilde{\mathcal{U}}$. On the contrary, if $\widetilde{\ell} > [((\kappa^{*-} - \kappa^-)/2), ((\kappa^{*+} - \kappa^+)/2)]$, then $\widetilde{\mathcal{U}}(0) \geq [((\kappa^{*-} - \kappa^-)/2), ((\kappa^{*+} - \kappa^+)/2)]$. So, $\widetilde{\mathcal{U}}(0) + \widetilde{\ell} > [((\kappa^{*-} - \kappa^-)/2), ((\kappa^{*+} - \kappa^+)/2)] + [((\kappa^{*-} - \kappa^-)/2), ((\kappa^{*+} - \kappa^+)/2)] = [\kappa^{*-} - \kappa^-, \kappa^{*+} - \kappa^+]$. This implies that $0_{\widetilde{\ell}}(\widetilde{\kappa}^*, q_{\widetilde{\kappa}})\widetilde{\mathcal{U}}$. Hence, $0_{\widetilde{\ell}} \in \vee(\widetilde{\kappa}^*, q_{\widetilde{\kappa}})\widetilde{\mathcal{U}}$. □

Lemma 2. *Let $\widetilde{\mathcal{U}}$ be an IVFS of X. Then, $(\hbar * v)_{\widetilde{\ell}} \in \widetilde{\mathcal{U}}$ and $v_{\widetilde{j}} \in \widetilde{\mathcal{U}}$ imply $(\hbar)_{\min\{\widetilde{\ell},\widetilde{j}\}} \in \vee(\widetilde{\kappa^*}, q_{\widetilde{\kappa}})\widetilde{\mathcal{U}} \Leftrightarrow \widetilde{\mathcal{U}}(\hbar) \geq \min$ $\left\{\widetilde{\mathcal{U}}(\hbar * v), \widetilde{\mathcal{U}}(v), [((\kappa^{*-} - \kappa^-)/2), ((\kappa^{*+} - \kappa^+)/2)]\right\}$.*

Proof. ($\Rightarrow$) On the contrary, suppose that $\widetilde{\mathcal{U}}(\hbar) < \min$ $\left\{\widetilde{\mathcal{U}}(\hbar * v), \widetilde{\mathcal{U}}(v), [((\kappa^{*-} - \kappa^-)/2), ((\kappa^{*+} - \kappa^+)/2)]\right\}$ for some $\hbar, v \in X$. Choose $\widetilde{\ell} \in D(0, ((\kappa^* - k)/2]$ such that $\widetilde{\mathcal{U}}(\hbar) < \widetilde{\ell} \leq \min\left\{\widetilde{\mathcal{U}}(\hbar * v), \widetilde{\mathcal{U}}(v), [((\kappa^{*-} - \kappa^-)/2), ((\kappa^{*+} - \kappa^+)/2)]\right\}$. Then, $(\hbar * v)_{\widetilde{\ell}} \in \widetilde{\mathcal{U}}$ and $v_{\widetilde{\ell}} \in \widetilde{\mathcal{U}}$, but $\hbar_{\widetilde{\ell}} \in \vee(\widetilde{\kappa^*}, q_{\widetilde{\kappa}})\widetilde{\mathcal{U}}$, which is not possible. Thus, we have shown that

$$\widetilde{\mathcal{U}}(\hbar) \geq \min\left\{\widetilde{\mathcal{U}}(\hbar * v), \widetilde{\mathcal{U}}(v), \left[\frac{\kappa^{*-} - \kappa^-}{2}, \frac{\kappa^{*+} - \kappa^+}{2}\right]\right\}. \tag{10}$$

This implies that $\hbar_{\min\{\widetilde{\ell},j\}}(\widetilde{\kappa^*}, q_{\widetilde{\kappa}})\widetilde{\mathcal{U}}$. Hence, $\hbar_{\min\{\widetilde{\ell},j\}} \in \vee(\widetilde{\kappa^*}, q_{\widetilde{\kappa}})\widetilde{\mathcal{U}}$, as required.

By combining Lemmas 1 and 2, we have the following theorem. $\quad\square$

Theorem 4. *An IVFS $\widetilde{\mathcal{U}}$ of X is an IV $(\in, \in \vee(\widetilde{\kappa^*}, q_{\widetilde{\kappa}}))$-FI of $X \Leftrightarrow$*

(1) $\widetilde{\mathcal{U}}(0) \geq \min\left\{\widetilde{\mathcal{U}}(\hbar), [((\kappa^{*-} - \kappa^-)/2), ((\kappa^{*+} - \kappa^+)/2)]\right\}$ and

(2) $\widetilde{\mathcal{U}}(\hbar) \geq \min\left\{\widetilde{\mathcal{U}}(\hbar * v), \widetilde{\mathcal{U}}(v), [((\kappa^{*-} - \kappa^-)/2), ((\kappa^{*+} - \kappa^+)/2)]\right\}$

for all $\hbar, v \in X$.

Lemma 3. *Let $\widetilde{\mathcal{U}}$ be an IV $(\in, \in \vee(\widetilde{\kappa^*}, q_{\widetilde{\kappa}}))$-FI of X such that $\hbar \leq v$. Then, $\widetilde{\mathcal{U}}(\hbar) \geq \min\left\{\widetilde{\mathcal{U}}(v), [((\kappa^{*-} - \kappa^-)/2), ((\kappa^{*+} - \kappa^+)/2)]\right\}$.*

($\Leftarrow$) Let $(\hbar * v)_{\widetilde{\ell}} \in \widetilde{\mathcal{U}}$ and $v_{\widetilde{j}} \in \widetilde{\mathcal{U}}$ for all $\widetilde{\ell}, \widetilde{j} \in D(0, 1]$. Then, $\widetilde{\mathcal{U}}(\hbar * v) \geq \widetilde{\ell}$ and $\widetilde{\mathcal{U}}(v) \geq \widetilde{j}$. Thus,

$$\widetilde{\mathcal{U}}(\hbar) \geq \min\left\{\widetilde{\mathcal{U}}(\hbar * v), \widetilde{\mathcal{U}}(v), \left[\frac{\kappa^{*-} - \kappa^-}{2}, \frac{\kappa^{*+} - \kappa^+}{2}\right]\right\}$$
$$\geq \min\left\{\widetilde{\ell}, \widetilde{j}, \left[\frac{\kappa^{*-} - \kappa^-}{2}, \frac{\kappa^{*+} - \kappa^+}{2}\right]\right\}. \tag{11}$$

Now, if $\min\{\widetilde{\ell}, \widetilde{j}\} \leq [((\kappa^{*-} - \kappa^-)/2), ((\kappa^{*+} - \kappa^+)/2)]$, then $\widetilde{\mathcal{U}}(\hbar) \geq \min\{\widetilde{\ell}, \widetilde{j}\}$ and $(\hbar)_{\min\{\widetilde{\ell},j\}} \in \widetilde{\mathcal{U}}$; otherwise, i.e., when $\min\{\widetilde{\ell}, \widetilde{j}\} > [((\kappa^{*-} - \kappa^-)/2), ((\kappa^{*+} - \kappa^+)/2)]$, then $\widetilde{\mathcal{U}}(\hbar) \geq [((\kappa^{*-} - \kappa^-)/2), ((\kappa^{*+} - \kappa^+)/2)]$. So, we have

$$\widetilde{\mathcal{U}}(\hbar) + \min\{\widetilde{\ell}, \widetilde{j}\} > \left[\frac{\kappa^{*-} - \kappa^-}{2}, \frac{\kappa^{*+} - \kappa^+}{2}\right] + \left[\frac{\kappa^{*-} - \kappa^-}{2}, \frac{\kappa^{*+} - \kappa^+}{2}\right] = [\kappa^{*-} - \kappa^-, \kappa^{*+} - \kappa^+]. \tag{12}$$

Proof. Let $\hbar \leq v$ for $\hbar, v \in X$. Then, $\hbar * v = 0$. By hypothesis, we have

$$\widetilde{\mathcal{U}}(\hbar) \geq \min\left\{\widetilde{\mathcal{U}}(\hbar * v), \mathcal{U}(v), \left[\frac{\kappa^{*-} - \kappa^-}{2}, \frac{\kappa^{*+} - \kappa^+}{2}\right]\right\}$$
$$= \min\left\{\widetilde{\mathcal{U}}(0), \mathcal{U}(v), \left[\frac{\kappa^{*-} - \kappa^-}{2}, \frac{\kappa^{*+} - \kappa^+}{2}\right]\right\}$$
$$\geq \min\left\{\widetilde{\mathcal{U}}(v), \left[\frac{\kappa^{*-} - \kappa^-}{2}, \frac{\kappa^{*+} - \kappa^+}{2}\right]\right\}. \tag{13}$$
$\quad\square$

Lemma 4. *Let $\widetilde{\mathcal{U}}$ be an IV $(\in, \in \vee(\widetilde{\kappa^*}, q_{\widetilde{\kappa}}))$-FI of X. Then, for any $\hbar, v, z \in X$, $\hbar * v \leq z \Rightarrow \widetilde{\mathcal{U}}(\hbar) \geq \min\{\widetilde{\mathcal{U}}(v), \widetilde{\mathcal{U}}(z), [((\kappa^{*-} - \kappa^-)/2), ((\kappa^{*+} - \kappa^+)/2)]\}$.*

Proof. Suppose that $\hbar * v \leq z$ for $\hbar, v, z \in X$. Then, we have

$$\widetilde{\mathcal{U}}(\hbar) \geq \min\left\{\widetilde{\mathcal{U}}(\hbar * v), \mathcal{U}(v), \left[\frac{\kappa^{*-} - \kappa^-}{2}, \frac{\kappa^{*+} - \kappa^+}{2}\right]\right\}$$
$$\geq \min\left\{\min\left\{\widetilde{\mathcal{U}}(z), \left[\frac{\kappa^{*-} - \kappa^-}{2}, \frac{\kappa^{*+} - \kappa^+}{2}\right]\right\}, \widetilde{\mathcal{U}}(v), \left[\frac{\kappa^{*-} - \kappa^-}{2}, \frac{\kappa^{*+} - \kappa^+}{2}\right]\right\} \tag{14}$$
$$= \min\left\{\widetilde{\mathcal{U}}(v), \mathcal{U}(z), \left[\frac{\kappa^{*-} - \kappa^-}{2}, \frac{\kappa^{*+} - \kappa^+}{2}\right]\right\}.$$
$\quad\square$

Theorem 5. *Every IV $(\in, \in \vee(\widetilde{\kappa^*}, q_{\widetilde{\kappa}}))$-FI of BCK-algebra X is an IV $(\in, \in \vee(\widetilde{\kappa^*}, q_{\widetilde{\kappa}}))$-FS of X.*

Proof. Let $\widetilde{\mathcal{U}}$ be an IV $(\in, \in \vee(\widetilde{\kappa^*}, q_{\widetilde{\kappa}}))$-FI of X and $v, \hbar \in X$. As $v * \hbar \leq v$ in X, by Lemma 3, we have

$$\widetilde{\mathcal{U}}(v * \hbar) \geq \min\left\{\widetilde{\mathcal{U}}(v), \left[\frac{\kappa^{*-} - \kappa^{-}}{2}, \frac{\kappa^{*+} - \kappa^{+}}{2}\right]\right\}. \quad (15)$$

$$\begin{aligned}
\widetilde{\mathcal{U}}(v * \hbar) &\geq \min\left\{\widetilde{\mathcal{U}}(v), \left[\frac{\kappa^{*-} - \kappa^{-}}{2}, \frac{\kappa^{*+} - \kappa^{+}}{2}\right]\right\} \\
&\geq \min\left\{\min\left\{\widetilde{\mathcal{U}}(v * \hbar), \mathcal{U}(\hbar), \left[\frac{\kappa^{*-} - \kappa^{-}}{2}, \frac{\kappa^{*+} - \kappa^{+}}{2}\right]\right\}, \left[\frac{\kappa^{*-} - \kappa^{-}}{2}, \frac{\kappa^{*+} - \kappa^{+}}{2}\right]\right\} \\
&\geq \min\left\{\widetilde{\mathcal{U}}(v), \widetilde{\mathcal{U}}(\hbar), \left[\frac{\kappa^{*-} - \kappa^{-}}{2}, \frac{\kappa^{*+} - \kappa^{+}}{2}\right]\right\}.
\end{aligned} \quad (16)$$

Hence, $\widetilde{\mathcal{U}}$ is an IV $(\in, \in\vee(\widetilde{\kappa^*}, q_{\widetilde{\kappa}}))$-FS of X. $\qquad\square$

Example 4. Consider a BCK-algebra $X = \{0, 1, 2, 3\}$ with the binary operation $*$ as defined in Table 3.

Consider the IV $(\in, \in\vee(\widetilde{\kappa^*}, q_{\widetilde{\kappa}}))$-FS $\widetilde{\mathcal{U}}$ of X, where $\widetilde{\mathcal{U}}: X \longrightarrow D[0, 1]$ is defined by

$$\widetilde{\mathcal{U}}(\hbar) = \begin{cases} [0.3, 0.4], & \text{if } \hbar = 0, \\ [0.1, 0.2], & \text{if } \hbar \in \{1, 2\}, \\ [0.2, 0.3], & \text{if } \hbar = 3. \end{cases} \quad (17)$$

Choose $\widetilde{\kappa^*} = [0.8, 0.9]$ and $\widetilde{\kappa} = [0.1, 0.2]$. Then, $\widetilde{\mathcal{U}}$ is not an IV $(\in, \in\vee(\widetilde{\kappa^*}, q_{\widetilde{\kappa}}))$-FI of X as $0_{\widetilde{\ell}=[0.3,0.3]} = (1 * 3)_{\widetilde{\ell}=[0.3,0.3]} \in \widetilde{\mathcal{U}}$ and $3_{\widetilde{j}=[0.2,0.2]} \in \widetilde{\mathcal{U}}$ but $1_{\min\{\widetilde{\ell},\widetilde{j}\}=[0.2,0.2]} \overline{\in\vee(\widetilde{\kappa^*}, q_{\widetilde{\kappa}})} \widetilde{\mathcal{U}}$.

Theorem 6. *Let $\widetilde{\mathcal{U}}$ be an IV $(\in, \in\vee(\widetilde{\kappa^*}, q_{\widetilde{\kappa}}))$-FS of X. Then, $\widetilde{\mathcal{U}}$ is an IV $(\in, \in\vee(\widetilde{\kappa^*}, q_{\widetilde{\kappa}}))$-FI $\Leftrightarrow$ for all $v, \hbar, z \in X$ such that $v * \hbar \leq z$ implies $\widetilde{\mathcal{U}}(v) \geq \min\{\widetilde{\mathcal{U}}(\hbar), \widetilde{\mathcal{U}}(z), [((\kappa^{*-} - \kappa^{-})/2), ((\kappa^{*+} - \kappa^{+})/2)]\}$.*

Proof. ($\Rightarrow$) It follows from Lemma 4.

($\Leftarrow$) Let $\widetilde{\mathcal{U}}$ be an IV $(\in, \in\vee(\widetilde{\kappa^*}, q_{\widetilde{\kappa}}))$-FS such that for all $v, \hbar, z \in X$ with $v * \hbar \leq z$ imply $\widetilde{\mathcal{U}}(v) \geq \min\{\widetilde{\mathcal{U}}(\hbar), \widetilde{\mathcal{U}}(z), [((\kappa^{*-} - \kappa^{-})/2), ((\kappa^{*+} - \kappa^{+})/2)]\}$. As $v * (v * \hbar) \leq \hbar$, by hypothesis,

$$\widetilde{\mathcal{U}}(v) \geq \min\left\{\widetilde{\mathcal{U}}(v * \hbar), \widetilde{\mathcal{U}}(\hbar), \left[\frac{\kappa^{*-} - \kappa^{-}}{2}, \frac{\kappa^{*+} - \kappa^{+}}{2}\right]\right\}. \quad (18)$$

Hence, $\widetilde{\mathcal{U}}$ is an IV $(\in, \in\vee(\widetilde{\kappa^*}, q_{\widetilde{\kappa}}))$-FI of X. $\qquad\square$

Theorem 7. *Let $\widetilde{\mathcal{U}}$ be an IVFS of X. Then, $\widetilde{\mathcal{U}}$ is an IV $(\in, \in\vee(\widetilde{\kappa^*}, q_{\widetilde{\kappa}}))$-FI of $X \Leftrightarrow$ the set $\widetilde{\mathcal{U}}_{\widetilde{\ell}}(\neq \varnothing)$ is an ideal of X for each $\widetilde{\ell} \in D(0, ((\kappa^* - \kappa)/2)]$.*

Proof. ($\Rightarrow$) Let $\widetilde{\ell} \in D(0, ((\kappa^* - \kappa)/2)]$ such that $\widetilde{\mathcal{U}}_{\widetilde{\ell}} \neq \varnothing$. By Theorem 4, we have

$$\widetilde{\mathcal{U}}(0) \geq \min\left\{\widetilde{\mathcal{U}}(\hbar), \left[\frac{\kappa^{*-} - \kappa^{-}}{2}, \frac{\kappa^{*+} - \kappa^{+}}{2}\right]\right\}, \quad (19)$$

Since $\widetilde{\mathcal{U}}$ is an IV $(\in, \in\vee(\widetilde{\kappa^*}, q_{\widetilde{\kappa}}))$-FI of X, we have

with $\hbar \in \widetilde{\mathcal{U}}_{\widetilde{\ell}}$. It follows that $\widetilde{\mathcal{U}}(0) \geq \min\{\widetilde{\ell}, [((\kappa^{*-} - \kappa^{-})/2), ((\kappa^{*+} - \kappa^{+})/2)]\} = \widetilde{\ell}$. Therefore, $0 \in \widetilde{\mathcal{U}}_{\widetilde{\ell}}$.

Next, suppose that $\hbar * v \in \widetilde{\mathcal{U}}_{\widetilde{\ell}}$ and $v \in \widetilde{\mathcal{U}}_{\widetilde{\ell}}$. Then, $\widetilde{\mathcal{U}}(\hbar * v) \geq \widetilde{\ell}$ and $\widetilde{\mathcal{U}}(v) \geq \widetilde{\ell}$. Again, by Theorem 4, we have

$$\begin{aligned}
\widetilde{\mathcal{U}}(\hbar) &\geq \min\left\{\widetilde{\mathcal{U}}(\hbar * v), \mathcal{U}(v), \left[\frac{\kappa^{*-} - \kappa^{-}}{2}, \frac{\kappa^{*+} - \kappa^{+}}{2}\right]\right\} \\
&\geq \min\left\{\widetilde{\ell}, \left[\frac{\kappa^{*-} - \kappa^{-}}{2}, \frac{\kappa^{*+} - \kappa^{+}}{2}\right]\right\} = \widetilde{\ell}.
\end{aligned} \quad (20)$$

Therefore, $\hbar \in \widetilde{\mathcal{U}}_{\widetilde{\ell}}$. Hence, $\widetilde{\mathcal{U}}_{\widetilde{\ell}}$ is an ideal of X.

($\Leftarrow$) Suppose that $\widetilde{\mathcal{U}}_{\widetilde{\ell}}$ is an ideal of X for all $\widetilde{\ell} \in D(0, ((\kappa^* - k)/2)]$. If $\widetilde{\mathcal{U}}(0) < \min\{\widetilde{\mathcal{U}}(\hbar), [((\kappa^{*-} - \kappa^{-})/2), ((\kappa^{*+} - \kappa^{+})/2)]\}$ for some $\hbar \in X$, then $\exists \widetilde{\ell} \in D(0, ((\kappa^* - k)/2)]$ such that $\widetilde{\mathcal{U}}(0) < \widetilde{\ell} \leq \min\{\widetilde{\mathcal{U}}(\hbar), [((\kappa^{*-} - \kappa^{-})/2), ((\kappa^{*+} - \kappa^{+})/2)]\}$. It follows that $\hbar \in \widetilde{\mathcal{U}}_{\widetilde{\ell}}$ but $0 \notin \widetilde{\mathcal{U}}_{\widetilde{\ell}}$, a contradiction. Therefore, $\widetilde{\mathcal{U}}(0) \geq \min\{\widetilde{\mathcal{U}}(\hbar), [((\kappa^{*-} - \kappa^{-})/2), ((\kappa^{*+} - \kappa^{+})/2)]\}$. Also, if $\widetilde{\mathcal{U}}(\hbar) < \min\{\widetilde{\mathcal{U}}(\hbar * v), \widetilde{\mathcal{U}}(v), [((\kappa^{*-} - \kappa^{-})/2), ((\kappa^{*+} - \kappa^{+})/2)]\}$ for some $\hbar, v \in X$, then $\exists \widetilde{\ell} \in D(0, ((\kappa^* - k)/2)]$ such that

$$\widetilde{\mathcal{U}}(\hbar) < \widetilde{\ell} \leq \min\left\{\widetilde{\mathcal{U}}(\hbar * v), \widetilde{\mathcal{U}}(v), \left[\frac{\kappa^{*-} - \kappa^{-}}{2}, \frac{\kappa^{*+} - \kappa^{+}}{2}\right]\right\}. \quad (21)$$

It follows that $\hbar * v \in \widetilde{\mathcal{U}}_{\widetilde{\ell}}$ and $v \in \widetilde{\mathcal{U}}_{\widetilde{\ell}}$ but $\hbar \notin \widetilde{\mathcal{U}}_{\widetilde{\ell}}$, which is again a contradiction. Therefore, $\widetilde{\mathcal{U}}(\hbar) \geq \min\{\widetilde{\mathcal{U}}(\hbar * v), \widetilde{\mathcal{U}}(v), [((\kappa^{*-} - \kappa^{-})/2), ((\kappa^{*+} - \kappa^{+})/2)]\}$. Hence, $\widetilde{\mathcal{U}}$ is an IV $(\in, \in\vee(\widetilde{\kappa^*}, q_{\widetilde{\kappa}}))$-FI of X. $\qquad\square$

Definition 7. Let $\widetilde{\mathcal{U}}$ be an IVFS of X. The set

$$[\widetilde{\mathcal{U}}]_{\widetilde{\ell}} = \left\{\hbar \in X | \hbar_{\widetilde{\ell}} \in\vee\left(\widetilde{\kappa^*}, q_{\widetilde{\kappa}}\right)\widetilde{\mathcal{U}}\right\}, \quad \text{where } \widetilde{\ell} \in D(0, 1], \quad (22)$$

is called an $(\in\vee(\widetilde{\kappa^*}, q_{\widetilde{\kappa}}))$-level subset of $\widetilde{\mathcal{U}}$.

Theorem 8. *Let $\widetilde{\mathcal{U}}$ be an IVFS of X. Then, $\widetilde{\mathcal{U}}$ is an IV $(\in, \in\vee(\widetilde{\kappa^*}, q_{\widetilde{\kappa}}))$-FI of $X \Leftrightarrow$ the $(\in\vee(\widetilde{\kappa^*}, q_{\widetilde{\kappa}}))$-level subset $[\widetilde{\mathcal{U}}]_{\widetilde{\ell}}$ of $\widetilde{\mathcal{U}}$ is an ideal of X for each $\widetilde{\ell} \in D(0, 1]$.*

Table 3: Cayley Table of the binary operation*.

$*$	0	1	2	3
0	0	0	0	0
1	1	0	1	0
2	2	2	0	0
3	3	3	3	0

Proof. ($\Rightarrow$) Suppose $\widetilde{\mathcal{U}}$ is an interval-valued $(\in, \in \vee (\widetilde{\kappa^*}, q_{\widetilde{\kappa}}))$-FI of X. Take any $\hbar \in [\widetilde{\mathcal{U}}]_{\widetilde{\ell}}$. Then, $\hbar_{\widetilde{\ell}} \in \vee (\widetilde{\kappa^*}, q_{\widetilde{k}}) \widetilde{\mathcal{U}}$. So, $\widetilde{\mathcal{U}}(\hbar) \geq \widetilde{\ell}$ or $\widetilde{\mathcal{U}}(\hbar) + \widetilde{\ell} > [\kappa^{*-} - \kappa^-, \kappa^{*+} - \kappa^+]$. Now, by Theorem 4, we have $\widetilde{\mathcal{U}}(0) \geq \min\{\widetilde{\mathcal{U}}(\hbar), [((\kappa^{*-} - \kappa^-)/2), ((\kappa^{*+} - \kappa^+)/2)]\}$. Thus, $\widetilde{\mathcal{U}}(0) \geq \min\{\widetilde{\ell}, [((\kappa^{*-} - \kappa^-)/2), ((\kappa^{*+} - \kappa^+)/2)]\}$ when $\widetilde{\mathcal{U}}(\hbar) \geq \widetilde{\ell}$. If $\widetilde{\ell} > [((\kappa^{*-} - \kappa^-)/2), ((\kappa^{*+} - \kappa^+)/2)]$, then $\widetilde{\mathcal{U}}(0) \geq [((\kappa^{*-} - \kappa^-)/2), ((\kappa^{*+} - \kappa^+)/2)]$ implies $0 \in [\widetilde{\mathcal{U}}]_{\widetilde{\ell}}$. Also, if $\widetilde{\ell} \leq [((\kappa^{*-} - \kappa^-)/2), ((\kappa^{*+} - \kappa^+)/2)]$, then $\widetilde{\mathcal{U}}(0) \geq \widetilde{\ell}$ implies $0 \in [\widetilde{\mathcal{U}}]_{\widetilde{\ell}}$. Similarly, $0 \in [\widetilde{\mathcal{U}}]_{\widetilde{\ell}}$ when $\widetilde{\mathcal{U}}(\hbar) + \widetilde{\ell} > [\kappa^{*-} - \kappa^-, \kappa^{*+} - \kappa^+]$.

Next, take any $\hbar * v \in [\widetilde{\mathcal{U}}]_{\widetilde{\ell}}$ and $v \in [\widetilde{\mathcal{U}}]_{\widetilde{\ell}}$. Then, $(\hbar * v)_{\widetilde{\ell}} \in \vee (\widetilde{\kappa^*}, q_{\widetilde{k}}) \widetilde{\mathcal{U}}$ and $v_{\widetilde{\ell}} \in \vee (\widetilde{\kappa^*}, q_{\widetilde{k}}) \widetilde{\mathcal{U}}$, i.e., either $\widetilde{\mathcal{U}}(\hbar * v) \geq \widetilde{\ell}$ or $\widetilde{\mathcal{U}}(\hbar * v) + \widetilde{\ell} > [\kappa^{*-} - \kappa^-, \kappa^{*+} - \kappa^+]$ and either $\widetilde{\mathcal{U}}(v) \geq \widetilde{\ell}$ or $\widetilde{\mathcal{U}}(v) + \widetilde{\ell} > [\kappa^{*-} - \kappa^-, \kappa^{*+} - \kappa^+]$. By assumption, $\widetilde{\mathcal{U}}(\hbar) \geq \min\{\widetilde{\mathcal{U}}(\hbar * v), \widetilde{\mathcal{U}}(v), [((\kappa^{*-} - \kappa^-)/2), ((\kappa^{*+} - \kappa^+)/2)]\}$. Thus, the following cases arise. $\qquad\square$

Case 1. Let $\widetilde{\mathcal{U}}(\hbar * v) \geq \widetilde{\ell}$ and $\widetilde{\mathcal{U}}(v) \geq \widetilde{\ell}$. If $\widetilde{\ell} > [((\kappa^{*-} - \kappa^-)/2), ((\kappa^{*+} - \kappa^+)/2)]$, then

$$\widetilde{\mathcal{U}}(\hbar) \geq \min\left\{\widetilde{\mathcal{U}}(\hbar * v), \widetilde{\mathcal{U}}(v), \left[\frac{\kappa^{*-} - \kappa^-}{2}, \frac{\kappa^{*+} - \kappa^+}{2}\right]\right\}$$
$$\geq \min\left\{\widetilde{\ell}, \left[\frac{\kappa^{*-} - \kappa^-}{2}, \frac{\kappa^{*+} - \kappa^+}{2}\right]\right\}$$
$$= \left[\frac{\kappa^{*-} - \kappa^-}{2}, \frac{\kappa^{*+} - \kappa^+}{2}\right],$$
(23)

and so, $\hbar_{\widetilde{\ell}} (\widetilde{\kappa^*}, q_{\widetilde{k}}) \widetilde{\mathcal{U}}$. If $\widetilde{\ell} \leq [((\kappa^{*-} - \kappa^-)/2), ((\kappa^{*+} - \kappa^+)/2)]$, then

$$\widetilde{\mathcal{U}}(\hbar) \geq \min\left\{\widetilde{\mathcal{U}}(\hbar * v), \widetilde{\mathcal{U}}(v), \left[\frac{\kappa^{*-} - \kappa^-}{2}, \frac{\kappa^{*+} - \kappa^+}{2}\right]\right\}$$
$$\geq \min\left\{\widetilde{\ell}, \left[\frac{\kappa^{*-} - \kappa^-}{2}, \frac{\kappa^{*+} - \kappa^+}{2}\right]\right\}$$
$$= \widetilde{\ell}.$$
(24)

So, $\hbar_{\widetilde{\ell}} \in \widetilde{\mathcal{U}}$. Hence, $\hbar_{\widetilde{\ell}} \in \vee (\widetilde{\kappa^*}, q_{\widetilde{k}}) \widetilde{\mathcal{U}}$.

Case 2. Let $\widetilde{\mathcal{U}}(\hbar * v) \geq \widetilde{\ell}$ and $\widetilde{\mathcal{U}}(v) + \widetilde{\ell} \geq [\kappa^{*-} - \kappa^-, \kappa^{*+} - \kappa^+]$. If $\widetilde{\ell} > [((\kappa^{*-} - \kappa^-)/2), ((\kappa^{*+} - \kappa^+)/2)]$, then

$$\widetilde{\mathcal{U}}(\hbar) \geq \min\left\{\widetilde{\mathcal{U}}(\hbar * v), \widetilde{\mathcal{U}}(v), \left[\frac{\kappa^{*-} - \kappa^-}{2}, \frac{\kappa^{*+} - \kappa^+}{2}\right]\right\}$$
$$\geq \min\{\widetilde{\ell}, ([\kappa^{*-} - \kappa^-, \kappa^{*+} - \kappa^+] - \widetilde{\ell}),$$
$$\cdot \left[\frac{\kappa^{*-} - \kappa^-}{2}, \frac{\kappa^{*+} - \kappa^+}{2}\right]\}$$
$$= [\kappa^{*-} - \kappa^-, \kappa^{*+} - \kappa^+] - \widetilde{\ell},$$
(25)

i.e., $\widetilde{\mathcal{U}}(\hbar) + \widetilde{\ell} > [\kappa^{*-} - \kappa^-, \kappa^{*+} - \kappa^+]$, and thus, $\hbar_{\widetilde{\ell}} (\widetilde{\kappa^*}, q_{\widetilde{k}}) \widetilde{\mathcal{U}}$. If $\widetilde{\ell} \leq [((\kappa^{*-} - \kappa^-)/2), ((\kappa^{*+} - \kappa^+)/2)]$, then

$$\widetilde{\mathcal{U}}(\hbar) \geq \min\left\{\widetilde{\mathcal{U}}(\hbar * v), \widetilde{\mathcal{U}}(v), \left[\frac{\kappa^{*-} - \kappa^-}{2}, \frac{\kappa^{*+} - \kappa^+}{2}\right]\right\}$$
$$\geq \min\{\widetilde{\ell}, ([\kappa^{*-} - \kappa^-, \kappa^{*+} - \kappa^+] - \widetilde{\ell}),$$
$$\cdot \left[\frac{\kappa^{*-} - \kappa^-}{2}, \frac{\kappa^{*+} - \kappa^+}{2}\right]\} = \widetilde{\ell},$$
(26)

and so, $\hbar_{\widetilde{\ell}} \in \widetilde{\mathcal{U}}$. Hence, $\hbar_{\widetilde{\ell}} \in \vee (\widetilde{\kappa^*}, q_{\widetilde{k}}) \widetilde{\mathcal{U}}$.

Similarly, in other two cases, i.e., when $\widetilde{\mathcal{U}}(\hbar * v)) + \widetilde{\ell} > [\kappa^{*-} - \kappa^-, \kappa^{*+} - \kappa^+]$, $\widetilde{\mathcal{U}}(v) \geq \widetilde{\ell}$, and $\widetilde{\mathcal{U}}(\hbar * v) + \widetilde{\ell} > [\kappa^{*-} - \kappa^-, \kappa^{*+} - \kappa^+]$, $\widetilde{\mathcal{U}}(v) + \widetilde{\ell} > [\kappa^{*-} - \kappa^-, \kappa^{*+} - \kappa^+]$, we have $\hbar_{\widetilde{\ell}} \in \vee (\widetilde{\kappa^*}, q_{\widetilde{k}}) \widetilde{\mathcal{U}}$. Hence, in each case, $\hbar_{\widetilde{\ell}} \in \vee (\widetilde{\kappa^*}, q_{\widetilde{k}}) \widetilde{\mathcal{U}}$, and thus, $\hbar \in [\widetilde{\mathcal{U}}]_{\widetilde{\ell}}$.

($\Leftarrow$) Let $[\widetilde{\mathcal{U}}]_{\widetilde{\ell}}$ be an ideal of X for all $\widetilde{\ell} \in D(0, 1]$. On the contrary, let

$$\widetilde{\mathcal{U}}(0) < \min\left\{\widetilde{\mathcal{U}}(\hbar), \left[\frac{\kappa^{*-} - \kappa^-}{2}, \frac{\kappa^{*+} - \kappa^+}{2}\right]\right\}, \quad (27)$$

with $\hbar \in X$. Then, $\exists \widetilde{\ell} \in D(0, 1]$ such that $\widetilde{\mathcal{U}}(0) < \widetilde{\ell} \leq \min\{\widetilde{\mathcal{U}}(\hbar), [((\kappa^{*-} - \kappa^-)/2), ((\kappa^{*+} - \kappa^+)/2)]\}$. It follows that $\hbar \in [\widetilde{\mathcal{U}}]_{\widetilde{\ell}}$, but $0 \notin [\widetilde{\mathcal{U}}]_{\widetilde{\ell}}$, which is not possible. Therefore,

$$\widetilde{\mathcal{U}}(0) \geq \min\left\{\widetilde{\mathcal{U}}(\hbar), \left[\frac{\kappa^{*-} - \kappa^-}{2}, \frac{\kappa^{*+} - \kappa^+}{2}\right]\right\}. \quad (28)$$

Also, if $\widetilde{\mathcal{U}}(\hbar) < \min\{\widetilde{\mathcal{U}}(\hbar * v), \widetilde{\mathcal{U}}(v), [((\kappa^{*-} - \kappa^-)/2), ((\kappa^{*+} - \kappa^+)/2)]\}$ for some $\hbar, v \in X$, then $\exists \widetilde{\ell} \in D(0, 1]$ such that

$$\widetilde{\mathcal{U}}(\hbar) < \widetilde{\ell} \leq \min\left\{\widetilde{\mathcal{U}}(\hbar * v), \widetilde{\mathcal{U}}(v), \left[\frac{\kappa^{*-} - \kappa^-}{2}, \frac{\kappa^{*+} - \kappa^+}{2}\right]\right\}. \quad (29)$$

It follows that $\hbar * v \in [\widetilde{\mathcal{U}}]_{\widetilde{\ell}}$ and $v \in [\widetilde{\mathcal{U}}]_{\widetilde{\ell}}$ but $\hbar \notin [\widetilde{\mathcal{U}}]_{\widetilde{\ell}}$, which is again a contradiction. Therefore, $\widetilde{\mathcal{U}}(\hbar) \geq \min\{\widetilde{\mathcal{U}}(\hbar * v), \widetilde{\mathcal{U}}(v), [((\kappa^{*-} - \kappa^-)/2), ((\kappa^{*+} - \kappa^+)/2)]\}$. Hence, $\widetilde{\mathcal{U}}$ is an IV $(\in, \in \vee (\widetilde{\kappa^*}, q_{\widetilde{\kappa}}))$-FI of X.

4. Interval-Valued $(\in, \in \vee (\widetilde{\kappa^*}, q_{\widetilde{\kappa}}))$-Fuzzy Commutative Ideals

Throughout the following sections, X denotes BCK-algebras unless stated otherwise.

Definition 8. Let X be a BCK-algebra. An IVFS $\widetilde{\mathcal{U}}$ is called an interval-valued $(\in, \in \vee (\widetilde{\kappa^*}, q_{\widetilde{\kappa}}))$-fuzzy commutative ideal (in short, IV $(\in, \in \vee (\widetilde{\kappa^*}, q_{\widetilde{\kappa}}))$-FCI) if for all $v, p, \hbar \in X$:

(1) $\hbar_{\widetilde{\ell}} \in \widetilde{\mathcal{U}}$ implies $0_{\widetilde{\ell}} \in \vee (\widetilde{\kappa^*}, q_{\widetilde{\kappa}})\widetilde{\mathcal{U}}$

(2) $((v * p) * \hbar)_{\widetilde{\ell}} \in \widetilde{\mathcal{U}}$ and $\hbar_{\widetilde{j}} \in \widetilde{\mathcal{U}}$ imply $(v * (p * (p * v)))_{\min\{\widetilde{\ell}, j\}} \in \vee (\widetilde{\kappa^*}, q_{\widetilde{\kappa}})\widetilde{\mathcal{U}}^j$

Example 5. Consider a BCK-algebra $X = \{0, 1, 2, 3\}$ with the binary operation $*$ as defined in Table 4.

Define $\widetilde{\mathcal{U}}: X \longrightarrow D[0, 1]$ by

$$\widetilde{\mathcal{U}}(\hbar) = \begin{cases} [0.5, 0.6], & \text{if } \hbar = 0, \\ [0.3, 0.4], & \text{if } \hbar \in \{1, 2\}, \\ [0.1, 0.2], & \text{if } \hbar = 3. \end{cases} \tag{30}$$

Choose $\widetilde{\kappa^*} = [0.2, 0.3]$ and $\widetilde{\kappa} = [0.1, 0.2]$. Then, it is easy to see that $\widetilde{\mathcal{U}}$ is an IV $(\in, \in \vee (\widetilde{\kappa^*}, q_{\widetilde{\kappa}}))$-FCI of X.

Theorem 9. *An IVFS $\widetilde{\mathcal{U}}$ of X is an IV $(\in, \in \vee (\widetilde{\kappa^*}, q_{\widetilde{\kappa}}))$-FCI of $X \Leftrightarrow$*

(1) $\widetilde{\mathcal{U}}(0) \geq \min\{\widetilde{\mathcal{U}}(\hbar), [((\kappa^{*-} - \kappa^-)/2), ((\kappa^{*+} - \kappa^+)/2)]\}$ and

(2) $\widetilde{\mathcal{U}}(v * (p * (p * v))) \geq \min\{\widetilde{\mathcal{U}}((v * p) * \hbar), \widetilde{\mathcal{U}}(\hbar), [((\kappa^{*-} - \kappa^-)/2), ((\kappa^{*+} - \kappa^+)/2)]\}$

for all $v, p, \hbar \in X$.

Table 4: Cayley Table of the binary operation*.

*	0	1	2	3
0	0	0	0	0
1	1	0	0	1
2	2	1	0	2
3	3	3	3	0

Proof. $(\Rightarrow)$ Condition (1) follows from Lemma 1. To show that (2) holds in X, suppose, on the contrary, that (2) does not hold in X, so we have

$$\widetilde{\mathcal{U}}(v * (p * (p * v)))$$
$$< \min\left\{\widetilde{\mathcal{U}}((v * p) * \hbar), \widetilde{\mathcal{U}}(\hbar), \left[\frac{\kappa^{*-} - \kappa^-}{2}, \frac{\kappa^{*+} - \kappa^+}{2}\right]\right\}, \tag{31}$$

for some $v, p, \hbar \in X$. Choose $\widetilde{\ell} \in D[0, 1]$ such that $\widetilde{\mathcal{U}}(v * (p * (p * v))) < \widetilde{\ell} \leq \min\{\widetilde{\mathcal{U}}((v * p) * \hbar), \widetilde{\mathcal{U}}(\hbar), [((\kappa^{*-} - \kappa^-)/2), ((\kappa^{*+} - \kappa^+)/2)]\}$. Then, $((v * p) * \hbar)_{\widetilde{\ell}} \in \widetilde{\mathcal{U}}$ and $\hbar_{\widetilde{\ell}} \in \widetilde{\mathcal{U}}$, but $(v * (p * (p * v)))_{\widetilde{\ell}} \in \vee (\widetilde{\kappa^*}, q_{\widetilde{\kappa}})\widetilde{\mathcal{U}}$, which is not possible. Thus,

$$\widetilde{\mathcal{U}}(v * (p * (p * v)))$$
$$\geq \min\left\{\widetilde{\mathcal{U}}((v * p) * \hbar), \widetilde{\mathcal{U}}(\hbar), \left[\frac{\kappa^{*-} - \kappa^-}{2}, \frac{\kappa^{*+} - \kappa^+}{2}\right]\right\}, \tag{32}$$

for each $v, p, \hbar \in X$.

$(\Leftarrow)$ Suppose that conditions (1) and (2) hold in X. It follows from condition (1) and Lemma 1 that $\hbar_{\widetilde{\ell}} \in \widetilde{\mathcal{U}}$ implies $0_{\widetilde{\ell}} \in \vee (\widetilde{\kappa^*}, q_{\widetilde{\kappa}})\widetilde{\mathcal{U}}$. Let $((v * p) * \hbar)_{\widetilde{\ell}} \in \widetilde{\mathcal{U}}$ and $\hbar_{\widetilde{j}} \in \widetilde{\mathcal{U}}$ for all $\widetilde{\ell}, \widetilde{j} \in D(0, 1]$. Then, $\widetilde{\mathcal{U}}((v * p) * \hbar) \geq \widetilde{\ell}$ and $\widetilde{\mathcal{U}}(\hbar) \geq \widetilde{j}$. Thus,

$$\widetilde{\mathcal{U}}(v * (p * (p * v))) \geq \min\left\{\widetilde{\mathcal{U}}((v * p) * \hbar), \widetilde{\mathcal{U}}(\hbar), \left[\frac{\kappa^{*-} - \kappa^-}{2}, \frac{\kappa^{*+} - \kappa^+}{2}\right]\right\}$$
$$\geq \min\left\{\widetilde{\ell}, \widetilde{j}, \left[\frac{\kappa^{*-} - \kappa^-}{2}, \frac{\kappa^{*+} - \kappa^+}{2}\right]\right\}. \tag{33}$$

Now, if $\min\{\widetilde{\ell}, \widetilde{j}\} \leq [((\kappa^{*-} - \kappa^-)/2), ((\kappa^{*+} - \kappa^+)/2)]$, then $\widetilde{\mathcal{U}}(v * (p * (p * v))) \geq \min\{\widetilde{\ell}, \widetilde{j}\}$ implies $(v * (p * (p * v)))_{\min\{\widetilde{\ell}, j\}} \in \widetilde{\mathcal{U}}$; otherwise, i.e., when $\min\{\widetilde{\ell}, \widetilde{j}\} > [((\kappa^{*-} - \kappa^-)/2), ((\kappa^{*+} - \kappa^+)/2)]$, then $\widetilde{\mathcal{U}}(v * (p * (p * v))) \geq [((\kappa^{*-} - \kappa^-)/2), ((\kappa^{*+} - \kappa^+)/2)]$. So, we have

$$\widetilde{\mathcal{U}}(v * (p * (p * v))) + \min\{\widetilde{\ell}, \widetilde{j}\}$$
$$\geq \left[\frac{\kappa^{*-} - \kappa^-}{2}, \frac{\kappa^{*+} - \kappa^+}{2}\right] + \left[\frac{\kappa^{*-} - \kappa^-}{2}, \frac{\kappa^{*+} - \kappa^+}{2}\right] \tag{34}$$
$$= [\kappa^{*-} - \kappa^-, \kappa^{*+} - \kappa^+].$$

This implies that $(v * (p * (p * v)))_{\min\{\widetilde{\ell}, j\}}(\widetilde{\kappa^*}, q_{\widetilde{\kappa}}))\widetilde{\mathcal{U}}$. Therefore, $(v * (p * (p * v)))_{\min\{\widetilde{\ell}, j\}} \in \vee (\widetilde{\kappa^*}, q_{\widetilde{\kappa}})\widetilde{\mathcal{U}}$. Hence, $\widetilde{\mathcal{U}}$ is an IV $(\in, \in \vee (\widetilde{\kappa^*}, q_{\widetilde{\kappa}}))$-FCI of X. □

Theorem 10. *Every IV $(\in, \in \vee (\widetilde{\kappa^*}, q_{\widetilde{\kappa}}))$-FCI of BCK-algebra X is an IV $(\in, \in \vee (\widetilde{\kappa^*}, q_{\widetilde{\kappa}}))$-FI of X.*

Proof. Let $\widetilde{\mathcal{U}}$ be any IV $(\in, \in \vee (\widetilde{\kappa^*}, q_{\widetilde{\kappa}}))$-FCI of X and $v, \hbar \in X$. Then, we have

Table 5: Cayley Table of the binary operation*.

$*$	0	1	2	3	4
0	0	0	0	0	0
1	1	0	1	0	0
2	2	2	0	0	0
3	3	3	3	0	0
4	4	4	3	2	0

$$\widetilde{\mathcal{U}}(v) = \widetilde{\mathcal{U}}(v * (0 * (0 * v)))$$

$$\geq \min\left\{\widetilde{\mathcal{U}}((v * 0) * \hbar), \widetilde{\mathcal{U}}(\hbar), \left[\frac{\kappa^{*-} - \kappa^-}{2}, \frac{\kappa^{*+} - \kappa^+}{2}\right]\right\}$$

$$= \min\left\{\widetilde{\mathcal{U}}((v * \hbar), \widetilde{\mathcal{U}}(\hbar), \left[\frac{\kappa^{*-} - \kappa^-}{2}, \frac{\kappa^{*+} - \kappa^+}{2}\right]\right\}. \tag{35}$$

Hence, $\widetilde{\mathcal{U}}$ is an IV $(\in, \in\vee(\widetilde{\kappa^*}, q_{\widetilde{\kappa}}))$-FI of X. □

Example 6. Consider a BCK-algebra $X = \{0, 1, 2, 3, 4\}$ with the binary operation $*$ as defined in Table 5.

Choose $\widetilde{\kappa^*} = [0.7, 0.8]$ and $\widetilde{\kappa} = [0.2, 0.3]$. Then, $\widetilde{\mathcal{U}}$ is an IV $(\in, \in\vee(\widetilde{\kappa^*}, q_{\widetilde{\kappa}}))$-FI of X but is not an IV $(\in, \in\vee(\widetilde{\kappa^*}, q_{\widetilde{\kappa}}))$-FCI of X as $(0)_{\widetilde{\ell}=[0.2,0.2]} = (2 * (3 * (3 * 2)))_{\widetilde{\ell}=[0.2,0.2]} \in \widetilde{\mathcal{U}}$ and $(0)_{\widetilde{j}=[0.3,0.3]} \in \widetilde{\mathcal{U}}$ but $(2 * (3 * (3 * 2)))_{\min\{\widetilde{\ell,j}\}=[0.2,0.2]} = (2)_{\widetilde{\ell}=[0.2,0.2]} \in\vee(\widetilde{\kappa^*}, q_{\widetilde{\kappa}})\widetilde{\mathcal{U}}$.

Theorem 11. *Let $\widetilde{\mathcal{U}}$ be an IV $(\in, \in\vee(\widetilde{\kappa^*}, q_{\widetilde{\kappa}}))$-FI of BCK-algebra X. Then, $\widetilde{\mathcal{U}}$ is an IV $(\in, \in\vee(\widetilde{\kappa^*}, q_{\widetilde{\kappa}}))$-FCI of $X \Leftrightarrow$ for all $v, p \in X$,*

$$\widetilde{\mathcal{U}}(v * (p * (p * v))) \geq \min\left\{\widetilde{\mathcal{U}}(v * p), \left[\frac{\kappa^{*-} - \kappa^-}{2}, \frac{\kappa^{*+} - \kappa^+}{2}\right]\right\}. \tag{37}$$

Proof. $(\Rightarrow)$ Let $\widetilde{\mathcal{U}}$ be an IV $(\in, \in\vee(\widetilde{\kappa^*}, q_{\widetilde{\kappa}}))$-FCI of X. Then, for all $v, p, \hbar \in X$, we have

$$\widetilde{\mathcal{U}}(v * (p * (p * v)))$$

$$\geq \min\left\{\widetilde{\mathcal{U}}((v * p) * \hbar), \widetilde{\mathcal{U}}(\hbar), \left[\frac{\kappa^{*-} - \kappa^-}{2}, \frac{\kappa^{*+} - \kappa^+}{2}\right]\right\}. \tag{38}$$

By taking $\hbar = 0$, we have

$$\widetilde{\mathcal{U}}(v * (p * (p * v))) \geq \min\left\{\widetilde{\mathcal{U}}((v * p) * 0), \widetilde{\mathcal{U}}(0), \left[\frac{\kappa^{*-} - \kappa^-}{2}, \frac{\kappa^{*+} - \kappa^+}{2}\right]\right\}$$

$$= \min\left\{\widetilde{\mathcal{U}}(v * p), \left[\frac{\kappa^{*-} - \kappa^-}{2}, \frac{\kappa^{*+} - \kappa^+}{2}\right]\right\}. \tag{39}$$

$(\Leftarrow)$ Let $v, p, \hbar \in X$. By assumption, we have

$$\widetilde{\mathcal{U}}(v * p) \geq \min\left\{\widetilde{\mathcal{U}}((v * p) * \hbar), \widetilde{\mathcal{U}}(\hbar), \left[\frac{\kappa^{*-} - \kappa^-}{2}, \frac{\kappa^{*+} - \kappa^+}{2}\right]\right\}. \tag{40}$$

By assumption and equation (40), we have

$$\widetilde{\mathcal{U}}(v * (p * (p * v))) \geq \min\left\{\widetilde{\mathcal{U}}(v * p), \left[\frac{\kappa^{*-} - \kappa^-}{2}, \frac{\kappa^{*+} - \kappa^+}{2}\right]\right\}$$

$$\geq \min\left\{\widetilde{\mathcal{U}}((v * p) * \hbar), \widetilde{\mathcal{U}}(\hbar), \left[\frac{\kappa^{*-} - \kappa^-}{2}, \frac{\kappa^{*+} - \kappa^+}{2}\right]\right\}. \tag{41}$$

Hence, $\widetilde{\mathcal{U}}$ is an IV $(\in, \in\vee(\widetilde{\kappa^*}, q_{\widetilde{\kappa}}))$-FCI of X. □

5. Conclusion

The aim of this paper is to present a general form of interval-valued fuzzy ideals of BCK/BCI-algebras. In fact, we introduced the concepts of interval-valued $(\in, \in\vee(\widetilde{\kappa^*}, q_{\widetilde{\kappa}}))$-fuzzy (subalgebras) ideals and interval-valued $(\in\vee(\widetilde{\kappa^*}, q_{\widetilde{\kappa}}), \in\vee(\widetilde{\kappa^*}, q_{\widetilde{\kappa}}))$-fuzzy ideals of BCK/BCI-algebras. In addition, interval-valued $(\in, \in\vee(\widetilde{\kappa^*}, q_{\widetilde{\kappa}}))$-fuzzy commutative ideals were defined, and some essential properties were discussed. Moreover, the relationship

$$\widetilde{\mathcal{U}}(\hbar) = \begin{cases} [0.5, 0.6], & \text{if } \hbar = 0, \\ [0.4, 0.5], & \text{if } \hbar = 1, \\ [0.0, 0.1], & \text{if } \hbar \in \{2, 3, 4\}. \end{cases} \tag{36}$$

between $(\in, \in \vee(\widetilde{\kappa}^*, q_{\widetilde{\kappa}}))$-fuzzy ideals and interval-valued $(\in, \in \vee(\widetilde{\kappa}^*, q_{\widetilde{\kappa}}))$-fuzzy commutative ideals is considered. In this present study, we conclude the following cases:

(1) If we take $\widetilde{\kappa}^* = [1, 1]$ and $\widetilde{\kappa} = [0, 0]$, then interval-valued $(\in, \in \vee(\widetilde{\kappa}^*, q_{\widetilde{\kappa}}))$-fuzzy subalgebras and interval-valued $(\in, \in \vee(\widetilde{\kappa}^*, q_{\widetilde{\kappa}}))$-fuzzy ideals reduce to the concepts of interval-valued $(\in, \in \vee q)$-fuzzy subalgebras and interval-valued $(\in, \in \vee q)$-fuzzy ideals of X as introduced in [34]

(2) If we take $\widetilde{\kappa}^* = [1, 1]$ and $\widetilde{\kappa} = \widetilde{\kappa}$, then interval-valued $(\in, \in \vee(\widetilde{\kappa}^*, q_{\widetilde{\kappa}}))$-fuzzy subalgebras and interval-valued $(\in, \in \vee(\widetilde{\kappa}^*, q_{\widetilde{\kappa}}))$-fuzzy ideals reduce to the concepts of interval-valued $(\in, \in \vee q_{\widetilde{\kappa}})$-fuzzy subalgebras and interval-valued $(\in, \in \vee q_{\widetilde{\kappa}})$-fuzzy ideals of X as introduced in [37]

Consequently, the notions introduced in this paper, i.e., $(\in, \in \vee(\widetilde{\kappa}^*, q_{\widetilde{\kappa}}))$-fuzzy subalgebras and $(\in, \in \vee(\widetilde{\kappa}^*, q_{\widetilde{\kappa}}))$-fuzzy ideals, are more general than $(\in, \in \vee q_{\widetilde{\kappa}})$-fuzzy subalgebras and $(\in, \in \vee q_{\widetilde{\kappa}})$-fuzzy ideals. In future work, one may extend these concepts to various algebraic structures such as rings, hemirings, LA-semigroups, semi-hypergroups, semi-hyperrings, BL-algebras, MTL-algebras, $R0$-algebras, MV-algebras, EQ-algebras, and lattice implication algebras.

Data Availability

No data were used to support this study.

Conflicts of Interest

The authors declare that there are no conflicts of interest.

Acknowledgments

References

[1] S. R. Barbhuiya and K. D. Choudhury, "($\in$, $\in$ Vq)-interval-valued fuzzy dot d-ideals of d-algebras," *Advanced Trends in Mathematics*, vol. 3, pp. 1–15, 2015.

[2] Y. B. Yun, "On (α, β)-fuzzy ideals of BCK/BCI-algebras," *Scientiae Mathematicae Japonicae*, pp. 101–105, 2004.

[3] M. Akram, N. Yaqoob, and J. Kavikumar, "Interval-valued $(\widetilde{\theta}, \widetilde{\delta})$-fuzzy KU-ideals of KU-algebras," *International Journal of Pure and Applied Mathematics*, vol. 92, no. 3, pp. 335–349, 2014.

[4] S. M. Mostafa, M. A. Abd-Elnaby, and O. R. Elgendy, "Interval-valued fuzzy KU-ideals in KU-algebras," *International Mathematical Forum*, vol. 6, no. 64, pp. 3151–3159, 2011.

[5] Y. B. Jun, "Interval-valued fuzzy subalgebras/ideals in BCK-algebras," *Scientiae Mathematicae*, vol. 3, no. 3, pp. 435–444, 2000.

[6] M. Aslam, S. Abdullah, and S. Aslam, "Characterization of regular LA-semigroup by interval-valued $(\overline{\alpha}, \overline{\beta})$-fuzzy ideals," *Afrika Matematika*, vol. 25, no. 3, pp. 1–18, 2013.

[7] A. L. Narayanan and T. Manikantan, "Interval-valued fuzzy interior ideal in semigroups," in *Proceedings of the 19th Annual Conference of the Ramanujan Mathematical Society*, Agra, India, July 2004.

[8] R. Biswas, "Rosenfeld's fuzzy subgroups with interval-valued membership functions," *Fuzzy Sets and Systems*, vol. 63, no. 1, pp. 87–90, 1994.

[9] N. Yaqoob, R. Chinram, A. Ghareeb, and M. Aslam, "Left almost semigroups characterized by their interval valued fuzzy ideals," *Afrika Matematika*, vol. 24, no. 2, pp. 231–245, 2013.

[10] N. Yaqoob, "Interval-valued intuitionistic fuzzy ideals of regular LAsemigroups," *Thai Journal of Mathematics*, vol. 11, no. 3, pp. 683–695, 2013.

[11] D. S. Lee and C. H. Park, "Interval-valued $(\in, \in \vee q)$ fuzzy ideals in rings," *International Mathematical Forum*, vol. 4, no. 13, pp. 623–630, 2009.

[12] A. Ahmad, M. Aslam, and S. Abdullah, "Interval-valued (α, β),-fuzzy hyperideals of semihyperring," *U.P.B. Scientific Bulletin, Series A*, vol. 75, no. 2, pp. 69–86, 2013.

[13] Y. B. Jun and K. H. Kim, "Interval-valued fuzzy r-subgroups of near-rings," *Indian Journal of Pure and Applied Mathematics*, vol. 33, no. 1, pp. 71–80, 2002.

[14] A. Khan, F. Hussain, A. Hadi, and S. A. Khan, "A decision making approach based on multi-fuzzy bipolar soft sets," *Journal of Intelligent & Fuzzy Systems*, vol. 37, no. 2, pp. 1879–1892, 2019.

[15] A. Khan, M. Izhar, and M. M. Khalaf, "Generalised multi-fuzzy bipolar soft sets and its application in decision making," *Journal of Intelligent & Fuzzy Systems*, vol. 37, no. 2, pp. 2713–2725, 2019.

[16] N. Malik and M. Shabir, "Rough fuzzy bipolar soft sets and application in decision-making problems," *Soft Computing*, vol. 23, no. 5, pp. 1603–1614, 2019.

[17] G. Ali, M. Akram, A. N. A. Koam, and J. C. R. Alcantud, "Parameter reductions of bipolar fuzzy soft sets with their decision-making algorithms," *Symmetry*, vol. 11, no. 8, p. 949, 2019.

[18] T. Mahmood, "A novel approach towards bipolar soft sets and their applications," *Journal of Mathematics*, vol. 2020, Article ID 4690808, 11 pages, 2020.

[19] M. Akram and G. Ali, "Hybrid models for decision-making based on rough Pythagorean fuzzy bipolar soft information," *Granular Computing*, vol. 5, no. 1, pp. 1–15, 2020.

[20] D. Al-Kadi and G. Muhiuddin, "Bipolar fuzzy BCI-implicative ideals of BCI-algebras," *Annals of Communications in Mathematics*, vol. 3, no. 1, pp. 88–96, 2020.

[21] A. Al-masarwah, A. G. Ahmad, and G. Muhiuddin, "Doubt N-ideals theory in BCK-algebras based on N- structures," *Annals of Communication in Mathematics*, vol. 3, no. 1, pp. 54–62, 2020.

[22] G. Muhiuddin, D. Al-Kadi, and A. Mahboob, "Hybrid structures applied to ideals in BCI-algebras," *Journal of Mathematics*, vol. 2020, Article ID 2365078, 7 pages, 2020.

[23] G. Muhiuddin and A. M. Al-roqi, "Cubic soft sets with applications in BCK/BCI-algebras," *Annals of Fuzzy Mathematics and Informatics*, vol. 8, no. 2, pp. 291–304, 2014.

[24] G. Muhiuddin, A. M. Al-roqi, and S. Aldhafeeri, "Filter theory in MTL-algebras based on Uni-soft property," *Bulletin of the Iranian Mathematical Society*, vol. 43, no. 7, pp. 2293–2306, 2017.

[25] G. Muhiuddin and A. M. Al-roqi, "Unisoft filters in R0-algebras," *Journal of Computational Analysis and Applications*, vol. 19, no. 1, pp. 133–143, 2015.

[26] Y. B. Jun, G. Muhiuddin, M. A. Ozturk, and E. H. Roh, "Cubic soft ideals in BCK/BCI-algebras," *Journal of Computational Analysis and Applications*, vol. 22, no. 5, pp. 929–940, 2017.